

AD-768 616

**PLUME CONTAMINATION EFFECTS PREDICTION.
THE CONTAM COMPUTER PROGRAM, VERSION II**

R. J. Hoffman, et al

McDonnell Douglas Astronautics Company

Prepared for:

Air Force Rocket Propulsion Laboratory

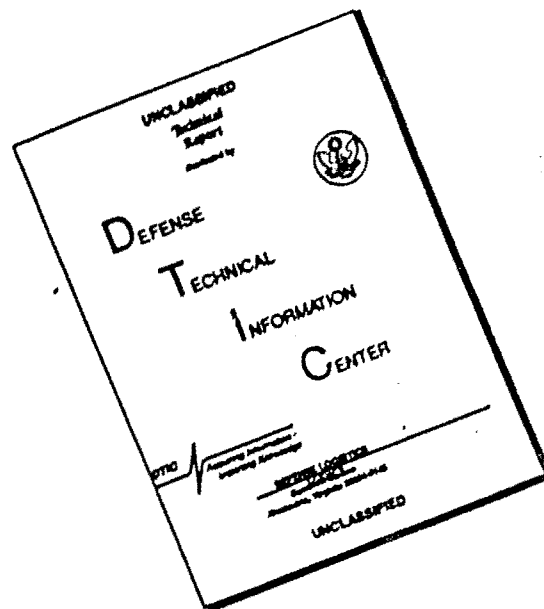
August 1973

DISTRIBUTED BY:

NTIS

**National Technical Information Service
U. S. DEPARTMENT OF COMMERCE
5285 Port Royal Road, Springfield Va. 22151**

DISCLAIMER NOTICE



THIS DOCUMENT IS BEST QUALITY AVAILABLE. THE COPY FURNISHED TO DTIC CONTAINED A SIGNIFICANT NUMBER OF PAGES WHICH DO NOT REPRODUCE LEGIBLY.

UNCLASSIFIED

SECURITY CLASSIFICATION OF THIS PAGE (When Data Entered)

AD 768616

REPORT DOCUMENTATION PAGE		READ INSTRUCTIONS BEFORE COMPLETING FORM
1. REPORT NUMBER AFRPL-TR-73-46	2. GOVT ACCESSION NO.	3. RECIPIENT'S CATALOG NUMBER
4. TITLE (and Subtitle) Plume Contamination Effects Prediction The Contam Computer Program Version II		5. TYPE OF REPORT & PERIOD COVERED Final Aug 1970 to April 1973
7. AUTHOR(s) R. J. Hoffman, W. T. Webber, S. S. Cherry, F. Cramer, W. D. English, R. G. Oeding, G. Yanow and Capt J. Ross Nunn, USAF		6. PERFORMING ORG. REPORT NUMBER
9. PERFORMING ORGANIZATION NAME AND ADDRESS McDonnell Douglas Astronautics Co. Huntington Beach, California		8. CONTRACT OR GRANT NUMBER(s) FO4611-72-C-0037
11. CONTROLLING OFFICE NAME AND ADDRESS Air Force Rocket Propulsion Laboratory (DY) Edwards, CA 93523		10. PROGRAM ELEMENT, PROJECT, TASK AREA & WORK UNIT NUMBERS
14. MONITORING AGENCY NAME & ADDRESS (if different from Controlling Office)		12. REPORT DATE August 1973
		13. NUMBER OF PAGES 221 / 765
		15. SECURITY CLASS. (of this report) UNCLASSIFIED
		15a. DECLASSIFICATION/DOWNGRADING SCHEDULE N/A
16. DISTRIBUTION STATEMENT (of this Report) APPROVED FOR PUBLIC RELEASE; DISTRIBUTION UNLIMITED		
17. DISTRIBUTION STATEMENT (of the abstract entered in Block 20, if different from Report)		
18. SUPPLEMENTARY NOTES Reproduced by NATIONAL TECHNICAL INFORMATION SERVICE U S Department of Commerce Springfield VA 22151		
19. KEY WORDS (Continue on reverse side if necessary and identify by block number) Computer Rocket Exhaust Plume Contamination Satellite Contamination Liquid Rocket Performance		
20. ABSTRACT (Continue on reverse side if necessary and identify by block number) The effect of rocket exhaust plume impingement on sensitive vehicle surfaces is an area of continuing concern in the design of spacecraft, missiles and reentry vehicle systems. Specifically, the contamination and subsequent degradation of functional surfaces, such as solar cells, thermal control coatings, optical lenses, optical view ports, and highly reflective surfaces, have resulted in compromises of mission effectiveness. The objective of this study was to develop a single computer code capable of predicting the production,		

DD FORM 1 JAN 73 1473

EDITION OF 1 NOV 65 IS OBSOLETE

UNCLASSIFIED

SECURITY CLASSIFICATION OF THIS PAGE (When Data Entered)

transport, and deposition of engine and plume contaminants, and the change in absorptivity, emissivity, reflectivity, and transmissivity of a functional spacecraft surface, such as thermal control coatings and optical view ports and lenses, resulting from plume contaminant deposition or mechanical abrasion (sand blasting). Both bipropellants and monopropellants have been treated. Surface chemical reaction with a deposited plume contaminant layer was not treated. Analytical models and computer subprograms have been developed and integrated to form the CONTAM computer program. Complete User's manuals for each of the computer subprograms as well as the CONTAM program are included in this report, along with details of the analysis and numerical methods. A sample case illustrating the CONTAM program's capability is presented.

FOREWORD

This report was prepared for the Air Force Rocket Propulsion Laboratory (AFRPL), United States Air Force, Edwards, California, under Contracts F04611-70-C-0076 and F04611-72-C-0037, by the McDonnell Douglas Astronautics Company (MDAC), Huntington Beach, California. The Air Force program monitors for this study were Dr. L. P. Quinn (RTSP) and James R. Nunn, Capt., USAF (RTSP). The study was performed during the period August 1970 to April 1973, and the final report submitted to AFRPL for approval on May 15, 1973. The results of the initial contract were previously reported in AFRPL-TR-71-109, December 1971.

The MDAC study manager for this project was Mr. R. J. Hoffman, Supervisor, Plume Effects, Aero/thermodynamics and Nuclear Effects Department. Mr. W. T. Webber acted as Principal Investigator for the study and Task Leader for the bipropellant contamination production task. Other members of the Plume Effects Group included Mr. R. G. Oeding, Task Leader, Contaminant Transport and Chemical Kinetics; Mr. F. Cramer, Task Leader, Monopropellant Contamination; Dr. G. Yanow, Task Leader, Final Report and Programming; and Mr. S. S. Cherry, Task Leader, Contamination Experiment. Dr. D. W. English, Propulsion Department was the Task Leader for the Surface Effects Portion of the study. Capt. J. R. Nunn, USAF provided valuable information concerning system application of the CONTAM Computer Program and continuing support for which we are grateful.

This technical report has been reviewed and is approved.

ABSTRACT

The effect of rocket exhaust plume impingement on sensitive vehicle surfaces is an area of continuing concern in the design of spacecraft, missiles, and reentry vehicle systems. Specifically, the contamination and subsequent degradation of functional surfaces, such as solar cells, thermal control coatings, optical lenses, optical view ports, and highly reflective surfaces, have resulted in compromises of mission effectiveness. The objective of this study was to develop a single computer code capable of predicting the production, transport, and deposition of engine and plume contaminants, and the change in absorptivity, emissivity, reflectivity, and transmissivity of a functional spacecraft surface, such as thermal control coatings and optical view ports and lenses, resulting from plume contaminant deposition or mechanical abrasion (sand blasting). Both bipropellants and monopropellants have been treated. Surface chemical reaction with a deposited plume contaminant layer was not treated. Analytical models and computer subprograms have been developed and integrated to form the CONTAM computer program. Complete User's manuals for each of the computer subprograms as well as the CONTAM program are included in this report, along with details of the analysis and numerical methods. A sample case illustrating the CONTAM program's capability is presented.

CONTENTS

I	INTRODUCTION	1
II	OBJECTIVES AND SCOPE	9
	1. Objectives	9
	2. Scope	9
III	MODEL DESCRIPTION	11
	1. Combustion Chamber Contaminant Production	11
	a. Feed Systems	12
	b. Atomization	12
	c. Chamber Calculations	15
	d. Wall Calculations	15
	e. Comparison with Experimental Results	15
	2. Contaminant Transport	18
	3. Chemical Kinetics and Condensation in the Nozzle and Plume Flow Field	19
	a. Chemical Kinetics Model	20
	b. Condensation Model	20
	4. Deposition, Abrasion, and Surface Effects	21
	a. Solar Absorptivity	22
	b. Hemispherical Emissivity	22
	c. Surface Abrasion	23
	d. Material Deposition	23
IV	THE CONTAM COMPUTER PROGRAM	25
	1. General Description	25
	a. Combustion Chamber Contaminant Production	27
	b. Contaminant Transport	27
	c. Chemical Kinetics and Condensation	29
	d. Deposition and Surface Property Effects	29
	2. Program Description	29
	3. Program Structure	30
	4. Program Data Interfaces	30
	a. TCC Data	30
	b. <u>N₂H₄</u> Data	30
	c. <u>TDMAIN</u>	30
	d. <u>SLINES</u> Data	32
	e. <u>KINCON</u>	32

5.	Program User's Manual	32
a.	Input to CONTAM	32
b.	Program NAMELISTS	33
c.	CONTAM NAMELISTS	33
d.	Nonstandard Format Inputs	35
V	SAMPLE CASE	37
1.	Definition of Sample Case	37
2.	Contaminant Production—The TCC Program	37
a.	TCC Input-Sample Case (R-6C Engine)	38
b.	TCC Output-Sample Case (R-6C Engine)	59
3.	Contaminant Transport—The MULTRAN Program	61
4.	Kinetics and Condensation—The KINCON Program	130
5.	Surface Effects Determinations	158
VI	EXPERIMENTAL DETERMINATION OF GAS DEPOSITION RATE ON CRYOGENICALLY COOLED SURFACES	165
1.	Objective and Approach	167
2.	Experimental Facility	167
a.	Vacuum System	167
b.	Gas Supply and Feed System	169
c.	QCM Electronics and Sensor	171
3.	Test Procedure	172
4.	Data Reduction	173
a.	Steady-State Mass Deposition Flux	173
b.	Inviscid, Continuum, Incident Mas Flux	173
c.	Pitot Pressure Measurements	174
d.	Sensor Surface Temperature	176
5.	Reduced Data	176
a.	Ammonia (NH ₃) Results	176
b.	Carbon Dioxide (CO ₂) Results	178
c.	Water Vapor (H ₂ O) Results	181
d.	Composite Summary of Sticking Coefficients on Gold and Silver	183
e.	Vacuum Evaporation	184
6.	Interpretation of Results	185
7.	Recommendations for the Future Effort	186
a.	System Hardware Changes	187
b.	Additional Tests	188
VII	CONCLUSIONS AND RECOMMENDATIONS	189
VIII	REFERENCES	191

FIGURES

1	Liquid Bipropellant Plume Impingement (22-lb Thrustor MMH-NTO, O/F = 1.65)	2
2	Deposition Effects of Rocket Exhaust after Continuous Long-Duration Firing	4
3	Effect of Thrustor Exhaust Continuous Long- Duration Firing—ZnO-KSiO ₃ and Spinel Coatings	5
4	Effect of Thrustor Continuous Long-Duration Firing on Glass Sample	6
5	Schematic Diagram of Analytical Model Elements and Related Computer Programs	13
6	Types of Plume Contamination Damage	16
7	Comparison of Experimental and Calculated Wall-Film Contaminant Production as Function of Propellant/Hardware Temperature	17
8	Static Pressure and Temperature Profiles for Condensing Nozzle Flow (Sample Case 1:90% H ₂ , 10% N ₂ Mixture, P ₀ = 1.25 psia, T ₀ = 1,000°R, Cone Angle = 6 deg)	21
9	Contaminant Effects Physical Model-Heat Rejection Radiators	22
10	Schematic of Plume Contamination Effects Prediction Computer Program, CONTAM	26
11	Schematic of Contamination Processes and Related Subprograms	28
12	CONTAM Structure	31
13	Facility Schematic	168
14	Sketch of QCM Sensor/Shroud Installation	169
15	Sonic Nozzle Configuration	170

16	Pitot Pressure Results for Ambient Temperature Air	175
17	Sticking Coefficient for NH_3 on Gold	177
18	Sticking Coefficient for NH_3 on Silver	178
19	Comparison of Sticking Coefficient for NH_3 on Gold and Silver	179
20	Sticking Coefficient for CO_2 on Gold	179
21	Sticking Coefficient for CO_2 on Silver	180
22	Comparison of Sticking Coefficient for CO_2 on Gold and Silver	180
23	Sticking Coefficient for H_2O on Gold	181
24	Sticking Coefficient for H_2O on Silver	182
25	Comparison of Sticking Coefficient for H_2O on Gold and Silver	182
26	Sticking Coefficient for NH_3 , CO_2 , and H_2O on Gold	183
27	Sticking Coefficient for NH_3 , CO_2 , and H_2O on Silver	184

Section I

INTRODUCTION

The effect of rocket exhaust plume impingement on sensitive vehicle surfaces is an area of continuing concern in the engineering design of spacecraft, missiles, boosters, and RV systems. Specifically, the contamination and subsequent degradation of functional surfaces, such as solar cells, thermal control coatings, optical lenses, optical view ports, highly reflective (mirrored) surfaces, and sealants, have resulted in compromises of mission effectiveness.

To illustrate the deposition of contaminants problem, several photographic examples of contamination occurring as the result of actual bipropellant engine firings will be presented. These examples were taken from a series of contamination experiments conducted by MDAC under the MOL program.

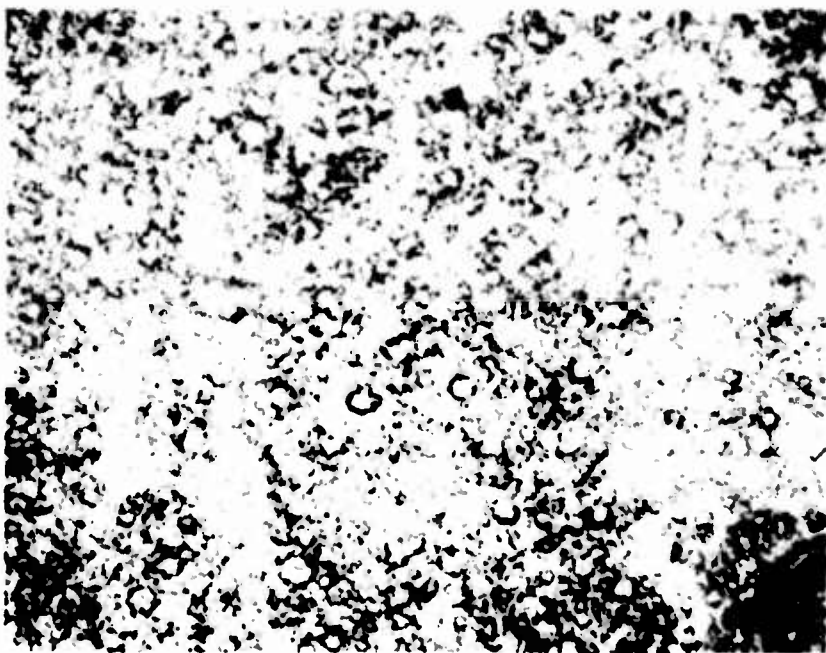
Figure 1 compares a control surface (no impingement) with a surface which has been exposed to normal impingement by the exhaust plume of a liquid bipropellant engine (MMH-NTO). Evidence of surface damage is apparent, and was postulated to be caused by condensed droplets in the core of the plume flow.

During a vacuum chamber subscale thruster test by MDAC at AEDC, a 1-lb thrust Marquardt MMH-NTO rocket engine was fired horizontally so that the exhaust products would impinge upon a vertically oriented test panel containing several surface specimens. Surface specimens included thermal control coatings, polished metal, and specialized glass lenses.

During pulse-mode operation of the motor, copious quantities of brownish, viscous liquid were observed about the nozzle lip and upon the lower external surface of the motor. This liquid exhibited considerable activity, bubbling while suspended from the motor lower external surface apparently due to some boiling and/or decomposition phenomenon. An impingement pattern of sorts was visible upon the test panel that appeared symmetrical but did not agree well (qualitatively) with theoretical predictions of the gas-phase impingement region. The region within the symmetric impingement pattern was coated with viscous liquid and/or solid material that increased in quantity with the number of pulses to which the panel was exposed; the coloration of this material was difficult to identify, but was definitely darker than the panel. Above and below the symmetric impingement region liquids were splattered in very large quantities, particularly near and below the rocket motor where semisolid formations of brownish color were noted; deposition of this variety seemed randomly distributed and was observed fore and aft of the nozzle exit plane. The amount of liquid generated by the rocket motor



a. CONTROL SAMPLE SHIELDED FROM DIRECT IMPINGEMENT



b. SAMPLE EXPOSED TO NORMAL EXHAUST IMPINGEMENT

Figure 1. Liquid Bipropellant Plume Impingement Effects (22-lb Thruster MMH-NTO, O/F = 1.65)

varied inversely with pulse duration, with maximum amount generated during the 16-msec "minimum impulse" pulses. Thermal control coatings exposed to these exhaust products were visibly coated and suffered losses in reflectance. Similarly, transparent samples suffered transmittance losses. After certain periods of liquid buildup upon the panel, brownish liquids ran down the panel surface. During long-duration firings in excess of several hundred seconds, a well-defined symmetric impingement pattern was noted upon the panel. It was difficult to discriminate between liquid and solid formations at this point. The symmetric impingement region gained further definition by virtue of a continuous ridge of solid and/or viscous liquid deposits at the symmetric impingement region boundaries. Posttest microphotography revealed that glass surfaces were coated with micron-sized droplets, even though the incidence angle of exhaust products was (theoretically) very small or nonexistent. Deposits upon the panel and surface samples displayed phase instability at standard temperature and pressure (STP) conditions, changing from solid to liquid to solid when disturbed physically or environmentally. When the chamber was repressurized to facility ambient conditions, much of the material deposited upon the panel became less viscous and ran off the panel.

Figures 2 through 4 show some of the deposits observed after various duty cycles.

This report will present the results of a 27-month study for the Air Force Rocket Propulsion Laboratory to develop an analytical model and computer program system for the prediction of spacecraft functional surface contamination effects caused by interactions with liquid bipropellant rocket exhaust plumes. Emphasis has been placed on development of computer codes to describe the complex two-phase combustion gas-dynamic processes occurring in a bipropellant combustor and the thermodynamic and kinetic nonequilibrium processes occurring during a two-phase nozzle and plume expansion. The operation of monopropellant hydrazine (N_2H_4) combustors has also been included in this study.

This report is divided into six discrete parts: the main body of the report and five appendixes. In the main body, emphasis is placed on describing the operating characteristics of the integrated Plume Contamination Effects Prediction Computer Program, CONTAM. A description of the program, User's Manual, and sample case run illustrating the ability of CONTAM to predict contaminant production, transport, and condensation are presented.

Each of the subprograms of CONTAM are described in detail in a separate appendix as follows:

Appendix A TCC

Transient Combustion Chamber Dynamics
Computer Program (a bipropellant contaminant production model)

Appendix B MULTRAN

Multiphase Nozzle and Plume Transport
Computer Program (a multiphase nozzle and plume flow field characterization model)



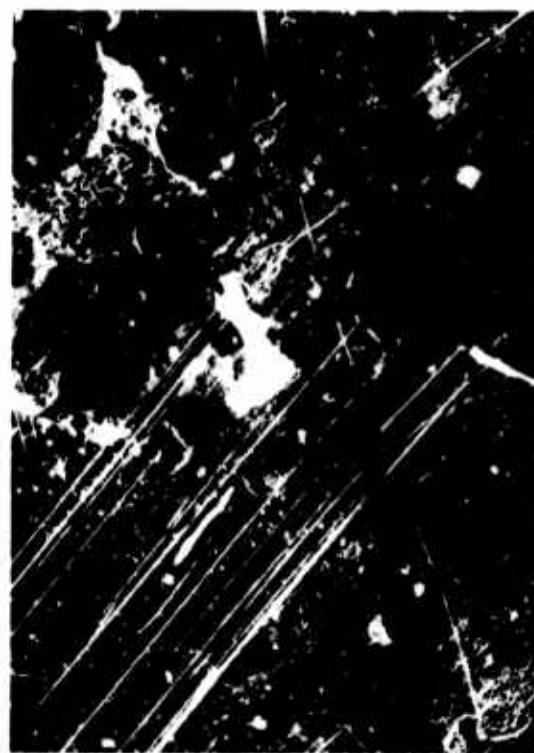
(a) NEAR-FIELD DEPOSITS ON PANEL



(b) NEAR-FIELD DEPOSITS ON PANEL

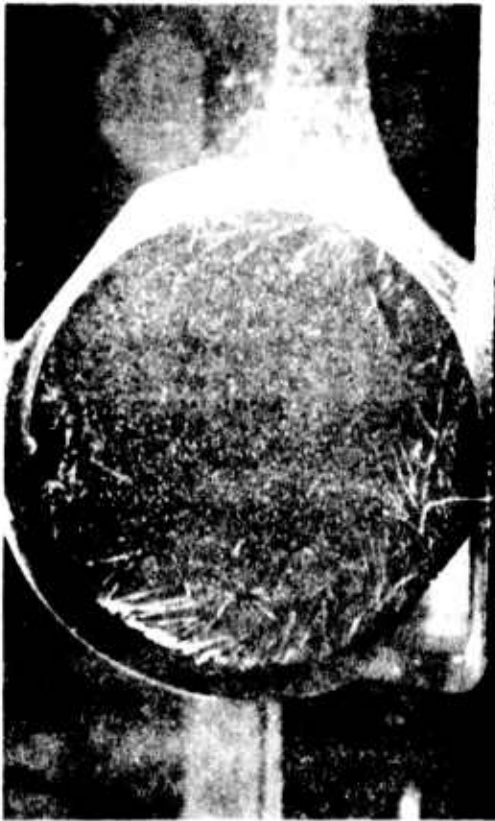


(c) SCHDAHL TAPE SAMPLE SHOWING DEPOSITS

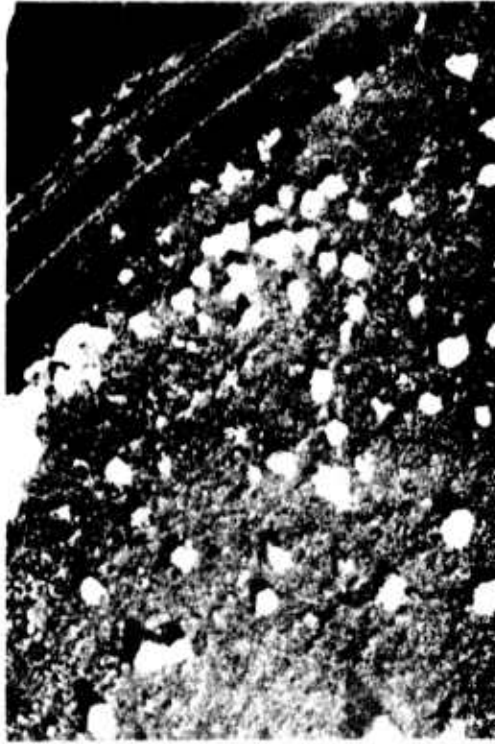


(d) 15X MAGNIFICATION OF (c)

Figure 2. Deposition Effects of Rocket Exhaust Impingement after Continuous Long-Duration Firing



(a) ZnO-KSiO₃ COATING SHOWING FRAGMENTATION



(b) 15X MAGNIFICATION OF (a)



(c) BLACK SPINEL COATING SHOWING DEPOSITS



(d) 30X MAGNIFICATION OF (c)

Figure 3. Effect of Thruster Exhaust Continuous Long-Duration Firing—ZnO-KSiO₃ and Spinel Coatings



(a) HORIZON SENSOR LENS
SHOWING DEPOSITS



(b) 80X MAGNIFICATION OF (a)

Figure 4. Effect of Thrustor Exhaust Continuous Long-Duration Firing on Glass Sample

Appendix C KINCON

**Nonequilibrium Chemical Kinetics and
Condensation Computer Program (a multi-
phase reacting gas streamtube model)**

Appendix D SURFACE

**Deposition and Surface Effects Computer
Program (a plume impingement, deposition,
abrasion, and surface contamination effects
model)**

Appendix E N₂H₄

**Monopropellant Combustion Chamber
Dynamics Program**

In addition to the sample case in the main body of the report, each appendix contains a sample case illustrating additional capabilities of the particular subprogram. Detailed operating information for each subprogram is contained in the User Manual section of each appendix.

This report has been loose-leaf bound to facilitate updating of the various User's Manuals, either by MDAC or other Government and industry users. The authors would greatly appreciate comments, corrections, additions, and suggestions for inclusion in future updates to be distributed to all users. Please send comments to:

R. J. Hoffman
A3-833-BBBO-28
McDonnell Douglas Astronautics Company
5301 Bolsa Avenue
Huntington Beach, California 92647

Qualified persons may obtain copies of the CONTAM computer program by addressing a request to:

AFRPL/DOE
Edwards AFB
Edwards, California 93523

Section II

OBJECTIVES AND SCOPE

1. OBJECTIVES

The objective of the study was to develop a single computer code capable of predicting the production, transport, and deposition of engine and plume contaminants and the change in absorptivity, emissivity, reflectivity, and transmissivity of a functional spacecraft surface, such as thermal control coatings and optical view ports and lenses, resulting from plume contaminant deposition or mechanical abrasion (sand blasting). Surface chemical reaction with a deposited plume contaminant layer is not treated.

The study was divided into five main areas:

- (1) Improvement of predictive technology for the characterization of reactive, multiphase rocket nozzle and exhaust plume flows containing propellant contaminants and nonequilibrium combustion products, including condensables.
- (2) Continued development of an analytical model to predict the production of contaminants in bipropellant rocket-engine combustion chambers.
- (3) Development of a semiempirical model to predict changes in surface properties of functional spacecraft surfaces (resulting from deposition or abrasion).
- (4) Integration and coupling of existing computer programs and newly developed computer programs to achieve a systems engineering design tool for the prediction of contaminant effects on spacecraft surfaces.
- (5) Verification of the contamination prediction model by comparison with experimental data.

2. SCOPE

The study was restricted to the development of predictive methods for the production, transport, and deposition of contaminants from hydrazine monopropellant and hydrazine-family fuels in combination with nitrogen tetroxide and to changes in thermal and optical surface properties of common thermal-control paints and optical lenses. The model development has considered RCS engines in the 5- to 600-lb thrust range; the validity of the model for much larger engines has not been assessed.

SECTION III MODEL DESCRIPTION

Section IV describes the CONTAM plume contamination effects prediction computer program system developed during this study. The analytical models associated with each link of the CONTAM program are discussed in detail in the appropriate appendix. In this section, a summary description of the analytical models employed in the CONTAM system is given.

The general objectives of the study were to construct a single analytical model capable of predicting the effects of bipropellant and monopropellant plume impingement contamination on optical and thermal spacecraft surfaces based only on a knowledge of available engine operating conditions, engine/spacecraft configuration geometries, and spacecraft orbital parameters. To this end, it was necessary to construct a model for the production of contaminants in bipropellant and monopropellant combustion chambers (unburned propellants ejected through nozzle throat); transport of these contaminants by the expanding gases in the nozzle and exhaust plume; chemical nonequilibrium composition of plume species; condensation of plume species in the expanding plume; abrasion damage and deposition resulting from plume impingement; and, finally, the changes in thermal and optical surface properties, absorptivity, emissivity, transmissivity, and reflectivity resulting from contaminant deposition and/or abrasion damage. In addition, the model considers the effect of engine duty cycle and spacecraft radiant energy transfer on the rate of contaminant deposition over an entire mission profile.

The feasibility of constructing a valid model, considering all of the above aspects, relied heavily upon the existence of several models and computer codes which could be used as a basis for construction of the overall contamination effects prediction model. Several new portions of the model and computer subprograms were developed. Figure 5 schematically illustrates the computation flow logic and the related computer codes. Details of each computer code can be found in the appropriate appendix.

1. COMBUSTION CHAMBER CONTAMINANT PRODUCTION (See Appendixes A and E for further details)

Unburned propellant and intermediate products of combustion (liquid phase) ejected from the combustion chamber are considered first as a source of contaminants. Referring to Figure 5, the Transient Combustion Chamber (TCC) Dynamics Program, developed at MDAC, is used to calculate contaminant production from bipropellant thrust chambers. The contaminant production from monopropellant hydrazine thrust chambers is calculated using a modified version of the program developed at UARL by A. S. Kesten, et al (References 1 and 2).

TCC PROGRAM

Contaminant material is produced by the combustor of a bipropellant rocket engine when unburned propellant vapor passes through the throat, when partially burned propellant droplets pass through the throat or when fuel and oxidizer droplets strike a cold chamber wall to form a liquid film of hydrazine nitrate which is moved downstream by chamber gas shear forces. When the unburned propellant or intermediate reaction products are ejected from a rocket engine, they may be transported in the plume and deposited on nearby sensitive spacecraft surfaces, changing their thermal or optical properties.

The sequence of combustion related events in the rocket engine combustion chamber is calculated by numerically integrating the differential and algebraic equations which describe the basic processes of the feed system, injector, and combustion chamber. Figure A-1 in Appendix A is a drawing of the rocket system.

a. Feed Systems

The feed systems are approximated with single lumped parameters representing the inertial and resistive aspects of the feed system, the rate of acceleration of flow being proportional to the amount that the instantaneous pressure drop exceeds the instantaneous pressure losses in the system. The opening and closing of the valves are modeled by varying the feed system resistance as a function of time. Flow reversals or initial start conditions, which result in partially or fully gas-filled feed lines, are simulated by varying both the resistance and inertia of the feed system as functions of time.

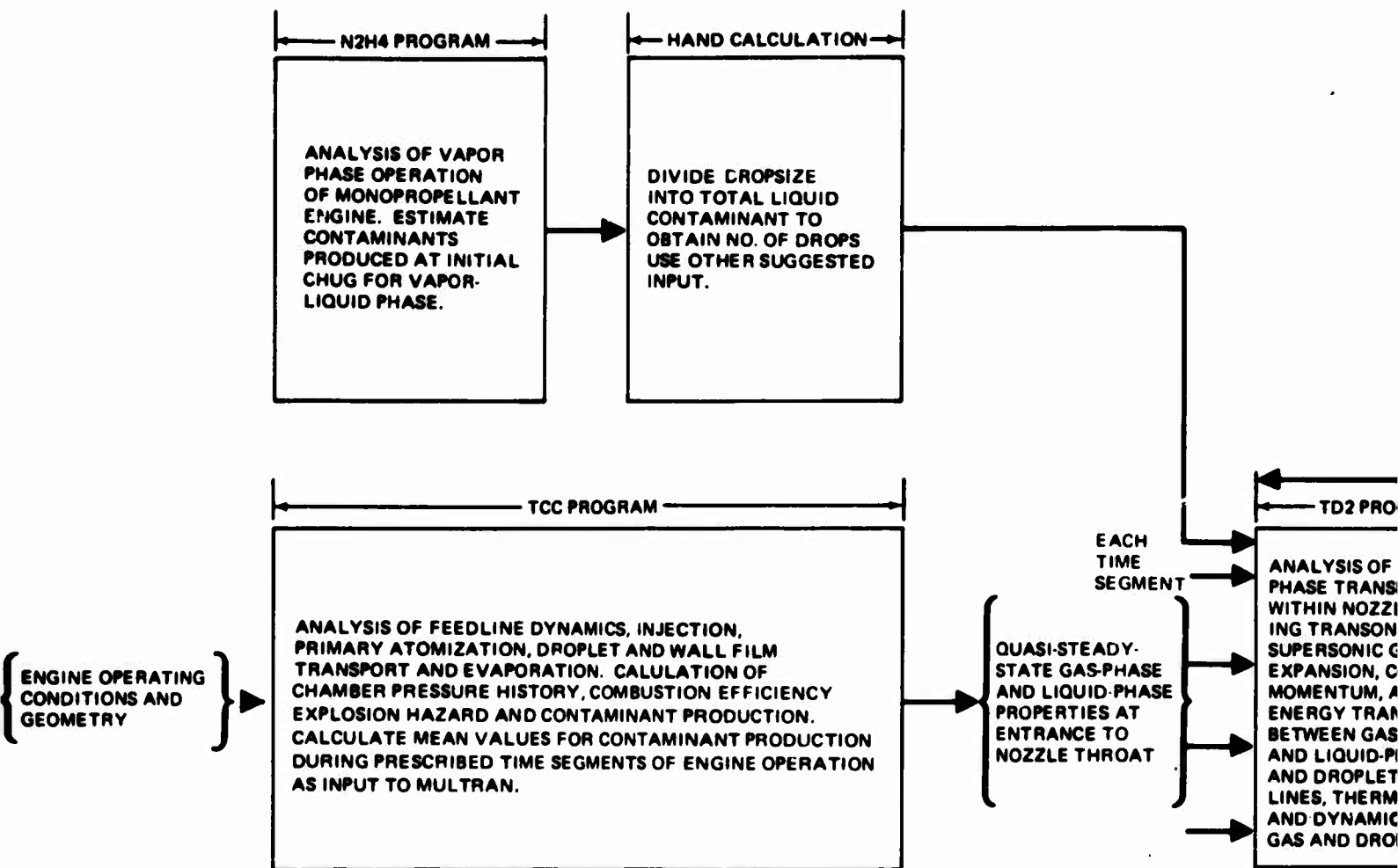
b. Atomization

The atomization process is calculated for one of several modes, depending on the chamber pressure. If the injected propellant is sufficiently supersaturated, the stream is presumed to flash-atomize. The flash-atomization process resembles the gas-atomization process, with the gas being supplied by the explosive growth of bubbles in the supersaturated stream. The flash atomization process gives relatively fine droplets, on the order of 40 microns in diameter.

When the chamber pressure is sufficiently high that the injected propellant streams do not flash, the atomization occurs by the impingement of the fuel and oxidizer streams. The median droplet diameter is obtained from an equation based on the orifice diameters, injection velocities, relative momentum of the streams, and physical properties of the propellants.

When only one stream is being injected during a start transient, there can be no impingement and droplet formation is calculated based on singlestream breakup.

The injected propellant moves from the injection point to the impingement point along the direction of injection. After impingement, the



INPUT DATA

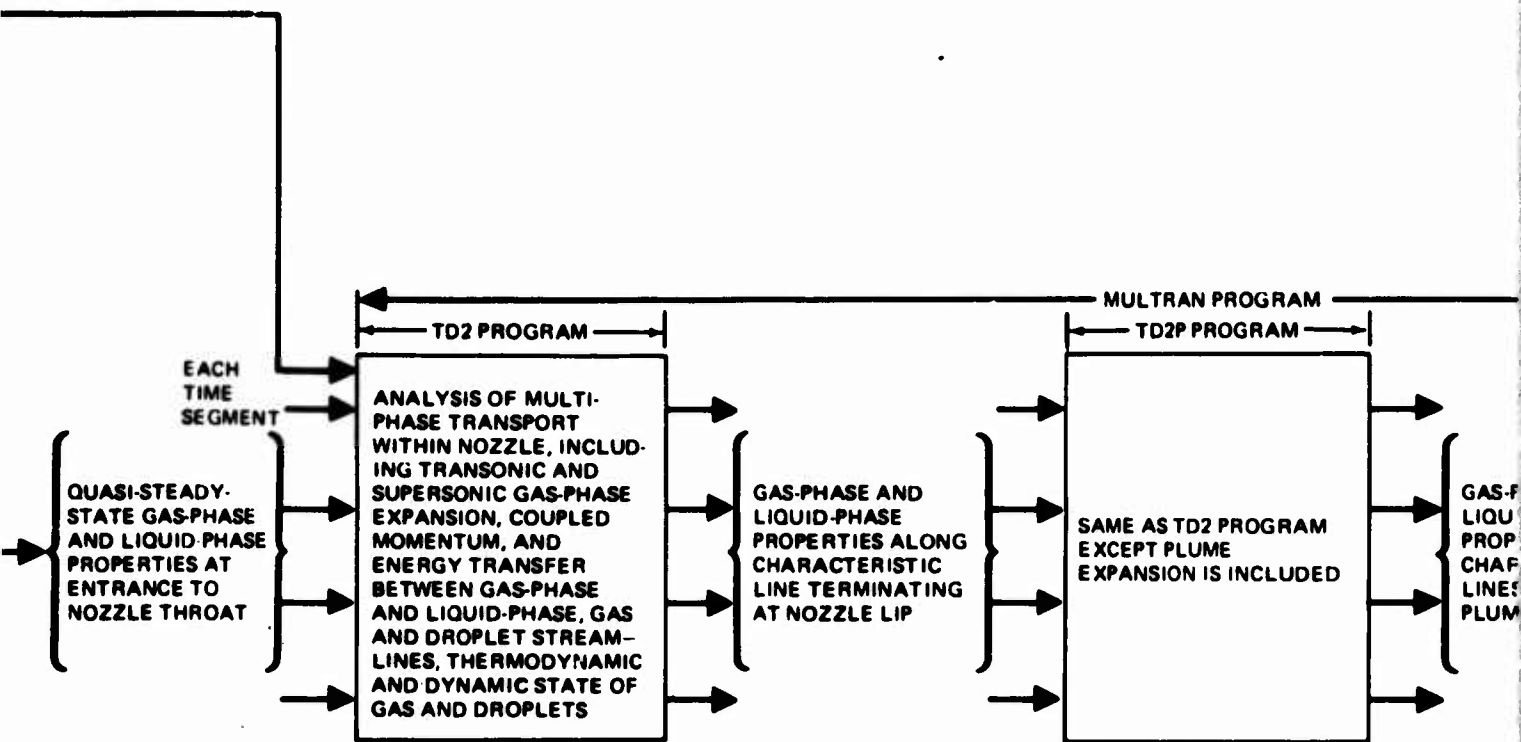
- FEEDLINE CHARACTERISTICS
- INJECTOR AND COMBUSTOR GEOMETRY
- PROPELLANT TANK PRESSURES AND TEMPERATURES
- PROPELLANT VALVE TIMING AND RAMP CHARACTERISTICS
- PULSE WIDTH AND DUTY CYCLE
- PROPELLANT PROPERTIES
- COMBUSTOR WALL TEMPERATURE
- ETC

TCC OUTPUT (TIME DEPENDENT)

- CHAMBER PRESSURE AND TEMPERATURE
- AMOUNT OF UNBURNED PROPELLANTS
- AMOUNT OF LIQUID PROPELLANTS EJECTED FROM CHAMBER
- SIZE AND VELOCITY DISTRIBUTION OF EJECTED PROPELLANT DROPLET
- AMOUNT OF LIQUID DEPOSITED ON CHAMBER WALL
- AMOUNT OF LIQUID WALL FILM EJECTED FROM CHAMBER

TD2 INPUT (AVERAGED OVER EACH TIME SEGMENT)

- CHAMBER PRESSURE AND TEMPERATURE
- DISTRIBUTION OF SIZE AND NUMBER OF DROPLETS ENTERING THROAT



TD2 INPUT (AVERAGED OVER EACH TIME SEGMENT)

- CHAMBER PRESSURE AND TEMPERATURE
- DISTRIBUTION OF SIZE AND NUMBER OF DROPLETS ENTERING THROAT

TD2P INPUT (FOR EACH TIME SEGMENT)

- STATIC GAS TEMPERATURE, PRESSURE, VELOCITY, AND FLOW DIRECTION
- LIQUID DROPLET TEMPERATURE, DENSITY, VELOCITY, SIZE DISTRIBUTION, AND FLOW DIRECTION

TD2P OUTPUT

- STATIC PRESSURE, DIRECTION
- LIQUID DENSITY, DISTRIBUTION

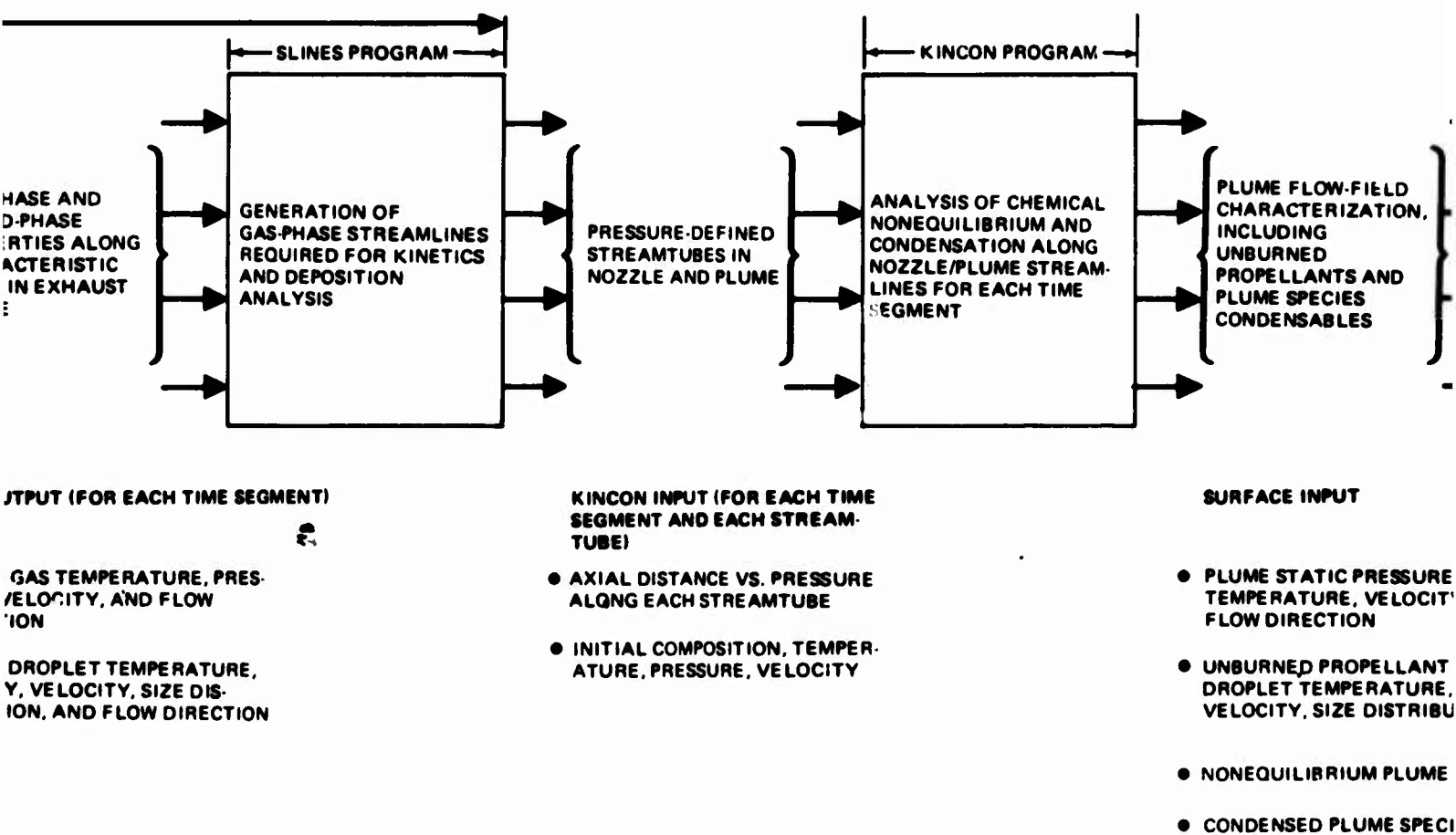
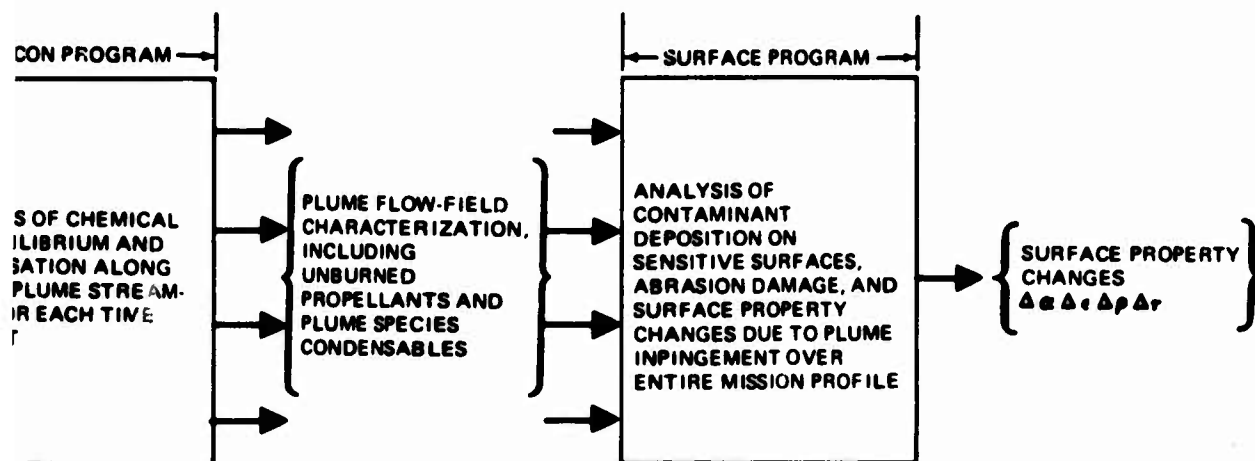


Figure 5. Schematic Diagram



SURFACE INPUT

- PLUME STATIC PRESSURE, TEMPERATURE, VELOCITY AND FLOW DIRECTION
- UNBURNED PROPELLANT LIQUID DROPLET TEMPERATURE, DENSITY, VELOCITY, SIZE DISTRIBUTION
- NONEQUILIBRIUM PLUME COMPOSITION
- CONDENSED PLUME SPECIES

Figure 5. Schematic Diagram of Analytical Model Elements and Related Computer Programs

stream moves in the direction of the resultant angle. The stream moves in this new direction until its atomization is complete, after which its two-dimensional trajectory is determined by the aerodynamic drag forces.

c. Chamber Calculations

The vapors or gases that fill the combustion chamber are derived from several sources: vapor from flashing propellant streams; material evaporated from propellant droplets; evaporation of material deposited on the combustion chamber walls and from the ignitor if one is used. Fuel and oxidizer vapor from these sources are axially cumulated in the chamber at each time interval, while the amounts calculated to flow through the nozzle are subtracted. This gives current values for the chamber-gas mass and stoichiometry, and the axial addition rate of mass. These are used to calculate the pressure, temperature, molecular weight, and velocity distribution in the chamber. The simplifying assumption is made that at any instant the pressure is constant throughout the chamber, and the gas is well mixed. Hypergolic ignition is based upon global vapor-phase chemical kinetics, and extinguishment is based upon a quenching distance correlation.

d. Wall Calculations

When a computed propellant droplet moves radially to the location of the combustion chamber wall, its fuel or oxidizer mass is added to the axial distribution of fuel or oxidizer previously deposited on the chamber wall. In calculating the axial and tangential velocities of the liquid material on the wall, each axial element of fluid is treated as an inertial free body acted upon by shear from the wall and gas, spin-induced forces, mass and momentum increments from the impinging droplets, from evaporation, from entrainment, and by convection at the upstream and downstream boundaries of the element. Evaporation is calculated based upon heat transfer from the gas during the firing, and by heat transfer from the wall coupled to vacuum evaporation during the "off" periods.

The heat transfer and entrainment associated with each axial segment of wall is calculated using the correlations of Gator, with corrections being made for mass transfer and rippling. The shear stress and heat transfer coefficients are correlated with local Reynolds numbers which are reevaluated at each axial segment of the chamber each time interval.

For ease of visualization, many of the calculations may be presented as computer plots or computer produced motion pictures.

e. Comparison with Experimental Results

Contamination from a conventional bipropellant RCS engine takes one or more of three forms: reacted or unreacted propellant vapor; incompletely burned droplets expelled through the throat; and unburned propellant that impinges upon the chamber wall and is eventually ejected from the nozzle lip. Figure 6 shows typical values for the amounts, directions, sizes, and velocities of the material making up these three forms for one particular small engine and one particular duty cycle.

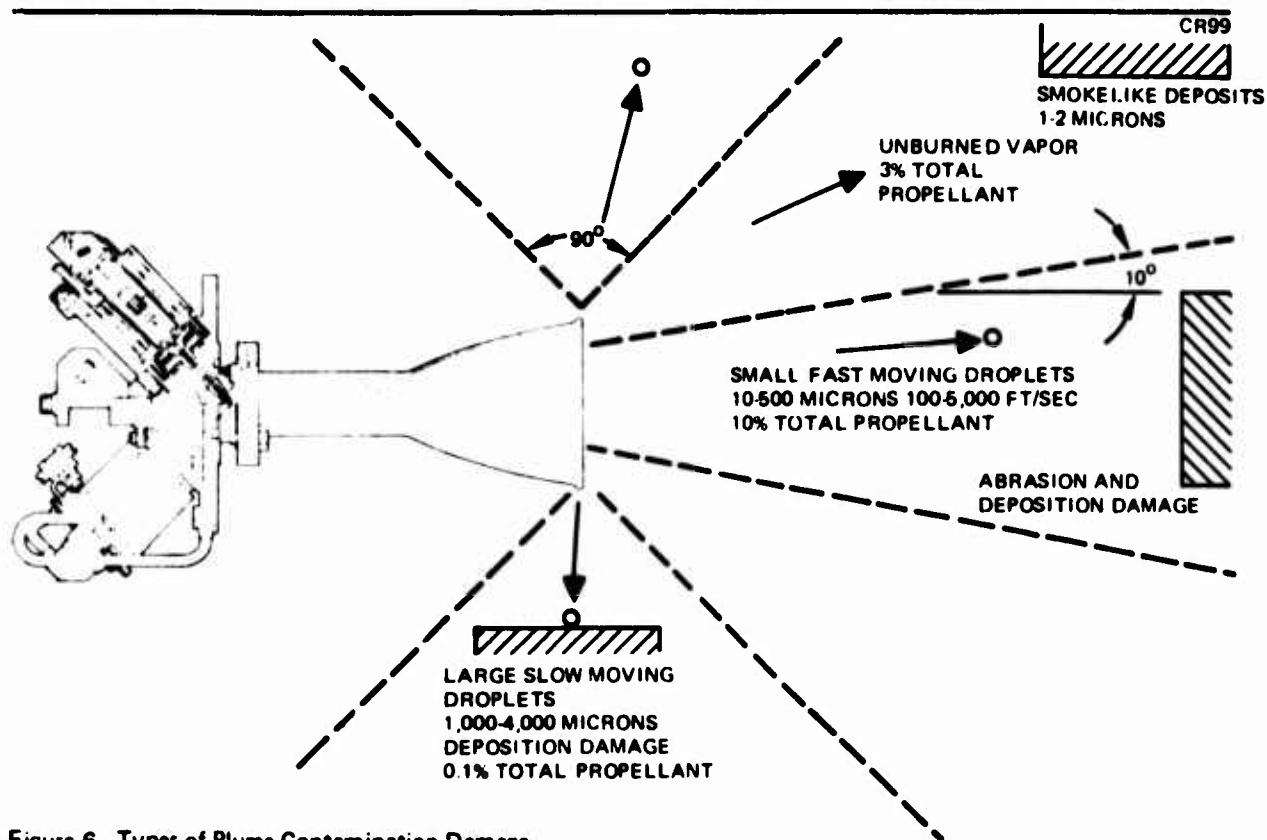


Figure 6. Types of Plume Contamination Damage

The vapors of fuel, oxidizer, or combustion products emitted during preignition, ignition, steady state, or postcutoff dribble periods will form plumes that can impinge upon various surfaces with the possibility of deposition and in-situ reaction. Contamination from this source usually takes the form of a hazy deposit of smoke-like particles (fairly uniform in size, 1 to 2 microns).

The fuel and oxidizer droplets, which are too large to burn completely in the chamber and which are centrally directed, will pass through the nozzle throat. These particles will be accelerated by aerodynamic forces both upstream and downstream of the throat, and can attain quite high velocities, which gives this class of particles the capability of doing considerable damage by abrasion.

The third form of contamination is the propellant that impinges upon the chamber wall and is then dragged downstream under the influence of shear forces from the combustion product gases. If this wall-film material is able to move to the nozzle lip without being thermally destroyed, it will be thrown off as large droplets in directions roughly normal to the axis of the chamber. This material is generally dark colored and shows the effects of thermal decomposition.

Figure 4 shows a horizon sensor lens exposed to wall-film contamination from an RCS engine operated in a vacuum chamber.

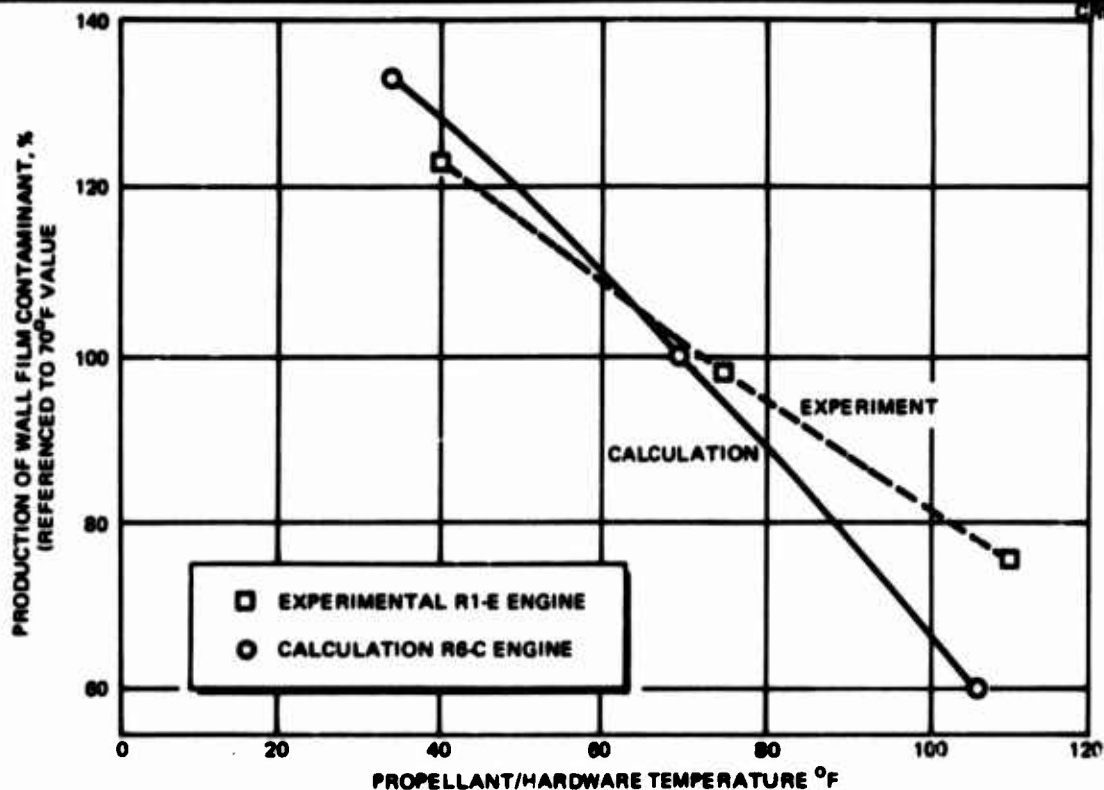


Figure 7. Comparison of Experimental and Calculated Wall-Film Contaminant Production as Function of Propellant/Hardware Temperature

Quantitative experimental data on contaminant production are still rather scarce. However, two recent papers have been published describing contaminant production from pulse-mode firings of the 22-pound Marquardt R1-E engine (References 3 and 4). This engine is very similar in design, but larger than the 5-pound Marquardt R6-C engine, which has been thoroughly parametrically analyzed, using the TCC program. Many aspects of the experimental firings of the R1-E engine agree with the trends calculated for the R6-C engine.

Martinkovic found that contaminant production was a function of injector temperature. His measurements for the temperature trend of the R1-E engine show good agreement with our calculations for the R6-C engine as shown in Figure 7. The absolute values for contaminant expelled as wall-film were also in good agreement. The Martinkovic 22-pound R1-E engine experimentally produced 0.772 mg of wall-film per 17 msec pulse at 75°F; i. e., about 1 part per thousand of total injected propellant ended up as wall-film contaminant. Our calculations for the 5-pound R6-C engine indicated that 0.33 mg of wall-film would be produced for each 17 msec pulse at 70°F; i. e., about 2 parts per thousand of total injected propellant. This is in agreement with the well-known trend toward increased contaminant production with decreased engine size.

Other indications of the accuracy of the TCC program are to be found in its excellent predictions of low-frequency combustion instability, start transients, popping amplitudes, spiking tendency, and pulse-mode specific impulse or total impulse versus pulse-width. These are discussed in some detail in Appendix A.

N2H4: Monopropellant Combustion Chamber Dynamics Program (See Appendix E for further details)

Contaminant production data is generated for monopropellant engines by the program N2H4, based on the transient and steady-state programs originally developed by Kesten, Smith, and Smith of UARL (References 1 and 2) and modified by F. B. Cramer of MDAC. In monopropellant engines, "normal" operation will produce primarily NH_3 , N_2 , H_2 , and N_2H_4 vapors. However, during cold starts or "chugging", droplets of liquid hydrazine will also be formed as a contaminant.

The original UARL program only treated the smooth vapor phase decomposition problem. MDAC modifications have extended the program to estimate "hard start" characteristics as an alternative option. In particular, the peak pressure, time to the pressure peak, mass of liquid hydrazine ejected, and the masses of the vapor constituents are printed out. This program will not calculate beyond the start transient when calculating a cold (hard) start; however, even in its present form, this computer program gives information when cannot be obtained any other way.

The smooth monopropellant decomposition calculations are carried out using a slug flow model. That is, the vapor (vaporization is assumed to occur instantaneously) formed upon contact with the catalyst bed is modeled one dimensionally.

The MDAC N2H4 monopropellant "hard start" subprogram is based in large part on curve fits of experimental data obtained from various engine firings. At present no monopropellant program will effectively follow a cold start after the initial pressure surge. The current MDAC program does provide working information about this initial pressure peak and then shuts down with a printout of the estimated start transient operational characteristics.

2. CONTAMINANT TRANSPORT (See Appendix B for further details).

Having defined the average amount of liquid phase contaminant ejected from the combustor for each pulse segment (see Subsection III. 1) the two-phase nozzle and plume flow is then computed for transient and steady state pulse segments, using method-of-characteristics computer programs described by Nickerson and Kliegel in (Reference 5) and modified by Gabbert and Hoffman (Reference 6). In Figure 5, these programs are identified as TD2 and TD2P. Variations in chamber pressure, chamber temperature, droplet velocity, and droplet-size distribution produce considerably different two-phase flow fields for each of the pulse segments (preignition, ignition, steady state, and tailoff) and therefore require a unique analysis for each pulse segment.

Because several contaminant sources originate upstream of the nozzle exit plane (for example, unburned propellant and nonequilibrium condensed fuel nitrate species), it is necessary to obtain a complete characterization of the multiphase flow at the nozzle exit, including droplet/particle

distributions (size, velocity, temperature, and species) as well as an axisymmetric distribution of the gas-phase flow. The extreme radial compression of droplet/particle laden regions indicates the need for accurate information concerning the combustor and nozzle transport of condensables as input to the plume analysis.

Starting at the convergent nozzle sections, up to 10 droplet groups are considered as an approximation to the distribution of condensed phase material produced in the combustion chamber. The concentrations, distribution, and trajectories of each droplet/particle group are considered at each mesh point in the axisymmetric method-of-characteristics flow analysis throughout the entire nozzle and plume. Fully coupled momentum exchange (drag) between the gas and droplet/particle phase is considered, including rarefaction effects. The results (output) of this program set provide the initial conditions (input) for the impingement model and subsequently, the surface effects analysis.

While the transport model will provide information about the dynamic condition and flux of species arriving in the vicinity of a functional surface submerged in an exhaust plume, the kinetic/condensation model and the deposition model are required to provide information regarding the chemical composition and amount of plume exhaust material actually deposited on the submerged surface.

3. CHEMICAL KINETICS AND CONDENSATION IN THE NOZZLE AND PLUME FLOW FIELD (See Appendix C for further details)

In addition to unburned propellant droplets, many liquid-bipropellant exhausts contain condensed phases as an important contaminant source. The primary condensables in bipropellant plumes are thought to be H_2O and nitrate salts of the fuel. One of the major study objectives was to review existing data on plume condensables and to model the mechanism of condensation analytically in rocket nozzles and exhaust plumes. A thermodynamic nonequilibrium nucleation and condensation model has been developed and is discussed in detail in Appendix C. The MDAC Streamtube Chemical Kinetics and Condensation Computer Program, identified in Figure 5 as KINCON, has provided the framework for development of this portion of the model. A preliminary study, using the combined chemical kinetics and condensation model, was performed to size condensation characteristics in the nozzle and plume, corresponding to typical engine operating regimes (both transient and steady state). The relative effect of condensation as a contaminant source, relative to combustion chamber sources, is yet to be determined, although it is thought to be an important factor in contamination of surfaces beyond the central core of the plume where heavy, unburned propellant droplets seem to dominate.

The modeling of this phase of the contaminant-production problem requires (1) the chemical kinetic analysis of the expanding exhaust gases and (2) a realistic analysis of the condensation process.

a. Chemical Kinetics Model

The chemical kinetic processes in the nozzle and plume are calculated along streamlines utilizing the MDAC KINCON computer program. The KINCON program possesses several unique features which make it well suited for analyzing the nozzle/plume chemical kinetics. These features include (1) a fully implicit numerical integration scheme that permits the rapid integration of the full set of kinetic equations (up to 40 species and 150 reactions) with complete numerical stability; (2) capability to treat the addition (or subtraction) of mass, momentum, and energy to the streamtube by specifying the specific rate as a function of streamtube distance; (3) reaction-rate screening capability, which identifies reactions and species that are unimportant and need not be considered in the calculation of a specific species concentration or fluid property in any particular application.

Principal assumptions inherent in the use of the streamtube kinetics model include the following: (1) the flow is one-dimensional, steady, and inviscid; (2) each component of the gas mixture is a perfect gas; and (3) internal degrees of freedom of each component are in equilibrium.

b. Condensation Model

It is well known that condensation of a rapidly expanding supersonic flow does not occur at the point in the flow where the gas equilibrium temperature reaches the saturated vapor temperature of the particular species in question. Instead, condensation is delayed and eventually occurs as a "condensation shock" or condensation zone downstream of the equilibrium condensation point. Although this phenomenon is not thoroughly understood, it may be caused by a number of factors, including (1) lack of nucleation material on which condensables may form and (2) inability of the surrounding gas phase to readily remove heat from the condensing material.

To treat condensation effects in rapidly expanding gases, a kinetic model of the condensation process utilizing the classical liquid drop theory was adopted. The condensation phenomenon, as described by this model, occurs as a result of two distinct processes: (1) nucleation and (2) droplet growth.

As saturated vapor conditions are reached in a rapid expansion, sufficient surface area will not usually exist for the condensation required to maintain equilibrium ($P_v = P_{vs}$), and a supersaturated condition results ($P_v > P_{vs}$). The nucleation process (spontaneous self-nucleation) occurs in the expanding supersaturated vapor and involves the clustering of vapor molecules to give rise to very small nuclei (radius of 10 to 100 Å). Only nuclei reaching the critical drop radius r^* can exist and grow. The critical drop size is determined from thermodynamic equilibrium considerations and represents the size at which the drop has an equal probability of either evaporating or growing.

Figure 8 illustrates the effects of condensation on the flow static pressure and temperature. Following the saturation point, the vapor continues to expand along the frozen gas isentrope until a suitable number of

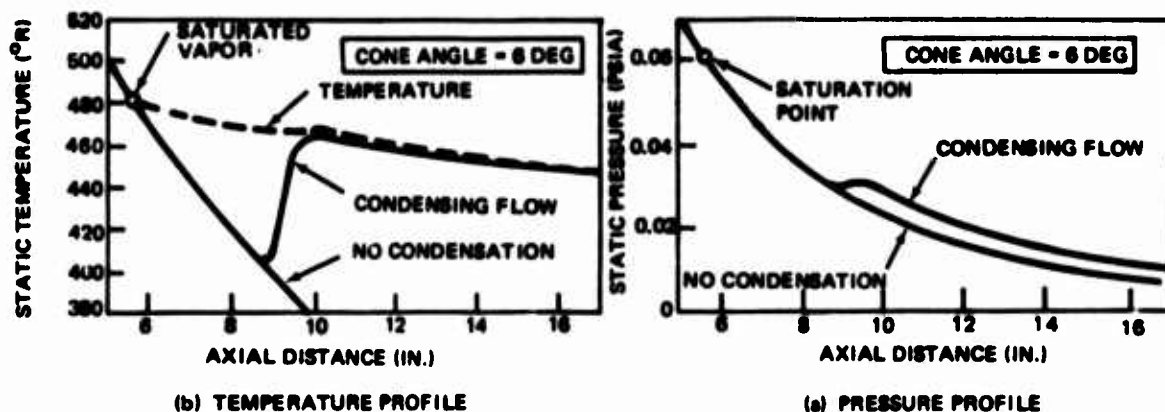


Figure 8. Static Pressure and Temperature Profiles for Condensing Nozzle Flow (Sample Case 1: 90% H_2 , 10% N_2 Mixture, $P_0 = 1.25$ Psia, $T_0 = 1,000^\circ R$, Cone Angle = 6 Deg)

nuclei are formed and the droplet growth process begins. At this point, the effects of condensation are observed. Both the static pressure and temperature increase rapidly with the temperature approaching the saturated-vapor temperature. The expansion then continues along a different isentrope corresponding to a new gas mixture.

4. DEPOSITION, ABRASION, AND SURFACE EFFECTS (See Appendix D for further details)

An analytical model for the prediction of plume contaminant deposition, surface abrasion due to liquid and solid particle impingement, and changes in thermal and optical surface properties due to deposition or abrasion has been completed.

Development of a surface effects model was based heavily upon experimental data relating plume species deposition and mechanical abrasion characteristics to changes in α and ϵ , in the case of thermal surfaces; and changes in transmissivity and reflectivity, in the case of optical surfaces. Such data are scarce for realistic plume-deposition products, such as MMH-nitrate, although recent experiments have provided some data.

The first step in developing a model to predict surface property changes, based on a computed amount of abrasion or deposition, is to examine the possible interactions of plume material with spacecraft surfaces. The model developed accounts for plume-induced changes in α and ϵ on thermal control surfaces, such as heat-rejection radiators and optical surfaces.

0

a. Solar Absorptivity

The absorptivity of the system is primarily determined by the characteristics of the external surface upon which the external radiation falls. The average or net absorptivity α_{net} of the radiator can be taken as the mean of the absorptivity of each type of absorptive surface α_i times the area of each type A_i . Generally, α_i is a simple term, easily determined or calculated, but in some instances, such as a transparent deposit, terms related to the thickness and internal parameters of the deposit become important.

b. Hemispherical Emissivity

When contaminant deposits are thin, it is assumed that they offer little resistance to heat flux through the layer. The emissivity of the surface is assumed to be that of the contaminant layer. For thick layers of deposits, the impedance to heat flow through the layer is also modeled.



Figure 9. Contaminant Effects Physical Model-Heat Rejection Radiators

c. Surface Abrasion

Abrasion can occur on either or both of the coated or uncoated portions of the radiator surface. Abrasion of the radiator coating affects the heat flux in a step-function fashion. If only the thermal-control coating is abraded, the effect is simply that of decreasing the original coating thickness without affecting the absorptivity or the emissivity. If the abrasion proceeds far enough, it will penetrate through the coating and expose an area of the metal plate substrate. The abrasion of the metal surface, both that originally present and that exposed by removal of the coating, will alter its α_p and ϵ_p significantly. The abraded area of the metal will consist of two parts, the part that was originally bare and now abraded, plus all that was exposed when the coating is abraded away. It is assumed that in any area where the abrasion is sufficient to remove the coating, the flow field will attack the metal at once.

d. Material Deposition

A deposit of material from the plume, randomly located on the exterior of the spacecraft radiator, acts simply like an additional coating through which the heat must be transferred. The deposit may be transparent (crystalline, glassy, or liquid), or it may be opaque due to either its basic nature or to particle sizes.

Opaque deposits affect the heat flux in a manner identical to the thermal-control coating. The situation can become more complex if the deposit forms a transparent film. Such films are not completely transparent at all wavelengths, and therefore a complex interaction occurs.

Radiant energy impinging from the environment is partly reflected, partly absorbed, and partly transmitted into the film at the outer surface in accordance with the usual ρ , α , and τ coefficients. As the energy passes through the thickness of the film, more of it is absorbed. At the bottom surface with the opaque paint or metal, the energy is either absorbed or reflected. That portion of the radiation that is reflected from the substrate then passes outward through the film, and again, part is absorbed. When the energy again reaches the outer surface, the part that strikes the surface at less than the critical angle is radiated away; but the portion that strikes the surface at an angle equal to, or greater than, the critical angle cannot escape and is eventually absorbed. A similar process also occurs for the emission of energy from and through the transparent layer.

SECTION IV

THE CONTAM COMPUTER PROGRAM

1. GENERAL DESCRIPTION

This section describes the integrated computer program, CONTAM, which has been developed to provide an engineering design tool for the prediction of plume contaminant effects on sensitive spacecraft surfaces arising from direct plume impingement. Figure 10 illustrates the component subprograms of the CONTAM program. The CONTAM program is capable of independently running any of the subprograms or of running the entire analysis sequentially. Except for TCC or N2H4, each program is dependent upon the output of previous programs. It is suggested that CONTAM be run sequentially, with an examination of each subprogram's output before the subsequent subprogram is called since improper data inputs can result in excessive computer run time. When run independently, the capabilities of each of the subprograms may be extended to solve problems associated with: combustion dynamics; nozzle and plume multiphase flow field characterization; nonequilibrium streamtube chemical kinetics and condensation; and impingement, deposition, abrasion, and surface property changes - not necessarily associated with plume contamination.

The subprogram SURFACE has not been fully integrated into CONTAM at the present time. This program is based for the most part on very large tables of experimental data, and in the current version of the program system, the memory requirements of this particular subroutine are considerably greater than any of the other programs. Consequently, while all the rest of CONTAM has now been overlayed via "Cell Loader", SURFACE has been left in the normal "SCOPE" loader overlay structure.

Each of the major subprograms of CONTAM are described in detail in separate appendixes as follows:

Appendix A <u>TCC</u>	Transient Combustion Chamber Dynamics Computer Program (a bipropellant contaminant production model)
Appendix B <u>MULTRAN</u>	Multiphase Nozzle and Plume Transport Computer Program (a multiphase nozzle and plume flow field characterization model)
Appendix C <u>KINCON</u>	Nonequilibrium Chemical Kinetics and Condensation Computer Program (a multiphase reacting gas streamtube model)

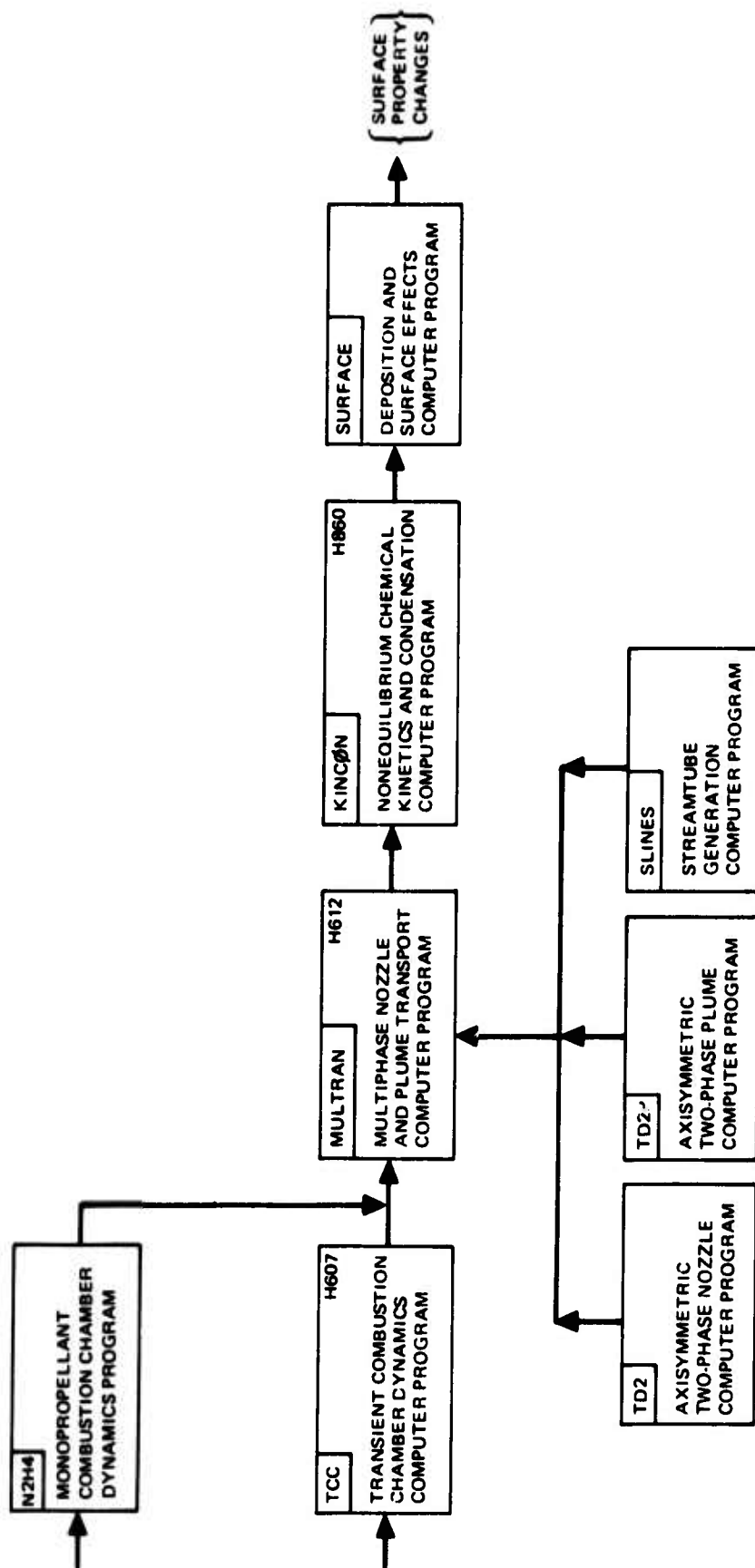


Figure 10. Schematic of Plume Contamination Effects Prediction Computer Program, CONTAM

Appendix D <u>SURFACE</u>	Deposition and Surface Effects Computer Program (a plume impingement, deposition, abrasion, surface contamination effects model)
Appendix E <u>N2H4</u>	Monopropellant Combustion Chamber Dynamics Program

This section concentrates on describing the operation of the integrated or controlling program CONTAM, and the interfacing of the various subprograms. The reader is referred to the appropriate appendix for detailed information concerning the operation of the individual subprograms.

The CONTAM program is written in FORTRAN IV. The primary version of the system includes the option of a monopropellant engine, subprogram N2H4, and requires 150,000 words of memory. However, a secondary version which only has a dummy N2H4 program, i. e., to be used with bipropellant engines only, can be run in only 120,000 words of memory. The cell loader directives for each of these editions are illustrated in this report. The program SURFACE has not been incorporated into CONTAM proper at this time for reasons previously explained in the report, and in its present form SURFACE requires 240,000 words of memory to execute. All aspects of the programming system have been written to run on a CDC 6000 series computer.

a. Combustion Chamber Contaminant Production

Unburned propellant and intermediate products of combustion (gas and liquid phase) ejected from the combustion chamber are considered first as a source of contaminants. Referring to Figure 11, the Transient Combustion Chamber Dynamics (TCC) subprogram or the monopropellant combustion chamber dynamic subprogram (N2H4) are used to generate contaminant production data. The results of the TCC or N2H4 subprograms are time dependent and require interface manipulation for subsequent modeling and analyses since the transport model treats the flow as steady state. After examination of the production of contaminants during the entire transient pulse, representative "time slices" are chosen so that gas and liquid properties may be averaged over the time intervals for use as input to the MULTRAN subprogram. The required output from TCC includes: chamber pressure, chamber temperature, droplet size distribution, droplet velocity, and mass flux of gas and droplets.

b. Contaminant Transport

Having defined the average amount of gas and liquid phase ejected from the combustor for each pulse segment, the two-phase nozzle and plume flow is then computed for each steady state pulse segment, using method-of-characteristics computer subprogram MULTRAN (subprograms TD2, TD2P, and SLINES are included in MULTRAN).

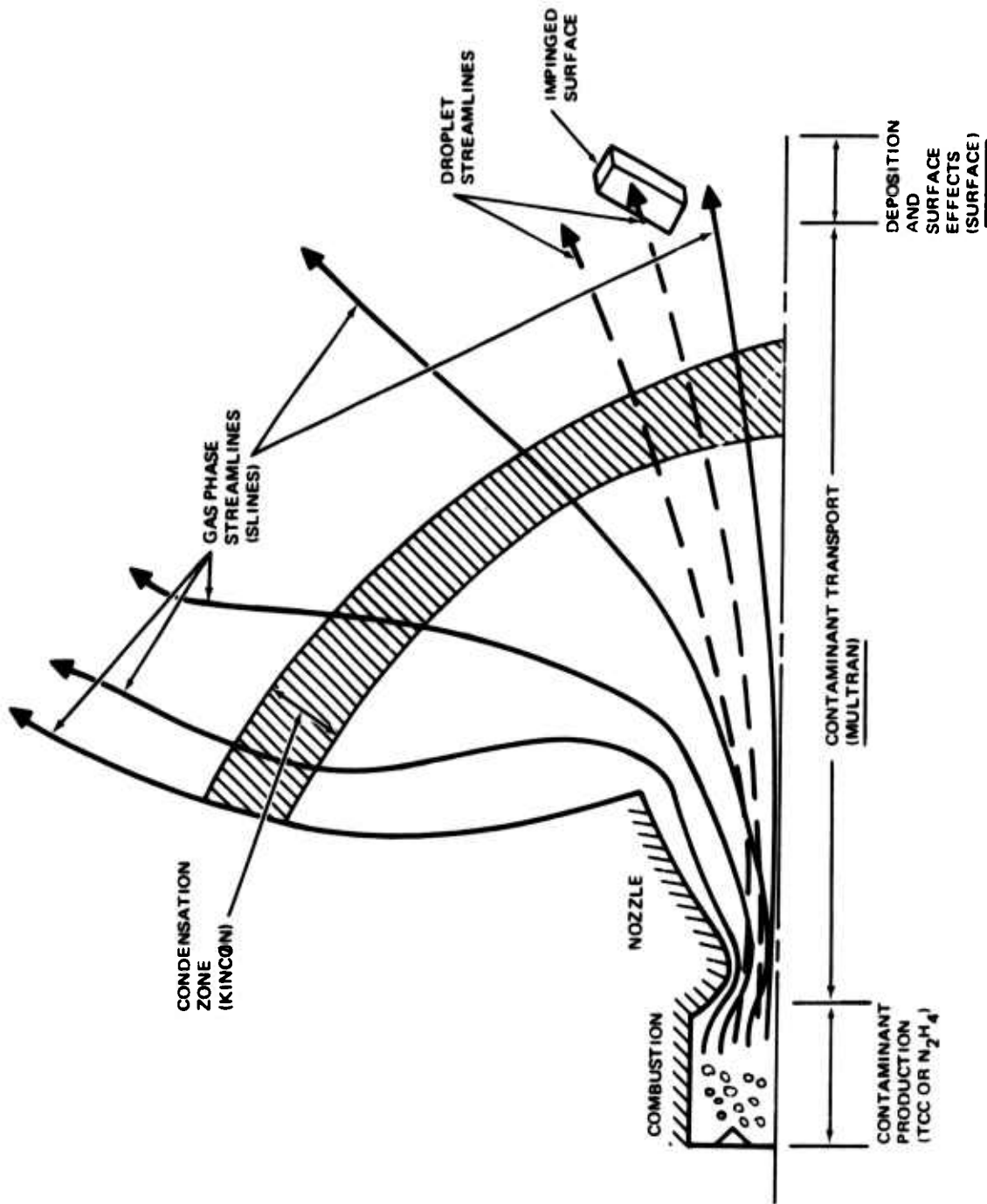


Figure 11. Schematic of Contamination Processes and Related Subprograms

Computer subprogram SLINES was developed to provide the necessary interface between the TD2, TD2P and the KINCON subprograms. Basically, SLINES interpolates between points on each characteristic line to provide exhaust gas properties for points on a streamline. A streamline is defined as that line which runs through the throat, nozzle, and plume, bounding a given constant percentage of the mass flow between it and the nozzle axis.

c. Chemical Kinetics and Condensation

In addition to unburned propellant droplets, many liquid-bipropellant exhausts contain condensed phase products of combustion as an important contaminant source. The formation of condensables in liquid propellant exhausts has been analytically modeled. The KINCON subprogram predicts the nozzle and plume condensation effects utilizing a classical nucleation and droplet growth model. It also provides the gas-phase chemical kinetics analysis along streamlines.

d. Deposition and Surface Property Effects

The flux of contaminants approaching a surface submerged in a bipropellant plume, as determined above, provides the starting point for the analysis of liquid and solid deposition on impinged surfaces. A model has been developed to account for the accommodation of momentum and energy upon impact of liquid and solid particles and to predict the amount and state (thin film, thick film, droplets, crystals, etc.) of the deposited materials. Damage and changes in surface properties due to mechanical abrasion and/or deposition are also treated in this subprogram, SURFACE. The surface property changes considered are absorptivity, emissivity, reflectivity, and transmissivity.

2. PROGRAM DESCRIPTION

This section describes the structure and logic of the Plume Contaminant Effects Prediction Computer Program, CONTAM. Particular emphasis is placed on the description of the main program, the cell loader structure, and the data interface between the various subprograms. Detailed descriptions of the subprograms may be found in the appropriate appendix.

The CONTAM program is structured so that any one subprogram may be run independently or any number of the subprograms may be run sequentially. Only the main program and required subprograms as defined by cell loader directive, reside in computer core during operation.

The main program (EXEC) was coded to perform the required selection of the various subprograms. It initializes certain logical control variables, accepts control variables through input, and provides overall logic control for the program. It also provides overlay communication.

3. PROGRAM STRUCTURE

The makeup of CONTAM is illustrated by Figure 12, a list of the various subprograms of the overall system.

4. PROGRAM DATA INTERFACES

The resultant data from the various subprograms reside on magnetic tape or disc file for use by subsequent subprograms.

The data interface has been designed so that the input and output data to a particular subprogram are preserved subsequent to the running of that subprogram, while at the same time, the number of logical file units used are minimized by reusing logical files. This means that while the user may run each program independently but sequentially, if the data output from a particular subprogram is not acceptable for some reason, the input data file to that subprogram has been preserved so that the user has a "restart" capability without having to restart from the initial subprogram of the sequence.

a. TCC Data

Data output from TCC is written on to logical file 9 (in addition to the NAMELIST'S RESRT1 and RESRT2) for subsequent use in the cases of multiple pulses or reprints of the results. "Movie" information is stored on TAPE 13. In addition, TCC uses files 1, 16, and 48 internally. File 1 contains the variable data used by the plotting routine in the subroutine GRAPHS; files 16 and 48 are required for the system plotting package. A quick visual inspection of the final printout of TCC will allow the user to choose the correct inputs for MULTRAN.

b. N2H4 Data

When using the monopropellant option, the needed input for MULTRAN is obtained by quick visual inspection of the printed output from N2H4.

c. TDMAIN

TDMAIN is the driver program for TD2 and TD2P. It also defines the overlay structure for COMMON block storage used by both of these programs.

The input logical file number for the TD2 program is 10. The TD2 subprogram provides data output on two logical files; 8 and 12. Logical file 8 contains data required to be input to the TD2P subprogram. Logical file 12 provides input data for the SLINES subprogram and the deposition and surface effects subprogram, SURFACE.

Subprogram TD2P receives its input data from logical file 8. TD2P provides output data on logical files 9 and 12. File 9 contains radiation and

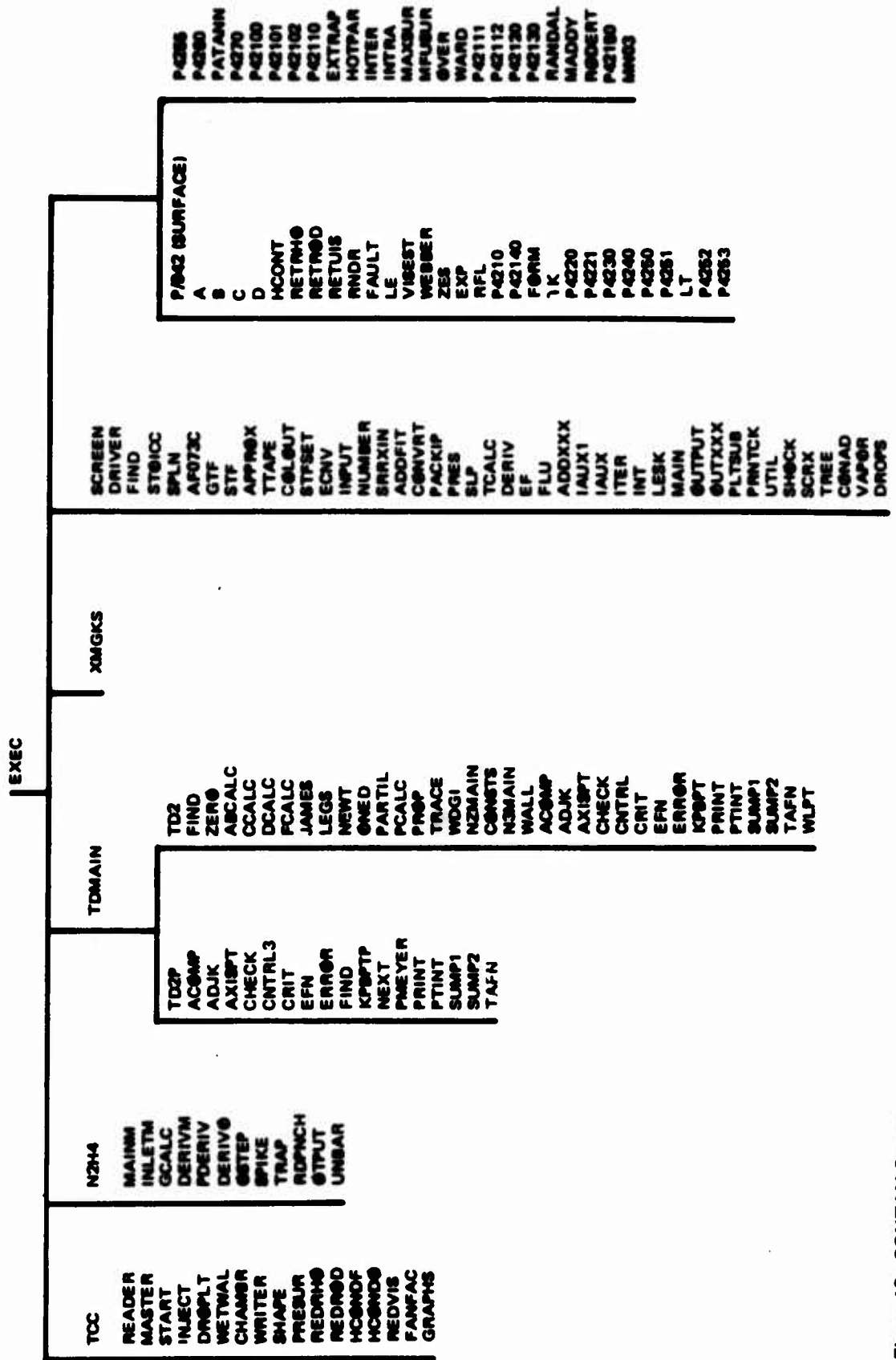


Figure 12. CONTAM Structure

force field data. File 12 contains the contaminant properties data. The subroutine which writes on file 12 is common to both TD2 and TD2P. It is located in the main overlay level so that it is accessible to both subprogram overlay levels.

d. SLINES Data

The SLINES subprogram reads data from logical file 12 which has been generated by subprograms TD2 and TD2P. It generates the streamline data and writes this data on logical file 8 for use by the KINCON subprogram.

e. KINCON

The KINCON subprogram uses five logical file units. The file unit numbers are 1, 4, 8, 11, and 12. Files 1 and 11 are scratch files used internally by the subprogram. File 1 contains the initial conditions and area ratio table to be used in the condensation calculation. File 11 contains reaction tables. Files 4 and 8 are input files. File 4 is an optional input which contains a list of thermal properties in JANAF format. Since logical file 4 is an optional input, if it is not used as such, it will default to an internally used file by the subprogram. If the logical file 4 input is not exercised, the thermal properties data must be input by punched cards (see Appendix C). The subprogram will then write JANAF thermal properties on logical file 4 from the punched card input. Obviously, with the appropriate control cards, file 4 may then be saved for subsequent use. File 8 contains the streamline properties required by the KINCON subprogram. Logical file 12 is the output tape of the subprogram and contains the multiphase and kinetic results to be used by the deposition and surface effects subprogram, SURFACE.

5. PROGRAM USER'S MANUAL

a. Input to CONTAM

Punched card input is required. Logical file 4 input is optional, but the option must be specified in the card input.

The punched card inputs required are of three types; NAMELISTS, some nonstandard format, and variable formats. Subsection 5. b describes the general nature of the data input through the various NAMELISTS and indicates the subprograms to which they apply. For a detailed description of the contents of the various NAMELISTS, the user should refer to the appropriate Appendix for each subprogram as listed in subsection of this section. A detailed description of the variable format inputs will also be found in the appropriate appendix. Section 5. d discusses the nonstandard format data and the required stacking (organization) of the punched cards.

Section V presents a sample case which includes a data listing, the resulting output, and a "day file" from the CDC 6500 computer system. The "day file" is included to illustrate the required system control cards and their proper sequence.

In addition to the aforementioned inputs, there are the data interfaces which are required by the various subprograms and discussed in Subsection 4 of this section. These interface data should be considered as inputs when running the subprograms independently.

b. Program NAMELISTS

Table I presents a list of the names of each NAMELIST and the subprograms to which they correspond. To determine the details and parameters contained in each NAMELIST, the user should refer to the appropriate Appendix as listed in Subsection 1 of this section. NAMELISTS required by CONTAM (the main program) are described in the Subsection 5. c.

c. CONTAM NAMELISTS

Two NAMELISTS are required by the main program, CONTAM, to provide control of the overall program. They are:

- (1) NAMELIST/NCASE/
- (2) NAMELIST/IPATH/

Table I
NAMELIST AND SUBPROGRAM

NAMELIST Name	Subprogram
NCASE	CONTAM(EXEC)
IPATH	CONTAM(EXEC)
PROCED	TCC
PRTDIR	TCC
RESRT1	TCC
RESRT2	TCC
STEADY	STDST
ENGINE	N2H4
CATLST	N2H4
CONTRL	N2H4
DATA	TD2
DATAP	TD2P
SID	XMGKS(SLINES)
THERMO	TTAPE(KINCON)
PROPEL	INPUT(KINCON)

There are eight NAMELIST sets in SURFACE, refer to Appendix D

There is only one parameter in the NAMelist/NCASE/. It is ICASE. ICASE is an integer variable which tells the program how many pulse segments are to result from the transient pulse output of the TCC subprogram. Each pulse segment is considered a "case." Each subsequent subprogram in the sequence must operate on each pulse segment (case), one segment at a time. The default value is ICASE = 1, which is recommended for most applications.

NAMelist/IPATH/ contains ten variables. However, only two of the variables are required per run (sequential mode). The variable list for NAMelist/IPATH is:

- TC
- BIPROP
- SSCP
- NOZZLE
- PLUME
- SLINES
- MGKS
- SURFAC
- KMODE
- NSL

Each variable except KMODE and NSL is logical. For example:

TC = T, BIPROP = T,

The above example indicates that the subprogram to be run will be TCC. If the data input were changed to

TC=T, BIPROP=F,

the program run would be N2H4. When running the MULTRAN portion of CONTAM, the user may desire to run sequentially during a single run the programs TD2, TD2P, and SLINES. In this instance, the data input would read

NOZZLE=T, SLINES=T.

In the case the subprogram KINCON is to be run, KMODE and NSL may also be required.

The variable KMODE is used only when the KINCON subprogram is run independently. If used, it is input as the integer variable "one." It indicates that certain options will be exercised in the operation of the KINCON subprogram. These options are described in Appendix C.

The variable NSL is required only when the KINCON subprogram is run independently. NSL indicates the number of streamlines that will be analyzed by the KINCON subprogram. If subprogram SLINES is run in

conjunction with the KINCON subprogram, any NSL value input here will be overridden by the value of NSL input for the SLINES subprogram.

d. Nonstandard Format Inputs

All of the nonstandard format punched card inputs are used by the KINCON subprogram. The names of these inputs are:

- Thermodynamic Data (Optional)
- Title Card
- Species Cards
- Reaction Cards

The format for the data on these cards is detailed in Appendix C.

Section V

SAMPLE CASE

This section presents a data listing and printed output for a sample case run in the sequential mode on the CDC 6500 computer system.

1. DEFINITION OF SAMPLE CASE

The sample case is chosen to illustrate the application of the successive subprograms of CONTAM for the prediction of the contamination effects resulting from a typical firing of a real rocket engine. The engine chosen for these computations is the Marquardt R-6C. The R-6C is a commercially available NTO-MMH rocket engine having a nominal thrust of 5 pounds and designed for pulse-mode operation. It is an excellent choice for experimental vacuum-chamber studies of contaminant production because of its small size, which makes it easier to maintain vacuum in the test chamber, and its short pulse capability which can be used to aggravate the production of contaminants. The effect of the small engine size, however, must be considered in designing the experiment. The R-6C is being used in an experimental contaminant effects study currently underway at NASA Lewis Research Center under the direction of Dr. Herman Mark. It is hoped that the computed values for contaminant production, transport, deposition, and surface effects can be experimentally verified by comparison with experiments such as those being run at NASA Lewis Research Center.

A pulse width of 17 milliseconds was chosen for these computations. This duration corresponds to a minimum impulse bit firing. Minimum impulse bit firings are particularly important for production of contaminant material, and are commonly employed for limit-cycle pointing corrections on vehicles which must maintain a prescribed attitude.

In our calculations, the engine is fired with its walls initially clean and with its dribble volumes both initially empty, but with the lines full of propellant behind the valves. This initial condition would be easier to match experimentally than any prescribed axial accumulation of fuel and oxidizer on the wall or partially filled dribble volumes. The chamber, injector, and tankage were initially set to room temperature values, again for ease of experimental comparison. The line lengths, line diameters, tank pressures, and other installation and operational variables were chosen to agree with the NASA Lewis vacuum chamber installation.

2. CONTAMINANT PRODUCTION - THE TCC PROGRAM

The TCC (transient combustion chamber) program calculates contaminant production by digital integration of the time-dependent engine processes, i. e., propellant flow, atomization, and combustion of the

injected droplets. The calculated two-dimensional trajectories for the burning droplets determine how much propellant is deposited on the wall, and how much passes through the throat unburned. The trajectories for the ejected unburned droplets are calculated up to the throat by the TCC subprogram, and in the nozzle and plume by the MULTRAN subprogram. The unburned propellant which is deposited on the combustion chamber wall is subjected to burnoff and axial flow from the action of the hot, fast-moving chamber gases. The amount of this wall film material which survives and passes through the throat is calculated by the TCC subprogram. Experimental firings of small pulsing engines show that much of this material accumulates on the nozzle lip during each firing, and is blown off during the succeeding start transient. The droplet size, initial direction of flight, and subsequent trajectory of this material may be defined statistically from experimental firings, but is outside of the present scope of the CONTAM program.

a. TCC Input-Sample Case (R-6C Engine)

Input data for the TCC program are broken down into several large blocks of related data. The block headings are: General Instructions, Time-Average Performance Values, Droplet Trajectory Plot, Flow Rate Overrides, Operating Conditions, Ignition Description, Fuel Feed System, Oxidizer Feed System, Atomization Parameters, Fuel Properties, Oxidizer Properties, Product Properties, Thrust Coefficient Table, Adduct Properties, Contaminant Viscosity, Valve Timing, Multi-Ring Injector, and Combustion Chamber Profile.

Loading such an extensive array of input information can never be easy; however, considerable effort has been made to make it as easy as possible. Wherever possible the input units chosen are those which are obtainable directly from a blueprint, engine test, literature reference, or standard engine performance computer program.

Certain of the data blocks, i. e., Fuel Properties and Oxidizer Properties, remain fixed for particular materials and can be passed on from one data set to another uncharged. The Product Property Deck for a particular propellant combination and pressure can also be reused when appropriate. Having such subdecks on hand for the common propellant constituents and combinations greatly facilitates loading the input for the TCC subprogram. When subdecks are created with the injector and chamber characteristics for particular engines, these can be used for a variety of operating conditions or for a variety of feed-system configurations, i. e., line lengths and diameters, restrictor areas, etc.

(1) Origin of Engine and Propellant Data

The known physical properties of nitrogen tetroxide and monomethylhydrazine were taken from the Battelle "Liquid Propellant Handbook" (Reference 7) and the Aerojet publication "Performance and Properties of Liquid Propellants" (Reference 8). The burning-rate coefficient for monomethylhydrazine was estimated to be halfway between the experimental values given for hydrazine and UDMH by Dykema and Greene (Reference 9). The burning-rate coefficient for NTO was calculated using Godsaves' equation. The equilibrium combustion gas properties of chamber temperature,

mean molecular weight, gamma, and vacuum thrust coefficient for an expansion area ratio of 40 were calculated, using the MDAC thermochemistry program H099 and the JANNAF (Reference 10) values for heats of formation. The chamber dimensions, injector parameters, and valve ramp durations come from the manufacturer, while the feed system values were supplied by NASA Lewis Research Center.

The ignition parameters, activation energy, and frequency factor multiplied by heat of reaction are the experimental values measured for NTO and MMH by Seamans, Vanpee, and Agosta (Reference 11). The fuel and oxidizer droplet size correction factors are taken from Rocketdyne Report R-8455 by L. J. Zajac (Reference 12). The fuel and oxidizer fan lengths are taken to be the same multiple of orifice diameter as for another motor where this value could be taken from NACA TN 3835 (Reference 13), and then experimentally verified by measuring chugging frequency and chugging amplitude. The distance to single-stream breakup is taken to be the same multiple of orifice diameter as shown in the photographs of NACA TN 3835. The flash cone angle was taken from photographs of flashing streams in the thesis of Brown (Reference 14). The drop size distribution is from NACA TN 4222 (Reference 15). The fraction of propellant hitting the wall which is presumed to stick is suggested by film-coolant injection effectiveness values published by B. L. McFarland (Reference 16). (Using a value of 1.0 for the fraction sticking when the film coolant is injected tangentially and a value of 0.5 for nontangential injections appears to give good agreement with experiment.) Experimental chamber wall temperature histories for small motors have also been published by McFarland (Reference 17).

The decomposition temperature for the MMH nitrate was taken from the paper of Perlee, Christos, Miron, and James (Reference 18). The values used for the density, vapor specific heat, latent heat and viscosity of the MMH nitrate and its solutions, and the accommodation coefficients for MMH and NTO are estimated values since no experimental values have ever been published.

The details of the fuel and oxidizer feed systems were unknown, while the flow rates and overall pressure drops were known. For this reason equivalent feed system orifice diameters were obtained using the flow override option. These values were obtained in an earlier computer run and are incorporated into the data input used for this run.

(2) Input Data for TCC Subprogram (Marquardt R6C Engine)

Title information is input via a variable format on the first card of the data deck. At present a title 58 characters long may be input.

The first card in the data for the TCC program is a variable format card which is used to introduce the hollerith information used as a printed heading for the TCC data (see Table II).

(IHO, 10X, * MARQUARDT R-6C ENGINE, SAMPLE CASE
FOR CONTAM *)

This card begins in card column 1 and extends to card column 70 inclusive. The hollerith title is inserted between the asterisks.

Table II
INPUT DATA FOR MARQUARDT R-6C ENGINE TCC

DDD1 Array Number	Variable	Value	Comments/Source
GENERAL INSTRUCTIONS			
9	Punch for restart flag (1.0 or 0.0)	1.0	Punch a card deck giving final distribution of propellant mass on the wall, i. e. RESRT1 & RESRT2
10	Work from tape flag (1.0 or 0.0)	0.0	Calculate chamber processes instead of taking values from a prewritten output tape
11	K BUG flag	0.0	Do not print a large set of diagnostic values at the K BUGTH iteration
12	No movie tape flag (1.0 or 0.0)	0.0	Write an output tape to be used to make chamber movies
201	Stop time	0.03 sec	Terminate calculations at a model time of 0.030 seconds
202	Time interval	0.0001 sec	Use an integrating time interval of 0.0001 (based upon previous experience)
203	Print one out of	10	A propellant disposition summary is printed for every tenth time interval
204	Plot one out of	30	A wall-film thickness profile is plotted for every 30th time interval
205	Film vertical exaggeration	20	The wall-film thickness is exaggerated by a factor of 20 for the combustion chamber movie

Table II
INPUT DATA FOR MARQUARDT R-6C ENGINE TCC (Continued)

DDD1 Array Number	Variable	Value	Comments/Source
206	Start movie iteration	150	Motion picture frames will be produced starting with the 150th iteration
207	End movie iteration	150	Motion picture frames will be produced ending with the 150th iteration
208	Data review only flag	0.0	The program will compute the chamber processes instead of stopping after printing out the input data set and values derived from the flow overrides

TIME-AVERAGE PERFORMANCE VALUES

313	Start time 1	0.0 sec	The first time slice for average values starts at 0.0 sec
314	Finish time 1	0.015	The first time slice for average values ends at 0.015 sec
315	Start time 2	0.015 sec	The second time slice for average values starts at 0.015 sec
316	Finish time 2	0.017 sec	The second time slice for average values ends at 0.017 sec
317	Start time 3	0.017 sec	The third time slice for average values starts at 0.017 sec
318	Finish time 3	0.030 sec	The third time slice for average values ends at 0.030 sec

Table II
INPUT DATA FOR MARQUARDT R-6C ENGINE TCC (Continued)

DDCI Array Number	Variable	Value	Comments/Source
DROPLET TRAJECTORY PLOT			
209	Fuel trajectory group	3.0	A trajectory will be plotted for the third fuel size group
210	Oxidizer trajectory group	0.0	Only one droplet can be plotted per run. Either fuel or oxidizer depending upon whether 209 or 210 is given a non zero value
211	Trajectory start time	0.015/sec	The fuel droplet trajectory will be plotted for the fuel droplet injected when the model time is 15 milliseconds
212	Injector ring	1.0	The fuel droplet trajectory is for a droplet originating from the first ring
FLOW RATE OVERRIDES			
213	Fuel flow rate	0.0 lb/sec	No fuel feed system values are being calculated. (Flow rate at which experimental pressure drops are known)
214	Total pressure drop	0.0 psi	Fuel-side orifice diameter is not being calculated (fuel tank pressure - chamber pressure)
215	Valve pressure drop	0.0 psi	Fuel valve port area is not being calculated

Table II
INPUT DATA FOR MARQUARDT R-6C ENGINE TCC (Continued)

DDD1 Array Number	Variable	Value	Comments/Source
216	Injector pressure drop	0.0 psi	Injector orifice discharge coefficients are not being calculated
61	Percent of total fuel flow which passes through ring 1	0.0	Injector orifice discharge coefficients are not being calculated
62	Percent of total fuel flow which passes through ring 2	0.0	Injector orifice discharge coefficients are not being calculated
63	Percent of total fuel flow which passes through ring 3	0.0	Injector orifice discharge coefficients are not being calculated
217	Oxidizer flow rate	0.0 lb/sec	No oxidizer feed system values are being calculated
218	Total pressure drop	0.0 psi	Oxidizer-side orifice diameter is not being calculated
219	Valve pressure drop	0.0 psi	Oxidizer valve port area is not being calculated
220	Injector pressure drop	0.0 psi	Injector orifice discharge coefficients are not being calculated
85	Percent of total oxidizer flow which passes through ring 1	0.0	Injector orifice discharge coefficients are not being calculated
86	Percent of total oxidizer which passes through ring 2	0.0	Injector orifice discharge coefficients are not being calculated
87	Percent of total oxidizer which passes through ring 3	0.0	Injector orifice discharge coefficients are not being calculated

Table II
INPUT DATA FOR MARQUARDT R-6C ENGINE TCC (Continued)

DDD1 Array Number	Variable	Value	Comments/Source
OPERATING CONDITIONS			
13	Fuel tank pressure	180 psia	NASA Lewis
14	Fuel tank temperature	294°K	Approximate room temperature
15	Fuel tank psi/sec	0.0	Fuel tank pressure is not rising or falling
16	External pressure	1×10^{-6} psia	Estimated vacuum environment
17	Oxidizer tank pressure	165. psia	NASA Lewis
18	Oxidizer tank temperature	294°K	Approximate room temperature
19	Oxidizer tank psi/sec	0.0	Oxidizer tank pressure is not rising or falling
21	Injector initial temperature	294. °K	Approximate room temperature
22	Throat initial temperature	294°K	Approximate room temperature
25	Injector maximum temperature	350°K	Estimated
26	Half-rise time	10.0 sec	Estimated
27	Injector minimum temperature	294. °K	Approximate room temperature
28	Half-fall time	100.0 sec	Estimated
29	Throat maximum temperature	1,400°K	Estimated, based on values for similar engines

Table II
INPUT DATA FOR MARQUARDT R-6C ENGINE TCC (Continued)

DDD1 Array Number	Variable	Value	Comments/Source
30	Half-rise time	10 sec	Estimated-see McFarland for experi- mental curves of similar engines (Reference 17)
31	Throat minimum temperature	294°K	Approximate room temperature
32	Half-fall time	100.0 sec	Estimated
IGNITION DESCRIPTION			
33	Assigned ignition delay	0.0 sec	Not used when chemi- cal kinetic values are specified
34	Igniter port location	0.0 in. from injector	No igniter used
35	Igniter fuel flow rate	0.0 lb/sec	No igniter used
36	Igniter oxidizer flow rate	0.0 lb/sec	No igniter used
37	Activation energy	5,200 cal/ mole	Seamans, Vanpee, and Agosta (Reference 11)
38	Frequency factor x heat of reaction	3.4×10^{14} (cc/mole sec) x (cal/mole)	Seamans, Vanpee, and Agosta
39	Perfect mixing flag	0.0	Use normal ignition calculations
40	No axial mixing flag	0.0	Use normal ignition calculations
FUEL FEED SYSTEM			
41	Fuel line length	480 in.	NASA Lewis Research Center
42	Fuel line diameter	0.189151 in.	NASA Lewis Research Center

Table II
INPUT DATA FOR MARQUARDT R-6C ENGINE TCC (Continued)

DDD1 Array Number	Variable	Value	Comments/Source
43	Fuel restrictor diameter	0.016728 in.	Calculated from pressure drop and flow rate values
44	Fuel venturi diameter	0.0 in.	No venturi used
45	Fuel valve port area	0.0281 in. ²	No valve restriction when open — line area used
46	Fuel check valve flag	0.0	Reverse flow in feed system is possible
47	Fuel valve opening ramp duration	0.001 sec	Manufacturer
48	Fuel valve closing ramp duration	0.001 sec	Manufacturer
57	Fuel initial void volume	0.00113 in. ³	Set equal to dribble volume for initially empty condition
59	Fuel transition volume	0.0 in. ³	No hot fuel in injector
60	Fuel dribble volume	0.00113 in. ³	Manufacturer
OXIDIZER FEED SYSTEM			
65	Oxidizer line length	480 in.	NASA Lewis Research Center
66	Oxidizer line diameter	0.189151 in.	NASA Lewis Research Center
67	Oxidizer restrictor diameter	0.020997 in.	Calculated from pressure drop and flow rate values
68	Oxidizer venturi diameter	0.0	No venturi used
69	Oxidizer valve port area	0.0281 in. ²	No valve restriction when open — line area used

Table II
INPUT DATA FOR MARQUARDT R-6C ENGINE TCC (Continued)

DDD1 Array Number	Variable	Value	Comments/Source
70	Oxidizer check valve flag	0.0	Reverse flow in oxidizer feed system is possible
71	Oxidizer valve open- ing ramp duration	0.001 sec	Manufacturer
72	Oxidizer valve closing ramp duration	0.001 sec	Manufacturer
81	Oxidizer initial void volume	0.000580 in. ³	Set equal to dribble volume for initially empty condition
83	Oxidizer transition volume	0.0 in. ³	No hot oxidizer in injector
84	Oxidizer dribble volume	0.000580 in. ³	Manufacturer
89	Fuel drop factor	0.50	Droplet size correc- tion factor for injector orifices which are nonturbulent, not flowing full or non- circular. L. J. Zajac's value for laminar flow (Reference 12)
90	Oxidizer drop factor	0.50	Droplet size correc- tion factor for injector orifices which are non- turbulent, not flowing full or noncircular. L.J. Zajac's value for laminar flow
91	Fuel fan length with 90-deg impingement, balanced momentum	3.0 orifice diameters	Estimated from NACA TN 3835. (Refer- ence 13). No experi- mental data for orifices this small

Table II
INPUT DATA FOR MARQUARDT R-6C ENGINE TCC (Continued)

DDD1 Array Number	Variable	Value	Comments/Source
92	Oxidizer fan length with 90-deg impinge- ment, balanced momentum	3.0 orifice diameters	Estimated from NACA TN3835. No experimental data for orifices this small.
93	Hold at triple point flag	0.0	Assume flashing propellant equilibrates with chamber pres- sure even though freezing occurs
94	No initial dribble flag	1.0	The quill-type Marquardt injector is not likely to dribble during start before the dribble volume fills completely
95	Flash cone angle	30 deg	Apex angle of flashing liquid spray taken from photographs of R. Brown (Refer- ence 14)
96	Single-stream breakup distance given in orifice diameters	10	Estimated from photo- graphs of single- stream breakup. See NACA TN3835 (Refer- ence 13)
97-101	Drop size distribution table	0.198, 0.759 1.0, 1.23, 2.3045	Taken from experi- mental values of NACA TN 4222 (Refer- ence 15)
102	No wall breakup flag	0.0	Streams are assumed to atomize on wall impact
103	Drop rebound velocity ratio	1.0	Droplets which bounce off wall are assumed perfectly elastic

Table II
INPUT DATA FOR MARQUARDT R-6C ENGINE TCC (Continued)

DDDI Array Number	Variable	Value	Comments/Source
104	Fraction sticking	0.5	One-half the streams and droplets impacting with the cold wall are assumed to bounce and the remainder stick. B. L. McFarland data (Reference 16)
105	No fuel flash flag	0.0	The fuel stream is permitted to flash atomize when the correlations indicate that it should
106	No oxidizer flash flag	0.0	The oxidizer stream is permitted to flash atomize when the correlations indicate that it should
107	No entrainment flag	0.0	The material deposited on the chamber walls is permitted to entrain when the correlations indicate that it should
108	Delete droplet means flag	0.0	The D ₃₀ , D ₃₁ , and D ₃₂ will be calculated for the chamber droplet population at each time interval
109	Fuel normal boiling point	360°K	Aerojet compilation (Reference 8)
110	Fuel freezing point	222°K	Aerojet compilation
111	Fuel critical temperature	594°K	Aerojet compilation
112	Fuel critical pressure	1, 195 psia	Aerojet compilation

Table II
INPUT DATA FOR MARQUARDT R-6C ENGINE TCC (Continued)

DDD1 Array Number	Variable	Value	Comments/Source
113	Fuel vapor specific heat at film temperature	0.995 cal/ gram °K	Value for propylene specific heat at 1500°K extrapolated from NBS C461. Structure similar to MMH. No data for MMH
114	Fuel liquid specific heat at 300°K	0.69 cal/ gram °K	Aerojet compilation
116	Fuel vapor molecular weight	46.074 grams/ gram mole	Aerojet compilation
117	Fuel latent heat of vaporization (at normal boiling point)	210 cal/gram	Aerojet compilation
118	Fuel latent heat of fusion	67.5 cal/gram	Battelle handbook (Reference 7)
119	Fuel liquid thermal conductivity	0.000545 cal/ cm °K	Aerojet compilation
120	Fuel accommodation coefficient	1.0	Strawman value, no data available
121	Reference temperature for fuel properties	300°K	Experimental values available at this temperature
122	Fuel density at reference temperature	0.88 gram/cc	Aerojet compilation
123	Fuel viscosity at reference temperature	0.0104 poise	Aerojet compilation
124	Fuel surface tension at reference temperature	47 dynes/cm	Battelle handbook
125	Fuel burning rate coefficient	0.0325 cm ² / sec	Dykema and Greene (Reference 9)

Table II
INPUT DATA FOR MARQUARDT R-6C ENGINE TCC (Continued)

DDD1 Array Number	Variable	Value	Comments/Source
126	Fuel monopropellant intercept (A)	0.0 cm/sec	Strand burning tests fitted $r = A + B P_c^n$ with r in cm/sec; P_c in psia
127	Fuel monopropellant coefficient (B)	0.0 cm/ sec psi ⁿ	MMH does not burn in liquid strand tests
128	Fuel monopropellant exponent (n)	0.0	
OXIDIZER PROPERTIES			
129	Oxidizer normal boiling point	294 °K	Aerojet compilation
130	Oxidizer freezing point	262 °K	Aerojet compilation
131	Oxidizer critical temperature	431 °K	Aerojet compilation
132	Oxidizer critical pressure	1,470 psia	Aerojet compilation
133	Oxidizer vapor specific heat at film temperature	0.298 cal/ gram °K	JANNAF tables for NO ₂ (Reference 10)
134	Oxidizer liquid specific heat at 300°K	0.36 cal/ gram °K	Aerojet compilation
136	Oxidizer vapor molecular weight	46.008 gram/ gram mole	Vapor mostly NO ₂ at high temperature or low pressure
137	Oxidizer latent heat of vaporization (at normal boiling point)	99.0 cal/gram	Aerojet compilation
138	Oxidizer latent heat of fusion	39.2 cal/gram	Battelle handbook

Table II
INPUT DATA FOR MARQUARDT R-6C ENGINE TCC (Continued)

DDD1 Array Number	Variable	Value	Comments/Source
139	Oxidizer liquid thermal conductivity	0.000306 cal/cm °K	Aerojet compilation
140	Oxidizer accommodation coefficient	1.0	Strawman value, no data available
141	Reference temperature for oxidizer properties	300°K	Experimental values available at this temperature
142	Oxidizer density at reference temperature	1.45 gram/cc	Aerojet compilation
143	Oxidizer viscosity	0.00446 poise	Aerojet compilation
144	Oxidizer surface tension	28 dyne/cm	Battelle handbook
145	Oxidizer burning rate coefficient	0.027 cm ² /sec	Calculated from Godsaves' equation
146	Oxidizer mono-propellant intercept (A)	0.0 cm/sec	Strand burning rate fitted to: $r = A + B p_c^n$ with r in cm/sec and P_c in psia
147	Oxidizer mono-propellant coefficient (B)	0.0 cm/sec psia	NTO does not burn in liquid strand tests
148	Oxidizer mono-propellant exponent (n)	0.0	NTO does not burn in liquid strand tests
PRODUCT PROPERTIES EQUILIBRIUM GAS TEMPERATURE			
149-159	Equilibrium combustion gas temperature at fuel fractions 0.0, 0.1, 0.2, ... 1.0	300; 2103 3084; 3397; 3061; 2368; 1705; 1433; 1344; 1266; 1190; in °K	From standard equilibrium thermochemistry calculations

Table II
INPUT DATA FOR MARQUARDT R-6C ENGINE TCC (Continued)

DDD1 Array Number	Variable	Value	Comments/Source
EQUILIBRIUM GAS MOLECULAR WEIGHT			
161-171	Equilibrium combustion gas mean molecular weight at fuel fractions 0.0, 0.1, 0.2, ... 1.0	46.008, 28.79, 26.41, 23.39, 19.88, 16.75, 14.41, 13.91, 14.00, 14.10, 14.29	From standard equilibrium thermochemistry calculations
EQUILIBRIUM GAS GAMMA			
173-183	Equilibrium combustion gas gamma at fuel fractions 0.0, 0.1, 0.2, ... 1.0	1.120, 1.252, 1.220, 1.217, 1.235, 1.268, 1.309, 1.299, 1.270, 1.247, 1.228	From standard equilibrium thermochemistry calculations
THRUST COEFFICIENT TABLE EQUILIBRIUM THRUST COEFFICIENT			
221-231	Vacuum thrust coefficients for the correct nozzle expansion area ratio of the motor, and fuel fractions of 0.0, 0.1, 0.2, ... 1.0	1.9240, 1.8028, 1.9082, 1.9617, 1.8470, 1.8122, 1.8680, 1.9331, 1.9294, 1.9224, 1.8959	These values were obtained from thermochemical calculations assuming equilibrium expansion. Values could be used from kinetics calculations or from steady-state experiments if they were available
232	Nozzle expansion area ratio	40	Manufacturer
ADDUCT PROPERTIES			
185	Contaminant mixture density	1 gram/cc	Strawman value, no experimental data
186	Contaminant vapor specific heat	1 cal/gram °K	Strawman value, no experimental data
187	Contaminant latent heat of vaporization	100 cal/gram	Strawman value, no experimental data

Table II
INPUT DATA FOR MARQUARDT R-6C ENGINE TCC (Continued)

DDD1 Array Number	Variable	Value	Comments/Source
188	Contaminant decomposition temperature	500°K	Perlee, Christos, Miron, and James (Reference 18)
CONTAMINANT VISCOSITY			
189-199	Contaminant mixture viscosity at fuel fractions 0.0, 0.1, 0.2 - 1.0	0.00446, 0.024, 0.043, 0.068, 0.081, 0.100, 0.082, 0.064, 0.046, 0.029, 0.0104 poise	Experimental values for pure fuel and pure oxidizer. Strawman values for MMH nitrate mixtures
VALVE TIMING			
233	Fuel valve opening time	0.0 sec	Time of first motion opening
234	Oxidizer valve opening time	0.0 sec	Time of first motion opening
235	Fuel valve closing time	0.017 sec	Time of first motion closing
236	Oxidizer valve closing time	0.017 sec	Time of first motion closing
237-264	Valve timing for 2nd, 3rd, 4th, 5th, 6th, 7th, and 8th pulses		Not being used
MULTI-RING INJECTOR FIRST RING FUEL HOLES			
49	Fuel hole diameter	0.0158 in.	Manufacturer
50	Fuel hole length	0.0625 in.	Estimated from engine drawing
51	Axial location of fuel hole	0.0 in.	Approximately flush with injector face

Table II
INPUT DATA FOR MARQUARDT R-6C ENGINE TCC (Continued)

DDD1 Array Number	Variable	Value	Comments/Source
52	Radial location of fuel hole	0.045 in.	Estimated from engine drawing
53	Fuel radial injection angle	-45 deg	Manufacturer
54	Discharge coefficient	1.0	Assumed value
55	Number of fuel holes in this ring	1.0	Manufacturer
56	Transverse angle	0.0	Manufacturer
OXIDIZER HOLES			
73	Oxidizer hole diameter	0.0186 in.	Manufacturer
74	Oxidizer hole length	0.0625 in.	Estimated from engine drawing
75	Axial location of oxidizer hole	0.0 in.	Approximately flush with injector face
76	Radial location of oxidizer hole	-0.045 in.	Estimated from engine drawing
77	Oxidizer radial injection angle	45 deg	Manufacturer
78	Discharge coefficient	1.0	Assumed value
79	Number of oxidizer holes this ring	1.0	Manufacturer
80	Transverse angle	0.0	Manufacturer

Table II
INPUT DATA FOR MARQUARDT R-6C ENGINE TCC (Continued)

DDD1 Array Number	Variable	Value	Comments/Source
SECOND RING			
265-272	Second fuel ring values equivalent to 49-56 for first fuel ring (This engine has no second ring)		
273-280	Second oxidizer ring values equivalent to 73-80 for first oxidizer ring (This engine has no second ring)		
THIRD RING			
281-288	Third fuel ring values equivalent to 49-56 for first fuel ring (This engine has no third ring)		
289-296	Third oxidizer ring values equivalent to 73-80 for first oxi- dizer ring (This engine has no third ring)		
COMBUSTION CHAMBER PROFILE			
297	Axial location of injector face	0.0 in.	
298	Diameter corre- sponding to above station	0.41735 in.	Scaled from print of the chamber
299-310	Six pairs of sta- tions and diame- ters, describing the chamber contour	0.25, 0.41735, 0.5, 0.41735, 0.75, 0.41735, 0.95872, 0.41735, 0.97363, 0.30607, 1.01436, 0.22461	Scaled from print of the chamber
311	Axial location of throat	1.07 in.	
312	Throat diameter	0.19479 in.	

The input data are introduced through two namelists, Namelist PROCED and Namelist PRTDIR. Namelist PROCED consists of a 319-word array DDD1. These values contain the detailed description of the motor, propellant, operating conditions, etc. Namelist PRTDIR consists of an 80-word array DDD2. These values are nonzero or zero to indicate which time-varying parameters are to be plotted as graphic output.

The input values to Namelist PROCED are printed out by the program along with headings in logical groupings which have been found to be convenient. The input values will be described in the order of this print, rather than in ascending order, as this will be a more logical presentation.

Namelist PRTDIR directs the program to produce graphics of the time-varying parameters which are desired. The default value for the members at this array is zero, and graphics are produced only for members which are given nonzero values. The graphics which can be produced are:

DDD2 array

<u>Number</u>	<u>Variable to be Plotted</u>
1.	Chamber pressure
2.	Fuel valve trace (fraction of wide-open port area)
3.	Oxidizer valve trace (fraction of wide-open port area)
4.	Fuel flow rate leaving tank
5.	Oxidizer flow rate leaving tank
6.	Total propellant flow rate leaving tanks
7.	Fuel injection rate
8.	Oxidizer injection rate
9.	Fuel (streams, fans, and droplets) mass in chamber
10.	Oxidizer (streams, fans, and droplets) mass in chamber
11.	Propellant (streams, fans, and droplets) mass in chamber
12.	Fuel mass on chamber wall
13.	Oxidizer mass on chamber wall
14.	Propellant mass on chamber wall
15.	Gas mass in chamber
16.	Mass fraction of the chamber gas which is fuel derived

17. Chamber temperature (gas phase)
18. Fuel evaporation rate
19. Oxidizer evaporation rate
20. Propellant evaporation rate
21. Gas outflow rate
22. Fuel droplet outflow rate
23. Oxidizer droplet outflow rate
24. Total droplet outflow rate
25. Fuel film outflow rate
26. Oxidizer film outflow rate
27. Total film outflow rate
28. Mass fraction of total outflow which is gas phase
29. All chamber contents – total explosion pressure capability
30. Mass of unatomized fuel streams and fans in chamber
31. Mass of unatomized oxidizer streams and fans in chamber
32. Mass of fuel droplets in chamber
33. Mass of oxidizer droplets in chamber
34. Gas and droplets only – total explosion pressure capability
35. Chamber wall adduct only – chamber explosion overpressure capability
36. D30 of all fuel droplets in chamber
37. D31 of all fuel droplets in chamber
38. D32 of all fuel droplets in chamber
39. D30 of all oxidizer droplets in chamber
40. D31 of all oxidizer droplets in chamber
41. D32 of all oxidizer droplets in chamber
42. Fuel injector void volume
43. Oxidizer injector void volume
44. Thrust

b. TCC Output-Sample Case (R-6C Engine)

The computer output is in the form of printout and computer graphics done on a Stromberg SD-4060 microfilm recorder operating in a SD-4020 emulation mode. Many of the output values are presented both in the form of printout and in the form of plots of variables versus time. It is generally easier to use the plots to follow the course of events in the chamber, but it is easier to use the printout to obtain exact numerical values, exact timing relationships, etc.

Since the complete set of graphics is expensive to produce in terms of computer time, it is best initially to request only the graphics which are really needed, plus chamber pressure, fuel injection rate and oxidizer injection rate (the three graphics which give the greatest amount of general information about the firing). If physical tape 9 and tape 13 are mounted before the computer calculations are done, they will record enough time-varying data that any additional graphics, additional time-slice average performance values, or motion picture frames that are desired can be recovered later from the tapes, without any additional combustion chamber calculations being required.

The information which is typically desired about the principal portions of a rocket engine firing is the duration, total impulse, fuel and oxidizer consumption and total contaminant production during the start transient; the same parameters for the cutoff transient; and the thrust level, fuel and oxidizer flow rates and contaminant production rate during the steady-state portion. It is obvious that for firings with sufficiently similar initial conditions such information can be used to estimate the mean performance level and cumulative contamination effects of longer or shorter pulses or of trains of pulses. For example, the total impulse of a pulse is simply the lumped impulse of the start transient plus the lumped impulse of the cutoff transient plus the steady-state duration multiplied by the steady-state thrust level. Total pulse specific impulse is obtained as the ratio of total pulse impulse to total pulse propellant consumption.

This segmental breakdown information cannot easily be obtained in a single pass through the computer, because it is not yet possible to describe "steady-state" in mathematical terms which will permit the computer to make satisfactory interval selections by itself (In typical pulse-mode firings, mathematical steady-state is never reached; however, the major parameters are sufficiently slow-varying that "steady-state" assumptions are useful engineering approximations. The procedure used is to perform the chamber calculations, recording data on tape 9 and tape 13. Next, inspect the graphics which are produced describing chamber pressure, propellant injection rates, wall accumulation, etc., and choose a time for the end of the start transient. Tape 9 can then be remounted, and the program instructed to work-from-tape in calculating interval values for the designated start transient, for the steady-state portion of the firing, and for the cutoff portion. Additional graphics, wall-film profiles, or combustion chamber "snap shots" or movies may be obtained in the same way. (Because of the details of the programming the only droplet trajectory which can be obtained from tape, is the single one specified in the original computer run, other trajectories can be estimated from the chamber "snapshots" however.)

The computer printout includes a recapitulation of the input values and the derived fuel and oxidizer properties versus temperature, followed by the values of the major system variables computed at each computing time interval. At each tenth time interval, there is a summary print which gives the disposition of the total mass of each propellant constituent injected up till that time, i. e., how much has been ejected in the gas phase, as droplets, or as wall film and how much is being retained as gas, as droplets, or as wall film.

Statements are printed to give the times when the oxidizer manifold fills, when the fuel manifold fills, when ignition occurs, and when extinguishment occurs. There are several error diagnostics programmed, but none are illustrated in the sample case.

A fairly detailed summary is given at the end of the computation, which includes mean values for the entire pulse. Entire pulse values are given for mixture ratio, C-Star, and specific impulse for three possible mass bases: propellant mass out of the tank, propellant mass through the injector, and propellant mass through the nozzle. The final summary also gives the propellant droplet size distribution for injected and ejected fuel and oxidizer, the fraction of injected propellant which is expelled or retained in seven different categories. The axial and radial mean velocities of the expelled droplets, and the axial distribution of unburned propellant deposited on the walls.

Approximately the same data can be obtained for any specified time-slice by using the data on tape 9 in a program rerun from tape. The time-slice calculations also give values to use as input to the MULTRAN Subprogram of CONTAM.

(1) Computer Printout

Printouts are reproduced illustrating the recapitulated input data for the R6-C engine, the curve-fitted values for fuel and oxidizer physical properties, the derived feed system values, the chamber description at the start of the run and excerpts from the voluminous time-varying description of the firing. Prints specifying manifold priming, ignition, extinguishment, and periodic propellant disposition summaries are illustrated.

A time-averaged interval print for the time-slice between 15 and 17 milliseconds is illustrated. Thrust, chamber pressure, propellant flow rate, mixture ratio, C-Star, I_{sp} , contaminant production, expelled droplet mean diameters, axial and radial velocity components are given. The final printout gives input values for the MULTRAN subprogram, which follows TCC in the CONTAM ensemble. Chamber pressure, chamber temperature, gas constant, specific heat, gamma, gas viscosity, and the densities, amounts and droplet size distribution are given in units compatible with MULTRAN.

(2) Computer Graphics

Only a small fraction of the computer graphics which can be called for are illustrated here. There are four general classes of graphics, the droplet trajectory plots, the time-varying parameter plots, the wall-film thickness plots, and frames from chamber movies.

The droplet trajectory plot shows the path followed by the fuel droplet of the third size group (median fuel droplet) injected 15 milliseconds after start from the first ring (the only ring in this motor). This graphic is drawn so as to fill the frame, and hence will show details of even small motions of the droplet in either the x or y direction. Because of this expansion to fill the frame, there is usually distortion because the x and y scales are generally not expanded to the same extent. Plots of x vs. t, y vs. t and y vs. x are produced, but only the y vs. x plot is illustrated here.

The time-varying parameter plots illustrated here are chamber pressure (psia), fuel injection rate (lb/sec), oxidizer injection rate (lb/sec), gas outflow rate (lb/sec), outflow rate for incompletely burned fuel droplets (lb/sec), outflow rate for incompletely burned oxidizer droplets (lb/sec), outflow rate for fuel film on the wall (lb/sec), and outflow rate for oxidizer film on the wall (lb/sec).

Wall-film thickness plots are shown for $T = 6.0$ milliseconds and $T = 9.0$ milliseconds. As in the case of the droplet trajectory plots, these are expanded to fill the frame, and thus are distorted by having a very large vertical exaggeration. This makes it possible to see details of the film which would not be visible otherwise.

The final type of graphic is a "motion picture frame," showing the outline of the chamber, the location of the droplet groups in the chamber and the (exaggerated) deposit of propellant film on the chamber wall. "Stills" or motion pictures of this kind are very valuable for aiding in the visualization of the very complex sequence of events which take place during the start and cutoff transients.

3. CONTAMINANT TRANSPORT—THE MULTRAN PROGRAM

The programs composing MULTRAN, TD2, TD2P, and SLINES are used to calculate the two-phase transonic and supersonic flow. The reader is referred to Appendix B for a detailed discussion of the computation methods.

The printout "Input Values for MULTRAN" of TCC supplies the input data for MULTRAN in the correct units, and this information has been used to generate the NAMELIST/DATA/, as illustrated. Using the results of the RC-6 engine, a calculation has been made for the fuel droplets. The given value for the ratio of droplet mass to gas mass has been taken directly from TCC, i.e. 0.123. However, some discussion is required in relation to the choice of droplet size used in the calculation.

THE INPUT DATA FOR THIS CASE ARE AS FOLLOWS

PROBLEM DESCRIPTION

HARQUARD M-AC ENGINE. SAMPLE CASE FOR CONTAM

GENERAL INSTRUCTIONS

PUNCH FOR RESTART WORK FROM TAPE MMUG END MOVIE TAPE

(9) 1.000000 (10) 0.000000 (11) 0.000000 (12) 0.000000

STOP TIME TIME INTERVAL PRINT ONE OUT OF FIVE OUT OF

(201) .030000 (202) .000100 (203) 10.000000 (204) 30.000000

FILM VERT. ENAG. START MOVIE ITER. END MOVIE ITER. DATA REVIEW ONLY

(205) 20.000000 (206) 150.000000 (207) 150.000000 (208) 0.000000

TIME-AVERAGE PERFORMANCE VALUES

START TIME 1 FINISH TIME 1 START TIME 2 FINISH TIME 2

(313) 0.000000 (314) .015000 (315) .015000 (316) .017000

START TIME 3 FINISH TIME 3

(317) .017000 (318) .010000 (

DROPLET TRAJECTORY PLOT

FUEL SIZE GROUP OXID SIZE GROUP INJECTION TIME INJECTION RING

(209) 3.000000 (210) 0.000000 (211) .015000 (212) 1.000000

FLOW RATE OVERRIDES

FUEL FLOW RATE TOTAL PRESS DROP VALVE PRESS DROP INJ PRESS DROP

(213) 0.000000 (214) 0.000000 (215) 0.000000 (216) 0.000000

PERCENT RING 1 PERCENT RING 2 PERCENT RING 3

(61) 0.000000 (62) 0.000000 (63) 0.000000 (64) 0.000000

OXID FLOW RATE TOTAL PRESS DROP VALVE PRESS DROP INJ PRESS DROP

(217) 0.000000 (218) 0.000000 (219) 0.000000 (220) 0.000000

PERCENT RING 1 PERCENT RING 2 PERCENT RING 3

(85) 0.000000 (86) 0.000000 (87) 0.000000 (88) 0.000000

OPERATING CONDITIONS

FUEL TANK PRESS FUEL TANK TEMP FUEL TANK PSI/SEC EXTERNAL PRESSURE

(13) 180.000000 (14) 294.000000 (15) 0.000000 (16) .000001

OXID TANK PRESS OXID TANK TEMP OXID TANK PSI/SEC

(17) 165.000000 (18) 294.000000 (19) .000000 (20) 0.000000

INJECT INIT TEMP THROAT INIT TEMP

(21) 294.000000 (22) 294.000000 (23) 0.000000 (24) 0.000000

INJECT MAX. TEMP HALF-RISE TIME INJECT MIN. TEMP HALF-FALL TIME

(25) 350.000000 (26) 10.000000 (27) 294.000000 (28) 100.000000

THROAT MAX. TEMP HALF-RISE TIME THROAT MIN. TEMP HALF-FALL TIME

(29) 1400.000000 (30) 10.000000 (31) 294.000000 (32) 100.000000

Reproduced from
best available copy.

IGNITION DESCRIPTION

ASSIGNED DELAY IGNITER PRMT LOC. FUEL FLOW RATE ORID FLOW RATE
(33) 0.000000 (34) 0.000000 (35) 0.000000 (36) 0.000000
ACTIVATION ENERGY FREQ. FACT. X Q PERFECT MIXING NO AXIAL MIXING
(37) 5200.000000 (38) 3.400000E+14 (39) 0.000000 (40) 0.000000

FUEL FEED SYSTEM

LINE LENGTH LINE DIAM RESTRICTOR DIAM VENTURI DIAM
(41) 480.000000 (42) .180151 (43) .016724 (44) 0.000000
VALVE AREA CHECK VALVES VALVE OPEN DT VALVE CLOSE DT
(45) .028100 (46) 0.000000 (47) .001000 (48) .001000
INIT. VOID VOLUME TRANSITION VOLUME WHIRL VOLUME
(57) .001130 (58) 0.000000 (59) 0.000000 (60) .001130

OXIDIZER FEED SYSTEM

LINE LENGTH LINE DIAM RESTRICTOR DIAM VENTURI DIAM
(65) 480.000000 (66) .180151 (67) .020997 (68) 0.000000
VALVE AREA CHECK VALVES VALVE OPEN DT VALVE CLOSE DT
(69) .028100 (70) 0.000000 (71) .001000 (72) .001000
INIT. VOID VOLUME TRANSITION VOLUME WHIRL VOLUME
(81) .000580 (82) 0.000000 (83) 0.000000 (84) .000580

ATOMIZATION PARAMETERS

FUEL DROP FACTOR ORID DROP FACTOR FUEL FAN MIN L/D ORID FAN MIN L/D
(89) .500000 (90) .500000 (91) 3.000000 (92) 3.000000
HOLD AT TRIPLE PT NO INIT. ORIBLE FLASH FOR ANGLE SINGLE STREAM L/D
(93) 0.000000 (94) 1.000000 (95) 30.000000 (96) 10.000000
DROP SIZE 1 DROP SIZE 2 DROP SIZE 3 DROP SIZE 4
(97) .198000 (98) .759000 (99) 1.000000 (100) 1.200000
DROP SIZE 5 NO MAIL BREAKUP DROP DESTINATION REACTION STICKING
(101) 2.304500 (102) 0.000000 (103) 1.000000 (104) .000100
NO FUEL FLASH NO ORID FLASH NO EXHAUSTANT CLEST DROP MEANS
(105) 0.000000 (106) 0.000000 (107) 0.000000 (108) 0.000000

FUEL PROPERTIES

BOILING POINT	FREEZING POINT	CRITICAL TEMP.	CRITICAL PRESS.
(109) 360.00000 (110) 222.00000 (111) 594.00000 (112) 1195.00000			
VAPOR CP.	LIQUID CP.		WGT. WEIGHT
(113) .995000 (114) .690000 (115) 0.00000 (116) 46.076000			
LATENT HEAT VAP.	LATENT HEAT FUS.	LIT. THERM. COND.	ACCOM. COEFF.
(117) 216.00000 (118) 67.50000 (119) .000545 (120) 1.00000			
REFERENCE TEMP.	DENSITY	VISCOSITY	SURFACE TENSION
(121) 300.00000 (122) .890000 (123) .014000 (124) 47.00000			
BURNING RATE K	WNOO. INTERCEPT WNOO.	COEFFICIENT	WNOO. EXPONENT
(125) .032500 (126) 0.00000 (127) 0.00000 (128) 0.00000			

OXIDIZER PROPERTIES

BOILING POINT	FREEZING POINT	CRITICAL TEMP.	CRITICAL PRESS.
(129) 294.00000 (130) 62.00000 (131) 431.00000 (132) 1470.00000			
VAPOR CP.	LIQUID CP.		WGT. WEIGHT
(133) .296000 (134) .360000 (135) 0.00000 (136) 46.00000			
LATENT HEAT VAP.	LATENT HEAT FUS.	LIT. THERM. COND.	ACCOM. COEFF.
(137) 99.00000 (138) 39.20000 (139) .000306 (140) 1.00000			
REFERENCE TEMP.	DENSITY	VISCOSITY	SURFACE TENSION
(141) 300.00000 (142) 1.450000 (143) .006400 (144) 26.00000			
BURNING RATE K	WNOO. INTERCEPT WNOO.	COEFFICIENT	WNOO. EXPONENT
(145) .027000 (146) 0.00000 (147) 0.00000 (148) 0.00000			

PRODUCT PROPERTIES
TABULAR PROPERTY DATA IS FOR FUEL FRACTIONS OF 0.0, 0.1, 0.2 - - - 1.0

EQUILIBRIUM GAS TEMPERATURE											
TEMP. 1	TEMP. 2	TEMP. 3	TEMP. 4	TEMP. 5	TEMP. 6	TEMP. 7	TEMP. 8	TEMP. 9	TEMP. 10	TEMP. 11	
(149) 300.00000 (150) 2103.00000 (151) 3084.00000 (152) 3397.00000											
(153) 3081.00000 (154) 2308.00000 (155) 1705.00000 (156) 1433.00000											
(157) 1344.00000 (158) 1266.00000 (159) 1190.00000 (160) 0.00000											
EQUILIBRIUM GAS MOL. WEIGHT											
MOL. WT. 1	MOL. WT. 2	MOL. WT. 3	MOL. WT. 4	MOL. WT. 5	MOL. WT. 6	MOL. WT. 7	MOL. WT. 8	MOL. WT. 9	MOL. WT. 10	MOL. WT. 11	
(161) 46.00000 (162) 28.79000 (163) 26.41000 (164) 23.30000											
(165) 19.00000 (166) 16.75000 (167) 16.41000 (168) 13.01000											
(169) 14.00000 (170) 14.10000 (171) 14.29000 (172) 0.00000											
EQUILIBRIUM GAS GAMMA											
GAMMA 1	GAMMA 2	GAMMA 3	GAMMA 4	GAMMA 5	GAMMA 6	GAMMA 7	GAMMA 8	GAMMA 9	GAMMA 10	GAMMA 11	
(173) 1.12000 (174) 1.25000 (175) 1.22000 (176) 1.21700											
(177) 1.23500 (178) 1.26000 (179) 1.30000 (180) 1.29000											
(181) 1.27000 (182) 1.24700 (183) 1.22800 (184) 0.00000											
THRUST COEFFICIENT TABLE											
EQUILIBRIUM THRUST COEFFICIENT											
CF VAC 1	CF VAC 2	CF VAC 3	CF VAC 4	CF VAC 5	CF VAC 6	CF VAC 7	CF VAC 8	CF VAC 9	CF VAC 10	CF VAC 11	EXP. AREA RATIO
(221) 1.92400 (222) 1.40200 (223) 1.90400 (224) 1.96170											
(225) 1.86700 (226) 1.81200 (227) 1.96000 (228) 1.93310											
(229) 1.92400 (230) 1.92400 (231) 1.89500 (232) 0.00000											

ADDUCT PROPERTIES

(185)	DENSITY	VAPOR CP.	LATENT HEAT	DECOMP. TEMP.
	1.000000 (186)	1.000000 (187)	100.000000 (188)	500.000000
	CONTAMINANT VISCOSITY			
(189)	VISCOSITY 1	VISCOSITY 2	VISCOSITY 3	VISCOSITY 4
	.000400 (190)	.020000 (191)	.003000 (192)	.000000
(193)	VISCOSITY 5	VISCOSITY 6	VISCOSITY 7	VISCOSITY 8
	.001000 (194)	1.000000 (195)	.002000 (196)	.000000
(197)	VISCOSITY 9	VISCOSITY 10	VISCOSITY 11	
	.000000 (198)	.020000 (199)	.010400 (200)	0.000000

FIRST PULS VALVE TIMING

FUEL VALVE OPEN	OXID VALVE OPEN	FUEL VALVE CLOSE	OXID VALVE CLOSE
(233) 0.000000	(234) 0.000000	(235) 0.017000	(236) 0.017000

SECOND PULS TIMING

FUEL VALVE OPEN	OXID VALVE OPEN	FUEL VALVE CLOSE	OXID VALVE CLOSE
(237) 0.000000	(238) 0.000000	(239) 0.000000	(240) 0.000000

THIRD PULS TIMING

FUEL VALVE OPEN	OXID VALVE OPEN	FUEL VALVE CLOSE	OXID VALVE CLOSE
(241) 0.000000	(242) 0.000000	(243) 0.000000	(244) 0.000000

FOURTH PULS TIMING

FUEL VALVE OPEN	OXID VALVE OPEN	FUEL VALVE CLOSE	OXID VALVE CLOSE
(245) 0.000000	(246) 0.000000	(247) 0.000000	(248) 0.000000

FIFTH PULS TIMING

FUEL VALVE OPEN	OXID VALVE OPEN	FUEL VALVE CLOSE	OXID VALVE CLOSE
(249) 0.000000	(250) 0.000000	(251) 0.000000	(252) 0.000000

SIXTH PULS TIMING

FUEL VALVE OPEN	OXID VALVE OPEN	FUEL VALVE CLOSE	OXID VALVE CLOSE
(253) 0.000000	(254) 0.000000	(255) 0.000000	(256) 0.000000

SEVENTH PULS TIMING

FUEL VALVE OPEN	OXID VALVE OPEN	FUEL VALVE CLOSE	OXID VALVE CLOSE
(257) 0.000000	(258) 0.000000	(259) 0.000000	(260) 0.000000

EIGHTH PULS TIMING

FUEL VALVE OPEN	OXID VALVE OPEN	FUEL VALVE CLOSE	OXID VALVE CLOSE
(261) 0.000000	(262) 0.000000	(263) 0.000000	(264) 0.000000

MULTI-RING INJECTOR

FIRST RING

FUEL HOLES

MOLE DIAMETER (49) .015000 (50)
 MOLE LENGTH (51) .062500 (52) 0.000000 (53) .045000
 RADIAL INJ. ANGLE (54) DISCHARGE COEFF. (55) 1.000000 (56) 0.000000
 NUMBER OF HOLES (57) 1.000000 (58) 0.000000
 TRANSVERSE ANGLE (59) 0.000000

OXIDIZER HOLES

MOLE DIAMETER (73) .010000 (74)
 MOLE LENGTH (75) .062500 (76) 0.000000 (77) -.045000
 RADIAL INJ. ANGLE (78) DISCHARGE COEFF. (79) 1.000000 (80) 0.000000
 NUMBER OF HOLES (81) 1.000000 (82) 0.000000
 TRANSVERSE ANGLE (83) 0.000000

SECOND RING

FUEL HOLES

MOLE DIAMETER (265) 0.000000 (266)
 MOLE LENGTH (267) 0.000000 (268) 0.000000 (269) 0.000000
 RADIAL INJ. ANGLE (270) DISCHARGE COEFF. (271) 0.000000 (272) 0.000000
 NUMBER OF HOLES (273) 0.000000 (274) 0.000000
 TRANSVERSE ANGLE (275) 0.000000

OXIDIZER HOLES

MOLE DIAMETER (275) 0.000000 (276)
 MOLE LENGTH (277) 0.000000 (278) 0.000000 (279) 0.000000
 RADIAL INJ. ANGLE (280) DISCHARGE COEFF. (281) 0.000000 (282) 0.000000
 NUMBER OF HOLES (283) 0.000000 (284) 0.000000
 TRANSVERSE ANGLE (285) 0.000000

THIRD RING

FUEL HOLES

MOLE DIAMETER (291) 0.000000 (292)
 MOLE LENGTH (293) 0.000000 (294) 0.000000 (295) 0.000000
 RADIAL INJ. ANGLE (296) DISCHARGE COEFF. (297) 0.000000 (298) 0.000000
 NUMBER OF HOLES (299) 0.000000 (300) 0.000000
 TRANSVERSE ANGLE (301) 0.000000

OXIDIZER HOLES

MOLE DIAMETER (299) 0.000000 (300)
 MOLE LENGTH (301) 0.000000 (302) 0.000000 (303) 0.000000
 RADIAL INJ. ANGLE (304) DISCHARGE COEFF. (305) 0.000000 (306) 0.000000
 NUMBER OF HOLES (307) 0.000000 (308) 0.000000
 TRANSVERSE ANGLE (309) 0.000000

COMBUSTION CHAMBER PROFILE

INJECTOR LOCATION	INJECTOR DIAMETER	AXIAL LOC. 2	CHAMBER DIAM. 2
(297)	0.00000 (298)	.417350 (299)	.250000 (300)
			.417350
AXIAL LOC. 3	CHAMBER DIAM. 3	AXIAL LOC. 4	CHAMBER DIAM. 4
(301)	.500000 (302)	.417350 (303)	.750000 (304)
			.417350
AXIAL LOC. 5	CHAMBER DIAM. 5	AXIAL LOC. 6	CHAMBER DIAM. 6
(305)	.958720 (306)	.417350 (307)	.973630 (308)
			.306070
AXIAL LOC. 7	CHAMBER DIAM. 7	THROAT PLANE	THROAT DIAM.
(309)	1.010360 (310)	.274610 (311)	1.070000 (312)
			.192790

INPUT UNITS ARE INCHES, PSIA, SECONDS AND DEGREES KELVIN.
PROPELLANT PROPERTIES ARE IN GRAMS/CC, POISE, DYNE/CM.

DERIVED FUEL PROPERTIES

REDUCED TEMP.	TEMPERATURE	LIO. ENTHALPY	VAP. ENTHALPY	VAPOR PRESSURE	LIO. DENSITY	VISCOSITY	SURFACE TENSION
.300000	170.200000	122.950000	145.000000	.000001	.994070	.200413	74.710000
.325000	193.050000	133.204500	359.704750	.000024	.980497	.127197	72.494632
.350000	207.900000	143.451000	374.500500	.000321	.966715	.083497	68.440005
.375000	222.750000	221.197500	389.336250	.002316	.952733	.050426	64.573200
.400000	237.600000	231.444000	404.112000	.011417	.938751	.039109	60.845205
.425000	252.450000	241.690500	418.847750	.046397	.924770	.027716	57.319396
.450000	267.300000	251.937000	433.663500	.144032	.910788	.020032	53.930744
.475000	282.150000	262.183500	448.439250	.405244	.896806	.014735	50.694609
.500000	297.000000	272.430000	463.215000	.970304	.882825	.011011	47.606346
.525000	311.850000	282.676500	477.990750	2.049199	.868843	.008366	44.661300
.550000	326.700000	292.923000	492.766500	4.119665	.854861	.006408	41.855208
.575000	341.550000	303.169500	507.542250	7.546474	.840879	.004970	39.103399
.600000	356.400000	313.416000	522.318000	12.990594	.826898	.003909	36.641594
.625000	371.250000	323.662500	537.093750	21.203941	.812916	.003433	34.225506
.650000	386.100000	333.909000	551.869500	33.664166	.798934	.003034	31.930919
.675000	400.950000	344.155500	566.645250	49.557001	.784953	.002694	29.753691
.700000	415.800000	354.402000	581.421000	71.756147	.770971	.002402	27.609749
.725000	430.650000	364.648500	596.196750	100.749887	.756989	.002151	25.735995
.750000	445.500000	374.895000	610.972500	137.866477	.743007	.001933	23.805800
.775000	460.350000	385.141500	625.748250	184.140620	.729026	.001743	22.138009
.800000	475.200000	395.388000	640.524000	240.836511	.715044	.001577	20.407937
.825000	490.050000	405.634500	655.299750	309.085094	.701062	.001432	18.443615
.850000	504.900000	415.881000	670.075500	390.008007	.687021	.001303	16.150055
.875000	519.750000	426.127500	684.851250	484.656476	.672935	.001189	13.277417
.900000	534.600000	436.374000	699.627000	594.004405	.658888	.001086	10.011953
.925000	549.450000	446.620500	714.402750	718.959165	.644826	.000998	6.619689
.950000	564.300000	456.867000	729.178500	860.315075	.630731	.000910	3.463114
.975000	579.150000	467.113500	743.954250	1018.704321	.470147	.000846	1.029307
1.000000	594.000000	477.360000	758.730000	1195.000000	.292011	.000390	.000000

DERIVED OXID PROPERTIES

REDUCED TEMP.	TEMPERATURE	LITQ. ENTHALPY	VAP. ENTHALPY	VAPOR PRESSURE	LIO. DENSITY	VISCOSITY	SURFACE TENSION
.30000	120.30000	46.548000	194.959400	.00000	1.865399	.365550	76.696121
.32500	140.07500	50.427000	198.170350	.00000	1.839178	.232006	72.873874
.35000	150.85000	54.306000	201.381300	.00000	1.812957	.152296	68.428405
.37500	161.62500	58.185000	204.592250	.00012	1.786736	.102920	64.554710
.40000	172.40000	62.064000	207.803200	.00103	1.760515	.071334	60.847856
.42500	183.17500	65.943000	211.014150	.00651	1.734294	.050553	57.302983
.45000	193.95000	69.822000	214.225100	.03206	1.708073	.036538	53.915301
.47500	204.72500	73.701000	217.436050	.01282	1.681852	.026877	50.608093
.50000	215.50000	77.580000	220.647000	.043714	1.655631	.020084	47.592715
.52500	226.27500	81.459000	223.857950	.129195	1.629410	.015223	44.648592
.55000	237.05000	85.338000	227.068900	.339885	1.603189	.011688	41.843223
.57500	247.82500	89.217000	230.279850	.809956	1.576968	.009080	39.172179
.60000	258.60000	93.096000	233.490800	1.774303	1.550747	.007130	36.631102
.62500	269.37500	96.975000	236.701750	3.614636	1.524526	.006261	34.215705
.65000	280.15000	100.854000	239.912700	6.914437	1.498305	.005533	31.921776
.67500	290.92500	104.733000	243.123650	12.519207	1.472084	.004913	29.745171
.70000	301.70000	108.612000	246.334600	21.599537	1.445863	.004381	27.681820
.72500	312.47500	112.491000	249.545550	35.711341	1.419642	.003923	25.727726
.75000	323.25000	116.370000	252.756500	56.852764	1.393421	.003525	23.878960
.77500	334.02500	119.249000	255.967450	87.511463	1.367200	.003180	22.131669
.80000	344.80000	123.128000	259.178400	130.701590	1.340979	.002877	20.482070
.82500	355.57500	127.007000	262.389350	189.982723	1.308419	.002611	18.938334
.85000	366.35000	130.886000	265.600300	269.498397	1.271923	.002377	16.145430
.87500	377.12500	134.765000	268.811250	373.918685	1.226564	.002169	13.273615
.90000	387.90000	138.644000	272.022200	508.479468	1.170403	.001985	10.009086
.92500	398.67500	142.523000	275.233150	678.929785	1.100147	.001821	6.617793
.95000	409.45000	146.402000	278.444100	891.495836	1.009387	.001674	3.462122
.97500	420.22500	150.281000	281.655050	1152.836831	.881741	.001543	1.029092
1.00000	431.00000	154.160000	284.866000	1470.000000	.549131	.000712	.000800

DERIVED FEED SYSTEM VALUES - INJECTION, RESTRICTOR, AND PORT AREAS REFER TO VENA CONTRACTA

FUEL SIDE VALUES

LINE AREA	INJECTION AREA	RESTRICTOR AREA	VENTURI AREA	VALVE PORT AREA	LINE RESISTANCE	INJ. RESISTANCE	LENGTH/AREA
2.810005E-02	1.960688E-04	2.197748E-04	2.810005E-02	2.810000E-02	498948	824932	17400.6

OXID SIDE VALUES

LINE AREA	INJECTION AREA	RESTRICTOR AREA	VENTURI AREA	VALVE PORT AREA	LINE RESISTANCE	INJ. RESISTANCE	LENGTH/AREA
2.810005E-02	2.717163E-04	3.462614E-04	2.810005E-02	2.810000E-02	201928	325379	17311.8

RING 1

FUEL INJ. AREA	PERCENT FUEL	OXID INJ. AREA	PERCENT OXID	AXIAL IMP. PT.	RADIAL IMP. PT.
1.960688E-04	100.0000	2.717163E-04	100.0000	4.500000E-02	1.748379E-16

STATION	DISTANCE	DIAMETER	AREA	UPSTREAM VOLUME	FUEL ON WALL	OXID ON WALL	WALL TEMPERATURE
1	0.00000000	0.173500	0.1860145	0.00000000	0.00000000	0.00000000	294.00000000
2	0.01700000	0.173500	0.1860145	0.0148378	0.00000000	0.00000000	294.00000000
3	0.02140000	0.173500	0.1860145	0.0292755	0.00000000	0.00000000	294.00000000
4	0.02100000	0.173500	0.1860145	0.04330133	0.00000000	0.00000000	294.00000000
5	0.02600000	0.173500	0.1860145	0.0585510	0.00000000	0.00000000	294.00000000
6	0.03500000	0.173500	0.1860145	0.0731464	0.00000000	0.00000000	294.00000000
7	0.04200000	0.173500	0.1860145	0.0876265	0.00000000	0.00000000	294.00000000
8	0.04900000	0.173500	0.1860145	0.1024643	0.00000000	0.00000000	294.00000000
9	0.05600000	0.173500	0.1860145	0.1171020	0.00000000	0.00000000	294.00000000
10	0.06300000	0.173500	0.1860145	0.1317394	0.00000000	0.00000000	294.00000000
11	0.07000000	0.173500	0.1860145	0.1463775	0.00000000	0.00000000	294.00000000
12	0.07700000	0.173500	0.1860145	0.1610153	0.00000000	0.00000000	294.00000000
13	0.08400000	0.173500	0.1860145	0.1756531	0.00000000	0.00000000	294.00000000
14	0.09100000	0.173500	0.1860145	0.1902904	0.00000000	0.00000000	294.00000000
15	0.09800000	0.173500	0.1860145	0.2049286	0.00000000	0.00000000	294.00000000
16	0.10500000	0.173500	0.1860145	0.2195663	0.00000000	0.00000000	294.00000000
17	0.11200000	0.173500	0.1860145	0.2342041	0.00000000	0.00000000	294.00000000
18	0.11900000	0.173500	0.1860145	0.2488418	0.00000000	0.00000000	294.00000000
19	0.12600000	0.173500	0.1860145	0.2634796	0.00000000	0.00000000	294.00000000
20	0.13300000	0.173500	0.1860145	0.2781173	0.00000000	0.00000000	294.00000000
21	0.14000000	0.173500	0.1860145	0.2927551	0.00000000	0.00000000	294.00000000
22	0.14700000	0.173500	0.1860145	0.3073924	0.00000000	0.00000000	294.00000000
23	0.15400000	0.173500	0.1860145	0.3220306	0.00000000	0.00000000	294.00000000
24	0.16100000	0.173500	0.1860145	0.3366684	0.00000000	0.00000000	294.00000000
25	0.16800000	0.173500	0.1860145	0.3513061	0.00000000	0.00000000	294.00000000
26	0.17500000	0.173500	0.1860145	0.3659439	0.00000000	0.00000000	294.00000000
27	0.18200000	0.173500	0.1860145	0.3805816	0.00000000	0.00000000	294.00000000
28	0.18900000	0.173500	0.1860145	0.3952194	0.00000000	0.00000000	294.00000000
29	0.19600000	0.173500	0.1860145	0.4098571	0.00000000	0.00000000	294.00000000
30	0.20300000	0.173500	0.1860145	0.4244949	0.00000000	0.00000000	294.00000000
31	0.21000000	0.173500	0.1860145	0.4391326	0.00000000	0.00000000	294.00000000
32	0.21700000	0.173500	0.1860145	0.4537704	0.00000000	0.00000000	294.00000000
33	0.22400000	0.173500	0.1860145	0.4684081	0.00000000	0.00000000	294.00000000
34	0.23100000	0.173500	0.1860145	0.4830459	0.00000000	0.00000000	294.00000000
35	0.23800000	0.173500	0.1860145	0.4976837	0.00000000	0.00000000	294.00000000
36	0.24500000	0.173500	0.1860145	0.5123214	0.00000000	0.00000000	294.00000000
37	0.25200000	0.173500	0.1860145	0.5269592	0.00000000	0.00000000	294.00000000
38	0.25900000	0.173500	0.1860145	0.5415969	0.00000000	0.00000000	294.00000000
39	0.26600000	0.173500	0.1860145	0.5562347	0.00000000	0.00000000	294.00000000
40	0.27300000	0.173500	0.1860145	0.5708724	0.00000000	0.00000000	294.00000000
41	0.28000000	0.173500	0.1860145	0.5855102	0.00000000	0.00000000	294.00000000
42	0.28700000	0.173500	0.1860145	0.6001479	0.00000000	0.00000000	294.00000000
43	0.29400000	0.173500	0.1860145	0.6147857	0.00000000	0.00000000	294.00000000
44	0.30100000	0.173500	0.1860145	0.6294234	0.00000000	0.00000000	294.00000000
45	0.30800000	0.173500	0.1860145	0.6440612	0.00000000	0.00000000	294.00000000
46	0.31500000	0.173500	0.1860145	0.6586990	0.00000000	0.00000000	294.00000000
47	0.32200000	0.173500	0.1860145	0.6733367	0.00000000	0.00000000	294.00000000
48	0.32900000	0.173500	0.1860145	0.6879745	0.00000000	0.00000000	294.00000000
49	0.33600000	0.173500	0.1860145	0.7026122	0.00000000	0.00000000	294.00000000
50	0.34300000	0.173500	0.1860145	0.7172500	0.00000000	0.00000000	294.00000000
51	0.35000000	0.173500	0.1860145	0.7318877	0.00000000	0.00000000	294.00000000
52	0.35700000	0.173500	0.1860145	0.7465255	0.00000000	0.00000000	294.00000000
53	0.36400000	0.173500	0.1860145	0.7611632	0.00000000	0.00000000	294.00000000
54	0.37100000	0.173500	0.1860145	0.7758010	0.00000000	0.00000000	294.00000000
55	0.37800000	0.173500	0.1860145	0.7904387	0.00000000	0.00000000	294.00000000
56	0.38500000	0.173500	0.1860145	0.8050765	0.00000000	0.00000000	294.00000000
57	0.39200000	0.173500	0.1860145	0.8197143	0.00000000	0.00000000	294.00000000
58	0.39900000	0.173500	0.1860145	0.8343520	0.00000000	0.00000000	294.00000000
59	0.40600000	0.173500	0.1860145	0.8489898	0.00000000	0.00000000	294.00000000
60	0.41300000	0.173500	0.1860145	0.8636275	0.00000000	0.00000000	294.00000000
61	0.42000000	0.173500	0.1860145	0.8782653	0.00000000	0.00000000	294.00000000

62	05270000	41735000	1360145	00929030	00000000	00000000	2040000000
63	06330000	41735000	1360145	00907500	00000000	00000000	2040000000
64	07410000	41735000	1360145	00921705	00000000	00000000	2040000000
65	08500000	41735000	1360145	009300163	00000000	00000000	2040000000
66	09550000	41735000	1360145	009514540	00000000	00000000	2040000000
67	10600000	41735000	1360145	009600210	00000000	00000000	2040000000
68	11690000	41735000	1360145	00907296	00000000	00000000	2040000000
69	12760000	41735000	1360145	00953673	00000000	00000000	2040000000
70	13800000	41735000	1360145	10100051	00000000	00000000	2040000000
71	14900000	41735000	1360145	10246420	00000000	00000000	2040000000
72	15970000	41735000	1360145	10324006	00000000	00000000	2040000000
73	17040000	41735000	1360145	10539103	00000000	00000000	2040000000
74	18110000	41735000	1360145	10445561	00000000	00000000	2040000000
75	19180000	41735000	1360145	10431934	00000000	00000000	2040000000
76	20250000	41735000	1360145	10478314	00000000	00000000	2040000000
77	21320000	41735000	1360145	11272467	00000000	00000000	2040000000
78	22390000	41735000	1360145	11271071	00000000	00000000	2040000000
79	23460000	41735000	1360145	11417449	00000000	00000000	2040000000
80	24530000	41735000	1360145	11563326	00000000	00000000	2040000000
81	25600000	41735000	1360145	11710204	00000000	00000000	2040000000
82	26670000	41735000	1360145	11856681	00000000	00000000	2040000000
83	27740000	41735000	1360145	12002459	00000000	00000000	2040000000
84	28810000	41735000	1360145	12149336	00000000	00000000	2040000000
85	29880000	41735000	1360145	12295714	00000000	00000000	2040000000
86	30950000	41735000	1360145	12442091	00000000	00000000	2040000000
87	32020000	41735000	1360145	12588469	00000000	00000000	2040000000
88	33090000	41735000	1360145	12734847	00000000	00000000	2040000000
89	34160000	41735000	1360145	12881224	00000000	00000000	2040000000
90	35230000	41735000	1360145	13027602	00000000	00000000	2040000000
91	36300000	41735000	1360145	13173980	00000000	00000000	2040000000
92	37370000	41735000	1360145	13320357	00000000	00000000	2040000000
93	38440000	41735000	1360145	13466735	00000000	00000000	2040000000
94	39510000	41735000	1360145	13613112	00000000	00000000	2040000000
95	40580000	41735000	1360145	13759490	00000000	00000000	2040000000
96	41650000	41735000	1360145	13905868	00000000	00000000	2040000000
97	42720000	41735000	1360145	14052246	00000000	00000000	2040000000
98	43790000	41735000	1360145	14198624	00000000	00000000	2040000000
99	44860000	41735000	1360145	14345002	00000000	00000000	2040000000
100	45930000	41735000	1360145	14491380	00000000	00000000	2040000000
101	47000000	41735000	1360145	14637758	00000000	00000000	2040000000

THE CALCULATED RUN PARAMETERS ARE PRINTED FOR EACH INTERVAL OF TIME FOLLOWING START

TIME MILLISEC	CHAMBER PRESS	IGNITION	FUEL FRACTION	CHAMBER TEMP K	MOL WT.	GAMMA	CP VAC
0.	1.000000E-06	0.	0.	294.000	46.0000	1.16004	2.00230
FUEL INJ RATE	0.	FUEL FLOW RATE	0.	FUEL VOID VOL	5.80000E-04	0.	OXID INJ TEMP
0.	0.	0.	0.	1.13000E-03	0.	0.	0.
FUEL DROP BURN	0.	FUEL FLAME RATE	0.	FUEL WALL BURN	0.	0.	OXID WALL EVAP
0.	0.	0.	0.	0.	0.	0.	0.
FUEL GAS MASS	0.	FUEL DROPLETS	0.	FUEL STREAMS	0.	0.	OXID ON WALL
0.	6.417895E-13	0.	0.	0.	0.	0.	0.
FUEL GAS EFFLUX	0.	FUEL DROP RATE	0.	FUEL FILM RATE	0.	1.00000	VAC THRUST LBP
0.	0.	0.	0.	0.	0.	0.	0.
FUEL DROP D32	0.	FUEL INJ. VEL.	0.	MAX. EXPLOSION	0.	0.	TOTAL IMPULS
0.	0.	0.	0.	0.	0.	0.	0.
INJECTED MASS	0.	GAS EXPELLED	0.	DROPS EXPELLED	0.	0.	WALL RETAINED
0.	0.0000000	0.0000000	0.0000000	0.0000000	0.0000000	0.0000000	0.0000000
OXID GRAMS	0.	0.0000000	0.0000000	0.0000000	0.0000000	0.0000000	0.0000000
TOTAL GRAMS	0.	0.0000000	0.0000000	0.0000000	0.0000000	0.0000000	0.0000000
FUEL DROPS INJECTED	0.	SUM N	0.	SUM D CUBED	0.	0.	TOTAL MOMENTUM
0.	0.	0.	0.	0.	0.	0.	0.
OXID DROPS INJECTED	0.	0.	0.	0.	0.	0.	0.
0.	0.	0.	0.	0.	0.	0.	0.

TIME MILLISEC	CHAMBER PRESS	IGNITION	FUEL FRACTION	CHAMBER TEMP K	MOL WT.	GAMMA	CP VAC
1.000000E-01	1.000000E-06	0.	0.	294.000	46.0000	1.16004	1.91020
FUEL INJ RATE	0.	FUEL FLOW RATE	0.	FUEL VOID VOL	5.793580E-04	0.	OXID INJ TEMP
0.	0.	4.049835E-04	3.397197E-04	1.128734E-03	0.	0.	294.000
FUEL DROP BURN	0.	FUEL FLAME RATE	0.	FUEL WALL BURN	0.	0.	OXID WALL EVAP
0.	0.	0.	0.	0.	0.	0.	0.
FUEL GAS MASS	0.	FUEL DROPLETS	0.	FUEL STREAMS	0.	0.	OXID ON WALL
0.	6.417895E-13	0.	0.	0.	0.	0.	0.
FUEL GAS EFFLUX	0.	FUEL DROP RATE	0.	FUEL FILM RATE	0.	1.00000	VAC THRUST LBP
0.	0.	0.	0.	0.	0.	0.	0.
FUEL DROP D32	0.	FUEL INJ. VEL.	0.	MAX. EXPLOSION	0.	0.	TOTAL IMPULS
0.	0.	0.	0.	1.020400E-06	7.447032E-08	1.000000E-10	0.

PAGES LIMITED

PAGES OMITTED

OXID MANIPOLD PILL0 AT 4.30 MILLISECONDS

TIME MILLISEC	CHAMBER PRESS	IGNITION	FUEL FRACTION	CHAMBER TEMP K	MOL WT.	GAMMA	CP VAC
4.30000	1.213017E-02	0.	0.	151.275	40.0000	1.10000	1.01020
FUEL INJ RATE	OXID INJ RATE	FUEL FLOW RATE	OXID FLOW RATE	FUEL VOID VOL	OXID VOID VOL	FUEL INJ TEMP	OXID INJ TEMP
0.	2.457067E-04	1.221300E-02	1.337023E-02	1.300507E-04	0.	200.000	200.000
FUEL DROP BURN	OXID DROP BURN	FUEL FLAME RATE	OXID FLAME RATE	FUEL WALL BURN	OXID WALL BURN	FUEL WALL EVAP	OXID WALL EVAP
0.	0.	0.	0.	0.	0.	0.	0.
FUEL GAS MASS	OXID GAS MASS	FUEL DROPLETS	OXID DROPLETS	FUEL STREAMS	OXID STREAMS	FUEL ON WALL	OXID ON WALL
0.	1.510001E-06	0.	0.	0.	0.	0.	0.
FUEL GAS EFFLUX	OXID GAS EFFLUX	FUEL DROP RATE	OXID DROP RATE	FUEL FILM RATE	OXID FILM RATE	GAS FRACTION	VAC THRUST LBP
0.	0.	0.	0.	0.	0.	1.00000	0.
FUEL DROP D32	OXID DROP D32	FUEL INJ. VEL.	OXID INJ. VEL.	MAX. EXPLOSION	MASS OUT OF TANK	INTEGRAL PCODY	TOTAL IMPULS0
0.	34.4300	0.	1.42052	3.907651E-02	6.203000E-05	1.210017E-06	0.
TIME MILLISEC	CHAMBER PRESS	IGNITION	FUEL FRACTION	CHAMBER TEMP K	MOL WT.	GAMMA	CP VAC
4.40000	.739785	0.	0.	203.334	40.0000	1.10000	1.01020
FUEL INJ RATE	OXID INJ RATE	FUEL FLOW RATE	OXID FLOW RATE	FUEL VOID VOL	OXID VOID VOL	FUEL INJ TEMP	OXID INJ TEMP
0.	1.352402E-02	1.233400E-02	1.352402E-02	9.99030E-05	0.	200.000	200.000
FUEL DROP BURN	OXID DROP BURN	FUEL FLAME RATE	OXID FLAME RATE	FUEL WALL BURN	OXID WALL BURN	FUEL WALL EVAP	OXID WALL EVAP
0.	0.	0.	0.	0.	0.	0.	0.
FUEL GAS MASS	OXID GAS MASS	FUEL DROPLETS	OXID DROPLETS	FUEL STREAMS	OXID STREAMS	FUEL ON WALL	OXID ON WALL
0.	6.664919E-07	0.	0.	0.	0.	0.	0.
FUEL GAS EFFLUX	OXID GAS EFFLUX	FUEL DROP RATE	OXID DROP RATE	FUEL FILM RATE	OXID FILM RATE	GAS FRACTION	VAC THRUST LBP
0.	1.370499E-05	0.	0.	0.	0.	1.00000	0.
FUEL DROP D32	OXID DROP D32	FUEL INJ. VEL.	OXID INJ. VEL.	MAX. EXPLOSION	MASS OUT OF TANK	INTEGRAL PCODY	TOTAL IMPULS0
0.	34.4300	0.	70.3004	2.10713	6.502553E-05	7.510000E-05	0.
TIME MILLISEC	CHAMBER PRESS	IGNITION	FUEL FRACTION	CHAMBER TEMP K	MOL WT.	GAMMA	CP VAC
4.50000	1.30110	0.	0.	226.000	40.0000	1.10000	1.01020
FUEL INJ RATE	OXID INJ RATE	FUEL FLOW RATE	OXID FLOW RATE	FUEL VOID VOL	OXID VOID VOL	FUEL INJ TEMP	OXID INJ TEMP
0.	1.367123E-02	1.245001E-02	1.367123E-02	0.000770E-05	0.	200.000	200.000
FUEL DROP BURN	OXID DROP BURN	FUEL FLAME RATE	OXID FLAME RATE	FUEL WALL BURN	OXID WALL BURN	FUEL WALL EVAP	OXID WALL EVAP
0.	0.	0.	0.	0.	0.	0.	0.
FUEL GAS MASS	OXID GAS MASS	FUEL DROPLETS	OXID DROPLETS	FUEL STREAMS	OXID STREAMS	FUEL ON WALL	OXID ON WALL
0.	1.150007E-06	0.	0.	0.	0.	0.	0.
FUEL GAS EFFLUX	OXID GAS EFFLUX	FUEL DROP RATE	OXID DROP RATE	FUEL FILM RATE	OXID FILM RATE	GAS FRACTION	VAC THRUST LBP
0.	7.240651E-04	0.	0.	0.	0.	1.00000	0.
FUEL DROP D32	OXID DROP D32	FUEL INJ. VEL.	OXID INJ. VEL.	MAX. EXPLOSION	MASS OUT OF TANK	INTEGRAL PCODY	TOTAL IMPULS0
0.	34.4300	0.	70.2416	8.24556	6.763772E-05	2.133130E-04	0.
							1.212050E-05

TIME MILLISEC 4.00000 CHAMBER PRESS 1.04017 IGNITION 0.0 FUEL FRACTION 0.0 CHAMBER TEMP K 235.722 MOL WT. 46.0000 GAMMA 1.10000 CP VAC 1.01020

FUEL INJ RATE 0.0 OXID INJ RATE 1.30122E-02 FUEL FLOW RATE 0.0 FUEL VOID VOL 0.0 FUEL INJ TEMP 290.000 OXID INJ TEMP 290.000

FUEL DROP BURN 0.0 OXID DROP BURN 0.0 FUEL FLASH RATE 0.0 FUEL WALL BURN 0.0 FUEL WALL EVAP 0.0 OXID WALL EVAP 0.0

FUEL GAS MASS 0.0 OXID GAS MASS 1.553034E-06 FUEL DROPLETS 0.0 OXID DROPLETS 2.360797E-06 FUEL ON WALL 0.0 OXID ON WALL 0.0

FUEL GAS EFFLUX 0.0 OXID GAS EFFLUX 1.280001E-03 FUEL DROP RATE 0.0 OXID DROP RATE 0.0 FUEL FILM RATE 0.0 OXID FILM RATE 0.0 GAS FRACTION 1.00000 VAC THRUST LOP .110012

FUEL DROP D32 0.0 OXID DROP D32 36.4300 FUEL INJ. VEL. 0.0 OXID INJ. VEL. 80.0500 MAX. EXPLOSION 7.027402E-05 MASS OUT OF TANK INTEGRAL PCODY TOTAL IMPULSE 2.331575E-05

FUEL MANIFOLD FILLS AT 4.70 MILLISECONDS

TIME MILLISEC 4.70000 CHAMBER PRESS 2.45292 IGNITION 0.0 FUEL FRACTION 0.0 CHAMBER TEMP K 242.950 MOL WT. 46.0000 GAMMA 1.10000 CP VAC 1.01020

FUEL INJ RATE 5.700540E-03 OXID INJ RATE 1.394732E-02 FUEL FLOW RATE 0.0 FUEL VOID VOL 0.0 FUEL INJ TEMP 290.000 OXID INJ TEMP 290.000

FUEL DROP BURN 0.0 OXID DROP BURN 0.0 FUEL FLASH RATE 0.0 FUEL WALL BURN 0.0 FUEL WALL EVAP 0.0 OXID WALL EVAP 0.0

FUEL GAS MASS 0.0 OXID GAS MASS 1.905043E-06 FUEL DROPLETS 0.0 OXID DROPLETS 3.116913E-06 FUEL ON WALL 0.0 OXID ON WALL 0.0

FUEL GAS EFFLUX 0.0 OXID GAS EFFLUX 1.765134E-03 FUEL DROP RATE 0.0 OXID DROP RATE 0.0 FUEL FILM RATE 0.0 OXID FILM RATE 0.0 GAS FRACTION 1.00000 VAC THRUST LOP .140223

FUEL DROP D32 0.0 OXID DROP D32 36.4300 FUEL INJ. VEL. 75.0200 OXID INJ. VEL. 80.0419 MAX. EXPLOSION 7.203501E-05 MASS OUT OF TANK INTEGRAL PCODY TOTAL IMPULSE 3.723002E-05

TIME MILLISEC 4.80000 CHAMBER PRESS 2.24926 IGNITION 0.0 FUEL FRACTION 0.0 CHAMBER TEMP K 246.161 MOL WT. 46.0000 GAMMA 1.10000 CP VAC 1.01020

FUEL INJ RATE 1.238290E-02 OXID INJ RATE 1.407670E-02 FUEL FLOW RATE 0.0 FUEL VOID VOL 0.0 FUEL INJ TEMP 290.000 OXID INJ TEMP 290.000

FUEL DROP BURN 0.0 OXID DROP BURN 0.0 FUEL FLASH RATE 0.0 FUEL WALL BURN 0.0 FUEL WALL EVAP 0.0 OXID WALL EVAP 0.0

FUEL GAS MASS 0.0 OXID GAS MASS 1.730209E-06 FUEL DROPLETS 0.0 OXID DROPLETS 2.016523E-06 FUEL ON WALL 0.0 OXID ON WALL 0.0

FUEL GAS EFFLUX 0.0 OXID GAS EFFLUX 2.190100E-03 FUEL DROP RATE 0.0 OXID DROP RATE 0.0 FUEL FILM RATE 0.0 OXID FILM RATE 0.0 GAS FRACTION 1.00000 VAC THRUST LOP .120001

FUEL DROP D32 0.0 OXID DROP D32 36.4300 FUEL INJ. VEL. 104.800 OXID INJ. VEL. 81.5423 MAX. EXPLOSION 7.350107E-05 MASS OUT OF TANK INTEGRAL PCODY TOTAL IMPULSE 5.000070E-05

TIME MILLISEC 4.90000 CHAMBER PRESS 2.10405 IGNITION 0.0 FUEL FRACTION 0.0 CHAMBER TEMP K 245.350 MOL WT. 46.0000 GAMMA 1.10000 CP VAC 1.01020

FUEL DROP D32 OXID DROP D32 OXID DROP D32 FUEL INJ. VEL. OXID INJ. VEL. MAX. EXPLOSION MASS OUT OF TANK INTEGRAL PCODT TOTAL IMPULSE
66.2836 32.6442 122.790 152.876 82.9406 503.949 8.341361E-05 2.145800E-02 1.839378E-03

TIME MILLISEC CHAMBER PRESS IGNITION FUEL FRACTION CHAMBER TEMP K MOL WT. GAMMA CP VAC
5.20000 122.790 1.00000 .290445 3167.72 23.6725 1.21728 1.95649
FUEL INJ RATE OXID INJ RATE FUEL FLOW RATE OXID FLOW RATE FUEL VOID VOL OXID VOID VOL FUEL INJ TEMP OXID INJ TEMP
1.110391E-02 1.411608E-02 1.110391E-02 1.411608E-02 0. 0. 296.800 296.800
FUEL DROP BURN OXID DROP BURN FUEL FLASH RATE OXID FLASH RATE FUEL WALL BURN OXID WALL BURN FUEL WALL EVAP OXID WALL EVAP
6.360410E-03 1.362439E-02 0. 0. 2.287712E-05 1.229790E-03 0. 0.
FUEL GAS MASS OXID GAS MASS FUEL DROPLETS OXID DROPLETS FUEL STREAMS OXID STREAMS FUEL ON WALL OXID ON WALL
1.020027E-06 2.510905E-06 4.121009E-06 3.773743E-06 0. 0. 2.487685E-07 1.049131E-06
FUEL GAS EFFLUX OXID GAS EFFLUX FUEL DROP RATE OXID DROP RATE FUEL FILM RATE OXID FILM RATE GAS FRACTION VAC THRUST LBP
5.367169E-03 1.444006E-02 0. 0. 8.440913E-04 0. .958024 7.10033
FUEL DROP D32 OXID DROP D32 FUEL INJ. VEL. OXID INJ. VEL. MAX. EXPLOSION MASS OUT OF TANK INTEGRAL PCODT TOTAL IMPULSE
67.7231 37.5291 147.500 81.8247 524.787 8.593500E-05 3.373795E-02 1.956485E-03

TIME MILLISEC CHAMBER PRESS IGNITION FUEL FRACTION CHAMBER TEMP K MOL WT. GAMMA CP VAC
5.20000 122.234 1.00000 .383619 3251.11 21.8660 1.22482 1.91100
FUEL INJ RATE OXID INJ RATE FUEL FLOW RATE OXID FLOW RATE FUEL VOID VOL OXID VOID VOL FUEL INJ TEMP OXID INJ TEMP
1.071286E-02 1.397226E-02 1.071286E-02 1.397226E-02 0. 0. 298.800 298.800
FUEL DROP BURN OXID DROP BURN FUEL FLASH RATE OXID FLASH RATE FUEL WALL BURN OXID WALL BURN FUEL WALL EVAP OXID WALL EVAP
7.310101E-03 1.063979E-02 0. 0. 3.154902E-05 1.648515E-03 0. 0.
FUEL GAS MASS OXID GAS MASS FUEL DROPLETS OXID DROPLETS FUEL STREAMS OXID STREAMS FUEL ON WALL OXID ON WALL
1.137867E-06 2.213720E-06 4.422606E-06 4.112740E-06 0. 0. 2.456338E-07 8.64766E-07
FUEL GAS EFFLUX OXID GAS EFFLUX FUEL DROP RATE OXID DROP RATE FUEL FILM RATE OXID FILM RATE GAS FRACTION VAC THRUST LBP
6.251291E-03 1.525698E-02 0. 0. 8.552996E-04 0. .968184 6.96645
FUEL DROP D32 OXID DROP D32 FUEL INJ. VEL. OXID INJ. VEL. MAX. EXPLOSION MASS OUT OF TANK INTEGRAL PCODT TOTAL IMPULSE
59.6643 42.7250 142.305 80.9865 540.494 8.640421E-05 4.596131E-02 2.651056E-03

TIME MILLISEC CHAMBER PRESS IGNITION FUEL FRACTION CHAMBER TEMP K MOL WT. GAMMA CP VAC
5.40000 125.661 1.00000 .363360 3180.79 21.1314 1.22858 1.88709
FUEL INJ RATE OXID INJ RATE FUEL FLOW RATE OXID FLOW RATE FUEL VOID VOL OXID VOID VOL FUEL INJ TEMP OXID INJ TEMP
1.035890E-02 1.363376E-02 1.035890E-02 1.363376E-02 0. 0. 296.800 296.800
FUEL DROP BURN OXID DROP BURN FUEL FLASH RATE OXID FLASH RATE FUEL WALL BURN OXID WALL BURN FUEL WALL EVAP OXID WALL EVAP
8.076173E-03 1.167602E-02 0. 0. 3.364882E-05 1.732222E-03 0. 0.
FUEL GAS MASS OXID GAS MASS FUEL DROPLETS OXID DROPLETS FUEL STREAMS OXID STREAMS FUEL ON WALL OXID ON WALL
1.267420E-06 2.176294E-06 4.633074E-06 4.340170E-06 0. 0. 2.422687E-07 7.076582E-07
FUEL GAS EFFLUX OXID GAS EFFLUX FUEL DROP RATE OXID DROP RATE FUEL FILM RATE OXID FILM RATE GAS FRACTION VAC THRUST LBP
7.208210E-03 1.378135E-02 9.515945E-05 4.972621E-04 0. 0. .970086 7.07616
FUEL DROP D32 OXID DROP D32 FUEL INJ. VEL. OXID INJ. VEL. MAX. EXPLOSION MASS OUT OF TANK INTEGRAL PCODT TOTAL IMPULSE
70.7768 45.2205 137.603 80.1636 546.911 9.082347E-05 5.852377E-02 3.350667E-03

PAGES OMITTED

PURL DROPS INJECTED	SUM N	SUM D	SUM D SQUARED	SUM D CUBED	TOTAL MOMENTUM
PURL DROPS EJECTED	4.951507E+04	6.710205E+03	2.072468E+01	9.485478E-02	9.790777E+01
OX10 DROPS INJECTED	1.407980E+05	5.922022E+02	3.252472E+00	2.334030E-02	1.327219E+02
OX10 DROPS EJECTED	1.210857E+07	1.450780E+01	1.593872E+01	1.138897E-01	1.280880E+02
	2.895551E+05	8.761333E+02	3.463457E+00	2.326202E-02	9.660762E+01

PERFORMANCE SUMMARY

PROPELLANT MASS BASIS	FUEL FLOW	OXID FLOW	MIXTURE RATIO	C STAR	VACUUM IOP
MASS OUT OF TANK - POUNDS	.000135	.000198	1.467980	3603.320247	215.821006
MASS THROUGH INJECTOR - POUNDS	.000099	.000198	2.003970	4041.357435	242.057205
MASS THROUGH NOZZLE - POUNDS	.000099	.000189	1.905046	4176.976893	256.299926
PRESSURE INTEGRAL - PSIA*SEC.	1.2538				
TOTAL VAC IMPULSE - POUND*SEC.	.0720				

DISPOSITION OF INJECTED PROPELLANT

	FUEL	OXID	TOTAL
FRACTION EXPELLED AS BURNT GAS	.733768	.767953	.716546
FRACTION EXPELLED AS UNBURNT VAPOR	.000000	.000695	.045027
FRACTION EXPELLED AS DROPS	.261026	.172629	.202255
FRACTION EXPELLED AS FILM	.004666	.001359	.002460
FRACTION RETAINED AS GAS+VAPOR	.000000	.003289	.002194
FRACTION RETAINED AS DROPS	0.000000	.000214	.000143
FRACTION RETAINED AS FILM	0.000000	.005062	.030595
TOTAL OF ABOVE VALUES	1.000000	1.000000	1.000000

TOTALS GREATER THAN 1.0 MAY INDICATE --

IGNITER FLOWS - NOT CLASSIFIED AS THROUGH-INJECTOR OR OUT-OF-TANK.

DEPLETION OF CHAMBER GAS MASS - THERE MAY BE AN APPRECIABLE MASS OF COLD VAPOR IN CHAMBER BEFORE START.

DEPLETION OF WALL-FILM, WHEN A FIRING IS STARTED WITH PROPELLANT-COATED WALLS.

MEAN DROP DIAMETER	INJECTED FUEL	EJECTED FUEL	INJECTED OXID	EJECTED OXID
D30 MICRONS	26.9441	56.4597	21.0576	41.2002
D51 MICRONS	33.3454	65.4097	26.2572	40.0354
D32 MICRONS	46.7350	77.9110	36.7903	58.1604
MEAN AXIAL VELOCITY FT/SEC	71.52	370.56	45.55	200.32
MEAN RADIAL VELOCITY FT/SEC		34.98		32.22

NOTE - THE ABOVE EJECTED DROPLET AND EJECTED FILM VALUES ARE AT THE THROAT PLANE, NOT THE EXIT PLANE.

DROP DIAMETER		INJECTED FUEL EJECTED FUEL		INJECTED OXID EJECTED OXID	
D MICRONS	LOG D	DROP SIZE DISTRIBUTION - CUMULATIVE MASS			
10	1.0000	0.0000	0.0000	0.0000	.0004
20	1.3010	.1988	.0000	.1988	.0026
30	1.4771	.1988	.0705	.1901	.1451
40	1.6021	.2000	.0726	.2305	.2380
50	1.6990	.2000	.1805	.4082	.3074
60	1.7762	.2344	.2354	.4452	.3964
70	1.8451	.3988	.2030	.5040	.3964
80	1.9031	.4473	.5113	.7454	.3964
90	1.9542	.5977	.5113	.7454	.3964
100	2.0000	.7965	.5113	.7454	.3964
110	2.0414	.7965	.5113	.7454	.3964
120	2.0792	.7965	.5113	.7454	.3964
130	2.1139	.7965	.5113	.7454	.3964
140	2.1461	.7965	.5113	.7454	.3964
150	2.1761	.7965	.5113	.7454	.3964
160	2.2041	.7965	.5113	.7454	.3964
170	2.2304	.7965	.5113	.7454	.3964
180	2.2553	.7965	.5113	.7454	.3964
190	2.2788	.7965	.5113	.7454	.3964
200	2.3010	.7965	.5113	.7454	.3964
210	2.3222	.7965	.5113	.7454	.3964
220	2.3424	.7965	.5113	.7454	.3964
230	2.3617	.7965	.5113	.7454	.3964
240	2.3802	.7965	.5113	.7454	.3964
250	2.3976	.7965	.5113	.7454	.3964
260	2.4150	.7965	.5113	.7454	.3964
270	2.4314	.7965	.5113	.7454	.3964
280	2.4472	.7965	.5113	.7454	.3964
290	2.4624	.7965	.5113	.7454	.3964
300	2.4771	.7965	.5113	.7454	.3964
310	2.4914	.7965	.5113	.7454	.3964
320	2.5051	.7965	.5113	.7454	.3964
330	2.5185	.7965	.5113	.7454	.3964
340	2.5315	.7965	.5113	.7454	.3964
350	2.5441	.7965	.5113	.7454	.3964
360	2.5563	.7965	.5113	.7454	.3964
370	2.5682	.7965	.5113	.7454	.3964
380	2.5798	.7965	.5113	.7454	.3964
390	2.5911	.7965	.5113	.7454	.3964
400	2.6021	.7965	.5113	.7454	.3964
410	2.6128	.7965	.5113	.7454	.3964
420	2.6232	.7965	.5113	.7454	.3964
430	2.6335	.7965	.5113	.7454	.3964
440	2.6435	.7965	.5113	.7454	.3964
450	2.6532	.7965	.5113	.7454	.3964
460	2.6628	.7965	.5113	.7454	.3964

FINAL CHAMBER CONDITION

STATION	GRAMS FUEL	GRAMS OXID	TEMPERATURE
1	0.0000000	0.0000000	294.0550001
2	0.0000000	0.0000000	294.06541702
3	0.0000000	0.0000000	294.07574602
4	0.0000000	0.0000000	294.08607502
5	0.0000000	0.0000000	294.09640402
6	0.0000000	0.0000000	294.10673303
7	0.0000000	0.0000000	294.11706203
8	0.0000000	0.0000000	294.12739103
9	0.0000000	0.0000000	294.13772003
10	0.0000000	0.0000000	294.14804904
11	0.0000000	0.0000000	294.15837804
12	0.0000000	0.0000000	294.16870704
13	0.0000000	0.0000000	294.17903604
14	0.0000000	0.0000000	294.18936505
15	0.0000000	0.0000000	294.19969405
16	0.0000000	0.0000000	294.21002305
17	0.0000000	0.0000000	294.22035205
18	0.0000000	0.0000000	294.23068106
19	0.0000000	0.0000000	294.24101006
20	0.0000000	0.0000000	294.25133906
21	0.0000000	0.0000000	294.26166806
22	0.0000000	0.0000000	294.27199707
23	0.0000000	0.0000000	294.28232607
24	0.0000000	0.0000000	294.29265507
25	0.0000000	0.0001800	294.30298407
26	0.0000000	0.0000000	294.31331308
27	0.0000000	0.0000000	294.32364208
28	0.0000000	0.0000000	294.33397108
29	0.0000000	0.0003907	294.34430008
30	0.0000000	0.0011394	294.35462909
31	0.0000000	0.0017110	294.36495809
32	0.0000000	0.0019425	294.37528709
33	0.0000000	0.0018591	294.38561609
34	0.0000000	0.0018097	294.39594510
35	0.0000000	0.0019008	294.40627410
36	0.0000000	0.0024201	294.41660310
37	0.0000000	0.0028713	294.42693210
38	0.0000000	0.0033592	294.43726111
39	0.0000000	0.0050914	294.44759011
40	0.0000000	0.0054253	294.45791911
41	0.0000000	0.0000000	294.46824811
42	0.0000000	0.0000000	294.47857712
43	0.0000000	0.0000000	294.48890612
44	0.0000000	0.0000000	294.49923512
45	0.0000000	0.0000000	294.50956412
46	0.0000000	0.0000000	294.51989313
47	0.0000000	0.0000000	294.53022213
48	0.0000000	0.0000000	294.54055113
49	0.0000000	0.0000000	294.55088013
50	0.0000000	0.0000000	294.56120914
51	0.0000000	0.0000000	294.57153814
52	0.0000000	0.0000000	294.58186714
53	0.0000000	0.0000000	294.59219614
54	0.0000000	0.0000000	294.60252515
55	0.0000000	0.0000000	294.61285415
56	0.0000000	0.0000000	294.62318315
57	0.0000000	0.0000000	294.63351216
58	0.0000000	0.0000000	294.64384116
59	0.0000000	0.0000000	294.65417016
60	0.0000000	0.0000000	294.66449916
61	0.0000000	0.0000000	294.67482817

02 0.0000000 0.0000000 294.68515717
03 0.0000000 0.0000000 294.68548617
04 0.0000000 0.0000000 294.70581517
05 0.0000000 0.0000000 294.71614418
06 0.0000000 0.0000000 294.72647318
07 0.0000000 0.0005445 294.73680218
08 0.0000000 0.0010738 294.74713118
09 0.0000000 0.0011987 294.75746019
10 0.0000000 0.0017505 294.76778919
11 0.0000000 0.0024917 294.77811819
12 0.0000000 0.0028482 294.78844719
13 0.0000000 0.0000000 294.79877620
14 0.0000000 0.0000000 294.80910520
15 0.0000000 0.0000000 294.81943420
16 0.0000000 0.0000000 294.82976320
17 0.0000000 0.0000000 294.84009221
18 0.0000000 0.0000000 294.85042121
19 0.0000000 0.0000000 294.86075021
20 0.0000000 0.0000000 294.87107921
21 0.0000000 0.0000000 294.88140822
22 0.0000000 0.0000000 294.89173722
23 0.0000000 0.0000000 294.90206622
24 0.0000000 0.0000000 294.91239522
25 0.0000000 0.0000000 294.92272423
26 0.0000000 0.0000000 294.93305323
27 0.0000000 0.0000000 294.94338223
28 0.0000000 0.0000000 294.95371123
29 0.0000000 0.0000000 294.96404024
30 0.0000000 0.0000000 294.97436924
31 0.0000000 0.0000000 294.98469824
32 0.0000000 0.0000000 294.99502724
33 0.0000000 0.0000000 295.00535625
34 0.0000000 0.0000000 295.01568525
35 0.0000000 0.0000000 295.02601425
36 0.0000000 0.02180000 295.03634325
37 0.0000000 0.0000000 295.04667226
38 0.0000000 0.0000000 295.05700126
39 0.0000000 0.0000000 295.06733026
40 0.0000000 0.0000000 295.07765926
41 0.0000000 0.0000000 295.08798827

PAGES OMITTED

PAGES OMITTED

TIME-AVERAGED INTERVAL PERFORMANCE VALUES

START TIME	.015000 SECONDS			
FINISH TIME	.017000 SECONDS			
INTERVAL LENGTH	.002000 SECONDS			
TOTAL IMPULSE	.010097 POUNDS/SEC	THRUST	5.000042 POUNDS	
CHAMBER PRESSURE INTEGRAL	.175390 PSIA/SEC	CHAMBER PRESSURE	87.600017 PSIA	
FUEL OUT OF TANK	.000014 POUNDS	FUEL FLOW RATE	.006979 POUNDS/SEC	
OXID OUT OF TANK	.000024 POUNDS	OXID FLOW RATE	.011994 POUNDS/SEC	
FUEL+OXID OUT OF TANK	.000038 POUNDS	TOTAL FLOW RATE	.018973 POUNDS/SEC	
MIXTURE RATIO	1.710620 OXID/FUEL			
C-STAR	4431.050000 FEET/SEC			
VAC. SPECIFIC IMPULSE	266.095743 SECONDS			

PROPELLANT EXPELLED THIS INTERVAL

	FUEL POUNDS	FUEL POUNDS/SEC	OXID POUNDS	OXID POUNDS/SEC
PRODUCTS OF COMBUSTION	.00001020	.005099	.00001994	.009972
UNBURNED VAPOR	0.00000000	0.000000	0.00000000	0.000000
UNBURNED DROPLETS	.00000372	.001059	.00000604	.002021
WALL FILM	0.00000000	0.000000	0.00000000	0.000000

EXPELLED DROPLET MEAN DIAMETER AND VELOCITY

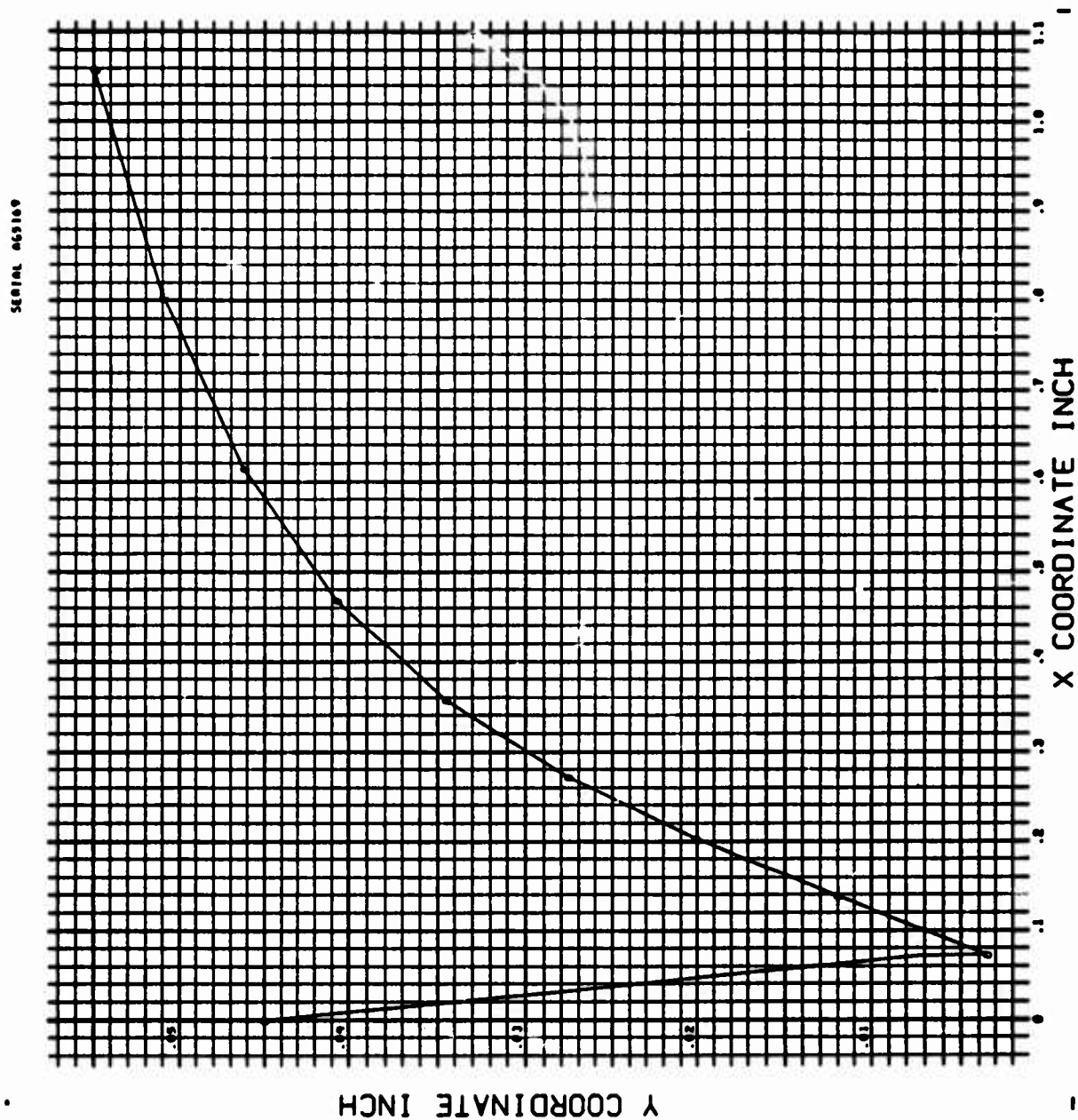
	FUEL DROPLETS	OXID DROPLETS
D30 MICRONS	56.015033	49.057094
D31 MICRONS	65.639041	56.009900
D32 MICRONS	70.266954	66.103060
AXIAL VELOCITY FT/SEC	391.921920	232.080445
RADIAL VELOCITY FT/SEC	39.373362	43.342769

INPUT VALUES FOR MULTIRAN

CHAMBER PRESSURE	87.600017 PSIA	
CHAMBER TEMPERATURE	5001.765005 DEG.R.	
GAS CONSTANT	2255.530752 FT*2/SEC*2 DEG.R	
GAS SPECIFIC HEAT	12331.905403 FT*2/SEC*2 DEG.R	
GAS GAMMA	1.224013	
GAS VISCOSITY	.000096 POUNDS/FT.SEC.	
		OXID DROPLETS
DROPLET DENSITY	55.260500 POUNDS/FT*3	91.391105 POUNDS/FT*3
MASS DROP8/MASS GAS	.123346	.134123

EXPULSED DROPLET SIZE DISTRIBUTION

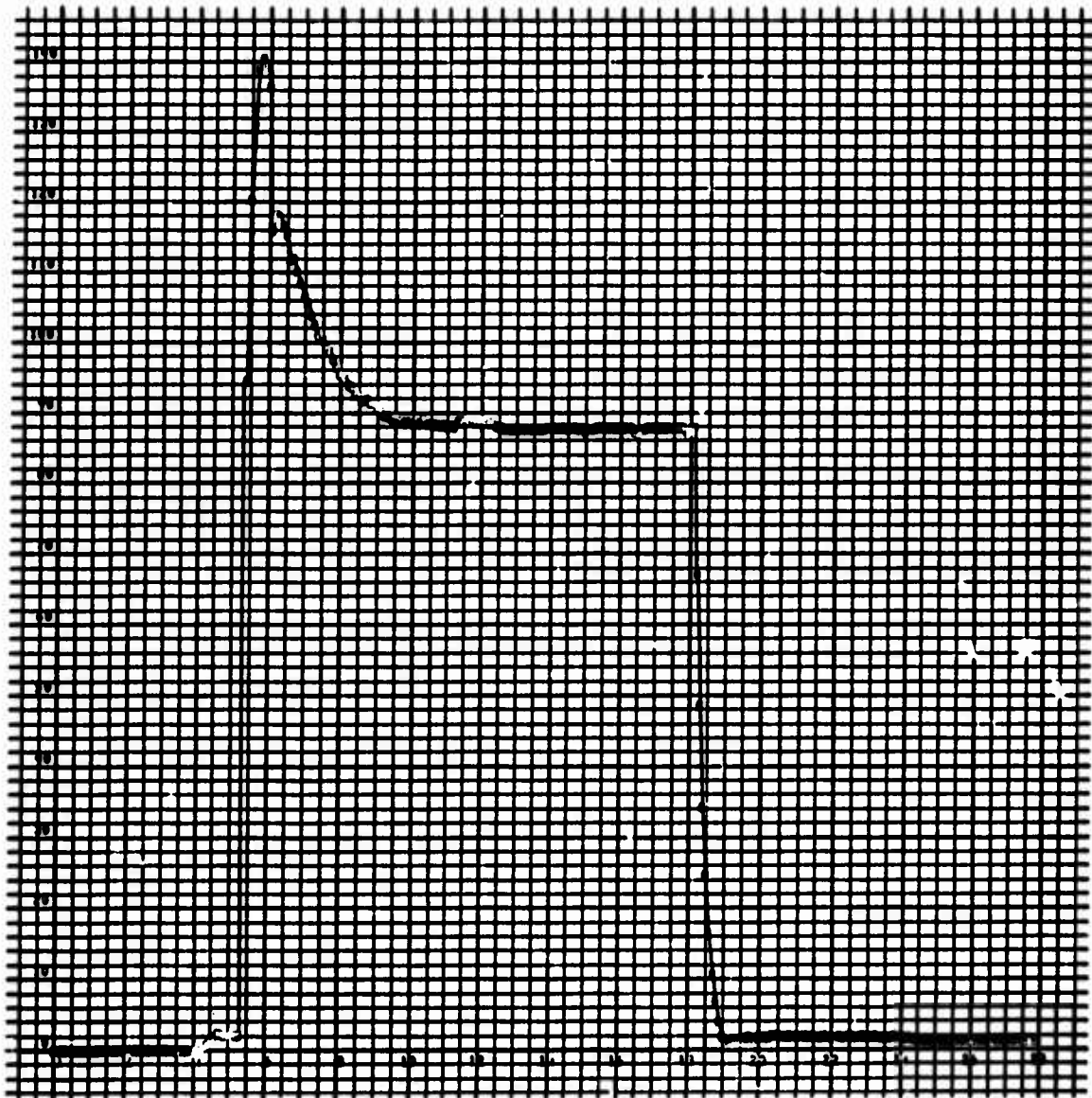
DIAM MICRON	RADIUS FEET	FUEL MASS FRACTION		OXID MASS FRACTION	
		INCREMENTAL	CUMULATIVE	INCREMENTAL	CUMULATIVE
10	1.640E-05	0.00000	0.00000	0.00000	0.00000
20	3.281E-05	0.00000	0.00000	0.00000	0.00000
30	4.921E-05	.003296	.003296	.109220	.109220
40	6.562E-05	0.00000	.003296	0.00000	.109220
50	8.202E-05	.110126	.201419	.245779	.355007
60	9.843E-05	.021192	.222611	0.00000	.355007
70	1.148E-04	0.00000	.222611	0.00000	.355007
80	1.312E-04	.204755	.509366	0.00000	.355007
90	1.476E-04	0.00000	.509366	0.00000	.355007
100	1.640E-04	0.00000	.509366	0.00000	.355007
110	1.804E-04	0.00000	.509366	0.00000	.355007
120	1.969E-04	0.00000	.509366	0.00000	.355007
130	2.133E-04	0.00000	.509366	.640993	1.000000
140	2.297E-04	0.00000	.509366	0.00000	1.000000
150	2.461E-04	0.00000	.509366	0.00000	1.000000
160	2.625E-04	0.00000	.509366	0.00000	1.000000
170	2.789E-04	.400634	1.000000	0.00000	1.000000



SERIAL A69169

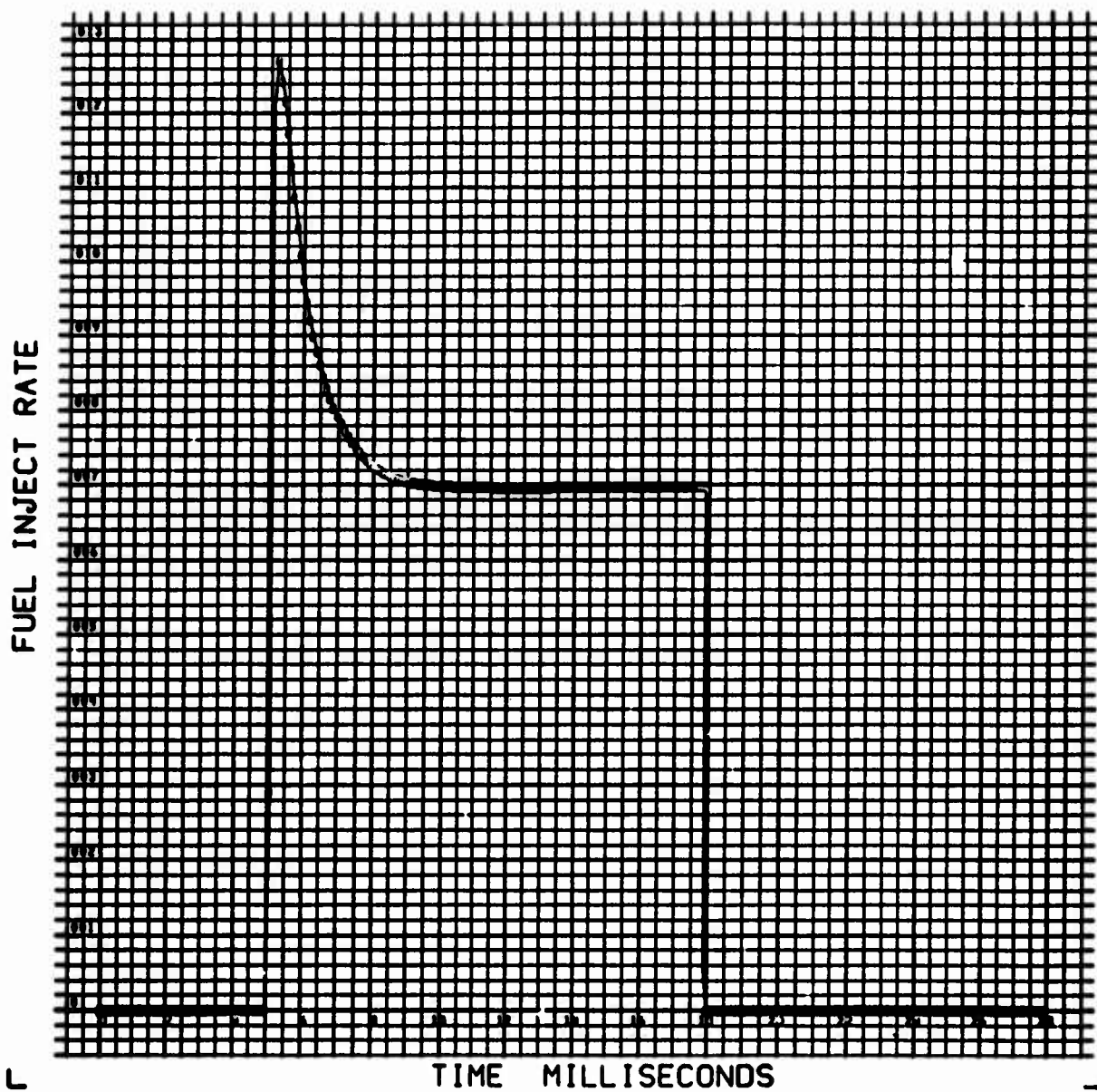
5 0-

CHAMBER PRESSURE



TIME MILLISECONDS

SERIAL A69169

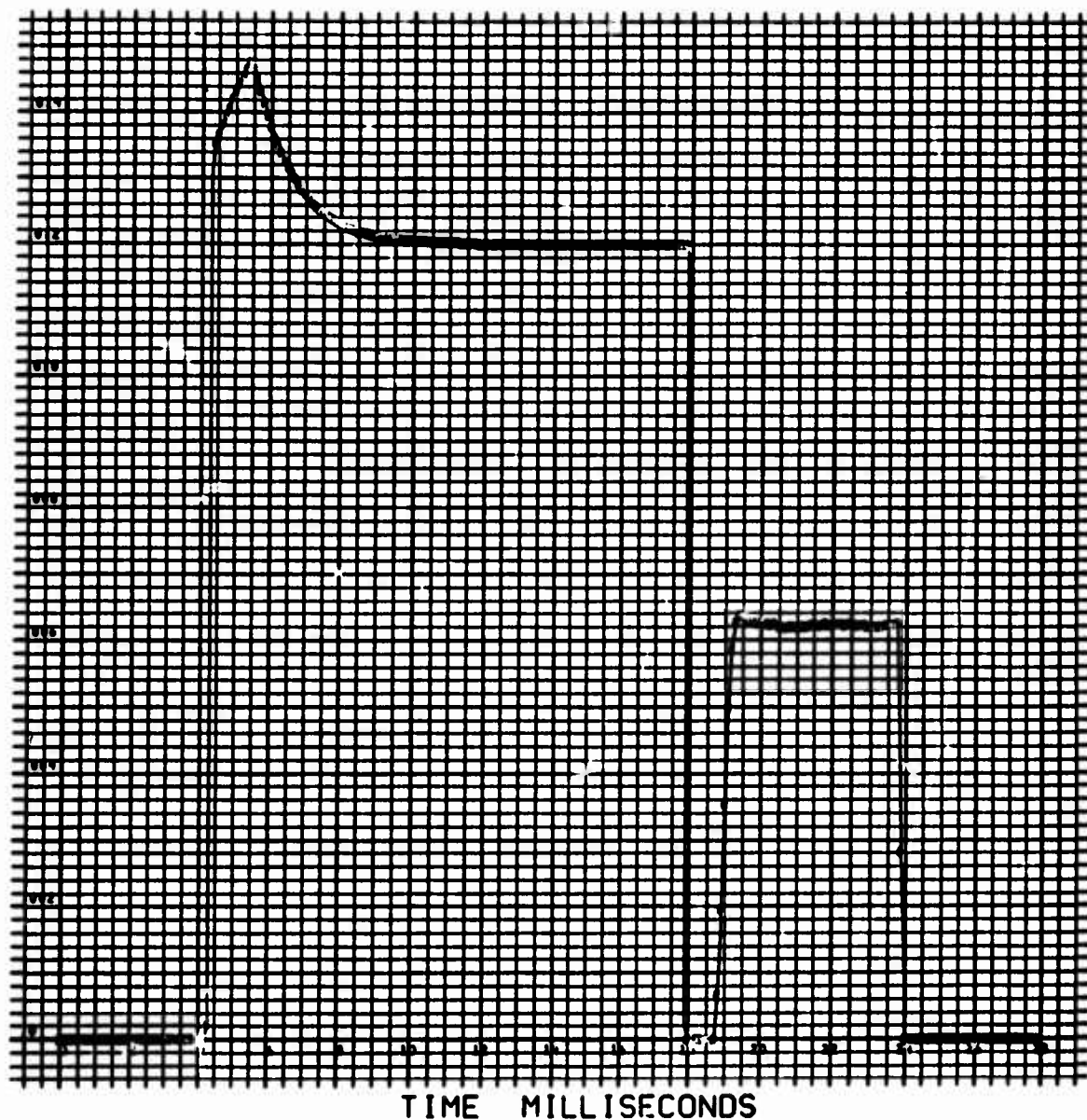


7

SERIAL 065109

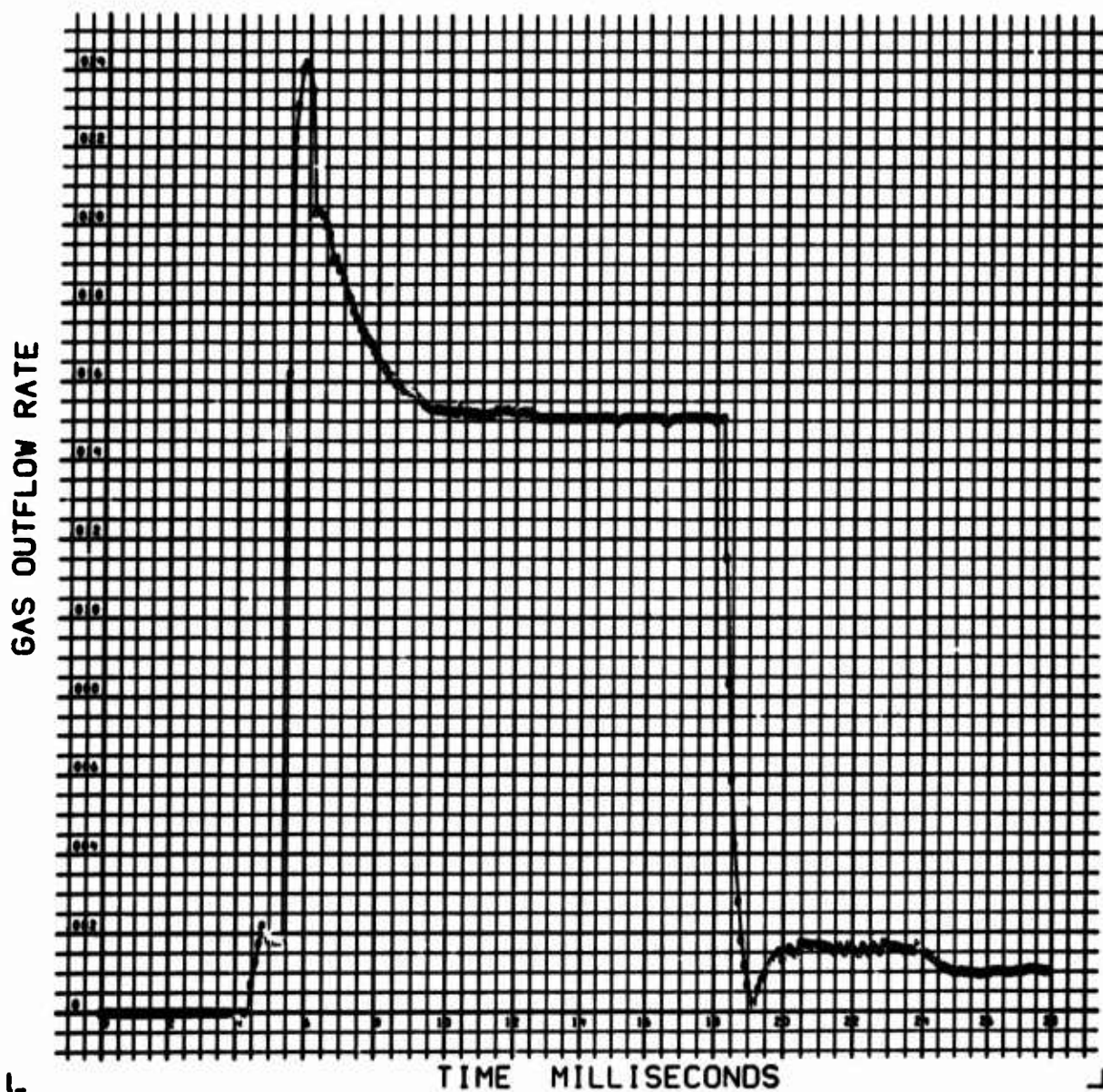
/ 07

OXID INJECT RATE

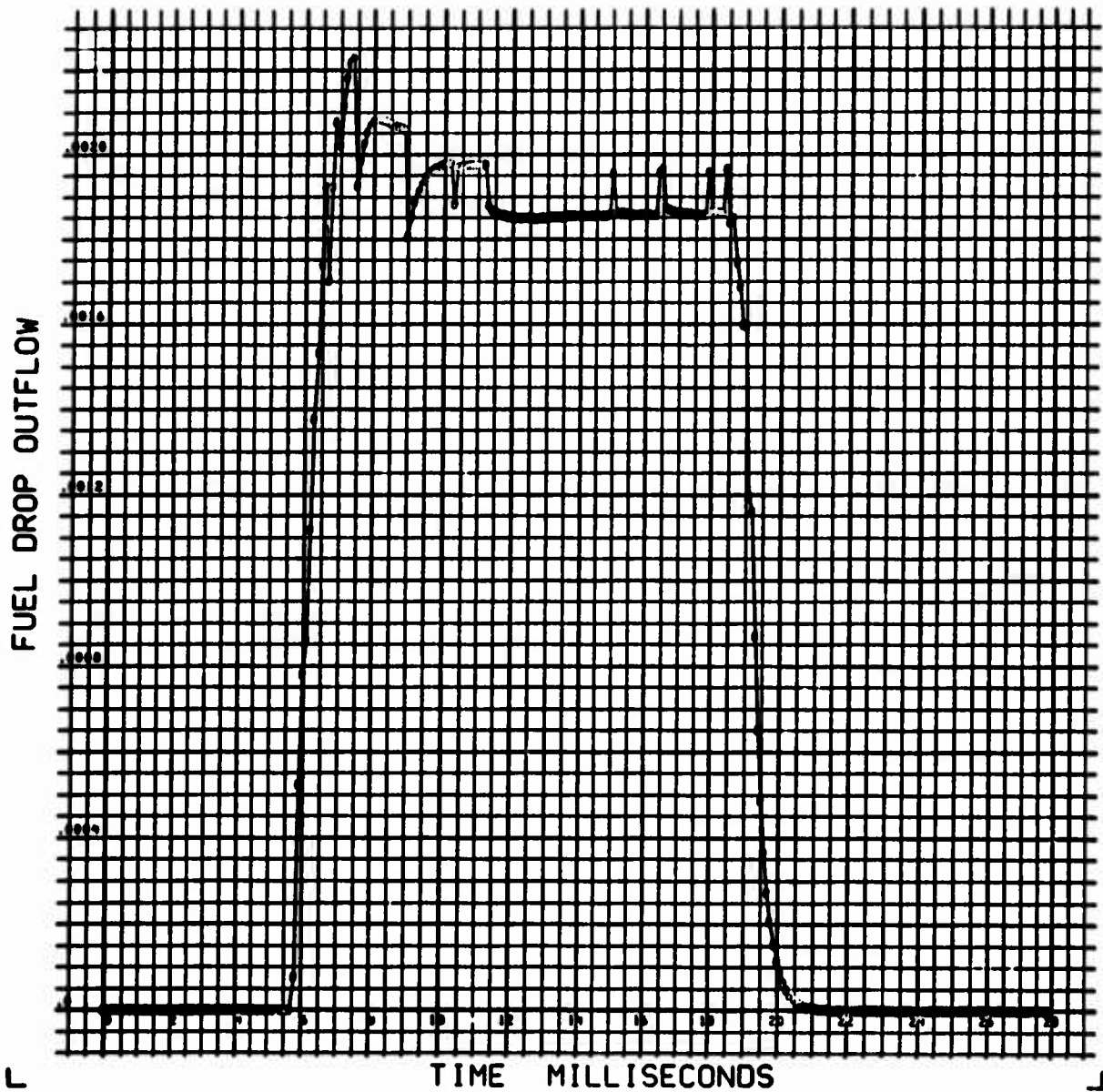


TIME MILLISECONDS

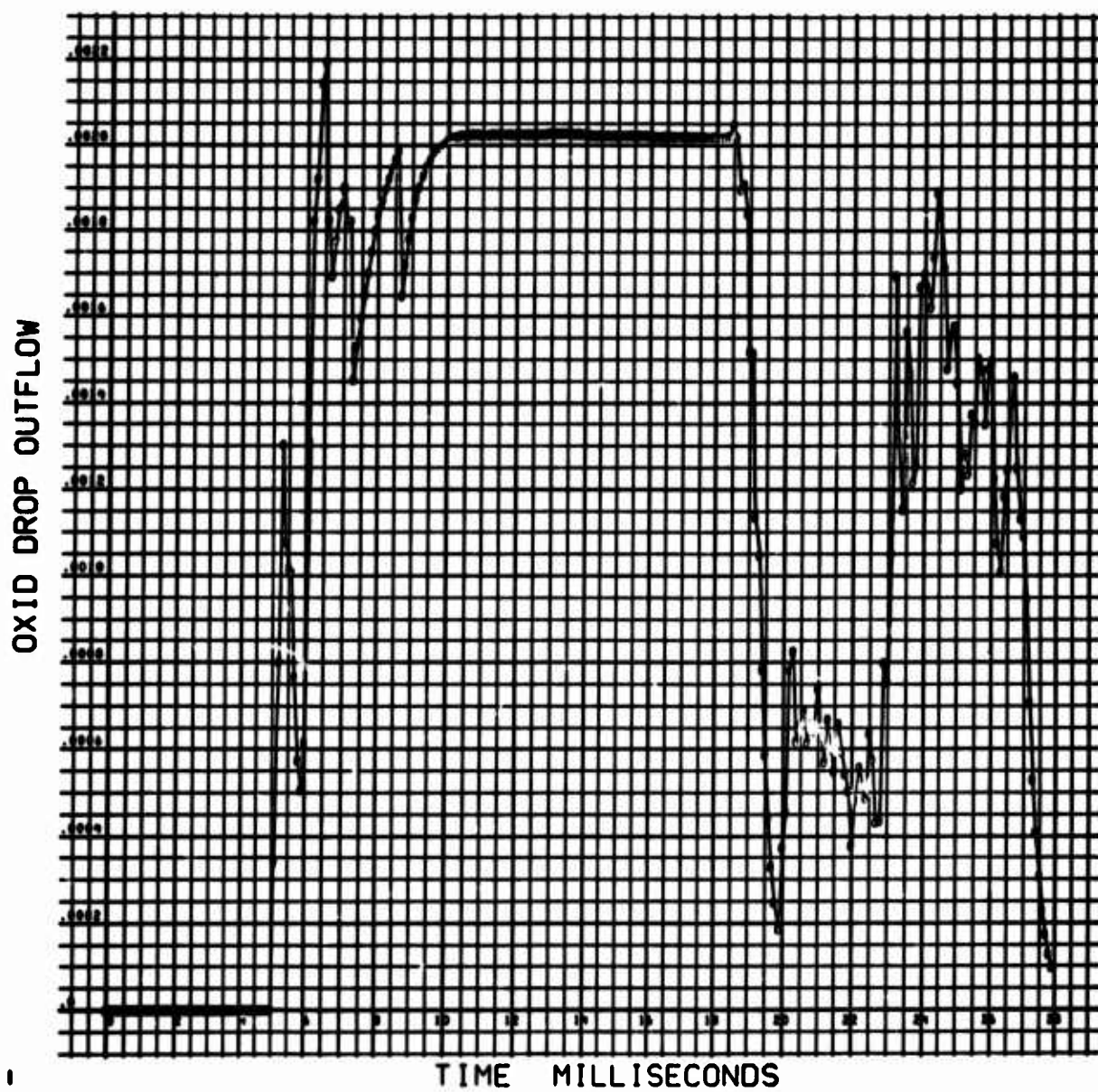
SERIAL AG9169



SERIAL 069109



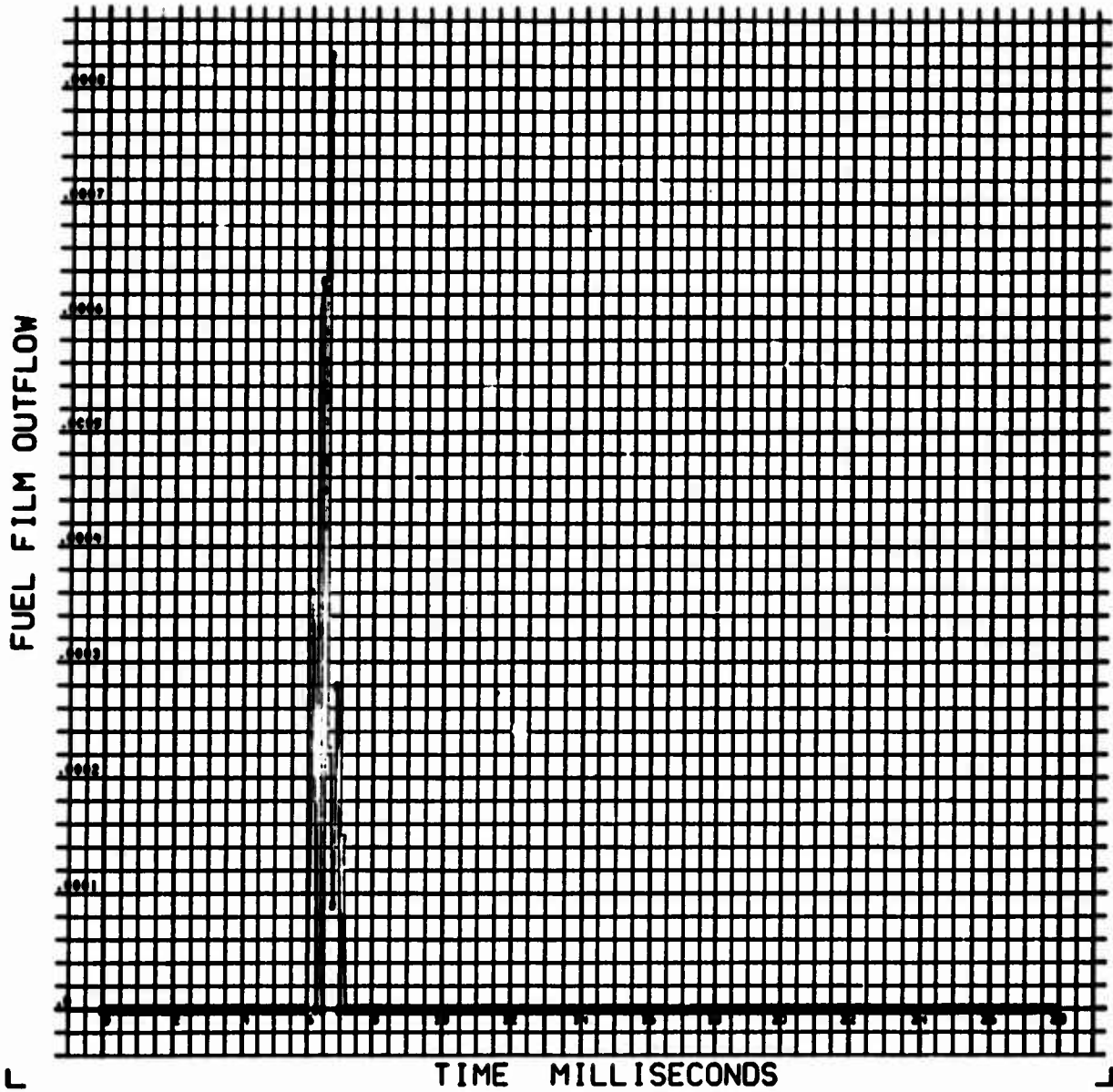
SERIAL AG9169



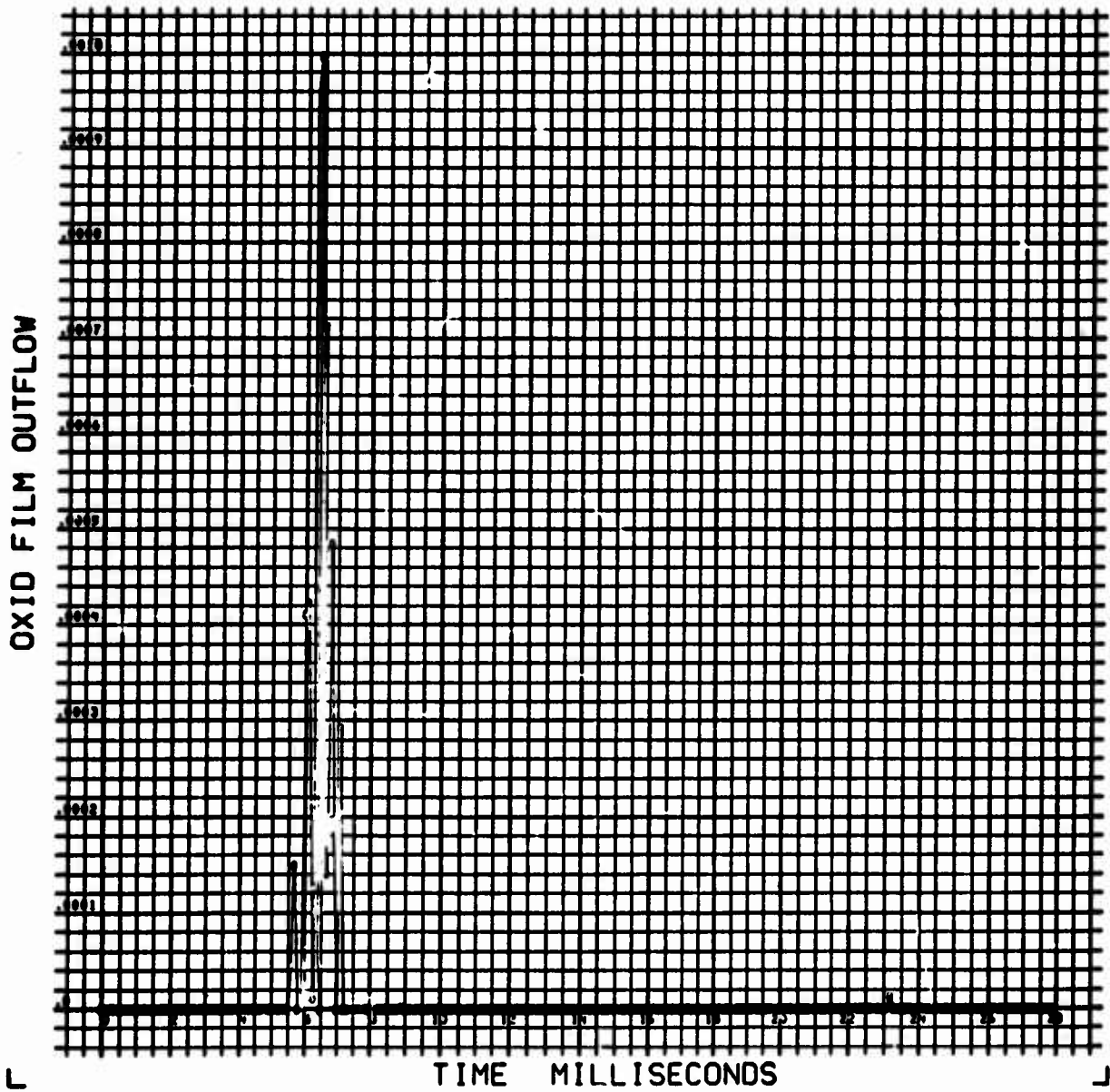
SERIAL A65169

12

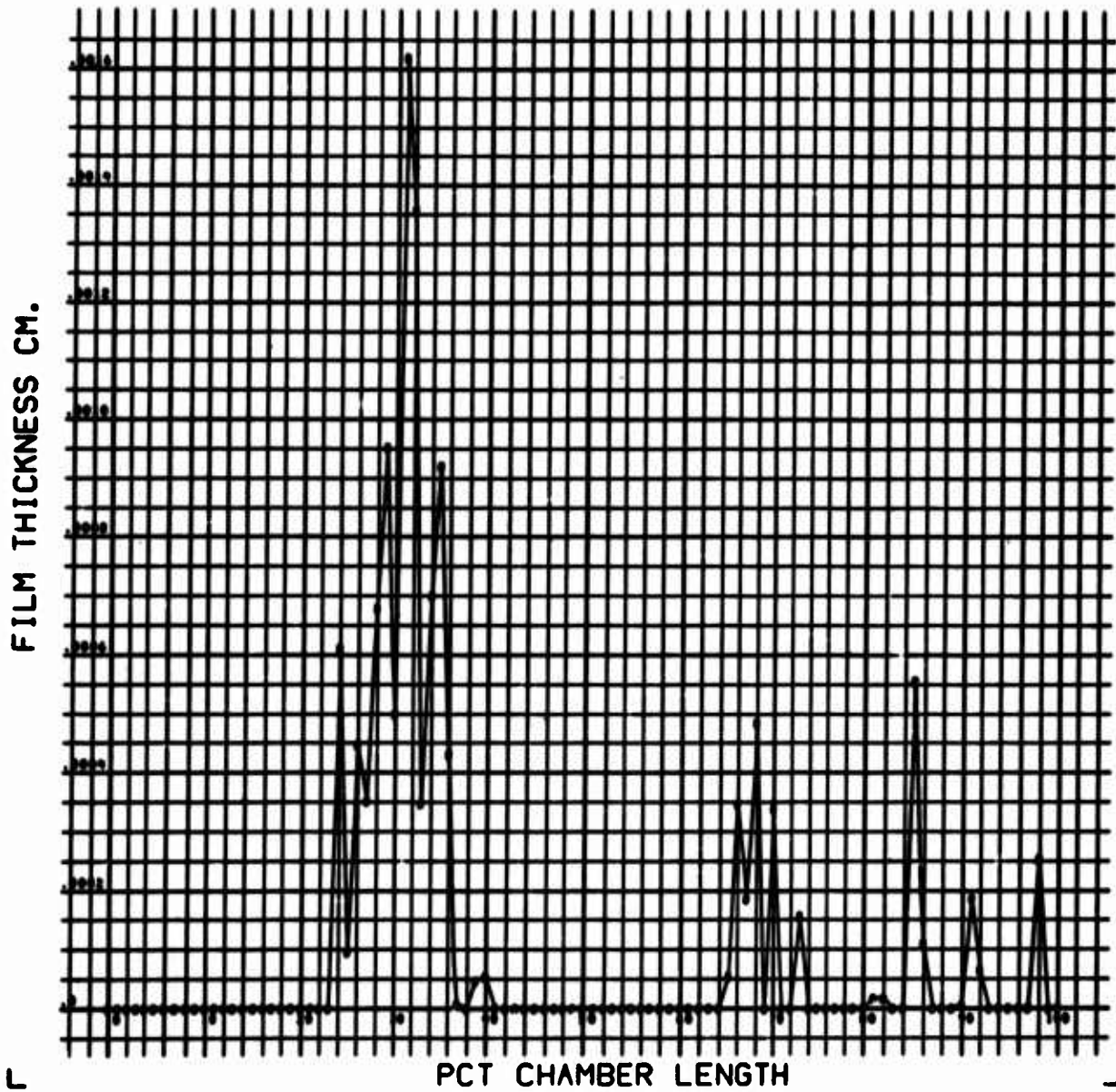
07



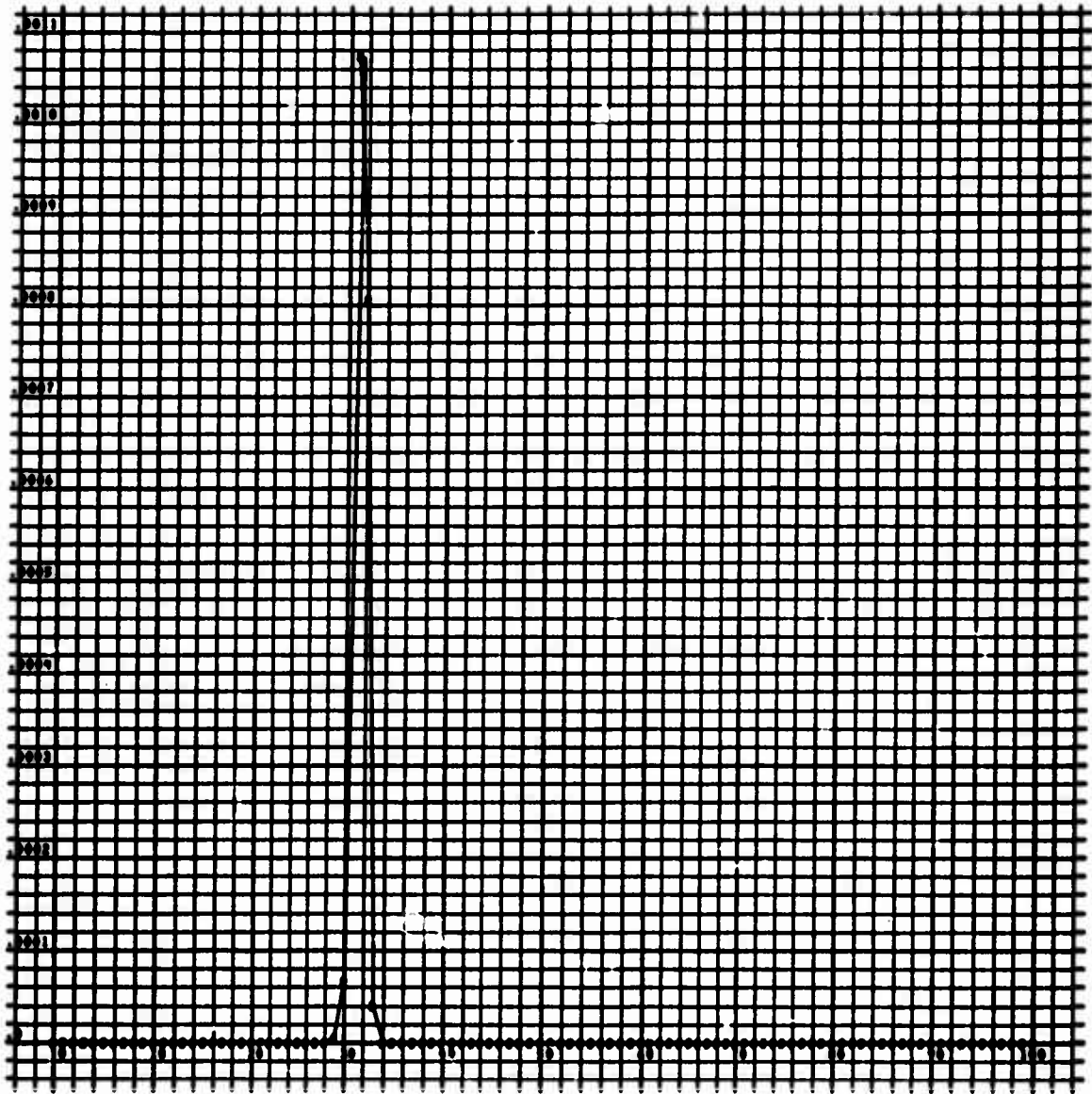
SERIAL 069109



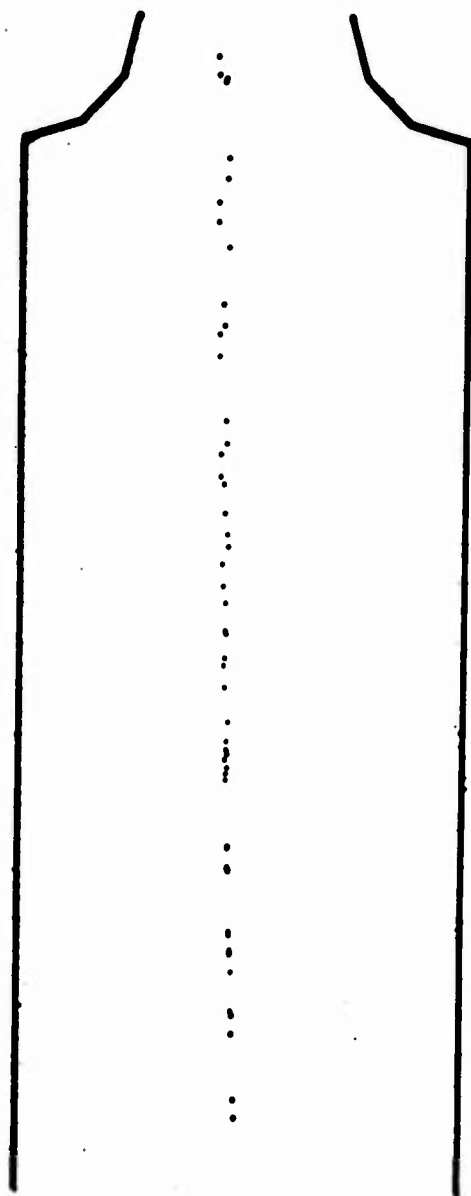
SERIAL 069169



FILM THICKNESS CM.



PCT CHAMBER LENGTH



Initial computer runs were made with the total particle population as given in the "Expelled Droplet Size Distribution Table" of the TCC output, that is, five droplet radii ranging in value from 1.6410^{-5} to 2.78910^{-4} feet. The limiting streamlines proved to be so close to one another that to retain computation accuracy the program used an extremely fine characteristic mesh. After several minutes of computer calculation, the solution was still very close to the start line, and further determinations of the flow using all particles sizes were not made because of the great expenditure of computer resources that would be needed.

The "Expelled Droplet Mean Diameter and Velocity" table of the TCC printout suggested that drops with a diameter on the order of 50 microns would be highly probable in the flow of this particular rocket motor, and consequently for the example droplets of this diameter were used. It should be noted that runs with 85μ droplet diameters and droplet to gas mass flow ratios of 25 percent have been made with no numerical difficulties in MULTRAN.

The input data and the last few pages of TD2 output are shown to illustrate the results of this part of CONTAM. The main function of TD2 is to produce a start tape, tape 8, for the plume flow calculations of TD2P. The additional NAMELIST/DATAP/used in TD2P is also shown. It should be noticed that a Prandtl-Meyer expansion angle of 60 degrees about the nozzle lip has been used. The flow calculation was carried out for a distance of 40 throat radii along the axis of the nozzle. This number was chosen to keep the overall calculation within reasonable computer time limits (including KINCON and SURFACE) and to match the requirements of the data that will be needed by SURFACE.

As with TD2 the last few pages of TD2P printout are presented to illustrate the results of the plume flow field calculation. Again as with TD2 the main task of TD2P is to produce a carry-on tape, tape 12, to be used by the Streamline Generation Program, SLINES.

The card input to SLINES is accomplished via the short NAMELIST/SID/. For example,

```
$SID NSL = 6, PCS(1) = 0.0, 0.25, 0.50, 0.80, 0.90, 0.99, $END
```

where the start of the NAMELIST begins in column two of the card. This input indicates that six streamlines will be determined for the limiting percentages of 0, 25, 50, 80, 90, and 99 percent of the total gas mass.

The output of this aspect of MULTRAN is adequately illustrated by the results for the streamlines shown. The printout is nondimensionalized or normalized in relation to the physical throat of the nozzle. Figures are given for axial, radial, and streamline distances. As will be shown below, the results of KINCON are given in terms of streamline distance, and the use of these tables will provide an avenue to interface the data points requested by SURFACE in axial and radial distance with the values given by KINCON.

A further discussion and interpretation of the MULTRAN outputs will be presented in the SURFACE section when the determination of the later programs inputs are made.

[illegible]

The image displays a dense, repeating pattern of small, dark, rectangular shapes arranged in horizontal rows. The pattern is highly regular and covers the entire frame, creating a textured, almost barcode-like appearance. The shapes are closely packed together, with minimal white space between them. The overall effect is a high-contrast, black and white texture that resembles a close-up of a perforated metal sheet or a digital data visualization.

106

[illegible]

LRC ID	N	REN	Z	ACF	TC	THETA	TC/160	PS/160	LC/160	SD/160	CF	ISP	IT
28	3	0.0000	3.72007	2.0465	3.03.1	7033.1	5.000	5.0576	2.0207	2.0200	0.0000	0.000	3
1	4.542040E-01	1.077553E-03	0.										
28	4	1.0304	7.08791	3.0225	2.049.0	8071.0	11.050	4.0333	0.1214	2.0270	0.0000	0.000	3
1	1.770131E-01	1.195535E-03	0.105057E-00	4.753309E-03	2.133400E-00	4.779331E-01	0.200000E-00						

LRC ID	N	REN	Z	ACF	TC	THETA	TC/160	PS/160	LC/160	SD/160	CF	ISP	IT
28	5	0.0000	3.72007	2.0465	3.03.1	7033.1	5.000	5.0576	2.0207	2.0200	0.0000	0.000	3
1	4.542040E-01	1.077553E-03	0.										
28	6	1.0304	7.08791	3.0225	2.049.0	8071.0	11.050	4.0333	0.1214	2.0270	0.0000	0.000	3
1	1.770131E-01	1.195535E-03	0.105057E-00	4.753309E-03	2.133400E-00	4.779331E-01	0.200000E-00						

LRC ID	N	REN	Z	ACF	TC	THETA	TC/160	PS/160	LC/160	SD/160	CF	ISP	IT
28	7	0.0000	3.72007	2.0465	3.03.1	7033.1	5.000	5.0576	2.0207	2.0200	0.0000	0.000	3
1	4.542040E-01	1.077553E-03	0.										
28	8	1.0304	7.08791	3.0225	2.049.0	8071.0	11.050	4.0333	0.1214	2.0270	0.0000	0.000	3
1	1.770131E-01	1.195535E-03	0.105057E-00	4.753309E-03	2.133400E-00	4.779331E-01	0.200000E-00						

APG ID	R	HEX	Z	ACH	Tn	VG	THETA	Y-FA	TO/TC	PC/PG	DC/DC	SDK/DC	CF	ISP	IT
84	3	0.0000	4.2242	2.723	3219.1	8074.3	0.000	0.000	0.000	0.000	0.000	0.000	0.000	0.00	9
1	3.4320	0.0000	1.1267	0.000	0.000	0.000	0.000	0.000	0.000	0.000	0.000	0.000	0.000	0.00	0
84	4	2.1004	4.7703	3.509	2496.5	9152.5	1.000	0.000	0.000	0.000	0.000	0.000	0.000	0.00	4
1	1.2663	0.0000	1.2351	0.000	0.000	0.000	0.000	0.000	0.000	0.000	0.000	0.000	0.000	0.00	0
84	5	0.2378	15.2723	4.032	1020.4	10713.7	2.000	0.000	0.000	0.000	0.000	0.000	0.000	0.00	2
1	0.0000	0.0000	0.0000	0.000	0.000	0.000	0.000	0.000	0.000	0.000	0.000	0.000	0.000	0.00	0
84	5	0.3231	15.5000	4.077	1507.0	10220.0	2.000	0.000	0.000	0.000	0.000	0.000	0.000	0.00	2
1	0.0000	0.0000	0.0000	0.000	0.000	0.000	0.000	0.000	0.000	0.000	0.000	0.000	0.000	0.00	0

TOTAL MASS FLO. = 3.347774E-C2

PC. POINTS = 32

APG ID	R	HEX	Z	ACH	Tn	VG	THETA	Y-FA	TO/TC	PC/PG	DC/DC	SDK/DC	CF	ISP	IT
84	3	0.0000	4.2242	2.723	3219.1	8074.3	0.000	0.000	0.000	0.000	0.000	0.000	0.000	0.00	9
1	3.4320	0.0000	1.1267	0.000	0.000	0.000	0.000	0.000	0.000	0.000	0.000	0.000	0.000	0.00	0
84	4	2.1004	4.7703	3.509	2496.5	9152.5	1.000	0.000	0.000	0.000	0.000	0.000	0.000	0.00	4
1	1.2663	0.0000	1.2351	0.000	0.000	0.000	0.000	0.000	0.000	0.000	0.000	0.000	0.000	0.00	0
84	5	0.2378	15.2723	4.032	1020.4	10713.7	2.000	0.000	0.000	0.000	0.000	0.000	0.000	0.00	2
1	0.0000	0.0000	0.0000	0.000	0.000	0.000	0.000	0.000	0.000	0.000	0.000	0.000	0.000	0.00	0
84	5	0.3231	15.5000	4.077	1507.0	10220.0	2.000	0.000	0.000	0.000	0.000	0.000	0.000	0.00	2
1	0.0000	0.0000	0.0000	0.000	0.000	0.000	0.000	0.000	0.000	0.000	0.000	0.000	0.000	0.00	0

IP= 50

YOUR NAME IS BEING USED FOR THE PROJECT

ON THE 15th OF 1971

SDATAP	
ZMAX	= 0.4E+02,
ZMA	= 0.6E+02,
APM	= -1,
APLOT = 1,	
POSS	= 6,
PCUT	= 0.1E+05,
SMIS	= 0.3E+02,
Q1	= 0.1E+01,
Q2	= 0.1E+01,
ARG	= 0.1E+01,
Q1	= 0.5E+01,
Q2	= 0.5E+01,
N1 = 5,	
N2 = 1,	
GAMMA	= 0.123E+01,
SEND	

[illegible]

[illegible]

Reproduced from
best available copy.

0.100000
20.22703
29.23736
31.00056
32.74097
34.42783
36.06049
37.64830
39.19237
40.69283
42.15035

0.00000
3.36802
3.72000
4.43009
5.02617
5.60340
6.17401
6.72977
7.27123
7.80000
8.31665

0.00000
0.00000
0.00000
0.00000
0.00000
0.00000
0.00000
0.00000
0.00000
0.00000
0.00000

0.00000
0.00000
0.00000
0.00000
0.00000
0.00000
0.00000
0.00000
0.00000
0.00000
0.00000

0.00000
0.00000
0.00000
0.00000
0.00000
0.00000
0.00000
0.00000
0.00000
0.00000
0.00000

0.00000
0.00000
0.00000
0.00000
0.00000
0.00000
0.00000
0.00000
0.00000
0.00000
0.00000

0.00000
0.00000
0.00000
0.00000
0.00000
0.00000
0.00000
0.00000
0.00000
0.00000
0.00000

0.00000
0.00000
0.00000
0.00000
0.00000
0.00000
0.00000
0.00000
0.00000
0.00000
0.00000

0.00000
0.00000
0.00000
0.00000
0.00000
0.00000
0.00000
0.00000
0.00000
0.00000
0.00000

0.00000
0.00000
0.00000
0.00000
0.00000
0.00000
0.00000
0.00000
0.00000
0.00000
0.00000

0.00000
0.00000
0.00000
0.00000
0.00000
0.00000
0.00000
0.00000
0.00000
0.00000
0.00000

0.00000
0.00000
0.00000
0.00000
0.00000
0.00000
0.00000
0.00000
0.00000
0.00000
0.00000

0.00000
0.00000
0.00000
0.00000
0.00000
0.00000
0.00000
0.00000
0.00000
0.00000
0.00000

0.00000
0.00000
0.00000
0.00000
0.00000
0.00000
0.00000
0.00000
0.00000
0.00000
0.00000

0.00000
0.00000
0.00000
0.00000
0.00000
0.00000
0.00000
0.00000
0.00000
0.00000
0.00000

0.00000
0.00000
0.00000
0.00000
0.00000
0.00000
0.00000
0.00000
0.00000
0.00000
0.00000

0.00000
0.00000
0.00000
0.00000
0.00000
0.00000
0.00000
0.00000
0.00000
0.00000
0.00000

0.00000
0.00000
0.00000
0.00000
0.00000
0.00000
0.00000
0.00000
0.00000
0.00000
0.00000


```

      2 2.00380 43.40174 5.2534 104.412 4.207 .24044 2.05022E-04 0.948312E-04 0.000000000
      3 1.000000E-01 1.73130E-03 3.45492E-03 5.20810E-03 4.82050E-03 0.140013E-02 0.000000E-00
      -----
      Z      S      F      F      F      F      F      F      F
      20 87.764 0.00000 0.00000 0.00000 0.00000 0.00000 0.00000 0.00000
      30 45.467 0.00133 0.00133 0.00133 0.00133 0.00133 0.00133 0.00133
      32 37.776 0.00332 0.00332 0.00332 0.00332 0.00332 0.00332 0.00332
      34 57.760 1.04057 1.04057 1.04057 1.04057 1.04057 1.04057 1.04057
      36 42.482 1.04056 1.04056 1.04056 1.04056 1.04056 1.04056 1.04056
      37 10.145 1.70464 1.70464 1.70464 1.70464 1.70464 1.70464 1.70464
      37 52.117 1.04056 1.04056 1.04056 1.04056 1.04056 1.04056 1.04056
      38 52.117 1.04056 1.04056 1.04056 1.04056 1.04056 1.04056 1.04056
      4 1.04056 1.04056 1.04056 1.04056 1.04056 1.04056 1.04056
      -----
      TOTAL MASS FLO = 3.11227E+02 1.00000E+00 1.00000E+00 1.00000E+00 1.00000E+00 1.00000E+00 1.00000E+00 1.00000E+00
      LOC ID # 1 1.00000E+00 1.00000E+00 1.00000E+00 1.00000E+00 1.00000E+00 1.00000E+00 1.00000E+00 1.00000E+00
      20 3 0.00000 0.00000 0.00000 0.00000 0.00000 0.00000 0.00000 0.00000
      3 1.00000E+00 1.00000E+00 1.00000E+00 1.00000E+00 1.00000E+00 1.00000E+00 1.00000E+00 1.00000E+00
      -----
      Z      S      F      F      F      F      F      F      F
      20 87.764 0.00000 0.00000 0.00000 0.00000 0.00000 0.00000 0.00000
      30 45.467 0.00133 0.00133 0.00133 0.00133 0.00133 0.00133 0.00133
      32 37.776 0.00332 0.00332 0.00332 0.00332 0.00332 0.00332 0.00332
      34 57.760 1.04057 1.04057 1.04057 1.04057 1.04057 1.04057 1.04057
      36 42.482 1.04056 1.04056 1.04056 1.04056 1.04056 1.04056 1.04056
      37 10.145 1.70464 1.70464 1.70464 1.70464 1.70464 1.70464 1.70464
      37 52.117 1.04056 1.04056 1.04056 1.04056 1.04056 1.04056 1.04056
      38 52.117 1.04056 1.04056 1.04056 1.04056 1.04056 1.04056 1.04056
      4 1.04056 1.04056 1.04056 1.04056 1.04056 1.04056 1.04056
      -----
      TOTAL MASS FLO = 3.11227E+02 1.00000E+00 1.00000E+00 1.00000E+00 1.00000E+00 1.00000E+00 1.00000E+00 1.00000E+00

```


Reproduced from
best available copy.

20	3	0.0000	3.10497	5.0449	1496.1	10719.0	0.000	.25444	2.5276341-04	9.934039E-04	0.11763	4
1	1.000474E-02	1.000327E-03	C.				5.000245E-03		0.1174201-03	4.940871E-02	0.200000E-02	
20	5	0.0338	41.0000	5.2305	1421.0	10740.2	0.000	.24101	1.097031E-04	7.040000E-04	0.04404	3
1	0.27345E-01	1.0-7274E-03	0.720347E-01	5.000	1421.0	10740.2	5.000347E-03		5.040021E-03	3.720449E-02	0.200000E-02	
<p>2 30 14497 3.00030 30 14445 .27540 41.00000 .00124 TOTAL MASS FLOW = 3.042040E-02 C. PCINYS = 3</p>												
LRC ID	M	REN	Z	ACN	YC	VC	YBYA-	YBYA-C	TS/100	PC/PCG	DS/DS	IT
30	3	0.0000	35.21375	5.0215	1471.2	10747.1	0.000	.25021	2.270533E-04	9.074439E-04	0.29510	3
1	0.310075E-01	1.0-7204E-03	0.				5.007030E-03		0.205170E-03	4.044324E-02	0.200000E-02	
30	2	0.2066	41.10002	5.0545	1456.7	10742.0	0.000	.24774	2.147332E-04	0.007795E-04	0.24012	3
1	0.012505E-01	1.0-7567E-03	1.74440E-01	5.005	1456.7	10742.0	5.00514E-03		0.200110E-03	4.411475E-02	0.200000E-02	
<p>2 40 94974 3.00000 40 10-42 .00100 TOTAL MASS FLOW = 3.042240E-02 C. PCINYS = 2</p>												
LRC ID	M	REN	Z	ACN	YC	VC	YBYA-	YBYA-C	TS/100	PC/PCG	DS/DS	IT
31	3	0.0000	41.0000	5.0449	1496.1	10719.0	0.000	.25444	2.5276341-04	9.934039E-04	0.11763	4
1	0.500000E-01	1.0-7274E-03	0.720347E-01	5.000	1421.0	10740.2	5.000347E-03		5.040021E-03	3.720449E-02	0.200000E-02	

T-501488 PL-16 RECORD HAS BEEN COMPLETED

OF THIS = 1.7.74 IN 1114 = 14.06

4. KINETICS AND CONDENSATION-- THE KINCON PROGRAM

The KINCON subprogram performs the chemical-kinetic and single-species condensation calculations along gas-phase streamlines as defined by the Multiphase Nozzle and Plume Transport program, MULTRAN. When operated in the sequential mode, KINCON accepts card input data describing the initial gas-phase composition, chemical reactions with rate coefficients, and pertinent integration control parameters. The streamline definition including initial streamline conditions (pressure, temperature, and velocity) and the streamline pressure distribution are obtained from the MULTRAN program via TAPE 8.

a. Description of Input

The chemical system (12 species and 24 reactions) describing the kinetics of MMH/NTO combustion products is a commonly used set and was obtained from the ODK (the ICRPG One-Dimensional Kinetic Nozzle Analysis Computer Program) kinetics library (Reference C-1 and C-2 in Appendix C). The rate constants were updated whenever possible with the latest values from the literature. The initial gas-phased chemical composition was obtained from thermochemical equilibrium results corresponding to the values calculated by the TCC subprogram.

A listing of the KINCON card input data for this sample case is presented. Nothing is entered in the namelist \$ THERMO since a master tape of thermodynamic data (in JANAF format) was attached to TAPE 4. The 12 chemical species with initial mass fractions follow the title card. The chemical reactions are specified in two groups; the three body dissociation and recombination reactions appearing before card END TBR REAX, and the binary exchange reactions following the END TBR REAX card. The rate constants for the reverse reaction are input on the same card as reaction, which is input in symbolic form. Integration control parameters and miscellaneous data follow the reaction cards in namelist \$PROPEL.

The normalizing factor for the streamline coordinate was taken as the throat radius, $RSTAR = 0.0972$ in. Initial step size (HI), minimum step size (HMIN), and maximum step size (HMAX) are input in values of the normalized streamline coordinate. DEL is the relative error criterion and represents a measure of the truncation error in the finite difference scheme. Every tenth integration step is output as specified by ND3.

```
$PROPEL RSTAR=0.0972, JPFLAG=1, DEL=0.01, ND3=10, HI=0.0001,  
HMAX=1.0, TCOND(1)=12*0.0, T=5881.8, AREPS=0.001, ETA=0.1,  
IDCOND=2, $END
```

At the initial step of each streamline a table of "Dissociation Recombination Reaction Rate Ratios" is printed as is shown. The kinetic results determined along the streamlines are based on the pressure at that point, and accordingly the next item printed out is a "Pressure Table", as illustrated. Results are shown for the 25 percent mass limiting streamline.

A further discussion and interpretations of the results of KINCON will be made in the next section when the inputs for SURFACE are determined.

BEGINNING OF STREAMLINE GENERATION PROGRAM

CP TIME = 17.875 MP TIME = 19.760

STREAMLINE 1 = 25.0000 PERCENT OF THE TOTAL MASS FLOW
 ZINIT = 0.00000 (NOMD)ENSIONAL = S/MC)
 ZINIT = 0.00000 (NOMD)ENSIONAL = S/MC)
 ZINIT = 5020.410383 (DEG. F)
 ZINIT = 2531.075-11 (FT/SEC)
 ZFINAL = 41.307145 (NOMD)ENSIONAL = Z/MC)
 MGRK = 96 (NO. OF PRESSURE TABLE POINTS)

POINT NO.	AXIAL DISTANCE (Z/MC)	RADIAL DISTANCE (R/MC)	STREAMLINE DISTANCE (S/MC)	PRESSURE (PSIA)
1	-8.00240E-01	5.309340E-01	0.	6.052867E+01
2	-7.72970E-01	5.25307E-01	0.1500001E-02	6.072800E+01
3	-6.77401E-01	5.234414E-01	1.914007E-01	6.10791E+01
4	-5.02071E-01	5.190000E-01	2.089495E-01	6.322472E+01
5	-4.06401E-01	5.132643E-01	3.024400E-01	6.12015E+01
6	-3.191291E-01	5.051534E-01	4.77938E-01	5.94389E+01
7	-2.05911E-01	4.82482E-01	5.7339E-01	5.73329E+01
8	-1.05921E-01	4.62977E-01	6.09170E-01	5.51830E+01
9	-1.05121E-01	4.61019E-01	7.04220E-01	5.29280E+01
10	-3.7318E-01	4.69864E-01	8.59285E-01	5.36730E+01
11	4.55279E-02	4.99530E-01	9.55172E-01	4.84270E+01
12	1.61040E-01	4.99927E-01	1.050470E+00	4.61440E+01
13	2.76438E-01	5.01132E-01	1.145830E+00	4.308974E+01
14	3.77689E-01	5.04044E-01	1.24212E+00	4.16019E+01
15	4.67218E-01	5.05694E-01	1.33661E+00	3.94742E+01
16	5.62094E-01	5.07074E-01	1.43231E+00	3.72403E+01
17	6.57986E-01	5.13319E-01	1.527970E+00	3.51806E+01
18	7.53380E-01	5.16102E-01	1.623060E+00	3.30200E+01
19	8.48778E-01	5.23030E-01	1.71661E+00	3.09014E+01
20	9.44100E-01	5.29022E-01	1.80923E+00	2.89094E+01
21	1.03744E-01	5.36651E-01	1.90205E+00	2.7033E+01
22	1.13480E-01	5.50613E-01	1.98287E+00	2.50344E+01
23	1.03664E+00	5.63331E-01	2.067450E+00	2.40121E+01
24	1.13254E+00	5.103824E-01	2.20397E+00	2.46290E+01
25	1.28180E+00	6.36154E-01	2.33825E+00	2.22278E+01
26	1.42797E+00	7.74544E-01	2.46098E+00	1.96139E+01
27	1.59714E+00	6.61518E-01	2.63037E+00	1.72763E+01
28	1.79857E+00	7.28612E-01	2.80449E+00	1.46189E+01
29	2.04375E+00	7.735974E-01	3.11010E+00	1.20249E+01
30	2.33724E+00	4.31979E-01	3.41196E+00	9.43350E+00
31	2.78451E+00	9.09463E-01	3.78099E+00	7.35120E+00
32	3.27934E+00	1.618282E+00	4.24804E+00	4.86015E+00
33	3.80134E+00	1.10000E+00	4.91259E+00	3.40017E+00
34	4.0374E+00	1.35723E+00	5.7099E+00	2.46059E+00
35	6.17637E+00	1.67329E+00	7.54204E+00	1.41772E+00
36	6.89125E+00	1.76430E+00	7.84918E+00	1.19491E+00
37	7.14913E+00	1.87125E+00	8.3517E+00	1.24820E+00
38	7.5004E+00	3.75900E+00	8.74001E+00	9.28008E+00
39	3.10191E+00	2.03530E+00	9.30224E+00	7.667830E+01
40	4.709501E+00	2.07548E+00	9.91197E+00	6.75440E+01
41	9.55990E+00	2.20372E+00	1.07766E+01	6.47890E+01
42	1.06022E+01	2.42213E+00	1.18617E+01	4.314720E+01
43	1.16601E+01	2.61328E+00	1.20203E+01	3.65467E+01
44	1.26601E+01	2.84444E+00	1.41744E+01	3.75444E+01

48	8.418947E+01	3.771230E+00	8.318141E+04	3.017091E+02
49	2.37280E+01	6.485940E+00	2.58532E+01	3.88279E+02
50	2.31370E+01	6.28820E+00	2.58435E+01	4.2718E+02
51	8.00657E+01	0.123080E+00	4.80942E+01	4.07906E+02
52	2.58673E+01	6.94653E+00	2.81446E+01	3.825290E+02
53	2.70193E+01	7.17187E+00	3.01857E+01	3.84244E+02
54	8.82724E+01	8.06690E+00	3.08032E+01	1.392130E+02
55	3.094907E+01	1.005757E+01	4.07207E+01	1.02112E+02

STEADY STATE FLOW 40.38000 PERCENT OF THE TOTAL PUMP FLOW
 Z1117 = 5.110000 (COEFFICIENTIAL - 1/400)
 Z1118 = 27.57200 (PSIA)
 Z1119 = 2000.349154 (DEG. F)
 Z1120 = 2000.349154 (F/SEC)
 Z1121 = 2000.349154 (COEFFICIENTIAL - 1/400)
 Z1122 = 2000.349154 (COEFFICIENTIAL - 1/400)

POINT NO.	AXIAL DISTANCE (Z/IN)	RADIAL DISTANCE (R/IN)	STREAMLINE DISTANCE (S/IN)	PRESSURE (PSIA)
1	0.000000	0.000000	0.000000	0.000000
2	0.000000	0.000000	0.000000	0.000000
3	0.000000	0.000000	0.000000	0.000000
4	0.000000	0.000000	0.000000	0.000000
5	0.000000	0.000000	0.000000	0.000000
6	0.000000	0.000000	0.000000	0.000000
7	0.000000	0.000000	0.000000	0.000000
8	0.000000	0.000000	0.000000	0.000000
9	0.000000	0.000000	0.000000	0.000000
10	0.000000	0.000000	0.000000	0.000000
11	0.000000	0.000000	0.000000	0.000000
12	0.000000	0.000000	0.000000	0.000000
13	0.000000	0.000000	0.000000	0.000000
14	0.000000	0.000000	0.000000	0.000000
15	0.000000	0.000000	0.000000	0.000000
16	0.000000	0.000000	0.000000	0.000000
17	0.000000	0.000000	0.000000	0.000000
18	0.000000	0.000000	0.000000	0.000000
19	0.000000	0.000000	0.000000	0.000000
20	0.000000	0.000000	0.000000	0.000000
21	0.000000	0.000000	0.000000	0.000000
22	0.000000	0.000000	0.000000	0.000000
23	0.000000	0.000000	0.000000	0.000000
24	0.000000	0.000000	0.000000	0.000000
25	0.000000	0.000000	0.000000	0.000000
26	0.000000	0.000000	0.000000	0.000000
27	0.000000	0.000000	0.000000	0.000000
28	0.000000	0.000000	0.000000	0.000000
29	0.000000	0.000000	0.000000	0.000000
30	0.000000	0.000000	0.000000	0.000000
31	0.000000	0.000000	0.000000	0.000000
32	0.000000	0.000000	0.000000	0.000000
33	0.000000	0.000000	0.000000	0.000000
34	0.000000	0.000000	0.000000	0.000000
35	0.000000	0.000000	0.000000	0.000000
36	0.000000	0.000000	0.000000	0.000000
37	0.000000	0.000000	0.000000	0.000000
38	0.000000	0.000000	0.000000	0.000000
39	0.000000	0.000000	0.000000	0.000000
40	0.000000	0.000000	0.000000	0.000000
41	0.000000	0.000000	0.000000	0.000000
42	0.000000	0.000000	0.000000	0.000000
43	0.000000	0.000000	0.000000	0.000000
44	0.000000	0.000000	0.000000	0.000000
45	0.000000	0.000000	0.000000	0.000000
46	0.000000	0.000000	0.000000	0.000000
47	0.000000	0.000000	0.000000	0.000000

49	5.7445E-01	9.7402E-01	4.0619E-01	1.1181E-03
50	2.9337E-01	1.1412E-01	2.1664E-01	3.6050E-07
51	2.3231E-01	1.4478E-01	2.6421E-01	1.0278E-07
52	4.0715E-01	1.7078E-01	4.6872E-01	7.9433E-04
53	3.5018E-01	1.5560E-01	4.2125E-01	1.2634E-03
54	3.7502E-01	1.4511E-01	4.4873E-01	1.3691E-03
55	3.8877E-01	1.4604E-01	5.1299E-01	1.0410E-03

.....
STREAMTUBE KINETICS/CONDENSATION CALCULATION
.....

STREAMTUBE NO. 1 CALCULATION PASS NO. 1

CHEMICAL KINETICS CALCULATION BEING PERFORMED
ON THIS PASS FOR PRESSURE DEFINED STREAMTUBE.

SPECIES RESULTING ON AFTER THERMODYNAMIC TAPE

1 M2	22 C2	43 C2F	64 C14	84 AL	104 G4H
2 M2	23 C2	44 C2F2	65 C2F4	85 ALP	105 PHOTON
3 O4	24 C2	45 C2F2	66 N2	86 ALP2	106 Z
4 O2	25 C4	46 d	67 N2	87 ALCL	107 MFI
5 O	26 C2	47 CL	68 HCO	88 ALCL2	108 MFI2
6 H	27 C4	48 CL2	69 HCO2	89 ALCL3	109 MFI3
7 H2O2	28 C4	49 N	70 C2H	90 ALF	110 MFI4
8 F2	29 C2H2	50 HCL	71 H2O2	91 ALF2	111 MFI5
9 HF	30 C4	51 CLF	72 H2O2	92 ALF3	112 MFI6
10 F	31 HCN	52 CNCL	73 COF2	93 ALCL	113 MFI7
11 M2	32 H2	53 CNF	74 N2	94 ALF	114 MFI
12 N2	33 H2	54 CF	75 NH	95 ALCLF	115 MFI2
13 N2	34 H2	55 C2F2	76 NH2	96 ALCL2F	116 MFI3
14 O2	35 HCL	56 O3	77 NH3	97 ALCLF2	117 MFI2
15 O2	36 HCL2	57 H2	78 NH	98 NH2	118 MFI4
16 E2	37 HCL3	58 N2O2	79 NH2	99 NH2O	119 MFI2
17 F2	38 HF	59 NA	80 NH3	100 NH2O	120 MFI1
18 S	39 HF2	60 NA2	81 M2H2	101 NH	121 MFI2
19 SF4	40 HF3	61 NAH	82 H2O2	102 M22	122 ME
20 SF6	41 HCL	62 CF2	83 H2O3	103 M2	123 CO2H
21 C	42 HCF	63 CF3			

Reproduced from
best available copy.

SEQUENTIAL MICON TEST CASE

CO	0.2017		
CO2	6.92E-02		
H2	0.020		
N2	0.42509741		
NO	0.002		
OH	0.00067		
O2	0.000764		
C	1.69E-11		
H2O	0.2736		
H	0.00119		
N	1.39E-06		
O	6.17E-04		
REACTIONS			
O2 = 2*O,	A=3.3E+17, N=1.7, P=0.0,		REACTION 1
N2 = 2*N,	A=9.6E+17, N=1.7, B=0.0,		REACTION 2
NO = N + O,	A=7.2E+15, N=0.5, B=0.0,		REACTION 3
H2 = 2*H,	A=5.0E+15, N=1.7, H=0.0,		REACTION 4
H2O = H + OH,	A=1.17E+17, N=0.7, H=0.0,		REACTION 5
OH = H + O,	A=2.3E+15, N=0.7, H=0.0,		REACTION 6
CO2 = CO + O,	A=5.1E+15, N=0.0, B=3.58,		REACTION 7
CO = C + O,	A=6.0E+07, N=0.7, H=50.0,		REACTION 8
END TMR REAX			
NO + O = O2 + N,	A=3.0E+11, N=0.5, H=7.13,		REACTION 9
NO + N = N2 + O,	A=5.0E+13, N=0.7, H=75.5,		REACTION 10
N2 + O2 = 2*NO,	A=1.0E+13, N=0.7, H=79.488,		REACTION 11
CO + O2 = CO2 + O,	A=1.0E+13, N=0.7, H=54.13,		REACTION 12
CO + N = C + NO,	A=1.3E+11, N=0.1, H=0.5,		REACTION 13
CO + O = C + O2,	A=2.4E+13, N=0.7, H=1.99,		REACTION 14
CO + H = C + OH,	A=1.2E+14, N=0.7, H=25.83,		REACTION 15

000 • H • 00 • OH,	A05,0E+11,	N00,0,	005,00,	REACTION 16
OH • 0 • H • 02,	A02,00E14,	N00,0,	005,0,	REACTION 17
OH • H2 • H20 • H,	A00,45E13,	N00,0,	000,1,	REACTION 18
000H • H20 • 0,	A09,79E13,	N00,0,	0010,0,	REACTION 19
H2 • 0 • 0 • OH • H,	A07,30E10,	N00,0,	000,0,	REACTION 20
H2 • 02 • 20H,	A04,90E23,	N02,0,	0009,7,	REACTION 21
NO • CO • CO2 • N,	A01,0E13,	N00,0,	009,93,	REACTION 22
NO • H • OH • H,	A03,4E13,	N00,0,	001,30,	REACTION 23
CO • CO • CO2 • C,	A01,0E13,	N00,7,	009,93,	REACTION 24

LAST CARD

SPECIES TABLE

1	CO	2	CO2
3	H2	4	H2
5	H2O	6	OH
7	O2	8	C
9	H2O	10	H
11	H	12	H

REACTION TABLE

THIRD BODY REACTION 1	A	1.000000E+00	B	0.	N	1.000000E+00
REACTANTS	H2					
PRODUCTS	C	0.0				
THIRD BODY REACTION 2	A	9.000000E+00	B	0.	N	1.000000E+00
REACTANTS	H2					
PRODUCTS	H	0.0				
THIRD BODY REACTION 3	A	7.200000E+00	B	0.	N	5.000000E+01
REACTANTS	NO					
PRODUCTS	H	0.0				
THIRD BODY REACTION 4	A	7.000000E+00	B	0.	N	1.000000E+00
REACTANTS	H2					
PRODUCTS	H	0.0				
THIRD BODY REACTION 5	A	1.170000E+00	B	0.	N	0.
REACTANTS	H2					
PRODUCTS	H	0.0				
THIRD BODY REACTION 6	A	2.500000E+00	B	0.	N	0.
REACTANTS	OH					
PRODUCTS	H	0.0				
THIRD BODY REACTION 7	A	5.100000E+00	B	0.	N	0.
REACTANTS	CO					
PRODUCTS	CO	0.0				
THIRD BODY REACTION 8	A	7.000000E+00	B	0.	N	0.
REACTANTS	CO					
PRODUCTS	C	0.0				
REACTION 9	A	3.000000E+00	B	7.130000E+00	N	5.000000E+01
REACTANTS	NO	0.0				
PRODUCTS	NO	0.0				
REACTION 10	A	5.000000E+00	B	7.500000E+00	N	0.
REACTANTS	NO	0.0				
PRODUCTS	H2	0.0				
REACTION 11	A	7.000000E+00	B	7.000000E+00	N	0.
REACTANTS	H2	0.0				
PRODUCTS	NO	0.0				
REACTION 12	A	1.900000E+00	B	5.450000E+00	N	0.
REACTANTS	CO	0.0				
PRODUCTS	CO	0.0				
REACTION 13	A	1.300000E+00	B	5.000000E+00	N	1.000000E+01
REACTANTS	CO	0.0				
PRODUCTS	C	0.0				
REACTION 14	A	7.000000E+00	B	1.000000E+00	N	0.
REACTANTS	CO	0.0				
PRODUCTS	C	0.0				
REACTION 15	A	1.200000E+00	B	2.500000E+00	N	0.
REACTANTS	CO	0.0				
PRODUCTS	C	0.0				

REACTION 16	AP	9.400000E+11	B= 1.000000E+00	N= 0.1
REACTANTS	CO2	* N		
PRODUCTS	CO	* OH		
REACTION 17	AP	2.700000E+10	B= 1.000000E+01	N= 0.1
REACTANTS	CH	* O		
PRODUCTS	H	* O2		
REACTION 18	AP	8.410000E+13	B= 2.010000E+01	N= 0.1
REACTANTS	OH	* H2		
PRODUCTS	H2O	* H		
REACTION 19	AP	9.750000E+13	B= 1.000000E+01	N= 0.1
REACTANTS	OH	* OH		
PRODUCTS	H2O	* O		
REACTION 20	AP	7.000000E+12	B= 0.1	N= 0.1
REACTANTS	H2	* N		
PRODUCTS	CH	* H		
REACTION 21	AP	4.900000E+23	B= 0.970000E+01	N= 2.500000E+00
REACTANTS	H2	* O2		
PRODUCTS	CH	* OH		
REACTION 22	AP	1.000000E+13	B= 9.930000E+00	N= 0.1
REACTANTS	NO	* CO		
PRODUCTS	CO2	* N		
REACTION 23	AP	0.100000E+10	B= 1.000000E+00	N= 0.1
REACTANTS	NO	* H		
PRODUCTS	CH	* N		
REACTION 24	AP	1.000000E+13	B= 9.530000E+00	N= 0.1
REACTANTS	CO	* CC		
PRODUCTS	CO2	* O		

DISSOCIATION RECOMBINATION REACTION RATE RATIOS

ALL REACTION RATE RATIOS INPUT AS 1.0

000100

1	0.	0.85060790E+01	-1.00000015E+01
2	9.5000416E-02	0.67200017E+01	-1.70737941E+01
3	1.7540749E-01	0.90079200E+01	-1.00000000E+01
4	2.40949521E-01	0.32247240E+01	-0.00052731E+01
5	3.0243907E-01	0.12501941E+01	-1.90220310E+01
6	4.7920000E-01	0.00000000E+01	-0.77514400E+01
7	5.73391971E-01	5.73329742E+01	-0.23970400E+01
8	6.40019014E-01	5.51634019E+01	-0.330773120E+01
9	7.0420000E-01	5.00000000E+01	-0.13444400E+01
10	8.3962000E-01	5.00036370E+01	-0.33992100E+01
11	9.35017175E-01	4.44270900E+01	-0.23042770E+01
12	1.0000000E+00	4.0444000E+01	-0.23000447E+01
13	1.1050000E+00	4.30007432E+01	-0.230000310E+01
14	1.24121470E+00	4.16401921E+01	-0.234070010E+01
15	1.3000000E+00	3.04074027E+01	-0.23000017E+01
16	1.4320000E+00	3.72340299E+01	-0.24020400E+01
17	1.5375752E+00	3.51100479E+01	-0.210792930E+01
18	1.6000000E+00	3.0000000E+01	-0.10000400E+01
19	1.71003374E+00	3.09001333E+01	-0.20564601E+01
20	1.81422511E+00	2.9020390E+01	-1.50734302E+00
21	1.9000000E+00	3.03403165E+01	-0.30400000E+01
22	1.9024607E+00	2.00344671E+01	-0.204711477E+01
23	2.30730095E+00	2.49121237E+01	-1.07071179E+01
24	2.0000000E+00	3.4444000E+01	-1.00734746E+01
25	2.3302041E+00	2.2227100E+01	-1.713357207E+01
26	2.40500477E+00	1.00139240E+01	-1.54640427E+01
27	2.0000000E+00	1.0000000E+01	-1.0000000E+01
28	2.0044920E+00	1.40100099E+01	-1.10794440E+01
29	3.11009975E+00	1.20924919E+01	-0.47600042E+00
30	2.0000000E+00	0.0000000E+01	-0.0000000E+01

31	3,700000718E+00	7,03913914E+00	-5,27672137E+00
32	4,270000000E+00	4,00101200E+00	-3,14004000E+00
33	4,700000000E+00	3,40000000E+00	-1,30000000E+00
34	5,700000000E+00	2,40000000E+00	-9,96744300E+01
35	7,34204049E+00	1,41177214E+00	-6,13237000E+01
36	7,10000000E+00	1,10000000E+00	-3,70000000E+01
37	8,33517710E+00	1,04020247E+00	-3,07004020E+01
38	8,79000000E+00	9,22000000E+01	-2,97014400E+01
39	9,70000000E+00	7,00000000E+01	-2,13000000E+01
40	9,91190951E+00	6,7940034E+01	-1,00441000E+01
41	1,17763502E+01	5,47400201E+01	-1,20097344E+01
42	1,10361702E+01	4,31472003E+01	-9,42000205E+02
43	1,20200308E+01	3,45467430E+01	-6,01377105E+02
44	1,41760208E+01	2,72300308E+01	-4,00723003E+02
45	1,57116007E+01	2,09135740E+01	-3,43049400E+02
46	1,74324003E+01	1,60036301E+01	-2,35004370E+02
47	1,90207040E+01	1,30002255E+01	-1,93300170E+02
48	1,93221000E+01	1,30001073E+01	-9,09144302E+03
49	1,99071074E+01	1,20120000E+01	-1,51097000E+02
50	2,10231404E+01	1,00312037E+01	-1,37500015E+02
51	2,20001051E+01	9,02015025E+02	-9,71172113E+03
52	2,50750432E+01	5,92441300E+02	-7,16359705E+03
53	2,80740100E+01	4,39424035E+02	-4,4100227E+03
54	3,20302030E+01	2,04131770E+02	-3,15041973E+03
55	3,97010510E+01	2,17304400E+02	-1,00707950E+03
56	4,13071054E+01	1,30413004E+02	-1,40972430E+03

INITIAL CONDITIONS KINETIC STREAMTUBE CALCULATION AXIAL POSITION = 0.

INPUT NORMALIZING INITIAL SCALE FACTOR (P1) 0.10000E+02

FLOW PROPERTIES

MACRO NUMBER 5.9104233E+01 COUPLING TERM A -9.07900044E+01
 PRESSURE (PSIA) 6.8580073E+01 COUPLING TERM B 1.2001002E+00
 TEMPERATURE (DEGR) 2.1523072E+02
 DENSITY (LB/FT3) 5.0010000E+03 INTEGRATION PARAMETERS
 ENTHALPY (BTU/LB) 2.1390922E+02 CURRENT STEP SIZE 1.0000000E+04
 GAS MOLECULAR WEIGHT 2.9545072E+03 PERCENT ENTHALPY CHANGE 0.
 HEAT CAPACITY (BTU/LB-DEGR) 5.2734014E+01 1.0 = SUMMATION C(1) -1.00340737E+11
 PRESSURE (PSIA) 6.8580073E+01 KINETIC RELATIVE ERROR 0.
 GAS CONST (FT2/SEC2/DEGR) 2.5264453E+03 GOVERNING EQUATION 0.
 SUM C(1)*H(1) (FT2/SEC2) 1.13420021E+07

CHEMICAL COMPOSITION

NO.	SPECIES	MACRO FRACTION	MOLE FRACTION	NO.	SPECIES	MACRO FRACTION	MOLE FRACTION
1	CO	2.017000E+01	1.417122E+01	2	CO2	0.220000E+02	2.919228E+02
3	H2	2.000000E+02	1.92243E+01	4	N2	4.250970E+01	2.906197E+01
5	H2O	0.000000E+00	1.511665E+02	6	OH	0.070000E+00	1.110031E+00
7	O2	7.040000E+04	4.600654E+04	8	C	1.090000E+11	2.709093E+11
9	H2O	2.730000E+01	2.090922E+01	10	H	1.150000E+03	2.245204E+02
11	H	1.300000E+00	1.050045E+00	12	O	0.170000E+04	2.500100E+04

KINETIC STREAMTUBE CONDITIONS AXIAL POSITION 1.50000E+03

FLOW PROPERTIES

MACH NUMBER 5.91986746E-01
 PRESSURE (PSIA) 6.8480752E-01
 VELOCITY (FT/SEC) 5.9566695E+08
 TEMPERATURE (DEG-R) 5.8733736E+03
 DENSITY (LB/FT3) 2.11624112E-02
 ENTHALPY-H0 (BTU/LB) 2.49649935E+03
 GAS MOLECULAR WEIGHT 1.9470972E-01
 HEAT CAPACITY(MTU/LB-DEG-R) 5.2722962E-01
 PRIMER-ORIGIN 1.87703943E+08
 GAS CONST(F72/SEC2/DEG-R) 2.52763041E-03
 SUM C(I)*M(I) (F72/SEC2) 1.13363626E+07

KINETIC COUPLING TERMS

COUPLING TERM A -8.98484298E-01
 COUPLING TERM B 1.19587304E+00

INTEGRATION PARAMETERS

CURRENT STEP SIZE 2.00000000E-04
 PERCENT ENTHALPY CHANGE -3.24842935E+03
 1.0 = SUMMATION C(I) -1.08256320E-11
 MAXIMUM RELATIVE ERROR 4.38474617E-03
 GOVERNING EQUATION 13

CHEMICAL COMPOSITION

NO.	SPECIES	MASS FRACTION	MOLE FRACTION	MOLEC/CC	NO.	SPECIES	MASS FRACTION	MOLE FRACTION	MOLEC/CC
1	CO	2.017276E+01	1.416631E-01	1.4856E+10	2	CO2	6.915671E-02	2.912221E-02	3.0349E+17
3	N2	2.002337E+02	1.984744E-01	2.04490E+10	4	N2	4.288974E-01	2.084734E-01	3.2306E+18
5	NO	1.998918E+03	1.318977E-03	1.3748E+10	6	OH	1.336444E-02	1.198726E-02	1.2371E+17
7	O2	7.01127E+04	4.67254E-04	4.9000E+15	8	C	1.823433E-11	2.986329E-11	3.1317E+08
9	H2O	2.350744E+01	9.881841E-01	2.1248E+10	10	H	1.156227E-03	2.256350E-02	2.3646E+17
11	N	1.436837E+00	2.01774E-04	2.1139E+13	12	O	6.242380E-04	7.874615E-04	8.0482E+15

KINETIC STREAMTUBE CONDITIONS AXIAL POSITION 3.50000E+03

FLOW PROPERTIES

MACH NUMBER 5.93202866E+01
 PRESSURE (PSIA) 6.84634830E+01
 VELOCITY (FT/SEC) 2.55948966E+03
 TEMPERATURE (DEG-R) 5.85429834E+03
 DENSITY (LB/FT3) 2.14094886E+02
 ENTHALPY-HR (BTU/LB) 2.49149337E+03
 GAS MOLECULAR WEIGHT 2.95393392E+01
 HEAT CAPACITY(BTU/LB-DEGR) 5.27891098E+01
 FROZEN SUMMA 1.27727090E+09
 GAS CONST(P72/SEC2/DEGR) 2.52912931E+03
 SUM C(1)H(1) (P72/SEC2) 1.13276337E+07

KINETIC COUPLING TERMS

COUPLING TERM A -8.09136830E+01
 COUPLING TERM B 1.00693470E+00
 INTEGRATION PARAMETERS
 CURRENT STEP SIZE 2.00000002E+04
 PERCENT ENTHALPY CHANGE -7.93211095E+03
 1.0 - SUMMATION C(1) -1.07972303E+11
 MAXIMUM RELATIVE ERROR 1.33963948E+03
 GOVERNING EQUATION 19

CHEMICAL COMPOSITION

NO.	SPECIES	MASS FRACTION	MOLE FRACTION	MOLES/CC	NO.	SPECIES	MASS FRACTION	MOLE FRACTION	MOLES/CC
1	CO	2.017555E-01	1.416038E-01	1.4877E+18	2	CO2	6.511285E-02	2.908534E-02	3.0558E+17
3	H2	2.006179E-02	1.956357E-01	2.0554E+18	4	N2	4.250976E-01	2.982987E-01	3.1340E+18
5	NO	1.000000E-03	1.318157E-03	1.3744E+16	6	OH	1.188343E-02	1.281128E+02	1.3460E+17
7	O2	7.376849E-04	4.684379E-04	4.8980E+15	8	C	1.998426E-11	3.257885E-11	3.4228E+00
9	H2O	2.723888E-01	2.971476E-01	3.1219E+18	10	H	1.171314E-03	2.284459E+02	2.4081E+17
11	H	1.492545E-06	2.094669E-06	2.18887E+13	12	O	6.408886E-04	7.985281E+04	8.3894E+19

KINETIC STEADY-STATE CONDITIONS AL POSITION 5,300000E-03

FLOW PROPERTIES

MACH NUMBER	5.9437204E-01	KINETIC COUPLING TERMS	
PRESSURE (PSIA)	4.8404134E-01	COUPLING TERM A	-7.4553702E-01
VELOCITY (FT/SEC)	2.1429000E-01	COUPLING TERM B	1.0177210E-00
TEMPERATURE (DEGR)	5.1832037E-03	INTEGRATION PARAMETERS	
DENSITY (LB/FT3)	2.1133349E-02	CURRENT STEP SIZE	2.0000000E-04
ENTHALPY (BTU/LB)	2.4148939E-03	PERCENT ENTHALPY CHANGE	-1.1949249E-02
GAS MOLECULAR WEIGHT	1.9448330E-01	1/J = SUMMATION (1/J)	-1.0775914E-11
HEAT CAPACITY (BTU/LB-DEGR)	5.1219671E-01	MAXIMUM RELATIVE ERROR	1.0904431E-03
PROBLEM NAME	1.1249940E-00	GOVERNING EQUATION	0
GAS CONST (FT2/SEC2/DEGR)	2.5105452E-03		
SUM C(1)M(1) (FT2/SEC2)	1.1110010E-07		

CHEMICAL COMPOSITION

NO.	SPECIES	MASS FRACTION	MOLE FRACTION	MOLEC/CC	NO.	SPECIES	MASS FRACTION	MOLE FRACTION	MOLEC/CC
1	CO	2.01774E-01	1.4153E-01	1.4005E-10	2	CO2	6.94000E-02	2.90944E-02	3.0377E-17
3	H2	2.00774E-02	1.9567E-01	2.0393E-10	4	H2	4.25007E-01	2.99131E-01	3.11379E-10
5	NO	1.99974E-03	1.30037E-03	1.3740E-10	6	OH	1.103667E-02	1.34420E-02	1.4147E-17
7	O2	7.95000E-04	4.05474E-04	4.0000E-15	8	C	2.140019E-11	3.511900E-11	3.0999E-00
9	H2O	2.710000E-01	2.96311E-01	1.1184E-10	10	H	1.191498E-03	2.322430E-02	2.4441E-17
11	N	1.942234E-00	7.163179E-00	7.2709E-13	12	O	6.85277E-04	6.415347E-04	8.8902E-19

KINETIC STEADY-STATE CONDITIONS AXIAL POSITION 3.34895E+01

FLOW PROPERTIES

MACH NUMBER	0.0784573E+00	KINETIC COUPLING TERMS
PRESSURE (PSIA)	2.9181132E+02	COUPLING TERM A
VELOCITY (FT/SEC)	1.1230918E+04	COUPLING TERM B
TEMPERATURE (DEGR)	1.8025923E+03	INTEGRATION PARAMETERS
DENSITY (LB/FT3)	4.2174768E+05	CURRENT STEP SIZE
ENTHALPY-H0 (BTU/LB)	1.7602499E+02	PERCENT ENTHALPY CHANGE
GAS MOLECULAR WEIGHT	1.9415918E+01	1.0 - SUMMATION C(I)
HEAT CAPACITY (BTU/LB-DEGR)	3.9724572E+01	MAXIMUM RELATIVE ERROR
PROPER GAMMA	1.9948222E+00	GOVERNING EQUATION
GAS CONST (FT2/SEC2/DEGR)	2.5147794E+03	13
SUM C(I)*H(I) (FT2/SEC2)	-4.8163690E+07	

CHEMICAL COMPOSITION

NO.	SPECIES	MASS FRACTION	MOLE FRACTION	MOLEC/CC	NO.	SPECIES	MASS FRACTION	MOLE FRACTION	MOLEC/CC
1	CO	1.972645E-01	1.381416E-01	1.3342E+15	2	CO2	7.216597E-02	3.214407E+02	7.7633E+14
3	H2	1.001552E+02	1.048495E-01	4.4422E+15	4	H2	4.255928E-01	2.978309E-01	7.1837E+19
5	H2O	2.012997E+03	1.319922E-03	1.1799E+13	6	OH	8.319894E-04	9.584488E-04	2.3180E+13
7	O2	1.099824E+03	4.741755E-04	1.6272E+13	8	C	4.190070E-12	6.842928E-12	1.6516E+09
9	H2O	2.802941E+01	3.051715E-01	7.3059E+15	10	H	2.031505E+03	3.953632E+02	9.5422E+14
11	H	1.078045E+07	9.340310E-07	9.14487E+09	12	O	2.888715E-04	3.538984E-04	8.8421E+13

KINETIC STREAMTUBE CONDITIONS AXIAL POSITION 3.40110E+01

FLOW PROPERTIES		KINETIC COUPLING TERMS	
MACH NUMBER	6.15930243E-00	COUPLING TERM A	9.15007303E-00
PRESSURE (PSIA)	2.41876414E-02	COUPLING TERM B	-0.12723442E-00
TEMPERATURE (DEG-R)	1.12320110E-00	INTEGRATION PARAMETERS	
DENSITY (LB/FT3)	9.73205504E-02	CURRENT STEP SIZE	2.04000000E-01
ENTHALPY (BTU/LB)	3.0009723E-03	PERCENT ENTHALPY CHANGE	1.41799700E-01
GAS MOLECULAR WEIGHT	1.00740130E-02	1.0 - SUMMATION C(1)	-1.4302000E-11
HEAT CAPACITY (BTU/LB-DEG-R)	1.00120127E-01	RELATIVE ERROR	9.0976509E-04
PROBEM GROSS	1.15903219E-00	GOVERNING EQUATION	13
GAS GROSS (FT2/SEC2)	2.3347790E-03		
SUM C(1)*H(1) (FT2/SEC2)	-4.04402940E-07		

Chemical Composition

NO.	SPECIES	MASS FRACTION	MOLEC/CC	NO.	SPECIES	MASS FRACTION	MOLE FRACTION	MOLEC/CC
1	CO	1.972054E+01	1.30145E-01	3	CO2	7.210703E-02	3.210001E-02	7.1010E+10
2	H2	1.001504E+02	1.000000E-01	4	HC	4.250000E-01	2.000000E-01	6.70000E+20
3	H2O	2.012057E+03	1.319022E-03	5	OH	0.200420E-04	9.540901E-04	2.1203E+13
7	O2	1.100020E+03	6.742999E-04	6	C	4.100770E-12	6.042037E-12	1.9834E+03
8	H2O	6.000000E-02	3.000000E-01	10	H	2.001000E-03	3.000000E-03	0.0001E+04
11	N	1.070302E+07	2.33004E-07	12	O	2.905143E-04	3.561017E-04	7.9200E+12

STEP SIZE HALVED AT 2 3.0459000E-01

KINETIC STREAMTUBE CONDITIONS AXIAL POSITION 3.62503E+01

FLOW PROPERTIES		KINETIC COUPLING TERMS	
MACH NUMBER	0.272608E+00	COUPLING TERM A	7.9481951E+00
PRESSURE (PSIA)	2.0710020E+02	COUPLING TERM B	-7.9590729E+00
VELOCITY (FT/SEC)	1.1590200E+04	INTEGRATION PARAMETERS	
TEMPERATURE (DEG-R)	9.3708061E+02	CURRENT STEP SIZE	1.0240000E+01
DENSITY (LB/FT3)	3.4483087E+05	PERCENT ENTHALPY CHANGE	1.4582787E+01
ENTHALPY (BTU/LB)	1.5750454E+02	1.0 - SUMMATION C(1)	-1.4489807E+11
GAS MOLECULAR WEIGHT	1.0115913E+01	MAXIMUM RELATIVE ERROR	1.7593469E+02
HEAT CAPACITY (BTU/LB-DEG-R)	3.8246297E+01	GOVERNING EQUATION	2
PRESENCE DATA	1.3580789E+00		
GAS CONDUCTIVITY (BTU/SEC2/DEG-R)	2.5147795E+03		
SUM C(1)*H(1) (FT2/SEC2)	-4.7196282E+07		

CHEMICAL COMPOSITION

NO	SPECIES	MASS FRACTION	MOLE FRACTION	NO	SPECIES	MASS FRACTION	MOLE FRACTION
1	CO	1.972441E+01	1.381370E-01	7	CO2	7.121072E+02	3.210974E+02
3	H2	1.801348E+02	1.84647E-01	4	H2O	4.250929E+01	2.978309E+01
5	NO	2.012897E+03	1.028802E+00	6	O2	8.220291E+04	9.490000E+04
7	O2	1.100240E+03	6.744952E+04	8	C	4.189401E+12	6.041934E+12
9	H2O	2.002949E+01	3.051922E-01	10	H	2.051920E+03	3.993304E+02
11	N	1.009841E+07	2.789744E+07	12	O	2.931449E+04	3.804114E+04

KINETIC STRUCTURE CONDITIONS AXIAL POSITION 3.99367E+01

FLOW PROPERTIES		KINETIC COUPLING TERMS	
ALICH NUMBER	6.61872787E+00	COUPLING TERM A	3.76682219E+00
PROBABILITY (PBLA)	1.56176724E+02	COUPLING TERM B	-5.0034351E+00
TEMPERATURE (TEMP)	2.32000000E+00	INTEGRATION PARAMETERS	
TEMPERATURE (TEMP)	8.56472748E+02	CURRENT STEP SIZE	
TEMPERATURE (TEMP)	2.71799715E+00	PERCENT ENTHALPY CHANGE	
TEMPERATURE (TEMP)	1.34934071E+00	PERCENT ENTHALPY CHANGE	
TEMPERATURE (TEMP)	1.96139103E+01	PERCENT ENTHALPY CHANGE	
TEMPERATURE (TEMP)	2.81429130E+01	PERCENT ENTHALPY CHANGE	
TEMPERATURE (TEMP)	1.30000000E+00	PERCENT ENTHALPY CHANGE	
TEMPERATURE (TEMP)	2.31477734E+03	PERCENT ENTHALPY CHANGE	
TEMPERATURE (TEMP)	-4.74676482E+07	PERCENT ENTHALPY CHANGE	

CHEMICAL COMPOSITION

NO.	SPECIES	MASS FRACTION	MOLEC/CC	NO.	SPECIES	MASS FRACTION	MOLEC/CC
1	CO	1.972010E+01	1.381303E+01	2	CO2	7.217330E+02	3.216730E+02
3	H2	2.002440E+00	1.040990E+01	4	H2O	4.890000E+01	2.070300E+01
5	H2	2.012937E+03	1.319822E+03	6	OH	8.138900E+04	9.377962E+04
7	O2	1.100700E+03	6.747614E+04	8	C	4.100703E+12	6.040026E+12
9	H2O	2.002440E+00	1.040990E+01	10	H	2.002440E+00	1.040990E+01
11	N	1.667214E+07	2.334599E+07	12	O	2.989295E+04	3.064736E+04

KINETIC STREAMTUBE CONDITIONS AXIAL POSITION 4.136718E-01

FLOW PROPERTIES

MACH NUMBER 6.74519482E-00
 PRESSURE (PSIA) 1.34413084E-02
 VISCOSITY (CP) 1.72410900E-04
 TEMPERATURE (DEG-R) 8.27423195E-02
 DENSITY (LB/FT3) 2.4488095E-05
 ENTHALPY-H0 (BTU/LB) 1.37447048E-02
 GAS MOLECULAR WEIGHT 1.94155185E-01
 HEAT CAPACITY (BTU/LB-DEG) 3.79501085E-01
 PROPER NAME 1234567890
 GAS CONST (FT2/SEC2) 2.54677938E-03
 SUM C111-M11 (FT2/SEC2) -4.67851282E-07

KINETIC COUPLING TERMS

COUPLING TERM A 5.0000000E-00
 COUPLING TERM B -5.10001033E-00
 INTEGRATION PARAMETERS
 CURRENT STEP SIZE 4.0000000E-01
 PERCENT ENTHALPY CHANGE 1.00707148E-01
 1,0 - SUMMATION C11 -1.03742705E-11
 MAXIMUM RELATIVE ERROR 2.00735007E-03
 GOVERNING EQUATION 12

CHEMICAL COMPOSITION

NO.	SPECIES	MOLES/CC	MOLE FRACTION	NO.	SPECIES	MOLES/CC	MOLE FRACTION	NO.	SPECIES	MOLES/CC	MOLE FRACTION
1	CO	1.97261E-01	1.38137E-01	2	CO2	7.21740E-02	3.21670E-02	4	NO2	4.7099E-14	
3	H2	1.09164E-02	1.54597E-01	4	N2	4.29802E-01	2.07630E-01	4	NO	4.0314E-13	
5	H2O	2.01993E-03	1.52502E-03	6	OH	0.09034E-04	9.33990E-04	1	NO2	1.0904E-13	
7	O2	1.10094E-03	6.74061E-04	8	C	4.10861E-12	6.84854E-12	1	NO2	1.0109E-03	
9	H2O	2.00294E-01	3.05184E-01	10	H	2.03125E-03	3.95279E-02	5	NO2	5.0003E-14	
11	H	1.04409E-07	8.8374E-07	12	O	3.01092E-04	3.68041E-04	5	NO2	5.0003E-13	

MAX AND MIN FOR REACTION PRODUCTION RATES

J,X(I),MAX,Z FOR MAX,...X(J)MIN,Z FOR MIN

1	4.5771280E+01	0.	-8.1496494E+09	4.1367149E+01
2	0.8594590E+09	0.	-9.4780042E+11	4.1367149E+01
3	2.8941173E+03	0.	1.33504720E+00	2.0910000E+01
4	4.7712442E+03	0.	3.04100737E+02	2.7390000E+01
5	2.2600079E+09	0.	-8.9031970E+00	4.1367149E+01
6	2.6116009E+03	5.5000000E+03	-9.1762804E+02	2.7470000E+01
7	2.58440627E+03	0.	-4.20720063E+03	4.1367149E+01
8	5.1272014E+16	0.	-1.05400074E+42	4.1367149E+01
9	2.12742817E+01	2.5000000E+02	-1.05455411E+09	4.1367149E+01
10	-4.92461407E+00	1.1590000E+01	-4.06562126E+04	1.7095000E+00
11	4.6426000E+03	1.5710000E+01	-7.02730405E+36	4.1367149E+01
12	-1.09695649E+00	3.0700000E+02	2.5687593E+10	4.1367149E+01
13	2.10043429E+07	0.	-2.05071173E+10	1.7950000E+01
14	9.0061303E+09	0.	1.77640027E+07	1.6350000E+01
15	3.49207040E+04	0.	-1.47023770E+17	4.1367149E+01
16	8.32370429E+03	0.	1.03433667E+00	2.0910000E+01
17	5.01300776E+03	5.0700000E+02	8.41251148E+03	7.3735000E+00
18	-1.0807964E+09	0.	2.0727270E+00	6.2150000E+01
19	-6.36994089E+03	0.	2.7794676E+09	3.1230000E+01
20	-1.00134943E+04	9.2000000E+03	2.39614913E+00	2.9230000E+01
21	-4.7796232E+00	2.9000000E+02	-4.7326221E+39	4.1367149E+01
22	3.43241200E+00	0.	-5.65240070E+09	4.1367149E+01
23	2.70328019E+01	0.	-6.76379349E+02	4.1367149E+01
24	6.7783525E+04	0.	-1.6506037E+00	4.1367149E+01

5. SURFACE EFFECTS DETERMINATIONS

The calculation of the effects of the impingement of the plume gas, large fuel and oxidizer droplets, and small condensation droplets upon the space vehicle appendages and surface is carried out in the segment SURFACE of CONTAM.

SURFACE is discussed in detail in Appendix D and the reader is referred to that section of the report for a complete description of all program overlays and inputs. The material that will be covered below will be directed at the problem of interfacing the outputs of TCC, MULTRAN, and KINCON with SURFACE.

It is assumed that the user has operated SURFACE under "STPFLG = 1" and has obtained a table listing the surface segments that the plume will impinge upon. In the sample case, a "p" value (one-half semi-latus rectum) of 0.14 has been used as a nominal value to obtain the data for thruster No. 2, as illustrated.

Thruster No. 2 is located 6 inches off the skin of the vehicle and 3.6 feet back from the leading tip. The thruster is part of the RCS.

Inspection of the table "Thruster-Based Coordinates of Plume-Impinged Segments" reveals that segments 52, 62, 72, 82, 91, 92, 93, 101, 102, and 103 will be impinged by the thruster plume. The outputs of the preceding programs will be interfaced with the input data required for SURFACE at location 52. This will amply demonstrate the techniques required to solve for the surface effects on any segment on the vehicle.

Referring back to the first kinetic streamtube condition printout of KINCON, the "Input Normalizing Axial Scale Factor (FT) is approximately 0.008. This figure is simply the throat radius of the nozzle given in the proper system of measure. By dividing the values obtained from SURFACE by this factor the whole problem is quickly converted into the normalized units employed in MULTRAN and KINCON, i. e., $R/RC = 62.5$ and $Z/RC = 215.6$.

At this point it is suggested as good practice to make a plot of R/RC vs Z/RC for the particle limiting streamline, obtained from the printout of TD2 and TD2P and the gas limiting mass streamlines, obtained from the printout of SLINES. The location of the nozzle wall can also be ascertained from TD2.

Referring to the first page of the characteristic calculation printout of the Gas-Particle Flow (Nozzle), e. g., TD2, any streamline identified by a "4" is part of the limiting particle streamline, and any printout identified by "5" is part of the boundary or in this case the nozzle wall. When looking at TD2P output the latter identification is not of concern since the calculations of TD2 end at the exit of the nozzle. The limiting particle streamline, however, continues and may be traced out to the end of the TD2P solution.

THRUSTOR-BASED COORDINATES
OF PLUME-IMPINGED SEGMENTS

FROM THRUSTOR NO. 2 WHEN P₀ = .14

SEG ID	AXIAL DIST Z (FT)	RADIAL DIST R (FT)	ANGULAR COORD THE(RAD)
52	1.72500	.5000	-1.5695
92	5.72500	.5000	-1.5695
72	5.72500	.5000	-1.5695
82	5.72500	.5000	-1.5695
91	5.72500	1.23798	-.70052
92	5.72500	.5000	-1.5695
93	5.72500	1.23798	.70052
101	6.72500	1.23798	-.70052
102	6.72500	.5000	-1.5695
103	6.72500	1.23798	.70052

* ANGLE FROM LINE JOINING
AXES OF SATELLITE AND THRUSTOR

USE COORDINATES Z AND R IN DETERMINATION OF PLUME CHARACTERISTICS
FOR INPUT TO REPLACE DEFAULT VALUES ON EDATA = TAPF11

The printout of SLINES or the Streamline Generation Program gives a table of various gas phase limiting mass streamlines in terms of Z/RC , R/RC , and S/RC . A direct plot of the first two items will produce the needed curve and correlation of this data with the last item will allow identification of proper KINCON information that will later be required as input to SURFACE.

The drawing shown displays the particle limiting streamline and the mass limiting gas phase streamlines for the values of 0.0, 25.0, 50.0, and 80.0 percent of the total mass. Inspection of this graph quickly reveals that the required location, as given by SURFACE, is far beyond the calculated data of CONTAM to this point of the solution.

When dealing with very small RCS engines, the normalizing factor of the throat radius will produce a characteristic grid mesh so fine in comparison to the characteristic size of the space vehicle that a computer solution taken out to this point is very costly. However, inspection of the streamline plot and the outputs of KINCON to the point they have been carried out demonstrate that the complete MOC calculation is not necessary. The streamlines have all become straight lines and the chemistry has frozen, thus enabling accurate and relatively simple extrapolation.

The methods suggested to obtain the required information at the called for SURFACE segments will now be discussed item by item, including the assumptions used whenever an extrapolation of MULTRAN or KINCON results is carried out.

Attention is directed to Appendix D. The array PLMCHR of the data set EDATA contains the needed input information for each of the segment locations called for. Note should be taken of the proper formats and the fact that three blank cards must precede input of the item NPMCR. These three cards may contain comments as they are not read by the program.

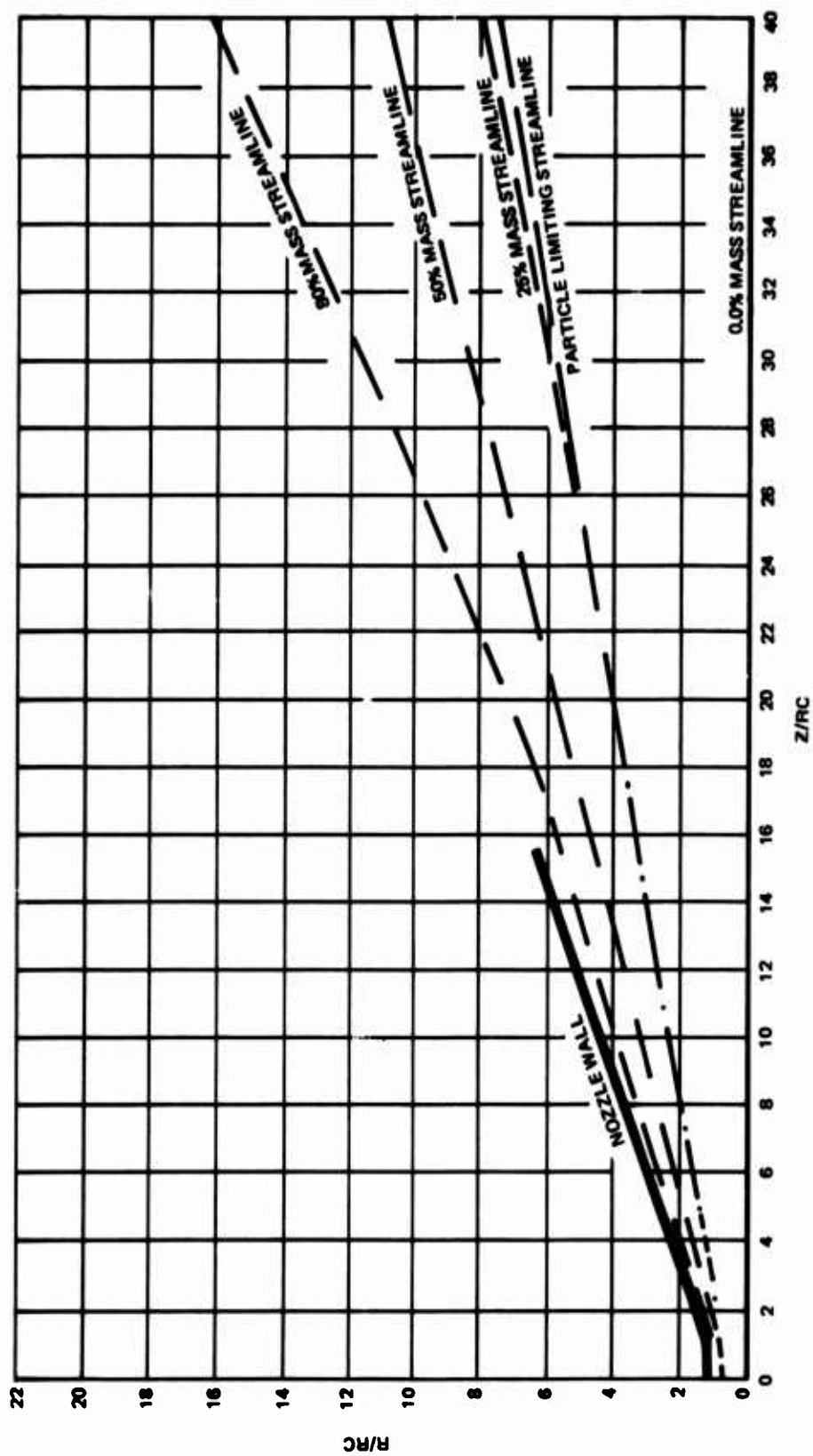
Extrapolation of the 25 percent mass limiting streamline and the particle limiting streamline data to the approximate region of interest on the surface have been used to obtain the data that will now be discussed.

PLMCHR(1) and PLMCHR(2)

SURFACE always assumes that two drop sizes will be given. The small droplet diameter will represent any products of condensation occurring in the plume, and the large droplet will refer to the fuel or oxidizer drops as predicted by TCC.

If the region of the plume of interest is hot or the density is very low (i. e., very few nucleation centers), no condensation will take place. In cooler regions of the plume of sufficient density, the condensation droplets formed will usually have a diameter of the order of one micron or less ($3.94E-05$ ft). This value is suggested for PLMCHR(1).

The large particle size was taken from TCC and MULTRAN; in this case 50 microns ($1.97E-03$ ft), and this value was used for PLMCHR(2).



PLMCHR(3)

The small droplet is assumed to move at the gas velocity. At the end of the KINCON solution the chemistry is frozen as indicated by the constant values of molefractions and the velocity of the gas is nearly constant.

Consequently, assuming the velocity to remain constant in value from this point will produce little or no error in the kinetic energy imparted to the surface of the vehicle. Accordingly, the last velocity figure from KINCON is taken as the input for PLMCHR(3), e.g., 11,417 ft/sec.

PLMCHR(4)

The item VPK in the output of TD2P is the particle velocity in units of ft/sec. The above argument certainly holds also in the case of the particles, and the last value given in TD2P is taken as input for PLMCHR(4). Referring back to the TD2P printout identified by "4", the value of 1,697 ft/sec is obtained.

PLMCHR(5) and PLMCHR(6)

The parameters of THETA-G and THETA-K of the TD2P output give the gas and particle streamline angles, respectively. Since the streamlines has become straight, it introduces no error to take the last values given for the particle limiting streamline as the inputs for PLMCHR(5) and PLMCHR(6). Care must be taken, however, to make sure the values given in MULTRAN in degrees are converted to radians, e.g., 0.170 and 0.218, respectively.

PLMCHR(7) and PLMCHR(8)

Since there are no small droplets present in this flow a very small number is input into PLMCHR(7), in this case say 10^{-6} . It should be noted that SURFACE will not accept "0" as an input here, but a very small value will accomplish the same task.

The mass flow rate for the larger droplets is not explicitly given in any of the outputs of the previous programs. This value may be determined in the following manner:

From the appropriate page of KINCON kinetics output a value for the gas density at the last S/RC position can be found, e.g., $2.44\text{E-}05 \text{ lb/ft}^3$. The value of density can be extrapolated from this last printout position to the surface point by using a "inverse square of the distance" procedure, i.e., using the radius vector distance at the end of the MOC calculation in comparison to the radius vector in the vicinity of the surface segment, a value for the gas density at the satellite of $8.39\text{E-}08 \text{ lb/ft}^3$ is calculated.

Referring back to the limiting particle TD2P output at the closest value of R/RC and Z/RC for the S/RC value used above gives the value for SDK/DG, the ratio of total particle density to gas density, 3.076. The product this value, the extrapolated gas density, and VPK, the particle velocity, give the estimation of the flow rate needed for input at PLMCHR(8), i.e., $4.38\text{E-}04 \text{ lb/ft}^2\text{-sec}$.

PLMCHR(9) through PLMCHR(31)

At stated earlier, the chemistry has frozen and, therefore, the mass fractions given in the later pages of output from KINCON remain unchanged and are assumed to continue to remain so until the surface point is reached. If any of the species called for in the PLMCHR list are not here, they are input in the proper array location as 0.0 (if the card is simply left blank that will also suffice in the case of EDATA). When a species on the PLMCHR list does exist, the mass fraction is read from the KINCON output and put into the proper position of the data card. In this case all that is matched is water and carbon, i. e., PLMCHR(15) = 0.2803 and PLMCHR(25) = 4.19E-12.

PLMCHR(34) through PLMCHR(53)

If there were any small drops present, they would probably be condensed water. Looking at the table of "Physico-Chemical Properties of Plume Deposits" in the output of SURFACE it is seen that the Code No. for water is "7". This value is input in PLMCHR(34). The mass percentage of water is entered into PLMCHR(35), in this case 100.0. Since no other items make up the composition of the small drops, PLMCHR(36) through PLMCHR(53) are set to 0.0 or left blank.

PLMCHR(54) through PLMCHR(73)

This portion of the data array is the same as the previous, only for the large drops. In this example only the fuel drops are considered, and reference to the SURFACE output gives a code No. of "3" for MMH. This is used as the input for PLMCHR(54) and PLMCHR(55) is set to 100.0. All other portions of this segment of the array are set to zero or left blank.

PLMCHR(84) through PLMCHR(86)

These three inputs describe the plume gas phase at the surface of the vehicle. SURFACE uses this information to determine any additional heat transfer to the surface of the satellite due to latent heat release upon condensation. In the case, such as this example, when the rocket motor is so relatively far from the surface, this additional heat release is very small. No significant error is introduced, accordingly, if the temperature, PLMCHR(84) for the plume is taken to be the last value given by KINCON, and the pressure and density, PLMCHR(85) and (86) are extrapolated from the last output of KINCON to the point on the surface via an "inverse square of the distance" method, i. e., PLMCHR(84) = 890°R, PLMCHR(85) = 4.69E-05 psia, and PLMCHR(86) = 8.39E-08 lb/ft³.

PLMCHR(87)

This input is not actually needed as SURFACE will calculate the viscosity. If this item is left blank, SURFACE makes the calculation. If a non-zero value is input, the program uses this figure rather than calculate one.

At this point the file EDATA is rewritten, as discussed in Appendix D. At the present time the portions of the program SURFACE are still being checked out, and consequently, this subprogram is not in a fully production status.

SECTION VI

EXPERIMENTAL DETERMINATION OF GAS DEPOSITION RATE ON CRYOGENICALLY COOLED SURFACES

NOMENC LATURE

<u>Symbol</u>	<u>Definition</u>	<u>Units</u>
A_t	Nozzle throat area	ft^2
C_D	Nozzle discharge coefficient	---
C_p	Specific heat at constant pressure	$\text{ft}^2/\text{sec}^2 - ^\circ \text{R}$
ΔF	QCM beat frequency	Hz
h	Axial distance between nozzle and sensor	in
K	QCM constant	$\text{gm}/\text{cm}^2 - \text{Hz}$
k	Hypersonic similarity parameter (Eq. 2)	---
M	Mach number	---
m	Mass flow rate	lb_m/sec
Δm	Mass deposited	gm/cm^2
$P_{c.}$	Nozzle stagnation pressure	mmHg or lb_f/ft^2
R	Gas constant	$\text{ft}^2/\text{sec}^2 - ^\circ \text{R}$
Re_D	Throat Reynolds number	---
r_e	Nozzle exit radius	in
T	Temperature	$^\circ \text{R}$
Δt	Time increment	sec
v	Velocity	ft/sec
v_{lim}	Limiting gas velocity (Eq. 3)	ft/sec
α	Sticking coefficient (deposited mass flux/ incident mass flux)	---
γ	Ratio of specific heats	---
θ	Flow angle	deg
ρ	Gas density	lb_m/ft^3
ρv	Incident mass flux	$\text{lb}_m/\text{ft}^2 - \text{sec}$ or $\text{gm}/\text{cm}^2 - \text{sec}$
<u>Subscripts</u>		
c	Nozzle stagnation condition	
e	Nozzle exit condition	

1. OBJECTIVE AND APPROACH

The objective of this experimental program was to measure the steady-state deposition rates of various gases on cryogenically cooled surfaces. These data will eventually be used to predict contamination effects on spacecraft borne optical devices and thermal control surfaces.

It was originally planned to perform these tests as functions of gas type, surface temperature, and prior surface deposit. The items actually covered consisted of variations in gas type (NH_3 , CO_2 , and H_2O) and surface material (gold and silver).

All testing was performed in a laboratory scale vacuum facility the key elements of which were: a gas supply system, sonic nozzle, LN_2 cooled shroud, measuring equipment, and a quartz crystal microbalance (QCM).

Each combination of gas type and surface materials was run as a function of incident mass flux (which was accomplished by varying the gas stagnation pressure). After data reduction the results were presented as the sticking coefficient (deposited mass flux/incident mass flux) versus incident mass flux. Other methods of data normalization are possible; e. g., sticking coefficient versus Knudsen number (based on gas properties at the surface); but these were not explored during the course of the present investigation.

2. EXPERIMENTAL FACILITY

The experimental facility consisted of four subassemblies:

1. Vacuum system.
2. Gas supply and feed system.
3. QCM electronics and sensor.
4. Measuring equipment.

Figure 13 is a schematic of the facility and indicates the functional and geometric relationship of the above subassemblies.

a. Vacuum System

The vacuum system consisted of a 14-in. -diameter glass belljar; a mechanical pump; and a 6-in.-diameter oil diffusion pump with an LN_2 cold trap. A Veeco Type RG-31X unit was employed to monitor the belljar pressure via a Veeco Type RG-75 ionization gage and the diffusion pump foreline pressure using a Veeco Type DV-1M thermocouple gage.

Feedthroughs were provided in the belljar baseplate to accommodate the shroud LN_2 lines, electrical power to the sensor, signals from the sensor, nozzle heater, and thermocouple leads.

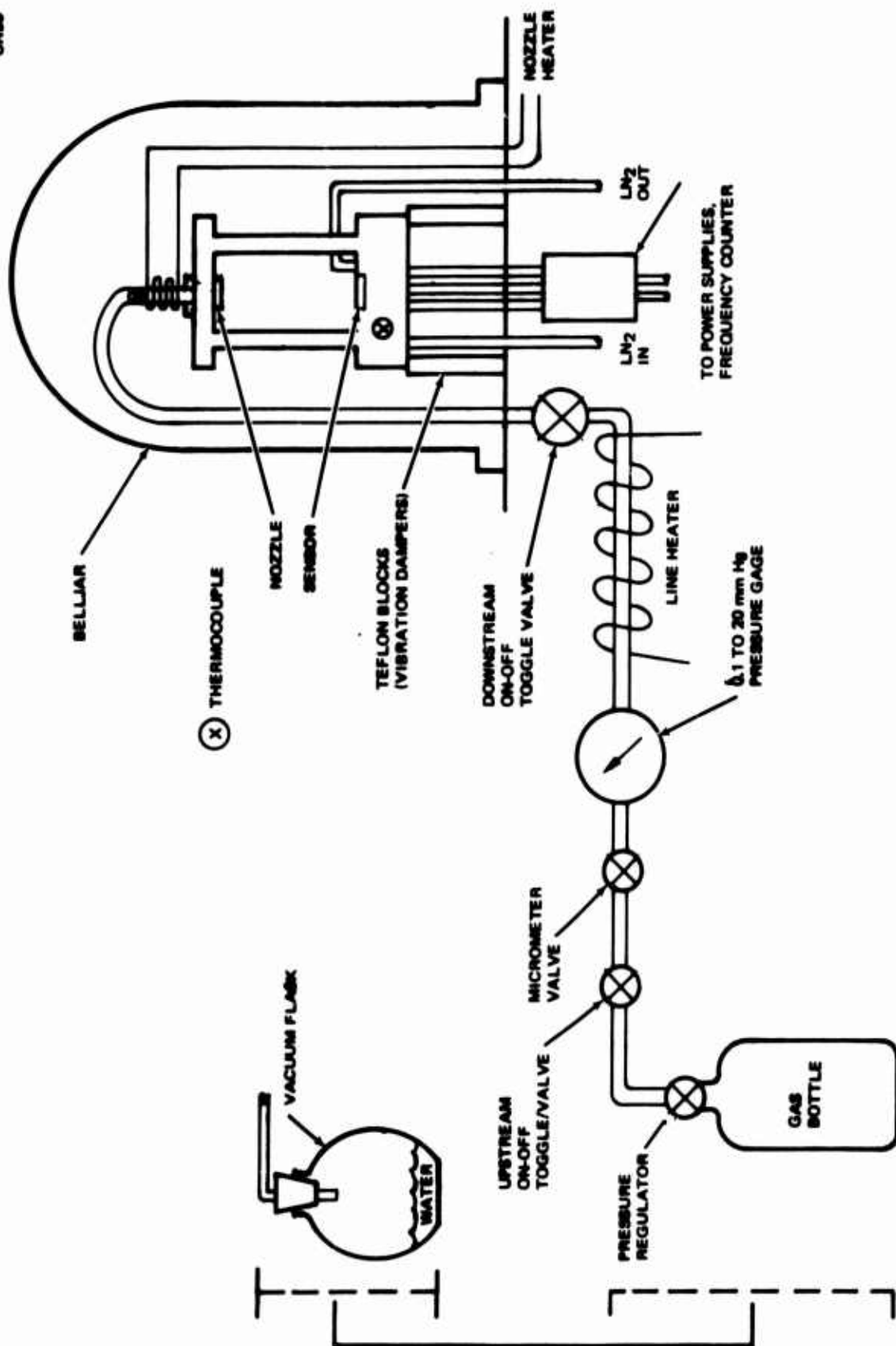


Figure 13. Facility Schematic

b. Gas Supply and Feed System

This system schematic is also shown in Figure 13 and includes the LN_2 cooled shroud (onto which is mounted the sonic orifice and QCM sensor). The CO_2 and NH_3 gases were supplied from commercially available cylinders while the water vapor was drawn from a vacuum flask.

An electrical line heater, powered by a Variac, was wrapped over the 1/4-in. stainless steel lines from the 0.1 to 20 mm Hg absolute pressure gage to the belljar baseplate in order to avoid NH_3 and H_2O condensation in the line. In addition, a bead heater was wrapped around the line just upstream of the nozzle orifice fitting (again, powered by a Variac). The use of these heaters was necessitated by evidence of nozzle plugging by condensed NH_3 during some of the earlier test runs.

Figure 14 presents a detailed cross section of the LN_2 cooled shroud. The nozzle orifice (Figure 15) was mounted in a Swagelock fitting and secured to the top of the shroud with two Teflon washers in order to provide some degree of thermal isolation. A copper-constantan thermocouple was inserted through the side of the feedline just upstream of the nozzle fitting such that the junction was within the gas stream. This reading was taken as the gas stagnation temperature because of the high contraction area ratio between the feedline and nozzle throat.

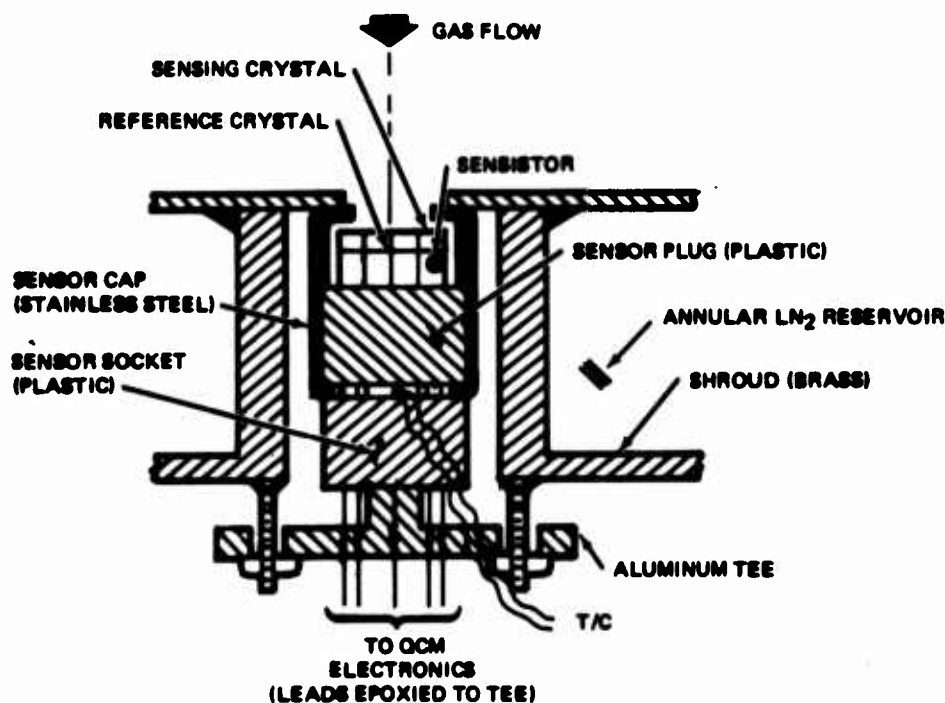


Figure 14. Sketch of QCM Sensor/Shroud Installation

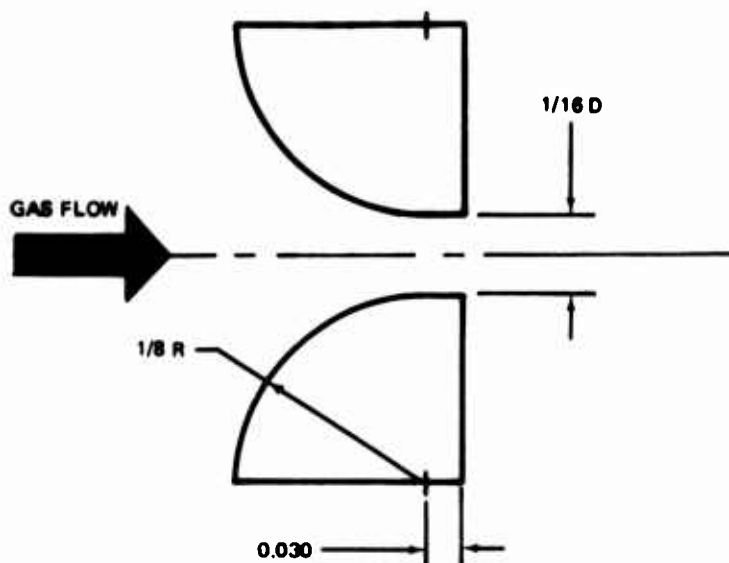


Figure 15. Sonic Nozzle Configuration

A second copper-constantan thermocouple was spot-welded to the outside of the shroud LN₂ reservoir and was used to verify the shroud cool-down. Typically, this reading very quickly approached the LN₂ boiling point at one atmosphere pressure and the use of this thermocouple became of secondary importance.

The QCM sensor was installed through the bottom of the shroud and was located at its forward edge by a smaller diameter lip within the brass shroud. The sensor was secured to this lip by an aluminum tee member which beared on the sensor plastic socket. This member was also a means of cooling the sensor by providing a conduction path from the sensor to the LN₂ reservoir. Additionally, the six leads from the sensor to its remote electronic package were bonded to the aluminum tee by a high thermal conductance, high electrical resistance epoxy (Wakefield Delta Bond 152). This design feature "short circuited" the energy being conducted from the warmer electronics package to the sensor. The shroud assembly was then loosely covered with aluminum foil with the foil being secured by wrapping it around the LN₂ lines. A narrow slit was made in the foil so that the sensor surface could be visually examined.

c. QCM Electronics and Sensor

The QCM system employed for this experimental program was manufactured by Faraday Laboratories, Inc., La Jolla, California, and consisted of an electronics package (Model 71-DE, Serial No. E8) and a series of plug-in crystal sensors.

The electronics was located on the test stand external to the LN_2 vacuum system since its specification indicated a minimum allowable temperature of -50°C . Electrical power was furnished by a standard 28-vdc supply while power for the sensor heater was furnished by a variable dc supply.

The QCM sensor consisted of two 10-MHz crystals matched to the temperature coefficient (so as to minimize beat frequency shifts with crystal temperature). The outer or sensing crystal was exposed to the incident gas stream and could be supplied with a variety of coatings. The program described herein used gold or silver plated sensing crystals. In addition, both crystals could be heated via an aluminum undercoat in order to drive off prior deposits. A solid-state sensistor was supplied to measure the crystal temperature; however, the manufacturer did not furnish calibration information for these units in the temperature range between -40°C and -200°C . To remedy this situation a copper-constantan thermocouple was spot-welded to the ground pin of the sensor plug and, the output of this thermocouple was one of the primary readings recorded during a test.

The mass deposited on the sensing crystal causes a change in its natural frequency of oscillation which when it is mixed with that of the inner, or reference, crystal causes a "beat" frequency (ΔF , the difference between the reference and sensing crystal frequencies) to be generated. This beat frequency was recorded on a digital frequency counter and was then related to the mass deposited by:

$$\Delta m(\text{gm/cm}^2) = K \Delta F (\text{Hz})$$

where K was either 4.1×10^{-9} or 3.5×10^{-9} gm/cm^2 -Hz depending on the sensor employed.

The manufacturer's specifications for the sensors indicated that they were capable of measuring deposits as low as 1.0×10^{-9} gm/cm^2 to as high as 1.0×10^{-3} gm/cm^2 .

d. Measuring Equipment

The voltage output of the copper-constantan thermocouples (in millivolts) located on the gas supply line, shroud, and sensor were measured on two Hewlett Packard Model 3440A digital voltmeters one of which employed

a H-P model 3433A high gain/auto range plug-in and the other with a H-P model 3444A dc multifunction plug-in. The output of the sensistor (in volts) was displayed on the DVM with the auto range plug-in. These units have a lowest scale of 100 millivolts which yielded three-digit representation of the thermocouple voltages.

A H-P Model 5245L digital electronic counter was used to display the sensor beat frequency and was set on its most sensitive scale of 0.1 vrms. The input to the counter was split to also drive a H-P Type 561B oscilloscope with a Type 3A72 dual-trace amplifier. The oscilloscope was used primarily during the initial facility setup to check for ground loops; subsequent usage was restricted to measuring the sensor output level.

3. TEST PROCEDURE

At the beginning of each day certain preparatory steps were taken prior to the initiation of the deposition runs. These included: evacuating the belljar, filling the thermocouple junction bath with an ice-water mixture, energizing the line and nozzle heaters (if NH_3 or H_2O was to be run), trimming the digital voltmeters against their internal checks, and filling the shroud with LN_2 to cool the sensor. The gas supply system was purged with dry GN_2 if a different gas was to be run.

The sensor cooldown period typically required 1 hour as evidenced by stabilizing of the sensistor and sensor thermocouple readings. At this point the micrometer valve was opened and adjusted to give the desired feed pressure and the clock was started. The beat frequency, gas stagnation thermocouple, and sensor thermocouple readings were manually recorded at time intervals which varied with the feed pressure; e. g., every 1 minute at 0.5 mm Hg and every 10 seconds at 4.0 mm Hg. The sensistor output was occasionally recorded and adjustments were made to the micrometer valve, if necessary, to maintain a constant feed pressure.

The run was terminated when the beat frequency reached 250 to 300 kHz (which corresponded to the maximum sensor loading of $1.0 \times 10^{-3} \text{ gm/cm}^2$) at which time the micrometer valve was adjusted to the next feed pressure. The upstream toggle valve was closed cutting off the gas flow and the sensor heater was energized to drive off the deposited material and return the sensor beat frequency to its nominal value. The next run was initiated by opening the upstream toggle valve and starting the clock.

The use of an automatic data recording system would be required in order to extend the gas feed pressure (and gas flowrate) to higher levels since it was not possible to manually record the data for time intervals less than 10 seconds.

It is to be noted that the sensor was not removed from the belljar once it was installed even though some change in the sensor nominal beat frequency was noted over a period of time. Earlier attempts to clean the gold plated sensors with a solvent usually resulted in removal of some of the gold. Two of these damaged units were returned to the manufacturer who successfully replated one of them with gold.

4. DATA REDUCTION

The reduction of all test data involved the following steps:

1. Determining the steady-state mass deposition flux.
2. Estimating the incident mass flux at the sensor location.
3. Calculating the sticking coefficient from the ratio of steps 1 and 2.

The final reduced data consisted of graphs showing the sticking coefficient versus incident mass flux for each of the gases and surfaces employed.

a. Steady-State Mass Deposition Flux

As previously mentioned the sensor beat frequency, ΔF , was recorded as a function of time, t . The first step in the data reduction process was to plot ΔF versus t and establish when this function achieved a constant slope. A typical result is presented in Figure 15 and indicates that approximately 5.5 minutes was required to establish a steady-state deposition condition for this particular run.

The corresponding steady-state mass deposition flux, $\Delta m/\Delta t$, was then found from:

$$\frac{\Delta m}{\Delta t} \text{ (gm/cm}^2\text{-sec)} = K \frac{\Delta F \text{ (Hz)}}{\Delta t \text{ (sec)}}$$

where K is a theoretical value supplied by the manufacturer and was either 4.1×10^{-9} or 3.5×10^{-9} depending on the particular sensor.

b. Inviscid, Continuum, Incident Mass Flux

The inviscid, continuum, incident mass flux, ρV , at the sensor location was calculated using the approximation by Roberts (Reference 19).

In this formulation the gas density is given by:

$$\rho = \rho_e \frac{k}{2} \left(\frac{r_e}{h} \right)^2 (\cos \theta)^k \quad (1)$$

$$k = \gamma(\gamma - 1) M_e^2 \quad (2)$$

The opening in the cap over the sensing crystal was 3/8 in. which indicated that this crystal subtended an angle of ± 3.7 deg; therefore, $(\cos \theta)^k$ was taken as unity (since $k \approx 0.45$).

The gas density at the nozzle exit was found from the measured feed pressure, stagnation temperature (T_c), gas constant (R), and isentropic expansion to an M_e zone. The value of $\gamma (= C_p/(C_p - R))$ was found from Reference 20 as a function of stagnation temperature. The gas velocity, ρV , at the sensor location was taken as the limiting gas velocity, i. e.:

$$V = V_{\text{lim}} = \sqrt{2 \gamma R T_c / (\gamma - 1)} \quad (3)$$

The inviscid, continuum, incident mass flux, ρV , was found by multiplying Equations (1) and (3).

c. Pitot Pressure Measurements

A pitot pressure probe was fabricated from 0.064 in. Od by 0.024 in. Id by 10 in. long stainless steel with a square lip and the pressure was measured on a Type 77 MKS Baratron Pressure Meter utilizing a secondary vacuum reference source.

The measured pitot pressure was divided by the feed (stagnation) pressure and with the normal shock total pressure relationship was used to calculate the free-stream Mach number. Results of these calculations for ambient temperature air, as shown in Figure 16, indicated that the free-stream Mach number was approximately 10.6 (over a feed pressure range of 0.5 to 3.0 mm Hg) while the Mach number found from the plume approximation (an extension of Equation 1) was 19.0. This difference is due to the rarefaction of the gas during the expansion process which "freezes" the velocity, static temperature, and Mach number. The error thus incurred amounts to overpredicting the air velocity by 2.2 percent when Equation (3) is employed, i. e., $V(M = 19)/V(M = 10.6) = 1.022$.

The inverse square dependency of density with distance (Equation 1) is still valid at the sensor location since it is a consequence of satisfying the conservation of mass. To more clearly illustrate this point Equation 1 may be rewritten (with $\cos \alpha = 1$) as:

$$\rho V = \rho_e \frac{k}{2} \left(\frac{r_e}{h} \right)^2 \sqrt{2 \gamma R (T_c - T) / (\gamma - 1)} \quad (4)$$

At some axial location, h_f , the static temperature (T) and velocity (V) "freeze" and the free-stream mass flux, ρV , still varies as $(h)^{-2}$. If it is assumed that the expansion suddenly freezes; i. e., the expansion follows continuum theory up to h_f and then T (and V) becomes constant; then the value of h_f can be calculated. For the air results cited above it was found that $h_f = 0.68$ in. compared to the nozzle/probe separation distance of 2.85 in.

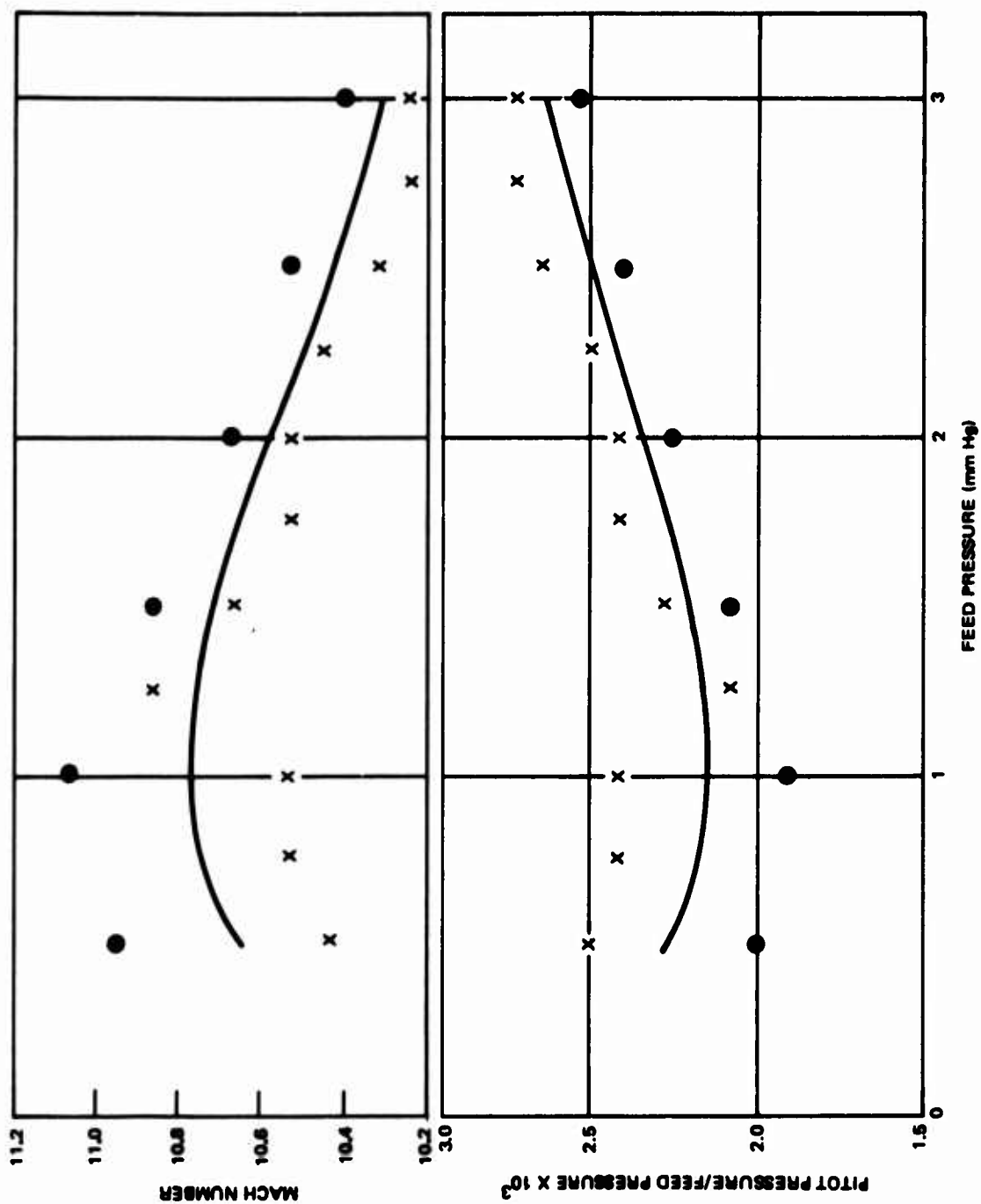


Figure 16. Pitot Pressure Results for Ambient Temperature Air

- (3) Multiplying the result from step 2 by the nozzle discharge coefficient corresponding to a square-edged orifice to arrive at the incident mass flux.*

The deposited mass flux was then divided by the incident mass flux to yield the sticking coefficient. The last step in the data reduction process involved performing least squares polynomial (cubic) curve fits to all test data. No attempt was made to preselect those data points to be used in this process; i. e., all data points were employed.

d. Sensor Surface Temperature

At the conclusion of the test program a small copper-constantan thermocouple was bonded directly to the sensing crystal of an inactive sensor. The shroud was then cooled with LN₂ and the reading of this thermocouple was compared to that attached to pin C of the sensor plug after a steady-state condition had been attained. It was found that the crystal was 5° C warmer than the plug thermocouple. (The latter thermocouple was thermally closer to the LN₂ reservoir than the former.) Therefore, all quoted surface temperatures were found by adding 5° C to the plug thermocouple reading.

5. REDUCED DATA

The finalized test data are presented for steady-state deposition of NH₃, CO₂, and H₂O on both gold and silver surfaces. Attempts were made to deposit O₂ and CH₄ in a flowing system but these were unsuccessful. Also presented are the results of a test performed to measure the NH₃ evaporation rate in a vacuum environment.

a. Ammonia (NH₃) Results

The NH₃ deposition rate on a gold plated QCM sensor was the first of the test series conducted and was subject to more data scatter than the subsequent tests. These data are presented in Figure 17** and depict the sticking coefficient (defined as the ratio of the deposited mass flux to the incident mass flux) as a function of the incident mass flux.

The tests conducted at an incident mass flux of approximately 2.5×10^{-6} gm/cm²-sec were the only ones which exhibited a reduction in the sticking coefficient with time, i. e., the deposition rate was larger at the beginning of the run than later on during the run. (A similar occurrence was noted in Figure 6 of Reference 23 for N₂ but no explanation was offered therein.)

*The use of the measured C_D's, in preference to those from Reference 22 would result in sticking coefficients on the order of 2-4.

**Surface temperature range noted on Figure 17 (and subsequent figures) refers to the minimum and maximum sensor temperatures recorded for all the data points. The variation in sensor temperature during the course of any one run was usually on the order of 2-3° C.

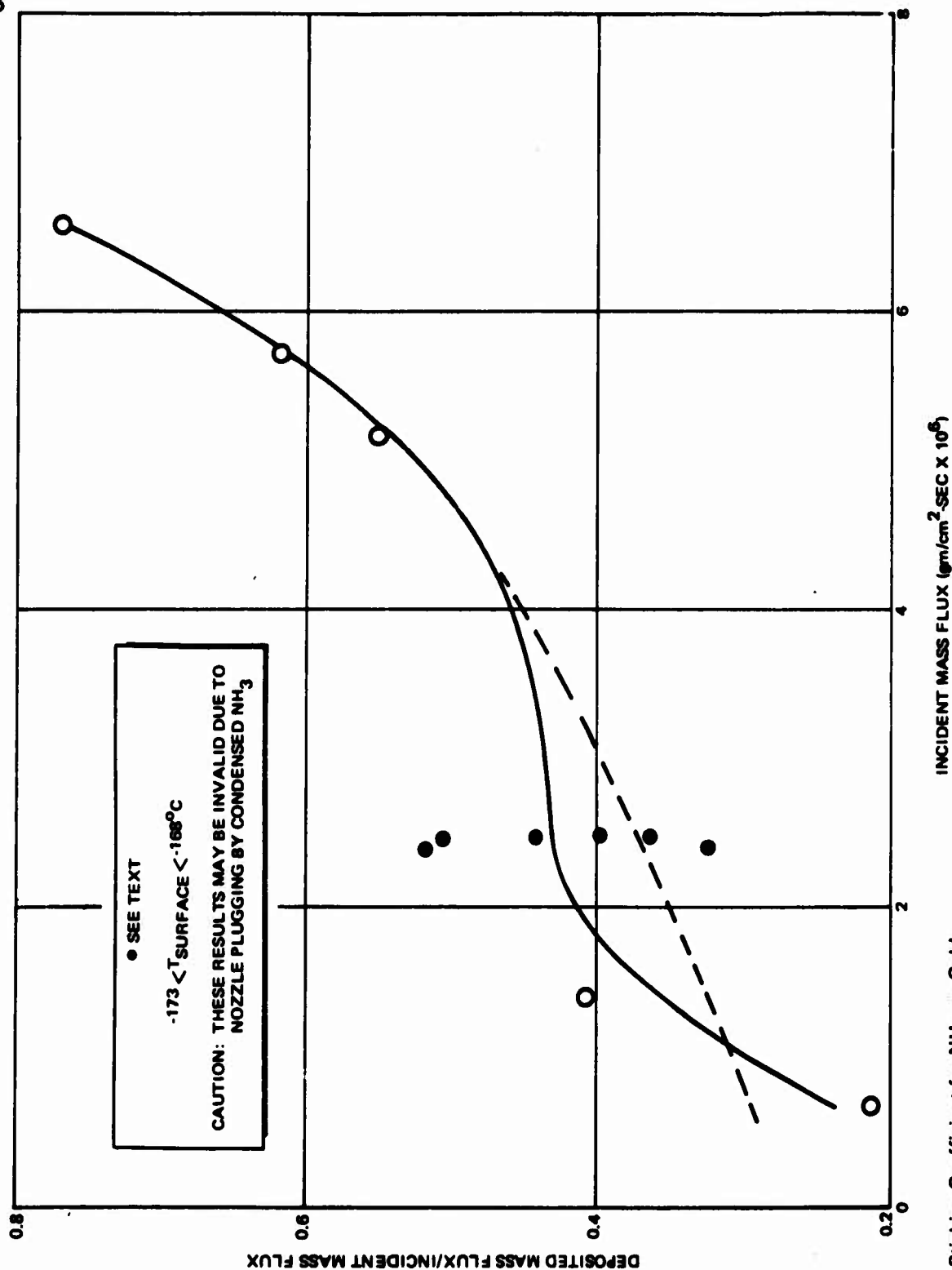


Figure 17. Sticking Coefficient for NH_3 on Gold

In point of time the NH_3 on gold results were the first ones obtained and these tests were performed prior to the installation of heaters on the gas supply line and nozzle. (These heaters were installed commencing with the H_2O on gold series to prevent condensation in the lines since saturated vapor was being withdrawn from the liquid flask.) Thus, there is some reason to suspect the NH_3 on gold results due to partial line plugging (especially at the higher ρv 's).

Corresponding results for NH_3 deposition rates on silver are shown in Figure 18. It is to be noted that the sticking coefficient was monotonically increasing with time to its steady-state value at each data point. Figure 19 compares the NH_3 sticking coefficient for both the gold and silver plated sensors. Both results agree up to a ρv of $2 \times 10^{-6} \text{ gm/cm}^2\text{-sec}$ with the gold results then exhibiting a lower sticking coefficient and different trend. (This difference is attributed to nozzle plugging by condensed NH_3 at the higher incident mass fluxes.)

b. Carbon Dioxide (CO_2) Results

The gold and silver results of sticking coefficient versus incident mass flux are presented in Figures 20 and 21, respectively. Both sets of data show very similar trends: a nearly linear increase of α with ρv followed by an asymptotic approach to an α of unity. This is more clearly depicted in Figure 22 which shows that $\alpha \approx 1$ for ρv between 10 to

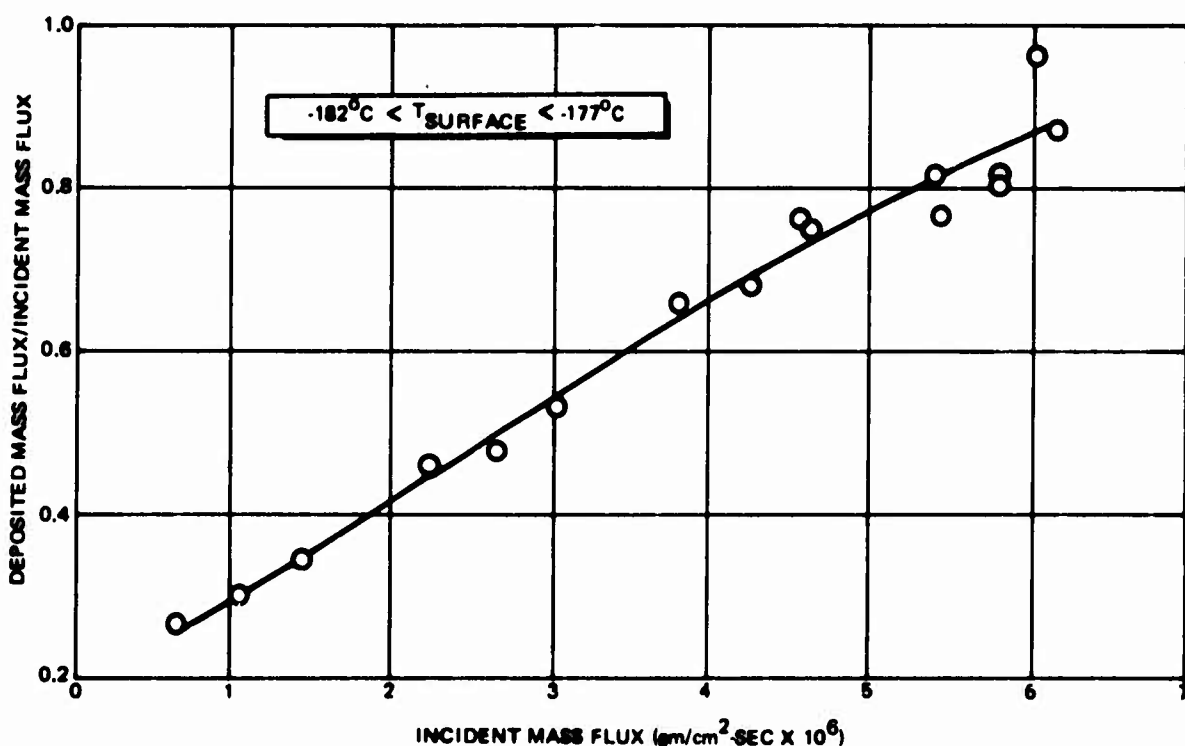
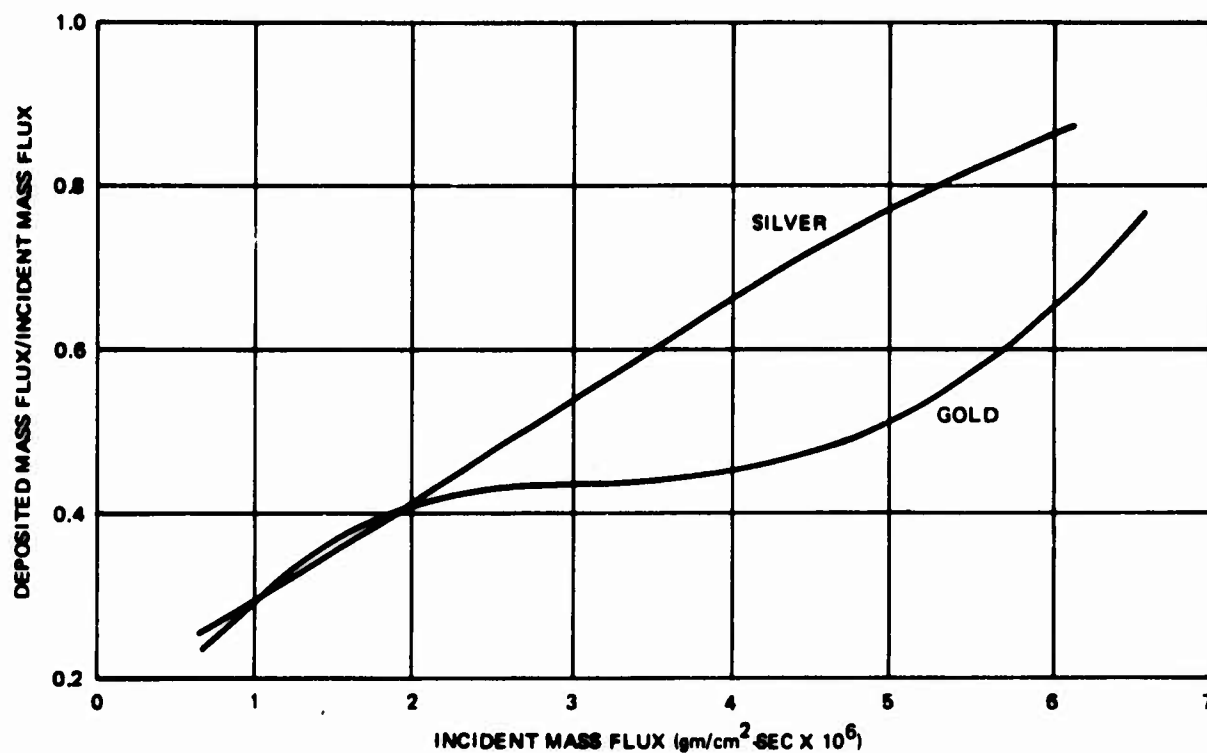
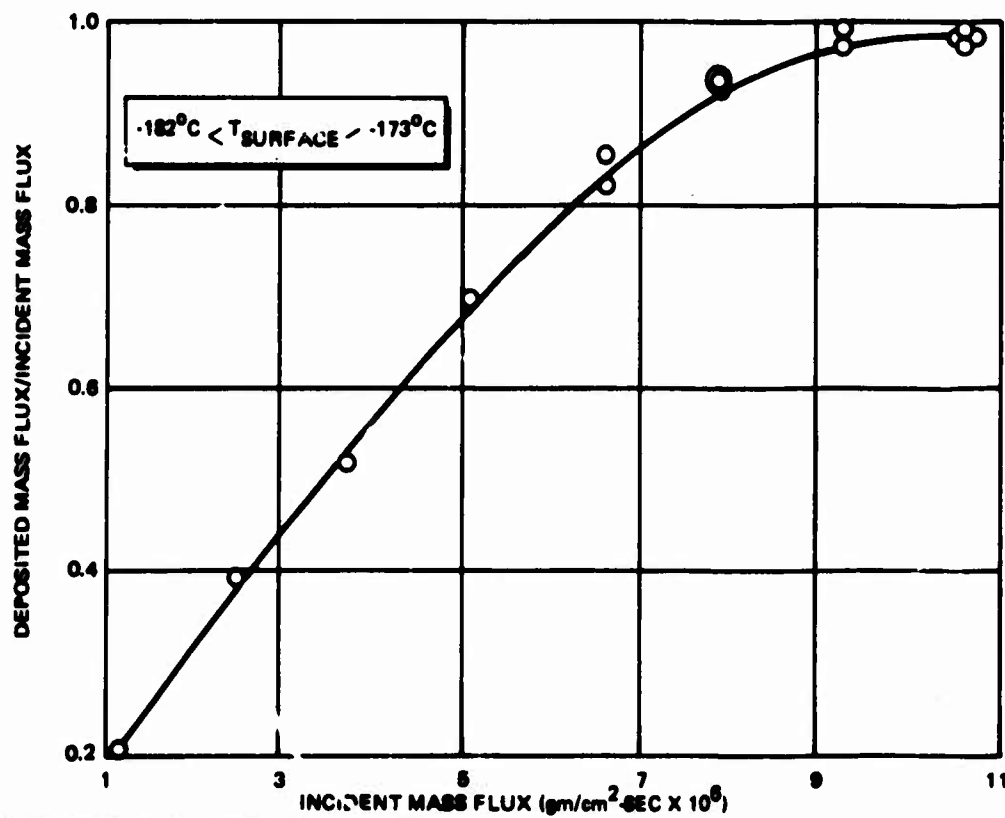


Figure 18. Sticking Coefficient for NH_3 on Silver

Figure 19. Comparison of Sticking Coefficient for NH_3 on Gold and SilverFigure 20. Sticking Coefficient for CO_2 on Gold

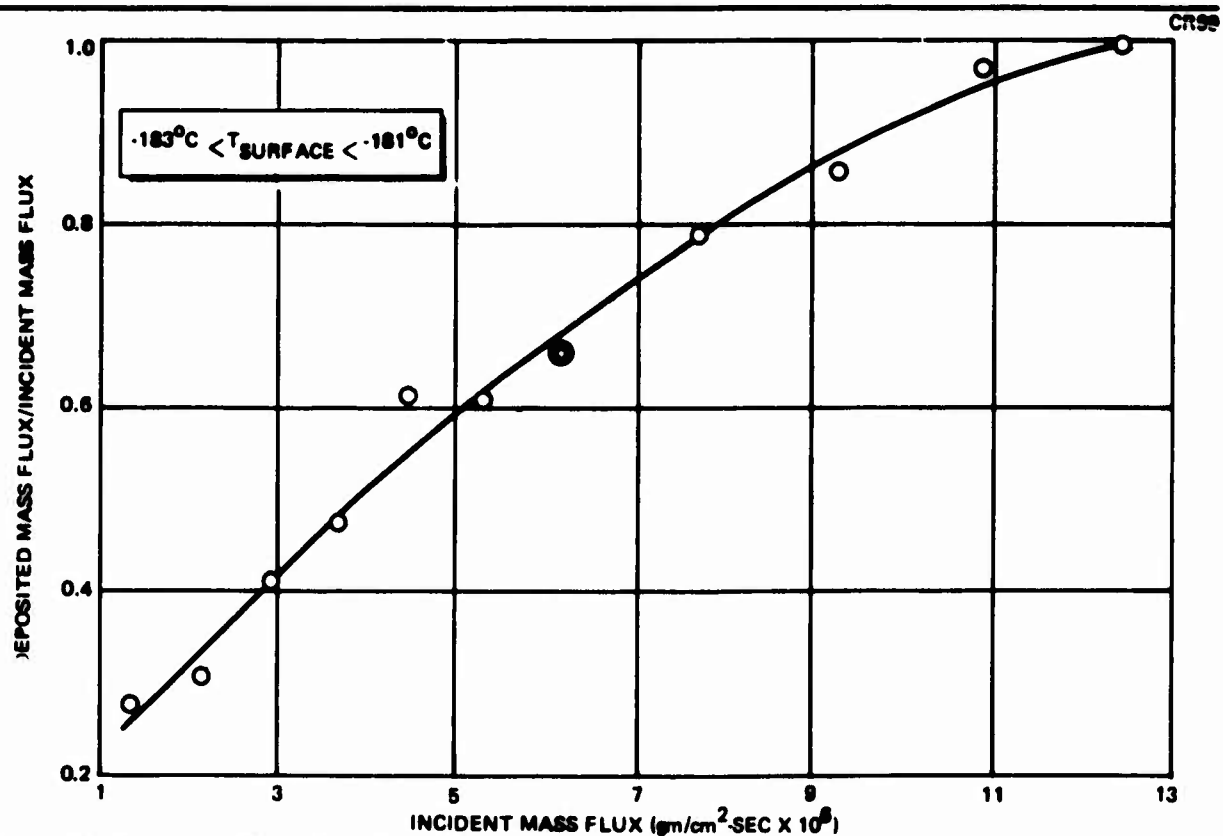


Figure 21. Sticking Coefficient for CO₂ on Silver

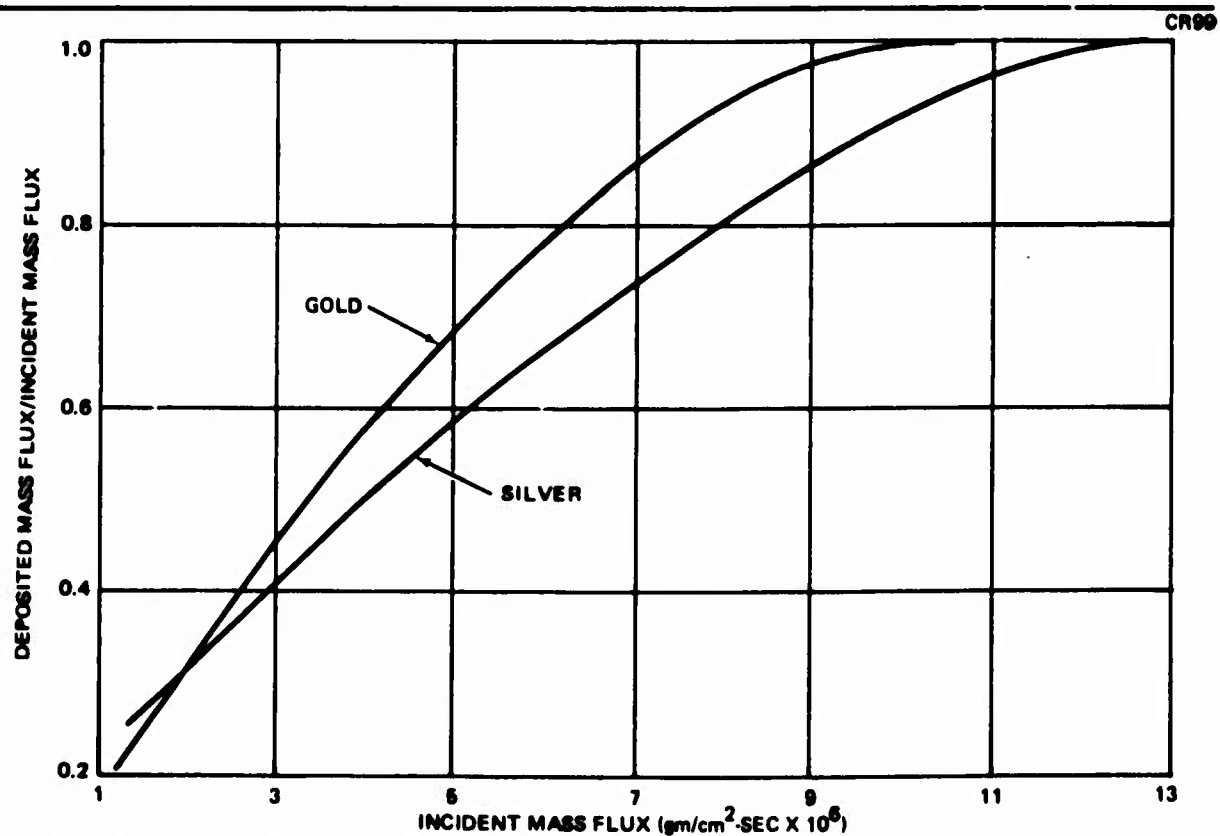


Figure 22. Comparison of Sticking Coefficient for CO₂ on Gold and Silver

$12.5 \times 10^{-6} \text{ gm/cm}^2\text{-sec}$. In addition, the differences in α between the gold and silver plated sensors were judged to be relatively minor, i. e., approximately a 19 percent difference at most. This observation, in conjunction with the close similarity in surface temperatures, indicates that there is essentially no difference in the steady-state α produced by the surface materials. This is supported by calculations which showed that at the sensor's upper measurement limit ($1 \times 10^{-3} \text{ gm/cm}^2$) there are approximately 2.5×10^4 monolayers of CO_2 deposited on the surface; i. e., the incident gas does not "see" the sensor surface.

The use of a theoretical clean surface would result in deposition rates which were dependent on the surface material due to differences in the potential energy function between the gas and the surfaces. However, it was not feasible to achieve this ideal condition nor accurately measure the deposition rate with the experimental setup, e. g., the buildup in feed pressure (incident flux) was too slow to attribute a measured deposition rate to a corresponding incident flux.

c. Water Vapor (H_2O) Results

The H_2O results for gold and silver surfaces are contained in Figures 23 and 24, respectively, while a cross-plot is shown in Figure 25.

The use of all the silver data points in the curve fit resulted in a dropoff in α at the higher values of V . A modified fit, as shown by the

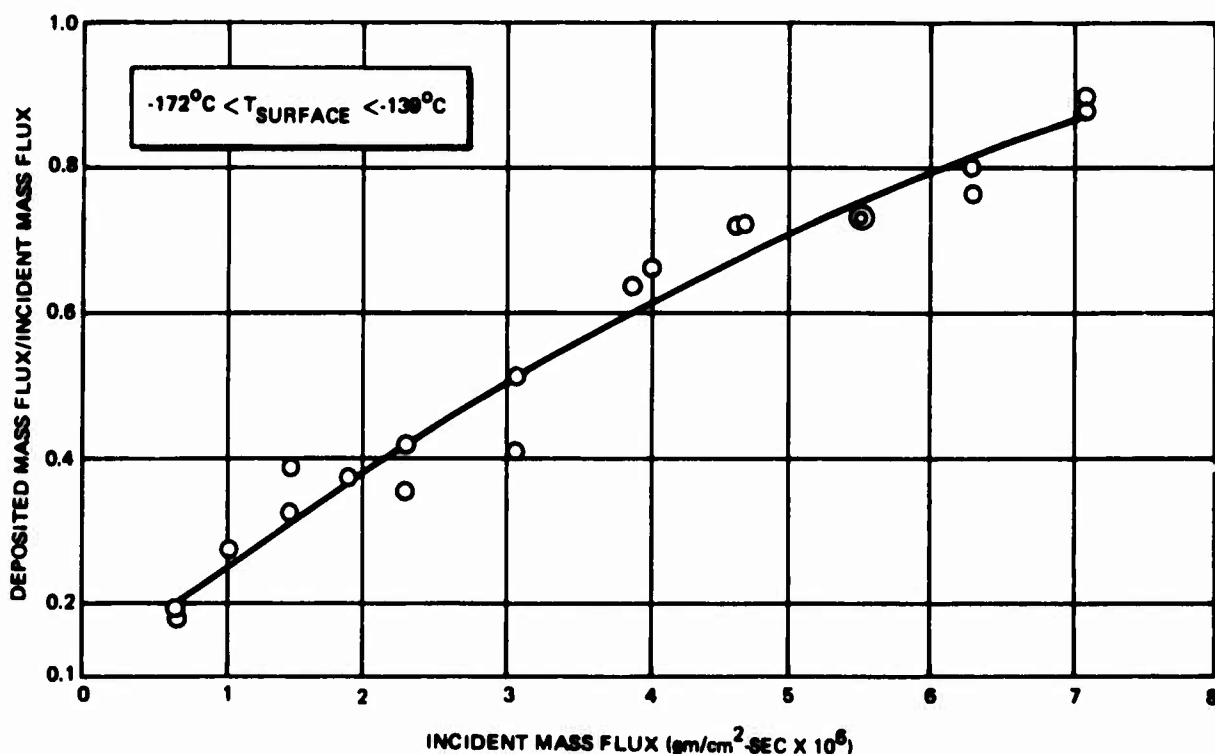
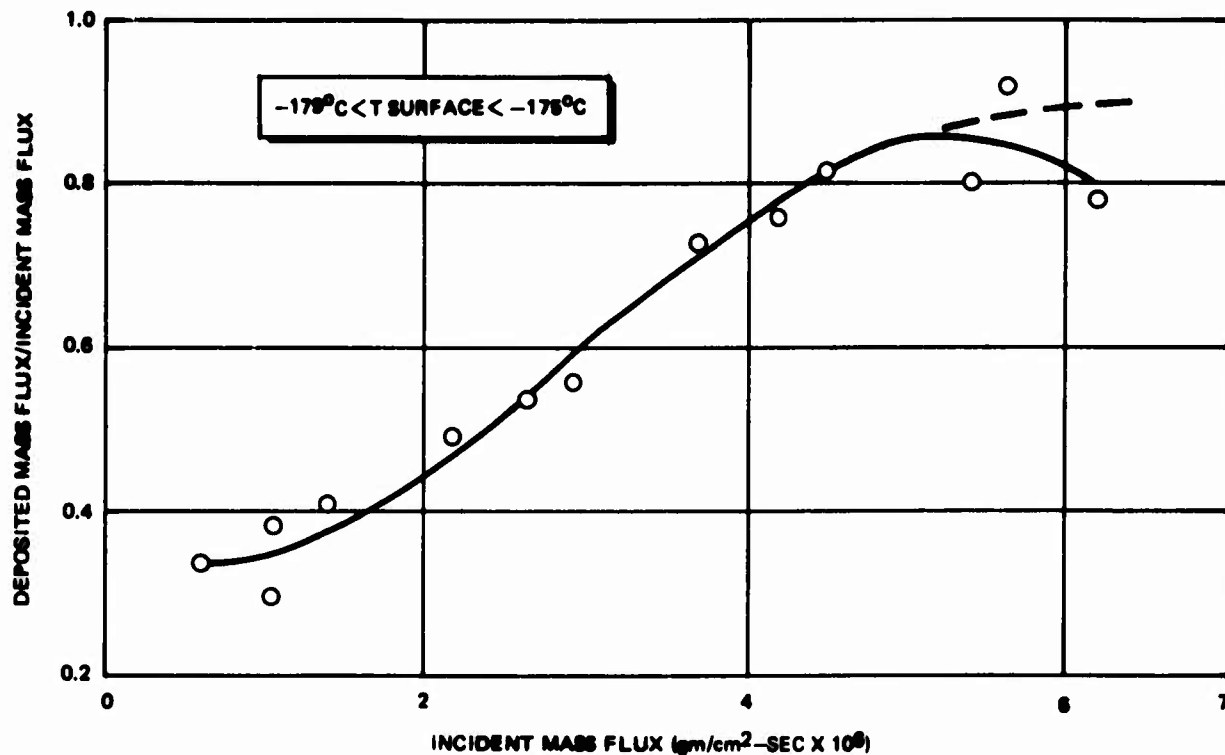
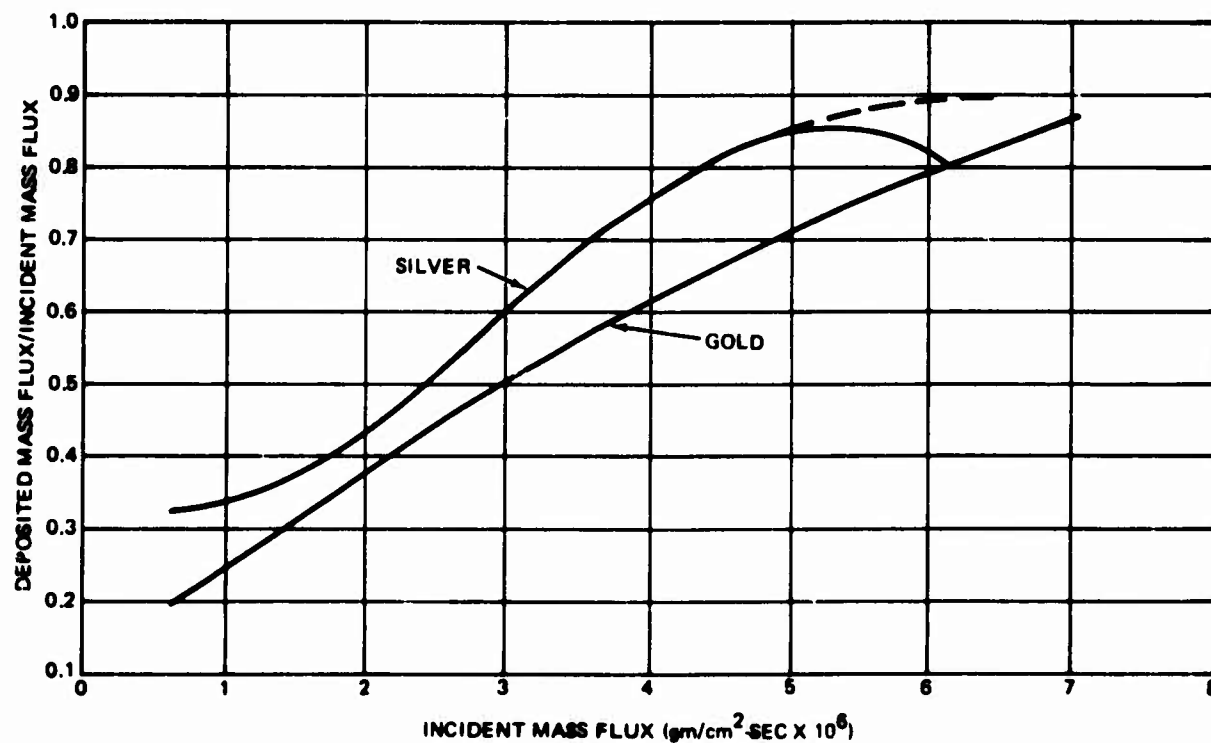


Figure 23. Sticking Coefficient for H_2O on Gold

Figure 24. Sticking Coefficient for H_2O on SilverFigure 25. Comparison of Sticking Coefficient for H_2O on Gold and Silver

dashed lines in Figures 24 and 25, was employed in this area and the resulting comparison (Figure 25) indicates the following:

1. The gold results were obtained over a much larger range in surface temperature.
2. The silver α 's for the H_2O are higher than the gold values (as opposed to the opposite trend for CO_2 shown in Figure 22) although they both appear to be approaching a common limit. This is probably due to the higher evaporation rate for the gold results which would produce lower net deposition rates, i. e., lower values of α .
3. The spread between the results is greater than those obtained for CO_2 with the maximum difference being 24 percent for $pV > 2 \times 10^{-6} \text{ gm/cm}^2 \text{-sec}$.

For engineering level contamination studies the H_2O results, especially item 3 above, suggest that there is essentially no difference between steady-state deposition on gold and silver surfaces.

d. Composite Summary of Sticking Coefficients on Gold and Silver

The reduced data for NH_3 , CO_2 , and H_2O on the gold plated sensor are shown in Figure 26 with the corresponding silver information presented

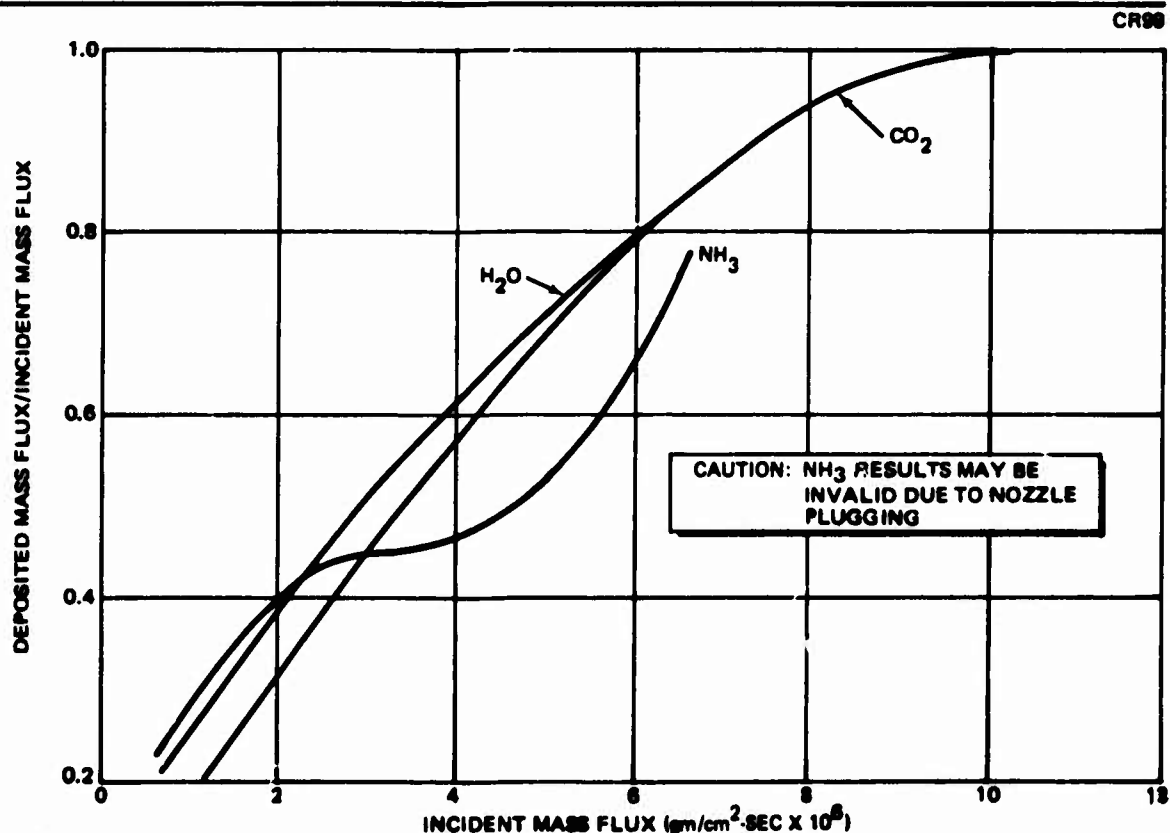


Figure 26. Sticking Coefficient for NH_3 , CO_2 , and H_2O on Gold

in Figure 27. The α for H_2O on gold is seen to approach, and then coincide with, the CO_2 results. It is to be noted that the surface temperature was significantly higher, 10 to 34° C, for the H_2O on gold than for the CO_2 test series. This higher temperature will cause a greater evaporation rate and a corresponding lower net deposition rate.

By comparison the NH_3 , CO_2 , and H_2O deposition results with a silver plated sensor (Figure 27) appear to be the most consistent set of data gathered: there were no anomalies concerning a decrease in α with time (as was the case with NH_3 on gold) since line and nozzle heaters were installed for all runs to prevent plugging; and, the maximum difference in surface temperature under any condition was 8° C. The α for CO_2 is seen to reach unity at an incident mass flux of $\approx 12.5 \times 10^{-6} \text{ gm/cm}^2\text{-sec}$ and it is apparent that both H_2O and NH_3 will achieve an α of unity at even lower values of V . (The more pronounced curvature of H_2O on silver at low ρV is due to the nozzle discharge coefficient effect which was more significant for these runs.)

e. Vacuum Evaporation

A preliminary vacuum evaporation experiment was performed wherein various amounts of heater current were applied to a gold sensor containing a prior NH_3 deposit. (The sensor manufacturer's specification indicated a 400 ma nominal heater current.) This test was planned to determine the evaporation rate as a function of surface temperature.

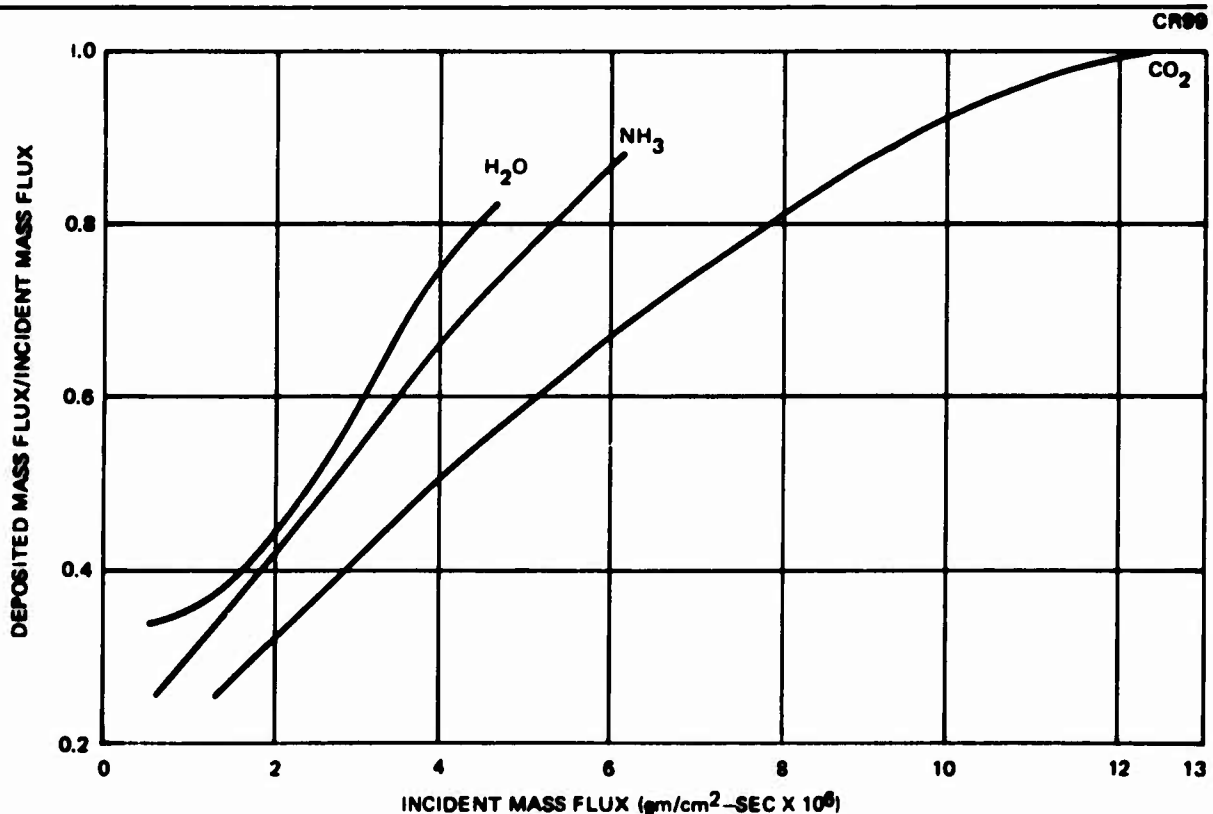


Figure 27. Sticking Coefficient for NH_3 , CO_2 , and H_2O on Silver

The results of this experiment were as follows:

- (1) With 100 ma heater current the sensor crystal stabilized at -171°C with a belljar pressure of 4.4×10^{-6} mm Hg. Additional evaporation was occurring at a rate of 7.823×10^{-8} gm/cm²-sec over an 18 minute time period.
- (2) With 200 ma heater current and the belljar at 4.0×10^{-6} mm Hg the sensor crystal stabilized at -169.5°C . An evaporation rate of 4.106×10^{-8} gm/cm²-sec was noted over a 92 minute time period.
- (3) With 300 ma heater current and the belljar at 3.6×10^{-6} mm Hg the sensor crystal stabilized at -167.5°C and the corresponding evaporation rate was 1.002×10^{-6} gm/cm²-sec averaged over a 13 minute time period.

The additional evaporation (item 1) was probably due to residual NH_3 gas in the belljar which condensed on the sensor even though the heater was partially activated. The other results (items 2 and 3) indicate that the evaporation rate is strongly dependent upon the surface temperature; i. e., a 2.0°C increase in surface temperature produced a factor of 24.4 increase in the evaporation rate.

6. INTERPRETATION OF RESULTS

All the data generated during the present investigation exhibited the common trend of increasing sticking coefficient (α) with increasing incident mass flux (ρV). In addition, each gas was run at essentially the same kinetic energy level as evidenced by the relatively small variation in stagnation temperature.

The deposition process involves the collisional transfer of energy from the incident molecule to the surface; and if this transfer is of sufficient magnitude or if the incident energy is low enough, then the molecule is "trapped" by the surface's potential energy field. This is clearly shown in Figure 6 of Reference 24 which presents the fraction trapped and thermal accommodation coefficient for argon on nickel as a function of incident energy. This particular study was theoretical in nature and considered only a single molecular impacting on a "clean" surface. Above a certain incident energy level there was no trapping predicted, i. e., $\alpha = 0$, while these results also shown that the thermal (energy) accommodation coefficient is $\approx 1/2$ when the sticking coefficient is 0, i. e., the molecule is partially accommodated to the surface energy without being trapped.

The present study involved vast numbers of incident molecules which possessed distributions of velocity (energy) about the mean flow velocity (energy). The results presented herein are qualitatively interpreted as follows;

a. Low values of incident mass flux, ρV , were obtained by low values of density, ρ , which implies fewer gas molecules in the path of the incident molecule.

b. Therefore, the incident molecule suffers few collisions and impacts the surface with small attenuation in its velocity (energy).

c. The reflected molecule also experiences few collisions after rebounding from the surface and has a low probability of being redirected back toward the surface for a second encounter.

d. Some of the incident molecules should be trapped by the surface at low ρV due to the distribution of velocity (energy) about the mean; i. e., statistically, a fraction of the incident molecules will have energies low enough to be trapped.

e. As the incident mass flux increases, through increases in ρ , a given molecule will undergo more collisions with those molecules which have already impacted the surface and will arrive at the surface with a reduced energy content, and the probability of trapping will increase.

f. Those molecules which have not been trapped during their first impact with the surface may experience collisions with molecules near the surface such that they are directed back toward the surface for an additional encounter(s), thereby increasing the trapping probability.

g. In the continuum limit the molecule will reach the surface with zero kinetic energy along the stagnation streamline. The deposition should then depend on whether the heat transfer rate to the surface is sufficiently high to permit extracting the sensible and latent energy from the gas.

The matter of particle density on surface effects has received attention in the area of surface damage due to high speed particles (Reference 25). In this instance increasing the incident particle flux did not produce a proportional increase in surface damage. Indeed, the relative (per particle) target damage was observed to rapidly diminish with increasing particle flux. This effect was attributed to shielding of the surface by particles which were already in the shock layer thereby causing significant energy attenuation of incoming particles and reduced damage per particle.

The above results have a direct parallel with the deposition experiment in that at high incident mass flux the incoming particle energy is attenuated to the point where they are more effectively trapped by the surface.

7. RECOMMENDATIONS FOR THE FUTURE EFFORT

Recommendations are contained, herein, for future effort in two areas:

- a. Improvements to experimental system hardware.
- b. Additional tests.

The recommended system hardware changes are based upon experience gained during the course of the present investigation and are suggested to improve the ease of data gathering, data reduction, and general flexibility of the system.

The additional tests proposed are those which would extend the range of the key parameters and thereby increase their applicability to full-scale systems.

a. System Hardware Changes

The sensor surface temperature is one of the key parameters to any deposition study and, for the present investigation, was difficult to control with any degree of precision. There was a tendency for the sensor temperature to increase with time during the course of a run due to heat transfer from the gas to the sensor. This drift can be corrected by redesigning the sensor/reservoir interface so that the sensor will be thermally closer to the reservoir.

A thermostatically controlled sensor electrical heater and/or controlled shroud LN_2 flow rate must be included in the design so that preselected sensor temperatures can be achieved without the necessity of opening the belljar. Attempts were made during the present investigation to increase the sensor temperature by, for example, inserting Teflon washers between the sensor cap and the reservoir, and by wrapping a small heater around the sensor cap. These attempts were very time consuming (requiring 3 hours just for a cooldown and warmup cycle) and produced either an insignificant temperature change or too large a change.

The incident mass flux, ρV , was varied during the present investigation by changing the stagnation pressure (and stagnation density) at a fixed nozzle/sensor separation distance. Variations in ρV could also be accomplished by changing the separation distance via a remotely controlled electric motor. The data thus generated would serve as a cross-check on the results presently available and would possibly allow the sensor to span the range from continuum to rarefied fluid mechanics.

A fast opening valve, externally controlled, must be placed as close to the nozzle as possible if it is desired to follow the transient portion of the deposition process. The present configuration had manually operated toggle valves outside the belljar and may have been responsible for the extended time period required to achieve a steady-state deposition rate (see Figure 16).

The need for an automatic data recording system becomes critical if results are to be obtained at higher values of incident mass flux. The test equipment employed for this investigation have BCD coded terminals on the chassis which can be connected directly to a recording system. If possible, the output of the frequency counter should be displayed on a stripchart so that

a quick check can be made of the run, e. g., the run could be terminated when the mass deposition flux achieved a constant value as evidenced by a linear variation of ΔF versus time. These plots could also be used as the first step in the data reduction process (as described in Subsection 4. a).

Higher rate vacuum pumps would also have to be used if mixtures of condensible/noncondensable gases are to be tested (Subsection 7. b).

b. Additional Tests

The primary additional test that is suggested involves measuring the deposition characteristics of a condensible/noncondensable gas mixture. This data will supply information as to whether the deposition rate of the condensible gas is a function of its partial density or of the total density. Commercially available mixtures of, for example, carbon dioxide in argon could be used at various CO₂ concentrations.

As mentioned in Subsection 7. a the attempts to systematically vary the sensor surface temperature were unsuccessful. However, the proposed system modifications should make it possible to more closely regulate this temperature so that gas deposition characteristics can be measured as a function of surface temperature. It is recommended that CO₂ be used for the initial series of tests and, based on these results, followed by NH₃ and H₂O.

The molecular weight ratios employed in the present investigation were NH₃: CO₂: H₂O: 1.0:2.584:1.058. It is suggested that a higher molecular weight gas such as SF₆ be tested to extend this ratio to 8.577 in order to establish if the deposition rates can be correlated in terms of molecular weight and/or inter-molecular force constants.

The effect of incident particle energy on deposition rate should be investigated. As discussed in Section VI, this is another key parameter in that it can indicate if a particle can be trapped by the surface's potential energy field. This will be somewhat difficult to simulate in the laboratory since high energies require high temperatures and the experimental facility may not be capable of achieving these conditions without a major redesign.

Section VII

CONCLUSIONS AND RECOMMENDATIONS

A computer program has been developed to predict the sensitivity to engine operating parameters and impingement geometry for the production and transport of bipropellant engine contaminants. An associated program to analyze the effect of plume impingement on sensitive thermal and optical surfaces in terms of changes in surface properties has also been completed. The contaminant production and contaminant transport models and subprograms have been checked out and seem to be working correctly, although verification with experimental data has not been attempted due to a lack of detailed experimental data relating engine operation to contaminant effects on surfaces.

Based on the analysis of a single engine, the Marquardt R-6C MMH/NTO 5-lb thruster, it appears that significant amounts of unburned fuel and oxidizer will be ejected from the engine during the transient portion of the pulse and that this contaminant may cause damage to sensitive thermal and optical surfaces if they are impinged upon by the central core of the plume, or if they are spattered with wall-film material blown off at the nozzle lip.

Section VIII
REFERENCES

1. D. B. Smith, E. J. Smith, and A. S. Kesten. Analytic Study of Catalytic Reactors for Hydrazine Decomposition, Computer Program Manual, Transient Model. United Aircraft Research Laboratories Report H910481-37, May 1969.
2. E. J. Smith, D. B. Smith, and A. S. Kesten. Analytical Study of Catalytic Reactors for Hydrazine Decomposition; One and Two Dimensional Steady-State Programs. United Aircraft Research Laboratories Report G910461-30, August 1968.
3. P. J. Martinkovic. Bipropellant Attitude Control engine exhaust contamination and its effect on Space borne equipment. 12th JANNAF Liquid Propulsion Meeting, Nov. 17-19, 1970, Las Vegas, Nevada. CPIA publication No. 201, Vol. 2, page 315.
4. R. C. Stechman and T. A. Thonet. The Effect of Rocket Exhaust Impingement on Spacecraft Surfaces During Pulsing Engine Duty Cycles. 12th JANNAF Liquid Propulsion Meeting, Nov. 17-19, 1970, Las Vegas, Nevada. CPIA publication No. 201, Vol. 1, page 869.
5. J. R. Kliegel and G. R. Nickerson. Axisymmetric Two-Phase Perfect Gas Performance Program. TRW 02874-6006-R000, April 3, 1967.
6. C. Gabbert and R. J. Hoffman. Reacting, Multiphase Plume Characterization and Plume Effects: Including Gas-Particle Impingement Heating. AIAA Paper No. 70-845, AIAA Fifth Thermophysics Conference, Los Angeles, California, June 29 to July 1, 1970.
7. A. W. Lemman, et al., Eds. Liquid Propellants Handbook. Battelle Memorial Institute, Columbus, Ohio, October 1955.
8. C. M. Beighley and W. R. Fish Ed., Performance and Properties of Liquid Propellants, Aerojet General Corporation.
9. O. W. Dykema and S. A. Greene. An Experimental Study of RP-1, UDMH and N₂H₄ Single-Droplet Burning in Air and in Oxygen. Research Report No. 59-41, Rocketdyne, Canoga Park, Calif., 1960.
10. D. R. Stull, et al., Eds. JANAF Thermochemical Tables. Thermal Research Laboratory, Dow Chemical Company, Midland, Michigan, August 1965.
11. T. F. Seamans, M. Vanpee, and V. D. Agosta. Development of a Fundamental Model of Hypergolic Ignition in Space-ambient Engines, AIAA Journal, Vol. 5, No. 9, September 1967.

12. L. J. Zajac. Correlation of Spray Drop size Distribution and Injector Variables. Rocket dyne Report No. R-8455, February 1971.
13. M.E. Heidmann, R. J. Priem, and J. C. Humphrey, A Study of Sprays Formed by two Impinging Jets. NACA TN 3835, 1957.
14. R. Brown. Sprays Formed by Flashing Liquid Jets. PhD Thesis, University of Michigan, 1961.
15. R.D. Ingebo. Drop-Size Distributions for Impinging-Jet Breakup in Airstreams Simulating the Velocity Conditions in Rocket Combustors. NACA TN 4222, 1950.
16. B. L. McFarland. Heat-Transfer Considerations in Internal Regeneratively (INTEREGEN) Cooled Thrust Chambers. ASME Space Technology and Heat Transfer Conference, Los Angeles, Calif.
17. B. L. McFarland and V. Jaqua. Space Storable Thruster Investigation. Rocketdyne Report No. 8415, NASA CR-72827, November 1971.
18. H.E. Perlee, T. Christos, Y. Miron, and H.K. James. Pre-ignition Phenomena in Small A-50/NTO Pulsed Rocket Engines, Journal of Spacecraft and Rockets, Vol. 5, No. 2, February 1968.
19. L. Roberts. The Action of a Hypersonic Jet on a Dust Layer. IAS Paper No. 83-58, January 1968.
20. R.A. Svehla. Estimated Viscosities and Thermal Conductivities of Gases at High Temperatures. NASA TR-132, 5 October 1961.
21. A.H. Shapiro. The Dynamics and Thermodynamics of Compressible Fluid Flow, Vol. I, The Ronald Press Co., 1958.
22. H. Ashkenas and F.S. Sherman. "The Structure and Utilization of Supersonic Free Jets in Low Density Wind Tunnels," in Rarefied Gas Dynamics, Supplement 3, Vol. II, edited by J.H. de Leuw, Academic Press, 1966.
23. W. Simon. Plume Backscatter Measurements Using Quartz Crystal Microbalances in JPL Molsink (Molecular Sink). JPL TM 33-540, 15 May 1972.
24. R.A. Owen, A. Bogan, and H.L. Chou. "Theoretical Prediction of Momentum and Energy Accommodation for Hypervelocity Gas Particles on an Ideal Crystal Surface," in Rarefied Gas Dynamics, Supplement 3, Vol. II, edited by J.H. de Leeuw, Academic Press, 1966.

Appendix A

TCC

**TRANSIENT COMBUSTION CHAMBER DYNAMICS
COMPUTER PROGRAM**

A Bipropellant Contaminant Production Model

Program Number H607

TABLE OF CONTENTS

Section		
A.1	INTRODUCTION	205
	a. The <u>TCC</u> Program	205
	b. Development of the MDAC Transient Combustion Chamber Program	206
	c. Scope	207
	d. Comparison with Experiment	210
A.2	ANALYSIS	218
	a. Program Structure	218
	b. Subroutine READER	220
	c. Subroutine START	220
	d. Subroutine INJECT	221
	e. Subroutine DROPLT	238
	f. Subroutine WETWAL	246
	g. Subroutine CHAMBR	251
	h. Subroutine WRITER	256
	i. Subroutine GRAPHS	257
	j. Utility Subroutines and Functions	258
	k. Limitations and Assumptions	260
A.3	NUMERICAL INTEGRATION METHOD	262
	a. Computational Methods for Droplet Arrays	263
A.4	PROGRAM USERS MANUAL	267
	a. Input	268
	b. Program Output	284
A.5	SAMPLE CASE	288
A.6	REFERENCES	288

ILLUSTRATIONS

Figure

A-1	Rocket System Diagram	207
A-2.	Calculated Chamber Pressure Versus Time During Low-Frequency Combustion Instability	211
A-3.	Research Rocket Engine	211
A-4.	Comparison of Calculated and Experimental Pulse Mode Firing	212
A-5.	Calculated Popping Amplitude Versus Time	213
A-6.	Calculated Fuel Flow Rate Versus Time	214
A-7.	Calculated Oxidizer Flow Rate Versus Time	215
A-8.	Calculated Resultant Stream Angle Versus Time	215
A-9.	Accumulation of Propellants on Chamber Wall Versus Time	216
A-10.	Calculated Chamber Pressure for Two Short Closely Spaced Pulses	217
A-11.	Progressive Buildup of Fuel on Wall Over Two Short Closely Spaced Pulses	217
A-12.	Injection Temperature Profile vs Flow from Tank	222
A-13.	Approximate Enthalpy of Monomethyl Hydrazine	224
A-14.	Feed System Schematic	226
A-15.	Preimpingement Trajectory of Propellant	234
A-16.	Droplet Circulation Criterion	241
A-17.	Burning Rate vs Reynolds Number	243
A-18.	Temperature vs Stoichiometry	244
A-19.	Molecular Weight vs Stoichiometry	254
A-20.	Gamma vs Stoichiometry	254

TABLES

Table		Page
A-I	Droplet Diameter Distributions Mid-Quintile Diameter/Median Diameter	235
A-II	Droplet Parameters	236
A-III	Sample Case for TCC Program	293

LIST OF ABBREVIATIONS AND SYMBOLS

A	Area, Acceleration, Molecular collision frequency
a	Acoustic velocity
B	Coefficient in vapor pressure equation
C	Specific heat, Coefficient
D	Diameter
E	Activation Energy, Accommodation Coefficient
F	Stoichiometry (mass fraction which is fuel)
f	Fanning friction factor
G	Entrainment parameter
H	Enthalpy
(I)	Subscript indicating a particular member of an array
K	Drop size distribution coefficient, Thermal conductivity
K'	Droplet burning rate coefficient
L	Length
M	Mass
N	Dimensionless modulus
P	Pressure
[P]	Parachor
Q	Heat of reaction
q	Volumetric flow rate, Heat flow rate, Quenching distance
R	Universal gas constant, Coefficient for resistance to flow
T	Temperature
t	Time
U	Chamber volume, Gas velocity
V	Velocity, Any time-dependent variable, Chamber volume
W _m	Molecular weight
X	Mass fraction which flashes, Axial location
Y	Radial location
β	Resultant stream angle
γ	Ratio of specific heats
Δ	Difference
ε	Expansion area ratio

δ	Thickness of a liquid film
μ	Viscosity
ρ	Density
σ	Surface tension
π	Ratio of Circumference to diameter of a circle

SUBSCRIPTS

c	Chamber, Critical point
cond.	Condensed phase
d	Drag, Difference
e	External, Effusion correction
F	Fuel, Thrust coefficient
film	Liquid film
flash	Flash threshold
fuel	Fuel
g	Gas
gas	Gas
i	Droplet group identifier, Chamber axial segment identifier
inj	Injection conditions
j	Jet conditions
L	At axial location L
l	Liquid
m	Wall film material
mn	Droplet mean $D_{mn} = \left[\frac{\sum N_i D_i^m}{\sum N_i D_i^n} \right]^{\frac{1}{m-n}}$
n	Injection group identifier
Nu	Nusselt number
O	Oxidizer, Orifice, Stagnant
Oxid	Oxidizer
P	Propellant p, At constant pressure
R	Resultant after impingement
r	Reduced variable (ratio to critical value), ripple correction

rel.	Relative
Re	Reynolds number
S	Surface
s	Spin-derived
Sat	Saturation conditions
Stream	Stream conditions
T	Throat, Total of fuel plus oxidizer, Tangential direction, Temperature correction
t	Tank
V	Vapor
Vap.	Vapor
w	Wall
We	Weber number
x	Component in the x direction
y	Component in the y direction

Appendix A

TCC

TRANSIENT COMBUSTION CHAMBER DYNAMICS COMPUTER PROGRAM

A Bipropellant Contaminant Production Model

A. 1 INTRODUCTION

a. The TCC Program

The computer program described in this appendix is a subprogram to the Plume Contamination Effects Prediction Computer Program, CONTAM, and performs the time-varying analysis of the chemical and physical processes occurring in the feed system, injector, combustion chamber, and nozzle-throat inlet of a bipropellant rocket-engine system operating under unsteady conditions. As a subprogram to CONTAM, the TCC program is the first link in the analysis of contamination effects, providing information about production of contaminants in the combustion chamber and the dynamic and thermodynamic state of combustion gases entering the nozzle throat. Unburned propellant droplet distributions and liquid wall film flow are computed for the entire transient pulse as well as gas-phase properties. TCC may also be used as an independent computer program on any third-generation computer with a core exceeding 104,000(8) words and a Fortran IV processor.

Development of the TCC program has been supported by MDAC Independent Research and Development over a period of approximately 5 years with additional modification supported by the current Air Force Rocket Propulsion Laboratory study. References A-1 through A-6 discuss the detailed modeling of the combustion processes included in the basic TCC program. Reference A-7 describes the development of the TCC program at the end of 1971, relates it to the earlier work in combustion chamber modeling, and gives an illustration of its use in doing a parametric variation study on a small rocket engine (the Marquardt R6-C). Reference A-8 illustrates the application of the TCC program to perform a detailed rocket engine analysis related to contaminant production and its potential effect upon a satellite. As far as is practical, this appendix will cover all aspects of the modeling and computer program.

b. Development of the MDAC Transient Combustion Chamber Program

The combustion chamber processes important to large rocket engines have been modeled successfully for several years using the method introduced by R. J. Priem and subsequently refined by others (References A-9 through A-12). In these methods, numerical integration is used to calculate the trajectories and evaporation rates of the propellant droplets, assuming steady conditions in the chamber and one-, two-, or three-dimensional flow of the gas and droplets.

This same basic analysis has been extended to include the more complex events of importance in small pulse-modulated rocket engines. Small rocket engines differ from large engines in two important ways: (1) the proximity of the injection points to the chamber wall, the larger surface-to-volume ratio of the chamber, off-nominal injection and atomization during the transients, and the wide-spread use of film-cooling makes deposition of unburned propellant on the walls much more important in small engines; (2) small rocket engines are typically used to control vehicle attitude or for minor trajectory corrections, where the firing duration is typically as short as 10 to 100 msec, thus the transient behavior of a small engine system is at least as important as the steady-state behavior.

The TCC program was started at MDAC in 1967 under IRAD funding as a general method for solving transient problems in liquid rocket engines, and in particular as a basis for aiding in the development of very fast response control engines. It very quickly became evident that the original one-dimensional program had the capability to model low-frequency combustion instability with great precision, that it had a considerable potential for assisting in the analysis of hard starts, and that it offered a feasible approach to the study of contaminant production in pulse-mode rocket engines.

Since 1970 the AFRPL has supported the extension of the program to model contaminant production in liquid bipropellant rocket engines. Under this support, the droplet trajectories were made two-dimensional (three-dimensional in some experimental versions) to model deposition of propellant on the walls, hypergolic ignition and extinguishment were modeled, the wall processes have been modeled with progressively greater precision, and the postfiring dribble and vacuum evaporation have been modeled.

The intent has always been to use the simplest acceptable mathematical approximation for each combustion chamber process but to model all of the processes which are known to be important. Thus, the program is quite general in its capabilities.

The operational problems that can currently be analyzed include vacuum hypergolic ignition and the start transient, pulse-mode specific impulse, low-frequency system instability, production of contaminant material in the plume and as wall film, explosion pressures that can be obtained from chamber detonations, and engine response to off-nominal operating conditions. Good agreement with experiment has generally been obtained.

The present program, however, is still incomplete, in that there are some important processes which are not yet represented, i. e., axial and radial variation in gas stoichiometry, secondary atomization of droplets, pressure waves in the propellant feed systems, heat transfer to and through the walls, etc. It is also obvious that the present experimental correlations for stream breakup distance and primary atomization droplet size, which were all obtained with large orifice sizes, form a very questionable basis for design or prediction when extrapolated to the very small injection orifice sizes found in pulse-mode engines. The complexities of very reactive impingement or stream blow-apart have not been modeled.

c. Scope

The transient combustion chamber program uses numerical integration of the detailed system processes to calculate the events in a rocket engine system operating under unsteady conditions. The system which is modeled consists of a pressure-fed bipropellant feed system, an injector, a combustion chamber, and a nozzle (Figure A-1).

The initial flow of propellant is calculated as the valves open, the fluids accelerate through the resistive-inertial feedlines, and the injector fills. If the vapor pressure of the first injected propellant is sufficiently above the initial chamber pressure, and the stream Weber number is sufficiently high, the atomization is calculated to take place by vacuum-flashing of the stream. If one stream is injected before the other and does not flash, it is calculated to undergo single-stream breakup if there is sufficient distance for it to do so.

CR98

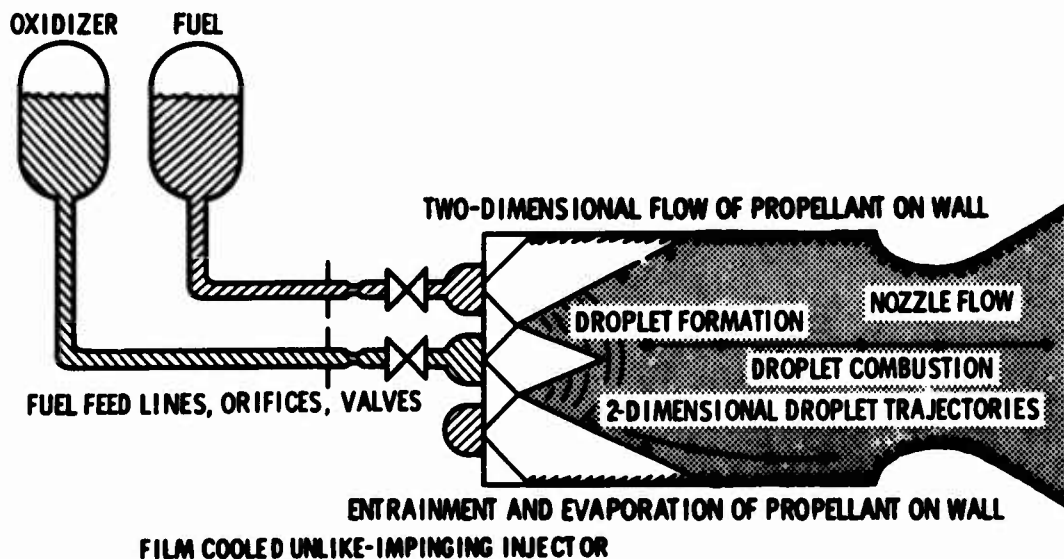


Figure A-1. Rocket System Diagram

Alternatively, it impinges upon the chamber wall, where part of it sticks as wall film and the rest is calculated to atomize by the wall impact. Later in the firing, atomization occurs by the impingement of the two unlike streams. The time-varying initial mean droplet size, the droplet size distribution, the initial droplet velocity vector, initial velocity distribution, and the distance traveled before the breakup process is completed are all calculated as time-varying functions of the injection and chamber parameters.

Two-dimensional trajectories of all of the droplets injected into the chamber are calculated with Reynolds-number-dependent drag coefficients recalculated for each droplet group at each time interval. The trajectories are followed until the droplets either burn completely, pass through the nozzle incompletely burned, or impact upon the wall. The normal bipropellant combustion rates of the droplets are based on droplet diameter and physical properties, droplet Reynolds number, combustion gas temperature and composition, and the presence or lack of ignition in the chamber. When a propellant constituent such as hydrazine has appreciable monopropellant character, this may also be modeled. The combustion rates are recalculated for each droplet group at each time interval to reflect the changing conditions in the chamber. The chamber gas properties are recalculated at each time interval, as is the chamber's velocity profile. The velocity profile is based on the axial distribution of contributions of vapor from burning droplets, igniter flows, vacuum flashing propellant streams, propellant burned off the wall-film and propellant vacuum-evaporated from the wall-film.

Hypergolic vacuum ignition is calculated in the vapor phase, based upon global chemical kinetics (Reference A-13). Various locations are examined to determine where ignition will occur first—the well-mixed vapors in the chamber, the most recently formed vapor mixture from the flashing streams, the boundary layer around the fuel droplets, or the boundary layer around the oxidizer droplets. Once ignition occurs anywhere, the entire chamber contents are presumed to ignite and will continue to burn until the criterion for extinguishment is met. Before ignition, the values for the temperature, molecular weight, and specific heat of the chamber gas are calculated, assuming well mixed but unreacted fuel and oxidizer vapor. After ignition, properties appropriate for equilibrium combustion products are used. After extinguishment, a distinction is drawn between quenched combustion gas and newly formed propellant vapors, so as to properly calculate reignition, if it occurs.

The film of liquid that builds up on the wall may flow in the axial and tangential directions, from its initial momentum, and under the influence of shear forces from the combustion gas and chamber wall. When the film has a tangential velocity component, the effects of spin-generated forces are considered. The film is partially burned off by the heat transfer from the hot combustion gases flowing past it. When threshold levels for an entrainment parameter are exceeded, entrainment from the liquid film is calculated. The axial variation in the wall-deposited material is approximated by dividing the chamber wall into 100 discrete axial segments. The deposition, flow, burnoff, entrainment, and vacuum evaporation from each segment are treated separately, so as to give the film thickness and composition profile and to correctly reflect the influence of unevenly distributed propellant. If the amount and rate of flow of the material on the wall are sufficiently high, some of the wall film material will be carried through the throat and ejected (one form of contaminant production).

The rate of burnoff from each axial segment of the wall is calculated from a heat transfer coefficient based upon the time-varying local Reynolds number, corrected for counter-current mass transfer and rippling of the surface. Entrainment from the surface is modeled based upon the local film thickness and velocity, the local velocity and density of the combustion gas, and the local surface tension of the film (Reference A-14).

When the local chamber wall temperature is sufficiently above the boiling temperature of the propellant droplets (at the momentary chamber pressure), an impacting droplet will bounce off instead of sticking (Reference A-15). When wall-film flows onto an axial segment that is sufficiently hot to cause the transition to film boiling, the film is detached from the surface, converted to a group of droplets, and entered into the ensemble of droplet groups in the chamber.

In calculating the axial and tangential velocities of the liquid material deposited on the wall, each axial element of fluid on the wall is treated at each time interval as an inertial free body being acted upon by shear from the wall, shear from the combustion gas, spin-induced forces, mass and momentum addition from the impinging droplets, mass and momentum loss from burnoff and entrainment, and with convection of fuel and oxidizer mass, axial and angular momentum at the upstream and downstream boundaries. The axial and tangential shear forces at the gas-liquid and liquid-wall interfaces are calculated based on correlations with appropriate local Reynolds numbers. It is presumed that the material in each axial segment is well-mixed at each time interval. When a hydrazine-derivative fuel and nitrogen tetroxide oxidizer are mixed on a wall segment, the neutralization reaction is presumed to take place to form the hydrazinium nitrate salt plus a remainder of whichever reactant is in excess of the stoichiometric ratio. This time-varying two-component system is used to estimate the physical properties of the wall film at each segment.

The assumption is implicitly made that injected fuel or oxidizer will react to give thermochemical equilibrium combustion products only when it is vaporized from the surface of a stream, droplet, or liquid film and the vapors subsequently are mixed with a mass of hot, ignited, combustion product gases.

After the valves have closed, the pressure in the chamber decays, most of the droplets leave the chamber, and the combustion in the chamber is calculated to be extinguished as soon as the time-varying calculated quenching distance exceeds the chamber diameter.

If the chamber pressure falls below the vapor pressure of the propellant in the injector dribble volumes, this material will flow out of the injector. The same technique is used to compute flow rate, atomization, and droplet trajectory as was used during the rest of the firing; with the exception that injector vapor pressure is now used instead of tank pressure to produce flow, and the flow impedances of the injector orifices are used instead of the whole system flow impedances. This dribbled material will be calculated to burn, be expelled through the throat unburned, or be deposited upon the chamber wall, depending upon the injector and chamber conditions.

When the chamber pressure falls below the vapor pressure of the material on the walls, it starts to evaporate, absorbing heat from the chamber

walls. The rate of evaporation from each segment of chamber length is calculated separately, based upon simultaneous solution of the Knudsen-Langmuir evaporation law and the heat transfer through the liquid film.

At any time, the propellant valves may be reopened to initiate a second pulse of firing. The propellant dribbled from the injector following the first pulse will constitute the injector void volume that must be filled to prime the injector for the second pulse; the propellant buildup on the walls will continue from the values attained during the vacuum evaporation following the first pulse, etc.

d. Comparison With Experiment

(1) Low Frequency Combustion Instability

The TCC program calculations were first tested by comparison with high-amplitude, low-frequency combustion instability produced in a small experimental engine (Reference A-16). The engine was operated with a family of four injectors, which differed only in impingement distance. The input to the program consisted of blueprint values for the engine and literature values for the propellant physical parameters, with no fitted coefficients of any kind. The calculated and experimental frequencies differed by no more than 7 percent while the amplitudes agreed within 5 percent for the entire family of injectors (References A-1 and A-2).

Figure A-2 shows the calculated chamber pressure for one of the injectors. It agrees in waveform with the experiment. The rate of rise is two to three times faster than the rate of fall, and it is cusped at the minimum points. The calculated fuel feedline flow rate was interesting in that it periodically assumed negative values; i. e., reverse flow. The integral of the reverse flow with time predicted a maximum backflow bubble volume of 0.4 cc. The back side of the injector was observed with high-speed motion picture photography through a transparent window, and the observed bubble size was in agreement with the calculations.

(2) Vacuum Hypergolic Start Transients

Figure A-3 illustrates a McDonnell Aircraft Company research engine that has been fired to investigate vacuum hypergolic start transients and pulse-mode behavior (Reference A-17). Figure A-4 shows a comparison of an experimental 25 msec duration pulse and a corresponding computed value. The two curves show surprisingly good agreement, especially in the prediction of events. The injector priming delay, the ignition delay, the initial surge from flash-atomized fuel, the succeeding pressure trough, the second pressure surge, the steady-state chamber pressure, and the cutoff delay are all in good agreement. The residual differences between the curves are associated with pressure waves in the experimental engine feed system, which was equipped with very long propellant lines. Pressure waves are not modelled by the lumped-parameter flow algorithm of the TCC program.

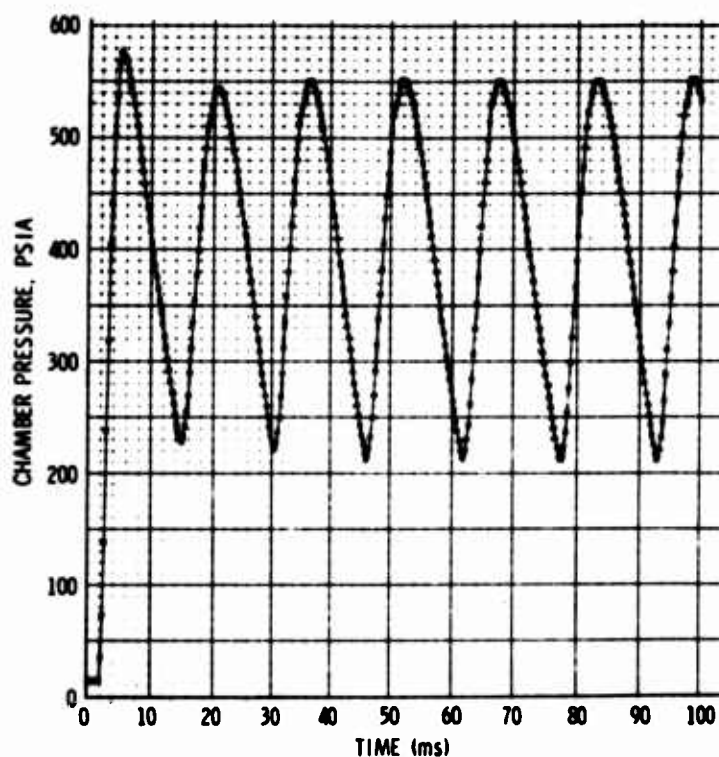


Figure A-2. Calculated Chamber Pressure Versus Time During Low-Frequency Combustion Instability

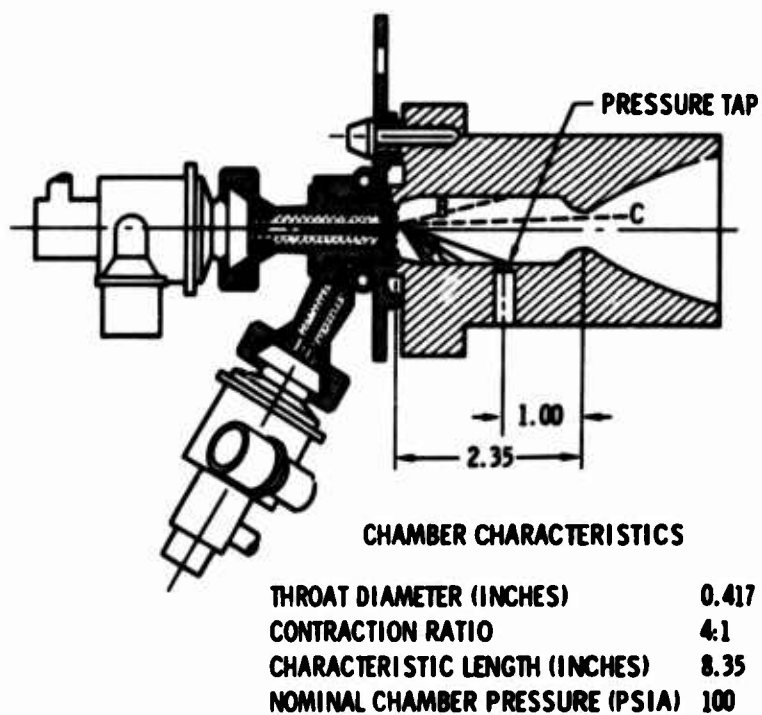


Figure A-3. Research Rocket Engine

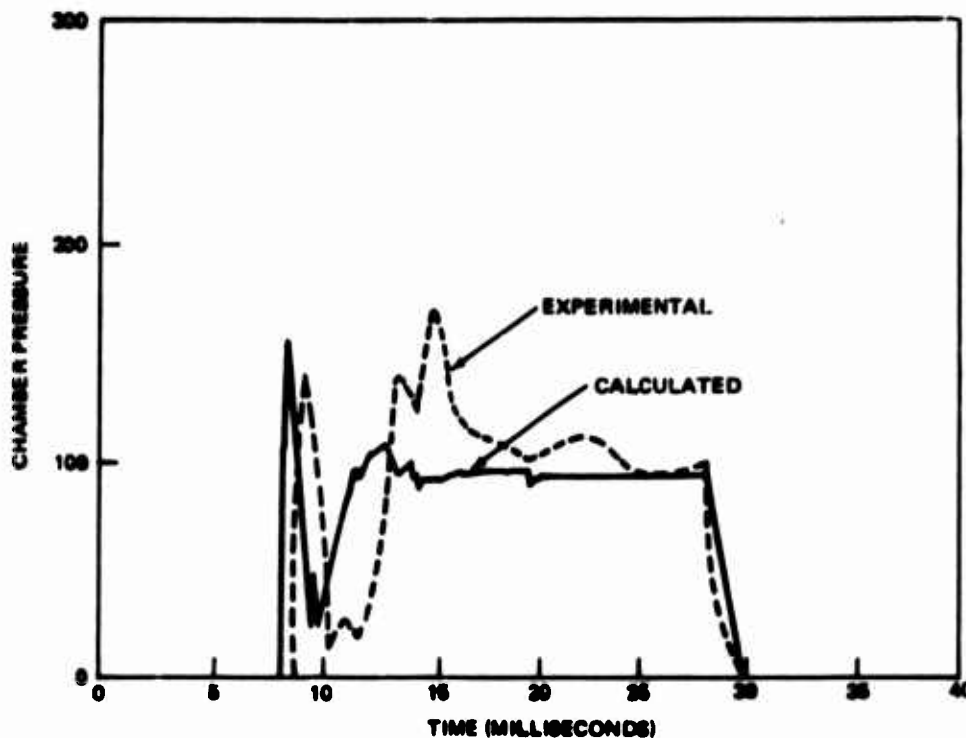


Figure A-4. Comparison of Calculated and Experimental High Altitude Start

(3) Contaminant Production

Contamination from a conventional bipropellant RCS engine takes one or more of three forms: reacted or unreacted propellant vapor (Reference A-18), incompletely burned droplets expelled through the throat (Reference A-19), and unburned propellant that impinges upon the chamber wall and is eventually ejected from the nozzle lip (Reference A-20). All of these sources are modeled by the TCC program. The only mode of contaminant production which has been experimentally measured is wall-film production. The wall-film production rate from the Marquardt R1-E engine was measured at three operating temperatures by P. J. Martinkovic. Calculations of wall film production from the similar R6-C engine have been calculated by the TCC program, and give acceptable agreement with experiment both in trend with operating temperature and in absolute values (See Section III of this report).

(4) Chamber Explosion Amplitude

Since the spatial distribution of unburned propellant in the form of streams, droplets, unreacted wall-film or hydrazinium-nitrate deposits is known in a time-dependent manner; it is possible to calculate the mean chamber pressure that could be produced at any instant by the explosive combustion of this material. The term "popping" is often used to describe the moderate amplitude explosions of the droplets and streams that may be periodically initiated by explosive reactions of the fuel and oxidizer streams near the impingement point. The stream hydraulic conditions and chamber conditions

that can produce impingement point explosions, and the conditions necessary for such an initiating explosion to propagate a detonation through the droplet spray contained in the chamber have been discussed in a number of publications (References A-21 through A-24).

Figure A-5 illustrates the calculated maximum volume-mean "popping" amplitude as a function of time for a particular 60-msec engine firing. Experimental bombings of this engine during the "steady-state" portions of the firing produced experimental chamber pressure amplitudes that had a mean value within 14 percent (or 1.2 experimental standard deviations) of the calculated value.

The time-dependent volume-mean chamber pressure amplitude that could result from a detonation of hydrazinium-nitrate deposits on the chamber walls is calculated in a similar way. Such detonations, which are often called "spikes", have been observed in a number of engines and can be quite destructive. Large transient accumulations of hydrazinium-nitrate have been calculated for two engines, which experimentally are known to produce "spikes" or "spikelike" behavior under certain conditions.

One of these engines is the McDonnell Aircraft Company research engine illustrated in Figure A-3 (Reference A-25). When this engine is operated in pulse mode under vacuum ambient conditions (using NTO and MMH propellants), the oxidizer flows from the injector dribble volume very much

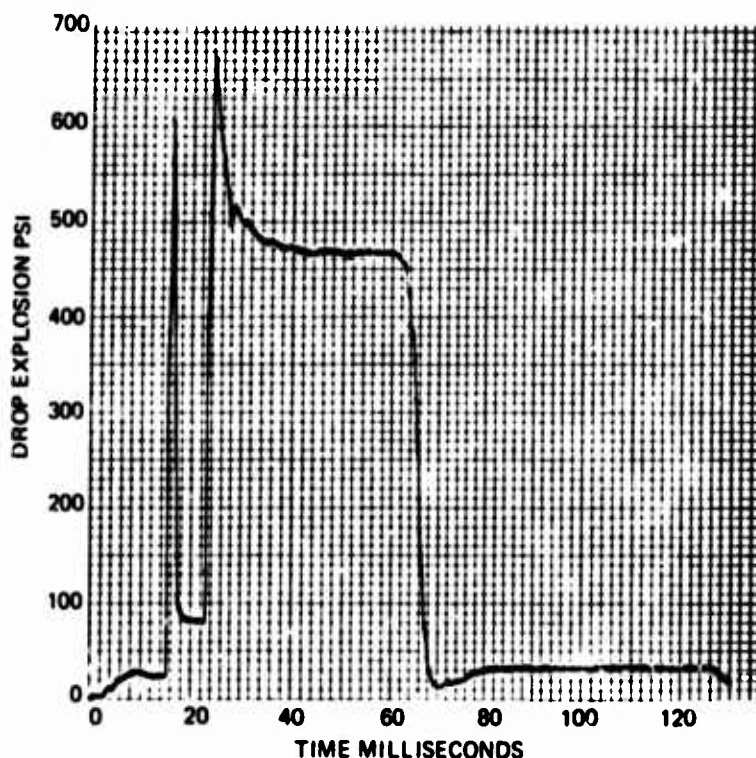


Figure A-5. Calculated Popping Amplitude Versus Time

faster than the fuel does at the end of a pulse because of its higher vapor pressure. Hence, in a train of very closely spaced pulses, successive engine pulses are likely to be started with imbalanced initial conditions, i. e., with an oxidizer dribble volume nearly empty and a fuel dribble volume nearly full. The firing of this engine (Figure A-4) has such an initial condition, corresponding to a previous pulse completed 95 msec prior to its start. The result of this initial condition is shown in Figures A-6 and A-7, which give the fuel and oxidizer flow rates as functions of time after first valve motion. The fuel side fills after 2.3 msec. This increases the resistance to flow and rather quickly limits the flow rate to a value about 40 percent greater than the steady-state value. The oxidizer side, however, takes 8.0 msec to fill, and in this time a flow rate almost 100 percent higher than the steady-state value is attained. The consequences are seen in Figure A-8, which shows the resultant stream momentum angle versus time. Between 2.3 and 8.0 msec, only fuel is entering the chamber. Consequently its momentum is centered along the axes of the fuel orifices, i. e., 35.5 degrees inward relative to the engine centerline. The fuel streams are flash-atomized to form a spray-cone of approximately 30-degree apex angle, as illustrated by A in Figure A-3. Some of the small droplets are turned sufficiently by the initial rush of vacuum vaporized fuel vapor to pass through the throat; however, much of this initial fuel is deposited on the chamber wall. When the oxidizer first enters the chamber 8.0 msec after first valve motion, its flow velocity is so disproportionately high that the resultant momentum angle is 13 degrees outward, as shown in Figure A-8 and as B in Figure A-3.

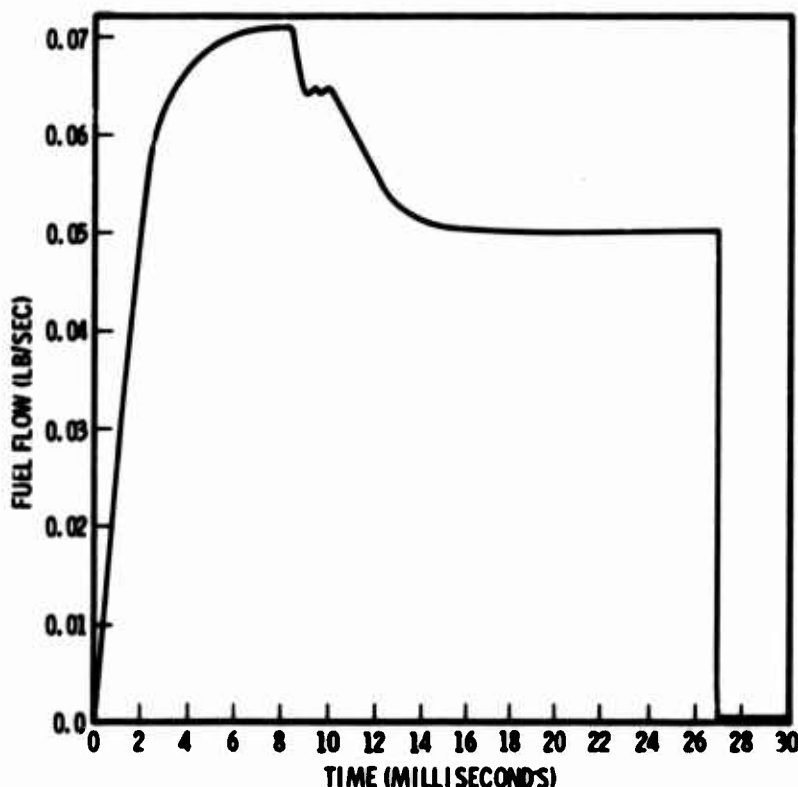


Figure A-6. Calculated Fuel Flow Rate Versus Time

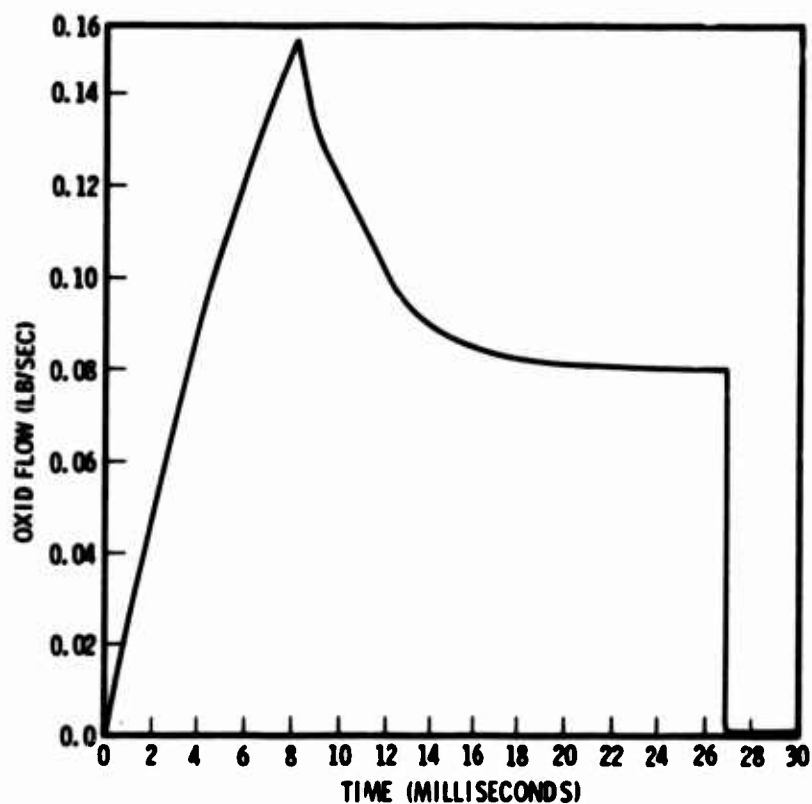


Figure A-7. Calculated Oxidizer Flow Rate Versus Time

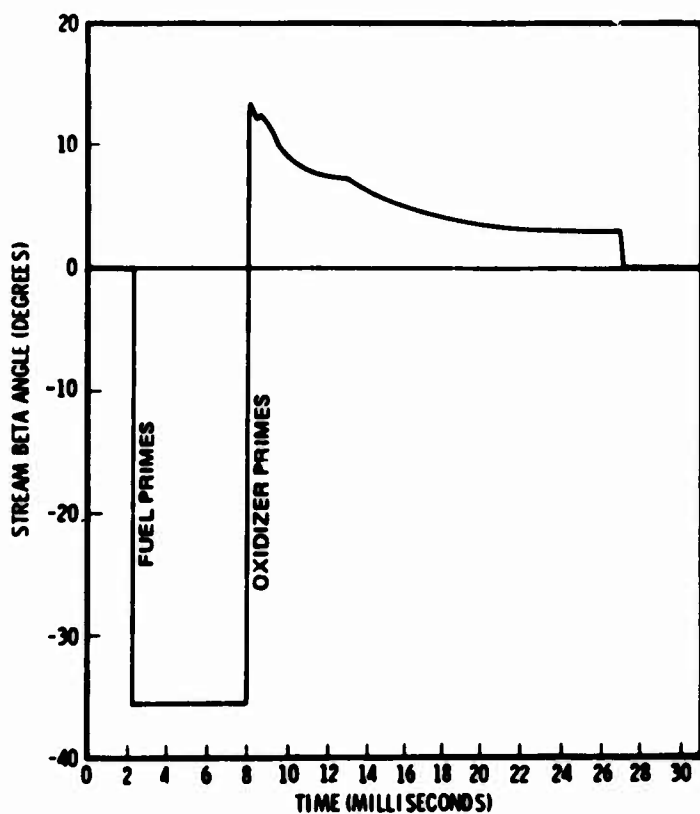


Figure A-8. Calculated Resultant Stream Angle Versus Time

Eventually the propellant flow rates settle to the design value of 3 degrees outward, C in Figure A-3; but in the meantime, 272 milligrams of mixed fuel and oxidizer have been deposited onto the chamber wall, as shown in Figure A-9. This material can be burned off completely in an additional 60 msec of steady operation; however, if it detonates at the worst possible time, a volume-mean chamber pressure of 2,000 to 3,000 psi is produced, depending upon whether the unburned droplets and streams contained in the chamber are detonated also.

This is in general agreement with experiment which gave local measured peak pressures as high as 7,000 psi, with volume-mean chamber pressures on the order of 1,500 to 3,000 psi.

Another engine, for which calculations have been made, only exhibits spikelike behavior when it is run cold and in short pulses. Both of these conditions contribute to the accumulation of detonable material. Again reasonable agreement between calculated and measured overpressures are obtained (References A-5 and A-26).

Figures A-10 and A-11 show the results of very closely spaced repetitive firings of another small RCS engine. This engine will burn its walls clean very quickly after a start transient, however with firings which are too short and too closely spaced, the wall-deposited propellant can build up over a series of pulses.

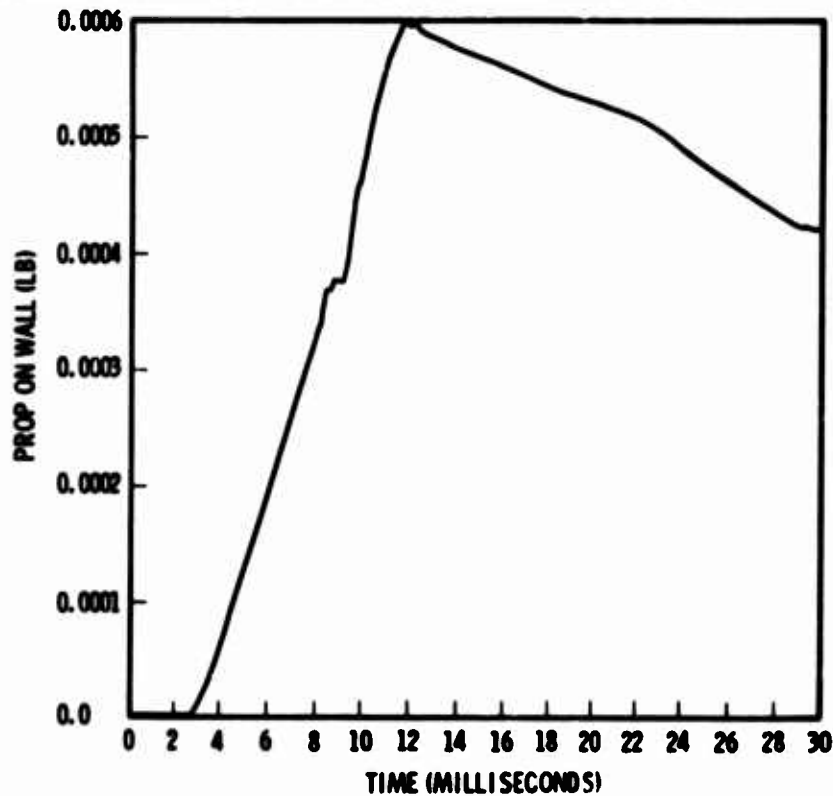


Figure A-9. Accumulation of Propellants on Chamber Wall Versus Time

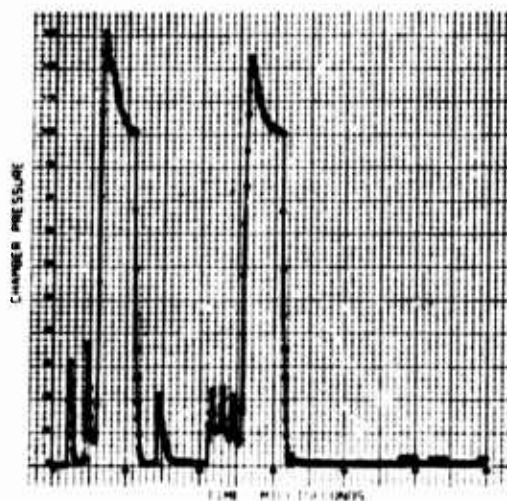


Figure A-10. Calculated Chamber Pressure for Two Short Closely Spaced Pulses

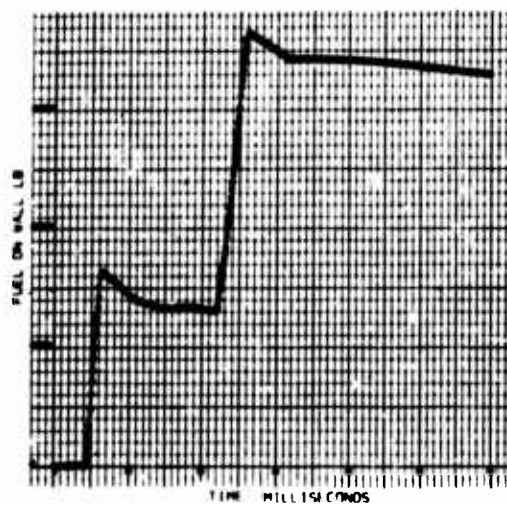


Figure A-11. Progressive Buildup of Fuel on Wall Over Two Short Closely Spaced Pulses

(5) Pulse-Mode Specific Impulse

The calculations of time-varying thrust and time integrated specific impulse are at present a rather uneven mixture of sophistication and oversimplification. The fully transient, two-dimensional treatment of the droplets, and the very detailed treatment of the wall-film behavior implies that the predicted variation of delivered specific impulse with pulse-width or with fraction of total fuel used as film-coolant should be accurate, and this has been verified by comparison with experiment.

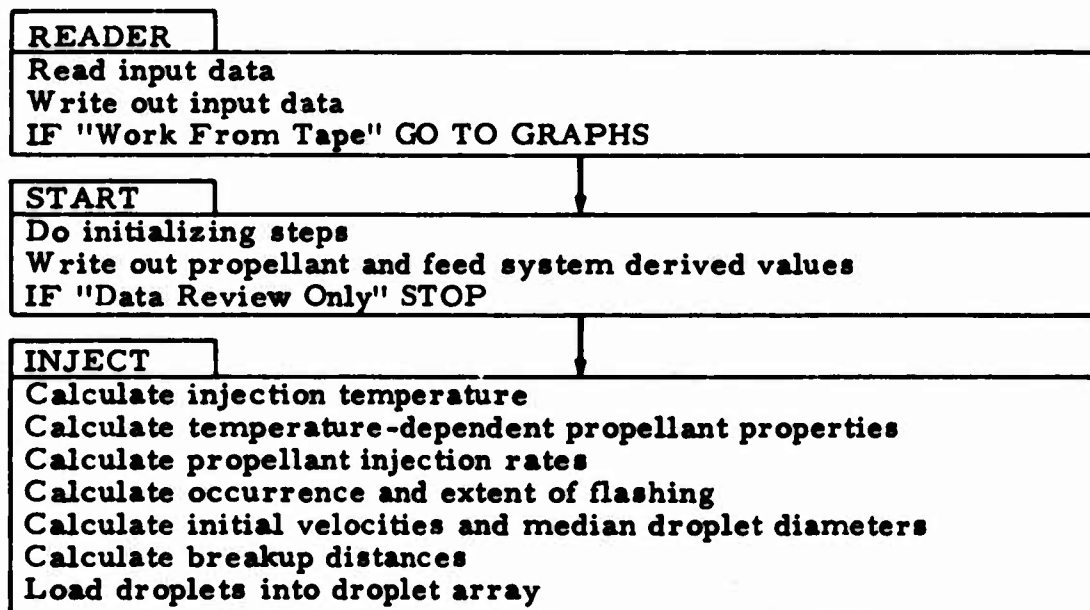
The absolute values for calculated specific impulse have also given good agreement with experimental values; however, this depends in part upon the fortuitous cancellation of errors arising from oversimplifications inherent in the present TCC program.

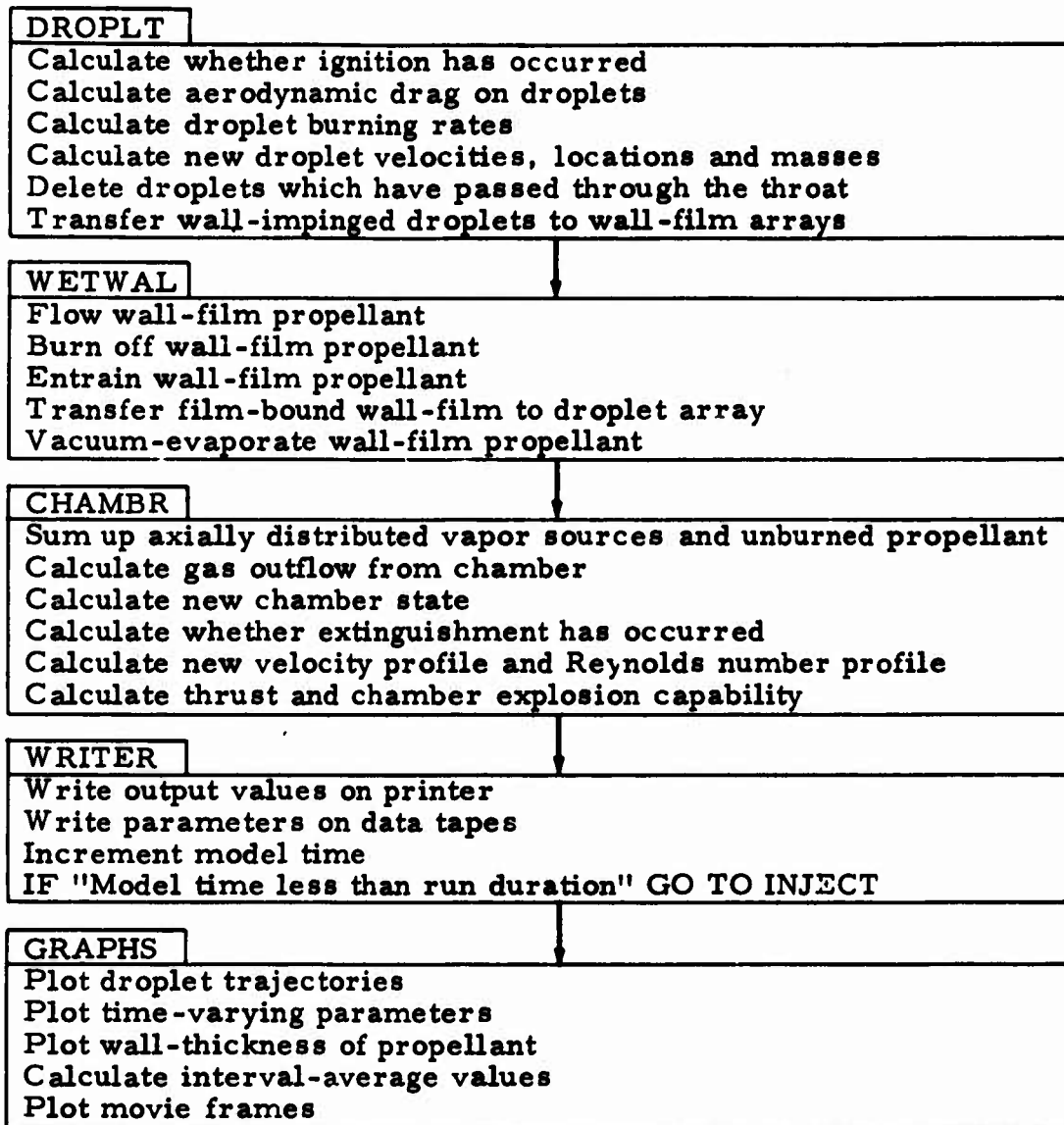
The most important simplifying assumptions are (1) treating the combustion gases in the chamber as being well-mixed, (2) ignoring wall-film evaporation from axial heat conduction in the chamber wall, (3) ignoring secondary breakup of the droplets, and (4) using equilibrium thrust coefficients. The result of these simplifying assumptions is that the characteristic velocity is calculated a few percent too low, while the thrust coefficient is calculated a few percent too high. It is pleasant, but fortuitous that the absolute values of calculated specific impulse have been almost identical with the corresponding experimental values.

A. 2 ANALYSIS

a. Program Structure

The following logical sequence of events, with subroutine names and functions, illustrates the order in which calculations are performed during combustion chamber calculations, and for the two other modes of operation.





It may be seen that there are three principal modes of running the program.

If a nonzero value is given to "Data Review only" input Data Value 208, then the input data are read and they are printed with identifying headings. The initializing steps are performed including calculations of propellant physical property correlations and any feed system values obtained from the flow-rate overrides. Because of the extensive input data required for TCC, it is strongly recommended that any new data deck be checked out with this optional mode of operation before proceeding to make calculations. The person trying to assemble a data deck for the first time will find the input data print of value in assigning DDD1 array subscripts correctly to his data.

The second mode of operation is used to do combustion chamber calculations. After the initializing steps, the successive time increments are calculated by passing repeatedly through the subroutines INJECT through WRITER. The time-varying parameters are calculated and printed, and large amounts of time-varying output is stored on tapes 9 and 13. After the entire run duration time has been calculated, subroutine GRAPHS is entered and any designated plots and interval-averaged performance values are produced. Producing all the possible graphics or interval values would be quite time-consuming and expensive, so it is best to ask only for the most descriptive parameters such as chamber pressure and fuel and oxidizer injection rates at this time.

After the first set of graphics and printout has been examined, it is reasonable to remount tapes 9 and 13 and rerun the program, specifying "work from tape," input Data Value 10. In this mode any new parameter plots can be produced from the values recorded on tape 9. Chamber "snapshots" or "movies" can be produced from tape 13 and the cumulated and mean rate values may be calculated for the start transient, the steady-state portion of the firing and for the tailoff. The times at which these portions begin and end must come from the user's judgment, after examining the available graphics and printout, with the criterion for the time assignments based upon his particular needs. The "work from tape" option may be repeated as many times as desired, so long as the data tapes remain intact.

b. Subroutine READER

The TCC program has taken several forms through the course of its development. The READER subroutine has always read the input data block and reprinted it with descriptive headings. The CONTAM version uses four NAMELIST reads. Other versions exist which use formatted FORTRAN reads or input editors.

c. Subroutine START

The START subroutine converts english unit input to metric CGS units which are used for calculation inside the program. Curve-fit parameters are derived for later use in the propellant property calculations. When flow override values are specified, the corresponding hardware values are calculated and used in place of any conflicting data which might have been read into the input data array. Valve port areas are calculated first if flow rates and valve pressure drops have been supplied. If flow rates and injector pressure drops have been specified, the injection orifice discharge coefficients are calculated next. This calculation assumes that all of the injector pressure drop is localized in the injection orifices. When these calculations are done for multiple-ring injectors, the relative flow rates through the various rings must be specified. This data input is specified as a set of percentage values, but the total flow through all the rings is normalized to unity, so fractional flow or flow ratios or actual flows can be used equally well. The final flow override

value which can be calculated is an equivalent orifice to represent all the losses except valve and injector in the entire feed system. This is particularly useful for modeling complex systems with long lines, many fittings, filters, bellows, etc. The required input data are the difference between tank pressure and chamber pressure at a specified propellant flow rate. In making this calculation, it is presumed that the venturi is not cavitating. The START subroutine does all of the initialization required to commence the combustion chamber calculations and prints out derived values for propellants, feed systems, and chamber shape.

d. Subroutine INJECT

(1) Chamber Wall and Injection Temperature

The injector end and the throat end of the chamber are each assigned asymptotic temperatures for the firing and nonfiring conditions of operation, and half-times for the approach to these values. The time-varying values for injector end temperature and throat temperature are computed from these values. The axially varying chamber wall temperature is linearly interpolated with chamber length between these two values at each computational time interval.

The thermal transient of the propellant delivered after valve opening is approximated by using the injector end temperature until an amount has flowed from the injector equal to the hot slug of fuel contained in the injector at valve opening time. Following this the injection temperature varies linearly with flowed volume, from the injector temperature to the tank temperature, where it remains for the remainder of the firing (Figure A-12). The propellant in the injector is presumed to warm up to injector temperature whenever the valves are closed, so repeated firings start with propellant initially at injector temperature.

(2) Propellant Physical Properties

The density, viscosity, surface tension, vapor pressure, and liquid enthalpy are evaluated at the injection temperature, and are important in determining the dribble flowrates, the onset and extent of stream flashing, the flashing or impinging stream atomization droplet size, and the ignition delay time.

The densities of the liquid propellants are obtained from a mathematical approximation to a general correlation of reduced density versus reduced temperature along the saturation line (Reference A-27). The critical density is obtained from the propellant density given at a reference temperature.

The viscosity is approximated from a mathematical approximation to a generalized correlation of reduced viscosity versus reduced temperature. The critical viscosity is obtained from the propellant viscosity given at a reference temperature.

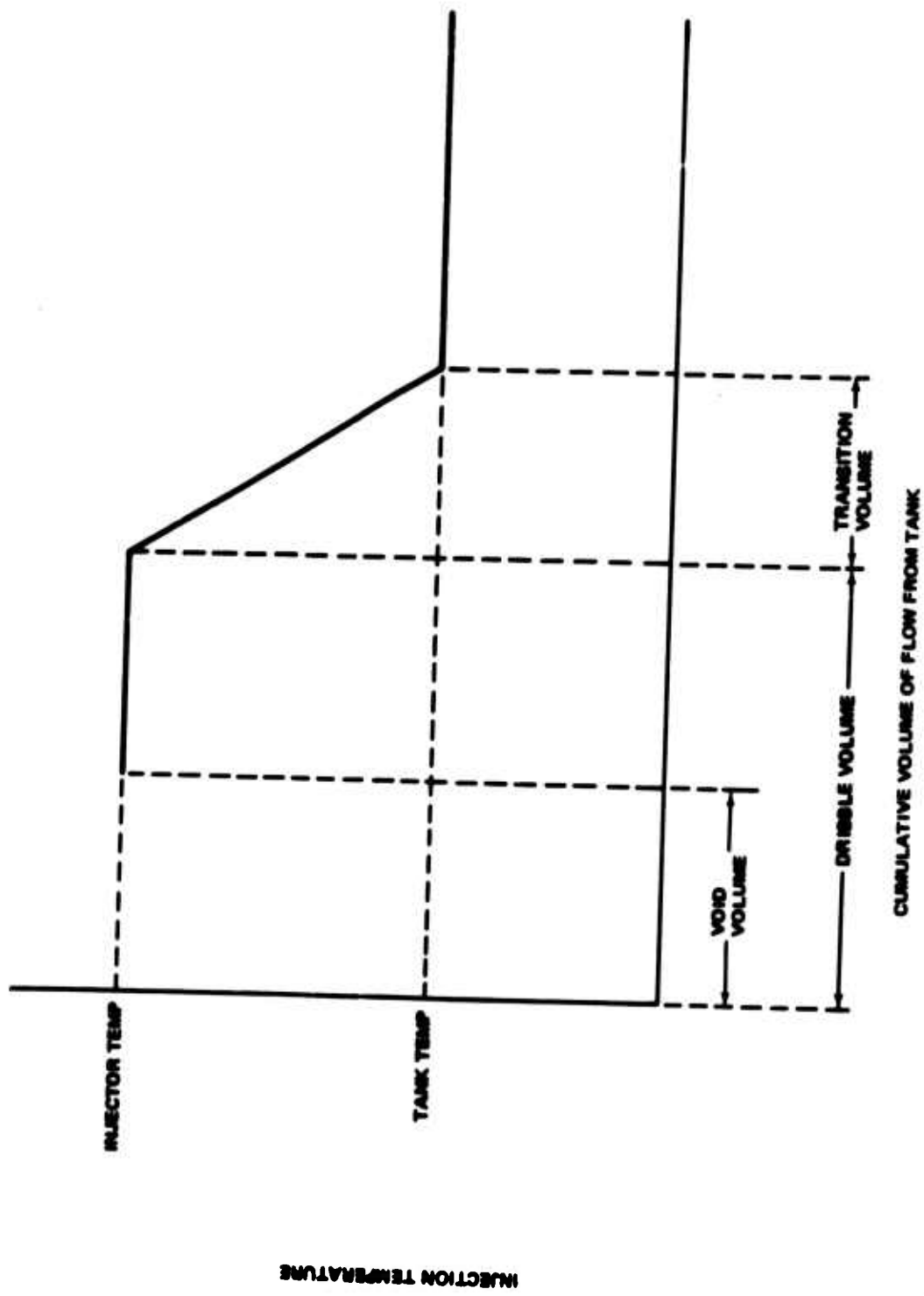


Figure A-12. Injection Temperature Profile Versus Flow from Tank

The surface tension is approximated using the parachor and a mathematical approximation to a generalized correlation of reduced density difference (liquid density-vapor density) versus reduced temperature along the saturation line. The parachor is a parameter which is closely related to the critical properties of a fluid.

$$[P] = \frac{W_m \sigma^{0.25}}{\rho_l - \rho_v} \quad (A-1)$$

For most materials it varies by no more than a few percent over the entire liquid range. The parachor for each propellant constituent is calculated from the propellant surface tension given at a reference temperature, and is used to calculate surface tension at other temperatures.

The vapor pressures of the propellants are obtained from a modification of the equation of Calingaert and Davis (Reference A-28):

$$\ln P = A - \frac{B}{T - C} \quad (A-2)$$

The value used for C is from an empirical correlation with the critical temperature of the material:

$$C = -7.39 + 0.03785 T_c + 0.000149 T_c^2 \quad (A-3)$$

A and B are evaluated for the fuel and oxidizer using the pressures and temperatures corresponding to the normal boiling point and the critical point.

Because of the scarcity of thermodynamic data for many propellants, the specific heats of vapor, liquid, and the solid form of each propellant are assumed to be constants which are neither temperature- nor pressure-dependent. When these values are supplemented by the melting point, heat of fusion, normal boiling point, latent heat of vaporization at the boiling point, and critical temperature, the straight-line relationship of Figure A-13 is obtained. This relationship is used to approximate the enthalpy of the vapor or condensed phases as a function of temperature.

(3) Feed System

The feed systems are approximated with single lumped parameters representing the inertial and resistive aspects of the feed systems:

$$\frac{dq}{dt} = \frac{P_t - P_c - \frac{1}{2} \rho R q |q|}{\rho \Sigma L/A} \quad (A-4)$$

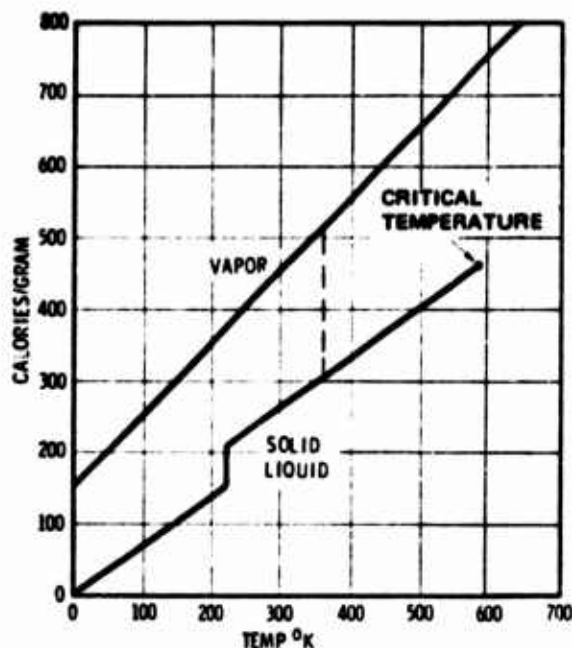


Figure A-13. Approximate Enthalpy of Monomethyl Hydrazine

where

q = volumetric flow rate through the line

P_t = tank pressure

P_c = chamber pressure

R = a coefficient representing the steady-flow pressure drop through the feed system

$\Sigma L/A$ = the summation of segment length divided by cross-sectional area for the series of segments which make up the feed system

Opening and closing of the valves are modeled by varying the value of R as a function of time. Flow reversals or initial start conditions which result in partially or fully gas-filled feedlines are simulated by varying both R and $\Sigma L/A$ as functions of time, so as to delete the resistive and inertial contribution of components which are not liquid filled at any particular instant. Equation A-4 does not model the compressibility of the propellant or the pressure waves in the lines. For cases in which wave action is important, a method-of-characteristics solution for a distributed parameter resistive-inertial-compressible feed system would be more accurate; however, the

present approximation is quite adequate to model flow events which take longer than five or six acoustic periods of the feed system (see Reference A-29).

After the valves close at the end of a firing, the chamber pressure decays, approaching the external pressure. When the chamber pressure falls below the vapor pressure of either propellant, it will start to flow from the dribble volume (the liquid-filled volume between the valve and the injector face). The flow rate out of the dribble volume is calculated using Equation A-4, but with R and $\Sigma L/A$ now restricted to the injector orifice values and with P_t replaced with the propellant vapor pressure evaluated at the injector temperature. As soon as the dribble volume is emptied, the dribble flow rate is set to zero.

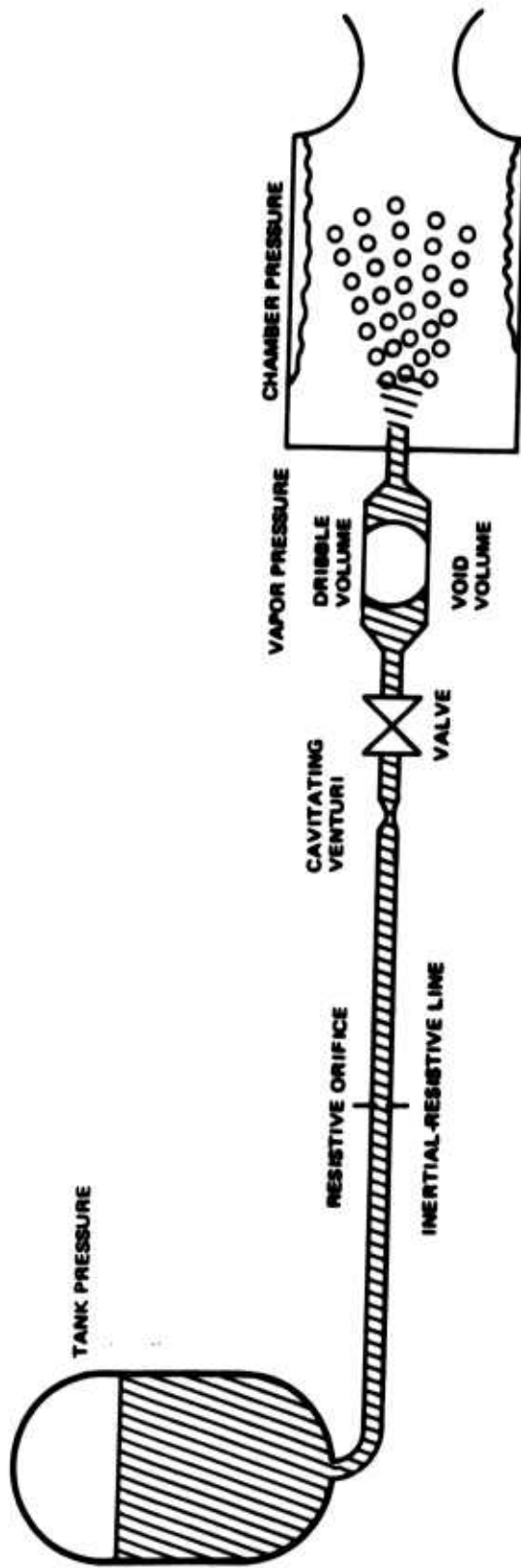
There are two optional assumptions which may be used to describe the injector priming process (Figure A-14). If a ring-type injector is being filled in a vacuum environment, some of the orifices will be wetted even before the ring volume is filled, and flow will be expected through these wetted orifices under the influence of the propellant vapor pressure. The initial dribble option is for this situation, and initial dribble flow rate is calculated the same as a postfiring dribble. The flow from the propellant tank into the dribble volume is calculated according to Equation A-4 but with R and $\Sigma L/A$ restricted to the values for the upstream hardware and with P_c replaced with the vapor pressure evaluated at the injector temperature. As soon as the injector is primed, the flow follows Equation A-4 as written.

The other injector priming option which may be used is appropriate for a smooth unbranched injector passage which would be expected to fill progressively from the valve out to the injector orifices without any dribbling of propellant before the passages are completely filled.

If high-amplitude combustion instability or high-amplitude pressure spikes temporarily reverse the flow in the propellant feedlines, the reverse flow is time-integrated to give the time-varying gas volume behind the injector. So long as there is gas behind the injector, the injection rate is set equal to zero, and the inertial and resistive contributions of the injector orifices are deleted from Equation A-4.

The static pressure in the throat of the cavitating venturi is monitored, and if it falls below the vapor pressure of the propellant, Equation A-4 is evaluated for the impedance of the upstream hardware only, with the venturi throat pressure set to the vapor pressure.

There are several complex modes that flow from the injector could take which have not been programmed in the current model. The propellant in the dribble volume could boil in a vacuum environment, with the well-mixed foam flowing through the orifice. Chugging or popping during the dribble periods could force noncondensable combustion gases into the dribble volumes to form foam at a pressure higher than the vapor pressure. If these modes of flow were found to be important they could be modeled.



PROGRAM OPTIONS

DRIBBLY CUT OFF



DRIBBLE ANYTIME THERE IS LIQUID IN THE INJECTOR AND VAPOR PRESSURE IS ABOVE CHAMBER PRESSURE

DRIBBLY START



DRIBBLE ANYTIME THERE IS LIQUID IN THE INJECTOR AND VAPOR PRESSURE IS ABOVE CHAMBER PRESSURE

NON-DRIBBLY START



NO DRIBBLE BEFORE FILLUP ON FIRST START



DRIBBLE BEFORE FILLUP ON SUBSEQUENT STARTS UNLESS INJECTOR DRIES UP COMPLETELY

Figure A-14. Feed System Schematic

(4) Flash Atomization and Flash Vaporization

The atomization process is calculated for one of several modes, depending upon the chamber pressure, the propellant injection temperature and the propellant injection rates. If the chamber pressure is sufficiently below the vapor pressure of the propellant at its injection temperature, the stream is presumed to flash atomize. If streams of both propellants are being injected and are not flashing, then impinging stream atomization is calculated. If only one stream is being injected, and it does not flash, the stream breaks up in a single-stream mode unless it hits the wall first, in which case it is calculated to break up by wall impact. If both streams are being injected, and only one of them flashes, the other stream is presumed to be unaffected by passing through the spray of small flashed droplets and behaves as though the other stream were absent.

Bushnell and Gooderum (Reference A-30) investigated the flashing of streams of water over a range of subatmospheric pressures, and found that the ratio of stream temperature to saturation temperature was almost a constant at the onset of flashing (with temperature measured on an absolute scale). Brown (Reference A-31) investigated the flashing of streams of superheated water at atmospheric pressure, varying temperature, orifice diameter, and stream velocity, and found that the temperature at the onset of flashing was a function of the stream Weber number. If these findings may be combined, the supersaturation temperature ratio at the onset of flashing may be represented as a function of stream Weber number. The following correlation is taken from the experimental data of Brown, but does not disagree with the data of Bushnell and Gooderum.

$$0 < N_{we} < 12.5 \quad \frac{T_{flash}}{T_{sat}} = 1.138 - 0.005 N_{we} \quad (A-5)$$

$$12.5 < N_{we} < 24 \quad \frac{T_{flash}}{T_{sat}} = 1.085 - 0.00353 N_{we} \quad (A-6)$$

$$24 < N_{we} \quad \frac{T_{flash}}{T_{sat}} = 1.0 \quad (A-7)$$

Where the Weber number is

$$N_{we} = \frac{\rho_g V_j D_o}{2\sigma} \quad (A-8)$$

There is a discontinuity in the function at a Weber number of 12.5 corresponding to some unknown change in the mechanism. The supersaturation temperature ratio is known to depend upon the surface roughness of the orifice; however, this effect has not been modeled in the TCC computer program, and the above relationship is for ordinary drilled holes, flowing full.

Brown has investigated the mean droplet diameter and droplet size distribution obtained when superheated water is flash-atomized at atmospheric pressure.

Gooderum and Bushell (Reference A-32) flashed water through drilled holes into a vacuum (~2 mm Hg) under otherwise comparable conditions and also obtained measurements of mean droplet diameter.

The functional effects of orifice size and temperature were quite different for the two experiments, probably due to the large differences in Weber number. Until the relationships are better understood, we will take 40 microns as a typical mean droplet diameter for the flash atomization of water, with reasonable values for orifice diameter, stream velocity, and degree of superheat. Brown described the flash atomization process as resembling the gas atomization process, with the gas being supplied by the explosive growth of bubbles in the superheated stream. For this reason we have applied a physical properties correction which would be suitable for the gas atomization process. The equation used in the program to describe flash atomization droplet size is:

$$\bar{D}_p = 0.0065 \left(\frac{\sigma_p \mu_p}{\rho_p} \right)^{0.25} \quad (A-9)$$

where

\bar{D}_p = median droplet diameter of propellant P, in centimeters

σ = surface tension of propellant, P

μ = viscosity of propellant, P

ρ = density of propellant, P

The drop size distribution obtained by flash atomization is much narrower than that obtained by impinging stream atomization.

When a stream of propellant is injected into a combustion chamber having a total pressure lower than the vapor pressure of the propellant, and if the Weber number is sufficiently high, then flash atomization will take place from explosive growth of vapor bubbles at nucleation sites in the stream. A certain amount of evaporation of propellant will occur during the flash atomization process. Following this, evaporation from the droplets will proceed, initially following the Langmuir-Knudsen law. If the chamber pressure increases to a value above the vapor pressure of one or both of the constituents, the vaporation can continue by molecular diffusion. Molecular-diffusion-evaporation can continue until the droplets have either equilibrated with the chamber vapors, are expelled through the throat, or impact upon the chamber wall. There are large areas of uncertainty in this complex process. One unknown is the amount of evaporation which takes place during the atomization

process, before the droplets are completely formed. Another is the chemical processes which could occur on the surface of a cold droplet of nitrogen tetroxide which is cryopumping vapors of hydrazine onto its surface.

Seamans, Vanpee, and Agosta (Reference A-13) have calculated the preignition chamber pressure history for the injection of one propellant component, based upon Langmuir-Knudsen evaporation of droplets having a mean diameter of 100 microns in a chamber 1 in. long. They found that the droplets had nearly equilibrated by the end of a time period (1.5 to 5.5 msec) corresponding to a nominal droplet residence time. Since their droplets were quite large for flash-atomized propellant, and since their chamber was quite small, it is reasonable to assume that phase equilibrium is generally attained, and to use this asymptotic value to describe the preignition evaporation.

The TCC program tests each portion of injected propellant by Equations (A-5 through A-8) to determine whether flashing occurs. If it does, the program calculates the fraction of the propellant which will vaporize to obtain local phase equilibrium at the instantaneous chamber pressure. The vapor formed is added to the vapors already in the chamber, the addition being made at the propellant injection point. The liquid which is unvaporized is assigned droplet properties, and the droplets are entered into the chamber droplet array. No further evaporation from or condensation on the droplets is calculated until they either impact upon the wall or until the ignition of the chamber contents occurs.

When liquid propellant is injected at a prescribed injection temperature, the relationships shown in Figure A-13 fix the injection enthalpy. The value of the chamber pressure at the time of injection is used in Equation (A-2) to determine the equilibrium temperature of the flashing propellant. When the enthalpies of the vapor and condensed-phase propellant are evaluated at the equilibrium flashing temperature, the fraction of the propellant which evaporates may be obtained:

$$H_{inj} = X \cdot H_{vap} + (1-X) H_{cond} \quad (A-10)$$

or

$$X = \frac{H_{inj} - H_{cond}}{H_{vap} - H_{cond}} \quad (A-11)$$

Since internal boiling and convective heat transfer inside the droplet both decrease after freezing of the surface, the program has the option of terminating the evaporation process once the liquid droplets have reached the triple point.

(5) Impinging Stream Atomization

When the chamber pressure is sufficiently high that the injected propellant streams do not flash, atomization occurs by either the impinging stream or single stream mode of breakup. The expression for droplet diameter

used in our program is based upon the work of Ingebo (Reference A-33), who examined the atomization of two identical streams of heptane, impinging at 90-degree included angle in air streams having velocities typical of rocket-engine thrust chambers. Ingebo correlated his data:

$$D_{30} = \frac{D_j}{0.30 \sqrt{D_j V_j} + 0.0125 D_j \Delta V} \quad (A-12)$$

where

D_{30} = volume-number-mean droplet diameter

D_j = injector orifice diameter

V_j = injection velocity

ΔV = velocity difference between the injected streams and the gas flow at the atomization point.

Preim et al reported (Reference A-9) that for rocket-engine conditions, where ΔV varies with axial distance from the injector, that 4,560 cm/sec (150 ft/sec) is an appropriate average value to use for ΔV .

Preim also offers a correction for liquid physical properties:

$$\frac{D_A}{D_B} = \left(\frac{\rho_B \sigma_A \mu_A}{\rho_A \sigma_B \mu_B} \right)^{1/4} \quad (A-13)$$

where

D_A = mean diameter obtained with fluid A

ρ = density

σ = surface tension

μ = viscosity

Equations (A-12 and (A-13) are combined, along with the above value for ΔV , the physical properties of heptane and the multiplier need to convert from volume-number-mean diameter to mass median diameter. This yields a more general expression for initial median droplet diameter expected from a symmetrical self-impinging doublet injecting a fluid of specified properties.

$$\bar{D} = \left[\frac{D_j}{0.20 \sqrt{D_j} V_j + 39 D_j} \right] \left[1.725 \left(\frac{\sigma \mu}{\rho} \right)^{1/4} \right] \quad (A-14)$$

This expression is still insufficiently general for the analysis of unlike impinging streams during transients, where the momenta of the two streams may be very different, or where one stream may be missing completely. In the absence of experimental data, a simplifying assumption is used to estimate the effects of relative stream momenta. The simplifying assumption is that a small element of liquid in the stream approaching the impingement point is not affected by the condition of the other stream except through the formation of a quasi-stationary planar stagnation surface which acts to redirect the stream into the initial planar flow pattern leading to the formation of the fan. This leads to the conclusion that stream velocity is not the variable controlling fan formation in Equation A-14, but rather the component of stream velocity relative to the resultant direction of the combined stream. This leads to the generalization:

$$\bar{D}_p = \left[\frac{D_p}{0.24 \sqrt{D_p} V_p \sin \left| \beta_p - \beta_R \right| + 39 D_p} \right] \left[1.725 \left(\frac{\sigma_p \mu_p}{\rho_p} \right)^{0.25} \right] \quad (A-15)$$

where

\bar{D}_p = median droplet diameter for propellant p

D_p = orifice diameter of the injector for propellant p

V_p = velocity of the jet of propellant p along its own centerline

β_p = angle of the stream of propellant p relative to the engine centerline

β_R = angle of the resultant stream relative to the engine centerline

The resultant angle of the combined fuel plus oxidizer stream is calculated assuming conservation of momentum in the axial and radial directions. When a stream which has not flashed intersects a stream which has flash-atomized, it is assumed that there is no momentum interaction; i. e., each stream continues in its original direction instead of being redirected to the "resultant" direction.

If a single stream impacts against the wall before it has traveled a sufficient distance to atomize in the single-stream mode, then atomization is presumed to take place by wall impact. Atomization by wall impact is based

upon Equation (A-15); however, the value used for relative velocity is simply the absolute value of the radial velocity of the stream, $|V_y|$ which is substituted for the term $V_p \sin |\beta_p - \beta_R|$.

Experimental verification of Equation (A-15) is still rather sketchy. It is obviously as correct as Ingebo's expression for the special case (symmetrical 90-degree impingement of heptane) from which it was derived. When only one stream is being injected, the stream angle and resultant angle are identical, and the following special case is obtained.

$$D_p = \frac{1}{39} \left[1.725 \left(\frac{\sigma_p \mu_p}{\rho_p} \right)^{0.25} \right] \quad (A-16)$$

This is an expression for single-stream breakup (with an assumed value for mean gas velocity) and was compared with the findings of Weiss and Worsham (Reference A-34) for this special case. The functional relationships appear to be in approximate agreement and the values predicted for mean droplet diameter under typical rocket conditions were in adequate agreement.

Since Equation (A-15) should account for stream impingement angle, it was compared with the findings of Heidmann and Foster (Reference A-35), who measured mean drop size as a function of impingement angle for symmetrical impinging streams. Again the predictions were in reasonable accord with the data. The droplet sizes obtained from the unlike impingement of streams of water and molten wax have been reported by Rocketdyne (Reference A-36). Evaluated at several points, the Rocketdyne droplet diameter values differed from the values of Equation (A-15) by no more than 5 percent.

All of the early experimental investigations of impinging stream atomization were done with turbulent flow through round orifices flowing full. Unfortunately most real engines have short, sharp-edged orifices with the flow detached. There are some, very small rocket engines whose orifices are in the laminar flow regime, and noncircular injection orifices are being used in some injectors. The effects of these parameters have recently been investigated by L. J. Zajac and others (Reference A-37). Detached flow and laminar flow each result in droplet diameters approximately half the correlation value of Equation (A-15). Droplet diameter correction factors may be used in TCC to account for these effects. The Zajac correction values for detached flow or laminar flow appear to give TCC results which agree with experiment.

(6) Atomization Distance

The distance which the impinged streams travel before the atomization is complete is calculated based upon investigations performed at NASA (References A-35 and A-38). The calculations used in this study presume that the distance to breakup is a prescribed number of orifice diameters in the absence of impingement (i. e., when $\beta_p - \beta_R = 0$ degrees), that it is as specified in Reference A-38 for impingement when $\beta_p - \beta_R = 45$ degrees, and that it varies linearly with $\sin(\beta_p - \beta_R)$ for intermediate values.

$$L_p = L_{45p} + \left(L_{op} - L_{45p} \right) \left(1 - \frac{\sin |\beta_p - \beta_R|}{\sin 45^\circ} \right) \quad (A-17)$$

L_p = fan length for complete atomization of propellant p

L_{45p} = experimental fan length for symmetrical 90-deg impingement

L_{op} = distance for single stream breakup of propellant p

β_p = injection angle of propellant p

β_R = resultant angle of the fuel plus oxidizer fan

When $\beta_p - \beta_R$ is greater than 45 degrees, L_p is taken equal to L_{45p} degrees. When the injected streams are flash-atomized, the droplets are presumed to be formed immediately at the injection point.

The atomization is completed at an axial location in the chamber equal to the impingement distance plus the breakup distance multiplied by the cosine of the resultant angle. This axial location is a droplet group property called XIMP (I) in the TCC program.

To approximate the relatively inert condition of the propellants prior to breakup, we assume that there are no combustion, aerodynamic drag, or momentum interaction between particles of injected propellant in the interval between the injection point and the point of droplet formation, i. e., when $X(I) < XIMP(I)$. Since the injection velocity is time-varying, this implies propellant bunching in this region. This behavior may be visualized from a plot of particle location versus time (Figure A-15). When the first propellant is injected, it is moving quite slowly due to the restriction of the partly opened valve and the inertia of the fluid in the lines. The propellant, which is injected a few milliseconds later, is moving much faster and overtakes the previously injected material.

Where the lines are close together, the bunching is most extreme, and the effects of velocity modulation produce the maximum effect in varying the arrival rate of propellant. In many rocket engines, this point of least-stable propellant flow is close to the location where droplets are formed and become available for combustion, i. e., XIMP (I). The injected propellant moves from the injection point to the impingement point along the direction of injection. After impingement, the stream moves in the direction of the resultant angle. It moves in this new direction until its atomization is complete, after which its two-dimensional trajectory is determined by the aerodynamic drag forces exerted by the chamber combustion gases. At the present time, the spreading of the fan is not modeled. When droplets are formed by flash-atomization, they are presumed to be formed at the injection point, and they are presumed to be immediately subject to aerodynamic forces and available for combustion.

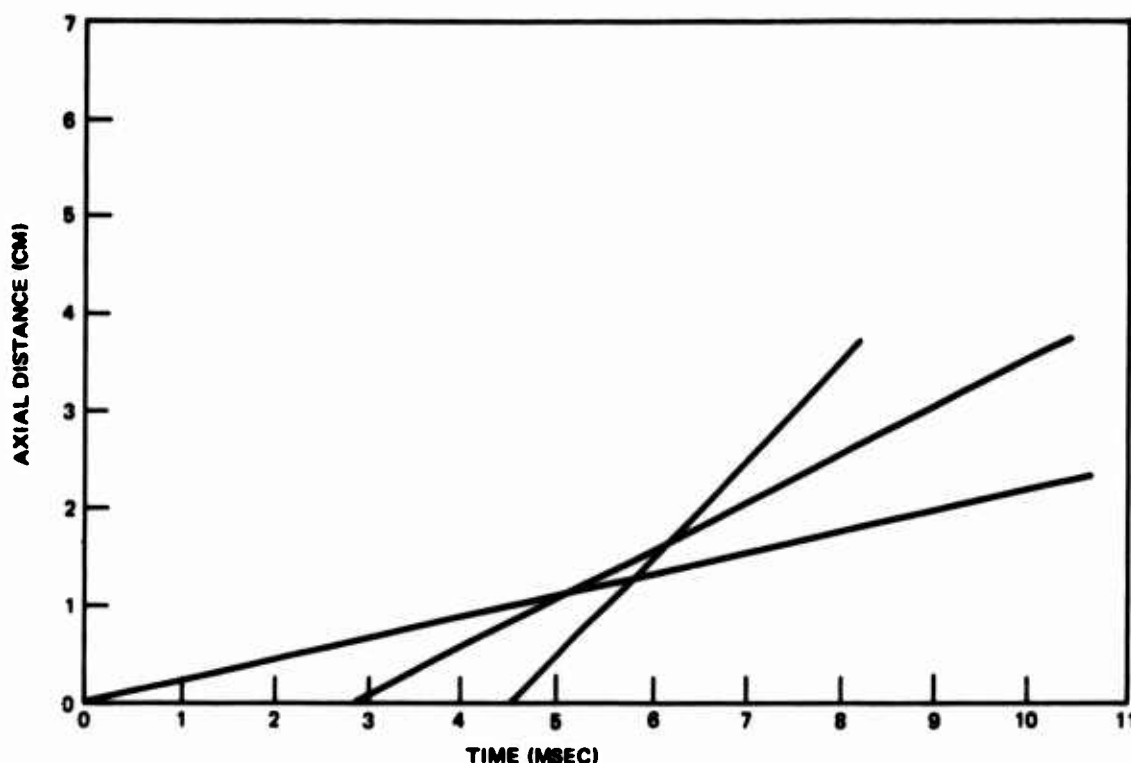


Figure A-15. Preimpingement Trajectory of Propellant

(7) Loading the Droplet Array

The droplets injected into a real combustion chamber are distributed in droplet size, initial direction, initial speed, in point of origin as newly formed drops, and possibly in composition, if the fuel and oxidizer are miscible and not excessively reactive. It is possible to model these distributed parameters by adding more than two droplet groups (one fuel, one oxidizer) to the droplet array during each computational time interval; however, the more droplet groups that are added, the more time-consuming the calculations become. If M values are used to approximate the distribution of each parameter and if N properties are treated as distributed, then the number of droplet groups per propellant is M^N . If M and N were each taken equal to five, then 6,250 droplet groups would have to be added to the computational array during each time interval, instead of the 10 which are presently added. The storage location requirement for the droplet array would increase from 12,000 to 7,500,000 and the computing time on a high-speed computer would increase from about 2 minutes to about 20 hours. Obviously great restraint must be exercised in "improving" the calculations by this particular approach. It is this particular problem which keeps the TCC model from using a truly three-dimensional formulation at this time. It is still possible that a three-dimensional version might be made economically practicable by restricting the initial directional variation to the larger droplet groups, as they are the only ones which can fly cross-wind any distance, and by introducing the directional variation in a time-dependent Monte Carlo approach where only a limited portion of the possible distribution is introduced at any given time iteration.

In the present computer program, the initial droplet diameter is the only parameter which is treated as distributed during "normal" operation; five values are used to approximate the experimental size distribution. For impinging stream atomization, the fifth mass quintile of the propellant has a droplet diameter approximately nine times that of the first quintile. This distribution is so wide that the distribution must be modeled if meaningful results are to be obtained.

During the periods that flash atomization is occurring, the droplet size distribution is much narrower, the fifth quintile diameter being only about twice the first quintile value (Reference A-31). However, at this time the initial directions of the droplets from the flashing stream are distributed over a cone having an apex angle of about 30 degrees. This distributed initial direction must be modeled in order to adequately describe the thickness profile of the propellant which is deposited on the chamber wall during the pre-ignition period.

For these reasons, only the droplet size distribution is modeled for impinging stream atomization, while only the initial direction distribution is modeled for flash atomization.

The droplet size distribution about the median value is approximated by dividing the injected mass of each propellant into five equal portions. Each of these portions is converted to a group of droplets having a diameter which is a prescribed multiple of the median droplet diameter. The droplet group size ratios come from a table of coefficients chosen to approximate the experimental droplet size distribution. The droplet diameter of the nth group is:

$$D_n = \bar{D} K_n \quad (A-18)$$

The coefficients used to represent Ingebo's experimental distribution, a Rocketdyne experimental distribution and a widely used analytical approximation are given in Table A-I.

Table A-I. DROPLET DIAMETER DISTRIBUTIONS
MID-QUINTILE DIAMETER/MEDIAN DIAMETER

	Ingebo Experimental (like doublets)	Log-Probability $\sigma = 2.4$	Rocketdyne Experimental (unlike doublets)
K_1	0.198	0.333	0.60
K_2	0.759	0.645	0.81
K_3	1.00	1.00	1.00
K_4	1.23	1.55	1.22
K_5	2.30	3.00	1.55

After the droplet diameters of the fuel or oxidizer size groups are calculated, the mass per droplet and number of droplets in the group can be computed. The mass of each droplet in the nth group is:

$$M_n = \rho \frac{\pi}{6} D_n^3 \quad (\text{A-19})$$

The number of droplets in the nth group is:

$$N_n = \frac{0.2 \rho q \Delta t}{M_n} \quad (\text{A-20})$$

The feed system and atomization calculations provide values for the mass, median droplet diameter, initial velocity, etc., for the propellant which is injected into the combustion chamber at each time interval. Each group of droplets injected at each time interval is described by twelve variables, shown in Table A-II.

Table A-II. DROPLET PARAMETERS

AM (I)	Mass per droplet
AN (I)	Number of droplets in this group
X (I)	Axial location
Y (I)	Radial location
V (I)	Axial velocity
VY (I)	Radial velocity
SPAMOM (I)	Specific angular momentum
XIMP (I)	Axial atomization point
NUMS (I)	A "packed" integer number containing flags indicating whether or not the droplet group has passed the impingement point, whether it is fuel or oxidizer from which ring it originated, and the iteration at which it was injected.
VM (I)	Axial velocity immediately after impingement
SYM (I)	Radial velocity immediately after impingement
DM (I)	Mass evaporated from this group this iteration

The four values packed into the integer NUMS may be visualized by writing NUMS as an 8-digit decimal integer

										k	k	k	k	l	l	m	n
--	--	--	--	--	--	--	--	--	--	---	---	---	---	---	---	---	---

n has a value of 1 before impingement, 0 after impingement

m has a value of 1 for a fuel droplet, 0 for an oxidizer droplet

ll has a value corresponding to the ring from which the droplet originated

kkkk has a value equal to the iteration at which the droplet was injected

As an example, a postimpingement fuel droplet which originated at the third ring during the 157th iteration would have a value for NUMS of 1570310.

NUMS may be assembled in the following manner:

$$\text{NUMS} = K * 10000 + \text{IMRING} * 100 + \text{IFRAC} * 10 + \text{IXIM}$$

The final complication of NUMS is that the iteration number is used only to designate whether a trajectory plot is to be made. For this reason, the iteration number is given a nonzero value only if the droplet is from the size group designated to be plotted.

The droplet array has 10 new droplet groups added to it from each injector ring at each integrating time interval, and has droplet groups deleted when the mass of the droplet falls to zero, the axial location exceeds the chamber length, or the radial location exceeds the chamber radius. This data array grows to represent the entire droplet population of the combustion chamber.

Each droplet group has the mathematical character of a vector in that 12 independent values are required for its description. The total droplet population of the chamber is then an array of droplet vectors or a matrix. The droplet population of the chamber can usually be adequately described using no more than 1,000 droplet groups or 12,000 computer storage locations. (The number is determined by the size of the integrating time interval.) The combustion chamber calculations consist of working on the array of droplet groups at each computational time interval to obtain the succeeding new value for droplet mass, droplet axial velocity, droplet radial velocity, droplet axial position, droplet radial position, and droplet evaporation rate. The storage locations reserved for the droplet group parameters are reused when the previous droplet group is burned completely, escapes through the throat, or sticks to the wall. If the droplet arrays fill up, leaving no place for newly injected propellant to go, an error message is printed and the calculations are stopped.

e. Subroutine DROPLT

(1) Ignition

Several types of ignition are modeled by the computer program. Calculations may be performed for sea-level or high-altitude ambient conditions, and for hypergolic or nonhypergolic propellants.

When a motor is being started at atmospheric pressure, using a liquid propellant igniter, it is assumed that droplets of the main propellants ignite instantaneously. When the fuel and oxidizer flow rates to the igniter and the axial location of the igniter port are specified, the initial composition, temperature, and axial velocity profile of the chamber gas are established. Although droplet ignition is presumed to be instantaneous, it would be erroneous to presume that the calculated start transient will necessarily be either smooth or simple, as experience has frequently shown it to be otherwise.

When nonvolatile hypergols are injected at atmospheric pressure, the ignition results from complex liquid and vapor phase processes and it is necessary to obtain ignition delay values from the published literature based on experimental tests. When such an ignition delay time is prescribed, the droplet burning rates are set to zero during the preignition period. The delay time is counted as starting only after both fuel and oxidizer streams have reached the impingement point in the chamber.

When volatile hypergolic pairs are injected under near-vacuum conditions, the ignition depends upon the physical processes which contribute to the production of reactive vapors in the chamber. The calculation of the ignition delay time in the vapor phase is based on an equation given by Seamans, Vanpee, and Agosta (Reference A-13):

$$\tau_{\text{ignition}} = \frac{RT^2 \rho_{\text{gas}} C_p}{EAQ C_{\text{fuel}} C_{\text{oxidizer}}} \text{Exp} \left(\frac{E}{RT} \right) \quad (\text{A-21})$$

where E, A and Q are the activation energy, frequency factor, and heat of reaction for the vapor phase reaction responsible for ignition. C_p is the specific heat of the vapor mixture in the combustion chamber and C_{fuel} or C_{oxidizer} are the concentrations of fuel and oxidizer vapor in the chamber gases.

This function may be evaluated in either of three ways. One option is to assume that there is no axial mixing of vapors. In this mode, the relative concentrations of fuel vapor and oxidizer vapor come from the relative amounts flashed at each instant. A second option is to assume that all the vapors in the chamber are well-mixed. In this mode, the values for fuel and oxidizer vapor concentration used in Equation (A-21) are derived from a mass balance on the chamber considering the entire previous history of vapor generation and outflow. The third option presumes that at any instant there will be some location in the chamber which has the optimum stoichiometry for the quickest possible ignition. This optimum stoichiometry is found by examining the well-mixed vapor composition in the chamber, as well as the most advantageous composition in the boundary layers surrounding

fuel droplets and oxidizer droplets (when they are present), the composition having the greatest value for $(C_{\text{fuel}} \times C_{\text{oxidizer}})$ is the one used in the ignition calculations. Any ignition delay time longer than the gas residence time is discarded, as external ignition is ineffective. Because of the necessity of calculating repeated ignitions and extinguishments, unreacted fuel and oxidizer vapors are distinguished from residual quenched combustion product gases in calculating the concentrations used in Equation (A-21).

The vapor-phase ignition delay time is recalculated at each time interval, and the chemical delay time is added to the model time at which the calculation is made to obtain a projected time of ignition. The smallest value for the projected time of ignition is retained. Ignition is presumed to occur when the model time exceeds the smallest value for projected ignition time.

(2) Droplet Drag

The aerodynamic drag, heat transfer, and diffusion rates associated with the droplets depend upon a number of dimensionless groups which characterize the regime of flow; thus, the Reynolds number, Mach number, and Knudsen number must be considered. The Reynolds number is of great importance to all of the transport processes. Drag coefficients and heat transfer coefficients are correlated with droplet Reynolds number. The Mach number of the flow about the droplets is generally less than 0.1 and its effects are ignored. The Knudsen numbers associated with the chamber processes have been calculated for a large number of conditions. The Knudsen numbers may be large for the first computational time interval, when the chamber pressure is taken equal to space ambient pressure; however, the Knudsen numbers have always been well into the continuum flow regime as soon as the first portion of either propellant is injected. Thus, free molecular flow effects should be negligible and are not considered in the correlations for vaporization rate, aerodynamic drag, and nozzle flow.

The velocity of the chamber gas relative to each droplet group must be calculated at each time interval in order to obtain the droplet aerodynamic drag and droplet combustion rate.

The absolute value of the chamber gas velocity relative to the droplet is:

$$V_{\text{rel.}} = \sqrt{(V_{\text{xgas}} - V(I))^2 + (V_{\text{ygas}} - VY(I))^2} \quad (\text{A-22})$$

The Reynolds number is calculated for each droplet group at each time interval based upon the droplet diameter (obtained from the droplet mass, presuming spherical geometry) and the velocity difference between the droplet and the gas.

$$D = \left(\frac{6M_i}{\pi \rho_i} \right)^{1/3} \quad (\text{A-23})$$

$$N_{Re} = \frac{\rho_{gas} D_{drop} V_{rel}}{\mu_{gas}} \quad (\text{A-24})$$

If the Reynolds number is less than 0.5, Stokes law acceleration is calculated:

$$A = \frac{18\mu_{gas} V_{rel}}{\rho_{drop} D^2} \quad (\text{A-25})$$

If the Reynolds number is greater than 0.5, the acceleration is calculated from the Newtonian drag law:

$$A = \frac{0.75 C_d \rho_{gas} V_{rel}^2}{\rho_{drop}} \quad (\text{A-26})$$

The drag coefficient data of Rabin (Reference A-39) are approximated by the functions:

$$0.5 < N_{Re} < 70 \quad C_d = 27 N_{Re}^{-0.84} \quad (\text{A-27})$$

$$70 < N_{Re} < 59,200 \quad C_d = 0.414 N_{Re}^{0.1433} \quad (\text{A-28})$$

$$59,200 < N_{Re} \quad C_d = 2.0 \quad (\text{A-29})$$

(3) Droplet Evaporation Rate Calculations

The evaporation rate (combustion rate) of a stable fuel or oxidizer droplet is determined by the heat transport to the droplet surface and diffusional mass transport away from it. In the regime encountered in a rocket combustion chamber, the vapor effusion from the droplet has a very large effect on the heat transport process, and the effect of the forced convective flow about the droplet is also of great importance. An additional, important factor in determining the droplet life history is the transport of heat from the surface of the droplet to its interior.

If the droplet has appreciable internal circulation, the convective transport of heat to the interior of the droplet will be large, and there will be a considerable unsteady period when the droplet is warming from its initial injection temperature to the final steady temperature at which it evaporates. The unsteady droplet evaporation problem may be solved by simultaneous calculation of the heat and mass transport about the droplet together with the droplet state (Reference A-40).

If the droplet lacks internal circulation, then heat transport into the interior of the droplet is negligible (Reference A-41), and all the heat which reaches the droplet surface is used in vaporizing the outermost layer of fluid. When this is the case, the droplet state and vapor diffusion equations need not be solved.

According to Bond and Newton (Reference A-42), as cited by Hughes and Gilliland (Reference A-43), droplets will only circulate when the surface shear forces are sufficient to overcome the surface tension forces. An approximate criterion for the onset of circulation is

$$\Delta V = \sqrt[3]{\frac{\sigma^2}{\mu_{\text{gas}} \rho_{\text{gas}} D}} \quad (\text{A-30})$$

where ΔV is the difference in velocity between droplet and combustion gas at which circulation will start. This threshold is illustrated in Figure A-16.

CR90

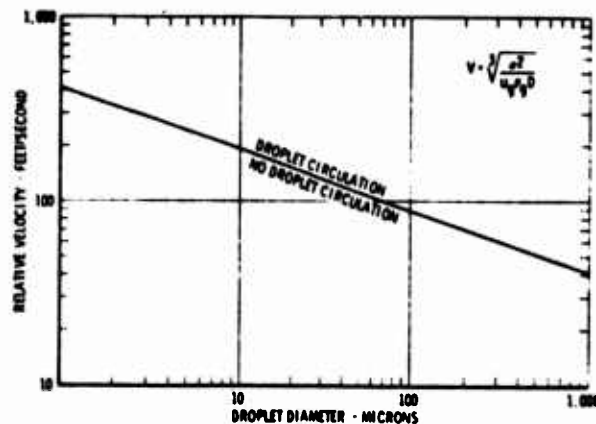


Figure A-16. Droplet Circulation Criterion

The gas properties in Figure A-16 are appropriate for a combustion chamber operating at 500 psia on liquid oxygen and RP-1. The surface tension is for room-temperature RP-1. According to this figure, circulation is expected in large droplets even at low relative velocity, but is not expected during most of the lifetime of the smallest droplets found in a rocket combustion chamber. In order to model accurately the evaporation of both large and small droplets in a time-varying environment, the presence or absence of circulation should be determined for each droplet group at each integration time interval, with heat transport into the droplet permitted only when circulation is present.

For the present calculations, the simplifying assumption is made that there is no heat transfer into the interior of any of the droplets. This permits accurate calculations for the small droplets responsible for much of rocket transient behavior, at the expense of accuracy in modeling the large droplets which largely determine combustion efficiency.

Heat transfer is correlated in terms of a Nusselt number. For a sphere

$$q = N_{NU} \pi K D \Delta T \quad (A-31)$$

where q is heat transfer rate and K is thermal conductivity of the vapor film.

From the assumption that all heat reaching the surface of the droplet goes to evaporate liquid

$$\dot{M} = \frac{q}{\Delta H} = \frac{N_{NU} \pi K D \Delta T}{\Delta H} \quad (A-32)$$

where \dot{M} is the rate of evaporation and ΔH is the sum of the latent heat of the liquid and the sensible heat required to raise it from the injection temperature.

A noneffusing sphere in a nonconvective environment has a Nusselt number of 2.0, but the value for a droplet evaporating into a high-temperature environment is much lower. Godsave (Reference A-44) gives a simple but adequate estimate for the heat transfer to a burning droplet, assuming that thermal conductivity and specific heat of the vapor film are constant. His equation may be rearranged

$$N_{NU} = 2.0 \left[\frac{\Delta H}{C_p \Delta T} \ln \left(1 + \frac{C_p \Delta T}{\Delta H} \right) \right] \quad (A-33)$$

The rate of fuel consumption from burning fuel-wetted spheres has been determined experimentally under forced convective conditions by several investigators (Reference A-45, A-46, and A-47). These experimental values are correlated (Figure A-17) by the equation

$$\frac{\dot{M} - \dot{M}_0}{\dot{M}_0} = 0.25 N_{Re}^{0.50} \quad (A-34)$$

where \dot{M}_0 and \dot{M} are nonconvective and convective consumption rates. This is rearranged and combined with Equations (A-32) and (A-33) to give

$$N_{NU} = \left[2.0 + 0.5 N_{Re}^{0.5} \right] \times \left[\frac{\Delta H}{C_p \Delta T} \ln \left(1 + \frac{C_p \Delta T}{\Delta H} \right) \right] \quad (A-35)$$

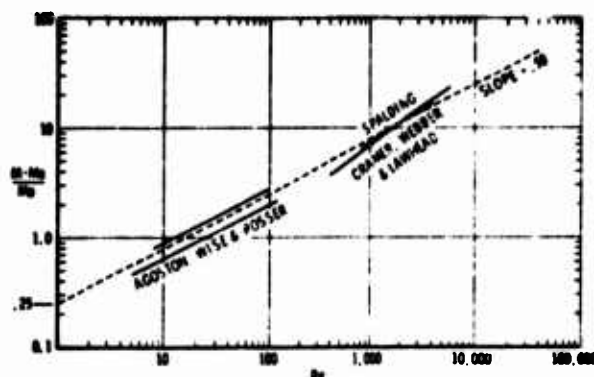


Figure A-17. Burning Rate Versus Reynolds Number

The term containing Reynolds number represents the effect of forced convection on a burning sphere. It is very similar in value to the correlation of Ranz and Marshall (Reference A-48) for the rate of evaporation from wetted spheres, but is preferred for this application because it was obtained in the presence of combustion and with temperature differences up to 3,000°K and Reynolds numbers up to 6,000. The Ranz and Marshall experiments were limited to temperature differences of 100°K and Reynolds numbers of 200.

Equations (A-32) and (A-35) may be combined to give

$$\dot{M} = \left(\frac{\pi K}{C_p} \right) D \left[2.0 + 0.5 N_{Re}^{0.5} \right] \times \ln \left[1 + \left(\frac{C_p}{\Delta H} \right) \Delta T \right] \quad (A-36)$$

which is the expression used to calculate the burning rate of a single droplet. In the computer calculations, $(\pi K/C_p)$ and $(C_p/\Delta H)$ are the parameters used to characterize the combustion properties of the fuel and oxidizer materials. These values are not treated as time-varying in the analysis in order to simplify the calculations. To obtain agreement with experimental burning rate values, C_p and K are evaluated at the arithmetic mean of the expected droplet surface and hot gas temperatures.

The temperature difference used in the burning-rate equation is the difference between the instantaneous droplet boiling temperature obtained from Equation (A-2), and the flame temperature or gas temperature surrounding the droplet.

The flame or gas temperature used in the burning-rate equation is obtained from the curve of chamber temperature versus composition (Figure A-18), the calculated composition of the chamber gas, and the known composition of the droplet which is carried as a subscripted variable. It is presumed that when a droplet of a given stoichiometry is evaporating into chamber gas having a different stoichiometry, every intermediate stoichiometry will be found in the diffusion zone surrounding the droplet and that the local temperature in the diffusion zone will correspond to the local stoichiometry. Thus the flame temperature used in the burning-rate equation

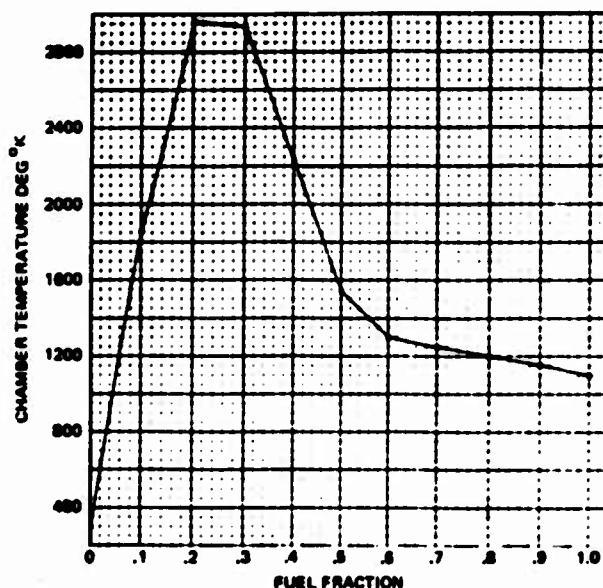


Figure A-18. Temperature Versus Stoichiometry

is the highest temperature found on the temperature versus composition curve in the interval between the chamber gas stoichiometry and the droplet stoichiometry.

There are many common propellant materials for which the vapor thermal conductivity is unknown in the 1,500 to 2,000°K temperature range. Nitric acid and UDMH are good examples. Experimental droplet burning rates have been obtained for these materials, and these burning rates may be used to infer this necessary information. Normally experimental burning rate data are given in terms of a burning rate constant, K'

$$\frac{dD^2}{dt} = -K' \quad (\text{A-37})$$

in terms of our droplet burning rate expression

$$K' = \frac{8K \Delta T}{\rho \Delta H} \left[\frac{\Delta H}{C_p \Delta T} \ln \left(1 + \frac{C_p \Delta T}{\Delta H} \right) \right] \quad (\text{A-38})$$

This expression is solved for K using the experimental value for K' . When the mean value for thermal conductivity is obtained this way, the droplet combustion equations are no longer being used to derive the burning rates from basic principles, but merely become functions for extending a burning rate measurement to a different flame temperature.

Some propellant materials have the capability of burning as a monopropellant. Examples are hydrazine, propyl nitrate, and hydrogen

peroxide. When the monopropellant burning rate is known as a function of chamber pressure from liquid strand tests, the burning rate may be entered, correlated in the form

$$r = A + BP^n \quad (\text{A-39})$$

where r is the burning rate in cm/sec and P is pressure in psia. The corresponding mass burning rate of a droplet is

$$\dot{M} = r \pi \rho D^2 \quad (\text{A-40})$$

When propellant droplets can burn as either a bipropellant or as a monopropellant, the computer program calculates the burning rate for each droplet group in both ways at each time interval, and the larger of the two values is used.

(4) Droplet Velocity and Location

The simplifying assumption is made that the combustion chamber contour consists of seven butted cylindrical segments or conical frustum shapes. The corresponding assumption for gas flow direction is that it consists of a series of butted parallel flows or radial source or sink flows. This permits easy evaluation of the axial and radial components of chamber gas velocity at any point in the chamber. The direction cosines of the relative wind producing aerodynamic forces on the droplet are

$$C_x = \frac{V_{x\text{gas}} - V(I)}{V_{\text{rel.}}} \quad (\text{A-41})$$

$$C_y = \frac{V_{y\text{gas}} - VY(I)}{V_{\text{rel.}}} \quad (\text{A-42})$$

where $V_{\text{rel.}}$ is the absolute value of relative velocity as defined in Equation (A-22).

After the droplet acceleration and direction cosines have been calculated, the new velocity and location of the droplet group are calculated

$$V_{X(t+\Delta t)} = V_{X(t)} + A C_X \Delta t \quad (\text{A-43})$$

$$V_{Y(t+\Delta t)} = V_{Y(t)} + A C_Y \Delta t \quad (\text{A-44})$$

$$X_{(t+\Delta t)} = X_{(t)} + V_{x(t)} \Delta t + 0.5 A C_X \Delta t^2 \quad (\text{A-45})$$

$$Y_{(t+\Delta t)} = Y_{(t)} + V_{Y(t)} \Delta t + 0.5 A C_Y \Delta t^2 \quad (\text{A-46})$$

When the axial location of a droplet group exceeds the length of the chamber, the droplet group is removed from the array and its mass is added to the summation of unburned droplets that escape from the chamber.

When the radial position of a droplet group exceeds the radial dimensions of the chamber—and certain other conditions are satisfied—the droplet group is removed from the array and its mass is added to the summation of propellant mass which is coating the chamber wall at that particular axial location.

The droplets which remain in the chamber have their new mass calculated

$$M_{(t + \Delta t)} = M_{(t)} - \dot{M} \Delta t \quad (A-47)$$

where the value used for \dot{M} comes from Equation (A-36) or (A-40).

Droplets are not permitted to decrease to negative masses. When the mass of droplet I decreases to zero all the other parameters for droplet group I are set to zero and the storage locations can then be used for a newly injected droplet group.

Each time that the mass decrement of a droplet is calculated from Equation (A-47), the value for the evaporation from that droplet group at that time interval is also calculated and is stored as DM(I) until it can be used in the summations which give the velocity profile in the chamber and the total burning rate for the chamber.

f. Subroutine WETWAL

(1) Wall-Film Flow Calculations

When a droplet group moves radially to the location of the combustion chamber wall, its fuel or oxidizer mass is deleted from the droplet array and is added to the appropriate location in a 100-member array which represents the axial distribution of fuel or oxidizer deposited on the chamber wall. At the same time its axial momentum and its tangential angular momentum are added to the corresponding locations in 100-member arrays holding these values. From these values the axial and tangential velocities, the gross stoichiometry, the masses of adduct and of free fuel or oxidizer can be calculated for each axial segment of chamber. The flows at each axial location may be regarded as two-dimensional in that axial and tangential momenta, velocities and drag forces are calculated, the wall treatment is one-dimensional, however, in that there is only one lumped value for the wall variables at each axial location. Tangential variation could easily be programmed, but computer time would increase considerably. The first process calculated for the wall film is change of velocity due to chamber gas shear force, wall shear force, and spin-generated axial force.

The gas shear force acting upon each axial segment of the liquid film is taken from pipe-flow theory:

$$F_g = f(N_{Re}) \pi D \Delta X \frac{1}{2} \rho_{gas} (V_{gas} - V_{film})^2 \quad (A-48)$$

f is the Fanning friction factor, evaluated as a function of Reynolds number based upon chamber gas density, local axial gas velocity, chamber diameter, and gas viscosity. D is local chamber diameter, ΔX is the length of the wall segment.

The shear force from the chamber wall is:

$$F_w = f(N_{Re}) \pi D \Delta X \frac{1}{2} \rho_{film} V_{film}^2 \quad (A-49)$$

here the Reynolds number is based upon the hydraulic radius of the film

$$N_{Re} = \frac{4 \delta V_{film} \rho_{film}}{\mu_{film}} \quad (A-50)$$

where δ is film thickness.

The spin-derived net axial force on element i is:

$$F_s = \left\{ \frac{\rho_i V_{Ti}^2 \delta_i^2 (D_i + \delta_i)}{D_i} - \frac{\rho_{i+1} V_{Ti+1}^2 \delta_{i+1}^2 (D_{i+1} + \delta_{i+1})}{D_{i+1}} + \left[\frac{\rho_i V_{Ti}^2 \delta_i}{D_i} + \frac{\rho_{i+1} V_{Ti+1}^2 \delta_{i+1}}{D_{i+1}} \right] \times \left[\frac{D_{i+1}^2 - D_i^2}{4} \right] \right\} \quad (A-51)$$

where ρ is film material density, V_T is tangential velocity of the film, δ is film thickness, and D is chamber diameter. The net force acting upon the element of fluid is the sum of the above contributions, and the resulting change in axial velocity of the element is

$$\Delta V = \frac{F_g - F_w + F_s}{M} \Delta t \quad (A-52)$$

The wall shear force acting in the tangential direction is:

$$F_T = f(N_{Re}) \pi D \Delta X \frac{1}{2} \rho_{film} V_{T film}^2 \quad (A-53)$$

where Reynolds number is:

$$N_{Re} = \frac{4 \delta V_{T film} \rho_{film}}{\mu_{film}} \quad (A-54)$$

The tangential velocity decrement for one time interval is:

$$\Delta V_T = \frac{F_T}{M} \Delta t \quad (A-55)$$

The axial flow calculation is very simple. The axial displacement of the material in segments i during one time interval is:

$$\Delta L_i = V_i \Delta t \quad (A-56)$$

The corresponding uniform mass flow across the downstream boundary is:

$$\Delta M_i = \frac{V_i M_i \Delta t}{\Delta X} \quad (\text{A-57})$$

where ΔX is the length of the chamber segment.

For a small axial displacement of the material on segment i (less than half the segment length) the corresponding fraction of the mass of segment i is removed from segment i and added to segment $i+1$. Corresponding fractions of the axial and tangential momentum of segment i and of the gross fuel and oxidizer composition of segment i are transferred as well. When larger displacements are involved (which is very rare), a different algorithm is used for the sake of stability. The large-displacement algorithm distributes the mass of segment i over several downstream segments in amounts proportional to what would result by shearing segment i from the initial shape of a rectangle to the final shape of a parallelogram, with the base still in place, but with the top removed far enough downstream to move the center of mass of the element one displacement distance. The mass which flows out of the downstream end of the chamber at each time interval is considered to be the wall-film contaminant production.

(2) Wall-Film Burnoff

The burnoff from each axial segment of the wall is calculated from a heat transfer coefficient taken from the work of Gator (Reference A-14). The heat transfer coefficient is basically a function of chamber Reynolds number based on length, but is corrected for "blowing" from the evaporating surface, rippling of the surface, and temperature ratio. Evaporation rate is:

$$\dot{M}_i = \frac{H_i A_i \Delta T_i}{\Delta H_i} C_{e_i} C_{r_i} C_{T_i} \quad (\text{A-58})$$

\dot{M}_i is the rate of burnoff of propellant from the i th wall segment. H_i and A_i are the heat transfer coefficient evaluated for the conditions at i and the chamber wall surface area of the i th segment. The value for H_i is calculated:

$$H_i = .0295 C_{p_{\text{gas}}} \rho_{\text{gas}} V_{i_{\text{gas}}} N_{\text{Re}_i}^{-0.2} (D_i/L_i)^{0.2} \quad (\text{A-59})$$

N_{Re_i} is the Reynolds number based on chamber diameter evaluated at the i th segment, and L_i is the downstream distance of the element.

The correction for simultaneous heat and mass transfer is calculated:

$$C_e = \left(\frac{\Delta H_i}{C_{p_i} \Delta T} \right) \ln \left(1.0 + \frac{C_{p_i} \Delta T}{\Delta H_i} \right) \quad (\text{A-60})$$

Where ΔH_i is the heat required to evaporate or pyrolyze unit mass of the propellant mixture at the i th wall segment, C_{pi} is the specific heat of the vapor produced and ΔT is the difference between the chamber gas temperature and the surface temperature of the evaporating propellant, the ripple correction is calculated:

$$C_r = 1.0 + 35.4466 \rho_{gas}^{-0.4} V_{gas}^{-0.8} \quad (A-61)$$

with the maximum value for C_r limited to 2.5. The temperature ratio correction is:

$$C_T = \left(\frac{T_{gas}}{T_{surface}} \right)^{0.25} \quad (A-62)$$

(3) Wall-Film Entrainment

Whenever the chamber gas shear stress is high enough and the surface tension small enough, the wall film will be expected to atomize from the surface and the droplets entrain into the combustion chamber gas. An entrainment parameter is calculated:

$$G_i = \frac{\rho_{gas}^{0.5} V_{gas_i}}{\sigma_i} \left(\frac{T_{gas}}{T_{surface}} \right)^{0.25} \quad (A-63)$$

Whenever the entrainment parameter is greater than 1.5 for an element of wall film, the entrainment rate for the element is calculated

$$\dot{M}_i = M_i V_i \left(1.0 - e^{-0.001313 (G_i - 1.5) \Delta X} \right) \quad (A-64)$$

The entrained mass is removed from the mass on the element at wall, and is presumed to burn immediately; i. e., it is added to the chamber gas array at the i th segment of the chamber.

(4) Wall-Film Detachment by Film Binding

It is well known that a liquid, boiling through contact with a hot surface, will detach itself from the surface when the surface temperature exceeds the equilibrium boiling temperature by too great a margin. This appears to be the mechanism responsible for the phenomenon illustrated in Figure 6 of McFarland's paper on internal regenerative cooling (Reference A-49), which shows the heat transfer coefficient from the hot chamber wall to a film of MMH decreasing as the chamber wall temperature increases from the boiling temperature to 1.5 times the boiling temperature. Below the boiling temperature, the heat transfer coefficient is appropriate for heat transfer to a nonboiling liquid film, while at 1.5 times the boiling temperature, the heat transfer is roughly what would be expected for heat transfer to saturated MMH vapor. This temperature ratio of 1.5 for detachment is not far from the value observed by Tamura and Tanasawa (Reference A-15) for the complete detachment of water from a hot surface. Several hydrocarbons

and alcohol appear to detach at considerably lower temperature ratios (1.15 to 1.3 times the boiling temperature). Attempts to correlate this behavior with the reduced temperature corresponding to equilibrium boiling (boiling temperature/critical temperature) as suggested by Bernath (References A-50 and A-51) were not successful.

In the TCC program, the wall film is detached from the wall whenever the liquid film advances onto a segment of wall surface having a temperature greater than 1.5 times the boiling temperature (because of hysteresis in the wetting process, droplets impinging against a dry portion of chamber wall are presumed not to adhere above a temperature ratio of 1.2). The detached wall film is converted to a group of droplets which are introduced into the droplet array. The diameter of the newly formed droplets is taken to be 3 times the thickness of the wall film from which they were produced. This ratio leaves the surface to volume ratio unchanged in the transformation from detached film to droplets. If the droplet formation was driven solely by surface tension forces, the droplet diameter to film thickness ratio would have to be higher than this. If droplet formation was aided appreciably by aerodynamic forces, the droplet diameter to film thickness ratio could be appreciably lower.

(5) Vacuum Evaporation Rate

When the chamber pressure falls below the vapor pressure of the fuel and oxidizer deposited on the wall, they undergo Knudsen-Langmuir evaporation, with heat simultaneously being transferred from the chamber wall.

The evaporating wall film is treated as being locally thermally quasi-steady (Reference A-52) and the local vacuum evaporation rate from each of the 100 axial segments of wall is presumed to balance the local heat transfer rate from the chamber wall to the evaporating surface. The expression for Knudsen-Langmuir evaporation is:

$$\dot{M}_{pi} = A_{pi} E_p \left(P_{vap p}(T_{si}) - P_c \right) \left(\frac{M_{w_p}}{2 \pi R T_{si}} \right)^{1/2} \quad (A-65)$$

Where \dot{M}_{pi} is the evaporation rate of constituent p from the i th axial segment of the chamber wall, A_{pi} is the exposed surface area of constituent p on the i th segment. E_p is the accommodation coefficient of constituent p . $P_{vap p}(T_{si})$ is the vapor pressure of constituent p at the local surface temperature T_s . P_c is the chamber pressure. M_{w_p} is the vapor molecular weight of constituent p , and R is the gas constant. The effects of the neutralization reaction removing fuel or oxidizer from the mixed layer with the consequent formation of hydrazinium nitrate, and the vapor pressure reduction from solution effects are considered roughly by decreasing the vapor pressure of the free fuel or oxidizer to be proportional to its mass fraction in the wall-film mixture. Raoult's law is not presumed to apply to the very nonideal components of the wall film, and the experimental phase behavior of these mixtures has never been determined. The hydrazinium nitrate itself is treated as being nonvolatile in accordance with the experimental

findings of H. H. Takimoto et al at the Aerospace Corporation (References A-53, A-54, and A-55). The expression for heat transfer through the wall film is:

$$\dot{M}_{pi} = \frac{A_{pi} K_p (T_{wi} - T_{si})}{\delta_i \Delta H_p} \quad (A-66)$$

Where K_p is thermal conductivity of constituent p , T_{wi} is the chamber wall temperature at segment i , δ_i is the thickness of coating on segment i , ΔH_p is the latent heat of evaporation of constituent p .

Equations (A-65) and (A-66) must be simultaneously solved to obtain the values of \dot{M}_{pi} and T_{si} . This is done by Newton iteration. The fuel and oxidizer deposited on each axial segment of chamber wall surface are presumed to be well-mixed, reacted to completion to give hydrazinium nitrate plus fuel or oxidizer excess, and are regarded as uniformly covering the entire area of the wall segment.

g. Subroutine CHAMBER

(1) Axial Summations of Propellant Vapor

The 100-member arrays DXMF and DXMO are used to bring together the axially distributed contributions of fuel and oxidizer vapor mass from the igniter (if one is used), from flash vaporization of super-heated fuel or oxidizer, from droplet vaporization, from burnoff of wall film, from fuel or oxidizer mist entrained from the wall film (and presumed to burn rapidly), and from wall-film material vacuum-evaporated by heat transfer from the chamber wall.

At the same time that the vapor source summations are being obtained, sums are obtained representing atomized fuel and oxidizer in the chamber and fuel and oxidizer which has been injected but which is not yet atomized (i. e. , streams and fans). These sums are used to obtain the chamber explosion capabilities of the engine.

Each member of the DXMF or DXMO array holds the production of fuel or oxidizer vapor at its particular axial location at that particular time interval. The DXMF and DXMO arrays are axially integrated to give the 100-member XMF and XMO arrays. Each member of these arrays holds the sum of all fuel or oxidizer vapor sources upstream of its axial location. These arrays are used to obtain the total vapor production at each time interval and to obtain the chamber gas velocity profiles.

(2) Gas Outflow from the Chamber

Conventional steady flow, compressible gas, nozzle flow equations are used to calculate the instantaneous mass flow rate through the nozzle throat. The use of these equations together with the assumption of constant pressure throughout the chamber restricts the validity of TCC

calculations to cases where the rate of change of pressure is sufficiently slow that only a small change in pressure occurs during a single acoustic time period of the chamber or nozzle.

The nozzle is sonic when

$$\frac{P_e}{P_c} \leq \left(\frac{2.0}{\gamma + 1} \right)^{\gamma/(\gamma - 1)} \quad (\text{A-67})$$

Subsonic mass flow rate is calculated

$$\dot{M}_T = A_T P_C \sqrt{\frac{2.0 \gamma W_m}{(\gamma - 1) R T_c}} \sqrt{\left[\left(\frac{P_e}{P_c} \right)^{2/\gamma} - \left(\frac{P_e}{P_c} \right)^{(\gamma + 1)/\gamma} \right]} \quad (\text{A-68})$$

Sonic flow rate is calculated:

$$\dot{M}_T = A_T P_C \sqrt{\frac{\gamma W_m}{R T_c} \left(\frac{2.0}{\gamma + 1} \right)^{(\gamma + 1)/(\gamma - 1)}} \quad (\text{A-69})$$

The rates at which fuel- and oxidizer-derived mass leave the chamber are

$$\dot{M}_F = \dot{M}_T \times F \quad (\text{A-70})$$

$$\dot{M}_O = \dot{M}_T \times (1 - F) \quad (\text{A-71})$$

where F is the mass fraction of the chamber gas which fuel-derived.

(3) Chamber Gas State

At each integration time interval, the expressions for flashing of the propellant streams, evaporation of droplets, burnoff of propellant on the walls, vacuum evaporation of propellant on the walls, and the assigned igniter flows are used to calculate the amounts of fuel-derived mass and oxidizer-derived mass which have been added to the chamber. Nozzle flow equations are used to calculate the amount of gas leaving the chamber, with the assumption being made that the material flowing through the nozzle has the same composition as the well-mixed material in the chamber. The new amounts of fuel-derived gas mass and oxidizer-derived gas mass contained in the chamber are then calculated:

$$M_{F(t+\Delta t)} = M_{f(t)} + \text{fuel evaporated} - \text{fuel exhausted} \quad (\text{A-72})$$

$$M_{O(t+\Delta t)} = M_{O(t)} + \text{oxidizer evaporated} - \text{oxidizer exhausted} \quad (\text{A-73})$$

The total mass of gas in the chamber is the sum of the fuel-derived and oxidizer-derived mass

$$M_T = M_F + M_O \quad (A-74)$$

The stoichiometry of the chamber gas is expressed in terms of the fraction of the total gas mass which is fuel-derived

$$F = \frac{M_F}{M_F + M_O} \quad (A-75)$$

When combustion is taking place in the chamber, the temperature, molecular weight, and thermal properties of the chamber gas are functions of the elemental compositions and heats of formation of the fuel and oxidizer, the stoichiometry and the chamber pressure. Since the composition and heat of formation of the fuel and oxidizer are fixed for a given set of propellants, and since the product composition is only a weak function of pressure, the temperature, molecular weight and thermal properties of the chamber gas are approximated as a function of F alone with only small error. Temperature, molecular weight and gamma are stored as 11-point tables with linear interpolation being used to obtain values for intermediate values of F . Figures A-18, A-19, and A-20 illustrate the values used for the white fuming nitric acid - UDMH propellant combination.

When the combustion chamber contents are not ignited, the gas properties are calculated for the unreacted fuel and oxidizer vapors, assuming ideal gas behavior.

After chamber temperature and molecular weight are estimated as functions of the gas stoichiometry, the chamber pressure is calculated

$$P_c = \frac{\rho R T}{W_m} \quad (A-76)$$

The density is obtained from the known total gas mass and total chamber volume, where U_c is chamber volume

$$\rho = \frac{M_T}{U_c} \quad (A-77)$$

(4) Extinguishment

Since the droplet population of the chamber declines very rapidly after the propellant valves are closed, the vacuum evaporation of fuel and oxidizer film on the wall becomes the major source of fuel and oxidizer vapors very shortly after valve closure. For this reason the criterion for extinguishment is based upon the combustion chamber gas state rather than upon the conditions in the droplet boundary layers. Extinguishment in the gas is predicted from experimental quenching distance values taken from data on the combustion of premixed gases (Reference A-56). Quenching distance of premixed gases is a function of the pressure, and of

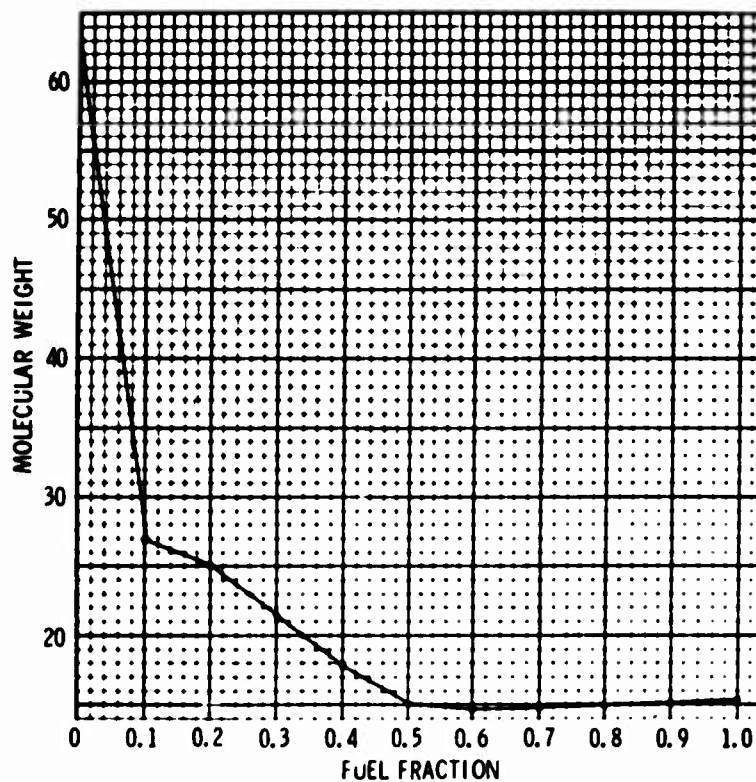


Figure A-19. Molecular Weight Versus Stoichiometry

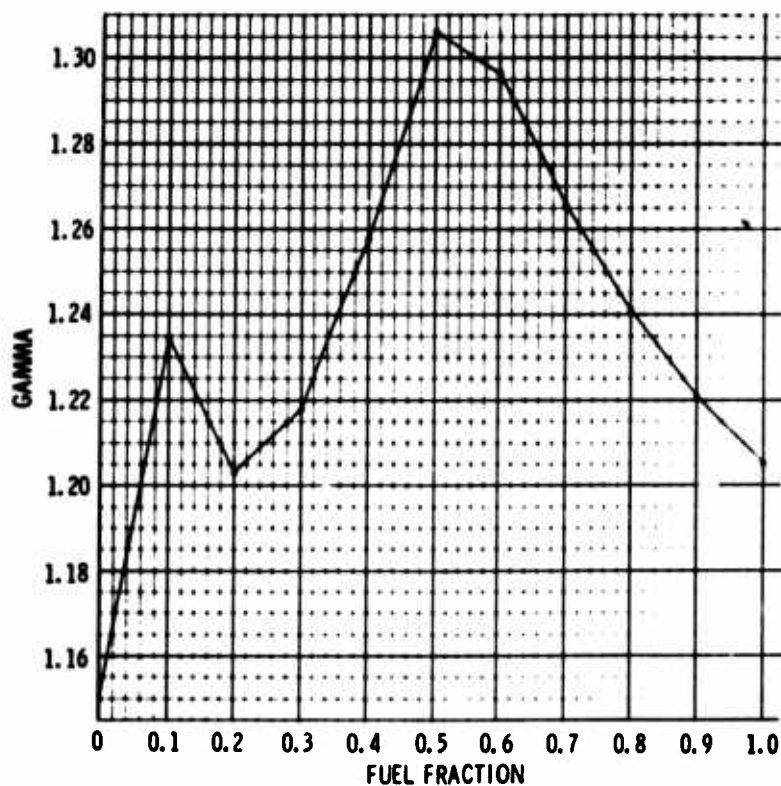


Figure A-20. Gamma Versus Stoichiometry

the initial temperature and stoichiometry of the combustible mixture. For the present purposes, the effects of stoichiometry and initial temperature can be lumped together in terms of the corresponding final gas temperature. The data on propane-air quenching distance are correlated adequately by:

$$q = 3.6 \times 10^{17} P^{-1.0} T^{-4.0} \quad (\text{A-78})$$

Where q is quenching distance in cm, P is pressure in dyne/cm², and T is equilibrium final gas temperature in °K. When the calculated value of q becomes larger than the chamber diameter, extinguishment is presumed to occur.

(5) Axial Gas Velocity

The axial gas velocity is calculated at 100 equally spaced axial locations at each integrating time interval to give the gas velocities used in the droplet drag and evaporation rate calculations, the wall burnoff calculations and the wall-film flow calculations during the next time interval. When velocities are required at intermediate locations, linear interpolation is used. The simplifying assumption is made that at any instant the pressure is constant throughout the chamber and the gas is well mixed. Since the computation time interval is typically of the order of 1 to 10 times the longitudinal acoustic period of the engine, the uniform chamber pressure assumption seems justified for engines with large contraction ratios.

The axial gas velocity at any axial location L_i may be obtained through the continuity equation, a mass balance on the chamber volume upstream of location L_i , and the assumption of uniform density throughout the chamber. The axial velocity at L_i is

$$V_i = \frac{\dot{M}_i}{\rho_{\text{gas}} A_i} \quad (\text{A-79})$$

where \dot{M}_i is the rate at which gas mass is flowing past the section at L_i and A_i is the cross-sectional area at L_i . The value for \dot{M}_i is obtained from a mass balance on the chamber volume upstream of L_i .

$$\dot{M}_i = \text{Evaporation rate upstream of } L_i - \text{accumulation rate upstream of } L_i \quad (\text{A-80})$$

$$\dot{M}_i = (XMF_i + XMO_i)/\Delta t - \frac{U_i}{U_{100}} \left[(XMF_{100} + XMO_{100})/\Delta t - \dot{M}_T \right] \quad (\text{A-81})$$

U_i is the chamber volume upstream of segment i , and U_{100} is the total chamber volume. \dot{M}_T is the mass flow rate through the nozzle.

Reynolds number, based upon chamber diameter, is calculated at 100 axial locations:

$$N_{\text{Re}_i} = V_i \rho_{\text{gas}} D_i / \mu_{\text{gas}} \quad (\text{A-82})$$

(6) Thrust Calculation and Explosion Potential

The vacuum thrust is calculated as the sum of the momentum rate of the ejected droplets and the theoretical vacuum thrust of the gas:

$$F = P_c A_t C_F + \frac{1}{\Delta t} \sum_{\text{droplets ejected}} V_i M_i \quad (\text{A-83})$$

When the chamber contents are ignited, the C_F is interpolated from a table of C_F versus stoichiometry of the chamber gas. When the chamber products are not ignited, C_F is interpolated from a table calculated for the mixture of unburned vapors. In calculating the C_F table for the vapors, first the ratio of exit pressure to chamber pressure must be obtained from the exit area ratio:

$$\frac{1}{\epsilon} = \left(\frac{\gamma+1}{2} \right)^{\frac{1}{\gamma-1}} \left(\frac{P_e}{P_c} \right)^{\frac{1}{\gamma}} \sqrt{\frac{\gamma+1}{\gamma-1} \left[1 - \left(\frac{P_e}{P_c} \right)^{\frac{\gamma-1}{\gamma}} \right]} \quad (\text{A-84})$$

This is solved for each value of γ using a Newton iteration. After the pressure ratio is obtained, the thrust coefficient is obtained:

$$C_F = \sqrt{\frac{2\gamma^2}{\gamma-1} \left(\frac{2}{\gamma+1} \right)^{\frac{\gamma+1}{\gamma-1}} \left[1 - \left(\frac{P_e}{P_c} \right)^{\frac{\gamma-1}{\gamma}} \right]} + \frac{P_e}{P_c} \epsilon \quad (\text{A-85})$$

Potential chamber explosion pressures are calculated, based on the assumption of well-mixed ideal-gas combustion products uniformly filling the chamber. Three assumptions are used: (1) that a "spike" or "total explosion" will involve all the fuel and oxidizer contained in the chamber, i. e., drops, streams, fans, gas and wall deposits, (2) that a "pop" will involve only gas, and drops (3) that an "adduct explosion" will involve only hydrazinium nitrate on the walls.

h. Subroutine WRITER

This subroutine prints 48 time-varying parameters at each time step and puts large volumes of time-varying data onto tapes 9 and 13.

At each Nth time step, where N is input data value 203, the cumulative amounts of injected fuel and oxidizer are printed, together with the cumulative amounts of the various forms in which oxidizer and fuel have been outflowed or accumulated. If a number has been specified for input data value 11, a large number of chamber parameters will be printed

characterizing the chamber state at that iteration. This print is most useful for clarifying chamber processes or diagnosing apparent program errors.

As soon as the prescribed model time has been calculated, or if the computer clock indicates that the time allocated for the calculations is expiring, end of file is written on tapes 9 and 13 and a summary print is written giving the average performance and contaminant production for the entire period of calculation. If data input value 9 has been given a nonzero value, masses of axially distributed wall deposits of fuel and oxidizer are punched out on cards. These can be used if it is desired to restart calculations at a later time with wall deposits corresponding to the values left at the end of this firing.

i. Subroutine GRAPHS

Subroutine GRAPHS can be entered either at the conclusion of a combustion chamber calculation or for use with data tapes 9 and 13 which hold output data recorded from a previous chamber calculation. If the program is being run from pre-recorded data tapes (indicated by a nonzero value on input data value 10), the information on tape 9 is transferred to disk storage to hasten the ensuing data handling processes and the number of records before end of file are counted for later use in subscripted read and write instructions. Any other necessary data is taken from the data array.

The first plots produced are droplet trajectory plots. Only the droplet specified during the initial combustion chamber calculation can be plotted and changing the droplet trajectory plot input data for re-runs from tape will not give trajectories for different droplets.

Next to be plotted are any time-varying parameters designated by non-zero values in namelist PRTDIR. These plots may be done either with or after the combustion chamber calculations, so long as the data tapes remain intact.

The third set of graphics to be produced is the set of wall-film thickness profiles. If a non-zero value N is given to input Data Number 204, either at the time of a combustion chamber calculation or later for a run from tapes, then the wall-film thickness profile is plotted at every Nth time iteration.

If time intervals are specified, the next output from subroutine GRAPHS is cumulative and time-averaged mean values for performance and contaminant production during the time intervals. The input values required for the MULTRAN subprogram are also produced for the specified time intervals.

The final output from subroutine GRAPHS is a set of snapshots or movie frames showing the combustion chamber contour, the instantaneous location of all droplet groups in the chamber and a wall-film thickness profile which may be given sufficient vertical exaggeration to make it easily visible.

These motion picture graphics give a very vivid description of the combustion chamber processes and make clear, in a very concrete way, many design problems which would go unnoticed if the data were presented in any other way.

j. Utility Subroutines and Functions

Most of the subroutines have available the statement functions PVAPF (TEMP) and PVAPØ(TEMP). These give the equilibrium vapor pressure of fuel or oxidizer in dynes per square centimeter when given the temperature in degrees Kelvin. The expressions used are:

$$P = e \left(A + \frac{B}{T-C} \right) \quad (A-86)$$

The minimum value allowed is either zero or the triple-point pressure, depending on whether FORTRAN variables PFRZF and PFRZØ are set equal to 0.0 or the values held in HOLDF and HOLDO, respectively. The maximum value allowed is the critical pressure.

TEMPF (PR) and TEMPO (PR) give the equilibrium boiling temperature of fuel or oxidizer in degrees Kelvin when the pressure is given in dynes per square centimeter. The expression used is:

$$T = C + \frac{B}{\ln p - A} \quad (A-87)$$

The minimum value permitted can be either 0.0 or the freezing point of the material, depending upon the value assigned to FORTRAN variables TFRZF and TFRZØ. The maximum values permitted are the critical temperatures.

HVAPF (TEMP) and HVAPO (TEMP) are values for the fuel vapor enthalpy and oxidizer vapor enthalpy in calories per gram as functions of temperature in degrees Kelvin. Contant C_p is assumed, and the zero datum is the solid at zero degrees Kelvin.

$$H = H_c + C_p T \quad (A-88)$$

TRIPØT (A, B) gives the length of the vector with an x component of 1.0, a Y component of Tan A, and a Z component of Tan B.

$$L = \sqrt{1 + \tan^2 A + \tan^2 B} \quad (A-89)$$

Subroutine SHAPE (X, DCHAM, ACHAM, UPVOL) is given an axial chamber station x and returns the chamber diameter, chamber cross-sectional area, and the upstream volume. Units are centimeters, square centimeters, and cubic centimeters. The chamber contour is linearly interpolated from an input table of 8 stations and diameters.

Functions HCONDF (TEMP) and HCONDØ (TEMP) approximate the enthalpies of liquid or solid phase fuel and liquid or solid phase oxidizer as functions of temperature. Constant C_p is assumed, and the solid phase is assumed to have the same heat capacity as the liquid. The latent heat of fusion is added above the melting point. Values are in calories per gram and degrees Kelvin.

$$T_{\text{freeze}} > T \quad H = C_p T \quad (\text{A-90})$$

$$T \geq T_{\text{freeze}} \quad H = C_p T + \Delta H_{\text{fusion}} \quad (\text{A-91})$$

Function REDRHO (TRED) approximates the reduced density of a liquid as a function of reduced temperature along the saturation line, based upon the curves of Hougen and Watson:

$$0.8 > T_r \quad \rho_{r(l)} = 3.97 - 1.91 T_r \quad (\text{A-92})$$

$$1.0 > T_r > 0.8 \quad \rho_{r(l)} = 1 + \sqrt{34.7 T_r - 25 T_r^2 - 9.7} \quad (\text{A-93})$$

$$T_r > 1.0 \quad \rho_{r(l)} = 1 \quad (\text{A-94})$$

Function REDROD (TRED) approximates the reduced density difference (reduced density of the liquid minus reduced density of the vapor) as a function of reduced temperature, along the saturation line. Based upon the curves of Hougen and Watson, the law of rectilinear diameters, and some supplementary physical property data:

$$0.8 > T_r \quad \rho_d = 3.97 - 1.91 T_r \quad (\text{A-95})$$

$$1.0 > T_r > 0.8 \quad \rho_d = -2.21 + 2.21 T_r + 2 \sqrt{34.7 T_r - 25 T_r^2 - 9.7} \quad (\text{A-96})$$

$$1.0 > T_r \quad \rho_d = 0.0 \quad (\text{A-97})$$

Function REDVIS (TRED) approximates the reduced viscosity of the liquid as a function of reduced temperature along the saturation line up to the critical temperature, and the reduced viscosity of the gas along the $P = 0$ line above the critical temperature.

$$0.6 > T_r \quad \mu_r = 0.55 T_r^{-5.68} \quad (\text{A-98})$$

$$1.0 > T_r \geq 0.6 \quad \mu_r = 2.0 T_r^{-3.15} \quad (\text{A-99})$$

$$T_r = 1.0 \quad \mu_r = 1.0 \quad (\text{A-100})$$

$$2.0 > T_r \geq 1.0 \quad \mu_r = 0.45 T_r \quad (A-101)$$

$$T_r > 2.0 \quad \mu_r = 0.572 T_r^{0.655} \quad (A-102)$$

Function FANFAC (REN) approximates the Fanning friction factor as a function of Reynolds number.

$$16 > Re \quad f = 1.0 \quad (A-103)$$

$$2,000 > Re > 16 \quad f = 16 Re^{-1.0} \quad (A-104)$$

$$Re > 2,000 \quad f = 0.06028 Re^{-0.2113} \quad (A-105)$$

k. Limitations and Assumptions

The particular processes which have been emphasized in the current program have been dependent upon the immediate interests or problems of the users. Thus many aspects of the start transient and contaminant production are well represented, while pressure wave action in the propellant feed lines, heat transfer in the chamber walls, and sophistication in the dynamics of the combustion gas are conspicuously absent. There are several obvious places where the precision or generality of the present program could be extended if there was a sufficient requirement for the added capability to justify the expense of programming and the longer computing time which goes with greater sophistication.

(1) Feed System

Compressibility of the propellant and the resulting wave action in the lines could be modeled using the method of characteristics. The pressure waves in the lines are important in determining the response of attitude control engines which have very fast valves and extended lines. The two-phase flow in the injector may be important during injector priming and during postrun dribbling under vacuum ambient conditions. Neither wave action nor two-phase flow is modeled at present.

(2) Chamber Gas Dynamics

The axial and transverse variation in gas stoichiometry could be modeled to replace the current assumption of well-mixed gas. This could be done by following discrete "slugs" of chamber gas along stream-tubes and summing the additions of fuel and oxidant vapor from the passage of the "slug" of gas through the droplet array. Doing this, together with a numerical approximation of eddy-diffusive mass exchange between stream-tubes, would permit much more accurate estimation of delivered performance especially in heavily film-cooled engines.

At present the combustion chamber gas state is imperfectly modeled. It is assumed that the chamber gas pressure, temperature, and density at the nozzle throat and at the injector end of the chamber are equal. No consideration is made of the fall in gas temperature associated with the large gas expansions at cutoff or during chugging. To model the expansion or compression of hot thermochemically equilibrated gas with concurrent arbitrary additions of fuel or oxidizer will probably require that equilibrium thermochemistry calculations be performed at each time step. There are current thermochemistry programs which possess sufficient speed and reliability to make this feasible, but it is not warranted for the present uses of the program.

(3) Droplet Trajectories and Secondary Atomization

The present program treats droplet trajectories as being only two-dimensional (axisymmetric). This means that the lateral spreading of the propellant fans is not modeled. Instead, all the propellant droplets are regarded as being initially directed down the centerline of the fan. This leads to predictions of wall deposition more localized than would be the case with a correct description of the fan. Changing the droplet trajectories to be fully three-dimensional would require only minor program changes but would give more precise results, at the expense of longer computing time.

It is well known that when droplets are subjected to sufficiently high relative gas velocities, they undergo secondary atomization, and that this can have an important effect in increasing the combustion efficiency of the chamber. This phenomenon is not presently modeled, but it should be considered if it ever became desirable to better approximate the actual delivered impulse of the engine.

(4) Wall Effects

The heat transfer to the nonwetted portions of the chamber walls is not presently calculated. This is a very interesting possibility, since the axial gas velocity profile, temperature, density, heat capacity, Reynolds number, and even heat transfer coefficients are already calculated for other uses. A simple two-dimensional mesh for unsteady heat transfer into the chamber walls would permit rather sophisticated calculations to be made, such as internal-regenerative cooling, and the effects of thermal soakback on the evaporation of deposited propellant and on subsequent hypergolic starts. Thermal histories for multiple-pulse firings could be calculated, including effects of quenching from propellant leads, from injector dribbling, etc.

(5) Experimental Uncertainties

In addition to the computational limitations of the program, there are some important processes and physical properties which are inadequately known.

The droplet sizes resulting from primary atomization of reactive unlike streams have never been investigated. There have been no experimental determinations of droplet size for the small orifice sizes and extremes of momentum imbalance which can be found in pulse-mode engines. This uncertainty as to correct droplet size is one restriction on the present use of the program. Very little is known about the droplet sizes produced when either an unatomized stream or large droplets impact upon the wall.

When film-coolant fuel flows onto a sufficiently hot segment of chamber wall it will film-bind, be detached and returned to the free volume of the chamber as droplets. The ensuing history of this fuel will depend very strongly on the droplet sizes which are produced; however, this atomization mechanism has never been studied.

The breakup distances for impinging-stream and single-stream atomization have been determined for only a very limited range of liquid velocities, gas densities, and orifice diameters. Further investigations are badly needed for smaller orifice diameters.

Very little is known about the impingement of droplets against the chamber wall. The fraction of impinging droplets which will stick to either a cold chamber wall or to a hot chamber wall is not known.

The effects of droplet size or velocity of approach is not known. The velocity of rebound from the wall and the amount of heat transfer between a bouncing droplet and a hot wall are unknown.

The physical properties of the hydrazinium nitrates and their solutions are completely unknown. Accommodation coefficients for the hydrazines, for nitrogen tetroxide, and for the hydrazinium nitrates are unknown, but because of the highly polar, highly associated nature of the molecules, they are certainly very far from unity.

A.3 NUMERICAL INTEGRATION METHOD

The numerical solution of sets of differential equations can be accomplished using a number of different techniques. The simplest technique is Euler's method. In this method, the next value for each dependent variable is obtained by linear extrapolation of the present value using the first derivative calculated at the present value. For a time-dependent function:

$$V(t + \Delta t) = V(t) + \frac{dV}{dt}(t) \Delta t \quad (A-106)$$

where V may be any variable value defined by a differential equation.

Other methods of numerical integration are available in which higher-order derivatives are calculated and used:

$$V(t + \Delta t) = V(t) + \frac{dV}{dt} \Delta t + \frac{1}{2} \frac{d^2V}{dt^2} \Delta t^2 + \dots + \frac{1}{n!} \frac{d^n V}{dt^n} \Delta t^n \quad (A-107)$$

The use of higher-order derivatives often allows larger values for Δt to be used without introducing excessive error or instability. A penalty must be paid for the use of the higher-order derivatives. In the present calculations, any higher-order derivatives would have to be estimated numerically by taking differences between previous values for the variables. Since 12,000 computer storage locations are required to contain the current values for the droplet array, the requirement that previous values be kept also would drastically increase the already large computer storage requirement. A further argument against the use of a higher-order integrating scheme is that many of the physical processes which are modeled do not have continuous derivatives. The feed system flow rates vary discontinuously when the dribble volumes fill up. The chamber gas properties and droplet burning rates vary discontinuously when the chamber contents ignite. The propellant primary atomization droplet size varies discontinuously when a decrease in chamber pressure or an increase in Weber number causes flashing to commence. When even the first derivative is not continuous, it is pointless to think of approximating higher-order derivatives.

One way that the Euler method can be improved in the solution of certain physical problems is by limiting variables to their physically defined asymptotic values. The time interval chosen for the calculations is based mostly upon the response time of the chamber pressure. If a fuel droplet is injected which is so small that it would burn up completely in less than one computing time interval, then Equation (A-106) would predict that it would burn to a negative diameter in one time interval and contribute more than 100 percent of its mass to the gas phase. Obviously a real burning droplet has an asymptotic value of zero for its diameter and mass. Hence it is appropriate to limit the derivative to a value which will just consume the droplet completely in one computational time interval. Doing this will obviously assign an incorrect value to the droplet burning rate, but will yield a value for chamber pressure at the end of the interval which is correct. Several other derivatives are limited to known asymptotic values. Droplets being accelerated by aerodynamic drag forces will not exceed the local velocity of the gas which is accelerating them, feed system flow rates will not accelerate past the steady-state flow rate corresponding to the current pressure drop. The instructions for limiting the value of the derivatives are all written so as to properly consider flow rates and velocities approaching from either side of the asymptotic value. It should be emphasized that this derivative-limiting procedure is to stabilize the calculations for exceptional conditions, and that most of the calculations are made according to Equation (A-106).

a. Computational Methods for Droplet Arrays

The methods used for the calculation of droplet combustion and trajectories differ according to the generality or restriction of the particular case. Three methods will be described to illustrate the similarities and differences. The first two methods illustrate the historical development of droplet analysis of rocket engine combustion chambers.

(1) Steady-State Chamber with Monodisperse Droplets

The simplest case is that of axially directed monodisperse droplets in a steady chamber. All of the droplets injected as a group at any particular time will behave alike, and the droplet group injected at any particular time will behave the same as any other group introduced at any other time. Thus, knowing the mass, velocity, and position history for any one droplet yields a general solution for the entire combustion chamber. The aerodynamic drag force and evaporation rate for a droplet may be computed, and the successive values for mass, velocity and location may be calculated for a sequence of time steps in a very straightforward manner:

$$M_{(t + \Delta t)} = M_{(t)} - \dot{M}_{(t)} \Delta t \quad (A-108)$$

$$V_{(t + \Delta t)} = V_{(t)} + \frac{F_{(t)}}{M_{(t)}} \Delta t \quad (A-109)$$

$$X_{(t + \Delta t)} = X_{(t)} + V_{(t)} \Delta t \quad (A-110)$$

$$U_{(t + \Delta t)} = U_{(t)} + \frac{1}{\rho A} N \dot{M}_{(t)} \Delta t \quad (A-111)$$

Where M is the mass of a droplet, \dot{M} is the evaporation rate of the droplet, V is the velocity of the droplet, F is the aerodynamic drag force acting on the droplet, X is the axial location of the droplet, U is the combustion gas velocity, N is the number of droplets in the group, ρ is the density of the combustion gas, and A is the cross-sectional area of the chamber. Since U and X are both functions of t , $U(X)$ is defined. This was the method used by Priem to evaluate chamber conditions with uniform droplets (Reference A-57).

(2) Steady-State Chamber with Distributed Droplet Sizes

When the droplets produced by the injector are distributed in initial diameter, the calculations are less straightforward. The small droplets are accelerated by aerodynamic forces much more rapidly than the large droplets, hence, if the droplets are initially together at some particular place and time, they will be separated a short interval of time later. For this reason, the same time interval cannot be used by all the different sized droplet groups to progress from one axial location to the next. In the steady-state chamber, no generality is lost by summing up combustion gas contributions from large, medium and small droplet groups which originated at different times, but which happen to be at the desired axial location in the chamber at the time the gas velocity summation is made. In marching down the chamber to develop the gas velocity profile, an axial distance interval is chosen, and then the time interval required for each different droplet size group to traverse the distance is calculated. The evaporation and acceleration effects for each droplet size group must be evaluated using its own correct time interval.

$$\Delta t_i = \frac{\Delta x}{V_{i(x)}} \quad (A-112)$$

$$M_{i(x + \Delta x)} = M_{i(x)} - \dot{M}_{i(x)} \Delta t_i \quad (A-113)$$

$$V_{i(x + \Delta x)} = V_{i(x)} + \frac{F_{i(x)}}{M_{i(x)}} \Delta t_i \quad (A-114)$$

$$U_{(x + \Delta x)} = U_{(x)} + \frac{1}{\rho A} \sum N_i M_{i(x)} \Delta t_i \quad (A-115)$$

The subscript i is used to distinguish between the various groups of different sized droplets. This is the method used by Priem (Reference A-9) and later by Lambiris (Reference A-58) to calculate chamber profiles with distributed droplet sizes. The Dynamic Science approach (Reference A-10) differed only in having groups of oxidizer droplets as well as fuel droplets.

It is apparent that the previous methods depend very strongly upon the assumption of steady conditions in the chamber and cannot be used to calculate the unsteady state. There are other more subtle restrictions, the methods cannot be used for droplets injected in the reverse direction, etc

(3) Unsteady-State Chamber with Distributed Droplets

The method used in the present program differs from the earlier methods. Instead of following one or a few droplet groups progressively down the length of the chamber, the entire chamber population of droplets is represented simultaneously and reexamined at each time interval. When this method is used, a larger computer memory is required in order to store the description of the entire droplet population of the chamber, and more computing time is required since all of the droplet groups constituting the entire population are examined at each time interval, however it is now possible to calculate time-varying behavior and it is simple to calculate droplet motion in one, two or three dimensions with no arbitrary restrictions. The mass, velocity and location for each droplet group in the chamber is recalculated at each time interval:

$$M_{i(t + \Delta t)} = M_{i(t)} - \dot{M}_{i(t)} \Delta t \quad (A-116)$$

$$V_{i(t + \Delta t)} = V_{i(t)} + \frac{F_{i(t)}}{M_{i(t)}} \Delta t \quad (A-117)$$

$$X_{i(t + \Delta t)} = X_{i(t)} + V_{i(t)} \Delta t \quad (A-118)$$

The forces, velocities, and locations may be treated as being one, two, or three dimensional with no difficulty.

The axial gas velocity may be calculated at any axial chamber location, based upon a mass balance on the upstream region. In its present form, this calculation depends upon the assumption that the gas in the chamber is well mixed and has a constant density (i. e. , no gradients in composition, temperature, or pressure).

$$U_x = \frac{\dot{M}_x}{A} \quad (A-119)$$

$$\dot{M}_x = \begin{array}{l} \text{Evaporation rate upstream of X-Accumulation Rate} \\ \text{Upstream of x} \end{array} \quad (A-120)$$

$$\dot{M}_x = \sum_{\text{All groups upstream of x}} N_i \dot{M}_i - \frac{V_x}{V_c} \left[\sum_{\text{All groups in chamber}} N_i \dot{M}_i - \dot{M}_{\text{Nozzle}} \right] \quad (A-121)$$

Where V_x is volume upstream of x and V_c is total chamber volume. In the present program the axial gas velocity is calculated at each of 100 equally spaced intervals and interpolated between these points. In the present program, also, vapor from other sources than droplets is considered; however, the principle remains the same.

(4) Integrating Time Interval

When gas is flowing from a chamber through a sonic throat, the mass flow rate is:

$$\dot{M}_t = A_t P_c \sqrt{\frac{\gamma W_m}{RT} \left(\frac{2}{\gamma+1} \right)^{(\gamma+1)/(\gamma-1)}} \quad (A-122)$$

The mass stored in the chamber is:

$$M = \frac{P_c V_c W_m}{RT} \quad (A-123)$$

The ratio of M/\dot{M} is often referred to as "gas residence time" and is a rough measure of how fast the chamber pressure can fall by flow through the nozzle. When Equations (A-122) and (A-123) are combined and simplified:

$$\text{gas residence time} = \frac{L_c \frac{A_c}{A_t}}{a_c \sqrt{\left(\frac{2}{\gamma+1} \right)^{(\gamma+1)/(\gamma-1)}}} \quad (A-124)$$

When this is evaluated using the values $\gamma = 1.25$, $(A_c/A_t) = 4$, $a_c = 3,600$ ft/sec and $L_c = 1.0$ inch, a value of 0.17 msec is obtained for gas residence time. It is obvious that if normal pressure changes are to be modeled with sufficient accuracy, the integrating time interval must be considerably less than the gas residence time of the particular chamber.

Fuel and oxidizer droplets are introduced at the injector end of the chamber and move downstream with a velocity which depends upon the axial injection velocity and the subsequent aerodynamic drag. To maintain sufficient accuracy in the calculation of the droplet trajectory and mass history, a sufficient number of calculations must be made during the stay time of a droplet in the chamber. Droplet stay time may be estimated as chamber length divided by average droplet axial velocity. A reasonable estimate for axial velocity is 100 ft/sec. Hence, for a chamber 1 inch long the droplet stay time is on the order of 0.8 msec.

In addition to the obvious restraints on maximum integrating time interval, there is a more subtle restraint on minimum time interval. At each time interval the axial gas velocity profile in the chamber is calculated based upon the mass of newly formed combustion gas which must be moved to restore the chamber to a uniform density and pressure. If an extremely short time interval is taken, it is possible that in some unusual cases, gas velocities will be calculated which are higher than are physically possible. This would introduce error in the velocity-sensitive functions such as droplet burning rate, drag, wall film flow and wall film burnoff. If the chamber is viewed as a closed-closed organ pipe a pressure relaxation physically requires one quarter of an acoustic period, i. e. ,

$$\Delta t = \frac{L_c}{2 a_c} \quad (A-125)$$

This sets 0.012 msec as a minimum time interval for a combustion chamber 1-inch long.

Since the maximum and minimum permissible time intervals often differ considerably, there is leeway to trade off computer expense against precision of calculation. Most of the computations reported here were done near the maximum acceptable value for time interval to reduce the computation expense.

A. 4 PROGRAM USER'S MANUAL

The TCC program is the first subprogram of the CONTAM computer program. It may be run as a subprogram to CONTAM or as an independent program. The TCC program requires 104,000 words of core and is written in FORTRAN IV.

a. Input

A complete data set consists of 600 data values; however, not all of these are required for every calculation. These are normally punched as four NAMELISTS; PROCED, PRTDIR, RESRT1, and RESRT2.

The 318 values in NAMELIST PROCED describe the engine, propellants, operating conditions, and a number of general instructions or choices of program options. The 80 values in NAMELIST PRTDIR are set to 1.0 or 0.0 to indicate which time-varying parameters should be plotted or not plotted.

The 101 values in NAMELIST RESRT1 are the masses of fuel-derived wall film left in the chamber at the end of a previous firing. The 101 values in NAMELIST RESRT2 are the masses of oxidizer-derived wall film left in the chamber at the end of a previous firing.

The first step performed by the program is to read the input data and then print it out along with descriptive headings. The values in NAMELIST PRTDIR are not printed out as they do not affect the accuracy of the combustion chamber calculations.

This printout makes it easy to review the data to ensure that all the values have been written, punched, and entered correctly. The first program option is to terminate the run at this point to permit a new set of data to be examined thoroughly before time is spent on calculations. The input data to this program are sufficiently complicated that occasional mistakes in entering the data may be expected and careful periodic examination of the contents of the data deck is highly recommended.

Certain of the data entries are not required for particular calculations and may be omitted (set to zero by the NAMELIST subroutine).

For a computation for which no motion picture is desired, NAMELIST PROCED items 205 through 207 may be omitted. When time-averaged values are not required, items 313 through 318 are omitted. When droplet trajectories are not desired, items 209 through 212 are omitted. When flow-rate override calculations are not desired, 61 to 64, 85 to 88, and 213 to 220 may be omitted.

For a computed vacuum hypergolic ignition, items 33, 34, 35, and 36 are omitted. When an igniter is used, items 33, 37, 38, 39, and 40 are omitted. When sea-level hypergolic ignition is being simulated by assigning a value for ignition delay, items 34, 35, 36, 37, 38, 39, and 40 are omitted. If injector heating of propellant and postfiring dribble are unimportant, the transition volumes (59 and 83) may be omitted. The monopropellant, burning-rate constants (126, 127, 128, 146, 147, 148) are omitted for materials which do not burn in a monopropellant mode.

When multiple pulses are not desired, 237 to 264 are omitted. When computations are being made for engines with less than three pairs of rings, no input values are required for rings which do not exist.

The option flags are all set to zero for "normal" calculations so that they may all be omitted unless an option is specifically desired.

If no time-varying parameter plots are required all of the values in NAMELIST PRTDIR may be omitted. To calculate a first start with a clean engine all values in NAMELISTS RESRT1 and RESRT2 should be omitted.

(1) Namelist Proced

An excellent way to assemble a data set for a new application is by having an old input data print to work from. If none is available, one can be obtained by running TCC with no input data except DDD1 (208) = 1.0, which will produce a "Data Review Only" print with no combustion chamber calculations attempted. The input data will be described in the order that they appear in the program input data print.

<u>DDD1 Subscript</u>	<u>Description</u>	<u>Units</u>
<u>GENERAL INSTRUCTIONS</u>		
9	Restart punch option (1.0 or 0.0, a nonzero value will cause a deck of cards to be punched at the conclusion of the run. These cards are input values for RESRT1 and RESRT2)	
10	Work from tape option (1.0 or 0.0, a nonzero value will cause the program to omit any combustion chamber calculations and work from prerecorded output data tapes)	
11	Debugging print option (a nonzero value K will cause diagnostic prints to be printed on the Kth time iteration)	
12	No movie tape option (a nonzero value will prevent a movie tape from being generated)	
201.	Model time at which the calculations will be terminated	seconds
202.	Integrating time Interval	seconds

<u>DDD1 Subscript</u>	<u>Description</u>	<u>Units</u>
203.	Number of time intervals between printing of propellant mass disposition prints	
204.	Number of time intervals between plotting of contaminant thickness profiles	
205.	Film vertical exaggeration (wall-film thickness exaggeration for motion picture frames)	
206.	Start movie iteration (time iteration at which the movie starts)	
207.	End movie iteration (time iteration at which the movie ends)	
208.	Data review option (When this flag is set to 1.0 the data are read, certain checks and initializing steps are made and the raw data and some derived information are printed out with headings; however, the chamber calculations are not performed. This makes it possible to check a new data deck for errors before proceeding with expensive calculations.)	(0.0 or 1.0)
<u>TIME-AVERAGE PERFORMANCE VALUES</u>		
313.	Time when the first interval starts	seconds
314.	Time when the first interval ends	seconds
315.	Time when the second interval starts	seconds
316.	Time when the second interval ends	seconds
317.	Time when the third interval starts	seconds
318.	Time when the third interval ends	seconds

DDD1 SubscriptDescriptionUnitsDROPLET TRAJECTORY PLOT

- | | | |
|------|--|-------------------|
| | Fuel trajectory group | (1.0 through 5.0) |
| 209. | (The chamber trajectory of one selected fuel or droplet group may be plotted each run. The chosen fuel size group is entered.) | |
| 210. | Oxid trajectory group | (1.0 through 5.0) |
| | (If a trajectory plot is wanted for an oxidizer droplet instead of a fuel droplet, the size group desired should be entered.) | |
| 211. | Trajectory start time | seconds |
| | (The trajectory is plotted for a fuel or oxidizer droplet which is injected at some chosen time. The time chosen should be entered.) | |
| 212. | Injector Ring | (1.0 through 3.0) |
| | (The droplet trajectory originates at the injector ring specified.) | |

FLOW-RATE OVERRIDES

Flow-rate overrides are provided for propellant feed systems where the internal dimensions are inadequately known, but where experimental values are available for flow rate versus pressure drop. To define the feed system resistances, it is necessary to specify a propellant flow rate, and the associated pressure drop.

- | | | |
|------|--|---------------|
| 213. | Fuel flow rate | pounds/second |
| 214. | Total fuel feed system pressure drop | psi |
| | (Tank pressure - chamber pressure. An orifice diameter will be calculated equivalent in resistance to the entire feed system except valve and injector.) | |

<u>DDD1 Subscript</u>	<u>Description</u>	<u>Units</u>
215.	Fuel valve pressure drop (A valve port area will be calculated.)	psi
216.	Fuel injector pressure drop	psi
61	Percent of fuel through ring 1 (Percentage flow, fractional flow, or actual flow in same units as 62 and 63. Discharge coefficients will be calculated.)	
62	Percent of fuel through ring 2	
63	Percent of fuel through ring 3	
217	Oxidizer flow rate	pounds/second
218	Total oxidizer feed system pressure drop (tank pressure - chamber pressure)	psi
219	Oxid valve pressure drop	psi
220	Oxid injector pressure drop	psi
85	Percent of oxidizer through ring 1 (Percentage, fractional, or actual flows in units compatible with 86 and 87.)	
86	Percent of oxidizer through ring 2	
87	Percent of oxidizer through ring 3	

OPERATING CONDITIONS

13	Fuel tank pressure	psi
14	Fuel tank temperature	degrees K
15	Fuel tank pressure-rate of change	psi/sec
16	External pressure	psi
17	Oxidizer tank pressure	psi
18	Oxidizer tank temperature	degrees K

<u>DDD1 Subscript</u>	<u>Description</u>	<u>Units</u>
19	Oxidizer tank pressure-rate of change	psi/sec
21	Injector initial temperature	degrees K
22	Throat initial temperature	degrees K
25	Injector maximum temperature (equilibrium temperature, firing)	degrees K
26	Half-rise time (half-time for injector heatup)	seconds
27	Injector minimum temperature (equilibrium temperature, nonfiring)	degrees K
28	Half-fall time (half-time for injector cooling)	seconds
29	Throat maximum temperature (equilibrium temperature, firing)	degrees K
30	Half-rise time (half-time for throat heatup)	seconds
31	Throat minimum temperature (equilibrium temperature, nonfiring)	degrees K
32	Half-fall time (half-time for throat cooling)	seconds
<u>IGNITION DESCRIPTION</u>		
33.	Assigned ignition delay (For sea-level hypergolic starts an experimental value for ignition delay time is entered)	seconds
34.	Igniter port location (If an external igniter is being used, the location, downstream of the injector, where the hot gases enter the chamber)	inches
35.	Igniter fuel flow rate (Flow rate of fuel through the igniter)	pounds/second

<u>DDD1 Subscript</u>	<u>Description</u>	<u>Units</u>
36.	Igniter oxidizer flow rate (Flow rate of oxidizer through the igniter)	pounds/second
37.	Activation energy (Activation energy of the global gas-phase ignition reaction)	(calories/mole)
38.	Frequency factor X Q (Molar collision frequency multiplied by the heat of reaction of the initiating reaction)	(cubic cm/mole/sec) X (calories/mole)
39.	Perfect mixing option (If this flag is set to 1.0, ignition will be calculated only for the well-mixed free-stream gases, ignoring the possibility of ignition in the boundary layers around droplets or on the wetted chamber walls)	(0.0 or 1.0)
40.	No axial mixing option (If this is marked with a 1.0, ignition will be calculated only for the newly flashed fuel and oxidizer vapors presuming no axial mixing of vapor and ignoring ignition in the boundary layer)	(0.0 or 1.0)

FUEL FEED SYSTEM

41	Fuel line length	inches
42	Fuel line diameter (I. D.)	inches
43	Restrictor diameter (The Vena Contracta diameter of a real restrictor, or a diameter equivalent to the resistance of a complex feed system)	inches
44.	Fuel Venturi diameter (Cavitating Venturi throat diameter)	inches

<u>DDD1 Subscript</u>	<u>Description</u>	<u>Units</u>
45	Fuel valve port area (port area * discharge coefficient)	square inches
46	Fuel check valve option (If nonzero, no reverse flow permitted in the fuel feed line)	(0.0 or 1.0)
47	Fuel valve opening time (Mechanical ramp duration, not electrical time)	seconds
48	Fuel valve closing time (Mechanical ramp duration, not electrical time)	seconds
57.	Initial void volume (Initial empty volume in the fuel feed system)	cubic inches
59.	Transition volume (Volume of fuel that flows while the injection temperature decreases from the injector temperature to the tank temperature.) (See Figure A-3.)	cubic inches
60.	Dribble Volume (Volume between the closed valve and the injector face)	cubic inches

OXIDIZER FEED SYSTEM

(65-72 and 81-84 are identical to
entries 41-48 and 57-60 except that
they describe the oxidizer feed system
instead of the fuel feed system)

ATOMIZATION PARAMETERS

- | | |
|-----|--|
| 89. | Fuel drop factor

(Correction factor for fuel droplet
median diameter - not needed for tur-
bulent flow through circular orifices
flowing full) |
|-----|--|

<u>DDD1 Subscript</u>	<u>Description</u>	<u>Units</u>
90.	Oxidizer drop factor (Correction factor for oxidizer droplet median diameter)	
91.	Fuel fan length (Distance between the impingement point and the point at which the fuel is atomized when the stream turns 45 degrees at impingement)	orifice diameters
92.	Oxidizer fan length	orifice diameters
93.	Hold at triple point option (When this flag is set to 1.0 a propellant stream flashing in a low pressure environment will not freeze, but will stop as triple-point liquid)	(0.0 or 1.0)
94.	No initial dribble option (When this flag is set to 1.0, no liquid will be injected until the void volume is filled, even when the injector-temperature vapor pressure is higher than the chamber pressure)	(0.0 or 1.0)
95.	Flash cone angle (This is the included apex angle of the cone of spray formed by a flashing stream)	degrees
96.	Showerhead length/orifice diameter ratio (The distance, in orifice diameters, that an unimpinged stream travels from the injection point to atomize completely)	orifice diameters
97-101.	Drop size 1 - drop size 5 (These are the diameter ratios of the droplet groups to the mass-median droplet)	

<u>DDD1 Subscript</u>	<u>Description</u>	<u>Units</u>
102.	No wall breakup option (When this flag is set to 1.0 an unatomized stream hitting the wall is not atomized by the impact)	(0.0 or 1.0)
103.	Drop restitution coefficient (The normal-velocity ratio for a droplet which hits the wall and bounces off)	
104.	Fraction sticking (The fraction of the droplets hitting the wall which stick to the wall instead of bouncing)	
105.	No fuel flash option (When this flag is set to 1.0, the injected fuel stream will not flash even when it is highly superheated)	(0.0 or 1.0)
106.	No oxidizer flash option (When this flag is set to 1.0, the injected oxidizer stream will not flash even when it is highly superheated)	(0.0 or 1.0)
107	No entrainment flag (A nonzero value will prevent any entrainment of wall film)	(0.0 or 1.0)
108	Delete droplet means (A nonzero value will prevent calculation of the chamber droplet size means at every time iteration)	(0.0 or 1.0)

FUEL PROPERTIES

109.	Fuel boiling point (The normal boiling point of the fuel)	degrees K
110.	Fuel freezing point	degrees K
111.	Fuel critical temperature	degrees K
112.	Fuel critical pressure	psia

<u>DDD1 Subscript</u>	<u>Description</u>	<u>Units</u>
113.	Fuel vapor specific heat (Fuel vapor specific heat at a temperature midway between the combustion gas and the droplet surface)	calories/gram/ °K
114.	Fuel liquid specific heat (Liquid fuel specific heat at the injection temperature)	calories/gram/ °K
115.	Blank	
116.	Fuel molecular weight (Molecular weight of fuel in the vapor phase)	grams/gram- mole
117.	Fuel latent heat of vaporization (Latent heat of vaporization of fuel at the normal boiling point)	calories/gram
118.	Fuel latent heat of fusion (Latent heat of fusion of the fuel at the freezing point)	calories/gram
119.	Fuel liquid thermal conductivity	calories/sec/ cm/°K
120.	Fuel accommodation coefficient (Coefficient for Langmuir-Knudsen vacuum evaporation rate)	
121.	Fuel reference temperature (Temperature at which values for density, viscosity, and surface tension are given)	degrees K
122.	Fuel density (Density of liquid fuel at the reference temperature)	grams/cm ³
123.	Fuel viscosity (Viscosity of liquid fuel at the reference temperature)	poises

<u>DDD1 Subscript</u>	<u>Description</u>	<u>Units</u>
124	Fuel surface tension (Surface tension of fuel at the reference temperature)	dynes/cm
125.	Fuel burning rate coefficient from droplet burning experiments ($-dD^2/dt$ for a burning fuel droplet in pure oxidizer vapor)	cm^2/sec
126.	Fuel monopropellant burning rate intercept	cm/sec
127.	Fuel monopropellant burning rate coefficient	$\text{cm}/\text{sec}/(\text{psia})^n$
128.	Fuel monopropellant burning rate exponent (Monopropellant burning rate values from liquid-strand experiments correlated by $r = A + BP^n$ where r is in centimeters per second and P is in psia)	

OXIDIZER PROPERTIES

129-148 Identical to 109-128 except that they describe the oxidizer instead of the fuel

PRODUCT PROPERTIES

EQUILIBRIUM GAS TEMPERATURE

149-159 Are the thermochemical equilibrium combustion product temperatures corresponding to fuel fractions of 0, 0.1, 0.2, ... 1.0 °K

EQUILIBRIUM GAS MOLECULAR WEIGHT

161-171 Are the mean molecular weights of the combustion products in thermochemical equilibrium at fuel fractions 0, 0.1, 0.2, ... 1.0

DDD1 SubscriptDescriptionUnitsEQUILIBRIUM GAS GAMMA

173-183 Are the values for frozen gamma of
the equilibrium combustion products
at fuel fractions 0, 0.1, 0.2, ... 1.0

THRUST COEFFICIENT TABLEEQUILIBRIUM THRUST
COEFFICIENT

221-231 Vacuum thrust coefficients are entered
for combustion product gases having
fuel fractions of 0., 0.1, 0.2, ... 1.0

232. Nozzle expansion area ratio

ADDUCT PROPERTIES

185. Density of the contaminant material gm/cm³
produced on the chamber wall

186. Specific heat of the gases produced by cal/gm/°K
the evaporation or pyrolysis of the
wall-film material

187. Latent heat of evaporation or heat of cal/cm
ablation of the wall-film material

188. Surface temperature of the wall-film degrees K
material during evaporation or
pyrolysis

CONTAMINANT VISCOSITY

189-199 Viscosity of the wall-film material at
the temperature to be expected on the
wall at fuel fractions 0, 0.1,
0.2, ... 1.0

MULTIPLE PULSE VALVE TIMING

233-264 Valve timing for the first through
eighth pulses of engine operation

233 Fuel valve, time of first motion seconds
opening on first pulse

234. Oxidizer valve, time of first motion seconds
opening on first pulse

<u>DDD1 Subscript</u>	<u>Description</u>	<u>Units</u>
234.	Fuel Valve, time of first motion closing on first pulse	seconds
236.	Oxidizer valve, time of first motion closing on first pulse	seconds
<u>MULTI-RING INJECTOR</u>		
<u>FIRST RING</u>		
<u>FUEL HOLES</u>		
49.	Fuel hole diameter (Injector hole size)	inches
50.	Fuel hole length (Injector hole length)	inches
51.	Axial location (Axial location of fuel injection point)	inches
52.	Radial location (Radial location of fuel injection point)	inches
53.	Injection angle (Outward angles counted as positive)	degrees
54.	Discharge coefficient	
55.	Number of fuel holes in this ring	
56.	Transverse angle (Used to impart swirl to film-coolant. Because of the two-dimensional drop-let calculations, transverse angle will not cause the propellant to approach the combustion chamber wall)	degrees
<u>OXIDIZER HOLES</u>		
73-80	Identical to entries 49-56 except that they describe the oxidizer holes instead of the fuel holes	

<u>DDD1 Subscript</u>	<u>Description</u>	<u>Units</u>
-----------------------	--------------------	--------------

SECOND RING

265-272	Describe the second ring fuel holes	
273-280	Describe the second ring oxidizer holes	

THIRD RING

281-288	Describe the third ring fuel holes	
289-296	Describe the third ring oxidizer holes	

COMBUSTION CHAMBER PROFILE

297.	Axial location of injector face (usually set to zero)	inches
298.	Injector face diameter	inches
299.	Axial location 2	inches
300.	Chamber diameter 2	inches
301-310	Pairs of axial stations and diameters describing the chamber contour	inches
311	Axial location of the throat plane	inches
312	Throat diameter	inches

(2) Namelist PRTDIR

Namelist PRTDIR directs the program to produce graphics of the time-varying parameters which are desired. The default value for the members at this array is zero, and graphics are produced only for members which are given non-zero values. The graphics which can be produced are:

<u>DDD 2 Subscript</u>	<u>Variable to be plotted</u>
------------------------	-------------------------------

1. Chamber pressure
2. Fuel valve trace (fraction of wide-open port area)
3. Oxidizer valve trace (fraction of wide-open port area)
4. Fuel flow rate leaving tank

DDD 2 Subscript

Variable to be plotted

5. Oxidizer flow rate leaving tank
6. Total propellant flow rate leaving tanks
7. Fuel injection rate
8. Oxidizer injection rate
9. Fuel (streams, fans and droplets) mass in chamber
10. Oxidizer (streams, fans and droplets) mass in chamber
11. Propellant (streams, fans and droplets) mass in chamber
12. Fuel mass on chamber wall
13. Oxidizer mass on chamber wall
14. Propellant mass on chamber wall
15. Gas mass in chamber
16. Mass fraction of the chamber gas which is fuel-derived
17. Chamber temperature (gas phase)
18. Fuel evaporation rate
19. Oxidizer evaporation rate
20. Propellant evaporation rate
21. Gas outflow rate
22. Fuel droplet outflow rate
23. Oxidizer droplet outflow rate
24. Total droplet outflow rate
25. Fuel film outflow rate
26. Oxidizer film outflow rate
27. Total film outflow rate
28. Mass fraction of total outflow which is gas phase
29. All chamber contents - total explosion pressure capability
30. Mass of unatomized fuel streams and fans in chamber

DDD 2 Subscript

Variable to be plotted

31. Mass of unatomized oxidizer streams and fans in chamber
32. Mass of fuel droplets in chamber
33. Mass of oxidizer droplets in chamber
34. Gas and droplets only - total explosion pressure capability
35. Chamber wall adduct only - chamber explosion over-pressure capability
36. D30 of all fuel droplets in chamber
37. D31 of all fuel droplets in chamber
38. D32 of all fuel droplets in chamber
39. D30 of all oxidizer droplets in chamber
40. D31 of all oxidizer droplets in chamber
41. D32 of all oxidizer droplets in chamber
42. Fuel injector void volume
43. Oxidizer injector void volume
44. Thrust

(3) Namelists RESRT 1 and RESRT 2

These Namelists contain the amounts of fuel and oxidizer left deposited on the chamber wall at the conclusion of a previously computed engine firing. These Namelists are punched by the program at the end of a calculation if the "Punch for restart" option has been given a non-zero value.

b. Program Output

(1) Input Print

The first print which is produced by the program is a recapitulation of the program input

(2) Propellant Property Print, Derived Feed System Values and Chamber Description

The second print produced is a table of calculated propellant properties versus temperature. These values can be compared with known experimental values to assure that the program physical properties subroutines are giving an adequate representation of the true values. The values printed are liquid enthalpy, vapor enthalpy, vapor pressure, liquid density, liquid viscosity, and surface tension. These are given for evenly spaced intervals of reduced temperature, with the corresponding absolute temperature also given. The units are calories/gram, psia, grams/cc, poise, dyne/cm, and degrees K.

If the flow overrides have been used, the values derived for effective valve port areas, orifice discharge coefficients and equivalent feed system orifice diameter are printed in square inches and inches.

The effective feed system component areas are given in square inches. The relative resistances to flow of the "line" (everything except valve and injector) and the injector are given in units of inches⁻⁴ ($1/A^2$). The inertial aspect of the feed system geometry is expressed in inches⁻¹ (L/A). The effective injection area (geometrical area * discharge coefficient) is given for each injector ring, and the percentage of total fuel and oxidizer flow through each ring is given. The axial and radial location of the impingement point is given for each ring in inches.

The combustion chamber is categorized by giving the axial location, diameter, cross-sectional area, upstream volume, mass of fuel on the wall, mass of oxidizer on the wall, and wall temperature for each of 100 equally spaced axial locations. The units are inches, square inches, cubic inches, grams, and degrees Kelvin.

(3) Print of Time-Varying Rocket System Parameters

At each integrating time interval, values are printed for 48 of the more important system variables. This print consists of six lines containing eight values per line.

The first line contains the model time in milliseconds, the chamber pressure in psia, the ignition state of the chamber (1.0 for ignited, 0.0 for unignited), the mass fraction of the gas or vapor in the chamber which is fuel-derived, the chamber temperature in degrees K, the mean molecular weight of the gases or vapors in the chamber, the specific heat ratio for the gases or vapors in the chamber and the vacuum thrust coefficient for the gas or vapor phase flowing from the chamber.

The second line contains the fuel and oxidizer injection rates in pounds per second, and the fuel and oxidizer feed-line flow rates in pounds per second. The injection flowrate and feed-line flowrate will differ when the injector is dribbling into a vacuum after the propellant valves close, or when a partially empty dribble volume is being filled before the injector primes. The void volumes on fuel and oxidizer sides of the injector are given in cubic inches. The dribble injection rate will decrease to zero when the dribble volume is emptied. The fuel and oxidizer injection temperatures are given in degrees Kelvin. The injection temperatures are equal to the injector temperature, until a volume of propellant has flowed out of the tank equal to the dribble volume, then the temperature linearly decreases to the tank temperature, with the decrease spread out over the prescribed transition volume.

The third line contains the evaporation rates of the fuel drop ensemble and the oxidizer drop ensemble in pounds per second. The fuel flash rate and oxidizer flash rate are given in pounds per second of vapor produced by the vacuum flashing of the injected streams. The rates of propellant burnoff from the wall is given for fuel and oxidizer in pounds per second. The heat for wall burnoff comes from heat transferred from the

chamber gases. The rates of vacuum evaporation from the wall are given for fuel and oxidizer in pounds per second. The heat for vacuum evaporation is transferred from the chamber wall through the propellant film to the evaporating surface.

The fourth line contains the mass of fuel-derived combustion gas or vapor in the chamber in pounds. The mass of oxidizer-derived gas or vapor is given similarly. The masses of fuel droplets and oxidizer droplets in the chamber are given in pounds. The masses of injected, but not yet atomized fuel and oxidizer are given under the headings Fuel Streams and Oxidizer Streams. The mass of fuel and oxidizer deposited on the walls are the final entries of the fourth line.

The first and second entries of the fifth line give the mass rate of efflux for fuel and oxidizer-derived vapors or combustion-product gases in pounds per second, the third and fourth entries are the mass rate of ejection through the throat for incompletely burned fuel drops and oxidizer drops in pounds per second. The rate at which propellant film on the wall is being flowed through the throat is given next in pounds per second. "Gas Fraction" is the instantaneous value for the fraction of the total mass efflux which is in the gas phase. The final entry on this line is thrust, in pounds force. The thrust includes the axial momentum rate of the expelled droplets, and the thrust from the gas phase products.

The sixth line starts with the sauter mean droplet diameter for all the fuel and oxidizer spray contained in the chamber this time interval. The next two entries give fuel and oxidizer stream injection velocities. The maximum explosion pressure is the pressure which would be attained if all the chamber contents (gas, streams, fans, droplets, and wall film) were well mixed and converted to equilibrium combustion products. The mass out of tank is total mass of propellant flowed from the propellant tanks from the start of the run, in pounds. The integral $PC \times DT$ is the area under the curve of chamber-pressure-versus time, in psia x seconds. Total impulse is the time integral of thrust in pound-force x seconds.

(4) Summary Prints and Special Messages

Other prints which may occur interspersed with the normal six line prints are summary prints and special messages. The most frequent special messages specify when ignition or extinguishment occurs in the combustion chamber, or when the fuel or oxidizer manifolds fill. Other special messages indicate minor errors, such as failure to converge to within 2 percent of the correct surface temperature during vacuum evaporation, or catastrophic errors such as calculation of a negative chamber pressure, or filling up the droplet array locations.

The propellant disposition summary, whose frequency is specified in data item 203 consists of seven lines of numbers. The first four lines give a mass balance for all fuel and oxidizer injected up to the present time. The masses, in grams, are given for total injected fuel, oxidizer and sum of fuel plus oxidizer, and the amounts expelled as gas, as droplets and as wall film. Also given are the masses currently retained as gas, as droplets and as wall film. The last five lines gives the numbers of fuel drops and

oxidizer drops injected and ejected up to the present time. The summation of droplet diameters, diameters squared, diameters cubed and axial momentum is also given, which makes it possible to calculate the mean diameters and mean axial velocities of expelled droplets for the interval between any two summary prints. If KBUG has been given a nonzero value, large numbers of diagnostic data will be printed on the KBUGTH iteration. These values will be of interest for trouble-shooting only.

(5) Final Performance Summary

After the last of the time-steps is printed, a performance summary is printed. The mass flowed out of tank is given, the mass flowed through the injector is given and the mass flowed through the nozzle is given. These values are not generally the same, because of filling or voiding of the injector dribble volumes, and because of increase or depletion of propellant mass stored in the combustion chamber in the forms of gas, droplets or streams, and wall film. The mixture ratio, C-Star, and specific impulse are calculated on each of these propellant mass bases. The pressure time integral for the entire pulse and the total impulse are also printed. The final print also gives the disposition of injected propellant for the entire firing. The fractions of injected fuel, oxidizer and total propellant expelled in the form of gas, unburned vapor, droplets and as wall film are given, and the fraction retained in the chamber as gas, droplets, and wall film are given. The mean diameters for injected and ejected fuel and oxidizer are given in microns. The mean axial and radial velocities are given for the ejected droplets in feet per second. The calculated size distribution for injected and ejected fuel and oxidizer is given. When this is plotted, it shows signs of the five-group approximation for injected droplet size, which is a computational artifact; however, also apparent are the real effects of flashing versus impinging stream atomization, the preferential burning or small droplets, the segregation by drag versus momentum effects, etc.

(6) Final Chamber Condition

The axial distribution of fuel wall film, oxidizer wall film, and temperature are given to show the input which would be used for a restart of the chamber for the next pulse. This print also reveals the potential for chamber explosion or contamination based on the wall-film propellant remaining in the chamber after cutoff.

(7) Time-Averaged Interval Performance Values

Up to three prints can be called per run, giving aggregate values and rates for prescribed intervals of time. These intervals are often chosen to represent the start transient, steady-state operation, and the cutoff transient. Having values for total impulse and propellant consumption for the transients and for thrust and propellant consumption rate during steady state makes it possible to estimate performance for pulses having similar initial conditions but different pulse duration, simply by summing up the total impulse and propellant consumption for the two transients together with appropriate amounts of steady-state operation. The average performance or

contamination production for different pulse-widths or pulse-trains may be estimated in a similar way. Input values required for MULTRAN are printed for these same time-averaged intervals.

(8) Computer Graphics

The computer graphics include the trajectory of the specified fuel or oxidizer drop, up to 44 time-varying system parameters plotted versus time, and a specified number of instantaneous profile plots of wall deposit thickness versus chamber length. The wall deposit plots may be eliminated by setting input item 204 to zero, motion picture frames are produced for the interval specified by input items 206 and 207. The desired time-varying system parameters are produced, by giving nonzero values to the corresponding subscripted flags in NAMELIST PRDIR.

A. 5 SAMPLE CASE

Table A-III consists of a sample case for the TCC program. Illustrated in the following order are; a listing of the control cards, and a representative sample of the prints and graphics produced.

The printer output consists of the input data print, and representative samples of each of the types of output prints. A sampling of computer graphics includes a droplet trajectory plot, chamber pressure, fuel injection rate, oxidizer injection rate, one wall-film thickness plot, and one frame of motion picture, showing the distribution of propellant droplets and wall-film in the combustion chamber.

A. 6 REFERENCES

- A-1. W. T. Webber. "Calculation of Low-Frequency Unsteady Behavior of Liquid Rockets from Droplet Combustion Parameters", Journal of Spacecraft and Rockets, Vol. 9, No. 4, April 1972.
- A-2. W. T. Webber and W. A. Gaubatz, "Calculation of Low-Frequency Combustion Instability in Liquid-Propellant Rocket Engines," Seventh JANNAF Combustion Meeting, Pasadena, California, October, 1970.
- A-3. W. T. Webber and W. A. Gaubatz, "Calculation of the Ignition and Start Transient of Liquid Propellant Rocket Engines," Paper No. 70-23, Western States Section, The Combustion Institute, Pasadena, California, October 26, 1970. Also published as McDonnell Douglas Astronautics Company paper MDAC WD-1439.
- A-4. W. T. Webber, W. A. Gaubatz, and R. J. Hoffman, "Calculation of Contaminant Production in Liquid Bipropellant Rocket Engines," JANNAF Sixth Plume Technology Meeting, March 1971. Also published as McDonnell Douglas Astronautics Company paper MDAC WD-1513, April 1971.

- A-5. W. T. Webber and R. J. Hoffman, "Calculation of Conditions Conducive of Spiking", Ninth JANNAF Combustion Meeting, Monterey, California, September, 1972. Also published as McDonnell Douglas Astronautics Company Paper MDAC WD-1968.
- A-6. W. T. Webber and R. J. Hoffman. A Mechanistic Model for Analysis of Pulse-Mode Engine Operation. AIAA Paper No. 72-1184, AIAA/SAE 8th Joint Propulsion Specialist Conference, New Orleans, La., November 1972. Also published as McDonnell Douglas Astronautics Company Paper MDAC WD-1969.
- A-7. R. J. Hoffman, W. D. English, R. G. Oeding, and W. T. Webber, "Plume Contamination Effects Prediction-The CONTAM Computer Program-Final Report and Program User's Manual," AFRPL-TR-71-109, December 1971.
- A-8. W. T. Webber, R. J. Hoffman, and J. R. Nunn, "Analysis of Potential Plume Contamination Effects Resulting from Two 300-Lb. Bipropellant Engines Operating in a Satellite Environment", AFRPL-TR-72-66, June 1972.
- A-9. R. J. Priem and M. F. Heidmann. "Propellant Vaporization as a Design Consideration for Rocket Engine Combustion Chamber", NASA TR R-67, 1960.
- A-10. M. R. Beltran, B. P. Breen, T. C. Kosvic, C. F. Sanders, R. J. Hoffman, and R. O. Wright. "Analysis of Liquid Rocket Engine Combustion Instability", AFRPL-TR-65-254, January 1966.
- A-11. L. P. Combs, "Liquid Rocket Performance Computer Model with Distributed Energy Release", Rocketdyne Report No. R-8888, NASA CR-114462, June 1972.
- A-12. W. D. Chadwick and L. P. Combs, "Pulse Mode Performance Model", Rocketdyne Report No. 8864, AFRPL TR-72-16, November, 1972.
- A-13. T. F. Seamans, M. Vanpee and V. D. Agosta. "Development of a Fundamental Model of Hypergolic Ignition in Space-Ambient Engines," AIAA Journal, Vol. 5, No. 9, P. 1616, September 1967.
- A-14. R. A. Gater and M. R. L'Ecuyer, "A Fundamental Investigation of the Phenomena that Characterize Liquid-Film Cooling" Report No. TM-69-1, Jet Propulsion Center, Purdue University, January 1969.
- A-15. Z. Tamura and Y. Tanasawa, "Evaporation and Combustion of a Drop Contacting with a Hot Surface", Seventh Symposium (International) on Combustion, Butterworths, London, 1959.
- A-16. R. B. Lawhead, R. S. Levine, and W. T. Webber, "Liquid-propellant Rocket Combustion Instability Studies-Final Summary Report Covering the Period 1 June 1954 to 30 November 1955", Rocketdyne Report R-122, 1956.

- A-17. J. C. Eschweiler and H. W. Wallace, "Liquid Rocket Engine Feed System Dynamics by the Method of Characteristics". Transactions ASME Journal of Engineering for Industry, November 1968.
- A-18. G. M. Arnett, "Lunar Excursion Module RCS Engine Vacuum Chamber Contamination Study," NASA, MSFC, Technical Memorandum No. 53859, July 8, 1969.
- A-19. H. H. Takimoto, and G. C. Denault, "Rocket Plume (N_2O_4/MMH) Impingement on Aluminum Surface," Journal of Spacecraft and Rockets, Vol. 7, No. 11, November 1970.
- A-20. P. J. Martinkovic, "Bipropellant Attitude Control Engine Exhaust Contamination and Its Effect on Space Borne Equipment," Twelfth JANNAF Liquid Propulsion Meeting, November 17-19, 1970, Las Vegas, Nevada. CPIA publication No. 201, Vol. 2.
- A-21. J. Houseman, "Jet Separation and Popping with Hypergolic Propellants", Seventh JANNAF Combustion Meeting, Pasadena, California, Oct. 1970.
- A-22. L. B. Zung and J. R. White, "Combustion Process of Impinging Hypergolic Propellants", Seventh JANNAF Combustion Meeting, Pasadena, California, Oct. 1970.
- A-23. W. H. Nurick and J. D. Cordill, "Final Report-Reactive Stream Separation Photography." Rocketdyne Report R-8490, Undated Circa 1971.
- A-24. B. R. Lawver, "A Model of the Hypergolic Propellant Pop Phenomena", Journal of Spacecraft and Rockets, Vol. 9, No. 4 April 1972.
- A-25. R. E. Martens, "Investigation of Hypergolic Ignition Spike Phenomena," 8th Liquid Propulsion Symposium, CPIA Publication No. 121, Vol. 1, October 1966.
- A-26. J. A. Nestlerode, "Acoustic Instability in Storable Propellant Rocket Motors," 5th ICRPG Combustion Conference, Johns Hopkins University, Applied Physics Laboratory, Maryland, October 1-3, 1968.
- A-27. O. A. Hougen and K. M. Watson. Chemical Process Principles John Wiley & Sons, 1950.
- A-28. Calingaert and Davis. Industrial and Engineering Chemistry, Vol. 17, page 1287, 1925.
- A-29. H. M. Paynter. "Fluid Transients in Engineering Systems." Handbook of Fluid Dynamics, McGraw-Hill Book Company, 1961.
- A-30. D. M. Bushnell and P. B. Gooderum. "Atomization of Superheated Water Jets at Low Ambient Pressures." Journal of Spacecraft and Rockets, Vol. 5, No. 2, February 1968.

- A-31. R. Brown. Sprays Formed by Flashing Liquid Jets. Ph. D. Thesis, University of Michigan, 1961.
- A-32. P. B. Gooderum and D. M. Bushnell. "Measurement of Mean Drop Sizes for Sprays from Superheated Water Jets." Journal of Spacecraft and Rockets, Vol. 6, No. 2, February 1969.
- A-33. R. D. Ingebo. Drop-Size Distributions for Impinging-Jet Breakup in Airstreams Simulating the Velocity Conditions in Rocket Combustors. NACA TN 4222, 1950.
- A-34. M. A. Weiss and C. H. Worsham. "Atomization in High Velocity Airstreams." Journal of the American Rocket Society, Vol. 29, No. 4, April 1959.
- A-35. M. F. Heidmann and H. H. Foster. Effect of Impingement Angle on Drop-Size Distribution and Spray Pattern of Two Impinging Water Jets. NASA TN D-872, 1961.
- A-36. R. A. Dickerson. "Like and Unlike Impinging Injection Element Droplet Sizes." Journal of Spacecraft and Rockets, Vol. 6, No. 11, November 1969.
- A-37. L. J. Zajac, "Correlation of Spray Dropsize Distribution and Injector Variables", Rocketdyne Report No. R-8455, February February 1971.
- A-38. M. E. Heidmann, R. J. Priem, and J. C. Humphrey. A Study of Sprays Formed by Two Impinging Jets. NACA TN 3835, 1957.
- A-39. E. Rabin, A. R. Schallenmueller, and R. B. Lawhead. Displacement and Shattering of Propellant Droplets. AFOSR TR 60-75, 1960.
- A-40. M. M. El Wakil, et al. Experimental and Calculated Temperature and Mass Histories of Vaporizing Fuel Drops. NACA TN 3490, 1956.
- A-41. J. G. Sotter. Nonsteady Evaporation of Liquid Propellant Drops. The Grossman Model JPL TR 32-1061, 1968.
- A-42. W. N. Bond and D. A. Newton. Phil. Mag. (7), 5, 794, 1928.
- A-43. R. R. Hughes and E. R. Gilliland. "The Mechanics of Drops." Chem. Eng. Prog., Vol. 28, No. 10, 1952.
- A-44. G. A. E. Godsave. "Studies of the Combustion of Drops in a Fuel Spray - The Burning of Single Drops of Fuel." Fourth Symposium on Combustion, Williams and Wilkins, 1953.
- A-45. D. B. Spalding. "The Combustion of Liquid Fuels." Fourth Symposium on Combustion, Williams and Wilkins, 1953.

- A-46. G. A. Agoston, H. Wise, and W. A. Rosser. "Dynamic Factors Affecting the Combustion of Liquid Spheres." Sixth Symposium on Combustion, Reinhold, 1956.
- A-47. W. T. Webber. Effects of Gas Motion on Heterogeneous Combustion etc. WADC TR 59-50, 1959.
- A-48. W. E. Ranz and W. R. Marshall. "Evaporation from Drops." Chem. Eng. Prog., Vol. 48, No. 4, 1952.
- A-49. B. L. McFarland, "Heat Transfer Considerations in Internal Regeneratively (INTEREGEN) Cooled Thrust Chambers", ASME Space Technology and Heat Transfer Conference, Los Angeles, California, June 1970, Paper Number 70-Ht/SpT-41.
- A-50. L. Bernath, "A Theory of Local-Boiling Burnout and its Application to Existing Data", Chem. Eng. Prog. Symp. Ser 56, No. 30, 95-116, 1960.
- A-51. L. S. Tong, "Boiling Heat Transfer and Two-Phase Flow", John Wiley & Sons, 1965.
- A-52. W. Juran and R. C. Stechman. "Ignition Transients in Small Hypergolic Rockets." Journal of Spacecraft and Rockets, Vol. 5, No. 3, March 1968.
- A-53. S. W. Mayer, D. Taylor and L. Schieler, "Preignition Products from Propellants at Simulated High-Altitude Conditions", Combustion Science and Technology, Vol. 1, 1969, P. 119-129.
- A-54. P. Breisacher, H. H. Takimoto, G. C. Denault and W. A. Hicks, "Simultaneous Mass Spectrometer Differential Thermal Analyses of Nitrate Salts of Monomethylhydrazine and Methylamine, Combustion and Flame, 14, 1970, P. 397-404.
- A-55. H. H. Takimoto, P. Breisacher, G. C. Denault and W. A. Hicks, "Vacuum Thermal Decompositions of the Nitrate Salts of Hydrazine". To be published in Combustion and Flame, 1972.
- A-56. H. C. Barnett and R. B. Hibbard, Ed. Basic Considerations in the Combustion of Hydrocarbon Fuels with Air. NACA Report 1300, 1957.
- A-57. R. J. Priem. Propellant Vaporization as a Criterion for Rocket Engine Design; Calculations of Chamber Length to Vaporize a Single n-Heptane Drop, NACA TN3985 July 1957.
- A-58. S. Lambiris, L. P. Combs, and R. S. Levine. "Stable Combustion Processes in Liquid Propellant Rocket Engines." Combustion and Propulsion. Fifth AGARD Colloquium: High Temperature Phenomena, the MacMillan Co., 1962.

[illegible]

THE INPUT DATA FOR THIS CASE ARE AS FOLLOWS

PROBLEM DESCRIPTION

ROCKETDYNE HS-2101 ENGINE - SAMPLE TEST CASE FOR PRODUCTION TCC

GENERAL INSTRUCTIONS

PUNCH FOR RESTART WORK FROM TAPE HANG NO MOVIE TAPE
(9) 0.00000 (10) 0.00000 (11) 50.00000 (12) 0.00000
STOP TIME TIME INTERVAL PRINT ONE OUT OF FIVE ONE OUT OF
(201) .02000 (202) .00020 (203) 10.00000 (204) 25.00000
FILM WEST, EXAG, START MOVIE TAIL, END MOVIE TAIL, DATA REVIEW ONLY
(205) 20.00000 (206) 10.00000 (207) 10.00000 (208) 0.00000

TIME-AVERAGE PERFORMANCE VALUES

START TIME 1 FINISH TIME 1 START TIME 2 FINISH TIME 2
(311) 0.00000 (312) 0.00000 (313) 0.00000 (314) 0.00000
START TIME 3 FINISH TIME 3
(315) 0.00000 (316) 0.00000

DROPLET TRAJECTORY PLOT

FUEL SIZE GROUP OXID SIZE GROUP INJECTION TIME INJECTOR RING
(209) 3.00000 (210) 0.00000 (211) .00500 (212) 2.00000

FLOW RATE OVERRIDES

FUEL FLOW RATE TOTAL PRESS DROP VALVE PRESS DROP INJ PRESS DROP
(213) 0.00000 (214) 0.00000 (215) 0.00000 (216) 0.00000
PERCENT RING 1 PERCENT RING 2 PERCENT RING 3
(61) 0.00000 (62) 0.00000 (63) 0.00000 (64) 0.00000
OXID FLOW RATE TOTAL PRESS DROP VALVE PRESS DROP INJ PRESS DROP
(217) 0.00000 (218) 0.00000 (219) 0.00000 (220) 0.00000
PERCENT RING 1 PERCENT RING 2 PERCENT RING 3
(85) 0.00000 (86) 0.00000 (87) 0.00000 (88) 0.00000

OPERATING CONDITIONS

FUEL TANK PRESS FUEL TANK TIIP FUEL TANK PSI/SEC EXTERNAL PRESSURE
(11) 240.00000 (12) 204.00000 (13) 0.00000 (14) 0.00000
OXID TANK PRESS OXID TANK TIIP OXID TANK PSI/SEC
(15) 240.00000 (16) 204.00000 (17) 0.00000 (18) 0.00000
INJECT INIT TEMP THROAT INIT TEMP
(21) 204.00000 (22) 204.00000 (23) 0.00000 (24) 0.00000
INJECT MAX, TEMP HALF-RISE TIME INJECT MIN, TEMP HALF-FALL TIME
(31) 300.00000 (32) 10.00000 (33) 204.00000 (34) 0.00000
THROAT MAX, TEMP HALF-RISE TIME THROAT MIN, TEMP HALF-FALL TIME
(35) 300.00000 (36) 10.00000 (37) 204.00000 (38) 0.00000

IGNITION DESCRIPTION

ASSIGNED DELAY IGNITER FORT LIG. FUEL FLOW RATE OXID FLOW RATE
 (33) 0.00000 (34) 0.00000 (35) 0.00000 (36) 0.00000
 ACTIVATION ENERGY FREQ. FACT. P O PERFECT MIXING NO AXIAL MIXING
 (37) 0.00000 (38) 0.00000 (39) 0.00000 (40) 0.00000

FUEL FEED SYSTEM

LINE LENGTH LINE DIAM RESTRICTOR DIAM VENTURI DIAM
 (41) 30.00000 (42) .40200 (43) .123500 (44) 0.00000
 VALVE AREA CHECK VALVES VALVE OPEN DT VALVE CLOSE DT
 (45) .015200 (46) 0.00000 (47) .001500 (48) .001500
 INIT. VOID VOLUME TRANSITION VOLUME DRIBBLE VOLUME
 (49) .010000 (50) 0.00000 (51) 0.00000 (52) .420000

OXIDIZER FEED SYSTEM

LINE LENGTH LINE DIAM RESTRICTOR DIAM VENTURI DIAM
 (53) 30.00000 (54) .40200 (55) .123500 (56) 0.00000
 VALVE AREA CHECK VALVES VALVE OPEN DT VALVE CLOSE DT
 (57) .017000 (58) 0.00000 (59) .001500 (60) .001500
 INIT. VOID VOLUME TRANSITION VOLUME DRIBBLE VOLUME
 (61) .010000 (62) 0.00000 (63) 0.00000 (64) .240000

ATOMIZATION PARAMETERS

FUEL DROP FACTOR OXID DROP FACTOR FUEL FAN MIN L/D OXID FAN MIN L/D
 (65) 0.00000 (66) 0.00000 (67) 0.00000 (68) 0.00000
 HOLD AT TRIPLE PT NO INIT. DRIEFILE FLASH CONE ANGLE SINGLE STREAM L/D
 (69) 0.00000 (70) 0.00000 (71) 0.00000 (72) 0.00000
 DROP SIZE 1 DROP SIZE 2 DROP SIZE 3 DROP SIZE 4
 (73) .00000 (74) .00000 (75) .00000 (76) .00000
 DROP SIZE 5 NO WALL DREAPUP DROP RESTITUTION FRACTION STICKING
 (77) 0.00000 (78) 0.00000 (79) 0.00000 (80) 0.00000
 NO FUEL FLASH NO OXID FLASH NO ENTRAINMENT DELETE DROP MEANS
 (81) 0.00000 (82) 0.00000 (83) 0.00000 (84) 0.00000

FUEL PROPERTIES

BOILING POINT	FREEZING POINT	CRITICAL TEMP.	CRITICAL PRESS.
(128) 300.00000 (128)	322.00000 (128)	394.00000 (128)	1125.00000 (128)
VAPOR CP.	LIQUID CP.		MOL. WEIGHT
(129) .00000 (129)	.00000 (129)	0.00000 (129)	46.09400 (129)
LATENT HEAT VAP.	LATENT HEAT FUS.	LIG. THERM. COND.	ACCOM. COEFF.
(130) 230.00000 (130)	67.00000 (130)	.00000 (130)	1.00000 (130)
REFERENCE TEMP.	DENSITY	VISCOSITY	SURFACE TENSION
(131) 300.00000 (131)	.00000 (131)	.00000 (131)	.00000 (131)
BURNING RATE M	MONO. INTERCEPT MONO.	COEFFICIENT MONO.	EXPONENT MONO.
(132) .00000 (132)	0.00000 (132)	0.00000 (132)	0.00000 (132)

OXIDIZER PROPERTIES

BOILING POINT	FREEZING POINT	CRITICAL TEMP.	CRITICAL PRESS.
(133) 204.00000 (133)	262.00000 (133)	431.00000 (133)	1470.00000 (133)
VAPOR CP.	LIQUID CP.		MOL. WEIGHT
(134) .29000 (134)	.36000 (134)	0.00000 (134)	46.08000 (134)
LATENT HEAT VAP.	LATENT HEAT FUS.	LIG. THERM. COND.	ACCOM. COEFF.
(135) 99.00000 (135)	39.20000 (135)	.00000 (135)	1.00000 (135)
REFERENCE TEMP.	DENSITY	VISCOSITY	SURFACE TENSION
(136) 300.00000 (136)	1.45000 (136)	.00460 (136)	20.00000 (136)
BURNING RATE M	MONO. INTERCEPT MONO.	COEFFICIENT MONO.	EXPONENT MONO.
(137) .02700 (137)	0.00000 (137)	0.00000 (137)	0.00000 (137)

PRODUCT PROPERTIES

TABULAR PROPERTY DATA IS FOR FUEL FRACTIONS OF 0.0, 0.1, 0.2 - - - 1.0

EQUILIBRIUM GAS TEMPERATURE

TEMP. 1	TEMP. 2	TEMP. 3	TEMP. 4
(149) 300.00000 (150) 2163.00000 (151) 3084.00000 (152) 3397.00000			
TEMP. 5	TEMP. 6	TEMP. 7	TEMP. 8
(153) 3061.00000 (154) 2360.00000 (155) 1769.00000 (156) 1433.00000			
TEMP. 9	TEMP. 10	TEMP. 11	
(157) 1344.00000 (158) 1266.00000 (159) 1190.00000 (160) 0.00000			

EQUILIBRIUM GAS MOL. WEIGHT

MOL. WT. 1	MOL. WT. 2	MOL. WT. 3	MOL. WT. 4
(161) 46.00000 (162) 20.70000 (163) 86.40000 (164) 33.30000			
MOL. WT. 5	MOL. WT. 6	MOL. WT. 7	MOL. WT. 8
(165) 50.00000 (166) 50.75000 (167) 54.40000 (168) 53.00000			
MOL. WT. 9	MOL. WT. 10	MOL. WT. 11	
(169) 54.00000 (170) 54.50000 (171) 54.80000 (172) 0.00000			

EQUILIBRIUM GAS GAMMA

GAMMA 1	GAMMA 2	GAMMA 3	GAMMA 4
(173) 1.12000 (174) 1.25000 (175) 1.22000 (176) 1.21700			
GAMMA 5	GAMMA 6	GAMMA 7	GAMMA 8
(177) 1.23500 (178) 1.26000 (179) 1.26900 (180) 1.26900			
GAMMA 9	GAMMA 10	GAMMA 11	
(181) 1.27000 (182) 1.24700 (183) 1.22000 (184) 0.00000			

THRUST COEFFICIENT TABLE

EQUILIBRIUM THRUST COEFFICIENT

CF VAC 1	CF VAC 2	CF VAC 3	CF VAC 4
(185) 0.00400 (186) 0.00800 (187) 0.00000 (188) 0.00000			
CF VAC 5	CF VAC 6	CF VAC 7	CF VAC 8
(189) 0.04500 (190) 0.01200 (191) 0.00000 (192) 0.00000			
CF VAC 9	CF VAC 10	CF VAC 11	EXP. AREA RATIO
(193) 0.00000 (194) 0.00000 (195) 0.00000 (196) 0.00000			

ADDUCT PROPERTIES

(185) DENSITY 3.00000 (186) VAPOR CP: 1.00000 (187) LATENT HEAT 500.00000 (188) DECOMP. TEMP: 500.00000

CONTAMINANT VISCOSITY

(189) VISCOSITY 1 .00400 (190) VISCOSITY 2 .02400 (191) VISCOSITY 3 .04300 (192) VISCOSITY 4 .06000
 (193) VISCOSITY 5 .00100 (194) VISCOSITY 6 .10000 (195) VISCOSITY 7 .00200 (196) VISCOSITY 8 .06400
 (197) VISCOSITY 9 .04000 (198) VISCOSITY 10 .02900 (199) VISCOSITY 11 .01040 (200) 0.00000

FIRST PULSE VALVE TIMING

FUEL VALVE OPEN OXID VALVE OPEN FUEL VALVE CLOSE OXID VALVE CLOSE
(233) 0.00000 (234) 0.00000 (235) 0.00000 (236) 0.00000

SECOND PULSE TIMING

FUEL VALVE OPEN OXID VALVE OPEN FUEL VALVE CLOSE OXID VALVE CLOSE
(237) 0.00000 (238) 0.00000 (239) 0.00000 (240) 0.00000

THIRD PULSE TIMING

FUEL VALVE OPEN OXID VALVE OPEN FUEL VALVE CLOSE OXID VALVE CLOSE
(241) 0.00000 (242) 0.00000 (243) 0.00000 (244) 0.00000

FOURTH PULSE TIMING

FUEL VALVE OPEN OXID VALVE OPEN FUEL VALVE CLOSE OXID VALVE CLOSE
(245) 0.00000 (246) 0.00000 (247) 0.00000 (248) 0.00000

FIFTH PULSE TIMING

FUEL VALVE OPEN OXID VALVE OPEN FUEL VALVE CLOSE OXID VALVE CLOSE
(249) 0.00000 (250) 0.00000 (251) 0.00000 (252) 0.00000

SIXTH PULSE TIMING

FUEL VALVE OPEN OXID VALVE OPEN FUEL VALVE CLOSE OXID VALVE CLOSE
(253) 0.00000 (254) 0.00000 (255) 0.00000 (256) 0.00000

SEVENTH PULSE TIMING

FUEL VALVE OPEN OXID VALVE OPEN FUEL VALVE CLOSE OXID VALVE CLOSE
(257) 0.00000 (258) 0.00000 (259) 0.00000 (260) 0.00000

EIGHTH PULSE TIMING

FUEL VALVE OPEN OXID VALVE OPEN FUEL VALVE CLOSE OXID VALVE CLOSE
(261) 0.00000 (262) 0.00000 (263) 0.00000 (264) 0.00000

MULTI-RING INJECTOR

FIRST RING

FUEL HOLES

HOLE DIAMETER (49) .029500 (50) .300000 (51) 0.000000 (52) .525000
 RADIAL INJ. ANGLE DISCHARGE COEFF. NUMBER OF HOLES TRANSVERSE ANGLE
 (53) .43.900000 (54) .099100 (55) 12.000000 (56) 0.000000

OXIDIZER HOLES

HOLE DIAMETER (73) .029000 (74) .375000 (75) 0.000000 (76) .440000
 RADIAL INJ. ANGLE DISCHARGE COEFF. NUMBER OF HOLES TRANSVERSE ANGLE
 (77) .34.000000 (78) .094100 (79) 18.000000 (80) 0.000000

SECOND RING

FUEL HOLES

HOLE DIAMETER (268) .017500 (269) .350000 (270) 0.000000 (271) .780000
 RADIAL INJ. ANGLE DISCHARGE COEFF. NUMBER OF HOLES TRANSVERSE ANGLE
 (272) .49.900000 (273) .099100 (274) 24.000000 (275) 0.000000

OXIDIZER HOLES

HOLE DIAMETER (273) .027000 (274) .345000 (275) 0.000000 (276) .400000
 RADIAL INJ. ANGLE DISCHARGE COEFF. NUMBER OF HOLES TRANSVERSE ANGLE
 (277) .32.800000 (278) .084100 (279) 24.000000 (280) 0.000000

THIRD RING

FUEL HOLES

HOLE DIAMETER (281) .016000 (282) .307500 (283) 0.000000 (284) 1.140000
 RADIAL INJ. ANGLE DISCHARGE COEFF. NUMBER OF HOLES TRANSVERSE ANGLE
 (285) .39.000000 (286) .469990 (287) 40.000000 (288) 0.000000

OXIDIZER HOLES

HOLE DIAMETER (290) 0.000000 (291) 0.000000 (292) 0.000000 (293) 0.000000
 RADIAL INJ. ANGLE DISCHARGE COEFF. NUMBER OF HOLES TRANSVERSE ANGLE
 (294) 0.000000 (295) 0.000000 (296) 0.000000 (297) 0.000000

COMBUSTION CHAMBER PROFILE

INJECTOR LOCATION	INJECTOR DIAMETER	AXIAL LOC. 2	CHAMBER DIAM. 2
(302)	0.00000 (306)	2.13000 (309)	1.50000 (300)
AXIAL LOC. 3	CHAMBER DIAM. 3	AXIAL LOC. 4	CHAMBER DIAM. 4
(303)	1.40000 (302)	3.00000 (303)	1.00000 (304)
AXIAL LOC. 5	CHAMBER DIAM. 5	AXIAL LOC. 6	CHAMBER DIAM. 6
(305)	2.14000 (304)	2.40000 (307)	2.70000 (308)
AXIAL LOC. 7	CHAMBER DIAM. 7	THROAT PLANE	THROAT DIAM.
(304)	2.00000 (301)	1.40000 (301)	3.12000 (302)

INPUT UNITS ARE INCHES, PSIA, SECONDS AND DEGREES KELVIN.
PROPELLANT PROPERTIES ARE IN GRAMS/GC, POISE, DYNE/CM,

DERIVED FUEL PROPERTIES

REDUCED TEMP., TEMPERATURE LJO, ENTHALPY HAP, ENTHALPY HAPOR, PRESSURE LJO, DENSITY VISCOSITY SURFACE TENSION

.30000	170.20000	122.95000	349.00000	.000001	.994670	.200013	70.710009
.32500	193.05000	133.20450	359.70475	.000020	.980697	.127197	72.494632
.35000	207.00000	145.48000	374.36000	.000321	.966715	.003407	68.440005
.37500	222.75000	221.19750	309.33625	.002316	.992733	.056420	64.972200
.40000	237.00000	231.44000	404.11200	.011017	.930751	.039199	60.009205
.42500	252.45000	241.60000	418.82750	.046307	.914270	.027246	57.320006
.45000	267.30000	251.93700	433.00300	.140632	.910708	.020032	53.930744
.47500	282.15000	262.10350	448.43025	.409244	.896806	.014739	50.004609
.50000	287.00000	272.43000	463.21000	.070306	.883025	.011014	47.604346
.52500	311.05000	282.67650	477.99075	2.000199	.868043	.008346	44.661300
.55000	326.70000	292.92300	492.76050	4.119665	.854061	.006400	41.095200
.57500	341.55000	303.16000	507.54225	7.560374	.840078	.004078	38.103300
.60000	356.40000	313.41000	522.31000	12.990590	.826090	.003009	36.641594
.62500	371.25000	323.66250	537.09375	21.203941	.812016	.003433	34.225506
.65000	386.10000	333.91000	551.86500	33.044466	.798034	.003034	31.800010
.67500	400.95000	344.15550	566.64250	49.557001	.784093	.002094	29.753691
.70000	415.80000	354.40200	581.42100	71.756147	.770971	.002402	27.607749
.72500	430.65000	364.64850	596.19475	106.700007	.756880	.002151	25.330005
.75000	445.50000	374.89500	610.97250	137.806477	.743007	.001933	23.005000
.77500	460.35000	385.14150	625.74025	184.149020	.729026	.001743	22.130009
.80000	475.20000	395.38800	640.52000	246.836511	.715044	.001577	20.402037
.82500	490.05000	405.63450	655.29075	309.005094	.697602	.001432	18.443619
.85000	504.90000	415.88100	670.07500	390.000007	.670221	.001303	16.150055
.87500	519.75000	426.12750	684.85125	484.454474	.640435	.001100	13.327447
.90000	534.60000	436.37400	699.62700	594.000405	.624008	.001000	10.011953
.92500	549.45000	446.62050	714.40275	716.959165	.596626	.000990	6.619009
.95000	564.30000	456.86700	729.17850	861.315075	.550031	.000910	3.443114
.97500	579.15000	467.11350	743.95425	1118.700321	.470167	.000046	1.020307
1.00000	594.00000	477.36000	758.73000	1195.000000	.292011	.000000	.000000

DERIVED OXID PROPERTIES

REDUCED TEMP., TEMPERATURE LIO, SATURATE VAPOR PRESSURE LIO, DENSITY VISCOSITY SURFACE TENSION

.30000	129.30000	46.54000	194.95940	.00000	1.065399	.365590	76.096121
.32500	140.07500	50.42700	198.17030	.00000	1.039170	.232006	72.473074
.35000	150.85000	54.30600	201.34300	.00000	1.013087	.183306	68.480408
.37500	161.62500	58.18500	204.59220	.00000	1.786736	.102920	64.554710
.40000	172.40000	62.06400	207.80320	.00000	1.760515	.071334	60.047056
.42500	183.17500	65.94300	211.01410	.00000	1.734304	.000593	57.308003
.45000	193.95000	69.82200	214.22510	.003206	1.708073	.036530	53.915301
.47500	204.72500	73.70100	217.43650	.012072	1.681852	.026077	50.000003
.50000	215.50000	77.58000	220.64700	.043714	1.655631	.020084	47.508215
.52500	226.27500	81.45900	223.85790	.129195	1.629410	.015223	44.648592
.55000	237.05000	85.33800	227.06890	.339045	1.603189	.011600	41.043223
.57500	247.82500	89.21700	230.27950	.68836	1.576968	.008000	38.138638
.60000	258.60000	93.09600	233.49000	1.774303	1.550747	.007130	36.631102
.62500	269.37500	96.97500	236.70170	3.614636	1.524526	.006261	34.219709
.65000	280.15000	100.85400	239.91270	6.914437	1.498305	.005333	31.821776
.67500	290.92500	104.73300	243.12390	12.519297	1.472084	.004913	29.749171
.70000	301.70000	108.61200	246.33400	21.999537	1.445863	.004381	27.081020
.72500	312.47500	112.49100	249.54400	36.51346	1.419642	.003803	25.707700
.75000	323.25000	116.37000	252.75400	54.052766	1.393421	.003525	23.070960
.77500	334.02500	119.24900	255.96450	87.511463	1.367200	.003100	22.131669
.80000	344.80000	123.12800	259.17450	136.504800	1.340979	.002677	20.408070
.82500	355.57500	127.00700	262.38450	189.908223	1.314758	.002611	18.436334
.85000	366.35000	130.88600	265.59450	269.490397	1.271923	.002377	16.145430
.87500	377.12500	134.76500	268.80450	378.848000	1.228084	.002040	13.823625
.90000	387.90000	138.64400	272.01450	508.479000	1.184003	.001909	10.009006
.92500	398.67500	142.52300	275.22450	678.929705	1.138147	.001821	6.017793
.95000	409.45000	146.40200	278.43450	891.490000	1.090007	.001674	3.408100
.97500	420.22500	150.28100	281.64450	1152.030000	.001741	.001543	1.029092
1.00000	431.00000	154.16000	284.85450	1478.000000	.001712	.000000	.000000

PUT DIFF VALUES

LINE AREA	INJECTION AREA	RESTRICTOR AREA	VENTURI AREA	VALVE PORT AREA	L'INE RESISTANCE INJ.	RESISTANCES LENGTH/AREA
1.24083	1.124405E+02	1.143200E+02	1.24083	1.150000E+02	1.70164	597.200
						100.751

OXID SIZE VALUES

LINE AREA	INJECTION AREA	RESTRICTOR AREA	VENTURI AREA	VALVE PORT AREA	LINE RESISTANCE INJ.	RESISTANCE LENGTH/AREA
.120923	1.362044E+02	1.620920E+02	.120923	1.708000E+02	94.1115	127.894
						303.277

RING 1

FUEL INJ. AREA	PERCENT FUEL	OXID. INJ. AREA	PERCENT OXID.	AXIAL INJ. PT.	AXIAL INJ. DIST.
2.769287E+03	24.4175	4.080485E+03	30.0048	5.194819E+02	475783

2

FUEL INJ. AREA	PERCENT FUEL	OXID INJ. AREA	PERCENT OXID	AXIAL INP. PT.	RADIAL IMP. PT.
4.334324E-03	35.5879	9.537905E-03	68.9982	5.459425E-03	1.324951

3 AUG 53

FUEL INJ. AREA	PERCENT FUEL	OXID INJ. AREA	PERCENT OXID	AXIAL IMP. PT.	RADIAL IMP. P.T.
4.33500E-03	39.9949	0.	0.	3.14000	.677000

CHAMBER DESCRIPTION

STATION	DISTANCE	DIAMETER	AREA	UPPER CASE VOLUME	FUEL ON WALL	OXYD ON WALL	WALL TEMPERATURE
1	0.00000000	2.4000000	4.63769733	0.00000000	0.00000000	0.00000000	294.00000000
2	0.31460000	2.4000000	4.63769733	0.00000000	0.00000000	0.00000000	294.00000000
3	0.62920000	2.4000000	4.63769733	0.00000000	0.00000000	0.00000000	294.00000000
4	0.94380000	2.4000000	4.63769733	0.00000000	0.00000000	0.00000000	294.00000000
5	1.25840000	2.4000000	4.63769733	0.00000000	0.00000000	0.00000000	294.00000000
6	1.57300000	2.4000000	4.63769733	0.00000000	0.00000000	0.00000000	294.00000000
7	1.88760000	2.4000000	4.63769733	0.00000000	0.00000000	0.00000000	294.00000000
8	2.20220000	2.4000000	4.63769733	0.00000000	0.00000000	0.00000000	294.00000000
9	2.51680000	2.4000000	4.63769733	0.00000000	0.00000000	0.00000000	294.00000000
10	2.83140000	2.4000000	4.63769733	0.00000000	0.00000000	0.00000000	294.00000000
11	3.14600000	2.4000000	4.63769733	0.00000000	0.00000000	0.00000000	294.00000000
12	3.46060000	2.4000000	4.63769733	0.00000000	0.00000000	0.00000000	294.00000000
13	3.77520000	2.4000000	4.63769733	0.00000000	0.00000000	0.00000000	294.00000000
14	4.08980000	2.4000000	4.63769733	0.00000000	0.00000000	0.00000000	294.00000000
15	4.40440000	2.4000000	4.63769733	0.00000000	0.00000000	0.00000000	294.00000000
16	4.71900000	2.4000000	4.63769733	0.00000000	0.00000000	0.00000000	294.00000000
17	5.03360000	2.4000000	4.63769733	0.00000000	0.00000000	0.00000000	294.00000000
18	5.34820000	2.4000000	4.63769733	0.00000000	0.00000000	0.00000000	294.00000000
19	5.66280000	2.4000000	4.63769733	0.00000000	0.00000000	0.00000000	294.00000000
20	5.97740000	2.4000000	4.63769733	0.00000000	0.00000000	0.00000000	294.00000000
21	6.29200000	2.4000000	4.63769733	0.00000000	0.00000000	0.00000000	294.00000000
22	6.60660000	2.4000000	4.63769733	0.00000000	0.00000000	0.00000000	294.00000000
23	6.92120000	2.4000000	4.63769733	0.00000000	0.00000000	0.00000000	294.00000000
24	7.23580000	2.4000000	4.63769733	0.00000000	0.00000000	0.00000000	294.00000000
25	7.55040000	2.4000000	4.63769733	0.00000000	0.00000000	0.00000000	294.00000000
26	7.86500000	2.4000000	4.63769733	0.00000000	0.00000000	0.00000000	294.00000000
27	8.17960000	2.4000000	4.63769733	0.00000000	0.00000000	0.00000000	294.00000000
28	8.49420000	2.4000000	4.63769733	0.00000000	0.00000000	0.00000000	294.00000000
29	8.80880000	2.4000000	4.63769733	0.00000000	0.00000000	0.00000000	294.00000000
30	9.12340000	2.4000000	4.63769733	0.00000000	0.00000000	0.00000000	294.00000000
31	9.43800000	2.4000000	4.63769733	0.00000000	0.00000000	0.00000000	294.00000000
32	9.75260000	2.4000000	4.63769733	0.00000000	0.00000000	0.00000000	294.00000000
33	10.06720000	2.4000000	4.63769733	0.00000000	0.00000000	0.00000000	294.00000000
34	10.38180000	2.4000000	4.63769733	0.00000000	0.00000000	0.00000000	294.00000000
35	10.69640000	2.4000000	4.63769733	0.00000000	0.00000000	0.00000000	294.00000000
36	11.01100000	2.4000000	4.63769733	0.00000000	0.00000000	0.00000000	294.00000000
37	11.32560000	2.4000000	4.63769733	0.00000000	0.00000000	0.00000000	294.00000000
38	11.64020000	2.4000000	4.63769733	0.00000000	0.00000000	0.00000000	294.00000000
39	11.95480000	2.4000000	4.63769733	0.00000000	0.00000000	0.00000000	294.00000000
40	12.26940000	2.4000000	4.63769733	0.00000000	0.00000000	0.00000000	294.00000000
41	12.58400000	2.4000000	4.63769733	0.00000000	0.00000000	0.00000000	294.00000000
42	12.89860000	2.4000000	4.63769733	0.00000000	0.00000000	0.00000000	294.00000000
43	13.21320000	2.4000000	4.63769733	0.00000000	0.00000000	0.00000000	294.00000000
44	13.52780000	2.4000000	4.63769733	0.00000000	0.00000000	0.00000000	294.00000000
45	13.84240000	2.4000000	4.63769733	0.00000000	0.00000000	0.00000000	294.00000000
46	14.15700000	2.4000000	4.63769733	0.00000000	0.00000000	0.00000000	294.00000000
47	14.47160000	2.4000000	4.63769733	0.00000000	0.00000000	0.00000000	294.00000000
48	14.78620000	2.4000000	4.63769733	0.00000000	0.00000000	0.00000000	294.00000000
49	15.10080000	2.4000000	4.63769733	0.00000000	0.00000000	0.00000000	294.00000000
50	15.41540000	2.4000000	4.63769733	0.00000000	0.00000000	0.00000000	294.00000000
51	15.73000000	2.4000000	4.63769733	0.00000000	0.00000000	0.00000000	294.00000000
52	16.04460000	2.4000000	4.63769733	0.00000000	0.00000000	0.00000000	294.00000000
53	16.35920000	2.4000000	4.63769733	0.00000000	0.00000000	0.00000000	294.00000000
54	16.67380000	2.4000000	4.63769733	0.00000000	0.00000000	0.00000000	294.00000000
55	16.98840000	2.4000000	4.63769733	0.00000000	0.00000000	0.00000000	294.00000000
56	17.30300000	2.4000000	4.63769733	0.00000000	0.00000000	0.00000000	294.00000000
57	17.61760000	2.4000000	4.63769733	0.00000000	0.00000000	0.00000000	294.00000000
58	17.93220000	2.4000000	4.63769733	0.00000000	0.00000000	0.00000000	294.00000000
59	18.24680000	2.4000000	4.63769733	0.00000000	0.00000000	0.00000000	294.00000000
60	18.56140000	2.4000000	4.63769733	0.00000000	0.00000000	0.00000000	294.00000000

61	1.88480000	2.08444444	5.65974886	12.6592409	0.00000000	294.00000000
62	1.91940000	2.64595956	5.51308837	12.78494312	0.00000000	294.00000000
63	1.94480000	2.41666667	5.36838881	12.88888889	0.00000000	294.00000000
64	1.97200000	2.57977778	5.22782346	13.12315892	0.00000000	294.00000000
65	2.00960000	2.50480000	5.08459905	13.28497779	0.00000000	294.00000000
66	2.04160000	2.18888889	4.91333333	13.44444444	0.00000000	294.00000000
67	2.07400000	2.47611111	4.81148631	13.59483764	0.00000000	294.00000000
68	2.10380000	2.44022222	4.67679790	13.74370070	0.00000000	294.00000000
69	2.13320000	2.48533333	4.54444444	13.88888889	0.00000000	294.00000000
70	2.16660000	2.34254400	4.3088189	14.02768125	0.00000000	294.00000000
71	2.19880000	2.27472000	4.06392550	14.15925112	0.00000000	294.00000000
72	2.23400000	2.20480000	3.88538888	14.33300443	0.00000000	294.00000000
73	2.26880000	2.13087200	3.59307041	14.39934980	0.00000000	294.00000000
74	2.29220000	2.07124000	3.36941154	14.5085979	0.00000000	294.00000000
75	2.32360000	2.08324000	3.18535048	14.6123367	0.00000000	294.00000000
76	2.35980000	1.93560000	2.94253123	14.70880453	0.00000000	294.00000000
77	2.38640000	1.86776000	2.73992980	14.79609026	0.00000000	294.00000000
78	2.43280000	1.43424000	3.6435314	14.86444432	0.00000000	294.00000000
79	2.44920000	1.89533000	2.5686663	14.98218490	0.00000000	294.00000000
80	2.48660000	1.77664000	2.47909196	15.04122097	0.00000000	294.00000000
81	2.53280000	1.74874000	2.38812815	15.13786559	0.00000000	294.00000000
82	2.54340000	1.71872000	2.3207319	15.19180993	0.00000000	294.00000000
83	2.57860000	1.68994000	2.24313300	15.28354515	0.00000000	294.00000000
84	2.60420000	1.66084000	2.16318121	15.33737941	0.00000000	294.00000000
85	2.63760000	1.53220000	2.09238144	15.39652206	0.00000000	294.00000000
86	2.65800000	1.48532000	2.01897190	15.46119768	0.00000000	294.00000000
87	2.70840000	1.37443200	1.84433322	15.53644802	0.00000000	294.00000000
88	2.73580000	1.54544000	1.87488539	15.58475964	0.00000000	294.00000000
89	2.76320000	1.51656000	1.85688842	15.64220998	0.00000000	294.00000000
90	2.78460000	1.48734000	1.73844336	15.6888332	0.00000000	294.00000000
91	2.82580000	1.45800000	1.67156704	15.73477779	0.00000000	294.00000000
92	2.85745000	1.42999200	1.60484264	15.80493315	0.00000000	294.00000000
93	2.88880000	1.40134000	1.54140008	15.86438888	0.00000000	294.00000000
94	2.92020000	1.39443200	1.5278452	15.90250471	0.00000000	294.00000000
95	2.95160000	1.38169560	1.51459556	15.95225999	0.00000000	294.00000000
96	2.98300000	1.38169560	1.50432001	15.98761835	0.00000000	294.00000000
97	3.01440000	1.37711840	1.48835495	16.0458472	0.00000000	294.00000000
98	3.04580000	1.37133280	1.47696329	16.09115972	0.00000000	294.00000000
99	3.07720000	1.36555520	1.46456407	16.13333842	0.00000000	294.00000000
100	3.10860000	1.35977760	1.45219728	16.18313286	0.00000000	294.00000000
101	3.14000000	1.35400000	1.43988293	16.22853836	0.00000000	294.00000000

THE CALCULATED RUN PARAMETERS ARE PRINTED FOR EACH INTERVAL OF TIME FOLLOWING START

TIME MILLISEC	CHAMBER PRESS	IGNITION	FUEL FRACTION	CHAMBER TEMP K	POL WT.	GAMMA	CF VAC
0.	1.00000E+06	0.	0.	204.000	46.0000	1.16944	2.09230
FUEL INJ RATE	OXID INJ RATE	FUEL FLOW RATE	OXID FLOW RATE	FUEL VOID VOL	OXID VOID VOL	FUEL INJ TEMP	OXID INJ TEMP
0.	0.	0.	0.	1.00000E+02	1.00000E+02	0.	0.
FUEL DROP BURN	OXID DROP BURN	FUEL FLASH RATE	OXID FLASH RATE	FUEL WALL BURN	OXID WALL BURN	FUEL WALL EVAP	OXID WALL EVAP
0.	0.	0.	0.	0.	0.	0.	0.
FUEL GAS PASS	OXID GAS PASS	FUEL DROPLETS	OXID DROPLETS	FUEL STREAMS	OXID STREAMS	FUEL ON WALL	OXID ON WALL
0.	7.14341E+11	0.	0.	0.	0.	0.	0.
FUEL GAS EFFLUX	OXID GAS EFFLUX	FUEL DROP RATE	OXID DROP RATE	FUEL FILM RATE	OXID FILM RATE	GAS FRACTION	VAC THRUST LBF
0.	0.	0.	0.	0.	0.	1.00000	0.
FUEL DROP D32	OXID DROP D32	FUEL INJ. VEL.	OXID INJ. VEL.	MAX. EXPLOSION PRESS OUT OF TANK	INTEGRAL PCODY	TOTAL IMPULSE	
0.	0.	0.	0.	0.	0.	0.	0.

FUEL GRAMS	OXID GRAMS	TOTAL GRAMS	INJECTED PASS	GAS EXPELLED	DROPS EXPELLED	WALL EXPELLED	GAS RETAINED	DROPS RETAINED	WALL RETAINED
0.0000000	0.0000000	0.0000000	0.0000000	0.0000000	0.0000000	0.0000000	0.0000000	0.0000000	0.0000000
0.0000000	0.0000000	0.0000000	0.0000000	0.0000000	0.0000000	0.0000000	0.0000000	0.0000000	0.0000000
SUM N	SUM D	SUM D SOLARED	SUM D CURED	SUM D	SUM D	SUM D	SUM D	SUM D	TOTAL MOMENTUM
0.	0.	0.	0.	0.	0.	0.	0.	0.	0.
FUEL DROPS INJECTED	OXID DROPS INJECTED	OXID DROPS EJECTED	0.	0.	0.	0.	0.	0.	0.
0.	0.	0.	0.	0.	0.	0.	0.	0.	0.

TIME MILLISEC	CHAMBER PRESS	IGNITION	FUEL FRACTION	CHAMBER TEMP K	POL WT.	GAMMA	CF VAC
0.20000	1.28978E+02	0.	0.143105	242.000	46.0072	2.12247	1.02383
FUEL INJ RATE	OXID INJ RATE	FUEL FLOW RATE	OXID FLOW RATE	FUEL VOID VOL	OXID VOID VOL	FUEL INJ TEMP	OXID INJ TEMP
1.00431E+03	1.00431E+03	0.00431E+03	0.00431E+03	0.00000E+00	0.00000E+00	204.000	204.000
FUEL DROP BURN	OXID DROP BURN	FUEL FLASH RATE	OXID FLASH RATE	FUEL WALL BURN	OXID WALL BURN	FUEL WALL EVAP	OXID WALL EVAP
0.	0.	0.00000E+00	0.00000E+00	0.	0.	0.	0.
FUEL GAS PASS	OXID GAS PASS	FUEL DROPLETS	OXID DROPLETS	FUEL STREAMS	OXID STREAMS	FUEL ON WALL	OXID ON WALL
0.00000E+00	0.00000E+00	0.00000E+00	0.00000E+00	0.	0.	0.	0.
FUEL GAS EFFLUX	OXID GAS EFFLUX	FUEL DROP RATE	OXID DROP RATE	FUEL FILM RATE	OXID FILM RATE	GAS FRACTION	VAC THRUST LBF
0.	0.	0.	0.	0.	0.	1.00000	0.
FUEL DROP D32	OXID DROP D32	FUEL INJ. VEL.	OXID INJ. VEL.	MAX. EXPLOSION PRESS OUT OF TANK	INTEGRAL PCODY	TOTAL IMPULSE	
0.00431	0.00431	0.00000	0.00000	0.00000E+00	0.00000E+00	0.	0.

TIME MILLISEC	CHAMBER PRESS	IGNITION	FUEL FRACTION	CHAMBER TEMP K	POL WT.	GAMMA	CF VAC
0.40000	5.12000E+02	0.	0.154770	294.200	46.0156	1.18003	1.00700

FUEL INJ RATE	OXID INJ RATE	FUEL FLOW RATE	OXID FLOW RATE	FUEL VOID VOL	OXID VOID VOL	FUEL INJ TEMP	OXID INJ TEMP
7.93995E-03	.110673	.127594	.127576	8.060621E-03	9.907373E-03	294.000	294.000
FUEL DROP BURN	OXID DROP BURN	FUEL FLASH RATE	OXID FLASH RATE	FUEL WALL BURN	OXID WALL BURN	FUEL WALL EVAP	OXID WALL EVAP
0.	0.	1.500467E-03	1.305194E-02	0.	0.	0.	0.
FUEL GAS PASS	OXID GAS PASS	FUEL DROPLETS	OXID DROPLETS	FUEL STREAMS	OXID STREAMS	FUEL ON WALL	OXID ON WALL
5.172141E-07	3.000317E-06	1.739264E-06	3.130992E-05	0.	0.	0.	0.
FUEL GAS EFFLUX	OXID GAS EFFLUX	FUEL DROP RATE	OXID DROP RATE	FUEL FILM RATE	OXID FILM RATE	GAS FRACTION	VAC THRUST LBF
1.050000E-04	6.500036E-04	0.	0.	0.	0.	1.00000	.149079
FUEL DROP D32	OXID DROP D32	FUEL INJ. VEL.	OXID INJ. VEL.	MAX. EXPLOSION	PASS OUT OF TANK	INTEGRAL PCODY	TOTAL IMPULSE
59.4369	34.4300	1.73247	13.0314	2.98693	7.522610E-05	1.302129E-05	2.1913970E-05

TIME MILLISEC	CHAMBER PRESS	IGNITION	FUEL FRACTION	CHAMBER TEMP K	POL HT.	GAMMA	CF VAC
.000000	9.037520E-02	0.	9.742290E-02	297.004	46.0144	1.13377	3.96179
FUEL INJ RATE	OXID INJ RATE	FUEL FLOW RATE	OXID FLOW RATE	FUEL VOID VOL	OXID VOID VOL	FUEL INJ TEMP	OXID INJ TEMP
1.304095E-02	.172605	.106206	.133921	7.774794E-03	9.940012E-03	294.000	294.000
FUEL DROP BURN	OXID DROP BURN	FUEL FLASH RATE	OXID FLASH RATE	FUEL WALL BURN	OXID WALL BURN	FUEL WALL EVAP	OXID WALL EVAP
0.	0.	1.733415E-03	1.969020E-02	0.	0.	0.	0.
FUEL GAS PASS	OXID GAS PASS	FUEL DROPLETS	OXID DROPLETS	FUEL STREAMS	OXID STREAMS	FUEL ON WALL	OXID ON WALL
8.107709E-07	7.548400E-06	3.597070E-06	6.297277E-05	0.	0.	0.	0.
FUEL GAS EFFLUX	OXID GAS EFFLUX	FUEL DROP RATE	OXID DROP RATE	FUEL FILM RATE	OXID FILM RATE	GAS FRACTION	VAC THRUST LBF
2.496312E-04	1.094575E-03	0.	0.	0.	0.	1.00000	.272236
FUEL DROP D32	OXID DROP D32	FUEL INJ. VEL.	OXID INJ. VEL.	MAX. EXPLOSION	PASS OUT OF TANK	INTEGRAL PCODY	TOTAL IMPULSE
59.4369	34.4300	2.53693	19.9492	5.05302	1.491094E-04	3.309633E-05	8.1346873E-05

TIME MILLISEC	CHAMBER PRESS	IGNITION	FUEL FRACTION	CHAMBER TEMP K	POL HT.	GAMMA	CF VAC
.000000	1.149430	0.	8.338025E-02	265.414	46.0133	1.13300	3.90414
FUEL INJ RATE	OXID INJ RATE	FUEL FLOW RATE	OXID FLOW RATE	FUEL VOID VOL	OXID VOID VOL	FUEL INJ TEMP	OXID INJ TEMP
1.324405E-03	.137806	.345000	.343030	8.344495E-03	9.844938E-03	294.000	294.000
FUEL DROP BURN	OXID DROP BURN	FUEL FLASH RATE	OXID FLASH RATE	FUEL WALL BURN	OXID WALL BURN	FUEL WALL EVAP	OXID WALL EVAP
0.	0.	0.	2.425405E-02	0.	0.	1.491094E-04	0.
FUEL GAS PASS	OXID GAS PASS	FUEL DROPLETS	OXID DROPLETS	FUEL STREAMS	OXID STREAMS	FUEL ON WALL	OXID ON WALL
1.020613E-04	1.173435E-05	3.200320E-04	1.000215E-04	2.040024E-06	0.	5.945370E-00	0.
FUEL GAS EFFLUX	OXID GAS EFFLUX	FUEL DROP RATE	OXID DROP RATE	FUEL FILM RATE	OXID FILM RATE	GAS FRACTION	VAC THRUST LBF
1.022742E-04	1.415707E-03	0.	0.	0.	0.	1.00000	.149079
FUEL DROP D32	OXID DROP D32	FUEL INJ. VEL.	OXID INJ. VEL.	MAX. EXPLOSION	PASS OUT OF TANK	INTEGRAL PCODY	TOTAL IMPULSE
59.4369	34.4300	1.73247	13.0314	2.98693	7.522610E-05	1.302129E-05	2.1913970E-05
IGNITE AT 1.00 MILLISECONDS							

TIME MILLISEC	CHAMBER PRESS	IGNITION	FUEL FRACTION	CHAMBER TEMP K	POL HT.	GAMMA	CF VAC
1.000000	3.76761	1.00000	9.917699E-02	2000.16	28.0317	1.24093	1.00300
FUEL INJ RATE	OXID INJ RATE	FUEL FLOW RATE	OXID FLOW RATE	FUEL VOID VOL	OXID VOID VOL	FUEL INJ TEMP	OXID INJ TEMP
1.707707E-02	.251040	.297201	.303762	4.594520E-03	9.647782E-03	294.000	294.000
FUEL DROP BURN	OXID DROP BURN	FUEL FLASH RATE	OXID FLASH RATE	FUEL WALL BURN	OXID WALL BURN	FUEL WALL EVAP	OXID WALL EVAP
0.	0.	0.	0.	0.	0.	0.	0.

7.730370E-03	3.299709E-02	0.	2.072920E-02	0.	0.	2.759505E-04	0.
FUEL GAS MASS	OXID GAS MASS	FUEL DROPLETS	OXID DROPLETS	FUEL STREAMS	OXID STREAMS	FUEL ON WALL	OXID ON WALL
2.530400E-06	2.299303E-09	1.704990E-06	1.590449E-04	0.264390E-06	0.	0.	0.
FUEL GAS EFFLUX	OXID GAS EFFLUX	FUEL DROP RATE	OXID DROP RATE	FUEL FILM RATE	OXID FILM RATE	GAS FRACTION	VAC THRUST LBF
4.909654E-04	5.009008E-03	0.	0.	0.	0.	1.00000	9.03730
FUEL DROP D32	OXID DROP D32	FUEL INJ. VEL.	OXID INJ. VEL.	MAX. EXPLOSION	PASS OUT OF TANK	INTEGRAL PC-DT	TOTAL IMPULSE
55.4369	34.4300	3.92173	29.1070	13.9555	3.667376E-04	8.205442E-04	2.135230E-03

TIME MILLISEC	CHAMBER PRESS	IGNITION	FUEL FRACTION	CHAMBER TEMP K	POL WT.	GAMMA	CF VAC
1.20000	3.01430	0.00000	2.280645E-02	752.203	42.0726	1.14071	1.00030
FUEL INJ RATE	OXID INJ RATE	FUEL FLOW RATE	OXID FLOW RATE	FUEL VOID VOL	OXID VOID VOL	FUEL INJ TEMP	OXID INJ TEMP
2.033408E-03	2.62790	3.48270	3.03000	3.430095E-03	3.270895E-03	294.002	294.002
FUEL DROP BURN	OXID DROP BURN	FUEL FLASH RATE	OXID FLASH RATE	FUEL WALL BURN	OXID WALL BURN	FUEL WALL EVAP	OXID WALL EVAP
4.441849E-03	4.475352	0.	0.	4.050420E-08	0.	0.	0.
FUEL GAS PASS	OXID GAS PASS	FUEL DROPLETS	OXID DROPLETS	FUEL STREAMS	OXID STREAMS	FUEL ON WALL	OXID ON WALL
2.020005E-04	1.603125E-04	0.003043E-07	4.024095E-08	0.020034E-06	5.000095E-06	1.700000E-07	0.
FUEL GAS EFFLUX	OXID GAS EFFLUX	FUEL DROP RATE	OXID DROP RATE	FUEL FILM RATE	OXID FILM RATE	GAS FRACTION	VAC THRUST LBF
4.004826E-03	4.001484E-02	0.	0.	0.	0.	1.00000	10.00000
FUEL DROP D32	OXID DROP D32	FUEL INJ. VEL.	OXID INJ. VEL.	MAX. EXPLOSION	PASS OUT OF TANK	INTEGRAL PC-DT	TOTAL IMPULSE
44.7094	33.8507	4.00434	30.3238	23.4432	0.000114E-04	1.402400E-03	4.020300E-03

FUEL MANIFOLD FILLS AT 1.40 MILLISECONDE

TIME MILLISEC	CHAMBER PRESS	IGNITION	FUEL FRACTION	CHAMBER TEMP K	POL WT.	GAMMA	CF VAC
2.40000	4.26377	1.00000	2.272097E-02	891.029	42.2601	1.14024	1.00707
FUEL INJ RATE	OXID INJ RATE	FUEL FLOW RATE	OXID FLOW RATE	FUEL VOID VOL	OXID VOID VOL	FUEL INJ TEMP	OXID INJ TEMP
0.032550E-03	0.270109	0.390529	0.17904	0.	0.713301E-03	294.002	294.002
FUEL DROP BURN	OXID DROP BURN	FUEL FLASH RATE	OXID FLASH RATE	FUEL WALL BURN	OXID WALL BURN	FUEL WALL EVAP	OXID WALL EVAP
2.031921E-03	0.152171	0.	0.	1.270710E-04	3.390903E-04	0.	9.794031E-03
FUEL GAS MASS	OXID GAS MASS	FUEL DROPLETS	OXID DROPLETS	FUEL STREAMS	OXID STREAMS	FUEL ON WALL	OXID ON WALL
2.751795E-06	1.230305E-04	0.	9.005240E-06	0.197534E-06	1.065973E-04	1.524940E-07	1.000790E-06
FUEL GAS EFFLUX	OXID GAS EFFLUX	FUEL DROP RATE	OXID DROP RATE	FUEL FILM RATE	OXID FILM RATE	GAS FRACTION	VAC THRUST LBF
2.130542E-03	9.193007E-02	0.	0.	0.	0.	1.00000	10.00000
FUEL DROP D32	OXID DROP D32	FUEL INJ. VEL.	OXID INJ. VEL.	MAX. EXPLOSION	PASS OUT OF TANK	INTEGRAL PC-DT	TOTAL IMPULSE
32.0361	23.1105	1.50009	31.2270	14.7074	0.717107E-04	2.000170E-03	0.000014E-03

EXTINGUISH AT 3.40 MILLISECONDE

TIME MILLISEC	CHAMBER PRESS	IGNITION	FUEL FRACTION	CHAMBER TEMP K	POL WT.	GAMMA	CF VAC
1.00000	3.41003	0.	1.001301E-02	697.243	46.0093	1.10072	1.00754
FUEL INJ RATE	OXID INJ RATE	FUEL FLOW RATE	OXID FLOW RATE	FUEL VOID VOL	OXID VOID VOL	FUEL INJ TEMP	OXID INJ TEMP
0.020051	0.274010	0.400052	0.470733	0.	7.960002E-03	294.002	294.002
FUEL DROP BURN	OXID DROP BURN	FUEL FLASH RATE	OXID FLASH RATE	FUEL WALL BURN	OXID WALL BURN	FUEL WALL EVAP	OXID WALL EVAP
0.	0.644002E-02	0.	0.	3.160996E-05	9.400036E-04	0.	9.000000E-03

7

FUEL GAS MASS	OXID GAS MASS	FUEL DROPLETS	OXID DROPLETS	FUEL STREAMS	OXID STREAMS	FUEL ON WALL	OXID ON WALL
2.30924E-04	1.14933E-04	0.408402E-09	0.	2.902370E-09	1.61392E-04	1.461617E-07	1.039008E-06
FUEL GAS EFFLUX	OXID GAS EFFLUX	FUEL DROPLETS	OXID DROPLETS	FUEL FILM RATE	OXID FILM RATE	GAS FRACTION	VAC THRUST LBF
2.26301E-03	.101923	0.	0.	0.	0.	1.00000	9.40073
FUEL DROP D32	OXID DROP D32	FUEL INJ. VEL.	OXID INJ. VEL.	MAX. EXPLOSION PASS OUT OF TANK	INTEGRAL PCODY	TOTAL IMPULS	
0.	14.4001	97.8423	31.0694	101.298	8.10732E-04	3.139942E-03	0.980108E-03
TIME MILLISEC	CHAMBER PRESS	IGNITION	FUEL FRACTION	CHAMBER TEMP K	VOL WT.	GAMMA	CF VAC
1.00000	2.00040	0.	1.90218E-02	694.768	46.0093	1.10073	1.02713
FUEL INJ RATE	OXID INJ RATE	FUEL FLOW RATE	OXID FLOW RATE	FUEL VOID VOL	OXID VOID VOL	FUEL INJ TEMP	OXID INJ TEMP
.49099	.20020	.490992	.521764	0.	7.096764E-03	204.002	204.002
FUEL DROP BURN	OXID DROP BURN	FUEL FLASH RATE	OXID FLASH RATE	FUEL WALL BURN	OXID WALL BURN	FUEL WALL EVAP	OXID WALL EVAP
0.	0.	0.	0.	2.132779E-05	3.930207E-05	0.	1.205307E-03
FUEL GAS MASS	OXID GAS MASS	FUEL DROPLETS	OXID DROPLETS	FUEL STREAMS	OXID STREAMS	FUEL ON WALL	OXID ON WALL
1.99400E-06	9.67264E-05	1.933042E-04	1.073614E-04	3.022102E-05	1.100794E-04	1.410961E-07	7.961430E-07
FUEL GAS EFFLUX	OXID GAS EFFLUX	FUEL DROPLETS	OXID DROPLETS	FUEL FILM RATE	OXID FILM RATE	GAS FRACTION	VAC THRUST LBF
1.778901E-03	8.79221E-02	0.	0.	0.	0.	1.00000	0.81009
FUEL DROP D32	OXID DROP D32	FUEL INJ. VEL.	OXID INJ. VEL.	MAX. EXPLOSION PASS OUT OF TANK	INTEGRAL PCODY	TOTAL IMPULS	
79.7001	0.	103.970	32.3096	199.610	1.049624E-03	3.717637E-03	1.010317E-02
TIME MILLISEC	CHAMBER PRESS	IGNITION	FUEL FRACTION	CHAMBER TEMP K	VOL WT.	GAMMA	CF VAC
2.00000	2.44340	0.	1.92348E-03	681.084	46.0093	1.10074	1.02713
FUEL INJ RATE	OXID INJ RATE	FUEL FLOW RATE	OXID FLOW RATE	FUEL VOID VOL	OXID VOID VOL	FUEL INJ TEMP	OXID INJ TEMP
.426330	.304240	.426340	.320430	0.	5.00440E-03	204.000	204.000
FUEL DROP BURN	OXID DROP BURN	FUEL FLASH RATE	OXID FLASH RATE	FUEL WALL BURN	OXID WALL BURN	FUEL WALL EVAP	OXID WALL EVAP
0.	0.	0.	0.	3.302440E-05	3.404740E-05	0.	3.30230E-03
FUEL GAS MASS	OXID GAS MASS	FUEL DROPLETS	OXID DROPLETS	FUEL STREAMS	OXID STREAMS	FUEL ON WALL	OXID ON WALL
1.48024E-04	8.30230E-05	8.00404E-04	2.37440E-04	8.23534E-05	8.23400E-05	3.73700E-05	3.03280E-05
FUEL GAS EFFLUX	OXID GAS EFFLUX	FUEL DROPLETS	OXID DROPLETS	FUEL FILM RATE	OXID FILM RATE	GAS FRACTION	VAC THRUST LBF
1.30456E-03	7.44790E-02	0.	0.	0.	0.	1.00000	0.70004
FUEL DROP D32	OXID DROP D32	FUEL INJ. VEL.	OXID INJ. VEL.	MAX. EXPLOSION PASS OUT OF TANK	INTEGRAL PCODY	TOTAL IMPULS	
33.7044	52.6756	100.330	33.7448	199.000	1.00440E-03	4.00437E-03	1.149900E-02
INJECTED MASS	GAS EXCELLED	DROPS EXCELLED	MALL EXCELLED	GAS RETAINED	DROPS RETAINED	MALL RETAINED	
FUEL GRAMS	.1201114	.00121925	0.0000000	.00075295	.1109433	.00034461	
OXID GRAMS	.19921271	.03711138	0.0000000	.03732768	.12464299	.00012040	
TOTAL GRAMS	.32233361	.13833063	0.0000000	.03808063	.23558623	.00046501	
FUEL CROPS INJECTED	SUM K	SUM D	SUM D SOLARED	SUP D CURED	TOTAL MOMENTUM		
FUEL CROPS EJECTED	3.04444E-04	9.426213E-03	3.502345E-01	3.754040E-01	8.912470E-02		
OXID CROPS INJECTED	0.	0.	0.	0.	0.		
OXID CROPS EJECTED	9.009707E-06	2.078201E-04	5.763653E-01	2.406875E-01	1.300639E-02		
IGNITE AT	2.20	MILLISECONDS					

V TIME MILLISEC CHAMBER PRESS IGNITION FUEL FRACTION CHAMBER TEMP K VOL WT. GAMMA CF VAC

2.2000	53.8935	1.00000	.363005	3102.41	21.1403	1.22050	1.00043
FUEL INJ RATE	OXID INJ RATE	FUEL FLOW RATE	OXID FLOW RATE	FUEL VOID VOL	OXID VOID VOL	FUEL INJ TEMP	OXID INJ TEMP
.400015	.293132	.400016	.016042	0.	4.76160E-03	294.002	294.002
FUEL DROP BURN	OXID DROP BURN	FUEL FLASH RATE	OXID FLASH RATE	FUEL WALL BURN	OXID WALL BURN	FUEL WALL EVAP	OXID WALL EVAP
.309709	.204112	0.	0.	5.409530E-05	3.292939E-05	0.	1.300073E-03
FUEL GAS MASS	OXID GAS MASS	FUEL DROPLETS	OXID DROPLETS	FUEL STREAMS	OXID STREAMS	FUEL ON WALL	OXID ON WALL
6.339787E-05	1.107667E-04	2.705000E-04	2.339004E-04	0.197334E-06	5.062630E-05	3.520133E-05	0.
FUEL GAS EFFLUX	OXID GAS EFFLUX	FUEL DROP RATE	OXID DROP RATE	FUEL FILM RATE	OXID FILM RATE	GAS FRACTION	VAC THRUST LBT
1.274002E-03	6.310611E-02	0.	0.	0.	0.	1.00000	140.844
FUEL DROP D32	OXID DROP D32	FUEL INJ. VEL.	OXID INJ. VEL.	MAX. EXPLOSION	PASS OUT OF TANK	INTEGRAL PCOST	TOTAL IMPULSE
73.0009	52.4714	312.256	33.8795	230.001	1.475150E-03	1.400500E-02	4.076700E-02

TIME MILLISEC	CHAMBER PRESS	IGNITION	FUEL FRACTION	CHAMBER TEMP K	POL WT.	SANNA	CF VAC
2.0000	61.4300	1.00000	.403104	3030.05	10.7000	0.83000	1.00000
FUEL INJ RATE	OXID INJ RATE	FUEL FLOW RATE	OXID FLOW RATE	FUEL VOID VOL	OXID VOID VOL	FUEL INJ TEMP	OXID INJ TEMP
.400015	.293132	.400016	.016042	0.	4.76160E-03	294.002	294.002
FUEL DROP BURN	OXID DROP BURN	FUEL FLASH RATE	OXID FLASH RATE	FUEL WALL BURN	OXID WALL BURN	FUEL WALL EVAP	OXID WALL EVAP
.309709	.204112	0.	0.	5.409530E-05	3.292939E-05	0.	1.300073E-03
FUEL GAS MASS	OXID GAS MASS	FUEL DROPLETS	OXID DROPLETS	FUEL STREAMS	OXID STREAMS	FUEL ON WALL	OXID ON WALL
6.339787E-05	1.107667E-04	2.705000E-04	2.339004E-04	0.197334E-06	5.062630E-05	3.520133E-05	0.
FUEL GAS EFFLUX	OXID GAS EFFLUX	FUEL DROP RATE	OXID DROP RATE	FUEL FILM RATE	OXID FILM RATE	GAS FRACTION	VAC THRUST LBT
1.274002E-03	6.310611E-02	0.	0.	0.	0.	1.00000	140.844
FUEL DROP D32	OXID DROP D32	FUEL INJ. VEL.	OXID INJ. VEL.	MAX. EXPLOSION	PASS OUT OF TANK	INTEGRAL PCOST	TOTAL IMPULSE
73.0009	52.4714	312.256	33.8795	230.001	1.475150E-03	1.400500E-02	4.076700E-02

TIME MILLISEC	CHAMBER PRESS	IGNITION	FUEL FRACTION	CHAMBER TEMP K	POL WT.	SANNA	CF VAC
2.0000	62.3290	1.00000	.400376	2864.35	10.9910	3.24436	1.03713
FUEL INJ RATE	OXID INJ RATE	FUEL FLOW RATE	OXID FLOW RATE	FUEL VOID VOL	OXID VOID VOL	FUEL INJ TEMP	OXID INJ TEMP
.407900	0.	.407902	.070953	0.	6.041700E-05	294.004	294.004
FUEL DROP BURN	OXID DROP BURN	FUEL FLASH RATE	OXID FLASH RATE	FUEL WALL BURN	OXID WALL BURN	FUEL WALL EVAP	OXID WALL EVAP
.239002	.203435	0.	0.	4.000003E-03	0.	0.	0.
FUEL GAS MASS	OXID GAS MASS	FUEL DROPLETS	OXID DROPLETS	FUEL STREAMS	OXID STREAMS	FUEL ON WALL	OXID ON WALL
0.007150E-05	1.140530E-04	3.410200E-04	1.710900E-04	0.197334E-06	1.000100E-05	0.374037E-05	0.
FUEL GAS EFFLUX	OXID GAS EFFLUX	FUEL DROP RATE	OXID DROP RATE	FUEL FILM RATE	OXID FILM RATE	GAS FRACTION	VAC THRUST LBT
.203514	.301237	0.	0.	0.	0.	1.00000	104.075
FUEL DROP D32	OXID DROP D32	FUEL INJ. VEL.	OXID INJ. VEL.	MAX. EXPLOSION	PASS OUT OF TANK	INTEGRAL PCOST	TOTAL IMPULSE
130.000	71.4440	312.046	0.	100.970	1.030240E-03	3.977000E-02	1.00000
OXID MANIFOLD FILLS AT 2.00 MILLISECONDS							

TIME MILLISEC	CHAMBER PRESS	IGNITION	FUEL FRACTION	CHAMBER TEMP K	POL WT.	SANNA	CF VAC
2.0000	63.0004	1.00000	.407304	2805.72	10.9910	3.24436	1.03713
FUEL INJ RATE	OXID INJ RATE	FUEL FLOW RATE	OXID FLOW RATE	FUEL VOID VOL	OXID VOID VOL	FUEL INJ TEMP	OXID INJ TEMP
.400015	.293132	.400016	.016042	0.	4.76160E-03	294.002	294.002

FUEL DROP BURN	OXID DROP BURN	FUEL FLASH RATE	OXID FLASH RATE	FUEL WALL BURN	OXID WALL BURN	FUEL WALL EVAP	OXID WALL EVAP
33030	37030	0.	0.	0.34300E-03	0.	0.	0.
FUEL GAS PASS	OXID GAS PASS	FUEL DROPLETS	OXID DROPLETS	FUEL STREAMS	OXID STREAMS	FUEL ON WALL	OXID ON WALL
0.00374E-00	0.14033E-00	3.74030E-04	3.73000E-04	0.13400E-04	1.13400E-04	7.00000E-05	0.
FUEL GAS EFFLUX	OXID GAS EFFLUX	FUEL DROP RATE	OXID DROP RATE	FUEL FILM RATE	OXID FILM RATE	GAS FRACTION	VAC THRUST LOP
32300	30030	0.	0.	0.	0.	1.00000	100.000
FUEL DROP D32	OXID DROP D32	FUEL INJ. VEL.	OXID INJ. VEL.	MAX. EXPLOSION	PASS OUT OF TANK	INTEGRAL PC-DT	TOTAL IMPULSE
330.342	02.2133	0.00.200	72.0033	300.000	0.13400E-03	0.00000E-02	1.00000
TIME MILLISEC	CHAMBER PRES	IGNITION	FUEL FRACTION	CHAMBER TEMP K	POL WT.	GAMMA	CF VAC
3.00000	53.3039	1.00000	.92200	2217.73	10.2300	1.27729	1.00000
FUEL INJ RATE	OXID INJ RATE	FUEL FLOW RATE	OXID FLOW RATE	FUEL VCD VOL	OXID VCD VOL	FUEL INJ TEMP	OXID INJ TEMP
.007752	.714990	.007754	.734905	0.	0.	294.000	290.000
FUEL DROP BURN	OXID DROP BURN	FUEL FLASH RATE	OXID FLASH RATE	FUEL WALL BURN	OXID WALL BURN	FUEL WALL EVAP	OXID WALL EVAP
.207370	.224970	0.	0.	2.02752E-03	0.	0.	0.
FUEL GAS PASS	OXID GAS PASS	FUEL DROPLETS	OXID DROPLETS	FUEL STREAMS	OXID STREAMS	FUEL ON WALL	OXID ON WALL
9.92134E-05	0.00000E-05	4.03902E-04	2.00670E-04	0.19753E-00	1.00003E-00	9.37025E-05	0.
FUEL GAS EFFLUX	OXID GAS EFFLUX	FUEL DROP RATE	OXID DROP RATE	FUEL FILM RATE	OXID FILM RATE	GAS FRACTION	VAC THRUST LOP
.227355	.220401	0.	0.	0.	0.	1.00000	100.000
FUEL DROP D32	OXID DROP D32	FUEL INJ. VEL.	OXID INJ. VEL.	MAX. EXPLOSION	PASS OUT OF TANK	INTEGRAL PC-DT	TOTAL IMPULSE
109.634	70.9309	112.012	82.0337	207.420	7.41509E-03	0.107467E-02	1.02203
TIME MILLISEC	CHAMBER PRES	IGNITION	FUEL FRACTION	CHAMBER TEMP K	POL WT.	GAMMA	CF VAC
3.20030	75.2507	1.00000	.42000	2704.00	10.5300	1.20914	1.00000
FUEL INJ RATE	OXID INJ RATE	FUEL FLOW RATE	OXID FLOW RATE	FUEL VCD VOL	OXID VCD VOL	FUEL INJ TEMP	OXID INJ TEMP
.400005	.723307	.400000	.723315	0.	0.	294.000	290.000
FUEL DROP BURN	OXID DROP BURN	FUEL FLASH RATE	OXID FLASH RATE	FUEL WALL BURN	OXID WALL BURN	FUEL WALL EVAP	OXID WALL EVAP
.209796	.454390	0.	0.	2.50400E-03	0.	0.	0.
FUEL GAS PASS	OXID GAS PASS	FUEL DROPLETS	OXID DROPLETS	FUEL STREAMS	OXID STREAMS	FUEL ON WALL	OXID ON WALL
1.00000E-04	1.30731E-04	4.27050E-04	3.41203E-04	0.19753E-00	1.01250E-00	1.009697E-04	0.
FUEL GAS EFFLUX	OXID GAS EFFLUX	FUEL DROP RATE	OXID DROP RATE	FUEL FILM RATE	OXID FILM RATE	GAS FRACTION	VAC THRUST LOP
.205035	.223703	0.	0.	0.	0.	1.00000	100.000
FUEL DROP D32	OXID DROP D32	FUEL INJ. VEL.	OXID INJ. VEL.	MAX. EXPLOSION	PASS OUT OF TANK	INTEGRAL PC-DT	TOTAL IMPULSE
109.606	55.3200	112.227	85.5900	302.000	7.45750E-03	7.61204E-02	1.01990
TIME MILLISEC	CHAMBER PRES	IGNITION	FUEL FRACTION	CHAMBER TEMP K	POL WT.	GAMMA	CF VAC
3.40000	91.0350	1.00000	.43000	3023.00	10.3000	1.24407	1.00000
FUEL INJ RATE	OXID INJ RATE	FUEL FLOW RATE	OXID FLOW RATE	FUEL VCD VOL	OXID VCD VOL	FUEL INJ TEMP	OXID INJ TEMP
.003000	.300000	.003000	.300000	0.	0.	294.000	290.000
FUEL DROP BURN	OXID DROP BURN	FUEL FLASH RATE	OXID FLASH RATE	FUEL WALL BURN	OXID WALL BURN	FUEL WALL EVAP	OXID WALL EVAP
.300074	.510003	0.	0.	3.00000E-03	0.	0.	0.
FUEL GAS PASS	OXID GAS PASS	FUEL DROPLETS	OXID DROPLETS	FUEL STREAMS	OXID STREAMS	FUEL ON WALL	OXID ON WALL
1.23517E-04	1.70000E-04	4.30000E-04	3.00000E-04	0.19753E-00	1.01250E-00	1.009697E-04	0.

FUEL GAS EFFLUX OXID GAS EFFLUX FUEL DROP RATE	OXID DROP RATE	FUEL FILM RATE	OXID FILM RATE	GAS FRACTION	VAC THRUST LBF
328003	3.000000E-05	0.	0.	0.00000	0.00000
FUEL DROP D32	OXID DROP D32	FUEL INJ. VEL.	OXID INJ. VEL.	MAX. EXPLOSION PASS OUT OF TANK	INTEGRAL PC-DT TOTAL IMPULSE
307.000	0.00000	0.00000	0.00000	0.00000	0.00000

TIME MILLISEC	CHAMBER PRESS	IGNITION	FUEL FRACTION	CHAMBER TEMP K	POL WT.	GAMMA	CF VAC
3.00000	104.125	1.00000	0.00000	3050.15	10.0716	1.00000	1.00000
FUEL INJ RATE	OXID INJ RATE	FUEL FLOW RATE	OXID FLOW RATE	FUEL VOID VOL	OXID VOID VOL	FUEL INJ TEMP	OXID INJ TEMP
0.075611	0.072543	0.075611	0.072543	0.	0.	204.000	204.000
FUEL DROP BURN	OXID DROP BURN	FUEL FLASH RATE	OXID FLASH RATE	FUEL WALL BURN	OXID WALL BURN	FUEL WALL EVAP	OXID WALL EVAP
0.394912	0.371517	0.	0.	0.140000E-03	0.091361E-04	0.	0.
FUEL GAS MASS	OXID GAS MASS	FUEL DROPLETS	OXID DROPLETS	FUEL STREAMS	OXID STREAMS	FUEL ON WALL	OXID ON WALL
1.316256E-04	1.97207E-04	4.416608E-04	4.125125E-04	0.107534E-06	1.031493E-06	1.300045E-04	0.1300973E-09
FUEL GAS EFFLUX	OXID GAS EFFLUX	FUEL DROP RATE	OXID DROP RATE	FUEL FILM RATE	OXID FILM RATE	GAS FRACTION	VAC THRUST LBF
0.310201	0.430973	5.000110E-03	4.310913E-03	0.	0.	0.02204	277.210
FUEL DROP D32	OXID DROP D32	FUEL INJ. VEL.	OXID INJ. VEL.	MAX. EXPLOSION PASS OUT OF TANK	INTEGRAL PC-DT TOTAL IMPULSE		
307.454	59.5703	100.225	03.5107	414.320	3.130000E-03	1.15310	1.30007

TIME MILLISEC	CHAMBER PRESS	IGNITION	FUEL FRACTION	CHAMBER TEMP K	POL WT.	GAMMA	CF VAC
3.00000	113.017	1.00000	0.00000	3096.52	20.2911	1.00000	1.00000
FUEL INJ RATE	OXID INJ RATE	FUEL FLOW RATE	OXID FLOW RATE	FUEL VOID VOL	OXID VOID VOL	FUEL INJ TEMP	OXID INJ TEMP
0.069007	0.071092	0.069007	0.071092	0.	0.	204.000	204.000
FUEL DROP BURN	OXID DROP BURN	FUEL FLASH RATE	OXID FLASH RATE	FUEL WALL BURN	OXID WALL BURN	FUEL WALL EVAP	OXID WALL EVAP
0.301411	0.02777	0.	0.	0.051040E-03	1.102011E-05	0.	0.
FUEL GAS MASS	OXID GAS MASS	FUEL DROPLETS	OXID DROPLETS	FUEL STREAMS	OXID STREAMS	FUEL ON WALL	OXID ON WALL
1.400047E-04	2.205752E-04	4.33562E-04	4.311006E-04	0.107534E-06	1.003860E-06	1.505094E-04	0.
FUEL GAS EFFLUX	OXID GAS EFFLUX	FUEL DROP RATE	OXID DROP RATE	FUEL FILM RATE	OXID FILM RATE	GAS FRACTION	VAC THRUST LBF
0.340050	0.510700	1.047394E-02	3.230009E-02	0.	2.910726E-05	0.00000	304.944
FUEL DROP D32	OXID DROP D32	FUEL INJ. VEL.	OXID INJ. VEL.	MAX. EXPLOSION PASS OUT OF TANK	INTEGRAL PC-DT TOTAL IMPULSE		
100.109	61.0034	100.973	02.0000	439.291	3.375900E-03	1.20042	1.307005

TIME MILLISEC	CHAMBER PRESS	IGNITION	FUEL FRACTION	CHAMBER TEMP K	POL WT.	GAMMA	CF VAC
4.00000	110.001	1.00000	0.00000	3143.07	30.7304	1.00000	1.00000
FUEL INJ RATE	OXID INJ RATE	FUEL FLOW RATE	OXID FLOW RATE	FUEL VOID VOL	OXID VOID VOL	FUEL INJ TEMP	OXID INJ TEMP
0.000000	0.000000	0.000000	0.000000	0.	0.	204.000	204.000
FUEL DROP BURN	OXID DROP BURN	FUEL FLASH RATE	OXID FLASH RATE	FUEL WALL BURN	OXID WALL BURN	FUEL WALL EVAP	OXID WALL EVAP
0.367000	0.000000	0.	0.	0.000000E-03	0.000000E-03	0.	0.
FUEL GAS MASS	OXID GAS MASS	FUEL DROPLETS	OXID DROPLETS	FUEL STREAMS	OXID STREAMS	FUEL ON WALL	OXID ON WALL
0.000000E-04	0.000000E-04	0.000000E-04	0.000000E-04	0.000000E-06	0.000000E-06	0.000000E-04	0.000000E-09
FUEL GAS EFFLUX	OXID GAS EFFLUX	FUEL DROP RATE	OXID DROP RATE	FUEL FILM RATE	OXID FILM RATE	GAS FRACTION	VAC THRUST LBF
0.000000	0.000000	0.000000E-02	0.000000E-02	0.	0.	0.00000	0.00000
FUEL DROP D32	OXID DROP D32	FUEL INJ. VEL.	OXID INJ. VEL.	MAX. EXPLOSION PASS OUT OF TANK	INTEGRAL PC-DT TOTAL IMPULSE		
100.000	0.00000	100.000	0.0000	0.00000	0.000000E-03	0.00000	0.00000

PAGES OMITTED

[illegible]

TIME MILLISEC	CHAMBER PRESS	IGNITION	FUEL FRACTION	CHAMBER TEMP K	POL WT.	GASRA	CF VAC
9.0000	112.114	1.00000	.33109	3250.79	22.2005	1.22269	1.98344
FUEL INJ RATE	OXID INJ RATE	FUEL FLOW RATE	OXID FLOW RATE	FUEL VOID VOL	OXID VOID VOL	FUEL INJ TEMP	OXID INJ TEMP
.407795	.623092	.407809	.633127	0.	0.	294.832	294.832
FUEL DROP BURN	OXID DROP BURN	FUEL FLASH RATE	OXID FLASH RATE	FUEL WALL BURN	OXID WALL BURN	FUEL WALL EVAP	OXID WALL EVAP
.298299	.680832	0.	0.	1.26622E+02	1.17702E+02	0.	0.
FUEL GAS PASS	OXID GAS PASS	FUEL DROPLETS	FUEL STREAMS	OXID STREAMS	FUEL ON WALL	OXID ON WALL	OXID ON WALL
1.223016E-04	2.466720E-04	4.319241E-04	5.666330E-07	1.306104E-04	5.165095E-04	5.511301E-03	5.511301E-03
FUEL GAS EFFLUX	OXID GAS EFFLUX	FUEL DROP RATE	OXID DROP RATE	FUEL FILM RATE	OXID FILM RATE	GAS FRACTION	VAC THRUST LBF
.307073	.625130	4.150191E-02	2.570504E-02	0.	0.	.930039	381.044
FUEL DROP D32	OXID DROP D32	FUEL INJ. VEL.	OXID INJ. VEL.	MAX. EXPLOSION	PASS OUT OF TANK	INTEGRAL PC-DOT	TOTAL IMPULSE
102.049	66.1092	93.6528	72.4866	510.546	9.956114E-03	.021500	2.20906

	XMFL	XMLO	DMF	DMO	GASV	RENCH
1	0	0	0	0	0	0
2	0	0	0	0	0	0
3	2,570279603E-04	0	0	0	0	0
4	0	0	0	0	0	0
5	0	0	0	0	0	0
6	2,2446514274E-02	5,924720110E-02	0	0	0	0
7	1,0709940785E-02	0	0	0	0	0
8	0	0	0	0	0	0
9	0	0	0	0	0	0
10	0	0	0	0	0	0
11	1,4323460710E-02	5,025040044E-02	0	0	0	0
12	1,1347483208E-04	0	0	0	0	0
13	1,1493631903E-02	0	0	0	0	0
14	1,4346546034E-05	0	0	0	0	0
15	1,0320828045E-03	0	0	0	0	0
16	1,0266235749E-02	5,8560199020E-02	0	0	0	0
17	2,2521854482E-05	0	0	0	0	0
18	3,1671825510E-04	0	0	0	0	0
19	2,015484095E-03	0	0	0	0	0
20	4,110273110E-03	0	0	0	0	0
21	3,0463070510E-03	2,4997994046E-02	0	0	0	0
22	3,0463070510E-03	3,107746317E-03	0	0	0	0
23	3,0463070510E-03	0	0	0	0	0
24	1,1234033254E-03	0	0	0	0	0
25	4,002239697E-03	0	0	0	0	0
26	3,0463070510E-03	0	0	0	0	0
27	1,0926075300E-03	4,279298937E-03	0	0	0	0
28	1,0689062076E-03	4,205703090E-03	0	0	0	0
29	0	0	0	0	0	0
30	0	0	0	0	0	0
31	4,104709430E-03	5,834545972E-03	0	0	0	0
32	3,272184080E-03	0	0	0	0	0
33	0	0	0	0	0	0
34	1,083077204E-03	0	0	0	0	0
35	1,101073722E-04	0	0	0	0	0
36	2,019609941E-04	0	0	0	0	0
37	2,077180307E-03	0	0	0	0	0
38	1,072703030E-03	0	0	0	0	0
39	3,002460117E-03	2,205214324E-03	0	0	0	0
40	0	0	0	0	0	0
41	0	0	0	0	0	0
42	0	0	0	0	0	0
43	0	0	0	0	0	0
44	1,408231248E-03	0	0	0	0	0
45	1,11223222E-03	0	0	0	0	0
46	3,098076120E-03	0	0	0	0	0
47	3,098076120E-03	1,999472240E-03	0	0	0	0
48	3,098076120E-03	0	0	0	0	0
49	3,098076120E-03	0	0	0	0	0
50	3,098076120E-03	0	0	0	0	0
51	3,098076120E-03	0	0	0	0	0
52	3,098076120E-03	0	0	0	0	0
53	3,098076120E-03	0	0	0	0	0
54	3,098076120E-03	0	0	0	0	0
55	3,098076120E-03	0	0	0	0	0
56	3,098076120E-03	0	0	0	0	0
57	3,098076120E-03	0	0	0	0	0
58	3,098076120E-03	0	0	0	0	0
59	3,098076120E-03	0	0	0	0	0
60	3,098076120E-03	0	0	0	0	0
61	3,098076120E-03	0	0	0	0	0
62	3,098076120E-03	0	0	0	0	0

63	9.0768216272E-04	0.1749320290E-04	1.1768944179E-04	17937.50377	51399.58234
64	0.7642288111E-04	1.4694258222E-03	1.6299172491E-04	10558.31588	52599.58749
65	1.1889748871E-03	3.4838555905E-05	0.7861761875E-04	10846.10803	53406.10803
66	1.2533030255E-03	0.	0.	19747.65981	54414.08947
67	0.	0.	0.	20308.37397	55182.09068
68	0.	0.	0.	10059.30094	59992.84400
69	0.	0.	0.5120198268E-05	21921.52437	56029.07817
70	0.	0.	0.	22690.77844	58383.31233
71	0.8821528827E-04	3.4474138147E-03	1.7214438189E-04	24323.85584	60803.57783
72	0.4497404573E-04	0.	0.	29776.30214	62409.76986
73	0.	0.	0.	27408.64037	64532.85040
74	0.	0.	0.	38338.81174	66444.47706
75	1.470828489E-03	1.1997184904E-03	2.713308723E-04	31518.83998	69388.38929
76	1.2225567264E-03	0.	0.	33796.92576	71018.14348
77	0.	0.	0.0285338245E-04	14384.88314	74488.83248
78	4.9066940676E-04	0.	2.50312743E-05	37813.18964	76194.28891
79	0.	1.0840456038E-05	7.565971599E-04	39339.98082	77977.38955
80	0.	0.	0.3889748871E-05	10648.15338	79381.34108
81	0.	0.	3.1239186194E-05	42821.19437	80886.83801
82	0.	0.	0.972277692E-05	43500.15329	82084.78886
83	0.5012287718E-04	1.4133234486E-03	1.332351317E-04	45285.84884	84814.88063
84	0.	0.	0.5713108414E-05	47088.04318	85932.88723
85	0.	0.	0.811883791E-05	48806.67933	87354.88417
86	0.	0.	0.328986636E-05	50643.88446	88447.88519
87	0.	0.	0.9733985199E-05	52649.90266	91081.77846
88	1.1798506197E-03	0.	5.4613.05143	92682.87481	92682.87481
89	0.	0.	0.9733985199E-05	54613.05143	94783.88566
90	9.5939902287E-04	0.	0.273373388E-05	56935.83331	94783.88566
91	0.	0.9321100199E-04	0.1374717128E-05	59256.80389	96783.88566
92	0.	0.	3.990949431E-04	61910.10988	99133.83228
93	0.	0.	0.183244384E-05	64537.81188	101367.38808
94	5.5687005436E-04	0.	0.102159204E-19	67180.90184	103334.31446
95	0.	0.	0.6807641319E-04	67921.97566	103977.5261
96	0.	0.	1.381861147E-18	68548.18874	104488.1883
97	3.7481313473E-04	0.	4.3818418342E-19	69112.66117	104923.5921
98	0.	0.	0.2464004200E-19	69825.58833	105562.9997
99	0.	0.	0.81186384E-18	70488.98343	106079.4348
100	0.	0.	3.398420699E-07	71118.44821	106683.3894
101	0.	0.	1.3212019598E-20	71698.37429	107838.8866
102	0.	0.	1.0440378188E-19	72311.63852	108486.8114

PAGES OMITTED

PERFORMANCE SUMMARY

PROPELLANT MASS BASIS	FUEL FLOW	OXID FLOW	MIXTURE RATIO	C-STAR	VACUUM -PS-
MASS OUT OF TANK - POUNDS	.004476	.006744	1.508812	4448.743965	244.883810
MASS THROUGH INJECTOR - POUNDS	.004196	.008065	1.940736	4076.936382	243.109846
MASS THROUGH NOZZLE - POUNDS	.003844	.004458	1.081583	4883.158841	387.144863
PRESSURE INTEGRAL - PSIA-SEC.	1.0755				
TOTAL VAC IMPULSE - POUND-SEC.	2.9711				

DISPOSITION OF INJECTED PROPELLANT			
	FUEL	OXID	TOTAL
FRACTION EXPELLED AS BURNT GAS	.732064	.770890	.757693
FRACTION EXPELLED AS UNBURNT VAPOR	.000049	.000337	.000371
FRACTION EXPELLED AS DROPS	.117300	.027528	.080088
FRACTION EXPELLED AS FILM	.003199	.001302	.002000
FRACTION RETAINED AS GAS-VAPOR	.000092	.010240	.010749
FRACTION RETAINED AS DROPS	.000434	.000030	.000463
FRACTION RETAINED AS FILM	.146771	.020307	.060644
TOTAL OF ABOVE VALUES	1.000000	1.000000	1.000000

TOTALS GREATER THAN 1.0 MAY INDICATE =

IGNITER FLAME - NOT CLASSIFIED AS THROUGH-INJECTOR OR OUT-OF-TANK.

DEPLETION OF CHAMBER GAS PASS - THERE MAY BE AN APPRECIABLE MASS OF COLD VAPOR IN CHAMBER BEFORE START.

DEPLETION OF WALL-FILM, WHEN A PIPING IS STARTED WITH PROPELLANT-COATED WALLS.

MEAN DROP DIAMETER	INJECTED FUEL	EJECTED FUEL	INJECTED OXID	EJECTED OXID
D30 MICRONS	33.5745	100.2649	25.9815	30.4274
D31 MICRONS	43.6456	136.3222	30.4125	37.3813
D32 MICRONS	65.3107	105.0307	45.4377	82.5429
MEAN AXIAL VELOCITY FT/SEC	73.43	321.46	53.17	560.21
MEAN RADIAL VELOCITY FT/SEC		83.81		114.38

NOTE - THE ABOVE EJECTED DROPLET AND EJECTED FILM VALUES ARE AT THE THROAT PLANE, NOT THE EXIT PLANE.

INJECTED FUEL EJECTED FUEL INJECTED OXIT EJECTED OXID

DROP DIAMETER

D MICRONS	LOG D	PROP SIZE DISTRIBUTION - CUMULATIVE MASS	INJECTED OXIT	EJECTED OXID
10	1.0000	0.0000	0.0000	0.0015
20	1.3010	0.0000	0.0000	0.0000
30	1.4771	0.0000	0.0000	0.0000
40	1.6021	0.0000	0.0000	0.0000
50	1.6982	0.0000	0.0000	0.0000
60	1.7787	0.0000	0.0000	0.0000
70	1.8451	0.0000	0.0000	0.0000
80	1.9011	0.0000	0.0000	0.0000
90	1.9487	0.0000	0.0000	0.0000
100	2.0000	0.0000	0.0000	0.0000
110	2.0414	0.0000	0.0000	0.0000
120	2.0797	0.0000	0.0000	0.0000
130	2.1139	0.0000	0.0000	0.0000
140	2.1441	0.0000	0.0000	0.0000
150	2.1701	0.0000	0.0000	0.0000
160	2.2041	0.0000	0.0000	0.0000
170	2.2364	0.0000	0.0000	0.0000
180	2.2653	0.0000	0.0000	0.0000
190	2.2788	0.0000	0.0000	0.0000
200	2.3010	0.0000	0.0000	0.0000
210	2.3227	0.0000	0.0000	0.0000
220	2.3424	0.0000	0.0000	0.0000
230	2.3617	0.0000	0.0000	0.0000
240	2.3802	0.0000	0.0000	0.0000
250	2.3979	0.0000	0.0000	0.0000
260	2.4150	0.0000	0.0000	0.0000
270	2.4314	0.0000	0.0000	0.0000
280	2.4472	0.0000	0.0000	0.0000
290	2.4624	0.0000	0.0000	0.0000
300	2.4771	0.0000	0.0000	0.0000
310	2.4914	0.0000	0.0000	0.0000
320	2.5051	0.0000	0.0000	0.0000
330	2.5185	0.0000	0.0000	0.0000
340	2.5315	0.0000	0.0000	0.0000
350	2.5441	0.0000	0.0000	0.0000
360	2.5563	0.0000	0.0000	0.0000
370	2.5682	0.0000	0.0000	0.0000
380	2.5798	0.0000	0.0000	0.0000
390	2.5911	0.0000	0.0000	0.0000
400	2.6021	0.0000	0.0000	0.0000
410	2.6128	0.0000	0.0000	0.0000
420	2.6232	0.0000	0.0000	0.0000
430	2.6335	0.0000	0.0000	0.0000
440	2.6435	0.0000	0.0000	0.0000
450	2.6532	0.0000	0.0000	0.0000
460	2.6628	0.0000	0.0000	0.0000

FINAL CHAMBER CONDITION

STATION	GRAMS FUEL	GRAMS OXID	TEMPERATURE
1	0.0000000	0.3000000	294.05100967
2	0.0000000	0.0000000	294.05523903
3	0.0000000	0.0000000	294.0844030
4	0.0000000	0.0000000	294.06173774
5	0.0000000	0.0000000	294.06490709
6	0.0000000	0.0000000	294.06030445
7	0.0000000	0.0000000	294.07140500
8	0.0000000	0.0000000	294.07473516
9	0.0000000	0.0000000	294.07700451
10	0.0000000	0.0000000	294.08123307
11	0.0000000	0.0000000	294.0844322
12	0.0000000	0.0000000	294.08533084
13	0.0000000	0.0000000	294.09090193
14	0.0000000	0.3000000	294.09423129
15	0.0000000	0.0000000	294.09740044
16	0.0000000	0.0000000	294.10072999
17	0.0035257	0.0000000	294.10397935
18	0.0105040	0.0000000	294.1072070
19	0.0105486	0.3000000	294.11047006
20	0.0146846	0.0000000	294.11372741
21	0.0371041	0.0000000	294.11692477
22	0.051724	0.0000000	294.1202012
23	0.0641497	0.0000000	294.12347946
24	0.0728246	0.0000000	294.1267481
25	0.0850915	0.0000000	294.12997419
26	0.0910610	0.0000000	294.13322354
27	0.1013241	0.0360000	294.13643288
28	0.0875043	0.0000000	294.13972225
29	0.0515705	0.0000000	294.14297100
30	0.0541848	0.0000000	294.14623080
31	0.0611077	0.0000000	294.14947831
32	0.0663949	0.0000000	294.15271967
33	0.0723197	0.0000000	294.15596002
34	0.0809378	0.0000000	294.15921030
35	0.0957347	0.0000000	294.16246773
36	0.102004	0.0000000	294.16572700
37	0.104993	0.0000000	294.16896444
38	0.120081	0.0000000	294.17221500
39	0.2253376	0.0000000	294.17544515
40	0.2097408	0.0000000	294.17871451
41	0.3391254	0.0000000	294.18196386
42	0.0000000	0.0000000	294.18521332
43	0.010129	0.0000000	294.18846257
44	0.0774622	0.0392516	294.19171192
45	0.0000000	0.0000000	294.19496428
46	0.0000000	0.0455510	294.19821003
47	0.0000000	0.0734466	294.20145999
48	0.0000000	0.0448530	294.20470924
49	0.0000000	0.0523922	294.20795870
50	0.0000000	0.0430227	294.21120805
51	0.0000000	0.0604440	294.21445741
52	0.0000000	0.0821272	294.21770676
53	0.0000000	0.08224204	294.22095612
54	0.0000000	0.0866454	294.22420547
55	0.0000000	0.08007608	294.22745483
56	0.0000000	0.0000000	294.23070410
57	0.0000000	0.0533517	294.23395344
58	0.0000000	0.0000000	294.23720209
59	0.0000000	0.0000000	294.24045224
60	0.0000000	0.0000000	294.24370160

61	.00000000	.00035111	294,24695095
62	0.00000006	0.00000000	294,25020031
63	0.00000000	0.00000000	294,25344966
64	0.00000000	0.00000000	294,25669902
65	.00000025	.00188410	294,25994837
66	.00000000	.00035063	294,26319773
67	0.00000000	.00074200	294,26644708
68	0.00000000	0.00000000	294,26969644
69	.00000045	.00035063	294,27294579
70	.00001043	.00015478	294,27619515
71	.00064110	.00043162	294,27944450
72	.00021320	.00035063	294,28269386
73	.00000059	0.00000000	294,28594321
74	.00000005	.00125041	294,28919256
75	.00000051	.00040004	294,29244192
76	.00000200	0.00000000	294,29569127
77	.00120004	.00042009	294,29894063
78	.00000000	.00035063	294,30219000
79	.00119716	.00124358	294,30543934
80	.00150366	.00035063	294,30868869
81	.00117633	.00035063	294,31193805
82	.00011260	.00012830	294,31518740
83	.00115060	.00150061	294,31843676
84	.00000000	.00040004	294,32168611
85	.00001210	.00035063	294,32493547
86	.00053922	.00030025	294,32818482
87	.00046040	.00035063	294,33143418
88	.00014005	.00035063	294,33468353
89	.00056020	.00030025	294,33793288
90	.00052761	.00035063	294,34118224
91	.00055209	.00035063	294,34443159
92	.00051220	.00070192	294,34768095
93	.00020130	.00035063	294,35093030
94	.00020070	.00121710	294,35417966
95	.00039367	.00119450	294,35742901
96	.00021741	.00040004	294,36067837
97	.00022333	0.00000000	294,36392772
98	.00064355	.00000022	294,36717708
99	.00017144	.00021230	294,37042643
100	.00009291	.00010043	294,37367579
101	.00010946	.00013047	294,37692514

TIME-AVERAGED INTERVAL PERFORMANCE VALUES

START TIME	0.00000 SECONDS		
FINISH TIME	.00000 SECONDS		
INTERVAL LENGTH	.00000 SECONDS		
TOTAL IMPULSE	1.69927 POUND-SEC	THRUST	312.44013 POUNDS
CHAMBER PRESSURE INTERVAL	.03990 PSI-SEC	CHAMBER PRESSURE	77.00728 PSI
FUEL OUT OF TANK	.00326 POUNDS	FUEL FLOW RATE	.403277 POUNDS/SEC
OXID OUT OF TANK	.004719 POUNDS	OXID FLOW RATE	.509903 POUNDS/SEC
FUEL-TO-OXID OUT OF TANK	.007949 POUNDS	TOTAL FLOW RATE	.999200 POUNDS/SEC
MIXTURE RATIO	1.412775 OXID/FUEL		
G-STAR	3614.315240 FEET/SEC		
VACUUM SPECIFIC IMPULSE	213.00000 SECONDS		

PROPELLANT EXPULSED THIS INTERVAL

FUEL	1.69927 POUNDS	OXID	2.22309 POUNDS	OXID-TO-FUEL RATIO	1.30841
PRODUCTS OF COMBUSTION	.00177090	.222309	.00324107	.403234	
UNBURNED VAPOR	.00000015	.000019	.00000127	.000159	
UNBURNED DROPLETS	.000000150	.00000000	.00000000	.000000	
WALL FILM	.00000025	.00000007	.00000007	.000503	

EXPULSED DROPLET MEAN DIAMETER AND VELOCITY

FUEL DROPLETS		OXID DROPLETS	
330 MICRONS	100.671961		50.640490
331 MICRONS	100.010000		00.100000
332 MICRONS	100.220731		00.270000
AXIAL VELOCITY FT/SEC	305.651774		050.333156
AXIAL VELOCITY MI/SEC	97.110000		100.000000

INLET VALUES FOR MILLMAN

CHAMBER PRESSURE 77.4F7272 PSIA

CHAMBER TEMPERATURE 588.3:3821 DEG.F.

GAS CONSTANT 1540.423837 F7002/SEC002 DEG.F.

GAS SPECIFIC HEAT 12486.472133 F7002/SEC002 DEG.F.

GAS GMPA 1.994773

GAS VISCOSITY .00092 POUNDS/FT.SEC.

FUEL DROPLETS OXID DROPLETS

DROPLET DENSITY 95.2F4500 POUNDS/FT003 91.391109 POUNDS/FT003

MASS DROPS/MASS GAS .052085 .015985

EXPULSED DROPLET SIZE DISTRIBUTION

FUEL MASS FRACTION

OXID MASS FRACTION

DIAM MICRON RADIUS FEET INCREMENTAL CUMULATIVE INCREMENTAL CUMULATIVE

10 1.640E-05 .00021 .06021 .00020 .00020

20 3.280E-05 .00122 .00143 .00740 .00740

30 4.920E-05 .00459 .00703 .01192 .01192

40 6.560E-05 .01592 .01640 .00140 .02120

50 8.200E-05 .00700 .01440 .00270 .02290

60 9.840E-05 .00393 .02233 .00000 .02290

70 1.148E-04 .01204 .03437 .00620 .02910

80 1.312E-04 .00260 .03697 .00000 .03070

90 1.476E-04 .00673 .07374 .00782 .03856

100 1.640E-04 .04633 .12007 .00045 .04036

110 1.804E-04 .00007 .14001 .00254 .04290

120 1.968E-04 0.00000 .16001 .01793 .06083

130 2.132E-04 .04950 .19760 .00000 .06083

140 2.296E-04 .00000 .22000 .00000 .06083

150 2.460E-04 .15400 .30600 .00000 .06083

160 2.624E-04 .06790 .40550 .00000 .06083

170 2.788E-04 0.00000 .40550 .00000 .06083

180 2.952E-04 .00207 .90622 .00000 .06083

Σ

190	3.1171-04	.000367	.600255	0.000000	1.000000
200	3.2421-04	.135209	.455444	0.000000	1.000000
210	3.4451-04	.219318	.604762	0.000000	1.000000
220	3.6091-04	.300000	.604762	0.000000	1.000000
230	3.7731-04	.300000	.604762	0.000000	1.000000
240	3.9371-04	.300000	.604762	0.000000	1.000000
250	4.1011-04	.300000	.604762	0.000000	1.000000
260	4.2651-04	.300000	.604762	0.000000	1.000000
270	4.4291-04	.300000	.604762	0.000000	1.000000
280	4.5931-04	.300000	.604762	0.000000	1.000000
290	4.7571-04	.300000	.604762	0.000000	1.000000
300	4.9211-04	.300000	.604762	0.000000	1.000000
310	5.0851-04	.300000	.604762	0.000000	1.000000
320	5.2491-04	.300000	.604762	0.000000	1.000000
330	5.4131-04	.300000	.604762	0.000000	1.000000
340	5.5771-04	.300000	.604762	0.000000	1.000000
350	5.7411-04	.300000	.604762	0.000000	1.000000
360	5.9051-04	.300000	.604762	0.000000	1.000000
370	6.0691-04	.300000	.604762	0.000000	1.000000
380	6.2331-04	.300000	.604762	0.000000	1.000000
390	6.3971-04	.300000	.604762	0.000000	1.000000
400	6.5611-04	.300000	.604762	0.000000	1.000000
410	6.7251-04	.300000	.604762	0.000000	1.000000
420	6.8891-04	.300000	.604762	0.000000	1.000000
430	7.0531-04	.300000	.604762	0.000000	1.000000

TIME-AVERAGED INTERVAL PERFORMANCE VALUES

START TIME	.002000 SECONDS				
FINISH TIME	.010000 SECONDS				
INTERVAL LENGTH	.002000 SECONDS				
TOTAL IMPULSE	.003454 POUNDS/SEC	THROUST	311.727101 POUNDS		
CHAMBER PRESSURE INTERVAL	.0274030 PSI/SEC	CHAMBER PRESSURE	112.010031 PSI		
FUEL OUT OF TANK	.003015 POUNDS	FUEL FLOW RATE	.407601 POUNDS/SEC		
OXID OUT OF TANK	.001307 POUNDS	OXID FLOW RATE	.053717 POUNDS/SEC		
FUEL-TO-OXID OUT OF TANK	.002123 POUNDS	TOTAL FLOW RATE	1.001499 POUNDS/SEC		
MIXTURE RATIO	1.003462 OXID/FUEL				
Q-STAR	4849.143899 FEET/SEC				
VAC. SPECIFIC IMPULSE	293.001910 SECONDS				

FUEL PILLANT EXPLED THIS INTERVAL

	FUEL POUNDS	FUEL POUNDS/SEC	OXID POUNDS	OXID POUNDS/SEC
PRODUCTS OF CORRUPTION	.00061451	.307255	.00125099	.625493
UNBURNED VAPOR	3.00000000	1.000000	0.00000000	0.000000
UNBURNED DROPLETS	.00000000	.000000	.00000000	.000000
BALL FILM	.00000000	.000000	.00000000	.000000

EXPERIMENTAL DROPLET MEAN DIAMETER AND VELOCITY

	FUEL DROPLETS	OXID DROPLETS
830 MICRONS	114.345511	92.797727
831 MICRONS	100.120420	70.000200
832 MICRONS	171.950610	90.550510
AXIAL VELOCITY FT/SEC	200.072000	997.102025
RADIAL VELOCITY FT/SEC	90.320700	130.003777

INPUT VALUES FOR MULTIAN

CHAMBER PRESSURE

115.016031 PSIA

CHAMBER TEMPERATURE

434.475200 DEG.R.

GAS CONSTANT

1080.428837 FT*2/SEC*2 DEG.R

GAS SPECIFIC HEAT

12233.345302 FT*2/SEC*2 DEG.R

GAS GRAVITY

1.098041

GAS VISCOSITY

.000098 POISE/FT.SEC.

FUEL DROPLETS

55.24900 PCOUNTS/FT*3

DROPLET DENSITY

OXID DROPLETS

PASS DROPS/MASS GAS

.344534

92.892103 PCOUNTS/FT*3

.027820

EXPILED DROPLET SIZE DISTRIBUTION

FUEL MASS FRACTION

OXID MASS FRACTION

INCREMENTAL CUMULATIVE

INCREMENTAL CUMULATIVE

DIAP MICRON RADIUS FEET

INCREMENTAL CUMULATIVE

INCREMENTAL CUMULATIVE

INCREMENTAL CUMULATIVE

INCREMENTAL CUMULATIVE

INCREMENTAL CUMULATIVE

INCREMENTAL CUMULATIVE

INCREMENTAL CUMULATIVE

INCREMENTAL CUMULATIVE

INCREMENTAL CUMULATIVE

INCREMENTAL CUMULATIVE

INCREMENTAL CUMULATIVE

INCREMENTAL CUMULATIVE

INCREMENTAL CUMULATIVE

INCREMENTAL CUMULATIVE

INCREMENTAL CUMULATIVE

INCREMENTAL CUMULATIVE

INCREMENTAL CUMULATIVE

INCREMENTAL CUMULATIVE

INCREMENTAL CUMULATIVE

INCREMENTAL CUMULATIVE

INCREMENTAL CUMULATIVE

INCREMENTAL CUMULATIVE

INCREMENTAL CUMULATIVE

INCREMENTAL CUMULATIVE

INCREMENTAL CUMULATIVE

INCREMENTAL CUMULATIVE

INCREMENTAL CUMULATIVE

INCREMENTAL CUMULATIVE

INCREMENTAL CUMULATIVE

INCREMENTAL CUMULATIVE

INCREMENTAL CUMULATIVE

INCREMENTAL CUMULATIVE

INCREMENTAL CUMULATIVE

INCREMENTAL CUMULATIVE

INCREMENTAL CUMULATIVE

INCREMENTAL CUMULATIVE

INCREMENTAL CUMULATIVE

INCREMENTAL CUMULATIVE

INCREMENTAL CUMULATIVE

INCREMENTAL CUMULATIVE

INCREMENTAL CUMULATIVE

INCREMENTAL CUMULATIVE

INCREMENTAL CUMULATIVE

INCREMENTAL CUMULATIVE

INCREMENTAL CUMULATIVE

V

190	3.1171-04	0.000000	.471000	0.000000	1.000000
200	3.2111-04	.253700	.000700	0.000000	1.000000
210	3.4131-04	0.000000	.000700	0.000000	1.000000
220	3.6091-04	0.000000	.000700	0.000000	1.000000
230	3.7731-04	0.000000	.000700	0.000000	1.000000
240	3.9571-04	0.000000	.000700	0.000000	1.000000
250	4.1011-04	0.000000	.000700	0.000000	1.000000
260	4.2651-04	0.000000	.000700	0.000000	1.000000
270	4.4291-04	0.000000	.000700	0.000000	1.000000
280	4.5931-04	0.000000	.000700	0.000000	1.000000
290	4.7571-04	0.000000	.000700	0.000000	1.000000
300	4.9211-04	0.000000	.000700	0.000000	1.000000
310	5.0851-04	0.000000	.000700	0.000000	1.000000
320	5.2491-04	0.000000	.000700	0.000000	1.000000
330	5.4131-04	0.001200	.000000	0.000000	1.000000
340	5.5771-04	0.000000	.000000	0.000000	1.000000
350	5.7411-04	0.000000	.000000	0.000000	1.000000
360	5.9051-04	0.000000	.000000	0.000000	1.000000
370	6.0701-04	0.000000	.000000	0.000000	1.000000
380	6.2341-04	0.000000	.000000	0.000000	1.000000
390	6.3981-04	0.000000	.000000	0.000000	1.000000
400	6.5621-04	0.000000	.000000	0.000000	1.000000
410	6.7261-04	0.000000	.000000	0.000000	1.000000
420	6.8901-04	0.000000	.000000	0.000000	1.000000
430	7.0541-04	.314000	1.000000	0.000000	1.000000

TIME-AVERAGED INTERVAL PERFORMANCE VALUES

START TIME	.01000 SECONDS			
STOP TIME	.01000 SECONDS			
INTERVAL LENGTH	.01000 SECONDS			
TOTAL IMPULSE	.66069 POUNDS/SEC	IMPULSE	64.00087 POUNDS	
CHAMBER PRESSURE INITIAL	.231372 PSI/SEC	CHAMBER PRESSURE	23.137104 PSI	
FUEL OUT OF TANK	.003434 POUNDS	FUEL FLOW RATE	.043415 POUNDS/SEC	
OXID OUT OF TANK	.009717 POUNDS	OXID FLOW RATE	.071744 POUNDS/SEC	
FUEL-TO-OXID OUT OF TANK	.002332 POUNDS	TOTAL FLOW RATE	.115159 POUNDS/SEC	
MIXTURE RATIO	1.652235 OXID/FUEL			
0-STAR	9315.756385 FEET/SEC			
VAC. SPECIFIC IMPULSE	562.770107 SECONDS			

PROPELLANT EXCELLED THIS INTERVAL

FUEL POUNDS	FUEL POUNDS/SEC	OXID POUNDS	OXID POUNDS/SEC
PRODUCTS OF COMBUSTION	.00014859	.004309	.00172465
UNBURNED VAPOR	.00000006	.000030	.0000306
UNBURNED DROPLETS	.00000000	.00000000	.00000000
WALL FILT	.00000042	.000042	.0000446

EXPLICIT DROPLETS WITH DIAMETER AND VELOCITY

FUEL DROPLETS	OXID DROPLETS
830 MICRONS	114.752712
831 MICRONS	144.112300
832 MICRONS	173.356381
AXIAL VELOCITY FT/SEC	254.836761
RADIAL VELOCITY FT/SEC	82.740222

INPUT VALUES FOR FULTON

CHAMBER PRESSURE 23.157164 PSIA
 CHAMBER TEMPERATURE 9217.225724 DEG.R.
 GAS CONSTANT 1600.430037 FT²/SEC² LB/LB.F
 GAS SPECIFIC HEAT 11420.639785 FT²/SEC² LB/LB.F
 GAS GAMMA 1.214009

GAS VISCOSITY 0.00009 POUNDS/FT.SEC.

FUEL PROPERTIES OXIDE DROPLETS

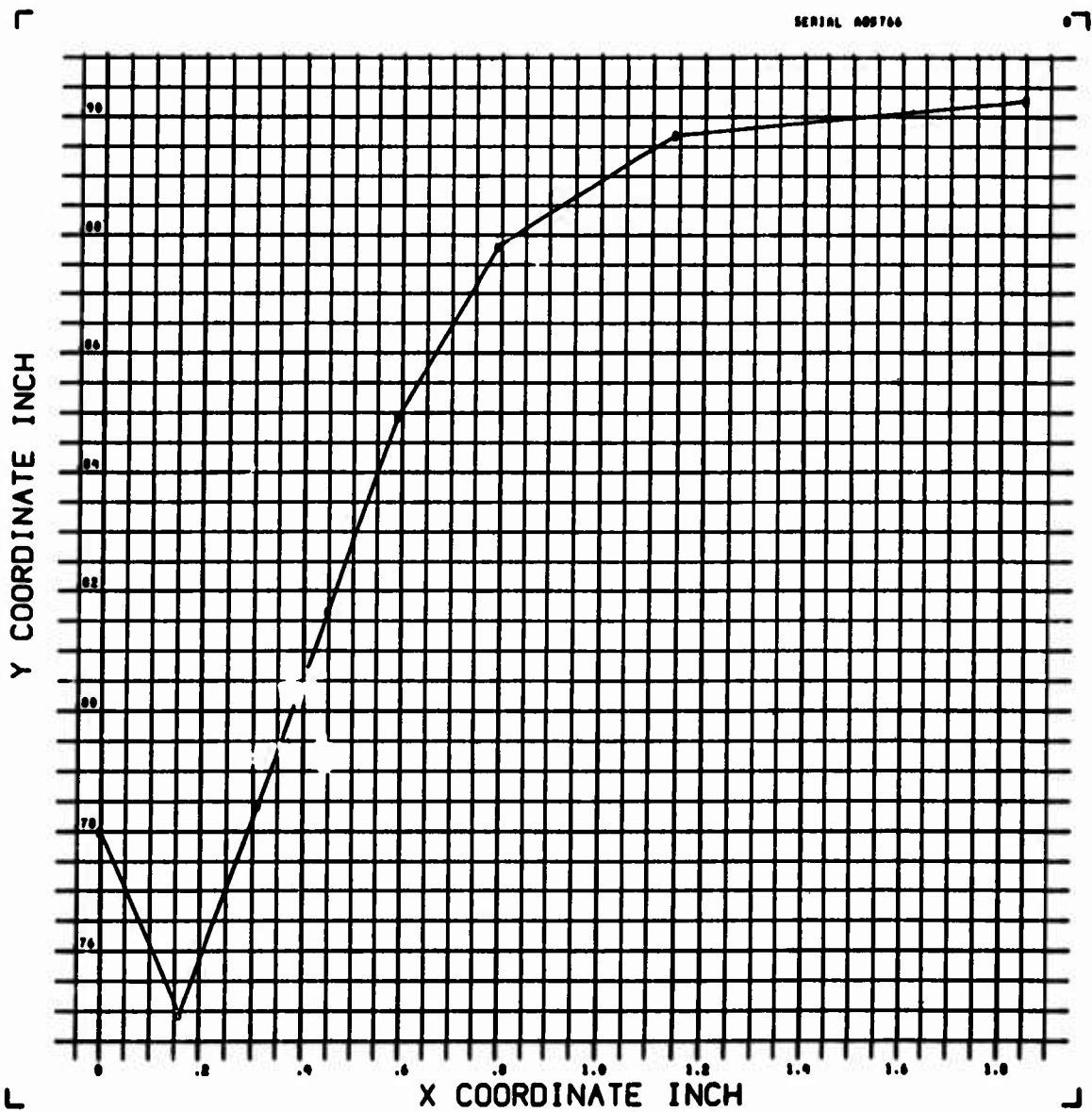
DROPLET DENSITY 5.274259 POUNDS/FT³ 0.139105 POUNDS/FT³
 MASS DROPS/MASS GAS 0.09247 0.037774

EXPILED DROPLET SIZE DISTRIBUTION

FUEL MASS FRACTION OXIDE MASS FRACTION

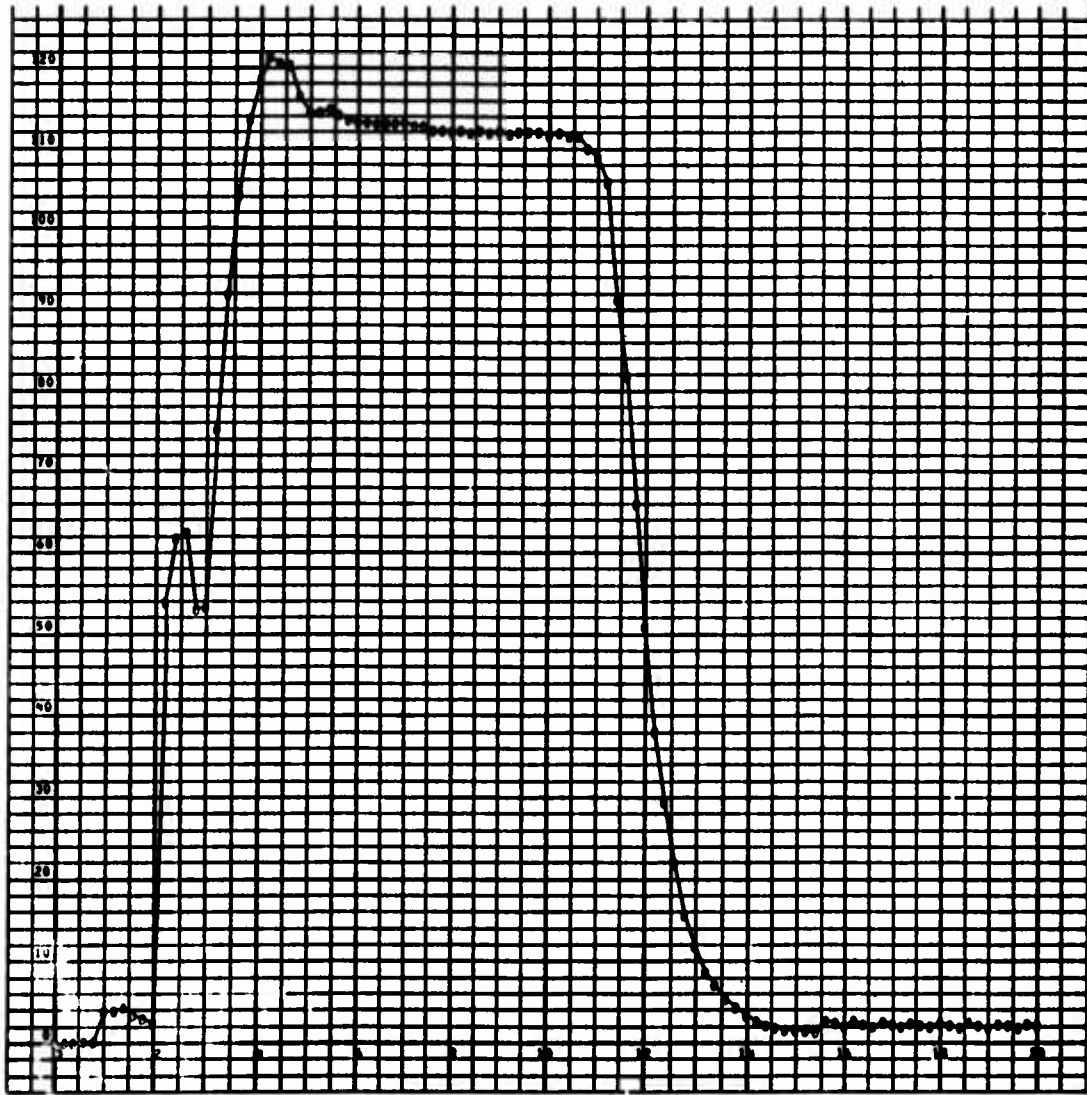
BIAM MICROH	RADIUS FEET	INCREMENTAL	CUMULATIVE	INCREMENTAL	CUMULATIVE
10	1.040E-05	0.000000	0.000000	0.003040	0.003040
20	3.201E-05	0.00127	0.00127	0.07763	0.080632
30	4.921E-05	0.010475	0.010630	0.34912	0.119715
40	6.562E-05	0.00041	0.000674	0.19285	0.131000
50	8.202E-05	0.07203	0.07277	0.00031	0.131931
60	9.843E-05	0.01313	0.07690	0.000000	0.131931
70	1.146E-04	0.01024	0.07715	0.000000	0.131931
80	1.312E-04	0.00005	0.07770	0.000000	0.131931
90	1.476E-04	0.047304	0.05084	0.000000	0.135367
100	1.640E-04	0.07025	0.09210	0.10624	0.331991
110	1.804E-04	0.01004	0.09310	0.12400	0.456350
120	1.969E-04	0.00370	0.093572	0.09142	0.465301
130	2.133E-04	0.01434	0.135000	0.00993	0.474894
140	2.297E-04	0.01020	0.144732	0.00910	0.483998
150	2.461E-04	0.24030	0.396271	0.000000	0.483998
160	2.625E-04	0.01110	0.497380	0.000000	0.483998
170	2.789E-04	0.22200	0.719380	0.000000	0.483998
180	2.953E-04	0.000000	0.719380	0.000000	0.483998

190	3.117L-04	.011353	..1975	0.000000	.995945
200	3.201L-04	.073477	.587952	0.000000	.995945
210	3.445L-04	.110618	.694569	.005002	.990846
220	3.609L-04	.015440	.734024	.009154	1.000000
230	3.773L-04	.008599	.754440	0.000000	1.000000
240	3.937L-04	0.000000	.734596	0.000000	1.000000
250	4.101L-04	0.000000	.734596	0.000000	1.000000
260	4.265L-04	0.000000	.734596	0.000000	1.000000
270	4.429L-04	0.000000	.734596	0.000000	1.000000
280	4.593L-04	0.000000	.734596	0.000000	1.000000
290	4.757L-04	0.000000	.734596	0.000000	1.000000
300	4.921L-04	0.000000	.734596	0.000000	1.000000
310	5.085L-04	0.000000	.734596	0.000000	1.000000
320	5.249L-04	.008422	.753010	0.000000	1.000000
330	5.413L-04	0.000000	.753010	0.000000	1.000000
340	5.577L-04	0.000000	.753010	0.000000	1.000000
350	5.741L-04	0.000000	.753010	0.000000	1.000000
360	5.905L-04	0.000000	.753010	0.000000	1.000000
370	6.070L-04	0.000000	.753010	0.000000	1.000000
380	6.234L-04	0.000000	.753010	0.000000	1.000000
390	6.398L-04	0.000000	.753010	0.000000	1.000000
400	6.562L-04	0.000000	.753010	0.000000	1.000000
410	6.726L-04	0.000000	.753010	0.000000	1.000000
420	6.890L-04	0.000000	.753010	0.000000	1.000000
430	7.054L-04	.246990	1.000000	0.000000	1.000000



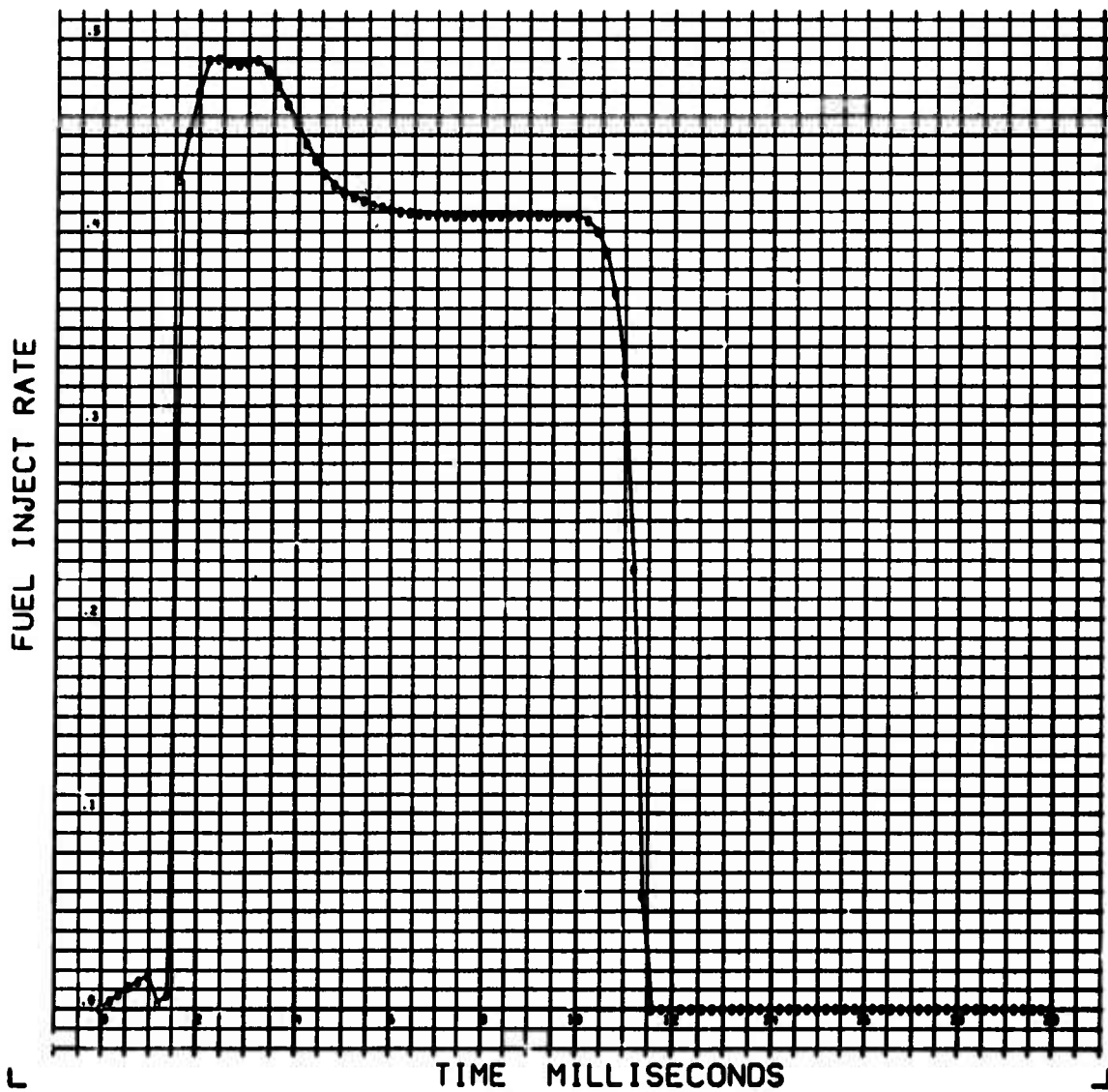
SERIAL A09760

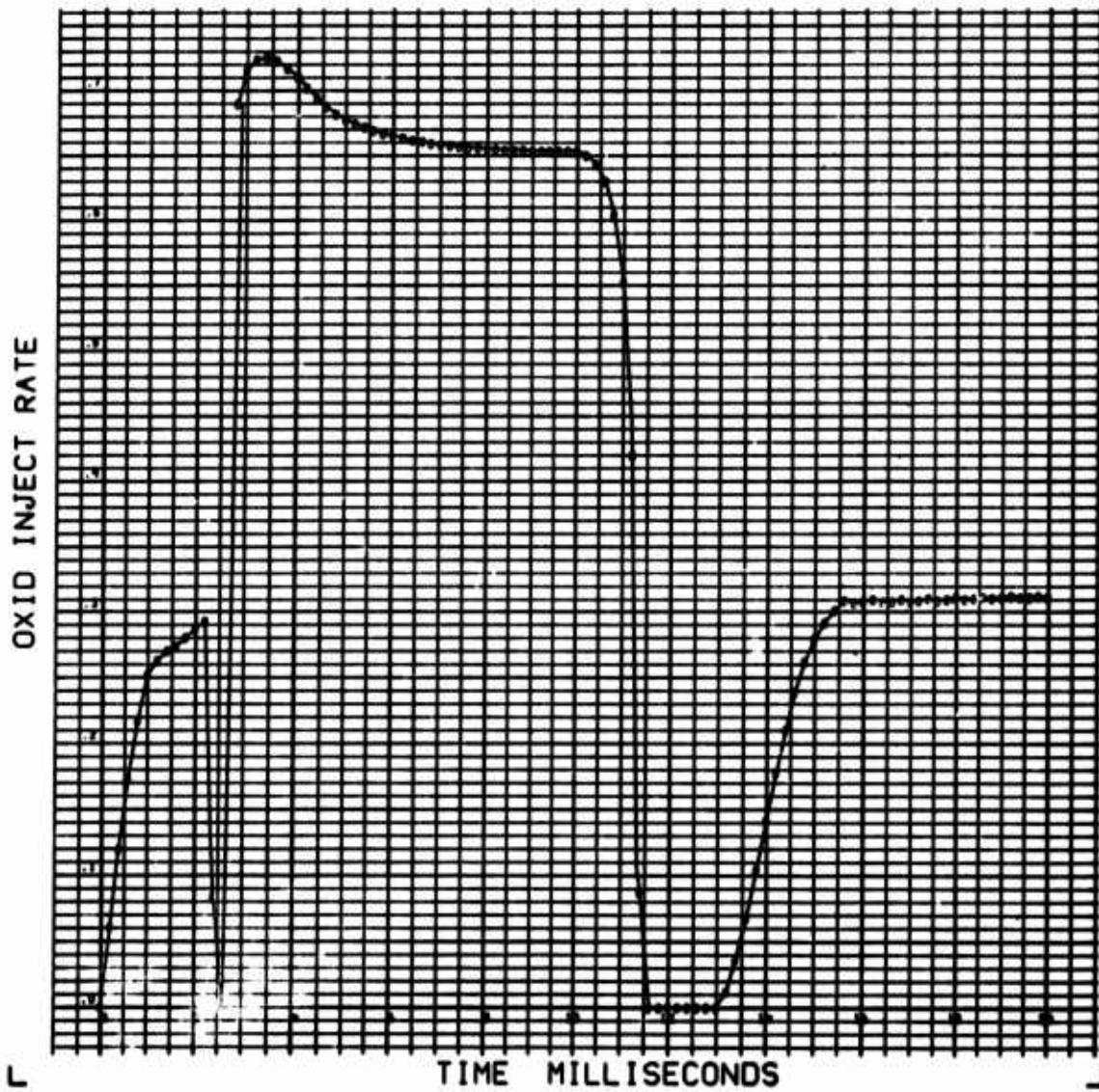
CHAMBER PRESSURE



TIME MILLISECONDS

SERIAL A05766

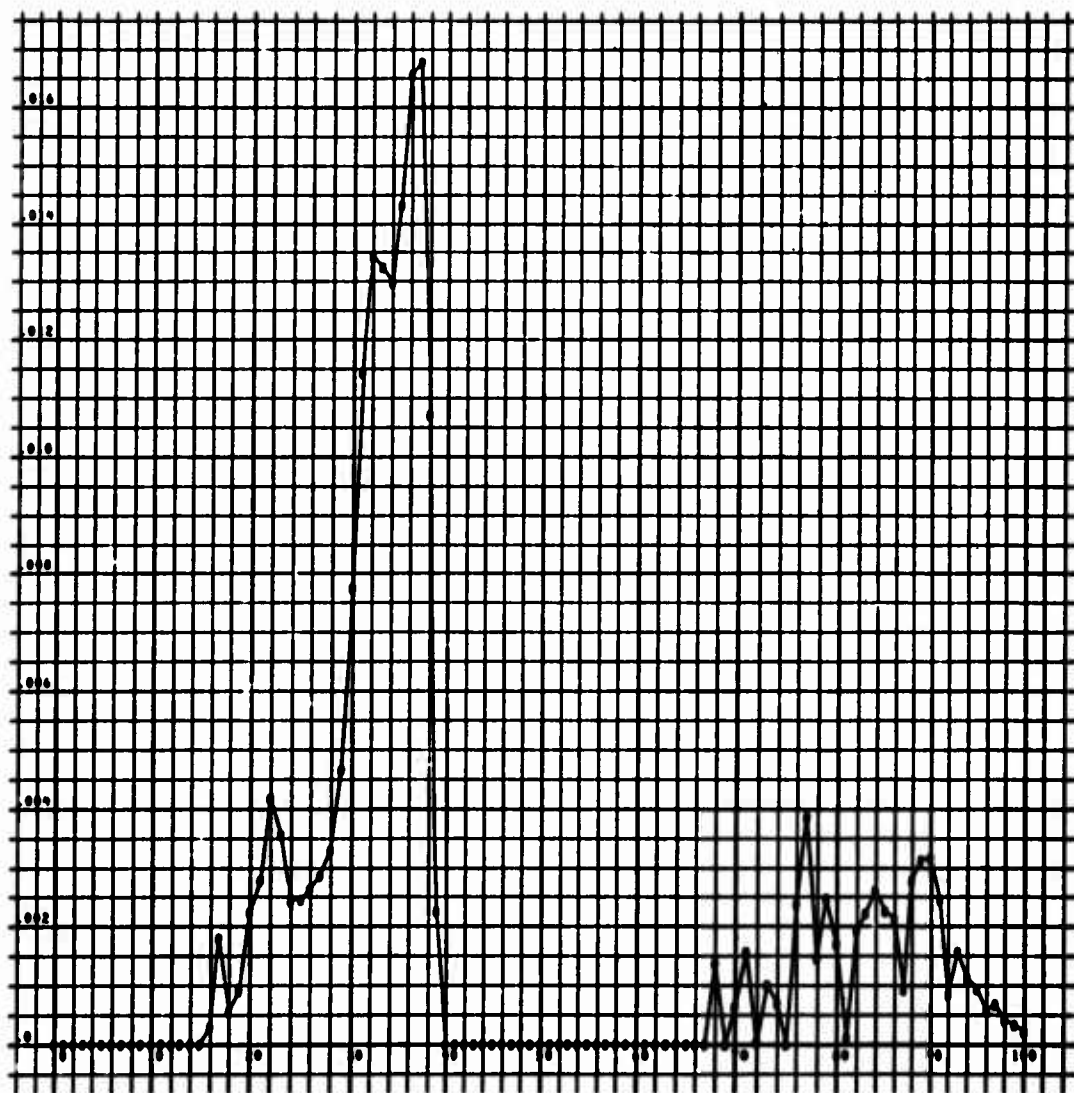




SERIAL A05766

10

FILM THICKNESS CM.

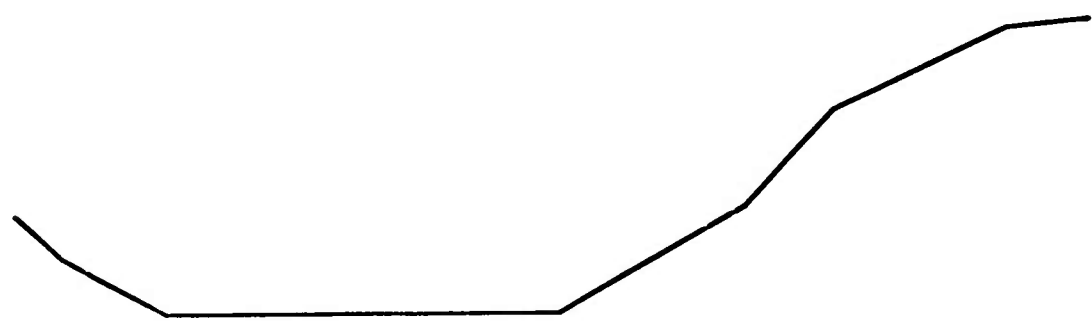
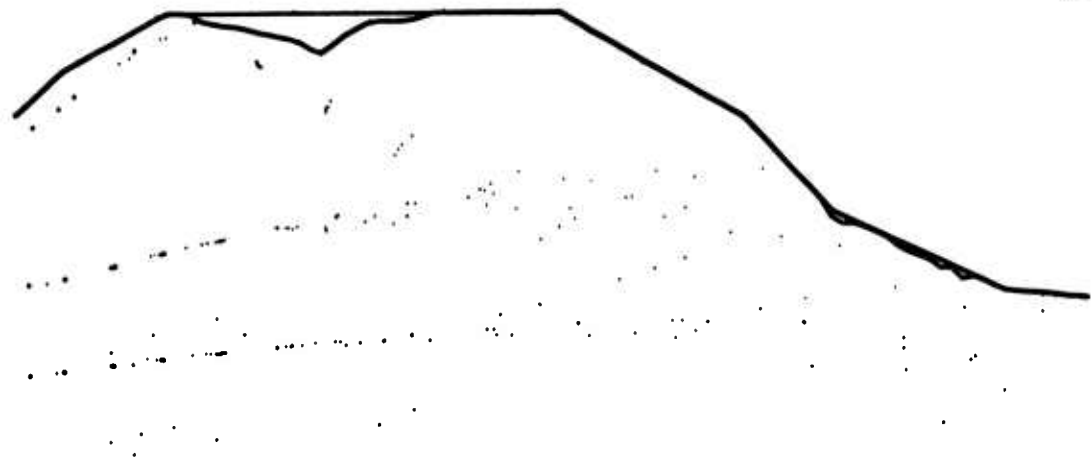


PCT CHAMBER LENGTH

「

1970 01/01

12 07
1970



Appendix B

MULTRAN

**MULTIPHASE NOZZLE AND PLUME TRANSPORT
COMPUTER PROGRAM**

**A Multiphase Nozzle and Plume Flow Field
Characterization Model**

Program Number H612

CONTENTS

B. 1	INTRODUCTION	341
	B. 1. a TD2	341
	B. 1. b TD2P	341
	B. 1. c SLINES	341
B. 2	ANALYSIS, INTEGRATION METHOD, AND SUBROUTINE STRUCTURE	341
B. 3	PROGRAM CELL LOADER STRUCTURE	344
B. 4	PROGRAM USER'S MANUAL	344
	B. 4. a TD2 Program Input	345
	B. 4. b TD2P Program Input	349
	B. 4. c TD2/TD2P Output Description	351
	B. 4. d SLINES Subprogram	356
B. 5	SAMPLE CASE	362

Appendix B

MULTRAN

MULTIPHASE NOZZLE AND PLUME TRANSPORT COMPUTER PROGRAM

A Multiphase Nozzle and Plume Flow Field Characterization Model

B.1 INTRODUCTION

The computer program described in this appendix is a subprogram to the Plume Contamination Effects Prediction Computer Program, CONTAM, and performs the subsonic, transonic, and supersonic computations required to define the steady-state multiphase flow field within a rocket nozzle and exhaust plume. The TCC program (Appendix A) provides the input to MULTRAN in terms of quasi-steady values of droplet distributions, and gas properties, averaged over specified portions of a transient engine pulse. The nozzle and plume flow field defined by MULTRAN provides the input data for the kinetics and condensation computation, KINCON (Appendix C), and subsequently for the deposition and surface efforts computations, SURFACE (Appendix D). MULTRAN may also be used as an independent computer program on any third generation computer with a core exceeding 120,000 words and a Fortran IV processor.

The MULTRAN program combines three previously independent programs:

- a. TD2, Axisymmetric Two-Phase Perfect Gas Performance Computer Program (developed by TRW for NASA/MSFC, reference B-1)
- b. TD2P, Axisymmetric Two-Phase Perfect Gas Plume Analysis Computer Program (developed by Dynamic Science and MDAC)
- c. SLINES, Streamline Generation Computer Program (developed by MDAC)

B.2 ANALYSIS, INTEGRATION METHOD, AND SUBROUTINE STRUCTURE

The axisymmetric two-phase analysis, numerical methods, and subroutine structure used in TD2, which also forms the basis for TD2P, is discussed in detail in Reference B-1; however, a very brief summary of the procedures given in the reference (as well as modifications necessary to treat contaminant transport) will be presented. The conservation equations of gas continuity, particle continuity, momentum, and energy in conjunction with the equations of the perfect gas law, particle drag and particle heat transfer

which govern an inviscid axisymmetric, two-phase mixture flow have been derived under the following assumptions:

- a. There are no mass or energy losses from the system
- b. The gas is inviscid except for its interactions with the condensed particles
- c. The volume occupied by the condensed particles is negligible
- d. The thermal (Brownian) motion of the condensed particles is negligible
- e. The condensed particles do not interact
- f. The condensed particle size distribution may be approximated by groups of different size spheres
- g. The internal temperature of the condensed particles is uniform
- h. Energy exchange between the gas and the condensed particles occurs only by convection
- i. The only forces on the condensed particles are viscous drag forces
- j. There is no mass transfer between the gas and the condensed phases.

The equations were put into the form of characteristic relationships in the reference where the characteristic directions are along gas streamlines, along gas mach lines, and along particle streamlines. It is found that the characteristics are real if the flow is supersonic ($M > 1$). Thus, the method-of-characteristics is used to compute the supersonic flow of a gas-particle mixture.

In the transonic flow region, however, solution for a gas-particle mixture is an extremely formidable task because the throat conditions are determined by the nozzle inlet geometry. Thus, to obtain initial conditions to start a characteristic calculation for a gas-particle system, the equations for the complete subsonic and transonic flow field in the nozzle inlet and throat regions must be solved. Qualitatively, it is found that the particle and gas streamlines diverge in the throat region, leading to the concentration of particles along the nozzle axis, greatly complicating the calculation of gas-particle flow properties in the nozzle throat. Mach number is found to be

less than one at the nozzle throat; hence, the transonic zone in a gas-particle flow extends downstream of the throat.

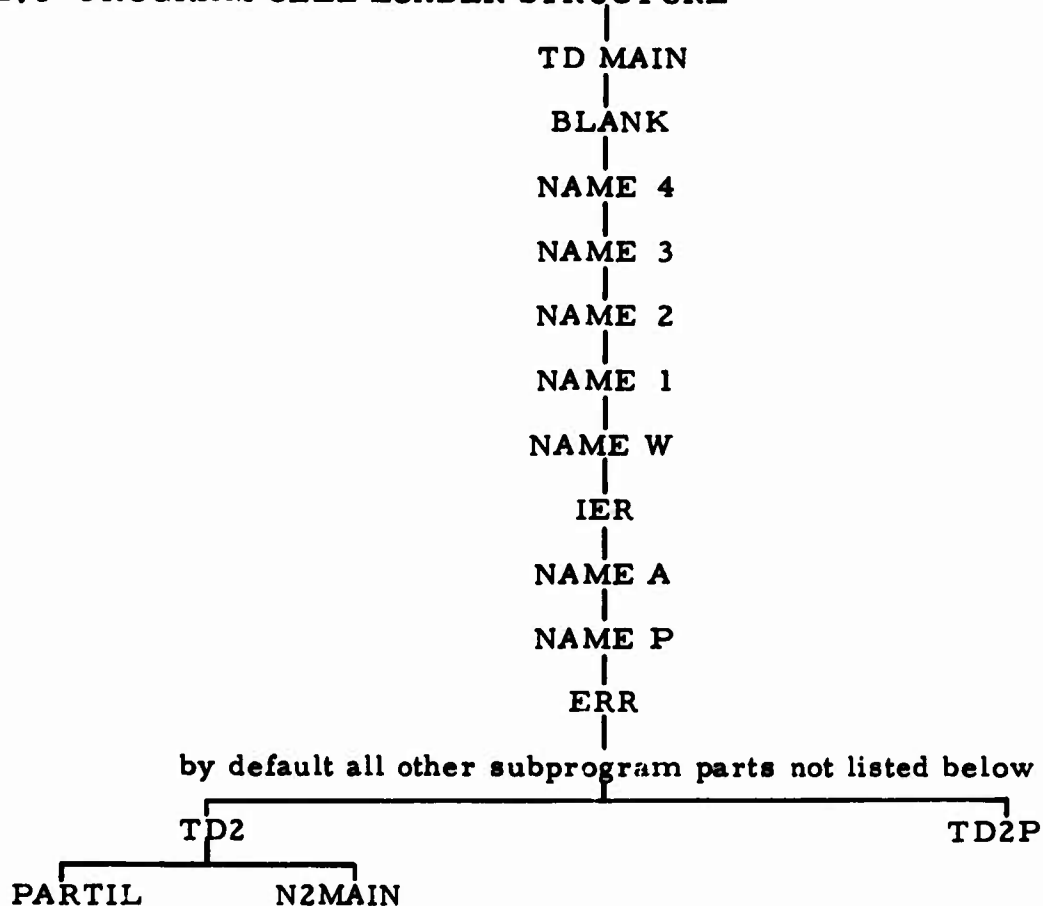
In view of the complexities involved, only approximate solutions to the equations governing the transonic flow of a gas-particle system can be obtained. In order to simplify the calculations, the nozzle inlet and throat geometry is assumed to consist of a conical inlet section joined smoothly to a constant radius of curvature throat section.

The following method as discussed in Reference B-1 is used to obtain approximate initial conditions for the characteristic calculations. In the conical inlet section, the flow is assumed to be a one-dimensional sink flow. The equations governing the one-dimensional flow of a gas-particle system are solved to obtain the flow properties on the sink line. The gas properties in the throat region are approximated by the perfect gas relationships, and particle trajectories are calculated through the throat region to determine the particle properties along the initial line. An average expansion coefficient is used which approximates the gas-particle expansion, including the effects of gas-particle nonequilibrium.

When adapting this method to contaminant transport predictions, certain modifications are necessary to better approximate the physical processes involved. Specifically, as discussed in Reference B-1, the particles in the nozzle inlet region are assumed to be directed with the gas in a one-dimensional sink flow (converging toward the axis). This assumption is reasonable for typical solid propellant engines where particle radii are usually less than 15μ and the gas-particle flow is near equilibrium. However, in the case of bipropellant exhausts, the unburned fuel and oxidizer droplets can range from 15μ to 100μ in radius and be far from equilibrium. The particle trajectories as computed up to the nozzle throat by the transient combustion chamber model TCC indicate that these large droplets travel in approximately straight lines parallel to the nozzle axis.

In order to better model bipropellant contaminant transport in the nozzle, the particle distributions and velocities are specified at the geometric throat from the TCC output. Particle trajectories are then computed from the throat to the supersonic start line assuming the velocity at the throat is parallel to the axis. The gas-phase properties in the transonic region are computed as before. An option is available for solid rocket exhausts which computes particles trajectories in the original manner as outlined in Reference B-1.

B.3 PROGRAM CELL LOADER STRUCTURE



B.4 PROGRAM USER'S MANUAL

This program was developed on the CDC 6500 computer using the FORTRAN IV language. Conversion to another computer system should be straightforward provided sufficient core storage (120,000 words) is available. The Program Cell Structure extends three levels deep including the executive level, when used as a subprogram to CONTAM: the MULTRAN driver program, TDMAIN, is used to define the overlay structure for common blocks that are the same in TD2 and TD2P.

The description of the input to and output from MULTRAN is divided into the following four subsections:

- B.4.a TD2 INPUT
- B.4.b TD2P INPUT
- B.4.c TD2/TD2P OUTPUT DESCRIPTION
- B.4.d SLINES Subprogram

A card listing for the complete input for the sample case is given in Subsection B.5

a. TD2 Program Input

The program input for the Axisymmetric Two-Phase Perfect Gas Performance Subprogram TD2 conforms to the I. B. M. NAMELIST format. All input items are read under control of the name \$DATA. The input items are divided into five types 1) Propellant Data, 2) Particle Data, 3) Inlet and Throat Parameters, 4) Characteristics mesh control data, 5) Nozzle Wall Contour Data.

For some input items, default values are assumed by the program. These items need not be input to the program if default values are desired.

\$DATA

(1) Propellant Data

<u>Item Name</u>	<u>Input Quantity</u>	<u>Units</u>
CAPN =	N, Viscosity temperature exponent	none
CPG =	C_{pg} , specific heat of gas at constant pressure	$\text{ft}^2/\text{sec}^2 \cdot R$
CPL =	C_{p_l} , particle heat capacity ($T_p > T_{p_m}$).	$\text{ft}^2/\text{sec}^2 \cdot R$
CPS =	C_{p_s} , particle heat capacity ($T_p < T_{p_m}$).	$\text{ft}^2/\text{sec}^2 \cdot R$
GAMMA =	γ , specific heat ratio, C_{pg}/C_{gv} .	none
GMGO =	μ_{g_o} , chamber gas viscosity coefficient	lb/ft sec
HPL =	h_{p_l} , liquid particle enthalpy ($T_p = T_{p_m}$).	ft^2/sec^2
HPS =	h_{p_s} , solid particle enthalpy ($T_p = T_{p_m}$).	ft^2/sec^2
ISOLID =	1, solid rocket exhaust 0, contaminant transport (default value)	none

<u>Item Name</u>	<u>Input Quantity</u>	<u>Units</u>
PC =	P_{g_o} , chamber pressure.	PSIA
PR =	P_r , Prandtl number.	none
RCAP =	R, gas constant.	$\text{ft}^2/\text{sec}^2 \cdot \text{R}$
SMP =	m_p , particle density.	lb/ft^3
TG0 =	T_{g_o} , chamber temperature	$^{\circ}\text{R}$
TPM =	T_{p_m} , particle solidification temperature.	$^{\circ}\text{R}$

(2) Particle Data

<u>Item</u>	<u>Input Quantity</u>	<u>Units</u>
R(1) =	r_{p_j} , the radius of each of n particles is to be input so that $r_{p_1} < r_{p_2} \dots < r_{p_n}$ set $r_{p_{n+1}} = 0$. n < 10 is required.	ft
WPWGT =	$\Sigma \dot{w}_{p_j} / \dot{w}_g$, ratio of particle to gas weight flow.	none
WPWT(1) =	$\dot{w}_{p_j} / \Sigma \dot{w}_{p_j}$, particle weight flow fractions corresponding to each of the above particle sizes, r_{p_j} .	none

(3) Inlet and Throat Parameters (Figure B-1)

<u>Item Name</u>	<u>Input Quantity</u>	<u>Units</u>	<u>Assumed Value</u>
DZI =	Δz , particle trajectory integration step size.	none	0.002
DZMIN =	Δz_{\min} , inlet step size parameter.	none	0.002
NILP =	N_i , number of initial line points.	none	15
RRT =	R_c , throat radius of curvature. A value $R_c \geq 2$ is required.	none	

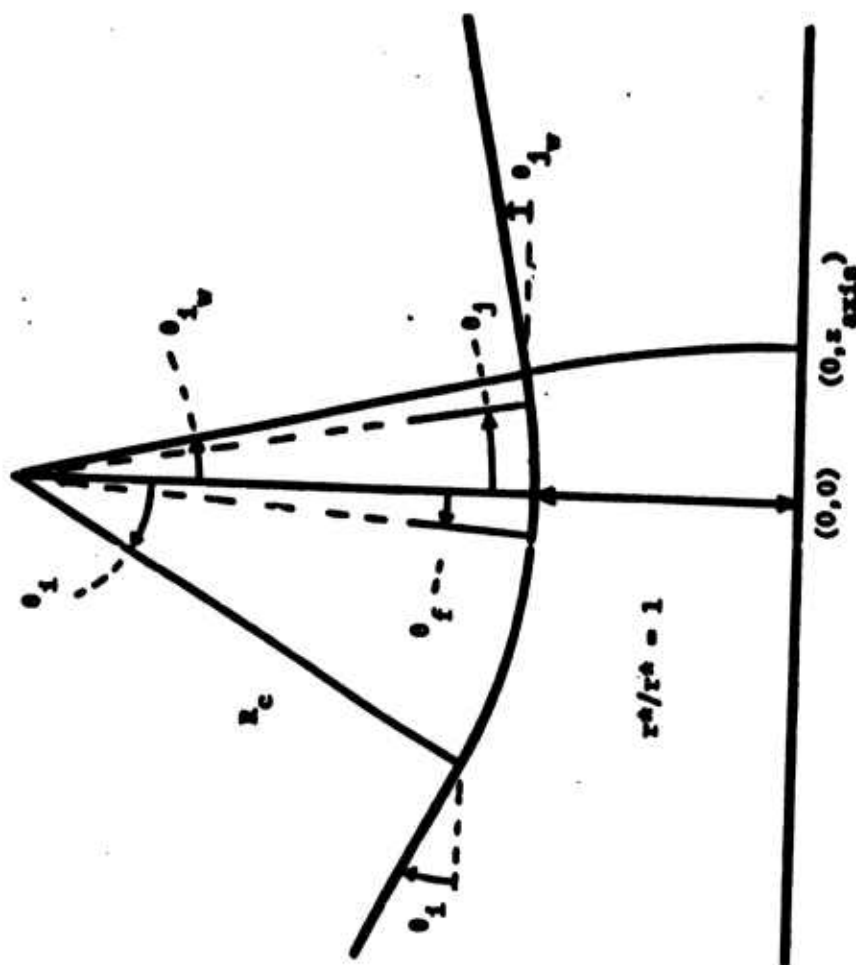


Figure B-1. Inlet and Throat Parameters

<u>Item Name</u>	<u>Input Quantity</u>	<u>Units</u>	<u>Assumed Value</u>
RT =	r^* , throat radius	ft	
SAUR(1) =	First estimates of x_o , u_o , α , β , and γ for the special throat expansion. Required only if $\theta_i > \theta_f$.	none	-0.15, 1, 0.5, 0.3, -1
THFD =	θ_f , faring angle ($\theta_f > \theta_i$ = no faring).	degrees	5.0
THID =	θ_i , inlet angle	degrees	
THIW =	θ_{i_w} , intersection of initial line and wall.	degrees	12.0
THJD =	θ_j , angle defining the zone farthest downstream	degrees	9.0
VAR(1) =	First estimates of x_o , u_o , α , β , and γ for the zone farthest upstream	none	0.3, 0, 0, 0.1, 0.1
ZAX =	z_{axis} , intersection of initial line and axis	none	
ZI =	n_i , number of upstream zones.	none	3.0
ZJ =	n_j , number of downstream zones.	none	2.0

(4) Characteristics Mesh Control Data

<u>Item Name</u>	<u>Input Quantity</u>	<u>Units</u>	<u>Assumed Value</u>
DL =	Δl , maximum LRC mesh width.	none	0.2
DTWI =	$\Delta \theta_w$, maximum flow angle change along the wall.	degrees	3.0
DR =	Δr , maximum RRC mesh width.	none	0.2
EW =	ϵ_w , end of nozzle wall criterion.	none	0.001
IMAX =	i_{max} , maximum number of iterations per mesh point.	none	5.0
N1 =	n_1 , select each n_1^{th} LRC for print.	none	1,000
N2 =	n_2 , print each n_2^{th} point on selected characteristics.	none	1.0

(5) Nozzle Wall Contour Data

<u>Item Name</u>	<u>Input Quantity</u>	<u>Units</u>
IWALL =	Option flag.	none
	0=> tabular input	
	1=> cone	
	2=> parabola	
	3=> circular arc	

If the wall is to be input in tabular form (IWALL = 0):

PW(1) = (r_i, z_i) , wall coordinates $i = 1, 2, \dots, n$ points. none
viz.: PW(1) = $r_1, z_1, r_2, z_2, \dots, r_n, z_n, 0, 0$.

Note:

(a) always mark the end of the table with two zeros.

(b) $n \leq 79$ is required.

If a cone, parabola, or circular arc contour is to be specified then:

THJW = θ_{j_w} , attachment angle for the contour; e.g., for a cone, the conical half angle. degrees

EPS = ϵ , nozzle expansion ratio (cone only). none

RWMAX = r_{\max} , nozzle exit radius (parabola or arc only). none

ZWMAX = z_{\max} , nozzle length from throat to exit (parabola or arc only). none

\$ END OF CASE.

NOTE:

A case is defined as the data included or implied between the \$DATA card and the \$ signifying the end of case. Whenever a value is input as data for a case, that value will remain set for succeeding cases until a new value is input. The values indicated as assumed by the program hold only until a different value is input. If more than one value is input for a given quantity within a case, the last value given will be used.

b. TD2P Program Input

The program input for the Axisymmetric Two-Phase Perfect Gas Plume Analysis computer subprogram is an extension of the input to the TD2 computer subprogram. Input to the TD2P computer subprogram consists of a binary start tape ((TAPE 8) or an extend disc storage file (TAPE 8) generated by the TD2 computer subprogram. The same NAMELIST data deck used for the TD2 calculation must be used for the TD2P calculation and is read from TAPE 8 automatically. The following input items must be inserted into the data deck following the TD2 data. Additional data for the TD2P subprogram is read under control of the name DATAP.

\$ DATAP

<u>Item Name</u>	<u>Input Quantity</u>	<u>Units</u>
PMA =	θ_{PM} , The Prandtl-Meyer expansion angle to be used at the nozzle lip.	degrees
NPM =	The number of Prandtl-Meyer points to be generated.	none
	NPM < 0 The maximum number (98-IP) of points will be generated.	
	NPM = 0 Points will be generated one degree apart unless less than 5 points would result.	
	NPM > 0 This number of points will be generated unless the maximum would be exceeded. If the maximum would be exceeded, points are placed one degree apart unless this would again exceed the maximum or would result in less than 5 points.	
ZMAX =	This item defines a cutoff plane for the calculations. The run will be terminated when an axis point is calculated located downstream of $Z = ZMAX$.	none
PCUT =	If a Pressure, P_g , is calculated such that the ratio P_g/P_{g0} drops below this value, no more points will be calculated on the characteristic.	none

<u>Item Name</u>	<u>Input Quantity</u>	<u>Units</u>
NPLOT =	Flag for auxiliary radiation output on tape unit 9, (see Description of Program Output). NPLOT = 0 deletes this output. NPLOT = 1 requests this output.	none
AREA =	Flag for auxiliary force field output on tape unit 9. This item is also used to represent the frontal surface area of a body in the plume, (see Description of Program Output). AREA = 0 deletes this output. AREA > 0 requests this output e. g., AREA = 1.	in. ²
EMIS =	ϵ_p , particle emissivity used for the radiation printout.	none
C1 =	C ₁ , force coefficient used for the force printout.	none
C2 =	C ₂ , force coefficient used for the force printout.	none

REMARKS

If the mesh width control items DL and DR have been input as part of the NAMELIST DATA deck, these items should be deleted for the plume input. The TD2P computer program will then assume values for these variables, minimizing the mesh points.

The last item printed at the end of a complete TD2 calculation is the item IP = nm, where nm is number of points used along the last running characteristic. Reference should be made to this number to determine if sufficient space is available (98-IP) for the Prandtl-Meyer expansion.

The TD2P computer subprogram is not suitable for running consecutive cases.

c. TD2/TD2P Output Description

Program output may be viewed in detail by examining the sample case in Section B. 5. The program output follows the sequence listed below:

For the one-dimensional inlet and the axisymmetric transonic throat calculations

- (1) The values k and \dot{m}_g for gas-particle equilibrium.
- (2) Initial and final conditions for the one-dimensional inlet integration.
- (3) Converged values for x_o , u_o , α , β , γ and f_1 , f_2 , f_3 , f_4 , f_5 for each transonic flow zone.
- (4) The corrected estimate for k , corrected values for x_o , u_o , α , β , and γ in the transonic zone containing the initial supersonic data line, corrected values for \dot{m}_g and \dot{m}_{pj} .
- (5) Items 2, 3, and 4 are iterated twice.
- (6) The gas-particle flow properties P_g , ρ_g , u_g , v_g , r , z , h_{pj} , ρ_{pj} , u_{pj} and v_{pj} along the initial supersonic data line.

For the supersonic method of characteristics calculations for the nozzle and plume, printout may occur after the completion of each mesh point calculation. Points for print are selected as follows:

The following points are always printed:

axis points.

Kth particle boundary points.

initial line points.

wall points.

Interior points are selected for print only along every n_1^{th} left running characteristic and only at every n_2^{th} position along these characteristics.

Inserted points are printed if all points are to be printed ($n_1 = n_2 = 1$).

The items printed are listed below in the order they appear, left to right, on the output sheet. A header is printed for identification purposes above each characteristic.

Row One:

<u>Item</u>	<u>Header</u>	<u>Meaning</u>	<u>Units</u>
LRC number	LRC	Left running characteristic number.	none
Ident. number	ID	Type of point (see below).	none
r	R	r position coordinate.	none
z	Z	z position coordinate.	none
M	MACH	Mach number.	none
T_g	TG	Gas temperature.	°R
V_g	VG	Gas velocity (scalar).	ft/sec
θ_g	THETA-G	Gas streamline angle	degrees
T_g / T_{g0}	TG/TG0	Ratio of gas temperature to chamber temperature.	none
P_g / P_{g0}	PG/PG0	Ratio of gas pressure to chamber pressure.	none
ρ_g / ρ_{g0}	DG/DG0	Ratio of gas density to chamber density.	none
$\sum^k \rho_{pj} / \rho_g$	SDK/DG	Ratio of total particle density to gas density.	none
C_F	CF	Thrust coefficient.	none
I_{sp}	ISP	Specific impulse.	sec.
iteration no.	IT	Number of iterations required.	none

Rows Two through K+1

A row is printed for each particle size, $k=1, \dots, K$.

<u>Item</u>	<u>Header</u>	<u>Meaning</u>	<u>Units</u>
k	K	Particle size number.	none
Re_k	REK	Particle Reynolds number	none
V_{pk}	VPK	Particle velocity (scalar).	ft/sec

<u>Item</u>	<u>Header</u>	<u>Meaning</u>	<u>Units</u>
θ_{pk}	THETA-K	Particle streamline angle.	degrees
T_{pk}	TPK	Particle temperature.	°R
ρ_{pk}/ρ_g	DPK/DG	Ratio of particle density to gas density.	none
ρ_{pk}/ρ_{p0}	DPK/DP0	Ratio of particle density to chamber particle density.	none
r_{pk}	RPK	Particle radius	ft

d. Additional Output

Table B-1 illustrates additional output options as discussed above.

(1) Force Field Print

If the force field auxiliary output is requested (AREA > 0) the following items will be computed and written on tape unit 9.

<u>Item</u>	<u>Units</u>
$F_g = \frac{C_1 A}{144g} \frac{\gamma}{2} P_g M^2$	lb _f
$F_{pk} = \frac{C_2 A}{144g} \rho_{pk} V_{pk}^2$	lb _f
$F_p = \sum_{k=1}^{k_{max}} F_{pk}$	lb _f
$F = F_g + F_p$	lb _f
F_p/F_g	None

The quantities C_1 and C_2 (which are nondimensional force coefficients) and A (which is surface area in square inches) are input as $C1$, $C2$, and $AREA$.

(2) Radiation Print

If the radiation auxiliary output is requested (NPLØT = 1) the following items will be computed and written on tape unit 9.

Table B-1. OPTIONAL OUTPUT - RADIATION AND FORCEFIELD PROPERTIES

[illegible]

<u>Item</u>	<u>Header</u>	<u>Meaning</u>	<u>Units</u>
<u>Row 1:</u>			
LRC number	LRC	Left characteristic number.	none
Ident. number	ID	Identification code.	none
r	R	r, radial coordinate	none
z	Z	z, axial coordinate	none
Rows 1 through k_{\max} (i. e., for each particle size $k = 1, \dots, k_{\max}$):			
N_{Pk}	NPK	Particle number density	number of particles/ft ³
q_1	RAD PK		BTU/sec
q_2	RAD BAR PK		BTU-number of particles/sec
\bar{T}_{Pk}^4	TPK 4		°R ⁴
Row $k_{\max} + 1$:			
\bar{T}_p^4	TBAR 4	Effective particle temperature	°R ⁴

where:

$$N_{Pk} = \frac{\rho_{Pk}}{\frac{4}{3} \pi r_{Pk}^3 m_p}$$

$$q_1 = \epsilon_p \sigma T_{Pk}^4 r_{Pk}^2$$

$$q_2 = \epsilon_p \sigma T_{Pk}^4 r_{Pk}^2 N_{Pk}$$

$$\sigma = 0.475834 \times 10^{-12} \text{ BTU/ft}^2\text{-sec-}^\circ\text{R}^4$$

$$\bar{T}_p^4 = \frac{\sum_{k=1}^{k_{\max}} T_{Pk}^4 N_{Pk} r_{Pk}^2}{\sum_{k=1}^{k_{\max}} N_{Pk} r_{Pk}^2}$$

d. SLINES Subprogram

This computer subprogram, SLINES, was developed to provide the necessary interface between the TD2 and TD2P subprograms and the KINCON subprogram. Basically, the program interpolates from data points on the characteristic lines (TD2 and TD2P results) to determine points of constant percentage of mass flow (bounded by axis and point of interest) running through the throat, nozzle, and plume.

Subsection (1) lists the program variables FORTRAN names, symbols, and definitions. Subsection (2) discusses the program logic interpolation equations and editing technique. Subsection (3) provides the user with the necessary operating information. Subsection B.5 provides input and output for a sample case of the MULTRAN program, which includes the output from SLINES (last portion).

(1) FORTRAN Variables

The FORTRAN names given are the names used throughout the program. The symbols are used in the text of this document.

<u>FORTTRAN NAME</u>	<u>SYMBOL</u>	<u>DEFINITION</u>
Z	Z	The axial distance of a point on a streamline.
R	R	The radial distance of a point on a streamline.
P	P	The pressure at a point on a streamline.
S	S	The distance from the initial point on a streamline to a given point on a streamline.
T	T	The temperature at a point on a streamline.
V	V	The velocity of the gas at a point on a streamline.
KD	i	The i^{th} point along a streamline. ($1 \leq i \leq n$)
JD	n	The total number of points along a streamline before editing.
ID	j	The streamline identification number. ($1 \leq j \leq m$)
NSL	m	The total number of streamlines.
K	k	A given point on a characteristic line. ($1 \leq k \leq \text{NPTS}$)

<u>FORTTRAN NAME</u>	<u>SYMBOL</u>	<u>DEFINITION</u>
NPTS	-	Total number of points on a given characteristic line.
N	N	The number of points on a streamline in the throat only.
PCM	η	The percentage of normalized integrated total mass flow pertaining to the point on a characteristic line.
PCS	ϵ	The percentage of normalized integrated total mass flow criteria for a streamline.
Z, R, P, S, T, V ZMGKS, RMGKS, PMGKS, TMGKS, VMGKS	X	The class of parameters pertaining to the properties of a point on a streamline or characteristic line. Each parameter is defined elsewhere in this glossary.
DSK	ΔS	The streamline distance criteria used in editing.
SX	S^{np}	The distance of the streamline from the supersonic start line through the nozzle and plume.
SID	-	The name of the namelist through which the user input data is provided.
TØTM	-	The integrated total mass flow along a characteristic line.
ZMGKS	-	The axial distance at a point on a characteristic line.
RMGKS	-	The radial distance at a point on a characteristic line.
PMGKS	-	The pressure at a point on a characteristic line.
TMGKS	-	The temperature at a point on a characteristic line.
ZINIT	-	The distance of the initial point on a streamline (ZINIT = S (j, 1) = 0).
PINIT	-	The pressure at the initial point of a streamline.

<u>FORTTRAN NAME</u>	<u>SYMBOL</u>	<u>DEFINITION</u>
TINIT	-	The temperature at the initial point of a streamline.
VINIT	-	The gas velocity at the initial point of a streamline.
MGKSK	-	The total number of points on a streamline after editing.
EXIT	-	The streamline distance of the last point on a streamline [EXIT = S(j, MGKSK)].

(2) Program Description

The program runs on the CDC 6500 computer system. It is written in FORTRAN IV and requires a field length less than 40,000g. A nominal case providing ten streamlines will require less than 7 central processor seconds and less than 20 peripheral processor seconds to execute.

The program includes five distinct functions:

1. Input
2. Streamline Location
3. Data Interpolation
4. Data Editing
5. Output

Each function is discussed in the subsequent paragraphs.

(a) Data Input

Two sources are required for data input: cards via NAMELIST which is user data allowing the program to know how many streamlines are desired and the percent mass flowing within a cylinder bounded by each streamline; and logical file TAPE 12 (tape or disc) which provides the program with data from the TD2 and TD2P subprograms on which to operate.

The data from the TD2 and TD2P subprograms consists of two records for each characteristic line. The first record tells how many points are on the characteristic line and the total integrated mass associated with the characteristic line. The second record contains the data designating the location, pressure and percentage of the normalized integrated total mass flow for each point on the characteristic line. The first requirements of the program is to provide initial temperature and velocity properties of each streamline. Therefore, the initial characteristic line has an additional record of data associated with it which gives the temperature and velocity properties associated with each point on the initial characteristic line. This

record follows the first two records, in order. The last record of both the TD2 and the TD2P subprograms contain a one word, negative number, record. This permits the program to know when there are no more characteristic lines provided by the respective programs.

(b) Streamline Location

The definition of a streamline is that line which runs through the throat, nozzle, and plume bounding a given constant percentage of the mass flow between it and the nozzle axis.

There are a discrete number of points on a characteristic line. The properties at any point usually will not meet the criteria for a point on the desired streamline, therefore, interpolation must be performed between the two input data points which bound the desired point on the streamline in order to obtain the necessary properties (location and pressure) on the streamline.

The initial point, with regard to distance along a streamline, is designated as the interpolated point on the initial TD2 subsonic start line. Each subsequent streamline point has a distance corresponding to:

$$S_i = S_{i-1} + \left[(Z_i - Z_{i-1})^2 + (R_i - R_{i-1})^2 \right]^{1/2}$$

where

S = the distance along the streamline

Z = axial distance along the streamline

R = radial distance along the streamline

i = the i^{th} point along the streamline ($1 \leq i \leq n$)

n = the total number of points along the streamline

As previously stated, $S_1 = 0$.

(c) Data Interpolation

Linear interpolation is used to locate a streamline point as follows:

$$X_{ji} = X_{k-1} + \left[\frac{\epsilon_j - \eta_{k-1}}{\eta_k - \eta_{k-1}} \right] \left[X_k - X_{k-1} \right]$$

where:

- X = the required streamline property (location, pressure, mass, etc.)
- ϵ = the percentage of normalized integrated total mass criteria for the streamline
- η = the percentage of normalized integrated total mass pertaining to the points on the characteristic line
- k = the point on the characteristic line having the greater value and bounding the streamline value
- k-1 = the point on the characteristic line having the lesser value and bounding the streamline value
- i = the i^{th} point along the streamline ($1 \leq i \leq n$)
- n = the total number of points along the streamline
- j = the streamline identification number ($1 \leq j \leq m$)
- m = the total number of streamlines

(d) Data Editing

There exists two reasons for editing the streamline data before output:

1. Due to the change in the nature of the characteristic lines at the supersonic start line in conjunction with the logic used previously in the program, there exists a redundant point along the axis streamline at the supersonic start line. This redundant point must be removed.
2. The KINCON program will accept a maximum of 101 data points for each streamline.

To locate the redundant point along the axial streamline, the points along that streamline are searched until two points are found which have no separation distance. The redundant point and its associated properties are removed from that streamline. In addition, the location of that point provides information as to the location of the supersonic start line and the number of points in the throat, along the streamline, which will be required for use in subsequent editing.

It is desirable that each point and its relevant properties along each streamline in the throat be provided as input to the KINCON program. Therefore these data are not edited. The remaining points along

the streamline, in the nozzle and plume, must be edited by some criteria which will limit the total number of points along the streamline to not more than 101. The criteria chosen is such that each point (exclusive of the last two points) in the nozzle and plume shall be separated by at least some distance determined by:

$$\Delta S_j = \frac{S_j^{np}}{100 - N_j}$$

where

ΔS = the distance criteria for editing

S^{np} = the distance of the streamline from the supersonic start line through the nozzle and plume

N = the number of points along the streamline through the throat to the supersonic start line

j = the streamline identification number

The last point along the streamline is always made available for output regardless of its distance from the previous point.

(e) Output

The output of this program is both printed and written onto a logical file (TAPE 8). The printed output is provided for the scrutiny of the user. The TAPE 8 file output is for use as input to the KINCON program. The written data contains only that information which is necessary for the operation of the KINCON program. The printed output provides the same data as the TAPE 8 file output but also contains other pertinent data which allows the user to determine the validity of the data. A sample of the printed output may be found in Subsection B. 5.

(3) Program User's Manual

Input to the computer program is divided into two subsections:

(a) NAMELIST/SID

(b) Logical File

Written output from the computer program is on logical file unit number 8. The sample case provided in Subsection B. 5 details the loadsheets for the NAMELIST card, and computer output.

(a) NAMELIST/SID

The NAMELIST feature permits the input of parameters without a format specification. The NAMELIST/SID contains two parameters:

1. NSL; the number of streamlines for which the program is to provide data.
2. PCS; an array of up to ten mass % values which provide the criteria for the streamline definition. The variable NSL determines the number of values which must be input.

The two permissible formats for PCS are:

1. PCS(1) = a, b, c,, j where a through j are the quantities corresponding to the PCS criteria.
2. PCS(2) = b, PCS(1) = a, PCS(4) = d, PCS(5) = e, PCS(7) = g, PCS(3) = c, and so on.

(b) Logical Files

The logical file input may be either tape or disc file. The unit number for the logical file is 12. This means that the logical file name used on the REQUEST or ATTACH card must be TAPE 12. The data on the logical file is provided from the TD2 and TD2P programs. The data is binary (unformatted).

B.5 SAMPLE CASE

Included in the section are the computer input and output for a sample case using the MULTRAN program as an independent program. The subprograms to MULTRAN, which are called sequentially are TD2, TD2P and SLINES. The use of MULTRAN as a subprogram to CONTAM for the analysis of contaminant transport is illustrated in Section 4 at the main text. To illustrate the use of MULTRAN as an independent program for other than bipropellant contaminant transport analysis, the sample case in this section is for a solid rocket motor nozzle and plume.

The calculation is performed for a typical solid propellant engine operating at a chamber pressure of 2,250 psia whose exhaust contains 13.6% Al_2O_3 by weight. The particle size distribution was obtained from experimental data of Radke, Delaney and Smith (Reference B-2). Six particle sizes are assumed with radius yielding weight flows as follows:

<u>Particle Size (ft x 10⁶)</u>	<u>Weight Fraction of Total Particles</u>
4.92	0.0214
9.84	0.1180
16.32	0.2390
22.90	0.3260
29.40	0.2344
36.20	0.0612
	1.0000

A complete set of Control Cards and Data Cards for the sample case are listed preceding the sample case.

B.6 REFERENCES

- B-1. G. R. Nickerson and J. R. Kliegel. Axisymmetric Two-Phase Perfect Gas Performance Program, TRW Systems Report No. 02874-6006-R000, Vol. I and II, April 1967.
- B-2. H. H. Radke, L. J. Delaney, and Lt. P. Smith. Exhaust Particle Size Data from Small and Large Solid Rocket Motors. San Bernardino Operations, Aerospace Corporation, Report No. TOR-1001 (S2951-18)-3, July, 1967.

17.28.46. AGO5202
 17.28.47.000070 CARDS READ
 17.28.47.3647.00002
 17.28.47.4612.5,450,530,300,70000,120000,
 17.28.47.10A0502 H -YANOW 00103700004104 40M607A 943248001
 17.28.47. REQUEST,SAVE,MI, (RESERVE)
 17.28.47. SAVE
 17.28.47. (20 ASSIGNED, REEL 55304)
 17.28.47. REQUEST,CON423,MI, (50207)
 17.29.05. (25 ASSIGNED, REEL 50207)
 17.29.05. REQUEST,H612CL,PF,
 17.29.05. REQUEST,NPR,PF,
 17.29.06. REWIND(CON423,SAVE)
 17.29.06. SKIPF(CON423,1,17)
 17.29.06. COPY8PT(CON423,NPR)
 17.29.22. RETURN(CON423)
 17.29.22. REWIND(NPR)
 17.29.22. MPL120000,
 17.29.22. DECIMAL-CP= 000 SEC.,PP= 020 SEC.,OCTAL=FL=070K,
 17.29.29. CELL(P=0)
 17.29.30. CELL DONE .308 CP SEC
 17.29.30. LOADER(CELOADR)
 17.29.30. NPR(CELL=H612CL)
 17.30.24. LOAD TIME 15.684 CP SEC
 17.36.00. STOP
 17.36.00. CURRENT PRU COUNT = 089
 17.36.03. CP 527.332 SEC,
 17.36.03. PP 137.466 SEC.
 17.36.03. MU 000.077
 AGO5202:000100 LINES PRINTED.

[illegible]

[illegible]

ZAX	=	0.8E+00,
ZI	=	0.3E+01,
ZJ	=	0.2E+01,
DZ1	=	0.2E+02,
IORDER	=	3,
ROWCON	=	0.0,
ISW1	=	0,
ISW2	=	0,
ISW3	=	0,
VAR	=	0.3E+00, 0.0, 0.0, 0.1E+00, 0.1E+00, 0.0,
FLAG	=	0.0,
TMJD	=	0.9E+01,
SAUR	=	-0.15E+00, 0.1E+01, 0.5E+00, 0.3E+00, -0.1E+01, 0.0,
TMFD	=	0.5E+01,
EPS	=	0.744E+01,
RHMAX	=	0.0,
ZHMAX	=	0.0,
IWALL	=	1,
TM1H	=	0.12E+02,
TMJ4	=	0.21E+02,
NTAPE	=	0,
SEND		

ROUTING OF TWO PHASE NOZZLE PROGRAM

CP TIME = 17.876 PP TIME = 114.208

GAS-PARTICLE FLOW (THROAT)

K BAR=1.1920711 WDB= 3332.313 EQUILIBRIUM CONDITIONS,
ONE DIMENSIONAL FLOW
Z0= -4.7154 MAX= -2.6697 STEP SIZE= .002000 U0= 423.346 YPI0= 6243.979 AG= 7.0920

Z0 -2.6697 A/AT= 1.91000 U0= 1416.955 UP(1) TP(1) K(1) L(1) 101.111 6
1277.097 0100.104 .07248 .00944 1330.710 0100.122 .73913 .72071
1271.853 0192.766 .09760 .00960 1219.674 0195.015 .06077 .01797
1179.875 0198.249 .03268 .78267 1146.351 0200.179 .00905 .75349

ITERATION NUMBER 3 1 VAR(1) F(1)
1 -1.4206234E+01 0.103097E+02
2 1.000000E+00 -1.500020E+07
3 4.032440E+01 -1.194304E+06
4 1.009247E+01 -2.497209E+06
5 -0.133400E+01 -5.429673E+08

ITERATION NUMBER 3 1 VAR(1) F(1)
1 1.001000E+01 1.313070E+08
2 3.744210E+01 4.002025E+09
3 3.136642E+01 -9.003210E+09
4 1.000000E+01 0.
5 4.002553E+01 0.

ITERATION NUMBER 3 1 VAR(1) F(1)
1 1.1992400E+01 4.437432E+07
2 5.202170E+01 -3.035533E+07
3 0.430921E+01 -1.076331E+08
4 3.017663E+01 0.
5 1.914239E+01 0.

ITERATION NUMBER 3 1 VAR(1) F(1)
1 -7.110120E+02 2.623500E+07
2 1.000000E+01 -1.076331E+07
3 4.021440E+01 4.397503E+08
4 4.403303E+01 0.
5 -0.140044E+01 0.

ITERATION NUMBER 6 1 VAR(1) F(1)
1 -3.017707E+01 1.100170E+07
2 1.077695E+00 -2.056725E+07
3 4.944704E+01 -3.936771E+07
4 1.137833E+01 -7.180030E+07
5 -7.090110E+01 -1.703261E+06

ITERATION NUMBER 3 1 VAR(1) F(1)
1 -3.030644E+01 4.584574E+07
2 1.214032E+00 -5.091102E+06
3 1.000000E+01 1.310002E+08
4 2.000000E+02 -0.036294E+08
5 -5.030420E+01 6.342695E+06

ITERATION NUMBER	4	1	VAR(I)	F(I)				
	1	-4.6130713E-01	2.189591E-08					
	2	1.800740E-00	-1.300004E-07					
	3	4.180801E-01	-1.362020E-07					
	4	-3.740539E-02	-2.334961E-07					
	5	-6.700077E-01	-6.751923E-07					
K BAR=1.1924305								
ITERATION NUMBER	5	1	VAR(I)	F(I)				
	1	-4.513352E-01	-3.673595E-08					
	2	1.2437840E-00	3.769721E-08					
	3	-6.023000E-01	1.900095E-07					
	4	-3.731108E-02	3.745425E-07					
	5	-4.662110E-01	1.699331E-06					
HDS= 3346.137 WDP(I)= 9.73060 93.69801100.76285148.35433106.66951 27.05097								
ONE DIMENSIONAL FLOW								
Z0	-4.7250	MAX= -2.66987	STEP SIZE= .002000	U0= 423.346 TP10= 6243.979 A0= 9.1300				
ITERATION NUMBER	3	1	VAR(I)	F(I)	TP(I)	K(I)	L(I)	I=1... 6
	1	0.7237	U0= 1423.034	UP(I)	6100.591	.93093	.91982	
	2	0.9779	.96457	1336.074	6100.591	.93093	.91982	
	3	0.83237	.90452	1222.133	6100.591	.93093	.91982	
	4	0.83237	.78175	1151.522	6100.591	.93093	.91982	
	5	-8.336973E-01	-6.349293E-06					
ITERATION NUMBER	3	1	VAR(I)	F(I)				
	1	-1.4295020E-01	8.163300E-02					
	2	1.000000E-00	-1.568214E-07					
	3	-7.05027E-01	-1.177787E-08					
	4	1.010670E-01	-2.465961E-06					
	5	-8.336973E-01	-6.349293E-06					
ITERATION NUMBER	1	1	VAR(I)	F(I)				
	1	2.466260E-01	-5.629523E-08					
	2	6.700100E-01	2.019432E-08					
	3	3.139023E-01	-3.521390E-06					
	4	1.927040E-01	0.					
	5	-6.213000E-01	0.					
ITERATION NUMBER	3	1	VAR(I)	F(I)				
	1	1.100000E-01	4.2381199E-07					
	2	5.575174E-01	-2.984232E-07					
	3	3.446331E-01	9.874914E-10					
	4	3.707000E-01	0.					
	5	1.924330E-01	0.					
ITERATION NUMBER	3	1	VAR(I)	F(I)				
	1	-7.100103E-02	2.015919E-07					
	2	7.700180E-01	-1.659082E-07					
	3	-6.030070E-01	3.889581E-08					
	4	4.491254E-01	0.					
	5	-9.272300E-01	0.					
ITERATION NUMBER	6	1	VAR(I)	F(I)				
	1	-3.019500E-01	1.147541E-07					
	2	2.076300E-00	-2.748071E-07					
	3	4.94367E-01	-4.119680E-07					
	4	1.130700E-01	-7.508982E-07					
	5	-6.070320E-01	-1.622000E-08					
ITERATION NUMBER	3	1	VAR(I)	F(I)				
	1	0.83237	4.587143E-07					
	2	1.213452E-00	-5.080133E-06					
	3	4.953908E-01	-1.361469E-06					

2	1.210720E+00	-3.000070E+00
3	4.9539044E+01	-1.3017406E+06
4	2.8997743E+02	-6.6923970E+08
5	-3.8341001E-01	8.3990129E-08

ITERATION NUMBER 4	I	VAR(I)	F(I)
	1	-4.6130382E-01	2.1792899E+08
	2	1.3437841E+00	-1.4953303E+07
	3	4.8115801E-01	-1.3543688E+07
	4	-3.7311429E+02	-2.3190490E+07
	5	-4.4081143E-01	-4.7520591E+07

K BAR=1.1924398

ITERATION NUMBER 6	I	VAR(I)	F(I)
	1	-4.6130382E-01	-9.8154769E+08
	2	1.3437841E+00	-9.0010217E+09
	3	4.8115801E-01	3.6394933E+07
	4	-3.7311429E+02	6.9702167E+07
	5	-4.4081143E-01	2.3908801E+08

WDQ= 3346.204 WDP(I)= 9.73479 53.69968108,76500148,35726106,67162 27,85112

***** CHANGE ZONES *****

Z	K	MPC	P
-1.25000	0.00000	0.00000	1992.78431
-1.25000	.04603	.00137	1992.84691
-1.25000	.09206	.00549	1993.09643
-1.25000	.13810	.01233	1993.91797
-1.25000	.18413	.02194	1994.11993
-1.25000	.23016	.03426	1994.91387
-1.25000	.27619	.04928	1995.91429
-1.25000	.32223	.06699	1997.13837
-1.25000	.36826	.08736	1998.60564
-1.25000	.41429	.11037	2000.33759
-1.25000	.46032	.13599	2002.39708
-1.25000	.50636	.16417	2004.68812
-1.25000	.55239	.19487	2007.39491
-1.25000	.59842	.22803	2010.38133
-1.25000	.64445	.26358	2013.79013
-1.25000	.69048	.30147	2017.60202
-1.25000	.73652	.34159	2021.83473
-1.25000	.78255	.38385	2026.50188
-1.25000	.82858	.42813	2031.81179
-1.25000	.87461	.47436	2037.16591
-1.25000	.92065	.52234	2043.15769
-1.25000	.96668	.57192	2049.57048
-1.25000	1.01271	.62293	2056.37582
-1.25000	1.05874	.67516	2063.53136
-1.25000	1.10478	.72840	2070.97892
-1.25000	1.15081	.78240	2078.64002
-1.25000	1.19684	.83687	2086.41717
-1.25000	1.24287	.89192	2094.18899
-1.25000	1.28890	.94602	2101.79899
-1.25000	1.33494	1.00000	2109.07218

TOTAL MASS FLOW = 3.5544769E+03

NO. POINTS = 30

VEL	T
1918.29121	6128.73483
1917.96691	6128.77583
1918.98782	6128.89967
1915.33069	6129.10884
1912.96348	6129.40749
1909.83779	6129.80129
1905.89329	6130.29724
1901.05812	6130.90383
1896.22295	6131.61042

1072,24740	6131,00074
1080,37457	6132,40771
1080,33260	6133,40646
1071,01388	6134,00023
1060,31110	6135,99490
1040,10221	6137,44651
1034,27212	6139,18477
1010,70556	6140,99867
1001,29216	6143,07397
1701,93018	6149,30220
1760,53096	6147,86036
1737,02426	6150,56970
1711,30497	6153,40387
1603,54102	6156,59830
1653,50369	6159,89283
1621,98012	6163,34098
1507,68906	6166,93121
1552,16054	6170,60736
1919,36013	6174,32739
1477,79873	6178,03231
1440,16790	6181,65083
1403,38020	6189,09809

Z	R	HPC	P
-1.16151	0.00000	0.00000	1968.19768
-1.16151	.04435	.00133	1968.27290
-1.16151	.08870	.00332	1968.49977
-1.16151	.13306	.01196	1968.88198
-1.16151	.17741	.02125	1969.42523
-1.16151	.22176	.03314	1970.13792
-1.16151	.26611	.04773	1971.03020
-1.16151	.31046	.06490	1972.11416
-1.16151	.35481	.08466	1973.40350
-1.16151	.39917	.10698	1974.91323
-1.16151	.44352	.13186	1976.65932
-1.16151	.48787	.15924	1978.65831
-1.16151	.53222	.18910	1980.92883
-1.16151	.57657	.22140	1983.48108
-1.16151	.62093	.25607	1986.33626
-1.16151	.66528	.29300	1989.50589
-1.16151	.70963	.33235	1993.00110
-1.16151	.75398	.37381	1996.82982
-1.16151	.79833	.41738	2000.99583
-1.16151	.84269	.46297	2005.49784
-1.16151	.88704	.51048	2010.32831
-1.16151	.93139	.55974	2015.47229
-1.16151	.97574	.61075	2020.90604
-1.16151	1.02009	.66324	2026.59563
-1.16151	1.06444	.71709	2032.49932
-1.16151	1.10880	.77213	2038.54585
-1.16151	1.15315	.82817	2044.67263
-1.16151	1.19750	.88496	2050.78378
-1.16151	1.24185	.94235	2056.76804
-1.16151	1.28620	1.00000	2062.49282

TOTAL MASS FLOW = 3.5393880E+03

NO. POINTS = 30

Z	R	HPC	P
-1.07302	0.00000	0.00000	1939.71774
-1.07302	.04283	.00129	1939.78092
-1.07302	.08566	.00517	1939.97127
-1.07302	.12849	.01163	1940.29126
-1.07302	.17131	.02067	1940.74492
-1.07302	.21414	.03227	1941.33778
-1.07302	.25696	.04644	1942.07675
-1.07302	.29979	.06315	1942.96995
-1.07302	.34262	.08222	1943.99995

-1,07302	1,0440	1,0440	1,0440
-1,07302	1,0444	1,0416	1,045,25651
-1,07302	1,0427	1,0442	1,046,67034
-1,07302	1,0410	1,0410	1,048,27875
-1,07302	1,04393	1,0433	1,050,09236
-1,07302	1,04675	1,0492	1,052,12127
-1,07302	1,0498	1,0498	1,054,37463
-1,07302	1,04241	1,0420	1,056,86012
-1,07302	1,04923	1,0479	1,059,98345
-1,07302	1,0488	1,0482	1,062,54775
-1,07302	1,0489	1,0482	1,065,75286
-1,07302	1,04372	1,04374	1,069,19465
-1,07302	1,04894	1,0488	1,072,80423
-1,07302	1,04937	1,0499	1,076,74703
-1,07302	1,04220	1,0496	1,080,82192
-1,07302	1,0492	1,0496	1,083,00015
-1,07302	1,02785	1,0487	1,089,42426
-1,07302	1,07068	1,0497	1,093,86693
-1,07302	1,11891	1,02127	1,098,32971
-1,07302	1,13633	1,0982	2002,74175
-1,07302	1,19916	1,93945	2007,01840
-1,07302	1,24199	1,00000	2011,09983

Z	R	MPC	P
-.98453	0.00000	0.00000	1906.87539
-.98453	.04149	.00126	1906.92239
-.98453	.08290	.00505	1907.06392
-.98453	.12435	.01135	1907.30154
-.98453	.16580	.02014	1907.63761
-.98453	.20725	.03152	1908.07619
-.98453	.24869	.04534	1908.62103
-.98453	.29014	.06170	1909.27734
-.98453	.33159	.08052	1910.05076
-.98453	.37304	.10182	1910.94728
-.98453	.41449	.12556	1911.97311
-.98453	.45594	.15178	1913.13441
-.98453	.49739	.18040	1914.43704
-.98453	.53884	.21142	1915.88624
-.98453	.58029	.24482	1917.48633
-.98453	.62174	.28056	1919.24030
-.98453	.66319	.31861	1921.14944
-.98453	.70463	.35894	1923.21267
-.98453	.74608	.40150	1925.42709
-.98453	.78753	.44629	1927.78928
-.98453	.82898	.49314	1930.27707
-.98453	.87043	.54211	1932.88758
-.98453	.91188	.59318	1935.59891
-.98453	.95333	.64604	1938.37937
-.98453	.99478	.70086	1941.20278
-.98453	1.03623	.75748	1944.02761
-.98453	1.07768	.81580	1946.80616
-.98453	1.11913	.87573	1949.48168
-.98453	1.16057	.93717	1952.98748
-.98453	1.20202	1.00000	1954.24593

	Z	R	HPC	P
1	0.89604	0.00000	0.00000	1869.19897
	0.89604	0.04021	0.00124	1869.22601
	0.89604	0.08042	0.00495	1869.30742
2	0.89604	0.12063	0.01113	1869.44405
	0.89604	0.16084	0.01978	1869.63730
	0.89604	0.20105	0.03089	1869.88904
	0.89604	0.24126	0.04447	1869.11989

-.89604	.47140	.04791	1870.40120
-.89604	.28147	.06090	1870.57740
-.89604	.32168	.07898	1871.01961
-.89604	.38189	.09990	1871.53084
-.89604	.40210	.12329	1872.11390
-.89604	.44231	.14901	1872.77156
-.89604	.48292	.17719	1873.50968
-.89604	.52273	.20779	1874.31768
-.89604	.56294	.24069	1875.20801
-.89604	.60319	.27598	1876.17584
-.89604	.64336	.31360	1877.21884
-.89604	.68357	.35394	1878.33279
-.89604	.72378	.39578	1879.51124
-.89604	.76399	.44023	1880.74513
-.89604	.80420	.48692	1882.02234
-.89604	.84441	.53586	1883.32728
-.89604	.88463	.58682	1884.64038
-.89604	.92484	.63995	1885.93759
-.89604	.96505	.69514	1887.18986
-.89604	1.00526	.75233	1888.36258
-.89604	1.04547	.81144	1889.41500
-.89604	1.08568	.87291	1890.29962
-.89604	1.12589	.93536	1890.96163
-.89604	1.16610	1.00000	1891.33829

TOTAL MASS FLOW = 3.5186764E+03

NO. POINTS = 30

Z	H	HPC	P
-.80756	0.00000	0.00000	1826.20444
-.80756	.03910	.00122	1826.20791
-.80756	.07821	.00486	1826.21844
-.80756	.11731	.01094	1826.23631
-.80756	.15642	.01945	1826.26199
-.80756	.19552	.03039	1826.29608
-.80756	.23463	.04379	1826.33926
-.80756	.27373	.05953	1826.39219
-.80756	.31283	.07773	1826.45547
-.80756	.35194	.09839	1826.52949
-.80756	.39104	.12137	1826.61433
-.80756	.43019	.14679	1826.70961
-.80756	.46929	.17460	1826.81436
-.80756	.50839	.20480	1826.92678
-.80756	.54748	.23738	1827.04413
-.80756	.58656	.27232	1827.16244
-.80756	.62567	.30961	1827.27633
-.80756	.66477	.34924	1827.37674
-.80756	.70388	.39119	1827.46064
-.80756	.74298	.43545	1827.51080
-.80756	.78208	.48206	1827.51940
-.80756	.82119	.53082	1827.49776
-.80756	.86029	.58189	1827.31800
-.80756	.89940	.63514	1827.07261
-.80756	.93850	.69064	1826.69415
-.80756	.97760	.74832	1826.15083
-.80756	1.01671	.80812	1825.40810
-.80756	1.05581	.87002	1824.41824
-.80756	1.09492	.93399	1823.13998
-.80756	1.13402	1.00000	1821.51809

TOTAL MASS FLOW = 3.5176283E+03

NO. POINTS = 30

Z	H	HPC	P
-.71907	0.00000	0.00000	1777.40965
-.71907	.03813	.00126	1777.38600
-.71907	.07625	.00480	1777.31900
-.71907	.11438	.01080	1777.19649

P	M-PJ	QMC	R13-FJ	U	U-PJ	V	V-PJ	W
2.0027200E+00	2.0047007E+01	5.430500E+03	1.230200E+03	1.054000E+00	5.197700E+01			
2.904300E+00	3.030790E+01	5.700250E+03	1.103000E+03	1.016772E+00	5.395300E+01			
J= 1	4.091017E+07	1.059090E+03	5.523310E+03	9.290120E+02				
3.040007E+00	3.122452E+01	5.741227E+03	1.004700E+03	9.742090E+01	5.000400E+01			
J= 1	4.070013E+07	1.120730E+03	5.502240E+03	8.000101E+02				
J= 2	4.970015E+07	6.095140E+03	5.245300E+03	6.579170E+02				
3.125349E+00	3.100200E+01	5.700031E+03	1.000730E+03	9.311220E+01	5.050000E+01			
J= 1	4.924124E+07	1.095330E+03	5.071130E+03	8.073470E+02				
J= 2	4.901520E+07	7.057730E+03	5.216030E+03	6.195400E+02				
J= 3	5.002000E+07	1.073700E+02	5.000000E+03	4.000000E+02				
3.173041E+00	3.200700E+01	5.0747130E+03	9.608320E+02	9.022000E+01	5.000200E+01			
J= 1	4.933720E+07	1.101470E+03	5.002100E+03	7.072000E+02				
J= 2	4.980200E+07	7.057730E+03	5.216030E+03	5.099000E+02				
J= 3	5.045500E+07	1.097000E+02	4.934010E+03	4.209750E+02				
J= 4	5.100000E+07	2.000000E+02	5.000000E+03	3.000000E+02				
3.205205E+00	3.230000E+01	5.457072E+03	9.270000E+02	8.015340E+01	0.042190E+01			
J= 1	4.939400E+07	1.135200E+03	5.030110E+03	7.000000E+02				
J= 2	4.993530E+07	7.109600E+03	5.109110E+03	5.759170E+02				
J= 3	5.049000E+07	1.093670E+02	4.925100E+03	4.100500E+02				
J= 4	5.100000E+07	2.000000E+02	5.000000E+03	3.000000E+02				
3.230400E+00	3.257420E+01	5.044000E+03	9.015071E+02	8.046400E+01	0.110470E+01			
J= 1	4.944200E+07	1.107150E+03	5.071250E+03	7.200000E+02				
J= 2	4.997410E+07	7.117110E+03	5.179320E+03	5.612000E+02				
J= 3	5.052010E+07	1.090000E+02	4.917100E+03	4.000000E+02				
J= 4	5.109100E+07	2.000000E+02	5.000000E+03	3.000000E+02				
J= 5	5.110040E+07	2.000000E+02	4.987300E+03	2.340000E+02				
J= 6	5.124300E+07	2.000000E+03	4.000000E+03	1.000000E+02				
3.351020E+00	3.359057E+01	5.000000E+03	7.702350E+02	7.733900E+01	6.093030E+01			
J= 1	4.905970E+07	1.111700E+03	5.000000E+03	6.233270E+02				
J= 2	5.010540E+07	7.133500E+03	5.130510E+03	4.833050E+02				
J= 3	5.060310E+07	1.093240E+02	4.874510E+03	3.500010E+02				
J= 4	5.110500E+07	2.000000E+02	4.910000E+03	2.000120E+02				
J= 5	5.135000E+07	2.000000E+02	4.900000E+03	2.000000E+02				
J= 6	5.154670E+07	2.000000E+03	4.000000E+03	1.000000E+02				
3.420700E+00	3.423707E+01	5.000000E+03	6.7927510E+02	7.0308730E+01	6.7545740E+01			
J= 1	4.970340E+07	1.111270E+03	5.032501E+03	5.530000E+02				
J= 2	5.021000E+07	7.102040E+03	5.097500E+03	4.750000E+02				
J= 3	5.080000E+07	1.072000E+02	4.843700E+03	3.150100E+02				
J= 4	5.110500E+07	2.000000E+02	4.662250E+03	2.000000E+02				
J= 5	5.140000E+07	2.000000E+02	4.520000E+03	1.000000E+02				
J= 6	5.160000E+07	2.000000E+03	4.415100E+03	1.000000E+02				
3.493517E+00	3.470434E+01	5.000000E+03	5.9557310E+02	6.327700E+01	6.001200E+01			
J= 1	4.994700E+07	1.110031E+03	5.033900E+03	4.875400E+02				
J= 2	5.030040E+07	7.032000E+03	5.069000E+03	3.797710E+02				
J= 3	5.090000E+07	1.050000E+02	4.700000E+03	2.779000E+02				
J= 4	5.120100E+07	2.000000E+02	4.635660E+03	2.124400E+02				
J= 5	5.153000E+07	2.000000E+02	4.497000E+03	1.657130E+02				
J= 6	5.173000E+07	2.000000E+03	4.390000E+03	1.270000E+02				
3.540040E+00	3.524657E+01	5.000000E+03	5.1779512E+02	5.624090E+01	7.2029270E+01			

J0 3	5120200E-07	1.002230E-04	0.710972E+03	0:
J0 4	5120004E+07	2.565099E-02	4.540310E+03	0:
J0 5	5104729E+07	1.90091E-02	4.410334E+03	0:
J0 6	5120333E+07	5.982493E-03	4.300417E+03	0:

GAS-PARTICLE FLOW(MOZZLE)

CP TIME = 109.403 PP TIME = 117.039

CHARACTERISTIC CALCULATION

Z	H	MPC	P
.00000	0.00000	0.00000	806.47852
.00075	.00031	.00003	805.88801
.00150	.00062	.00006	804.11508
.00225	.00093	.00009	801.13938
.00300	.00123	.00012	796.92102
.00375	.00154	.00015	791.40219
.00450	.00185	.00018	784.49723
.00525	.00216	.00021	776.80008
.00600	.00247	.00024	766.00584
.00675	.00278	.00027	754.84167
.00750	.00309	.00030	739.91732
.00825	.00340	.00033	723.28718
.00900	.00371	.00036	697.26940
.00975	.00402	.00039	691.82534
.01050	.00433	.00042	684.87000
.01125	.00464	.00045	674.57629
.01200	.00495	.00048	657.89568
.01275	.00526	.00051	639.81674
.01350	.00557	.00054	622.20708

TOTAL MASS FLOW = 3.0237998E+03 NO. POINTS = 19

LRC ID	R	K	REK	MACH	TO	VO	THETA=K	TPK	PG/PG0	DG/DG0	SDK/SD0	CF	ISF	IT
1	1.01677	.03954	1.7157	5102.0	592.1	13.372	.01633	.28436	.34834	0.00000	0.0000	0.000	0.00	0
2	1.07043	.08921	1.7986	4992.0	6120.3	13.707	.79073	.23029	.31336	0.00000	1.6752	217.92	4	

TOTAL MASS FLOW = 3.0237998E+03 NO. POINTS = 3

LRC ID	R	K	REK	MACH	TO	VO	THETA=K	TPK	PG/PG0	DG/DG0	SDK/SD0	CF	ISF	IT
1	1.01677	.03954	1.7157	5102.0	592.1	13.372	.01633	.28436	.34834	0.00000	0.000	0.00	0	
2	1.07043	.08921	1.7986	4992.0	6120.3	13.707	.79073	.23029	.31336	0.00000	1.6752	217.92	4	

LRC ID	R	K	REK	MACH	TO	VO	THETA=K	TPK	PG/PG0	DG/DG0	SDK/SD0	CF	ISF	IT
1	1.01677	.03954	1.7157	5102.0	592.1	13.372	.01633	.28436	.34834	0.00000	0.000	0.00	0	
2	1.07043	.08921	1.7986	4992.0	6120.3	13.707	.79073	.23029	.31336	0.00000	1.6752	217.92	4	

total mass flow = 3.0237956E+03 NO, POFW = 12

[illegible]

TOTAL MASS FLOW = 3.023798E+03 NO. POINTS = 14									
LOC ID	R	Z	REK	THETA-K	THETA-B	THETA-C	DPK/DQ	DPK/DPO	13P
K	REK	THETA-K	THETA-B	THETA-C	DPK/DQ	DPK/DPO	13P	13P	13P
0 14	00404	02165	1.4500	2479.3	9.193	0.075	0.075	0.075	0.075
1	2.31270E+01	5.40046E+01	7.61209E+00	5.23840E+03	3.39948E+03	9.35037E+03	9.35037E+03	9.35037E+03	9.35037E+03
2	8.14406E+01	5.20778E+01	6.18502E+00	5.30161E+03	2.18498E+02	0.01491E+02	0.01491E+02	0.01491E+02	0.01491E+02
3	2.06172E+02	4.93991E+01	4.17298E+00	5.36994E+03	5.20212E+02	1.43379E+01	1.43379E+01	1.43379E+01	1.43379E+01
4	3.99249E+02	4.73867E+01	3.17846E+00	5.41148E+03	7.99887E+02	2.12917E+01	2.12917E+01	2.12917E+01	2.12917E+01
5	5.27806E+02	4.99331E+01	2.93133E+00	5.44519E+03	6.21890E+02	1.71196E+01	1.71196E+01	1.71196E+01	1.71196E+01
6 4	0.8298	0.2982	1.6638	5184.8	9793.2	9.518	0.2476	0.2476	0.2476
1	1.76831E+01	5.53730E+01	8.14159E+00	5.21370E+03	3.39948E+03	9.35037E+03	9.35037E+03	9.35037E+03	9.35037E+03
2	7.78804E+01	5.27115E+01	6.18502E+00	5.30161E+03	2.18498E+02	0.01491E+02	0.01491E+02	0.01491E+02	0.01491E+02
3	1.99077E+02	4.89218E+01	5.12918E+00	5.34513E+03	5.22217E+02	1.40779E+01	1.40779E+01	1.40779E+01	1.40779E+01
4	3.49357E+02	4.79135E+01	4.07808E+00	5.39127E+03	7.98347E+02	2.15217E+01	2.15217E+01	2.15217E+01	2.15217E+01
5	5.12410E+02	4.84416E+01	3.19802E+00	5.42570E+03	6.21890E+02	1.71196E+01	1.71196E+01	1.71196E+01	1.71196E+01
6 4	0.9040	0.5132	1.6867	5124.4	9813.1	10.178	0.5199	0.5199	0.5199
1	1.76831E+01	5.53730E+01	8.14159E+00	5.21370E+03	3.39948E+03	9.35037E+03	9.35037E+03	9.35037E+03	9.35037E+03
2	7.78804E+01	5.27115E+01	6.18502E+00	5.30161E+03	2.18498E+02	0.01491E+02	0.01491E+02	0.01491E+02	0.01491E+02
3	1.99077E+02	4.89218E+01	5.12918E+00	5.34513E+03	5.22217E+02	1.40779E+01	1.40779E+01	1.40779E+01	1.40779E+01
4	3.49357E+02	4.79135E+01	4.07808E+00	5.39127E+03	7.98347E+02	2.15217E+01	2.15217E+01	2.15217E+01	2.15217E+01
5	5.12410E+02	4.84416E+01	3.19802E+00	5.42570E+03	6.21890E+02	1.71196E+01	1.71196E+01	1.71196E+01	1.71196E+01
6 4	0.94172	0.8476	1.7265	5072.9	9928.6	11.206	0.8166	0.8166	0.8166
1	1.76831E+01	5.53730E+01	8.14159E+00	5.21370E+03	3.39948E+03	9.35037E+03	9.35037E+03	9.35037E+03	9.35037E+03
2	7.78804E+01	5.27115E+01	6.18502E+00	5.30161E+03	2.18498E+02	0.01491E+02	0.01491E+02	0.01491E+02	0.01491E+02
3	1.99077E+02	4.89218E+01	5.12918E+00	5.34513E+03	5.22217E+02	1.40779E+01	1.40779E+01	1.40779E+01	1.40779E+01
4	3.49357E+02	4.79135E+01	4.07808E+00	5.39127E+03	7.98347E+02	2.15217E+01	2.15217E+01	2.15217E+01	2.15217E+01
5	5.12410E+02	4.84416E+01	3.19802E+00	5.42570E+03	6.21890E+02	1.71196E+01	1.71196E+01	1.71196E+01	1.71196E+01
6 4	1.88135	0.74890	1.8855	4968.3	6129.1	13.297	0.79493	0.79493	0.79493
1	1.76831E+01	5.53730E+01	8.14159E+00	5.21370E+03	3.39948E+03	9.35037E+03	9.35037E+03	9.35037E+03	9.35037E+03
2	7.78804E+01	5.27115E+01	6.18502E+00	5.30161E+03	2.18498E+02	0.01491E+02	0.01491E+02	0.01491E+02	0.01491E+02
3	1.99077E+02	4.89218E+01	5.12918E+00	5.34513E+03	5.22217E+02	1.40779E+01	1.40779E+01	1.40779E+01	1.40779E+01
4	3.49357E+02	4.79135E+01	4.07808E+00	5.39127E+03	7.98347E+02	2.15217E+01	2.15217E+01	2.15217E+01	2.15217E+01
5	5.12410E+02	4.84416E+01	3.19802E+00	5.42570E+03	6.21890E+02	1.71196E+01	1.71196E+01	1.71196E+01	1.71196E+01
6 4	1.87356	0.8746	1.9194	4816.6	6413.7	16.398	0.77866	0.77866	0.77866
1	1.76831E+01	5.53730E+01	8.14159E+00	5.21370E+03	3.39948E+03	9.35037E+03	9.35037E+03	9.35037E+03	9.35037E+03
2	7.78804E+01	5.27115E+01	6.18502E+00	5.30161E+03	2.18498E+02	0.01491E+02	0.01491E+02	0.01491E+02	0.01491E+02
3	1.99077E+02	4.89218E+01	5.12918E+00	5.34513E+03	5.22217E+02	1.40779E+01	1.40779E+01	1.40779E+01	1.40779E+01
4	3.49357E+02	4.79135E+01	4.07808E+00	5.39127E+03	7.98347E+02	2.15217E+01	2.15217E+01	2.15217E+01	2.15217E+01
5	5.12410E+02	4.84416E+01	3.19802E+00	5.42570E+03	6.21890E+02	1.71196E+01	1.71196E+01	1.71196E+01	1.71196E+01
6 5	1.16197	0.89520	2.0744	4684.8	6780.9	20.845	0.73769	0.73769	0.73769
Z	N	MPC	P						
1	0.1165	0.8644	0.7070						
2	0.0290	0.8227	0.7070						
3	0.0290	0.8227	0.7070						
4	0.0290	0.8227	0.7070						
5	0.0290	0.8227	0.7070						
6	0.0290	0.8227	0.7070						
7	0.0290	0.8227	0.7070						
8	0.0290	0.8227	0.7070						
9	0.0290	0.8227	0.7070						
10	0.0290	0.8227	0.7070						
11	0.0290	0.8227	0.7070						
12	0.0290	0.8227	0.7070						
13	0.0290	0.8227	0.7070						
14	0.0290	0.8227	0.7070						

[illegible]

3	1.77908E+02	5.13417E+03	6.10377E+00	5.26240E+03	4.14040E+04	2.00000E+00	1.00000E+00
4	3.17186E+02	4.92977E+03	5.10591E+00	5.13426E+03	5.23202E+02	1.33400E+01	1.00000E+00
5	4.70013E+02	4.76122E+03	4.27551E+00	5.37656E+03	8.02137E+02	2.04217E+01	2.00000E+00
7	4.91407	7.3702	1.7244	5.088.7	5912.8	11.074	0.1099
1	1.99392E+01	5.74202E+03	6.17333E+00	5.13255E+03	2.78024E+03	0.10000E+01	0.00000E+00
2	6.20578E+01	5.49071E+03	8.24042E+00	5.11208E+03	2.19093E+02	5.41305E+02	9.40000E+00
3	1.75657E+02	5.23172E+03	6.60050E+00	5.25391E+03	5.27230E+02	1.29786E+01	1.00000E+00
4	3.13208E+02	4.99685E+03	5.01174E+00	5.31432E+03	8.07730E+02	1.09823E+01	2.00000E+00
7	4.95277	7.7367	1.7725	5.005.6	6039.4	12.276	0.0094
1	1.40073E+01	5.00000E+03	1.00230E+01	5.07071E+03	5.49327E+03	7.07727E+03	1.00000E+00
2	6.47834E+01	5.60355E+03	9.25366E+00	5.15194E+03	2.22790E+02	5.17275E+02	9.40000E+00
3	1.73913E+02	5.31419E+03	7.01591E+00	5.21770E+03	5.33092E+02	1.23999E+01	1.00000E+00
7	4.01898	4.571	1.6715	4.074.9	6293.1	14.875	0.7799
1	1.57710E+01	6.4270E+03	1.03316E+01	4.95735E+03	3.50971E+03	7.18757E+03	4.92000E+00
2	6.70043E+01	5.01496E+03	1.11240E+01	5.01496E+03	2.29130E+02	4.17302E+02	9.40000E+00
4	1.10195	9.1122	2.039	4.098.7	6015.4	18.401	0.75179
1	1.50844E+01	6.30029E+03	1.02276E+01	4.79380E+03	3.50404E+03	6.13353E+03	4.92000E+00
7	4.12071	1.00185	2.1118	4.555.2	6864.6	21.000	0.72883
7	4.87163	7.4386	1.6961	5.103.0	9535.3	15.202	0.1647
1	1.29836E+01	5.0780E+03	8.09048E+00	5.13304E+03	3.39977E+03	8.20709E+03	4.92000E+00
2	6.23410E+01	5.43364E+03	7.01690E+00	5.21074E+03	2.11991E+02	5.10769E+02	9.40000E+00
3	1.70459E+02	5.13674E+03	6.16934E+00	5.28460E+03	5.20973E+02	1.34028E+01	1.00000E+00
4	3.05724E+02	4.93340E+03	5.11991E+00	5.33215E+03	8.11305E+02	2.04323E+01	2.00000E+00
5	4.50049E+02	4.90977E+03	4.72909E+00	5.38807E+03	8.73907E+02	1.91372E+01	2.00000E+00
6	6.27384E+02	4.67481E+03	3.17362E+00	5.39871E+03	1.75939E+02	4.45161E+02	3.00000E+00
7	4.80284	7.6370	1.7177	5.374.1	6092.0	10.884	0.1189
1	1.31230E+01	5.73413E+03	9.34197E+00	5.13818E+03	3.38813E+03	8.34215E+03	4.92000E+00
2	6.18100E+01	5.4362E+03	8.12615E+00	5.11150E+03	2.18178E+02	5.10769E+02	9.40000E+00
3	1.68036E+02	5.27900E+03	6.09131E+00	5.26240E+03	9.25222E+02	1.07322E+01	1.00000E+00
4	3.02573E+02	5.3543E+03	5.39237E+00	5.31214E+03	8.00383E+02	1.00348E+01	2.00000E+00
5	4.50735E+02	4.85285E+03	4.81061E+00	5.38466E+03	8.50092E+02	1.55139E+01	2.00000E+00
7	4.91947	7.8931	1.7485	5.333.4	5974.4	11.630	0.8535
1	1.33652E+01	5.4393E+03	1.02731E+01	5.02455E+03	3.40422E+03	8.00375E+03	4.92000E+00
2	6.15002E+01	5.20097E+03	8.00030E+00	5.19014E+03	2.20919E+02	5.12079E+02	9.40000E+00
3	1.67535E+02	5.2043E+03	7.24715E+00	5.23218E+03	5.20419E+02	1.25471E+01	1.00000E+00
4	2.90935E+02	5.3358E+03	6.17276E+00	5.25378E+03	8.12822E+02	1.25388E+01	2.00000E+00
7	4.94034	8.2797	1.8336	4.960.9	6116.2	13.018	0.79375
1	1.43655E+01	5.93400E+03	1.14046E+01	5.03095E+03	3.49190E+03	7.04994E+03	4.92000E+00
2	6.12037E+01	5.09397E+03	7.00730E+00	5.10371E+03	2.27208E+02	4.97032E+02	9.40000E+00
3	1.68122E+02	5.3248E+03	8.24072E+00	5.19208E+03	5.30892E+02	1.19421E+01	1.00000E+00
7	4.10394	8.9384	1.9100	4.918.6	6086.0	15.786	0.77103
1	1.53475E+01	6.16477E+03	1.39086E+01	4.90447E+03	3.51779E+03	6.01245E+03	4.92000E+00
2	6.46873E+01	5.91160E+03	1.20401E+01	4.97218E+03	2.31468E+02	4.45257E+02	9.40000E+00
7	4.12135	9.7537	2.0557	4.926.4	6734.2	19.587	0.74023
1	1.49436E+01	6.53774E+03	1.74103E+01	4.72612E+03	3.57138E+03	5.70297E+03	4.92000E+00
7	4.12396	1.7283	2.1315	4.528.2	697.9	21.000	0.72451

HPG

1.6932	7.7340	5.6909	723.20710
1.6935	8.2006	6.0119	684.22311
7.2326	8.3391	6.2191	672.49483
7.2349	8.3249	6.3961	653.45888
7.2363	8.3163	6.5725	633.51301

Z	H	MPC	P
1.29138	0.00000	0.00000	305.61352
1.29350	0.0744	0.0080	547.23438
1.40000	0.0732	0.0203	924.93375
1.50477	0.12072	0.0072	303.89711
1.56449	0.15939	0.0071	477.90374
1.62790	0.14202	0.0121	452.97050
1.71710	0.20005	0.0207	615.81352
1.74340	0.20001	0.02744	400.84440
1.78390	0.31744	0.0303	393.00030
1.82370	0.39795	0.0328	375.77682
1.86742	0.37080	0.0406	360.77631
1.90926	0.40920	0.0537	348.29775
1.95040	0.43907	0.0605	330.23538
1.99205	0.47096	0.0696	315.10461
2.03350	0.50220	0.0746	300.31066
2.07475	0.53394	0.0833	285.80339
2.11480	0.56434	0.0934	272.25030
2.15403	0.59405	0.1047	259.51040
2.19204	0.62293	0.11305	247.02712
2.22913	0.65350	0.1200	236.40420
2.26534	0.68237	0.1215	226.02564
2.30002	0.70800	0.1260	216.12085
2.37017	0.76729	0.1609	197.65629
2.43700	0.82271	0.17615	181.86256
2.50004	0.87603	0.1973	168.37233
2.55971	0.92714	0.2151	155.39480
2.61350	0.97335	0.23175	140.00090
2.66540	1.02001	0.24799	125.07089
2.72020	1.06664	0.26351	140.19745
2.77070	1.11706	0.28501	136.60097
2.84402	1.17306	0.30072	133.00276
2.91620	1.23513	0.33155	120.04796
2.99455	1.30211	0.35939	124.77717
3.02703	1.36903	0.37117	123.04139
3.11472	1.40437	0.40504	116.30030
3.17640	1.45032	0.42783	115.10264
3.27725	1.51175	0.46437	111.80080
3.30501	1.50511	0.47741	108.59534
3.40044	1.65277	0.51972	101.49204
3.52093	1.77001	0.58023	90.20260
3.52700	1.75106	0.56721	97.96432
3.63809	1.84372	0.6147	93.04499
3.73371	1.94007	0.65709	88.10767
3.87577	2.04104	0.72216	83.14203
3.93900	2.04400	0.75111	80.69367
4.00107	2.17710	0.8073	70.89269
4.10105	2.30372	0.8092	71.56140
4.25402	2.41092	0.93326	67.16206
4.36242	2.55529	1.00000	62.97695

TOTAL MASS FLOW = 5,9230369E+03

LRC ID	R	Z	MACH	T8	VG	THETA-G	TO/TGO	PR/P00	DS/DG0	SDK/DG	CF	ISP	IT
	K	REK	VPK				TPK			DPK/DP0		APK	

REP	2	0.00000	1.4485	1.7657	4.064.7	5.009.0	0.000	1.9430	23201	3	0.000	2.2187	0.000	0.00.0
A	1	0.00000	1.4485	1.7657	4.064.7	5.009.0	0.000	1.9430	23201 <td>3</td> <td>0.000</td> <td>2.2187</td> <td>0.000</td> <td>0.00.0</td>	3	0.000	2.2187	0.000	0.00.0
V	1	0.00000	1.4485	1.7657	4.064.7	5.009.0	0.000	1.9430	23201 <td>3</td> <td>0.000</td> <td>2.2187</td> <td>0.000</td> <td>0.00.0</td>	3	0.000	2.2187	0.000	0.00.0
3	1	0.00000	1.4485	1.7657	4.064.7	5.009.0	0.000	1.9430	23201 <td>3</td> <td>0.000</td> <td>2.2187</td> <td>0.000</td> <td>0.00.0</td>	3	0.000	2.2187	0.000	0.00.0

[illegible]

25	2	34306	1.94235	1.9979	4092.5	6530.5	4.86421E+00	4.72193E+03	1.242	74440	1.3285	1.2933	1.23701	0.0000	0.00	4	1.72323E+04	1.12400E+01	1.24000E+02	1.24000E+03	1.24000E+04	1.24000E+05	1.24000E+06	1.24000E+07	1.24000E+08	1.24000E+09	1.24000E+10	1.24000E+11	1.24000E+12	1.24000E+13	1.24000E+14	1.24000E+15	1.24000E+16	1.24000E+17	1.24000E+18	1.24000E+19	1.24000E+20	1.24000E+21	1.24000E+22	1.24000E+23	1.24000E+24	1.24000E+25	1.24000E+26	1.24000E+27	1.24000E+28	1.24000E+29	1.24000E+30	1.24000E+31	1.24000E+32	1.24000E+33	1.24000E+34	1.24000E+35	1.24000E+36	1.24000E+37	1.24000E+38	1.24000E+39	1.24000E+40	1.24000E+41	1.24000E+42	1.24000E+43	1.24000E+44	1.24000E+45	1.24000E+46	1.24000E+47	1.24000E+48	1.24000E+49	1.24000E+50	1.24000E+51	1.24000E+52	1.24000E+53	1.24000E+54	1.24000E+55	1.24000E+56	1.24000E+57	1.24000E+58	1.24000E+59	1.24000E+60	1.24000E+61	1.24000E+62	1.24000E+63	1.24000E+64	1.24000E+65	1.24000E+66	1.24000E+67	1.24000E+68	1.24000E+69	1.24000E+70	1.24000E+71	1.24000E+72	1.24000E+73	1.24000E+74	1.24000E+75	1.24000E+76	1.24000E+77	1.24000E+78	1.24000E+79	1.24000E+80	1.24000E+81	1.24000E+82	1.24000E+83	1.24000E+84	1.24000E+85	1.24000E+86	1.24000E+87	1.24000E+88	1.24000E+89	1.24000E+90	1.24000E+91	1.24000E+92	1.24000E+93	1.24000E+94	1.24000E+95	1.24000E+96	1.24000E+97	1.24000E+98	1.24000E+99	1.24000E+100	1.24000E+101	1.24000E+102	1.24000E+103	1.24000E+104	1.24000E+105	1.24000E+106	1.24000E+107	1.24000E+108	1.24000E+109	1.24000E+110	1.24000E+111	1.24000E+112	1.24000E+113	1.24000E+114	1.24000E+115	1.24000E+116	1.24000E+117	1.24000E+118	1.24000E+119	1.24000E+120	1.24000E+121	1.24000E+122	1.24000E+123	1.24000E+124	1.24000E+125	1.24000E+126	1.24000E+127	1.24000E+128	1.24000E+129	1.24000E+130	1.24000E+131	1.24000E+132	1.24000E+133	1.24000E+134	1.24000E+135	1.24000E+136	1.24000E+137	1.24000E+138	1.24000E+139	1.24000E+140	1.24000E+141	1.24000E+142	1.24000E+143	1.24000E+144	1.24000E+145	1.24000E+146	1.24000E+147	1.24000E+148	1.24000E+149	1.24000E+150	1.24000E+151	1.24000E+152	1.24000E+153	1.24000E+154	1.24000E+155	1.24000E+156	1.24000E+157	1.24000E+158	1.24000E+159	1.24000E+160	1.24000E+161	1.24000E+162	1.24000E+163	1.24000E+164	1.24000E+165	1.24000E+166	1.24000E+167	1.24000E+168	1.24000E+169	1.24000E+170	1.24000E+171	1.24000E+172	1.24000E+173	1.24000E+174	1.24000E+175	1.24000E+176	1.24000E+177	1.24000E+178	1.24000E+179	1.24000E+180	1.24000E+181	1.24000E+182	1.24000E+183	1.24000E+184	1.24000E+185	1.24000E+186	1.24000E+187	1.24000E+188	1.24000E+189	1.24000E+190	1.24000E+191	1.24000E+192	1.24000E+193	1.24000E+194	1.24000E+195	1.24000E+196	1.24000E+197	1.24000E+198	1.24000E+199	1.24000E+200	1.24000E+201	1.24000E+202	1.24000E+203	1.24000E+204	1.24000E+205	1.24000E+206	1.24000E+207	1.24000E+208	1.24000E+209	1.24000E+210	1.24000E+211	1.24000E+212	1.24000E+213	1.24000E+214	1.24000E+215	1.24000E+216	1.24000E+217	1.24000E+218	1.24000E+219	1.24000E+220	1.24000E+221	1.24000E+222	1.24000E+223	1.24000E+224	1.24000E+225	1.24000E+226	1.24000E+227	1.24000E+228	1.24000E+229	1.24000E+230	1.24000E+231	1.24000E+232	1.24000E+233	1.24000E+234	1.24000E+2
----	---	-------	---------	--------	--------	--------	-------------	-------------	-------	-------	--------	--------	---------	--------	------	---	-------------	-------------	-------------	-------------	-------------	-------------	-------------	-------------	-------------	-------------	-------------	-------------	-------------	-------------	-------------	-------------	-------------	-------------	-------------	-------------	-------------	-------------	-------------	-------------	-------------	-------------	-------------	-------------	-------------	-------------	-------------	-------------	-------------	-------------	-------------	-------------	-------------	-------------	-------------	-------------	-------------	-------------	-------------	-------------	-------------	-------------	-------------	-------------	-------------	-------------	-------------	-------------	-------------	-------------	-------------	-------------	-------------	-------------	-------------	-------------	-------------	-------------	-------------	-------------	-------------	-------------	-------------	-------------	-------------	-------------	-------------	-------------	-------------	-------------	-------------	-------------	-------------	-------------	-------------	-------------	-------------	-------------	-------------	-------------	-------------	-------------	-------------	-------------	-------------	-------------	-------------	-------------	-------------	-------------	-------------	-------------	-------------	-------------	-------------	-------------	--------------	--------------	--------------	--------------	--------------	--------------	--------------	--------------	--------------	--------------	--------------	--------------	--------------	--------------	--------------	--------------	--------------	--------------	--------------	--------------	--------------	--------------	--------------	--------------	--------------	--------------	--------------	--------------	--------------	--------------	--------------	--------------	--------------	--------------	--------------	--------------	--------------	--------------	--------------	--------------	--------------	--------------	--------------	--------------	--------------	--------------	--------------	--------------	--------------	--------------	--------------	--------------	--------------	--------------	--------------	--------------	--------------	--------------	--------------	--------------	--------------	--------------	--------------	--------------	--------------	--------------	--------------	--------------	--------------	--------------	--------------	--------------	--------------	--------------	--------------	--------------	--------------	--------------	--------------	--------------	--------------	--------------	--------------	--------------	--------------	--------------	--------------	--------------	--------------	--------------	--------------	--------------	--------------	--------------	--------------	--------------	--------------	--------------	--------------	--------------	--------------	--------------	--------------	--------------	--------------	--------------	--------------	--------------	--------------	--------------	--------------	--------------	--------------	--------------	--------------	--------------	--------------	--------------	--------------	--------------	--------------	--------------	--------------	--------------	--------------	--------------	--------------	--------------	--------------	--------------	--------------	--------------	--------------	--------------	--------------	------------

1	3.002014E+00	7.205920E+03	1.520320E+01	4.170000E+03	3.345800E+03	2.320240E+03	4.920000E+00
2	1.709260E+01	7.058220E+03	1.430800E+01	4.170000E+03	2.275117E+02	1.585035E+02	4.920000E+00
3	2.022130E+01	6.753800E+03	1.320500E+01	4.170000E+03	3.040187E+02	4.074537E+02	1.920000E+03
4	1.808930E+02	6.486400E+03	1.1234320E+01	4.170000E+03	9.590379E+02	6.059190E+02	2.290000E+05
5	1.357615E+02	6.205794E+03	1.1040270E+01	4.170000E+03	7.920570E+02	5.151710E+02	2.940000E+05
6	2.005117E+02	6.110782E+03	1.1114000E+01	4.170000E+03	2.350335E+02	1.040034E+02	3.920000E+05
20	2	1.00130	2.78004	0.053.0	7.669.4	15.920	6.6849
1	2.077359E+00	7.324170E+03	1.577100E+01	4.170000E+03	3.317021E+03	2.150010E+03	4.920000E+00
2	1.563556E+01	7.133600E+03	1.490800E+01	4.170000E+03	2.213168E+02	1.511222E+02	9.400000E+00
3	4.001105E+01	6.802020E+03	1.381345E+01	4.170000E+03	5.720094E+02	3.004159E+02	1.632000E+05
4	6.057372E+01	6.521132E+03	1.260701E+01	4.170000E+03	9.447008E+02	6.100768E+02	2.720000E+05
5	1.474352E+02	6.321870E+03	1.221690E+01	4.170000E+03	7.003095E+02	5.161035E+02	2.940000E+05
6	2.000337E+02	6.163306E+03	1.106000E+01	4.170000E+03	2.309255E+02	1.198755E+02	3.920000E+05
20	2	1.04000	2.84325	2.4449	4041.9	7.606.3	15.925
1	2.010911E+00	7.354650E+03	1.600742E+01	4.170000E+03	3.267899E+03	2.169942E+03	4.920000E+00
2	1.007122E+01	7.133100E+03	1.538770E+01	4.170000E+03	2.170108E+02	1.444707E+02	9.400000E+00
3	4.006161E+01	6.845540E+03	1.430245E+01	4.170000E+03	5.629442E+02	3.173735E+02	1.632000E+05
4	6.044570E+01	6.576352E+03	1.339080E+01	4.170000E+03	9.392575E+02	6.235685E+02	2.290000E+05
5	1.393594E+02	6.371300E+03	1.271710E+01	4.170000E+03	7.873705E+02	5.225100E+02	2.940000E+05
6	1.979453E+02	6.200700E+03	1.216171E+01	4.170000E+03	2.311702E+02	1.534727E+02	3.920000E+05
20	2	1.20000	2.70000	2.7000	4022.0	7.504.9	15.930
1	2.024000E+00	7.361920E+03	1.620796E+01	4.170000E+03	3.211441E+03	2.085755E+03	4.920000E+00
2	1.261340E+01	7.190600E+03	1.570200E+01	4.170000E+03	2.140067E+02	1.389923E+02	9.400000E+00
3	4.000442E+01	6.892250E+03	1.470300E+01	4.170000E+03	5.009997E+02	3.143302E+02	1.632000E+05
4	6.091190E+01	6.620900E+03	1.360830E+01	4.170000E+03	9.391215E+02	6.073393E+02	2.290000E+05
5	1.318920E+02	6.414040E+03	1.320100E+01	4.170000E+03	7.768005E+02	5.045003E+02	2.940000E+05
6	1.904700E+02	6.251070E+03	1.204771E+01	4.170000E+03	2.275500E+02	1.577268E+02	3.920000E+05
20	2	1.19051	2.97162	2.4664	4015.4	7.527.1	15.937
1	2.049700E+00	7.409320E+03	1.635310E+01	4.170000E+03	3.152074E+03	2.013300E+03	4.920000E+00
2	1.175283E+01	7.21210E+03	1.501489E+01	4.170000E+03	2.113302E+02	1.340466E+02	9.400000E+00
3	3.706257E+01	6.933360E+03	1.410441E+01	4.170000E+03	5.940961E+02	3.533497E+02	1.632000E+05
4	7.077020E+01	6.698790E+03	1.307700E+01	4.170000E+03	9.033133E+02	6.179005E+02	2.290000E+05
5	1.250466E+02	6.458762E+03	1.367480E+01	4.170000E+03	7.952049E+02	4.791487E+02	2.940000E+05
6	1.707095E+02	6.284562E+03	1.312800E+01	4.170000E+03	2.233590E+02	1.510961E+02	3.920000E+05
20	2	1.21706	3.04517	2.4007	3997.9	7.554.3	16.017
1	2.391340E+00	7.439450E+03	1.646575E+01	4.170000E+03	3.231049E+03	1.998005E+03	4.920000E+00
2	1.171130E+01	7.250920E+03	1.522220E+01	4.170000E+03	2.208221E+02	1.363298E+02	9.400000E+00
3	3.555331E+01	6.976052E+03	1.359570E+01	4.170000E+03	5.609244E+02	3.505714E+02	1.632000E+05
4	7.362914E+01	6.714870E+03	1.477130E+01	4.170000E+03	9.010706E+02	5.577250E+02	2.290000E+05
5	1.309435E+02	6.502270E+03	1.411230E+01	4.170000E+03	7.320977E+02	4.927371E+02	2.940000E+05
6	1.717307E+02	6.328066E+03	1.360202E+01	4.170000E+03	2.100033E+02	1.535354E+02	3.920000E+05
20	2	1.20000	2.70000	2.7000	4000.0	7.500.0	15.930
1	2.329204E+00	7.474802E+03	1.657626E+01	4.170000E+03	3.277650E+03	1.971103E+03	4.920000E+00
2	1.075967E+01	7.296407E+03	1.504550E+01	4.170000E+03	2.131071E+02	1.261613E+02	9.400000E+00
3	3.644020E+01	7.028110E+03	1.392090E+01	4.170000E+03	5.133491E+02	3.017423E+02	1.632000E+05
4	6.904812E+01	6.766461E+03	1.352051E+01	4.170000E+03	8.235775E+02	4.952828E+02	2.290000E+05
5	1.134883E+02	6.594774E+03	1.466941E+01	4.170000E+03	6.971056E+02	4.194234E+02	2.940000E+05
6	1.606700E+02	6.357702E+03	1.400515E+01	4.170000E+03	2.140000E+02	1.120000E+02	3.920000E+05
20	4	1.35920	3.21530	2.5215	3949.0	7.632.3	16.266
1	2.225157E+00	7.512020E+03	1.678082E+01	4.170000E+03	3.05012	1.07933	16.011
2	1.042766E+01	7.344020E+03	1.467607E+01	4.170000E+03	3.205550E+03	1.972898E+03	4.920000E+00
3	3.214175E+01	7.010070E+03	1.362800E+01	4.170000E+03	5.209973E+02	3.089040E+02	1.632000E+05
4	6.000000E+01	6.823700E+03	1.307700E+01	4.170000E+03	9.103710E+02	5.507765E+02	2.290000E+05
5	1.088472E+02	6.461170E+03	1.307090E+01	4.170000E+03	7.256350E+02	4.152168E+02	2.940000E+05
6	1.580600E+02	6.425210E+03	1.4597653E+01	4.170000E+03	2.006637E+02	1.121055E+02	3.920000E+05
20	2	1.30827	3.25050	2.5315	3937.6	7.609.0	16.333
1	2.222721E+00	7.536014E+03	1.675784E+01	4.170000E+03	3.04939	1.07839	16.013
2	1.042721E+00	7.336014E+03	1.467578E+01	4.170000E+03	3.205531E+03	1.946421E+03	4.920000E+00

2	1.451528E+02	6.513330E+03	1.170194E+01	4.32715E+03	2.081702E+02	1.100075E+02	9.121277E+02	4.700000E+03
26	1.54420	3.61186	2.6179	3833.6	780617	10.274	1.1330	1.0000
1	1.954146E+00	7.689034E+03	1.061895E+01	4.170000E+03	3.173947E+03	1.033532E+03	4.280000E+06	0.00
2	9.245175E+00	7.523038E+03	1.087458E+01	4.170000E+03	2.070504E+02	1.036202E+02	9.040000E+06	0.00
3	2.779005E+01	7.207188E+03	1.088783E+01	4.170000E+03	5.412121E+02	2.733331E+02	1.032000E+03	0.00
4	5.761252E+01	7.009518E+03	1.023152E+01	4.207564E+03	0.90017E+02	4.33290E+02	2.290000E+03	0.00
5	9.524893E+01	6.761895E+03	1.057956E+01	4.307937E+03	0.48353E+02	3.127574E+02	2.940000E+03	0.00
26	1.70941	3.81187	2.6912	3753.4	7940.7	16.816	.6055	0.00
1	1.923612E+00	7.815281E+03	1.07843E+01	4.170000E+03	3.202608E+03	1.545642E+03	4.920000E+06	0.00
2	9.739555E+00	7.642362E+03	1.07354E+01	4.170000E+03	2.114713E+02	1.017543E+02	9.040000E+06	0.00
3	2.699010E+01	7.391872E+03	1.072505E+01	4.170000E+03	5.272936E+02	2.497977E+02	1.032000E+03	0.00
4	5.574904E+01	7.128448E+03	1.062897E+01	4.170000E+03	0.073360E+02	3.024637E+02	2.290000E+03	0.00
26	1.93615	4.10220	2.8023	3634.2	8136.3	17.670	.98140	0.00
1	1.011654E+00	8.005904E+03	1.073584E+01	3.775383E+03	3.357703E+03	1.447639E+03	4.920000E+06	0.00
2	0.728219E+00	7.828834E+03	1.083908E+01	4.170000E+03	2.172613E+02	1.307000E+03	9.040000E+06	0.00
3	2.542198E+01	7.578390E+03	1.004245E+01	4.170000E+03	5.127545E+02	2.210000E+02	1.032000E+03	0.00
26	2.24246	4.51036	2.9512	3476.0	8379.0	10.946	.95616	0.00
1	1.608061E+00	8.249141E+03	1.01290E+01	3.541719E+03	3.483367E+03	1.310660E+03	4.920000E+06	0.00
2	7.385659E+00	8.079665E+03	1.010723E+01	4.170000E+03	2.100165E+02	0.237002E+03	9.040000E+06	0.00
26	2.48898	4.69191	3.0351	3392.0	8513.4	20.073	.94272	0.00
1	1.424204E+00	8.391333E+03	2.008626E+01	3.450111E+03	3.334602E+03	1.176710E+03	4.920000E+06	0.00
26	2.70383	4.90191	3.1147	3313.5	8635.3	21.030	.53016	0.00
26	2.72346	4.84873	3.1250	3302.5	8648.1	21.000	.52840	0.00
26	2.72676	4.96172	3.1276	3299.7	8652.7	21.000	.52795	0.00
IP=	54							

THOMPSON NOZZLE PROGRAM HAS BEEN COMPLETED

CP TIME W 203,487 PW TIME W 121,921

[illegible]

[illegible]~~| | | | | | |
|---|-----------|-----------|-----------|-----------|-----------|
| A | 0.492E-05 | 0.984E-05 | 0.163E-04 | 0.229E-04 | 0.294E-04 |
| | 0.362E-04 | 0.0 | 0.0 | 0.0 | 0.0 |~~

~~ROAF - DT 1417E-04~~

$\rho_{H_2O} = 0.0$

SNP = 0.25E+03,

~~FOUO - DT 6256-04~~

TPM = 0,417E+04,

000 = 0.1575E+03,

115-151

TWID = 0.3E+02.

```

NPWT      = 0.214E-01, 0.11AE+00, 0.239E+00, 0.326E+00, 0.234E+00,
           0.612E-01, 0.0, 0.0, 0.0, 0.0,

```

RT = 0.697E+00,

RRP - 0125E-011

WPMGT = 0.136E+00,

DZMIN = 0.2E-02,

TMD = 0.1E+04.

ZAX	=	0.0E+00,
Z1	=	0.15E+01,
ZJ	=	0.2E+01,
DZ1	=	0.2E+02,
ORDER	=	3,
SONCON	=	0.0,
LOW1	=	0,
LOW2	=	0,
LOW3	=	0,
VAR	=	0.3E+00, 0.0, 0.0, 0.1E+00, 0.1E+00, 0.0,
PLA0	=	0.0,
TMJD	=	0.9E+01,
SAUR	=	-0.15E+00, 0.1E+01, 0.2E+00, 0.3E+00, -0.1E+01, 0.0,
THP3	=	0.15E+01,
SP8	=	0.744E+01,
RHMAX	=	0.0,
ZHMAX	=	0.0,
IWALL	=	1,
TM14	=	0.12E+02,
THJW	=	0.1E+02,
NYAPE	=	0,
SEND		

ENDMP

ZMAX = 0.0E+02,

PMA = 0.1E+02,

MPH = 0.01,

NPLOT = 1,

NGASER = 0,

PGUT = 0.1E+02,

SMIS = 0.1E+00,

Q1 = 0.1E+01,

Q2 = 0.1E+01,

AREA = 0.1E+01,

BL = 0.1E+01,

BR = 0.1E+01,

N1 = 0.5,

N2 = 1,

GAMMA = 0.1E+01,

SEND

~~CP TIME = 209.491 PP TIME = 123.168~~

SIMPLE JET SPREADING

398

3	17400	415700	15000	4441200
3	31243	13039	30732	9807416
3	61918	140397	33801	9406141
3	73622	140633	37348	8906309
3	77611	152585	38502	8026799
3	98785	162789	42590	8366591
3	99617	168822	45889	8138848
4	12921	180091	49854	7632808
4	14231	181127	50304	7590372
4	28833	192478	55308	7138138
4	44642	204795	60897	6674878
4	55774	213482	66933	6364944
4	71395	225938	70795	5953134
4	88637	236237	77264	5536713
4	92809	242227	78864	5439748
5	12173	249283	82143	5231898
5	18975	259374	85440	5069286
5	27939	270379	92869	4780361
5	29094	273722	93347	4698118
5	31199	273930	94247	4618994
5	32474	273983	94474	4608022
5	33214	274537	94747	4588884
5	33863	275111	95820	4175644
5	34374	275786	95295	3972924
5	35303	276323	95567	3778853
5	36840	276882	95844	3591965
5	38672	277626	96119	3413203
5	37959	278314	96393	3241911
5	38338	278827	96668	3077843
5	39133	279767	96942	2922078
5	39972	280534	97215	2770921
5	40377	281330	97488	2626597
5	41637	282156	97759	2489862
5	42493	283013	98030	2353756
5	43335	283882	98300	2231926
5	44223	284824	98568	2112023
5	45129	285782	98835	1977503
5	46052	286776	99106	1888227
5	46882	287804	99383	1784803
5	47959	288879	99625	1688463
5	48927	289992	99884	1589964
5	49923	291147	100142	1499787
5	50938	292347	100397	1413931

TOTAL MASS FLOW = 6.822801E+03 NO. POINTS = 72

LRC ID	K	R	REX	Z	MACH	TPK	VG	THETA-K	THETA-G	TPK	PG/PG0	DPK/DP0	DG/DG0	SDK/DG	IT
3	3	0.0000	1.0263	1.9141	4753.7	6355.9	0.000	76059	1.79735E-01	2.31083E-01	2.31083E-01	2.31083E-01	2.31083E-01	123469	3
1	7.00095E+00	6.20360E+03	0	0	4.81847E+03	3.214057E+03	4.81847E+03	3.214057E+03	5.146125E+03	5.146125E+03	5.146125E+03	5.146125E+03	5.146125E+03	4.920000E+06	3
2	8.724005E+01	6.05137E+03	0	0	4.833987E+03	2.009455E+02	4.833987E+03	2.009455E+02	3.51637E+02	3.51637E+02	3.51637E+02	3.51637E+02	3.51637E+02	9.440000E+06	3
3	9.043986E+01	5.761861E+03	0	0	4.784914E+03	5.033354E+02	4.784914E+03	5.033354E+02	8.158042E+02	8.158042E+02	8.158042E+02	8.158042E+02	8.158042E+02	1.632000E+05	3
4	1.00003E+02	5.561665E+03	0	0	5.32521E+03	7.112505E+02	5.32521E+03	7.112505E+02	1.344476E+01	1.344476E+01	1.344476E+01	1.344476E+01	1.344476E+01	2.290000E+05	3
5	2.59997E+02	5.907996E+03	0	0	5.10138E+03	8.313333E+02	5.10138E+03	8.313333E+02	1.072740E+01	1.072740E+01	1.072740E+01	1.072740E+01	1.072740E+01	2.740000E+05	3
6	3.033533E+02	5.279916E+03	0	0	5.114085E+03	1.798950E+02	5.114085E+03	1.798950E+02	3.056567E+02	3.056567E+02	3.056567E+02	3.056567E+02	3.056567E+02	4.620000E+05	3
3	4	1.50002	4.05497	2.0000	3745.1	1922.6	15.225	99921	3.492891E-02	5.828917E-02	5.828917E-02	5.828917E-02	5.828917E-02	25398	3
1	1.054116E+00	7.60327E+03	1.559061E+01	4.170000E+03	4.170000E+03	3.215946E+03	4.170000E+03	3.215946E+03	1.378392E+03	1.378392E+03	1.378392E+03	1.378392E+03	1.378392E+03	4.920000E+06	3
2	7.070198E+00	7.643978E+03	1.593000E+01	4.170000E+03	4.170000E+03	2.094319E+02	4.170000E+03	2.094319E+02	8.976442E+03	8.976442E+03	8.976442E+03	8.976442E+03	8.976442E+03	9.840000E+06	3
3	2.970307E+01	7.393939E+03	1.598899E+01	4.170000E+03	4.170000E+03	5.211788E+02	4.170000E+03	5.211788E+02	2.077212E+02	2.077212E+02	2.077212E+02	2.077212E+02	2.077212E+02	1.132000E+05	3
4	4.982642E+01	7.135264E+03	1.516384E+01	4.170000E+03	4.170000E+03	8.228336E+02	4.170000E+03	8.228336E+02	3.686275E+02	3.686275E+02	3.686275E+02	3.686275E+02	3.686275E+02	2.290000E+05	3
5	8.264846E+01	6.90481E+03	1.57037E+01	4.224500E+03	4.224500E+03	6.918810E+02	4.224500E+03	6.918810E+02	2.965396E+02	2.965396E+02	2.965396E+02	2.965396E+02	2.965396E+02	2.740000E+05	3
6	1.237901E+02	6.709966E+03	1.588883E+01	4.313821E+03	4.313821E+03	2.891948E+02	4.313821E+03	2.891948E+02	8.723035E+02	8.723035E+02	8.723035E+02	8.723035E+02	8.723035E+02	3.820000E+05	3
3	4	1.72360	4.24447	2.7445	3684.3	8023.1	15.742	78950	3.241811E-02	5.499297E-02	5.499297E-02	5.499297E-02	5.499297E-02	22622	3

3.27120	1.66177	1.43411	70.97000
3.67011	1.29703	2.78892	90.73130
3.76239	1.38081	1.40552	87.05522
3.91878	1.47933	3.38837	82.78838
4.05457	1.59082	3.7736	70.59003
4.09140	1.60792	3.8782	77.46194
4.24447	1.72300	4.3229	72.94976
4.32442	1.78410	4.5621	70.68797
4.49176	1.91088	5.0775	66.88874
4.63748	2.08009	5.8082	61.72682
4.83919	2.17493	6.2090	57.35731
4.94089	2.25251	6.5481	59.01449
5.12094	2.39002	7.0077	51.32977
5.31458	2.54882	7.5882	47.23553
5.51238	2.74071	8.2953	46.78562
5.72493	2.97980	9.1449	43.32428
5.95940	3.27256	10.131	41.33139
6.23680	3.63680	11.261	33.94849
6.56033	4.07774	12.657	27.42883
6.93384	4.60221	14.3217	23.34900
7.35401	5.22079	16.3514	22.31852
7.82920	5.95288	18.781	21.17995
8.36481	6.81535	21.6402	19.89863
8.96688	7.83442	25.0442	18.77252
9.64008	9.03212	29.121	17.89958
10.39040	10.4048	33.9717	16.67785
11.22227	11.9692	39.6131	15.70530
12.14027	13.7527	46.083	14.78034
13.14924	15.8276	53.4013	13.98886

TOTAL MASS FLOW = 0.0020015-03 NO. OF WTS = 37

LRC ID	R	REK	Z	MACH	TS	VO	THEFAK	TPK	PG/POB	DPK/DPB	DPK/DPB	SDH/DB	IT
K				WPK									RPK
4	3	0.8800	1.9815	1.0734	4678.4	6495.2	0.000	.74726	1.363435E-01	2.892251E-01	2.892251E-01	1.23978	3
1	0.99872E+00	0.34317E+03	01				4.73081E+03	3.228152E+03	4.198330E+03	4.728000E+03	4.728000E+03		
2	2.938789E+01	6.14527E+03	01				4.81611E+03	2.190520E+02	3.210095E+02	3.210095E+02	3.210095E+02	9.440000E+04	
3	6.457716E+01	5.88522E+03	01				4.913997E+03	5.139032E+02	7.908205E+02	7.908205E+02	7.908205E+02	1.632000E+03	
4	1.702928E+02	3.68142E+03	01				4.987285E+03	8.371273E+02	1.244778E+01	1.244778E+01	1.244778E+01	2.870000E+03	
5	2.439739E+02	5.52972E+03	01				5.04512E+03	6.491344E+02	9.971932E+02	9.971932E+02	9.971932E+02	2.740000E+03	
6	3.411587E+02	5.591072E+03	01				5.08322E+03	1.892634E+02	2.890115E+02	2.890115E+02	2.890115E+02	3.120000E+03	
4	4	1.67739	4.42163	2.7555	3668.8	8036.1	14.908	.90670	3.018099E+02	9.149943E+02	9.149943E+02	1.23282	9
1	1.437181E+00	7.92194E+03	01				3.708974E+03	3.228173E+03	3.228173E+03	3.228173E+03	3.228173E+03	4.728000E+04	
2	6.980235E+00	7.75999E+03	01				4.170000E+03	2.102775E+02	7.959519E+03	7.959519E+03	7.959519E+03	9.440000E+04	
3	2.114632E+01	7.512454E+03	01				4.170000E+03	5.388139E+02	2.807349E+02	2.807349E+02	2.807349E+02	1.632000E+03	
4	4.363333E+01	7.254947E+03	01				4.170000E+03	8.358857E+02	3.234409E+02	3.234409E+02	3.234409E+02	2.870000E+03	
5	7.027778E+01	7.115190E+03	01				4.170000E+03	8.327807E+02	5.263494E+02	5.263494E+02	5.263494E+02	2.740000E+03	
6	1.075743E+02	6.811854E+03	01				4.24400E+03	2.804604E+02	7.887605E+03	7.887605E+03	7.887605E+03	3.120000E+03	
4	4	1.88497	4.68608	2.8174	3601.7	8143.4	15.711	.57027	2.788997E+02	4.838345E+02	4.838345E+02	1.23978	9
1	1.408159E+00	6.25223E+03	01				3.67895E+03	3.224333E+03	3.224333E+03	3.224333E+03	3.224333E+03	4.728000E+04	
2	6.881345E+00	7.85933E+03	01				4.170000E+03	2.124004E+02	7.943871E+03	7.943871E+03	7.943871E+03	9.440000E+04	
3	2.029320E+01	7.61270E+03	01				4.170000E+03	5.278999E+02	1.108900E+02	1.108900E+02	1.108900E+02	1.632000E+03	
4	4.193483E+01	7.353906E+03	01				4.170000E+03	8.359721E+02	2.961475E+02	2.961475E+02	2.961475E+02	2.870000E+03	
5	7.006159E+01	7.13916E+03	01				4.170000E+03	8.379748E+02	2.300003E+02	2.300003E+02	2.300003E+02	2.740000E+03	
4	4	2.03784	4.91291	2.9061	3509.2	8291.4	16.320	.56148	2.882574E+02	4.457114E+02	4.457114E+02	1.23978	9
1	1.235787E+00	6.16791E+03	01				3.56741E+03	3.183461E+03	3.183461E+03	3.183461E+03	3.183461E+03	4.728000E+04	
2	6.982320E+00	7.67888E+03	01				4.170000E+03	2.102775E+02	7.959519E+03	7.959519E+03	7.959519E+03	9.440000E+04	
3	1.825413E+01	7.753084E+03	01				4.170000E+03	5.324648E+02	1.250994E+02	1.250994E+02	1.250994E+02	1.632000E+03	
4	4.005476E+01	7.483445E+03	01				4.170000E+03	8.07376E+02	2.657495E+02	2.657495E+02	2.657495E+02	2.870000E+03	
4	4	2.32121	5.29415	3.333	3377.0	8489.5	17.429	.54032	2.150958E+02	3.991194E+02	3.991194E+02	1.23978	9
1	1.237426E+00	6.365800E+03	01				3.43541E+03	3.383219E+03	3.383219E+03	3.383219E+03	3.383219E+03	4.728000E+04	

[illegible]

5	2	1.08399	3.92166	2.6634	3761.9	7073.6	15.339	109190	3.492245E-02	5.902003E-02	1.27161	3
1	1.070944E+00	7.762307E+03	1.29030E+01	4.17000E+03	3.109356E+03	1.360470E+03	4.92000E+03					
2	1.070944E+00	7.762307E+03	1.29030E+01	4.17000E+03	3.109356E+03	1.360470E+03	4.92000E+03					
3	2.361335E+01	7.260241E+03	1.26079E+01	4.17000E+03	2.117999E+02	2.117999E+02	1.93200E+03					
4	5.395236E+01	7.000304E+03	1.21370E+01	4.17440E+03	9.170564E+02	3.912336E+02	2.29000E+03					
5	0.790970E+01	8.777330E+03	1.19013E+01	4.17320E+03	7.729918E+02	3.129923E+02	2.90000E+03					
6	1.872602E+02	6.97650E+03	1.12617E+01	4.37143E+03	2.109943E+02	9.529235E+03	3.92000E+03					
5	2	1.45896	4.06057	2.6735	3740.1	7064.9	15.414	109070	3.309750E-02	5.940005E-02	1.26010	3
1	1.011746E+00	7.780022E+03	1.32749E+01	4.17000E+03	3.104325E+03	1.326076E+03	4.92000E+03					
2	1.011746E+00	7.780022E+03	1.32749E+01	4.17000E+03	3.104325E+03	1.326076E+03	4.92000E+03					
3	2.361335E+01	7.260241E+03	1.26079E+01	4.17000E+03	2.117999E+02	2.117999E+02	1.93200E+03					
4	5.395236E+01	7.000304E+03	1.21370E+01	4.17440E+03	9.170564E+02	3.912336E+02	2.29000E+03					
5	0.790970E+01	8.777330E+03	1.19013E+01	4.17320E+03	7.729918E+02	3.129923E+02	2.90000E+03					
6	1.872602E+02	6.97650E+03	1.12617E+01	4.37143E+03	2.109943E+02	9.529235E+03	3.92000E+03					
5	2	1.28774	4.13144	2.6922	3731.4	7020.4	12.546	109732	3.271157E-02	5.97906E-02	1.29510	3
1	1.021008E+00	7.613305E+03	1.31900E+01	4.17000E+03	3.109310E+03	1.320309E+03	4.92000E+03					
2	1.021008E+00	7.613305E+03	1.31900E+01	4.17000E+03	3.109310E+03	1.320309E+03	4.92000E+03					
3	2.361335E+01	7.260241E+03	1.26079E+01	4.17000E+03	2.117999E+02	2.117999E+02	1.93200E+03					
4	5.395236E+01	7.000304E+03	1.21370E+01	4.17440E+03	9.170564E+02	3.912336E+02	2.29000E+03					
5	0.790970E+01	8.777330E+03	1.19013E+01	4.17320E+03	7.729918E+02	3.129923E+02	2.90000E+03					
6	1.872602E+02	6.97650E+03	1.12617E+01	4.37143E+03	2.109943E+02	9.529235E+03	3.92000E+03					
5	2	1.31250	4.25547	2.7699	3711.3	7051.1	13.737	109381	3.194471E-02	5.992010E-02	1.26254	3
1	1.022201E+00	7.64999E+03	1.32907E+01	4.17000E+03	3.109477E+03	1.324330E+03	4.92000E+03					
2	1.022201E+00	7.64999E+03	1.32907E+01	4.17000E+03	3.109477E+03	1.324330E+03	4.92000E+03					
3	2.361335E+01	7.260241E+03	1.26079E+01	4.17000E+03	2.117999E+02	2.117999E+02	1.93200E+03					
4	5.395236E+01	7.000304E+03	1.21370E+01	4.17440E+03	9.170564E+02	3.912336E+02	2.29000E+03					
5	0.790970E+01	8.777330E+03	1.19013E+01	4.17320E+03	7.729918E+02	3.129923E+02	2.90000E+03					
6	1.872602E+02	6.97650E+03	1.12617E+01	4.37143E+03	2.109943E+02	9.529235E+03	3.92000E+03					
5	2	1.40032	4.36495	2.7320	3694.5	7000.1	13.010	109004	3.290436E-02	5.960011E-02	1.26601	3
1	1.015791E+00	7.603035E+03	1.33001E+01	4.17000E+03	3.109477E+03	1.324330E+03	4.92000E+03					
2	1.015791E+00	7.603035E+03	1.33001E+01	4.17000E+03	3.109477E+03	1.324330E+03	4.92000E+03					
3	2.361335E+01	7.260241E+03	1.26079E+01	4.17000E+03	2.117999E+02	2.117999E+02	1.93200E+03					
4	5.395236E+01	7.000304E+03	1.21370E+01	4.17440E+03	9.170564E+02	3.912336E+02	2.29000E+03					
5	0.790970E+01	8.777330E+03	1.19013E+01	4.17320E+03	7.729918E+02	3.129923E+02	2.90000E+03					
6	1.872602E+02	6.97650E+03	1.12617E+01	4.37143E+03	2.109943E+02	9.529235E+03	3.92000E+03					
5	2	1.51663	4.59243	2.7893	3694.4	6935.9	13.360	109503	2.840265E-02	4.955931E-02	1.25953	3
1	1.021008E+00	7.613305E+03	1.31900E+01	4.17000E+03	3.109310E+03	1.320309E+03	4.92000E+03					
2	1.021008E+00	7.613305E+03	1.31900E+01	4.17000E+03	3.109310E+03	1.320309E+03	4.92000E+03					
3	2.361335E+01	7.260241E+03	1.26079E+01	4.17000E+03	2.117999E+02	2.117999E+02	1.93200E+03					
4	5.395236E+01	7.000304E+03	1.21370E+01	4.17440E+03	9.170564E+02	3.912336E+02	2.29000E+03					
5	0.790970E+01	8.777330E+03	1.19013E+01	4.17320E+03	7.729918E+02	3.129923E+02	2.90000E+03					
6	1.872602E+02	6.97650E+03	1.12617E+01	4.37143E+03	2.109943E+02	9.529235E+03	3.92000E+03					
5	2	1.64050	4.73153	2.7941	3619.2	6895.5	13.794	109707	2.670296E-02	4.911276E-02	1.25575	3
1	1.013348E+00	7.603035E+03	1.33001E+01	4.17000E+03	3.109477E+03	1.324330E+03	4.92000E+03					
2	1.013348E+00	7.603035E+03	1.33001E+01	4.17000E+03	3.109477E+03	1.324330E+03	4.92000E+03					
3	2.361335E+01	7.260241E+03	1.26079E+01	4.17000E+03	2.117999E+02	2.117999E+02	1.93200E+03					
4	5.395236E+01	7.000304E+03	1.21370E+01	4.17440E+03	9.170564E+02	3.912336E+02	2.29000E+03					
5	0.790970E+01	8.777330E+03	1.19013E+01	4.17320E+03	7.729918E+02	3.129923E+02	2.90000E+03					
6	1.872602E+02	6.97650E+03	1.12617E+01	4.37143E+03	2.109943E+02	9.529235E+03	3.92000E+03					
5	2	1.78074	4.76025	2.8002	3610.2	6828.5	14.721	109764	2.700324E-02	4.900010E-02	1.25139	3
1	1.023045E+00	7.603035E+03	1.33001E+01	4.17000E+03	3.109477E+03	1.324330E+03	4.92000E+03					
2	1.023045E+00	7.603035E+03	1.33001E+01	4.17000E+03	3.109477E+03	1.324330E+03	4.92000E+03					
3	2.361335E+01	7.260241E+03	1.26079E+01	4.17000E+03	2.117999E+02	2.117999E+02	1.93200E+03					
4	5.395236E+01	7.000304E+03	1.21370E+01	4.17440E+03	9.170564E+02	3.912336E+02	2.29000E+03					
5	0.790970E+01	8.777330E+03	1.19013E+01	4.17320E+03	7.729918E+02	3.129923E+02	2.90000E+03					
6	1.872602E+02	6.97650E+03	1.12617E+01	4.37143E+03	2.109943E+02	9.529235E+03	3.92000E+03					
5	2	1.81079	4.70097	2.8295	3595.7	6160.3	14.974	109732	2.619526E-02	4.965094E-02	1.22073	3

2 4.000000E+01 0.000000E+00 3.000000E+00 4.100000E+03 0.230000E+02 0.000000E+00 4.000000E+02
6 2.074020E+01 7.750385E+03 3.700000E+00 4.100000E+03 1.072000E+02 1.000000E+00 3.000000E+02

Z		M		MPC	
7.92999	0.00000	0.00000	0.00000	22.45309	
9.13394	0.00020	0.00012	0.00012	22.12103	
0.31194	0.00000	0.00000	0.00000	21.41000	
0.55112	0.00000	0.00000	0.00000	20.57674	
0.83185	0.00000	0.00000	0.00000	19.55660	
9.13776	0.00000	0.00000	0.00000	18.41228	
9.53769	0.00000	0.00000	0.00000	17.15101	
7.03527	0.00000	0.00000	0.00000	16.21449	
10.12254	0.00000	0.00000	0.00000	15.20207	
10.35236	0.00000	0.00000	0.00000	14.00673	

TOTAL MASS FLOW = 0.022000E+03 M3, POINTS = 10

LRC ID	K	M	Z	MACH	TG	VG	THETA-K	THETA-G	TU/T00	TPK	DPK/DG	PG/PG0	UG/DG0	SDK/DG	IT
31	3	0.00000	4.20454	3.1100	3273.0	0.0000	0.0000	0.0000	0.0000	0.0000	0.0000	0.0000	0.0000	0.0000	0
1	0.23000E+02	3.37194E+03	0.0												
2	9.72417E+01	4.45420E+03	0.0												
3	4.92012E+01	4.26432E+03	0.0												
4	1.82077E+01	7.90835E+03	0.0												
5	2.42514E+01	7.35337E+03	0.0												
6	3.70217E+01	7.49363E+03	0.0												
31	5	0.02435	10.37491	3.3369	3308.4	0.0000	0.0000	0.0000	0.0000	0.0000	0.0000	0.0000	0.0000	0.0000	0
1	2.00000E+01	3.79797E+03	0.0												
2	1.21177E+01	3.97033E+03	0.0												
3	3.91566E+01	3.49339E+03	0.0												
4	0.90000E+01	3.26272E+03	0.0												
5	1.02502E+01	3.23156E+03	0.0												
6	2.50015E+01	7.75152E+03	0.0												

Z		M		MPC	
3.20454	0.00000	0.00000	0.00000	21.50363	
4.93394	0.00020	0.00012	0.00012	20.64755	
9.73723	0.00000	0.00000	0.00000	20.00000	
9.32323	0.00000	0.00000	0.00000	18.99101	
9.35544	0.00000	0.00000	0.00000	17.05905	
7.74293	0.00000	0.00000	0.00000	16.02028	
10.04569	0.00000	0.00000	0.00000	15.70044	
10.36355	0.00000	0.00000	0.00000	14.79428	
10.57491	0.00000	0.00000	0.00000	14.20358	

TOTAL MASS FLOW = 0.022000E+03 M3, POINTS = 9

LRC ID	K	M	Z	MACH	TG	VG	THETA-K	THETA-G	TU/T00	TPK	DPK/DG	PG/PG0	UG/DG0	SDK/DG	IT
32	3	0.00000	0.70774	3.1400	3247.0	0.0000	0.0000	0.0000	0.0000	0.0000	0.0000	0.0000	0.0000	0.0000	0
1	1.04397E+01	4.59267E+03	0.0												
2	1.00000E+00	0.00000E+00	0.0												
3	4.07057E+01	8.30273E+03	0.0												
4	1.16719E+01	8.34744E+03	0.0												
5	2.15034E+01	7.79247E+03	0.0												
6	3.44010E+01	7.54136E+03	0.0												

Z		M		MPC	
3.70774	0.00000	0.00000	0.00000	20.12334	
0.95529	0.00000	0.00000	0.00000	19.30027	
8.24593	0.00000	0.00000	0.00000	18.29765	
9.58202	0.00000	0.00000	0.00000	17.10062	
9.98597	0.00000	0.00000	0.00000	15.90030	
10.00000	0.00000	0.00000	0.00000	14.00000	

DATE/TIME 12:00 10:00
 10.61935 0.67445 0.1193 14.20420

TOTAL MASS FLOW = 6.822800E+03 NO. POINTS = 7

LRC ID	R	Z	MACH	TQ	VG	THETA-K	TPK	THETA-G	TQ/TGO	PG/PQO	DPK/DG	DG/DGO	SDK/DG	IT
K	REK		VPK									DPK/DPG		RPK
33	3	0.0000	9.21114	3.1784	3214.7	8679.3	0.000	.51435	0.221992E+03	1.598533E+02	1.23529	5		
1	1.95437E+01	0.63025E+03	0				3.24141E+03	3.13898E+03	3.13898E+03	3.13898E+03	3.13898E+03	3.13898E+03	3.13898E+03	3.13898E+03
2	1.127812E+00	0.538044E+03	0				3.28033E+03	1.806670E+02	2.187017E+03	2.187017E+03	2.187017E+03	2.187017E+03	2.187017E+03	2.187017E+03
3	4.421175E+00	3.347309E+03	0				3.652121E+03	1.806670E+02	2.187017E+03	2.187017E+03	2.187017E+03	2.187017E+03	2.187017E+03	2.187017E+03
4	1.077322E+01	3.102787E+03	0				4.170000E+03	7.856612E+02	7.856612E+02	7.856612E+02	7.856612E+02	7.856612E+02	7.856612E+02	7.856612E+02
5	1.984023E+01	7.852205E+03	0				4.170000E+03	6.753791E+02	7.940705E+03	7.940705E+03	7.940705E+03	7.940705E+03	7.940705E+03	7.940705E+03
6	3.171771E+01	7.635338E+03	0				4.170000E+03	2.009256E+02	2.432107E+03	2.432107E+03	2.432107E+03	2.432107E+03	2.432107E+03	2.432107E+03

Z H MPC

9.21114 0.0000 0.0000 18.49948
 9.51178 0.0027 17.20022
 9.86123 0.0126 16.41997
 10.26952 0.0334 15.24799
 10.59013 0.0566 14.38028

TOTAL MASS FLOW = 6.822800E+03 NO. POINTS = 5

LRC ID	R	Z	MACH	TQ	VG	THETA-K	TPK	THETA-G	TQ/TGO	PG/PQO	DPK/DG	DG/DGO	SDK/DG	IT
K	REK		VPK									DPK/DPG		RPK
34	3	0.0000	9.82280	3.2256	3169.0	8745.2	0.000	.50704	7.339437E+03	1.447518E+02	1.23598	5		
1	2.199315E+01	0.686322E+03	0				3.203216E+03	3.152421E+03	3.152421E+03	3.152421E+03	3.152421E+03	3.152421E+03	3.152421E+03	3.152421E+03
2	1.127812E+00	0.538044E+03	0				3.28033E+03	1.806670E+02	2.187017E+03	2.187017E+03	2.187017E+03	2.187017E+03	2.187017E+03	2.187017E+03
3	4.421175E+00	3.347309E+03	0				3.652121E+03	1.806670E+02	2.187017E+03	2.187017E+03	2.187017E+03	2.187017E+03	2.187017E+03	2.187017E+03
4	9.872749E+00	8.40397E+03	0				3.553001E+03	4.716801E+02	5.020335E+03	5.020335E+03	5.020335E+03	5.020335E+03	5.020335E+03	5.020335E+03
5	1.984023E+01	8.166733E+03	0				4.170000E+03	7.856612E+02	8.379480E+03	8.379480E+03	8.379480E+03	8.379480E+03	8.379480E+03	8.379480E+03
6	2.875556E+01	7.923144E+03	0				4.170000E+03	6.753791E+02	7.170513E+03	7.170513E+03	7.170513E+03	7.170513E+03	7.170513E+03	7.170513E+03

Z H MPC

9.82280 0.0000 0.0000 16.51373
 10.18421 0.11892 15.48992
 10.50690 0.26092 14.38470

TOTAL MASS FLOW = 6.822800E+03 NO. POINTS = 3

LRC ID	R	Z	MACH	TQ	VG	THETA-K	TPK	THETA-G	TQ/TGO	PG/PQO	DPK/DG	DG/DGO	SDK/DG	IT
K	REK		VPK									DPK/DPG		RPK
35	3	0.0000	10.55917	3.2774	3119.3	8815.8	0.000	.49909	6.468893E+03	1.296139E+02	1.23595	5		
1	1.921080E+01	0.757862E+03	0				3.153947E+03	3.161745E+03	3.161745E+03	3.161745E+03	3.161745E+03	3.161745E+03	3.161745E+03	3.161745E+03
2	1.127812E+00	0.538044E+03	0				3.210252E+03	1.924031E+02	1.924031E+02	1.924031E+02	1.924031E+02	1.924031E+02	1.924031E+02	1.924031E+02
3	3.061272E+01	8.464624E+03	0				3.454232E+03	4.745373E+02	4.745373E+02	4.745373E+02	4.745373E+02	4.745373E+02	4.745373E+02	4.745373E+02
4	8.886162E+00	8.23925E+03	0				4.010123E+03	7.866674E+02	7.866674E+02	7.866674E+02	7.866674E+02	7.866674E+02	7.866674E+02	7.866674E+02
5	1.984023E+01	8.003081E+03	0				4.170000E+03	6.701448E+02	6.701448E+02	6.701448E+02	6.701448E+02	6.701448E+02	6.701448E+02	6.701448E+02
6	2.568892E+01	7.762458E+03	0				4.170000E+03	2.040794E+02	1.944965E+03	1.944965E+03	1.944965E+03	1.944965E+03	1.944965E+03	1.944965E+03

THOMPSON PLUME PROGRAM HAS BEEN COMPLETED

CP TIME - 229,132 PP TIME - 131,990

BEGINNING OF STREAMLINE GENERATION PROGRAM

CP TIME = 325.153 PP TIME = 133.690

STREAMLINE(1) = 0.00000 PERCENT OF THE TOTAL MASS FLOW
 ZINIT = 0.000000 (NONDIMENSIONAL - Z/RC)
 PINIT = 1992.764306 (PSIA)
 RINIT = 0.128734634 (IN, R)
 VINIT = 1918.291211 (FT/SEC)
 ZFINAL = 11.072805 (NONDIMENSIONAL - Z/RC)
 NNNNN = 62 (NO. OF PRESSURE TABLE POINTS)

POINT NO.	AXIAL DISTANCE (Z/RC)	RADIAL DISTANCE (R/RC)	STREAMLINE DISTANCE (S/RC)	PRESSURE (PSIA)
1	-1.250000E+00	0.	0.	1.992764E+03
2	-1.161511E+00	0.	8.848896E-02	1.968198E+03
3	-1.073022E+00	0.	1.709779E-01	1.939710E+03
4	-9.845331E-01	0.	2.694669E-01	1.906875E+03
5	-8.960442E-01	0.	3.539559E-01	1.869199E+03
6	-8.073332E-01	0.	4.424448E-01	1.828204E+03
7	-7.190662E-01	0.	5.309338E-01	1.777410E+03
8	-6.305773E-01	0.	6.194227E-01	1.727201E+03
9	-5.420885E-01	0.	7.079117E-01	1.669341E+03
10	-4.535994E-01	0.	7.964007E-01	1.652289E+03
11	-3.651104E-01	0.	8.848896E-01	1.604440E+03
12	-2.766214E-01	0.	9.733786E-01	1.550396E+03
13	-1.881325E-01	0.	1.061368E+00	1.480280E+03
14	-9.964350E-02	0.	1.150357E+00	1.430930E+03
15	0.000000E+00	0.	1.238849E+00	1.378494E+03
16	7.733442E-02	0.	1.327334E+00	1.317779E+03
17	1.658234E-01	0.	1.415823E+00	1.246342E+03
18	2.543124E-01	0.	1.504312E+00	1.166490E+03
19	3.428013E-01	0.	1.592801E+00	1.116877E+03
20	4.312903E-01	0.	1.681290E+00	1.057315E+03
21	5.197793E-01	0.	1.769779E+00	9.884789E+02
22	6.082684E-01	0.	1.858268E+00	9.093337E+02
23	6.967575E-01	0.	1.946757E+00	8.201986E+02
24	7.852466E-01	0.	2.035246E+00	7.210735E+02
25	8.737357E-01	0.	2.123735E+00	6.119484E+02
26	9.622248E-01	0.	2.212224E+00	4.928233E+02
27	1.050715E+00	0.	2.300715E+00	3.636982E+02
28	1.139206E+00	0.	2.389206E+00	2.245731E+02
29	1.227697E+00	0.	2.477697E+00	7.546078E+01
30	1.316188E+00	0.	2.566188E+00	1.856425E+01
31	1.404679E+00	0.	2.654679E+00	3.954678E+00
32	1.493170E+00	0.	2.743170E+00	3.517745E+00
33	1.581661E+00	0.	2.831661E+00	2.998862E+00
34	1.670152E+00	0.	2.920152E+00	2.731407E+00
35	1.758643E+00	0.	3.008643E+00	2.560348E+00
36	1.847134E+00	0.	3.097134E+00	2.245598E+00
37	1.935625E+00	0.	3.185625E+00	2.059835E+00
38	2.024116E+00	0.	3.274116E+00	1.820713E+00
39	2.112607E+00	0.	3.362607E+00	1.644164E+00
40	2.201098E+00	0.	3.451098E+00	1.441947E+00
41	2.289589E+00	0.	3.539589E+00	1.276404E+00
42	2.378080E+00	0.	3.628080E+00	1.113051E+00
43	2.466571E+00	0.	3.716571E+00	9.816917E+00
44	2.555062E+00	0.	3.805062E+00	8.618269E+00

45	3,412,309/E+00	0:	2,432,000/E+00	1,069,011E+01
46	4,178,995E+00	0:	5,428,095E+00	6,730,091E+01
47	4,377,391E+00	0:	5,627,391E+00	5,969,166E+01
48	4,582,991E+00	0:	5,832,991E+00	5,127,508E+01
49	5,018,630E+00	0:	6,268,630E+00	4,140,130E+01
50	5,489,336E+00	0:	6,739,336E+00	3,227,560E+01
51	5,979,387E+00	0:	7,229,387E+00	2,374,049E+01
52	6,424,582E+00	0:	7,674,582E+00	2,192,847E+01
53	6,754,447E+00	0:	8,004,447E+00	2,106,570E+01
54	6,971,979E+00	0:	8,221,979E+00	2,235,275E+01
55	7,162,996E+00	0:	8,412,996E+00	2,341,774E+01
56	7,377,977E+00	0:	8,627,977E+00	2,368,815E+01
57	7,580,912E+00	0:	8,830,912E+00	2,336,997E+01
58	7,929,992E+00	0:	9,179,992E+00	2,265,369E+01
59	8,284,540E+00	0:	9,534,540E+00	2,156,363E+01
60	8,707,735E+00	0:	9,957,735E+00	2,012,334E+01
61	9,211,141E+00	0:	1,046,114E+01	1,849,948E+01
62	9,828,055E+00	0:	1,107,280E+01	1,651,373E+01

STREAMLINE(2) = 20.00000 PERCENT OF THE TOTAL MASS FLOW

ZINIT = 0.000000 (NONDIMENSIONAL - S/RC)

PINIT = 2007.023437 (PSIA)

TINIT = 6136.189482 (DEG, R)

VINIT = 1858.421023 (FT/SEC)

ZFINAL = 11.132001 (NONDIMENSIONAL - Z/RC)

MGKSK = 55 (NO. OF PRESSURE TABLE POINTS)

POINT NO.	AXIAL DISTANCE (Z/RC)	RADIAL DISTANCE (R/RC)	STREAMLINE DISTANCE (S/RC)	PRESSURE (PSIA)
1	-1.250000E+00	5.095139E-01	0.	2.007823E+03
2	-1.181511E+00	5.471089E-01	8.934319E-02	1.981789E+03
3	-1.073022E+00	5.351643E-01	1.786434E-01	1.951099E+03
4	-9.845331E-01	5.235767E-01	2.678898E-01	1.915393E+03
5	-8.960442E-01	5.125879E-01	3.570847E-01	1.874112E+03
6	-8.075552E-01	5.021362E-01	4.461629E-01	1.826909E+03
7	-7.190662E-01	4.924377E-01	5.351817E-01	1.773265E+03
8	-6.305773E-01	4.798007E-01	6.221908E-01	1.749073E+03
9	-5.420883E-01	4.706441E-01	7.138592E-01	1.704692E+03
10	-4.535994E-01	4.655492E-01	8.024947E-01	1.693410E+03
11	-3.651104E-01	4.607004E-01	8.911160E-01	1.999818E+03
12	-2.766214E-01	4.562891E-01	9.797152E-01	1.532589E+03
13	-1.881325E-01	4.514948E-01	1.068334E+00	1.477028E+03
14	-9.964358E-02	4.472651E-01	1.156891E+00	1.418022E+03
15	-1.115454E-02	4.476713E-01	1.245354E+00	1.351434E+03
16	7.733442E-02	4.467961E-01	1.333848E+00	1.283990E+03
17	1.659828E-01	4.469979E-01	1.422337E+00	1.213008E+03
18	2.543124E-01	4.478593E-01	1.510830E+00	1.144993E+03
19	3.428013E-01	4.500540E-01	1.599346E+00	1.075117E+03
20	4.312703E-01	4.528003E-01	1.687871E+00	1.008222E+03
21	7.488261E-01	4.493781E-01	2.005423E+00	7.812043E+02
22	8.566563E-01	4.714112E-01	2.067308E+00	7.514840E+02
23	9.457896E-01	5.118846E-01	2.214308E+00	6.781239E+02
24	1.081492E+00	5.659717E-01	2.356396E+00	6.086027E+02
25	1.215880E+00	5.996573E-01	2.496241E+00	5.426303E+02
26	1.347829E+00	6.339898E-01	2.632583E+00	4.808801E+02
27	1.478018E+00	6.644708E-01	2.766293E+00	4.256136E+02
28	1.605764E+00	6.903317E-01	2.896631E+00	3.769050E+02
29	1.734712E+00	7.145966E-01	3.027842E+00	3.338399E+02
30	1.870469E+00	7.414044E-01	3.166220E+00	2.937517E+02
31	2.013737E+00	7.710104E-01	3.312517E+00	2.572703E+02
32	2.164889E+00	8.040390E-01	3.468798E+00	2.238389E+02
33	2.330585E+00	8.411768E-01	3.637043E+00	1.927253E+02
34	2.508448E+00	8.831555E-01	3.819793E+00	1.651280E+02
35	2.702929E+00	9.308437E-01	4.019988E+00	1.424400E+02
36	2.880634E+00	9.534257E-01	4.199147E+00	1.279978E+02
37	3.104043E+00	1.000583E+00	4.427479E+00	1.142637E+02
38	3.350347E+00	1.053528E+00	4.689277E+00	1.017809E+02
39	3.646197E+00	1.113960E+00	4.981361E+00	8.968903E+01
40	4.103559E+00	1.208693E+00	5.448431E+00	7.426068E+01
41	4.261335E+00	1.241399E+00	5.609758E+00	6.970852E+01
42	4.488760E+00	1.286978E+00	5.841509E+00	6.396294E+01
43	4.776931E+00	1.346223E+00	6.135706E+00	5.737539E+01
44	5.051074E+00	1.400334E+00	6.415924E+00	5.208451E+01
45	5.369631E+00	1.463867E+00	6.739969E+00	4.667151E+01
46	5.691198E+00	1.527228E+00	7.067720E+00	4.200858E+01
47	6.006214E+00	1.599825E+00	7.443809E+00	3.738804E+01
48	6.445995E+00	1.674527E+00	7.836756E+00	3.327434E+01
49	6.868851E+00	1.755874E+00	8.267366E+00	2.945093E+01

99	1.670972E+00	1.921437E+00	0./0002/E+00	2.018700E+01
99	7.758104E+00	1.922456E+00	9.164204E+00	2.326210E+01
99	0.208934E+00	2.007000E+00	9.680842E+00	2.074170E+01
99	0.000007E+00	2.000200E+00	1.021071E+01	1.850027E+01
99	9.175906E+00	2.100375E+00	1.001410E+01	1.653063E+01
99	9.085334E+00	2.270053E+00	1.113200E+01	1.476005E+01

STREAMLINE(3) = 40.00000 PERCENT OF THE TOTAL MASS FLOW

ZINIT = 0.000000 (NONDIMENSIONAL = Z/RC)

PINIT = 2020.304204 (PSIA)

TINIT = 6146.272736 (DEG. R)

VINIT = 1774.130855 (FT/SEC)

ZFINAL = 10.000240 (NONDIMENSIONAL = Z/RC)

NHRSK = 53 (NO. OF PRESSURE TABLE POINTS)

POINT NO.	AXIAL DISTANCE (Z/RC)	RADIAL DISTANCE (R/RC)	STREAMLINE DISTANCE (S/RC)	PRESSURE (PSIA)
1	-1.250000E+00	7.993263E+01	0.	2.020364E+03
2	-1.101911E+00	7.806301E+01	9.044084E+02	1.999334E+03
3	-1.073022E+00	7.823021E+01	1.808096E+01	1.969110E+03
4	-9.845331E-01	7.446223E+01	2.710474E+01	1.929349E+03
5	-8.960442E-01	7.270222E+01	3.611940E+01	1.879629E+03
6	-8.075552E-01	7.116973E+01	4.510722E+01	1.827471E+03
7	-7.190662E-01	6.969157E+01	5.407407E+01	1.768371E+03
8	-6.309773E-01	6.737240E+01	6.317710E+01	1.707699E+03
9	-5.420883E-01	6.608657E+01	7.207029E+01	1.712268E+03
10	-4.535994E-01	6.585182E+01	8.095848E+01	1.650323E+03
11	-3.651104E-01	6.509649E+01	8.983955E+01	1.582554E+03
12	-2.766214E-01	6.443928E+01	9.871282E+01	1.509524E+03
13	-1.881325E-01	6.381041E+01	1.075840E+00	1.464486E+03
14	-9.964550E-02	6.347573E+01	1.164393E+00	1.392430E+03
15	-1.115454E-02	6.325974E+01	1.252908E+00	1.318565E+03
16	7.733442E-02	6.317235E+01	1.341401E+00	1.242894E+03
17	1.650254E-01	6.323238E+01	1.429694E+00	1.170601E+03
18	2.543124E-01	6.344533E+01	1.518404E+00	1.094832E+03
19	3.428013E-01	6.382685E+01	1.606975E+00	1.023362E+03
20	4.312905E-01	6.428911E+01	1.695501E+00	9.499904E+02
21	6.958348E-01	6.425414E+01	1.960126E+00	7.520804E+02
22	7.157167E-01	6.449937E+01	1.981189E+00	7.413817E+02
23	8.589733E-01	6.554050E+01	2.126889E+00	6.852187E+02
24	9.923979E-01	7.406691E+01	2.272506E+00	5.866850E+02
25	1.130975E+00	7.852728E+01	2.418085E+00	5.093910E+02
26	1.270927E+00	8.500992E+01	2.564680E+00	4.597092E+02
27	1.411687E+00	8.757255E+01	2.713010E+00	3.766447E+02
28	1.554924E+00	9.223460E+01	2.863643E+00	3.152831E+02
29	1.700849E+00	9.899627E+01	3.017140E+00	2.679867E+02
30	1.849608E+00	1.018316E+00	3.173560E+00	2.298486E+02
31	2.001063E+00	1.069874E+00	3.332307E+00	2.043768E+02
32	2.157280E+00	1.113380E+00	3.495571E+00	1.877317E+02
33	2.322368E+00	1.163310E+00	3.668062E+00	1.727810E+02
34	2.497280E+00	1.215889E+00	3.850704E+00	1.585191E+02
35	2.684496E+00	1.271782E+00	4.046088E+00	1.447972E+02
36	2.883954E+00	1.331547E+00	4.256222E+00	1.316152E+02
37	3.104899E+00	1.396021E+00	4.484462E+00	1.189184E+02
38	3.344782E+00	1.466142E+00	4.734389E+00	1.088099E+02
39	3.551928E+00	1.496188E+00	4.943698E+00	9.730349E+01
40	3.824086E+00	1.563240E+00	5.223945E+00	8.658189E+01
41	4.133380E+00	1.639992E+00	5.542573E+00	7.822393E+01
42	4.490515E+00	1.727859E+00	5.910495E+00	6.620898E+01
43	5.058952E+00	1.869191E+00	6.496197E+00	5.354862E+01
44	5.297917E+00	1.919020E+00	6.700920E+00	4.984898E+01
45	5.540771E+00	1.988783E+00	6.992638E+00	4.522623E+01
46	5.903051E+00	2.079678E+00	7.366147E+00	4.003772E+01
47	6.249294E+00	2.189033E+00	7.722716E+00	3.589092E+01
48	6.651287E+00	2.265316E+00	8.137068E+00	3.169258E+01
49	7.053885E+00	2.365294E+00	8.553836E+00	2.811520E+01

51	1.023201E+00	2.190130E+00	7.032400E+00	2.427730E+01
52	6.012009E+00	2.603084E+00	9.539086E+00	2.118088E+01
53	8.551713E+00	2.740610E+00	1.009004E+01	1.745773E+01
54	9.104974E+00	2.800050E+00	1.000025E+01	1.406274E+01

STREAMLINE(4) = 60.00000 PERCENT OF THE TOTAL MASS FLOW
 ZINIT = 0.000000 (NONDIMENSIONAL = Z/RC)
 PINIT = 2099.317024 (PSIA)
 TINIT = 6198.412074 (DEG. R)
 VINIT = 1667.048615 (FT/SEC)
 ZFINAL = 9.872043 (NONDIMENSIONAL = Z/RC)
 NGKSK = 51 (NO. OF PRESSURE TABLE POINTS)

POINT NO.	AXIAL DISTANCE (Z/RC)	RADIAL DISTANCE (R/RC)	STREAMLINE DISTANCE (S/RC)	PRESSURE (PSIA)
1	-1.250000E+00	9.920203E+01	0.	2.053317E+03
2	-1.101911E+00	9.803900E+01	9.212605E+02	2.019760E+03
3	-1.073022E+00	9.413889E+01	1.840790E+01	1.983745E+03
4	-9.845331E+01	9.172810E+01	2.757930E+01	1.935960E+03
5	-8.940442E+01	8.945967E+01	3.671435E+01	1.884962E+03
6	-8.075552E+01	8.735829E+01	4.580934E+01	1.827239E+03
7	-7.190662E+01	8.543783E+01	5.486423E+01	1.762209E+03
8	-6.305778E+01	8.307788E+01	6.402242E+01	1.702140E+03
9	-5.420883E+01	8.131964E+01	7.296032E+01	1.714942E+03
10	-4.535994E+01	8.007624E+01	8.188279E+01	1.642099E+03
11	-3.651104E+01	7.867938E+01	9.078811E+01	1.563922E+03
12	-2.766214E+01	7.883383E+01	9.967693E+01	1.480801E+03
13	-1.881325E+01	7.811676E+01	1.085548E+00	1.442231E+03
14	-9.964890E+02	7.769563E+01	1.174137E+00	1.360893E+03
15	-1.115454E+02	7.749157E+01	1.262660E+00	1.277440E+03
16	7.733442E+02	7.739161E+01	1.351151E+00	1.193909E+03
17	1.666284E+01	7.754934E+01	1.439654E+00	1.111047E+03
18	2.543124E+01	7.787151E+01	1.528202E+00	1.035539E+03
19	3.428013E+01	7.842469E+01	1.616863E+00	9.610006E+02
20	4.312703E+01	7.911941E+01	1.705821E+00	8.818990E+02
21	6.404910E+01	7.948469E+01	1.914815E+00	7.171705E+02
22	6.831918E+01	8.089020E+01	1.959684E+00	6.938981E+02
23	8.208237E+01	8.519107E+01	2.103522E+00	6.094299E+02
24	9.586595E+01	8.971488E+01	2.249067E+00	5.219971E+02
25	1.098846E+00	9.449184E+01	2.397169E+00	4.365488E+02
26	1.241424E+00	9.957831E+01	2.548932E+00	3.630940E+02
27	1.387119E+00	1.050121E+00	2.704047E+00	3.011235E+02
28	1.536911E+00	1.108124E+00	2.864304E+00	2.503525E+02
29	1.689155E+00	1.166725E+00	3.027810E+00	2.382321E+02
30	1.845097E+00	1.224722E+00	3.194188E+00	2.200608E+02
31	2.004881E+00	1.282237E+00	3.364008E+00	2.028064E+02
32	2.169482E+00	1.339840E+00	3.538381E+00	1.867033E+02
33	2.339102E+00	1.397222E+00	3.717460E+00	1.715002E+02
34	2.515892E+00	1.455829E+00	3.903712E+00	1.571620E+02
35	2.703448E+00	1.517803E+00	4.101240E+00	1.434188E+02
36	2.902740E+00	1.583449E+00	4.311067E+00	1.302547E+02
37	3.116761E+00	1.653752E+00	4.536339E+00	1.177633E+02
38	3.347799E+00	1.729630E+00	4.779452E+00	1.059889E+02
39	3.599726E+00	1.811720E+00	5.044482E+00	9.475904E+01
40	3.876663E+00	1.901948E+00	5.335747E+00	8.411116E+01
41	4.180742E+00	1.9941327E+00	5.671143E+00	7.649671E+01
42	4.421066E+00	2.028190E+00	5.895324E+00	6.749181E+01
43	4.776991E+00	2.127592E+00	6.264866E+00	5.886322E+01
44	5.189428E+00	2.243407E+00	6.893254E+00	5.058813E+01
45	5.849836E+00	2.431184E+00	7.379841E+00	4.019394E+01
46	6.081545E+00	2.497727E+00	7.620915E+00	3.722404E+01
47	6.410979E+00	2.591157E+00	7.963338E+00	3.354102E+01
48	6.835616E+00	2.714446E+00	8.405517E+00	2.855930E+01
49	7.245205E+00	2.838023E+00	8.83339E+00	2.293517E+01
50	7.645205E+00	2.838023E+00	8.83339E+00	2.293517E+01

50 1.14072E+00 2.77902E+00 7.39341E+00 2.174030E+01
 51 0.230201E+00 3.107557E+00 9.072043E+00 1.329414E+01

STREAMLINE(5) = 00.00000 PERCENT OF THE TOTAL MASS FLOW
 ZINIT = 0.000000 (NONDIMENSIONAL = S/RC)
 PINIT = 2001.133171 (PSIA)
 TINIT = 6171.009471 (DEG, R)
 VINIT = 1540.268632 (FT/SEC)
 ZFINAL = 0.927407 (NONDIMENSIONAL = Z/RC)
 NPKPK = 49 (NO. OF PRESSURE TABLE POINTS)

POINT NO.	AXIAL DISTANCE (Z/RC)	RADIAL DISTANCE (R/RC)	STREAMLINE DISTANCE (S/RC)	PRESSURE (PSIA)
1	-1.250000E+00	1.165602E+00	0.	2.001153E+03
2	-1.101911E+00	1.130092E+00	9.509707E-02	2.041593E+03
3	-1.073022E+00	1.097600E+00	1.096254E-01	1.996673E+03
4	-9.849331E-01	1.066449E+00	2.034392E-01	1.946094E+03
5	-8.960442E-01	1.037064E+00	3.704929E-01	1.889211E+03
6	-8.075992E-01	1.011402E+00	4.607962E-01	1.825507E+03
7	-7.190662E-01	9.877304E-01	5.603946E-01	1.754245E+03
8	-6.305773E-01	9.650792E-01	6.522592E-01	1.702298E+03
9	-5.420803E-01	9.463754E-01	7.423069E-01	1.711576E+03
10	-4.535994E-01	9.317509E-01	8.319962E-01	1.627907E+03
11	-3.651104E-01	9.193739E-01	9.213465E-01	1.539209E+03
12	-2.766214E-01	9.093322E-01	1.010403E+00	1.445803E+03
13	-1.881325E-01	9.010397E-01	1.099239E+00	1.409973E+03
14	-9.964390E-02	8.967191E-01	1.187895E+00	1.318953E+03
15	-1.115454E-02	8.943137E-01	1.276377E+00	1.227595E+03
16	7.733442E-02	8.943339E-01	1.364866E+00	1.136380E+03
17	1.096234E-01	8.970428E-01	1.453399E+00	1.050140E+03
18	2.543124E-01	9.020271E-01	1.542025E+00	9.662164E+02
19	3.420013E-01	9.097239E-01	1.630848E+00	8.871731E+02
20	4.312903E-01	9.190701E-01	1.719883E+00	8.019944E+02
21	5.022934E-01	9.290423E-01	1.871182E+00	6.751031E+02
22	6.339070E-01	9.435163E-01	1.924744E+00	6.411890E+02
23	6.736233E-01	9.540290E-01	1.969715E+00	6.151247E+02
24	7.099375E-01	9.641490E-01	1.999595E+00	5.933811E+02
25	8.049062E-01	1.021289E+00	2.167464E+00	4.676299E+02
26	1.020040E+00	1.072109E+00	2.337134E+00	3.828910E+02
27	1.170395E+00	1.126309E+00	2.491682E+00	3.104579E+02
28	1.317804E+00	1.184700E+00	2.650235E+00	2.860143E+02
29	1.467747E+00	1.243497E+00	2.811279E+00	2.649001E+02
30	1.620764E+00	1.302714E+00	2.975370E+00	2.447127E+02
31	1.777414E+00	1.362600E+00	3.143107E+00	2.256445E+02
32	1.938407E+00	1.423949E+00	3.313219E+00	2.079709E+02
33	2.104190E+00	1.485942E+00	3.492182E+00	1.906389E+02
34	2.275866E+00	1.548842E+00	3.675180E+00	1.747092E+02
35	2.454364E+00	1.614049E+00	3.865223E+00	1.594490E+02
36	2.640553E+00	1.681259E+00	4.063171E+00	1.454033E+02
37	2.836097E+00	1.751344E+00	4.270897E+00	1.322361E+02
38	3.044096E+00	1.825000E+00	4.491623E+00	1.197027E+02
39	3.265661E+00	1.903023E+00	4.727123E+00	1.080707E+02
40	3.504190E+00	1.990207E+00	4.980414E+00	9.700275E+01
41	3.762350E+00	2.080229E+00	5.254490E+00	8.655562E+01
42	4.044566E+00	2.182889E+00	5.554105E+00	7.672922E+01
43	4.355951E+00	2.293656E+00	5.884230E+00	6.749932E+01
44	4.688167E+00	2.411200E+00	6.141260E+00	6.139253E+01
45	4.957402E+00	2.448390E+00	6.506607E+00	5.374610E+01
46	5.356128E+00	2.571373E+00	6.923066E+00	4.651960E+01
47	5.819210E+00	2.714963E+00	7.408707E+00	3.963260E+01
48	6.084686E+00	2.984964E+00	8.220397E+00	1.981126E+01
49	6.080650E+00	3.101666E+00	8.527407E+00	1.590489E+01

END OF STREAMLINE GENERATION PROGRAM
MGKS INPUT TAPE HAS BEEN PREPARED

CP TIME = 327,523 PP TIME = 137,101

Appendix C

KINCON

**NONEQUILIBRIUM CHEMICAL KINETICS
AND CONDENSATION COMPUTER
PROGRAM**

**A Multiphase Reacting Gas
Streamtube Model**

Program Number H360

CONTENTS

C. 1	INTRODUCTION	431
C. 2	ANALYSIS	433
	C. 2. a Conservation Equations	433
	C. 2. b Condensation Equations	438
C. 3	NUMERICAL METHOD	440
C. 4	CELL LOADER STRUCTURE	443
C. 5	PROGRAM SUBROUTINES	443
	C. 5. a Initialization Subroutines Description	443
	C. 5. b One-Dimensional Kinetic Expansion Subroutines Description	453
	C. 5. c Plotting Subroutines Description	478
C. 6	PROGRAM USER'S MANUAL	480
	C. 6. a Operation Mode	481
	C. 6. b \$THERMØ	482
	C. 6. c Thermodynamic Data	483
	C. 6. d Title Card	487
	C. 6. e Species Cards	487
	C. 6. f Reaction Cards	488
	C. 6. g \$PRØPEL	489
C. 7	SAMPLE CASES	498
	C. 7. a Reaction-Rate Screening Case	498
	C. 7. b Oblique Shock Case	498
	C. 7. c Normal Shock-Stagnation Streamline Case	498
	C. 7. d Automated Kinetics and Condensation Case	498
C. 8	REFERENCES	521

TABLES

C-I	Species Residing on Master Thermodynamic Tape	485
C-II	Sample Listing for Thermodynamic Function Cards for N ₂	486
C-III	Card Listing for Rate-Screening Case	500
C-IV	Sample Reaction-Screening Output	502
C-V	Final Summary Output After Screening—Results of Original and Screened Runs	503
C-VI	Card Listing for Oblique Shock Calculation in Air	504
C-VII	Pressure Table	505
C-VIII	Shock Calculation	506
C-IX	Card Listing for Normal Shock Stagnation Streamline Calculation in Air	507
C-X	Input Velocity Distribution Table	508
C-XI	Sample Output for Normal Shock Calculation	509
C-XII	Kincon Sample Case—Data Listing	510
C-XIII	Streamline Generation Program	511
C-IV	Initial Conditions Kinetic Streamtube Calculation Axial Position = 0. Input Normalizing Axial Scale Factor (ft) 8.10000E-03	513
C-XV	Kinetic Streamtube Conditions Axial Position 2.41693E+01	514
C-XVI	Kinetic Streamtube Conditions Axial Position 3.52285E+01	515
C-XVII	Area Ratio Table	516

C-XVIII	Initial Conditions Kinetic Streamtube Calculation Axial Position = 2.49885E+01 Input Normalizing Axial Scale Factor (ft) 8.10000E-03	518
C-XIX	Kinetic Streamtube Conditions Axial Position 2.70052E+01	519
C-XX	Kinetic Streamtube Conditions Axial Position 2.90277E+01	520

LIST OF ABBREVIATIONS AND SYMBOLS

A, a	Cross-sectional area of the streamtube
a_j, b_j	Reaction-rate parameters
C_p	Specific heat at constant pressure
c_i	Mass fraction of i^{th} species
f_i	Free energy of i^{th} species
g	Mass fraction of condensed phase
\dot{H}	Energy addition rate, per unit normalized length, per unit initial streamtube mass flux
h	Enthalpy
h'	Enthalpy of condensed phase
J	Nucleation rate, critical-size nuclei formed per unit volume, per unit time
k	Boltzmann constant
K_j	Equilibrium constant
k_j, k_{kj}	Reaction-rate parameters
\dot{M}	Momentum flux, per unit normalized length, per unit initial streamtube mass flux
M_j	Third-body reaction term
\bar{M}_i	Chemical symbol for the i^{th} species
m	Mass addition rate, per unit normalized length per unit initial streamtube mass flux
m_{ji}	Reaction-rate ratio
m_i	Molecular weight of i^{th} species
N_a	Avogadro's number
n	Total number of species

n_j	Reaction-rate parameters
P, P_i	Pressure and partial pressure of i^{th} species, respectively
R	Gas constant of the mixture
\mathcal{R}	Universal gas constant
r^*	Normalization factor for x
r^{**}	Critical droplet radius
\dot{s}_i	i^{th} species mass addition rate, per unit normalized length, per unit initial streamtube mass flux
T	Temperature
V	Flow velocity
X_j	Species production-rate term
x	Axial distance
γ	Ratio of specific heats
σ	Surface tension
η	Condensation coefficient
ν_{ij}, ν'_{ij}	Stoichiometric coefficients
ρ	Density
ω_i	Production rate of i^{th} species

SUBSCRIPT

D	Droplet
L	Liquid
V	Vapor
VS	Saturated vapor
i	i^{th} species
j	j^{th} reaction

Appendix C

KINCON

NONEQUILIBRIUM CHEMICAL KINETICS AND CONDENSATION COMPUTER PROGRAM

A Multiphase Reacting Gas Streamtube Model

C. 1 INTRODUCTION

The computer program described in this appendix is a subprogram to the Plume Contamination Effects Prediction Computer Program, CONTAM, and performs chemical-kinetic and single-species condensation calculations along gas-phase streamlines as computed by the Multiphase Nozzle and Plume Transport Computer Program, MULTRAN. KINCON may also be used as an independent computer program on any third-generation computer with a core exceeding 120, 000 words and a Fortran IV processor.

The present computer program is based on the ICRPG One-Dimensional Kinetic Nozzle Analysis Computer Program, ODK (References C-1 and C-2), and on modifications to the ODK by Dynamic Science Corporation under contract to McDonnell Douglas Astronautics Company (Reference C-3). The purpose of the original program was to provide an automated engineering tool for the kinetic analysis of one-dimensional chemically reacting gas systems. To this end, a number of options were included in the program to aid the user. These included a mass, momentum, and energy streamtube addition option, generalized oblique shock calculation, normal shock-stagnation streamline calculation, area-defined streamtube option, and a reaction screening option. Modifications performed under the present study include the addition of a thermodynamic nonequilibrium condensation model and the automation of the program to perform successive kinetics and condensation calculations for a series of streamlines.

Species and reactions are input to the program in symbolic form. The user may input arbitrary species (up to 40) and arbitrary gas phase reactions (up to 150). Specified third-body reaction rate ratios may be employed. A comprehensive library of thermochemical data is available as part of the computer program. This data may be expanded by input of tables punched directly from the JANAF format. Automatic plotting of temperature, density, and species concentration is available. A unique feature of the program is its ability to integrate—with complete numerical stability—the differential equations governing the kinetic system.

Section C. 2 contains a discussion of physical assumptions. The equations governing the inviscid, one-dimensional flow of a chemically reacting gas mixture are given in the form in which they are integrated in the computer program.

Section C. 3 contains a discussion of the integration method used in the computer program.

Section C. 4 contains a description of the program overlay structure.

Section C. 5 contains a detailed engineering and programming description of the logic and the calculations performed in the computer program.

Section C. 6 contains a program user's manual describing the use of the computer program with an explanation of the program input and output.

Section C. 7 contains input and output for a sample case.

C.2 ANALYSIS

The method of solution consists of integrating the conservation equations for the chemical system in such a form that the chemistry is generalized for binary exchange and dissociation-recombination reactions. Condensed phase products are considered by a single-species nonequilibrium condensation option.

a. Conservation Equations

The KINCON computer program integrates a set of simultaneous differential equations along a pressure-defined streamtube (i.e., $P(x)$ and $dP(x)/dx$ are known). These differential equations represent the conservation of species, mass, momentum, and energy for the system as expressed by Equations (C-5), (C-6), (C-7), and (C-8) below.

The conservation equations governing the inviscid flow of reacting gas mixtures have been given by Hirschfelder, Curtiss, and Bird (Reference C-4), Penner (Reference C-5), and others. The following basic assumptions are made in the derivation of these equations.

1. Mass (\dot{m} , \dot{s}_i), momentum (\dot{M}), and energy (\dot{H}) addition rates are defined for the system.
2. The gas is inviscid.
3. Each component of the gas is a perfect gas.
4. The internal degrees of freedom of each component of the gas are in equilibrium.

In one-dimensional flow, the conservation equations have the form¹

$$\text{species} \quad \frac{d}{dx} \left[(1 + \bar{m}) c_i \right] = \dot{s}_i + (1 + m) \frac{\omega_i r^*}{\rho V} \quad (\text{C-1})$$

$$\text{mass} \quad \frac{d}{dx} (1 + \bar{m}) = \dot{m} \quad (\text{C-2})$$

$$\text{momentum} \quad \frac{d}{dx} [(1 + \bar{m}) V] = \dot{M} - \frac{(1 + \bar{m})}{\rho V} \frac{dP}{dx} \quad (\text{C-3})$$

¹The independent variable, x , is taken as unitless with r^* as the conversion factor to units. The quantity $1 + \bar{m}$ represents the streamtube mass flux normalized by the initial streamtube mass flux; i.e., $1 + \bar{m} = (\rho Va)/(\rho Va)_0$.

energy

$$\frac{d}{dx} \left[(1 + \bar{m}) h_T \right] = \dot{H}, \quad (C-4)$$

$$h_T = \sum_{i=1}^n c_i h_i + \frac{V^2}{2}$$

If the expansion process is specified by the pressure distribution as a function of distance, Equations (C-1 through C-4) can be written as

$$\frac{dc_i}{dx} = \frac{\dot{s}_i - \dot{m}c_i}{1 + \bar{m}} + \frac{\dot{\omega}_i r^*}{\rho V} \quad (C-5)$$

$$\frac{dV}{dx} = \frac{\dot{M} - \dot{m}V}{1 + \bar{m}} - \frac{1}{\rho V} \frac{dP}{dx} \quad (C-6)$$

$$\frac{dT}{dx} = \frac{1}{C_p} \left[\frac{\dot{H} - \dot{m} h_T}{1 + \bar{m}} - \frac{V (\dot{M} - \dot{m}V)}{1 + \bar{m}} + \frac{1}{\rho} \frac{dP}{dx} - \sum_{i=1}^n h_i \frac{dc_i}{dx} \right] \quad (C-7)$$

$$\frac{d\rho}{dx} = \left[\frac{1}{P} \frac{dP}{dx} - \frac{1}{T} \frac{dT}{dx} - \frac{1}{R} \left(\sum_{i=1}^n R_i \frac{dc_i}{dx} \right) \right] \rho \quad (C-8)$$

where

$$C_p = \sum_{i=1}^n c_i C_{pi} \quad (C-9)$$

$$\gamma = \frac{C_p}{(C_p - R)} \quad (C-10)$$

$$h_i = \int_0^T C_{pi} dT + h_{i0} \quad (C-11)$$

For each component of the gas, the equation of state is

$$P_i = \rho_i R_i T \quad (C-12)$$

Summing over all the components of the mixture, the overall equation of state is obtained

$$P = \rho RT = \rho T \sum_{i=1}^n c_i R_i \quad (C-13)$$

The net species production rate ω_i for each species (component) is calculated from

$$\omega_i = \bar{m}_i \rho^2 \sum_{j=1}^n (\nu'_{ij} - \nu_{ij}) X_j \quad (C-14)$$

where

$$X_j = \left[K_j \prod_{i=1}^n c_i^{\nu_{ij}} - \rho^\lambda \prod_{i=1}^n c_i^{\nu'_{ij}} \right] k_j M_j \quad (C-15)$$

and λ depends on the order of the reaction and M_j is calculated only for dissociation-recombination reactions.

The equilibrium constant, K_j , is

$$K_j = e^{-\Delta F/RT} \quad (C-16)$$

$$\Delta F = \sum_{i=1}^n f_i \nu_{ij} - \sum_{i=1}^n f_i \nu'_{ij}$$

The computer program considers chemical reactions defined by the generalized chemical reaction equation

$$\sum_{i=1}^n \nu_{ij} \bar{M}_i = \sum_{i=1}^n \nu'_{ij} \bar{M}_i \quad (C-17)$$

where ν_{ij} and ν'_{ij} are the stoichiometric coefficients to be used in Equation (C-15) while \bar{M}_i represents the symbol for the i^{th} chemical species.

The reaction rates, k_j , for the j^{th} reaction appearing in Equation (C-15) are represented in the Arrhenius form

$$k_j = a_j T^{-n_j} e^{(-b_j/RT)} \quad (\text{C-18})$$

where

- a_j is the pre-exponential coefficient
- n_j is temperature dependence of the pre-exponential factor
- b_j is the activation energy

Since each dissociation-recombination reaction has a distinct reaction rate associated with each third body, the net production rate for each dissociation-recombination reaction should be calculated from

$$X_j = \sum_{k=1}^n \left[K_j \prod_{i=1}^n c_i^{\nu_{ij}} - \rho \prod_{i=1}^n c_i^{\nu'_{ij}} \right] c_k k_{kj} \quad (\text{C-19})$$

rather than Equation (C-15). However, Benson and Fueno (Reference C-6) have shown theoretically that the temperature-dependence of recombination rates is approximately independent of the third body. Assuming that the temperature dependence of recombination rates is independent of the third body, the recombination rate associated with the k^{th} species (third body) can be represented as

$$k_{kj} = a_{kj} T^{-n_j} e^{-b_j/RT} \quad (\text{C-20})$$

where only the constants a_{kj} are different for different species (third bodies). From Equation (C-19) it can be shown that

$$X_j = \left[K_j \prod_{i=1}^n c_i^{\nu_{ij}} - \rho \prod_{i=1}^n c_i^{\nu'_{ij}} \right] \left[\sum_{i=1}^n \frac{a_{ij}}{a_{kj}} c_i \right] a_{kj} T^{-n_j} e^{-b_j/RT} \quad (\text{C-21})$$

Thus, the recombination rates associated with each third body can be considered as in Equation (C-15) by calculating the general third body term M_j as

$$M_j = \sum_{i=1}^n m_{ji} c_i \quad (C-22)$$

where m_{ji} is the ratio a_{ij}/a_{kj} .

In order to numerically integrate Equations (C-1), (C-5), (C-6), and (C-7), it is necessary to input the following type of information concerning the chemical system:

Boundary Conditions:

x_o initial axial position

P_o initial pressure

T_o initial temperature

V_o Initial velocity

x_{max} final axial position

$P(x)$ table of pressure versus axial position

$dP(x)/dx$ table of pressure derivatives versus axial position

Species Information:²

\overline{M}_i species name

\overline{m}_i species molecular weight

$C_{pi}(T)$ species specific heat

$h_i(T)$ species enthalpy

$f_i(T)$ species free energy

²The items C_{pi} , h_i , and f_i are not available directly in the appropriate units. The computer program calculates these items for each species from the JANAF data for:

$$- \frac{H^\circ - H_{298}^\circ}{T} \quad \begin{matrix} C_p \text{ vs } T \\ \text{vs } T \\ \text{vs } T \end{matrix}$$

and

$$H_{f,298}^\circ$$

Reaction Information:

$$\sum_{i=1}^n \nu_{ij} \bar{M}_i \approx \sum_{i=1}^n \nu'_{ij} \bar{M}_i \quad \text{each reaction must be input in terms of its stoichiometric coefficients and constituent species}$$

a_j, n_j, b_j constants defining k_j , the reaction rates

m_{ji} third body reaction-rate ratios

Miscellaneous Information:

r^* normalization factor for x

Mass, Momentum, Energy, and Species Addition Functions:

$\dot{m}(x)$ mass addition rate, per unit normalized length, per unit initial streamtube mass flux

$\dot{M}(x)$ Momentum flux, per unit normalized length, per unit initial streamtube mass flux

$\dot{H}(x)$ energy addition rate, per unit normalized length, per unit initial streamtube mass flux

$\dot{s}_i(x)$ i^{th} species mass addition rate, per unit normalized length, per unit initial streamtube mass flux

A considerable amount of data (such as JANAF tables defining C_{pi} , h_i , and f_i , reaction rate parameters and cards defining chemical reactions) are available with the computer program. Details concerning input to the computer program are given in Subsection C.6.

For the area defined option including mass, energy, and momentum addition, the pressure profile is obtained by an iteration to obtain the pressure profile such that $\left| \frac{A(x) \text{ obtained} - A(x) \text{ input}}{A(x) \text{ input}} \right| < \epsilon$ where ϵ is an input convergence criteria.

b. Condensation Equations

Dropwise condensation of a single gaseous species is computed from classical liquid drop theory. In addition to the assumptions noted above, the condensation analysis assumes the following:

1. Condensed phase mass is uniformly distributed.
2. Droplets are spherical.
3. Droplets are small and follow gas streamlines.
4. Volume occupied by condensed phase is small compared to gas volume.

Two distinct processes are treated, nucleation and droplet growth. The nucleation process (spontaneous self-nucleation) occurs in the expanding supersaturated vapor and involves the clustering of vapor molecules to give rise to very small nuclei (radius of 10 to 100 Å). Only nuclei reaching the critical drop radius r^{**} can exist and grow. Critical drop radius is given by Frenkel (Reference C-7)

$$r^{**} = \frac{2\sigma}{\rho_L R_v T \ln\left(\frac{p_v}{p_{vs}}\right)} \quad (C-23)$$

The nucleation rate, J , represents the number of critical-size nuclei formed per unit volume per unit time and is calculated from the expression by Stever (Reference C-8)

$$J = \left(\frac{p_v}{kT}\right)^2 \frac{1}{\rho_L} \left(\frac{2\sigma m_i}{\pi N a}\right)^{1/2} \exp\left(-\frac{4\pi\sigma r^{**2}}{3 kT}\right) \quad (C-24)$$

Once a suitable number of nuclei are formed in the vapor, the process of droplet growth accounts for the actual condensation. Droplet growth occurs through the collision of vapor molecules and stable liquid droplets.

The net flux of vapor to the droplet surface is computed from kinetic theory considerations where droplets are typically smaller than the mean free path of the gas. The droplet growth equation of Hill (Reference C-9) is utilized

$$\frac{dr}{dx} = \frac{\eta}{\rho_L V} \frac{1}{(2\pi R_v)^{1/2}} (\beta - \beta_D) \quad (C-25)$$

where

$$\beta = \frac{p_v}{T^{1/2}}$$

$$\beta_D = \frac{p_D}{T_D^{1/2}}$$

Droplet temperature is assumed to be that of the saturated vapor.

The appropriate mass, momentum, and energy addition rates are computed internally from the following expressions

$$\begin{aligned}\dot{m} &= -\frac{dg}{dx} && \text{Mass} \\ \dot{M} &= \dot{m}V + g \frac{(1 - \bar{m})}{\rho V} \frac{dp}{dx} && \text{Momentum} \\ \dot{H} &= (1 - 2g) \dot{m}h' - (1 + \bar{m}) g \frac{dh'}{dx} && \text{Energy} \\ \dot{S}_i &= \dot{m}, i = \text{condensing species} && \text{Species} \\ &= 0 \text{ for other species}\end{aligned}$$

The rate-of-change of condensed-phase mass fraction, dg/dx , is evaluated by summing the mass of all droplets formed upstream of a specific location, x , as follows

$$\frac{dg}{dx} = \frac{4\pi\rho_L}{\rho V} \left[\frac{1}{3} r^{**}(x) J(x) \frac{A(x)}{A_0} + \frac{dr}{dx} \int_{x_0}^x r(x, \xi)^2 J(\xi) \frac{A(\xi)}{A_0} d\xi \right] \quad (C-26)$$

where the integral is replaced by a summation for numerical evaluation.

C.3 NUMERICAL METHOD

It has been shown (e. g., Reference C-10) that explicit methods of numerical integration are unstable when applied to relaxation equations [such as Equations (C-1), (C-5), (C-6), and (C-7)], unless the integration step size is of the order of the characteristic relaxation distance. Since in the near equilibrium flow regime the characteristic relaxation distance is typically many orders of magnitude smaller than characteristic physical dimensions of the system of interest, the use of explicit methods to integrate relaxation equations often results in excessively long computation times. An implicit integration method which is inherently stable in all flow situations (whether near equilibrium or frozen) is therefore used by the computer program. With this method, step sizes which are of the order of the physical dimensions of the system of interest can be used, reducing the computation time per case by several orders of magnitude when compared with conventional explicit integration methods.

Consider N first-order simultaneous differential equations

$$\frac{dy_i}{dx} = f_i(X, y_1, \dots, y_N) \quad i = 1, 2, \dots, N \quad (C-27)$$

with known partial derivatives (i. e. the Jacobian for the system)³

$$a_i = \frac{\partial f_i}{\partial x} \quad (C-28)$$

$$\beta_{i,j} = \frac{\partial f_i}{\partial y_j} \quad (C-29)$$

The following implicit difference equations are used by the computer program to determine the $y_{i,n+1}$, (the subscript n denotes the n^{th} integration step)

$$y_{i,n+1} = y_{i,n} + k_{i,n+1} \quad h = x_{n+1} - x_n \quad (C-30)$$

where

$$k_{i,n+1} = \left[f_{i,n} + a_{i,n} h + \sum_{j=1}^N \beta_{i,j,n} k_{j,n+1} \right] \cdot h \quad (C-31)$$

for the initial step and for restart (first order).

$$k_{i,n+1} = \frac{1}{3} \left[k_{i,n} + 2 \left(f_{i,n} + a_{i,n} h + \sum_{j=1}^N \beta_{i,j,n} k_{j,n+1} \right) \cdot h \right] \quad (C-32)$$

³The computer program uses analytic expressions for calculation of the partial derivatives, a_i , β_{ij} .

for equal steps (second order with $h = \text{previous } h$)

$$k_{i,n+1} = \frac{h_{n+1}^2}{(2h_{n+1} + h_n) \cdot h_n} \left[k_{i,n} + \left[f_{i,n} + a_{i,n} h_{n+1} + \sum_{j=1}^N \beta_{i,j,n} k_{j,n+1} \right] \cdot \frac{h_n}{h_{n+1}} (h_{n+1} + h_n) \right] \quad (C-33)$$

for unequal steps (2nd order with $h \neq \text{previous } h$)

A derivation of these equations is given in Reference C-2.

If the flow is frozen, the explicit form of the above equations can be used ($\beta_{ij} = 0$); i. e., Equations (C-31), (C-32), and (C-33) are each reduced from an NXN system of linear simultaneous equations to N explicit equations ($N = 3 + \text{number of species}$).

Control of the integration step size, h , is provided by calculating estimates for the truncation error and comparing these to an input criterion, δ .

The step size is halved if for any $i = 1, 2, \dots, N$

$$E_i > \delta$$

The step size is doubled if for all $i = 1, 2, \dots, N$

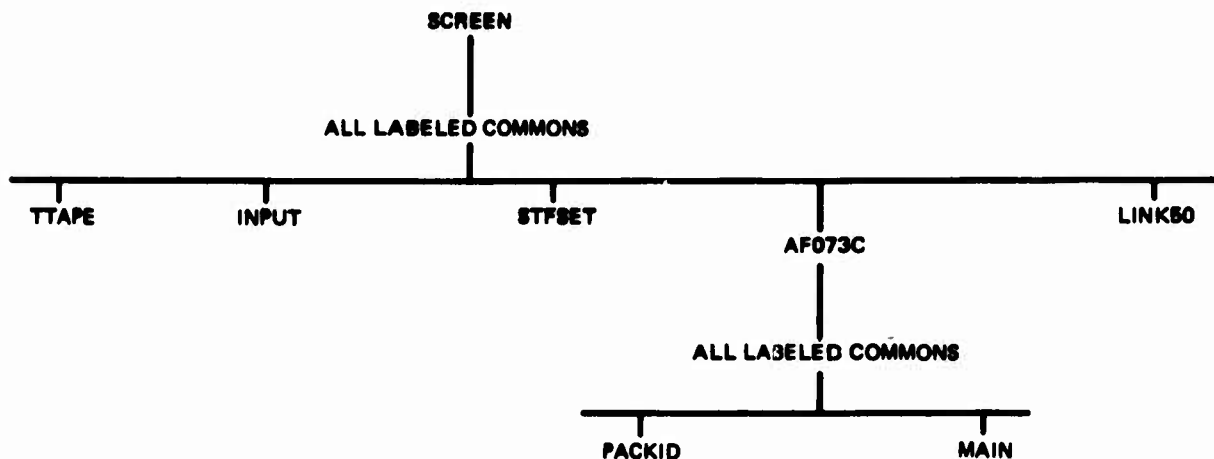
$$E_i < \frac{\delta}{10}$$

where

$$E_i = \left| \frac{k_{i,n+1} - 2k_{i,n} + k_{i,n-1}}{3k_{i,n+1} - k_{i,n}} \right| \quad (C-34)$$

The above expression for E_i is derived in Reference C-2.

C.4 CELL LOADER STRUCTURE



C.5 PROGRAM SUBROUTINES

This section contains a description of the program subroutines, and these commentaries are given in the order in which the subroutines appear.

The main program sets up master limits for the chemistry, initializes certain logical control variables, and calls subroutine **DRIVER**. This subroutine provides the overall logic control for the subprogram.

After the program is loaded, a master JANAF Thermochemical Data tape is prepared either from card input or by summary of the current master file in use.

a. Initialization Subroutines Description

(1) Program **SCREEN**

This subroutine provides overlay communication, defines the labeled common blocks, sets maximum limits for the chemical tables, and initializes certain logical control variables. It calls subroutine **DRIVER**.

(2) Subroutine **DRIVER**

This subroutine performs the overall logic for the program.

(3) Subroutine **FIND**

Provides indices of the table entries which bracket the value of a current variable. The subroutine saves its place in the table.

(4) Subroutine **STOICC**

Provides up to ten reactants indices and ten product indices from the master stoichiometric coefficient table.

(5) Subroutine **AF073C**

This subroutine provides linkage between the kinetic packing link and the kinetic expansion computations.

(6) Subroutine GTF

This subroutine computes the effective gas constant, gaseous heat capacity, γ , $\partial\gamma/\partial T$, $\partial\gamma/\partial C_i$ from the following formulae:

$$R = \sum_{i=1}^{NSP} C_i \cdot R_i$$

$$C_p = \sum_{i=1}^{NSP} C_i \cdot C_{p_i}$$

$$\gamma = \frac{C_p}{C_p - R}$$

$$\frac{\partial \gamma}{\partial T} = - \frac{\gamma \cdot (\gamma - 1)}{C_p} \cdot \sum_{i=1}^{NSP} C_i \cdot \frac{\partial C_{p_i}}{\partial T}$$

$$\frac{\partial \gamma}{\partial C_i} = \gamma \cdot (\gamma - 1) \cdot \left[\frac{R_i}{R} - \frac{C_{p_i}}{C_p} \right] \quad i = 1, \dots, NSP$$

(7) Subroutine SPLN

Performs cubic interpolation for a function and its first two derivatives. Given function values y_n and y_{n+1} and first derivative values y'_n and y'_{n+1} at x_n and x_{n+1} , this subroutine evaluates $y(x)$, $y'(x)$, and $y''(x)$ for $x_n \leq x < x_{n+1}$ using:

$$y = A(x - x_n)^3 + B(x - x_n)^2 + C(x - x_n) + D$$

$$y' = 3A(x - x_n)^2 + 2B(x - x_n) + C$$

$$y'' = 6A(x - x_n) + 2B$$

where:

$$A = \frac{1}{h^3} \cdot \left[(y'_{n+1} + y'_n) h - 2k \right]$$

$$B = -\frac{1}{h^2} \cdot \left[(y'_{n+1} + 2y'_n) h - 3k \right]$$

$$C = y'_n$$

$$D = y_n$$

$$h = x_{n+1} - x_n$$

$$k = y_{n+1} - y_n$$

(8) Subroutine STF

Using the SPLN interpolation subroutine, this subroutine computes the heat capacity and its temperature derivatives, enthalpy, and free energy, at the current temperature for all gaseous chemical species.

(9) Subroutine APPROX

This subroutine provides extension of the thermochemical data between the temperatures 9,000 and 20,000°R. A message is provided each time an approximation is calculated. The approximation formulae are given below with $X = 9,000^\circ\text{R}$:

$$C_{P_T} = C_{P_X}$$

$$H_T = H_X + C_{P_X} * \Delta T$$

$$F_T = F_X - \left[\frac{H_T^\circ - H_{298}^\circ}{T} - \frac{H_T^\circ - H_{298}^\circ}{X} - C_{P_T} \log \left(\frac{T}{X} \right) \right]$$

(10) Subroutine TTape

This subroutine generates a master JANAF thermochemical tape which is subsequently utilized by Subroutine STFSET. The tape is written in the binary mode with the thermodynamic functions in caloric units. The thermodynamic functions for each species include:

<u>Function</u>	<u>Units</u>
C_p°	cal/mole-°K
$H^\circ - H^\circ_{298}$	k-cal/mole
$-\frac{(F^\circ - H^\circ_{298})}{T}$	cal/mole-°K

given at 100°K temperature increments over the range 100°K to 5,000°K, inclusive. Reference may be made to Subsection C.6, the Program Users Manual, for a complete description of thermodynamic input format and output options.

(11) Subroutine COLOUT

Provides columnar output of species names for those species residing on the master thermo file.

(12) Subroutine ECVN

This subroutine translates a BCD string of characters, into one floating point numeric value. E, I, and F formats are permitted with the result always a floating point number. It is called by subroutine SPRXIN to decode numeric fields in the species and reactions cards.

(13) Subroutine INPUT

This subroutine performs specific case input for the program. It performs the following functions:

1. Variable initialization to nominal values.
2. Read title card.
3. Call subroutine SPRXIN to input the species and reactions cards.

4. Read \$PROPEL namelist for case input data.
5. Check input mole or mass fractions for unity ($\pm 1.0E-4$).
6. Read initial conditions and pressure table from Tape 8 when operated in automatic mode.

(14) Subroutine NUMBER

This subroutine converts a one-character BCD number to a FORTRAN integer number. It is called by subroutine ECVN to decode free field numeric data.

(15) Subroutine SPRXIN

This subroutine processes the species and reactions cards. Species symbols, numeric mass or mole fractions, symbolic reactions, and rate parameters are processed. Reference may be made to Subsection C. 6, the Program Users Manual, for a complete description of input requirements.

(16) Subroutine STFSET

This subroutine uses the master JANAF tape written by subroutine TTAPE, to generate a species thermal-function tape (KSTF) in blocked form for the kinetic calculations. The tabulated functions on the master tape are:

<u>Function</u>	<u>Units</u>
$Cp'_i = Cp^\circ_i$	cal/mole-°K
$H'_i = [H^\circ - H^\circ_{298}]_i$	kcal/mole
$F'_i = - \left[\frac{F^\circ - H^\circ_{298}}{T} \right]_i$	cal/mole-°K

For the kinetic calculations the above functions must be converted to the ft/sec²°R units system by the following:

<u>Function</u>	<u>Conversion</u>	<u>Internal Units</u>
Cp_i	$= [Cp'_i \cdot R_i] / 1.98726$	ft ² /sec ² · °R
H_i	$= \left(H'_i + \Delta H^\circ F_i \right) R_i \cdot 905.770$	ft ² /sec ²
F_i	$= F'_i / 1.98726$	unitless

These converted functions are then written in 900°R temperature blocks. The free energy and heat capacity derivatives are computed using the formulae below with $\Delta T = 180.0$.

The function derivatives are computed according to the following formulae:

$$\frac{d\eta}{dT}(i, T_1) = \frac{4 \cdot \eta(i, T_2) - 3 \cdot \eta(i, T_1) - \eta(i, T_3)}{2 \cdot \Delta T}$$

$$\frac{d\eta}{dT}(i, T_j) = \frac{\eta(i, T_j + \Delta T) - \eta(i, T_j - \Delta T)}{2 \cdot \Delta T}$$

$$\frac{d\eta}{dT}(i, T_{50}) = \frac{3 \cdot \eta(i, T_{50}) - 4 \cdot \eta(i, T_{49}) + \eta(i, T_{48})}{2 \cdot \Delta T}$$

where η_i may be species heat capacity Cp' or free energy F' .

(17) Subroutine ADDFIT

For mass, energy, momentum and species addition functions, this subroutine calculates addition function tables and their derivatives from the input tables using one of the following options:

1. Simple differencing.
2. Spline fit.
3. Input derivative tables.
4. Parabolic fit.

The addition functions are normalized, modified by the appropriate multiplicative constants if required, and output in tabular form.

If single species condensation option is utilized, addition functions are not input but computed internally. No operations are performed by ADDFIT.

(18) Subroutine CONVRT

This subroutine converts input data from the externally input units to internally used computation units. In order to conserve computation time during the kinetic expansion, parameters such as molecular weights are included in these conversions. Primed numbers are input quantities.

(a) Dissociation-Recombination Reaction Rate Ratio

Input units: unitless

Internal units: (lbs-mass/lb-mole)⁻¹

Formula: $XMM_{j,i} = XMM'_{j,i} / MW_i$

(b) Pre-exponential Reaction Rate Ratio

Dissociation-recombination reactions

Input units: cm, °K, g-mole, sec

Internal units: ft³, °R, lb-mole, sec

$$A_j = \frac{A'_j \cdot (.0160183)^{\eta \cdot 1.8} XN_j}{\prod_{i=1}^n MW_i^{\nu'_{ij}}}$$

Where η depends on the order of the reaction.

and

$$0.0160183 = \frac{3.531 \cdot 10^{-5} \text{ ft}^3}{1 \text{ cm}^3} \cdot \frac{1 \text{ g-mass}}{2.2 \cdot 10^{-3} \text{ lb-mass}}$$

(c) Exponential Term

Input units: kcal/mole

Internal units: °R

$$\text{Formula: } B_j = B'_j \cdot 905.770$$

where

$$905.770 = \frac{1000 \text{ cal}}{1 \text{ kcal}} \cdot \frac{1}{1.98726 \text{ cal/mole-}^\circ\text{K}} \cdot \frac{1.8^\circ\text{R}}{1.0^\circ\text{K}}$$

(d) Equilibrium Constant Multiplicative Factor

Input units: not input

Internal units: (lb-mass) - °R/ft³

Formula:

$$\text{DATEF(J)} = \frac{\prod_{i=1}^n \text{MW}_i^{\nu'_{ij}}}{\prod_{i=1}^n \text{MW}_i^{\nu_{ij}} \cdot 0.73034}$$

where

$$0.73034 = 49,721.011 \frac{\text{ft-poundsals}}{(\text{lb-mole}) \cdot ^\circ\text{R}} \cdot \frac{1 \text{ atmos}}{68,059.59 \text{ poundsals/ft}^2}$$

(e) Heats of Reaction

Input units: Kcal/mole (via heats of formation)

Internal units: °R

$$\text{Formula: } \text{DELH(J)} = \text{DELH(J)}' \cdot 905.770$$

(f) Pressure

Input units: PSIA

Internal units: pounds/ft²

Formula: $P = P' \cdot 4633.056$

where

$$4633.056 = \frac{144 \text{ in}^2}{1 \text{ ft}^2} \cdot 32.174 \frac{\text{ft}}{\text{sec}^2}$$

(19) Subroutine PACK1P

On the basis of those species currently being considered, this subroutine packs species and reaction information from the master tables into those control sections utilized by the kinetic calculation links.

The following is a description of the subroutine functions:

- a. The symbolic reactions and their input rate parameters are printed.
- b. Reaction mass balance is checked for a tolerance of $\pm 1.0 \text{ E-}10$.
- c. Heats of reaction are computed.

(20) Subroutine PRES

This subroutine provides a pressure table and its derivatives suitable for processing by the kinetic calculation links. For a normal shock stagnation streamline, velocity table and its derivatives are provided in a form suitable for processing by the kinetic calculation links.

(21) Subroutine SLP (X, Y, N, MFLAG, YP, W1, W2, W3, IFLAG)

The purpose of this subroutine is to supply derivatives for a tabulated function. The end point derivatives may be specified or are calculated internally by parabolic interpolation. Interior point derivatives may be found by a cubic spline fit procedure.

Calling Sequence:

- X is a table of independent variables, x_i
Y is a table of the dependent variables, y_i
N is the number of entries in each of the tables X, Y, and YP. $i = 1, \dots, N$

MFLAG this entry is a flag, m , such that

$m > 0$ implies x is equally spaced

$m < 0$ implies x is not equally spaced

$|m| = 1$ y' will be continuous

$|m| = 2$ y' and y'' will be continuous

YP is a table of the derivative, y'_i

W1 working storage of length N

W2 working storage of length N

W3 working storage of length N

IFLAG this entry is a flag, i , such that

$i = 0$ implies value for $YP(1)$ and $YP(N)$ will be calculated internally by parabolic differencing

$i = 1$ implies values for $YP(1)$ and $YP(N)$ will be input

Method:

The cubic spline fit procedure utilizes the interpolation formula given within the description of subroutine SPLN, i. e. :

$$y = A(x - x_0)^3 + B(x - x_0)^2 + C(x - x_0) + D$$

$$y' = 3A(x - x_0)^2 + 2B(x - x_0) + C$$

$$y'' = 6A(x - x_0) + 2B$$

The piecewise cubic fit to a tubular function by the above relations will yield a discontinuity in the second derivative y'' , between adjacent fits of:

$$y''_{1_{01}} - y''_{1_{12}} = \frac{1}{h_{01}} \left(2y'_0 + 4y'_1 - 6 \frac{k_{01}}{h_{01}} \right) - \frac{1}{h_{12}} \left(6 \frac{k_{12}}{h_{12}} - 4y'_1 - 2y'_2 \right)$$

where

$$h_{01} = x_1 - x_0$$

$$h_{12} = x_2 - x_1$$

$$k_{01} = y_1 - y_0$$

$$k_{12} = y_2 - y_1$$

The method consists of setting the left-hand side of the above relation equal to zero so that the second derivative is continuous across juncture points. As applied to a tabular function, the above procedure results in a set of linear simultaneous equations (tri-diagonal) to be solved for the y'_i , provided that values for y' at the end points are known.

(22) Subroutine TCALC

This is a dummy subroutine to permit the user to generate the addition function tables using his own supplied subroutine. It must be replaced with the appropriate TCALC routine and used in conjunction with the IADDOP = 2 option.

b. One-Dimensional Kinetic Expansion Subroutines Description

This link contains the one dimensional kinetic expansion subroutines.

The implicit integration method, used to integrate the fluid dynamic and chemical relaxation equations, requires the values of the partial derivatives of all total derivatives with respect to every variable. The program will generate a matrix of partial derivatives such that the entry in the n^{th} row and the m^{th} column is the partial derivative of $d[n]/dx$ with respect to m . This matrix is called BETA(I, J). The velocity, density, and temperature-fluid dynamic variables considered for every case reside in rows 1, 2, and 3 respectively. The chemical species occupy rows 4 through the number of species plus 3. The following notation will be used to denote partial derivatives:

$$\beta(A, B) = \frac{\partial \left[\frac{\partial A}{\partial x} \right]}{\partial B}$$

To facilitate the identification of program variables with the engineering notation, the following format will be used where applicable:

engineering notation—program variable—equation

The program will also generate a matrix which will be solved for the variable increments for each integration step. This matrix will expand or contract, depending on the number of chemical species to be considered.

The total derivatives f_i and partial derivatives β_{ij} have been separated into two components: (1) adiabatic component with no mass, momentum, or species addition, and (2) addition component due to mass, momentum, energy, or species addition. Subroutines DERIV and FLU calculate the adiabatic components and subroutine ADDXXX calculates the addition component. When no mass, momentum, energy, or species addition functions are input, the addition component calculations are bypassed.

For the single-species condensation option, subroutines CONAD, VAPOR and DRØPS compute the mass, momentum, and energy addition functions used by ADDXXX to calculate addition components.

(1) Subroutine DERIV

This subroutine computes the adiabatic components of total derivatives f_i and the partial derivatives $\beta(i, j)$ for the chemical relaxation equations.

Notation: i = Species subscript

j = Reaction subscript

l = Total number of chemical reactions

m = Number of dissociation-recombination reactions

n = Total number of gaseous species

The generalized chemical reaction which is handled by this subroutine is defined by:

$$\sum_{i=1}^n \nu_{ij} C_i \rightleftharpoons \sum_{i=1}^n \nu'_{ij} C_i$$

with:

$$\psi_{ij} = \nu'_{ij} - \nu_{ij}$$

The reverse reaction rate constant is defined by the equation:

$$k_j \quad SK(J) = A_j \cdot T^{-XN_j} \cdot \exp(-B_j/T)$$

The net production rate for a reaction is given by:

$$X_j \quad X(J) = \left[K_j \cdot \prod_{i=1}^n C_i^{\nu_{ij}} - \rho^\lambda \cdot \prod_{i=1}^n C_i^{\nu'_{ij}} \right] \cdot k_j \cdot M_j$$

where:

$\lambda = 1$ for a dissociation-recombination reaction

$= 0$ for a binary exchange reaction

and

$$M_j = \sum_{i=1}^n XMM_{j,i} \cdot C_i \quad \text{for a dissociation-recombination reaction}$$

$$= 1 \quad \text{for a binary exchange reaction}$$

The net individual species production rate is given by the equation:

$$\frac{dC_i}{dx} \quad FN(I) = \bar{K}_i \cdot \sum_{j=1}^l \psi_{ij} \cdot X_j$$

where:

$$\bar{K}_i = (MW_i \cdot \rho \cdot r^*)/V$$

The partial derivatives of the net species production rate with respect to the chemical species, the gas velocity, the gas density, and the gas temperature are:

$$\beta(C_k, C_i) \quad BT(I, K) = \bar{K}_i \cdot \sum_{j=1}^l \frac{\partial X_j}{\partial C_i} \quad \begin{array}{l} i = 1, \dots, NSP \\ k = 1, \dots, NSP \end{array}$$

$$\beta(C_i, V) \quad PHI(I, 1) = -\frac{1}{V} \frac{dC_i}{dx} \quad i = 1, \dots, NSP$$

$$\beta(C_i, \rho) \quad PHI(I, 2) = \frac{1}{\rho} \cdot \frac{dC_i}{dx} + \bar{K}_i \cdot \sum_{j=1}^m \frac{\partial X_j}{\partial \rho} \quad i = 1, \dots, NSP$$

$$\beta(C_i, T) \quad PHI(I, 3) = \bar{K}_i \sum_{j=1}^l \frac{\partial X_j}{\partial T} \quad i = 1, \dots, NSP$$

The equilibrium constants and their temperature derivatives are computed only for dissociation-recombination reactions; those quantities for the binary exchange reactions are computed by products and ratios of the dissociation-recombination reaction equilibrium constants and derivatives.

(2) Subroutine EF

This subroutine computes the dissociation-recombination reaction equilibrium constants and their temperature derivatives from the following formulae:

$$K_j \quad EK(J) = \frac{DATEF(J)}{T} \cdot \exp \left[\frac{-\Delta H_j}{T} - \sum_{i=1}^n Ft_i \cdot v_{ij} + \sum_{i=1}^n Ft_i \cdot v'_{ij} \right]$$

$$\frac{dK_j}{dT} \quad DKT(J) = \left[\frac{- \sum_{i=1}^n \left(\frac{Ht_i}{R_i} \right) \cdot v_{ij} + \sum_{i=1}^n \left(\frac{Ht_i}{R_i} \right) \cdot v'_{ij}}{T} - 1 \right] \cdot \frac{K_j}{T}$$

where:

Ft_i = species free energy at the current temperature

Ht_i = species enthalpy at the current temperature

ΔH_j = heat of reaction for the J^{th} reaction

$DATEF(j)$ = is discussed in Subsection C. 5. e(2)

(3) Subroutine FLU

This subroutine computes the adiabatic component of the total derivatives f_i and the partial derivatives α_i and $\beta_{(i,j)}$ for the fluid dynamic equations. Pressure defined fluid dynamic equations are used. The summation terms, energy exchange term B, the diabatic heat addition term A, the Mach number, and all the partial derivatives of these terms are computed. The pressure and its derivatives are obtained from the pressure table.

For a stagnation streamline calculation, the pressure derivatives are obtained from the relationship:

$$\frac{dP}{dx} = -\rho \cdot V \frac{dV}{dx}$$

where V and dV/dx are defined by input tables.

Notes: $\Phi(i, l)$, $l = 1, 2, 3$ are defined under Subroutine DERIV
 $\Phi(i, 1)$, = $\beta(C_i, V)$; $\Phi(i, 2)$ = $\beta(C_i, \rho)$; $\Phi(i, 3)$ = $\beta(C_i, T)$

The following relationships may be helpful:

$$f_i = \frac{dC_i}{dx}; f_i = \frac{r^* \cdot \omega_i \cdot R \cdot T}{P \cdot V}; \frac{dC_i}{dx} = \frac{\omega_i r^*}{\rho \cdot V}$$

Computation of the Summation Terms and their derivatives:

First Summation

$$S1 \quad S1 = \frac{1}{R} \cdot \sum_{i=1}^n \frac{dC_i}{dx} \cdot R_i$$

$$\frac{\partial S1}{\partial V} \quad DS1V = \frac{1}{R} \cdot \sum_{i=1}^n \Phi(i, 1) \cdot R_i$$

$$\frac{\partial S1}{\partial \rho} \quad DS1R\emptyset = \frac{1}{R} \cdot \sum_{i=1}^n \Phi(i, 2) \cdot R_i$$

$$\frac{\partial S1}{\partial T} \quad DS1T = \frac{1}{R} \cdot \sum_{i=1}^n \Phi(i, 3) \cdot R_i$$

$$\frac{\partial S1}{\partial C_i} \quad DS1C(I) = \frac{1}{R} \cdot \left[\sum_{i=1}^n \beta(C_j, C_i) \cdot R_j - S1 \cdot R_i \right]$$

$i = 1, \dots, NSP$

Second Summation

$$S2 \quad S2 = \frac{1}{R \cdot T} \cdot \sum_{i=1}^n \frac{dC_i}{dx} \cdot h_i$$

$$\frac{\partial S2}{\partial V} \quad DS2V = \frac{1}{R \cdot T} \cdot \sum_{i=1}^n \Phi(i, 1) \cdot h_i$$

$$\frac{\partial S_2}{\partial p} \quad DS_2 R\emptyset \quad = \quad \frac{1}{R \cdot T} \cdot \sum_{i=1}^n \Phi(i, 2) \cdot h_i$$

$$\frac{\partial S_2}{\partial T} \quad DS_2 T \quad = \quad \frac{1}{R \cdot T} \cdot \sum_{i=1}^n \left[\Phi(i, 3) \cdot h_i + \frac{dC_i}{dx} \cdot C_{p_i} \right] - \frac{S_2}{T}$$

$$\frac{\partial S_2}{\partial C_i} \quad DS_2 C(I) \quad = \quad \frac{1}{R} \cdot \sum_{j=1}^n \frac{\beta(C_j, C_i) \cdot h_i}{T} - S_2 \cdot R_i \quad \left. \vphantom{\sum_{j=1}^n} \right] \\ i = 1, \dots, NSP$$

Computation of the Energy Exchange Term B and its Derivatives:

$$B \quad BB \quad = \quad \frac{\gamma-1}{\gamma} \cdot S_2$$

$$\frac{\partial B}{\partial V} \quad DBBV \quad = \quad \frac{\gamma-1}{\gamma} \cdot \frac{\partial S_2}{\partial V}$$

$$\frac{\partial B}{\partial p} \quad DBBRO \quad = \quad \frac{\gamma-1}{\gamma} \cdot \frac{\partial S_2}{\partial p}$$

$$\frac{\partial B}{\partial T} \quad DBBT \quad = \quad \frac{\gamma-1}{\gamma} \cdot \frac{\partial S_2}{\partial T} + \frac{S_2}{\gamma^2} \cdot \frac{\partial \gamma}{\partial T}$$

$$\frac{\partial B}{\partial C_i} \quad DBBC(I) \quad = \quad \frac{\gamma-1}{\gamma} \cdot \frac{\partial S_2}{\partial C_i} + \frac{S_2}{\gamma^2} \cdot \frac{\partial \gamma}{\partial C_i} \quad i = 1, \dots, NSP$$

Computation of the Diabatic Heat Addition Term A and its Derivatives:

$$A \quad AA \quad = \quad S_1 - B$$

$$\frac{\partial A}{\partial V} \quad DAAV \quad = \quad \frac{\partial S_1}{\partial V} - \frac{\partial B}{\partial V}$$

$$\frac{\partial A}{\partial \rho} \quad \text{DAARO} \quad = \quad \frac{\partial S1}{\partial \rho} - \frac{\partial B}{\partial \rho}$$

$$\frac{\partial A}{\partial T} \quad \text{DAAT} \quad = \quad \frac{\partial S1}{\partial T} - \frac{\partial B}{\partial T}$$

$$\frac{\partial A}{\partial C_i} \quad \text{DAAC(I)} \quad = \quad \frac{\partial S1}{\partial C_i} - \frac{\partial B}{\partial C_i} \quad i = 1, \dots, \text{NSP}$$

Computation of the Mach Number and its Derivatives:

$$M^2 \quad \text{XM2} \quad = \quad \frac{V^2}{\gamma \cdot R \cdot T}$$

$$\frac{\partial M^2}{\partial V} \quad \text{DM2V} \quad = \quad \frac{2 \cdot M^2}{V}$$

$$\frac{\partial M^2}{\partial T} \quad \text{DM2T} \quad = \quad -\frac{M^2}{T} - \frac{M^2}{\gamma} \cdot \frac{\partial \gamma}{\partial T}$$

$$\frac{\partial M^2}{\partial C_i} \quad \text{DM2C(I)} \quad = \quad -M^2 \cdot \left[\frac{\partial \gamma}{\partial C_i} \cdot \frac{1}{\gamma} + \frac{R_i}{R} \right] \quad i = 1, \dots, \text{NSP}$$

$$\frac{dV}{dx} \quad \text{FNX(1)} \quad = \quad -\frac{1}{\rho \cdot V} \cdot \frac{dP}{dx}$$

$$\frac{\partial[\text{FNX(1)}]}{\partial x} \quad \text{AL(1)} \quad = \quad -\frac{1}{\rho \cdot V} \cdot \frac{d^2 P}{dx^2}$$

$$\beta(V, V) \quad \text{BETA (1, 1)} \quad = \quad -\frac{1}{V} \cdot \frac{dV}{dx}$$

$$\beta(V, \rho) \quad \text{BETA(1, 2)} \quad = \quad -\frac{1}{\rho} \cdot \frac{dV}{dx}$$

The Gas Density derivatives are Computed:

$$\frac{d\rho}{dx} \quad \text{FNX(2)} \quad = \quad \rho \cdot \left[\frac{dP}{dx} \cdot \frac{1}{\gamma \cdot P} - A \right]$$

$$\frac{\partial[\text{FNX(2)}]}{\partial x} \quad \text{AL(2)} \quad = \quad \frac{\rho}{\gamma \cdot P} \cdot \left[\frac{d^2 P}{dx^2} - \left(\frac{dP}{dx} \right)^2 \cdot \frac{1}{P} \right]$$

$$\beta(\rho, V) \quad \text{BETA(2, 1)} \quad = \quad - \rho \cdot \frac{\partial A}{\partial V}$$

$$\beta(\rho, \rho) \quad \text{BETA(2, 2)} \quad = \quad - \frac{1}{\rho} \cdot \frac{d\rho}{dx} - \rho \cdot \frac{\partial A}{\partial \rho}$$

$$\beta(\rho, T) \quad \text{BETA(2, 3)} \quad = \quad - \rho \cdot \frac{\partial A}{\partial T} - \frac{\rho}{P \cdot \gamma^2} \cdot \frac{\partial \gamma}{\partial T} \cdot \frac{dP}{dx}$$

$$\beta(\rho, C_i) \quad \text{BETA(2, i+3)} \quad = \quad - \frac{\rho}{\gamma^2 P} \cdot \frac{\partial \gamma}{\partial C_i} \cdot \frac{dP}{dx} - \rho \cdot \frac{\partial A}{\partial C_i} \quad i = 1, \dots, \text{NSP}$$

The Gas Temperature derivatives are computed:

$$\frac{dT}{dx} \quad \text{FNX(3)} \quad = \quad T \cdot \left[\frac{\gamma-1}{\gamma} \cdot \frac{1}{P} \cdot \frac{dP}{dx} - B \right]$$

$$\frac{\partial[\text{FNX(3)}]}{\partial x} \quad \text{AL(3)} \quad = \quad \frac{\gamma-1}{\gamma} \cdot \frac{T}{P} \cdot \left[\frac{d^2 P}{dx^2} - \left(\frac{dP}{dx} \right)^2 \cdot \frac{1}{P} \right]$$

$$\beta(T, V) \quad \text{BETA(3, 1)} \quad = \quad - T \cdot \frac{\partial B}{\partial V}$$

$$\beta(T, \rho) \quad \text{BETA(3, 2)} \quad = \quad - T \cdot \frac{\partial B}{\partial \rho}$$

$$\beta(T, T) \quad \text{BETA}(3, 3) = \frac{1}{T} \cdot \frac{dT}{dx} + T \cdot \frac{1}{Y^2 \cdot P} \cdot \frac{dP}{dx} \cdot \frac{\partial Y}{\partial T} - T \cdot \frac{\partial B}{\partial T}$$

$$\beta(T, C_i) \quad \text{BETA}(3, i+3) = T \cdot \left[\frac{1}{Y^2 \cdot P} \cdot \frac{dP}{dx} \cdot \frac{\partial Y}{\partial C_i} - \frac{\partial B}{\partial C_i} \right]$$

$$i = 1, \dots, \text{NSP}$$

For an adiabatic area defined calculation, the total derivatives f_i and the partial derivatives a_i and β_{ij} for the fluid dynamic equations are computed using the following area defined equations:

The area ratio and its derivatives are computed from:

$$a = Y^2$$

$$\frac{da}{dx} = 2 \cdot Y \cdot \frac{dY}{dx}$$

$$\frac{d^2 a}{dx^2} = 2 \cdot \left[Y \frac{d^2 Y}{dx^2} + \left(\frac{dY}{dx} \right)^2 \right]$$

where Y , dY/dx , $d^2 Y/dx^2$ are computed via interpolation in the table of derivatives of the input wall table generated in Subroutine SLP.

The Gas Velocity derivatives are computed:

$$\frac{dV}{dx} \quad \text{FNX}(1) = \frac{V}{M^2 - 1} \cdot \left[\frac{1}{a} \frac{da}{dx} - A \right]$$

$$\frac{\partial [\text{FNX}(1)]}{\partial x} \quad \text{AL}(1) = \frac{V}{M^2 - 1} \cdot \frac{1}{a} \cdot \left[\frac{d^2 a}{dx^2} - \frac{1}{a} \left(\frac{da}{dx} \right)^2 \right]$$

$$\beta(V, V) \quad \text{BETA}(1, 1) = \frac{1}{V} \cdot \frac{dV}{dx} - \frac{1}{M^2 - 1} \cdot \frac{dV}{dx} \cdot \frac{\partial M^2}{\partial V} - \frac{V}{M^2 - 1} \cdot \frac{\partial A}{\partial V}$$

$$\beta(V, \rho) \quad \text{BETA}(1, 2) = - \frac{V}{M^2 - 1} \cdot \frac{\partial A}{\partial \rho}$$

$$\beta(V, T) \quad \text{BETA}(1, 3) = - \frac{1}{M^2 - 1} \cdot \frac{dV}{dx} \cdot \frac{\partial M^2}{\partial T} - \frac{V}{M^2 - 1} \cdot \frac{\partial A}{\partial T}$$

$$\beta(V, C_i) \quad \text{BETA}(1, i+3) = - \frac{1}{M^2 - 1} \cdot \frac{dV}{dx} \cdot \frac{\partial M^2}{\partial C_i} - \frac{V}{M^2 - 1} \cdot \frac{\partial A}{\partial C_i}$$

$$i = 1, \dots, \text{NSP}$$

The Gas Density derivatives are computed:

$$\frac{d\rho}{dx} \quad \text{FNX}(2) = -\rho \cdot \left[\frac{M^2}{M^2 - 1} \cdot \left(\frac{1}{a} \cdot \frac{da}{dx} - A \right) + A \right]$$

$$\frac{\partial[\text{FNX}(2)]}{\partial x} \quad \text{AL}(2) = -\rho \cdot \frac{M^2}{M^2 - 1} \cdot \frac{1}{a} \cdot \left[\frac{d^2 a}{dx^2} - \frac{1}{a} \left(\frac{da}{dx} \right)^2 \right]$$

$$\beta(\rho, V) \quad \text{BETA}(2, 1) = \rho \cdot \left[\frac{1}{(M^2 - 1)^2} \cdot \left(\frac{1}{a} \frac{da}{dx} - A \right) \cdot \frac{\partial M^2}{\partial V} + \frac{1}{M^2 - 1} \cdot \frac{\partial A}{\partial V} \right]$$

$$\beta(\rho, \rho) \quad \text{BETA}(2, 2) = \frac{1}{\rho} \cdot \frac{d\rho}{dx} + \frac{\rho}{M^2 - 1} \cdot \frac{\partial A}{\partial \rho}$$

$$\beta(\rho, T) \quad \text{BETA}(2, 3) = \rho \cdot \left[\frac{1}{(M^2 - 1)^2} \cdot \left(\frac{1}{a} \frac{da}{dx} - A \right) \cdot \frac{\partial M^2}{\partial T} + \frac{1}{M^2 - 1} \cdot \frac{\partial A}{\partial T} \right]$$

$$\beta(\rho, C_i) \quad \text{BETA}(2, i+3) = \rho \cdot \left[\frac{1}{(M^2-1)^2} \cdot \left(\frac{1}{a} \frac{da}{dx} - A \right) \frac{\partial M^2}{\partial C_i} + \frac{1}{M^2-1} \cdot \frac{\partial A}{\partial C_i} \right] \quad i = 1, \dots, \text{NSP}$$

The Gas Temperature derivatives are computed:

$$\frac{dT}{dx} \quad \text{FNX}(3) = -T \cdot \left[(\gamma-1) \cdot \frac{M^2}{M^2-1} \cdot \left(\frac{1}{a} \frac{da}{dx} - A \right) + B \right]$$

$$\frac{\partial [\text{FNX}(3)]}{\partial x} \quad \text{AL}(3) = -T \cdot \frac{M^2}{M^2-1} \cdot \frac{\gamma-1}{a} \cdot \left[\frac{d^2 a}{dx^2} - \frac{1}{a} \cdot \left(\frac{da}{dx} \right)^2 \right]$$

$$\beta(T, V) \quad \text{BETA}(3, 1) = T \cdot \left[\frac{\gamma-1}{(M^2-1)^2} \left(\frac{1}{a} \frac{da}{dx} - A \right) \cdot \frac{\partial M^2}{\partial V} + \gamma-1 \cdot \frac{M^2}{M^2-1} \cdot \frac{\partial A}{\partial V} - \frac{\partial B}{\partial V} \right]$$

$$\beta(T, \rho) \quad \text{BETA}(3, 2) = T \cdot \left[\gamma-1 \cdot \frac{M^2}{M^2-1} \cdot \frac{\partial A}{\partial \rho} - \frac{\partial B}{\partial \rho} \right]$$

$$\begin{aligned} \beta(T, T) \quad \text{BETA}(3, 3) = & \frac{1}{T} \cdot \frac{dT}{dx} + T \cdot \left[\frac{\gamma-1}{(M^2-1)^2} \left(\frac{1}{a} \frac{da}{dx} - A \right) \frac{\partial M^2}{\partial T} + \gamma-1 \cdot \frac{M^2}{M^2-1} \cdot \frac{\partial A}{\partial T} - \frac{\partial B}{\partial T} \right. \\ & \left. - \frac{M^2}{(M^2-1)} \cdot \left(\frac{1}{a} \frac{da}{dx} - A \right) \frac{\partial \gamma}{\partial T} \right] \end{aligned}$$

$$\begin{aligned} \beta(T, C_i) \quad \text{BETA}(3, i+3) = & T \cdot \left[\frac{\gamma - 1}{(M^2 - 1)^2} \cdot \left(\frac{1}{a} \frac{da}{dx} - A \right) \cdot \frac{\partial M^2}{\partial C_i} \right. \\ & + \gamma - 1 \cdot \frac{M^2}{M^2 - 1} \cdot \frac{\partial A}{\partial C_i} - \frac{\partial B}{\partial C_i} - \frac{M^2}{M^2 - 1} \\ & \left. \cdot \left(\frac{1}{a} \frac{da}{dx} - A \right) \frac{\partial \gamma}{\partial C_i} \right] \quad i = 1, \dots, \text{NSP} \end{aligned}$$

(4) Subroutine ADDXXX

This subroutine calculates the addition component of the total derivatives f_i and the partial derivatives α_i and β_{ij} and calculates the total and partial derivatives.

The addition components of the total derivatives are presented below:

$$\left. \frac{dV}{dx} \right|_{\text{add}} = \frac{\dot{M} - \dot{m}V}{1 + \bar{m}}$$

$$\left. \frac{dC_i}{dx} \right|_{\text{add}} = \frac{\dot{S}_i - \dot{m}C_i}{1 + \bar{m}}$$

$$\left. \frac{dT}{dx} \right|_{\text{add}} = \frac{1}{C_p} \left[\frac{E - \dot{m} H_T}{1 + \bar{m}} - \frac{V(\dot{M} - \dot{m}V)}{1 + \bar{m}} - \sum_{i=1}^{\text{nsp}} h_i \left(\frac{\dot{S}_i - \dot{m} C_i}{1 + \bar{m}} \right) \right]$$

$$\left. \frac{d\rho}{dx} \right|_{\text{add}} = \frac{-\rho}{T} \left. \frac{dT}{dx} \right|_{\text{add}} - \sum_{i=1}^{\text{nsp}} \frac{R_i}{R} \rho \left. \frac{dC_i}{dx} \right|_{\text{add}}$$

On option the adiabatic and addition components of the total derivatives are output from this subroutine.

(5) Subroutine IAUX1 (HL, H, QK, RK, JX)

This subroutine performs implicit integration according to the method discussed in Subsection C.3. The increments for the chemical species concentrations and the fluid dynamic variables at the forward point are calculated by solving the appropriate set of nonhomogeneous algebraic equations.

The calling sequence parameters are:

HL—last integration step size

H —current integration step size

QK—last increments for variables

RK—computed increments for variables

JX— 1 initial 3 steps

2 general step

3 special step

4 restart step

The total derivatives, $f_{i,n}$, and partial derivatives, $\beta_{i,j,n}$ at the back point are calculated in subroutines DERIV and FLU.

The special step calculation is used only in halving the step size if required.

After each integration step, subroutine IAUX obtains the derivatives at the then current axial position.

For implicit integration the equations used are:

Initial Step and Restart

$$k_{i,1} = \left[f_{i,0} + \alpha_{i,0} h + \sum_{j=1}^N \beta_{i,j,0} k_{j,1} \right] \cdot h$$

General Step

$$k_{i,n+1} = \frac{1}{3} \left[k_{i,n} + 2 \cdot \left(f_{i,n} + \alpha_{i,n} h + \sum_{j=1}^N \beta_{i,j,n} k_{j,n+1} \right) \cdot h \right]$$

Special Step

$$k_{i, n+1} = \frac{h_{n+1}^2}{(2h_{n+1} + h_n) \cdot h_n} \left[k_{i, n} + \left[f_{i, n} + \alpha_{i, n} h_{n+1} + \sum_{j=1}^N \beta_{i, j, n} k_{j, n+1} \right] \cdot \frac{h_n}{h_{n+1}} (h_{n+1} + h_n) \right]$$

(6) Subroutine LAUX (HL, H, QK, RK, JX)

This subroutine performs the iteration for the area defined, mass energy, momentum addition calculation. If the problem is pressure defined or an adiabatic-area-defined calculation, this subroutine merely calls Subroutine LAUX1 and then updates the derivatives at the forward point by calling Subroutine DERIV.

For the area defined, mass, energy, momentum addition calculation, the iteration proceeds as described below.

Prediction:

$$\frac{dP}{dx} = R \cdot T \cdot \frac{d\rho}{dx} + R \cdot \rho \cdot \frac{dT}{dx}$$

where

$$\frac{d\rho}{dx} = -\frac{1}{a} \frac{da}{dx} \cdot \rho \cdot \frac{M^2}{(M^2 - 1)}$$

$$\frac{dT}{dx} = -\frac{1}{a} \frac{da}{dx} \cdot T \cdot (\gamma - 1) \cdot \frac{M^2}{(M^2 - 1)}$$

if

$$0.99 < M^2 < 1.01,$$

then

$$\frac{dP}{dx} = 0.005 \cdot \frac{P}{H}$$

if

$$\frac{da}{dx} = 0.0,$$

then dP/dx from the previous step is used as the first estimate.

Iteration: Subroutine ITER is called successively to use the secant method to provide new estimates for dP/dx such that

$$f(A_{\text{calc}} - A_{\text{input}}) < \epsilon$$

Convergence: Convergence is obtained when

$$\left| \frac{A_{\text{calc}} - A_{\text{input}}}{A_{\text{input}}} \right| < \epsilon$$

and the pressure at the forward point is computed from

$$P_{i+1} = P_i + \left. \frac{dP}{dx} \right|_i \cdot H$$

(7) ITER (F1, X1, XNEW, NØØ)

The purpose of this subroutine is to find the root or zero of the algebraic equation

$$f(X) = 0$$

using the method of secant or false position. In particular this subroutine is designed to take advantage of the fact that the secant method will always find the root of the above equation if the root has been spanned.

Calling Sequence:

- F1 is the value of the dependent variable, f ,
 corresponding to the value of X1. (Input)
- X1 is the value of the independent variable, X , which
 corresponds to F1. (Input)
- XNEW is the predicted or new value of the independent vari-
 able. (Output)
- NØØ is a flag such that
- NØØ = -1 the first time ITER is called. (Input)
- NØØ = +1 upon subsequent calls. (Output)

Restrictions:

The user is expected to check for convergence as there are no internal checks made in ITER. A literal must not be input to this subroutine.

Method:

Subroutine ITER utilizes the secant method predictor formula

$$X_{i+1} = X_i - f_i \cdot (X_i - X_{i-1}) / (f_i - f_{i-1})$$

where the subscript i refers to the current value of X and f except for the first iteration in which the value of X is perturbed only slightly. When the root has been spanned, the subroutine saves 2 back values of f and X in order that the root may always be straddled and thus found. The linkage to the subroutine is set up so that if bounds on the root are known, then the value of XNEW may be disregarded and bounded values may be used for the first two guesses. This type of linkage necessitates that the value of X1 must be set equal to XNEW or the bounded value of X . In order to accelerate convergence, if the error within the bounded domain of the dependent variable exceeds a ratio of 10, then the new value of X is set equal to one half of the range.

(8) Subroutine INT

Provides control for the implicit integration procedure, determines the proper set of nonhomogeneous equations to solve, and, after

each integration step, computes the next integration step size according to the following relations:

$$h_{n+2} = 2h_{n+1}, \quad \left| \frac{k_{i,n+1} - 2k_{i,n} + k_{i,n-1}}{3k_{i,n+1} - k_{i,n}} \right|_{\text{MAX}} < \frac{\delta}{10}$$

$$h_{n+2} = \frac{1}{2} h_{n+1}, \quad \left| \frac{k_{i,n+1} - 2k_{i,n} + k_{i,n-1}}{3k_{i,n+1} - k_{i,n}} \right|_{\text{MAX}} > \delta$$

$$h_{n+2} = h_{n+1}, \quad \frac{\delta}{10} \leq \left| \frac{k_{i,n+1} - 2k_{i,n} + k_{i,n-1}}{3k_{i,n+1} - k_{i,n}} \right|_{\text{MAX}} \leq \delta$$

On option, (JF=1) only the fluid dynamic variables are used in determining the next integration step size.

If the step size is halved for the fourth step, the integration is restarting using one-half the original step size.

The correspondence between equation number and physical property is:

<u>Equation Number</u>	<u>Property</u>
1	Velocity of gas
2	Density of gas
3	Temperature of gas
4 → NSP+3	Gaseous species mass fraction (1 → NSP) corresponds to (4 → NSP + 3)

(9) Subroutine LESK(Y)

This subroutine is a single precision linear equation solver which is used to perform the matrix inversions required by subroutine IAUX. Gaussian elimination is used with row interchange taking place to position maximum pivot elements after the rows are initially scaled.

(10) Subroutine MAIN

Provides overall logic control for the kinetic calculations, controls the shock calculation for both generalized oblique shock and the normal shock for the stagnation streamline, and prints the summary for the maximum and minimum reaction net production rates.

The normal shock calculation equations are presented below:

$$P_2 = \rho_1 V_1^2 + P_1 - (\rho_1 V_1) V_2$$

$$h_2 = \frac{V_1^2}{2} - \frac{V_2^2}{2} + h_1$$

$$T_2 = f(h_2)$$

$$\rho_2 = \frac{P_2}{R \cdot T_2}$$

(11) Subroutine OUTPUT

This subroutine provides conversion from internal computational units to output engineering units. The following output parameters are computed by this subroutine:

The pressure (in PSIA) is computed from:

$$P_{(PSIA)} = P/4633.056$$

The gaseous species mole fractions are computed from:

$$C_{i,m} = \frac{R_i}{R} \cdot C_i$$

The gas molecular weight is computed from:

$$MW = 49721.011/R$$

The percentage mass fraction change is computed from:

$$\Delta(\text{Mass Fraction}) = 100.0 \cdot \left(1.0 - \sum_{i=1}^n C_i \right)$$

The gas heat capacity is computed from:

$$C_{p_g} \text{ (BTU/LB-}^\circ\text{R)} = 3.9969 \cdot 10^{-5} \cdot C_{p_g}$$

The gas static enthalpy is computed from:

$$H_g \text{ (BTU/LB)} = 3.9969 \cdot 10^{-5} \sum_{i=1}^n C_i \cdot (h_i - 905.770 \cdot R_i \cdot \Delta H_{F_i}^\circ)$$

The percentage enthalpy change is computed from:

$$\Delta H_T = \frac{100 \cdot \left(H_c - \sum_{i=1}^{NSP} C_i \cdot h_i - v^2 / 2 \right)}{HREF}$$

where

$$HREF = \sum_{i=1}^{NSP} C_i \cdot (h_i - 905.770 \cdot R_i \cdot \Delta H_{F_i}^\circ)$$

evaluated at the initial conditions in Subroutine CØNVRT.

The real gas constant and frozen gamma [Subsection C. 5f(2) (EF)] the enthalpy in internal units, the kinetic coupling terms A and B [Subsection C. 5f(3) (FLU)], the maximum relative error [Subsection C. 5t(8) (INT)], and the species concentrations in molecules per cc are also output.

(12) Subroutine OUTXXX

This subroutine is identical except in name to subroutine UTIL. It is used during the iteration for θ , the shock angle, during a generalized oblique shock calculation.

(13) Subroutine PLTSUB

This subroutine saves the current values of the variables requested for plotting and generates the proper labels and formatting for processing by subroutine DSCPLT. Plot information is saved on logical unit IPTAPE.

(14) Subroutine PRNTCK

For the option to print starting at step ND1, printing every ND3rd step up to step ND2, this subroutine checks whether or not the current step should be printed. If it is to be printed this subroutine calls OUTPUT.

(15) Subroutine UTIL (F1, X1, XNEW, NOO)

The purpose of this subroutine is to find the root or zero of the algebraic equation

$$f(X) = 0$$

using the method of secant or false position. In particular this subroutine is designed to take advantage of the fact that the secant method will always find the root of the above equation if the root has been spanned.

Calling Sequence:

F1 is the value of the independent variable, f, corresponding to the value of X1. (Input)

X1 is the value of the independent variable, X, which corresponds to F1. (Input)

XNEW is the predicted or new value of the independent variable. (Output)

NOO is a flag such that

NOO = -1 the first time ITER is called. (Input)

NOO = +1 upon subsequence calls. (Output)

Restrictions:

The user is expected to check for convergence as there are no internal checks made in UTIL. A literal must not be input to this subroutine.

Method:

Subroutine UTIL utilizes the secant method predictor formula

$$X_{i+1} = X_i - f_i \cdot (X_i - X_{i-1}) / (f_i - f_{i-1})$$

where the subscript i refers to the current value of X and f except for the first iteration in which the value of X is perturbed only slightly. When the root has been spanned the subroutine saves 2 back values of f and X in order that the root may always be straddled and thus found. The linkage to the subroutine is set up so that if bounds on the root are known, then the value of $XNEW$ may be disregarded and bounded values may be used for the first two guesses. This type of linkage necessitates that the value of $X1$ must be set equal to $XNEW$ or the bounded value of X . In order to accelerate convergence, if the error within the bounded domain of the dependent variable exceeds a ratio of 10, then the new value of X is set equal to one half of the range.

(16) Subroutine SHOCK

This subroutine calculates the downstream oblique shock conditions for an arbitrary pressure rise. The chemistry is assumed frozen across the shock. The method used is an iteration on the shock angle, θ , using the following:

$$1. \quad \theta^{(0)} = \arcsin \left[\sqrt{\frac{\frac{P_2}{P_1} (\gamma_1 + 1) + (\gamma_1 - 1)}{2 \gamma_1 M_1^2}} \right]$$

$$2. \quad u_1^{(i+1)} = V_1 \sin \theta^{(i)}$$

$$3. \quad v_2^{(i+1)} = V_1 \cos \theta^{(i)}$$

$$u_2^{(i+1)} = \frac{P_1 - P_2 + \rho_1 \left[u_1^{(i+1)} \right]^2}{\rho_1 u_1^{(i+1)}}$$

$$H_2^{(i+1)} = H_1 + \frac{1}{2} \left[u_1^{(i+1)} \right]^2 - \frac{1}{2} \left[u_2^{(i+1)} \right]^2$$

$$4. \quad T_2^{(i+1)} = f(H_2^{(i+1)}), \text{ obtained by iteration using subroutine UTIL.}$$

$$5. \quad \rho_{2a}^{(i+1)} = \frac{P_2}{R T_2^{(i+1)}}$$

$$\rho_{2b}^{(i+1)} = \frac{\rho_1 u_1}{u_2^{(i+1)}}$$

$$6. \quad \text{if } \left| \frac{\rho_{2a}^{(i+1)} - \rho_{2b}^{(i+1)}}{\rho_{2a}^{(i+1)}} \right| < \epsilon \text{ go to 9.}$$

7. Call OUTXXX to obtain new value for $\theta^{(i)}$ using secant method

8. Go to 2.

9. Compute and output downstream conditions:

$$y_2 = \frac{C_P(T_2)}{C_P(T_2) - R}$$

$$v_2 = \sqrt{u_2^2 + v_2^2}$$

$$M_2 = \frac{v_2}{\sqrt{\gamma_2 R T_2}}$$

If the upstream Mach number is less than one, no shock calculation is possible and the calculation is terminated at this point.

If the specified conditions are inconsistent, i. e., if

$$\sqrt{\frac{\frac{P_2}{P_1} (\gamma_1 + 1) + (\gamma_1 - 1)}{2 \gamma_1 M_1^2}} > 1.0$$

a normal shock calculation is attempted using $\theta = \pi/2$ and no iteration. An error message is provided for both of the above error conditions.

(17) Subroutine SCRX

This subroutine screens the reaction set at each axial station for those reactions which are necessary to assure a relative accuracy for a specified chemical species. Summaries of an ordered set of those reactions which produce and those reactions which destroy the specified species, along with total production and destruction rates are provided.

The subroutine screens those reactions which produce or destroy the specified species and retains those which produce or destroy the species at a rate greater than the input criterion (a percentage of the total production or destruction per unit normalized length). A logical vector is generated with the entry TRUE if the reaction is required or FALSE if the reaction is not required.

(18) Subroutine TREE (L, LIND, N)

The purpose of this subroutine is to reorder an input vector L containing N components so that

$$L(1) \leq L(2) \leq \dots \leq L(N).$$

L may be either real or integer.

The vector LIND must be input as a vector of integers 1, 2, . . . N. The vector LIND will be output as a vector containing the integer numbers which were the original position numbers of the L components.

The method used by subroutine TREE is described by ALGORITHM 245, TREE SORT 3 by Robert W. Floyd, "Communications of the ACM." December, 1964.

(19) Subroutine CONAD

This subroutine calculates the mass, momentum, energy, and species addition functions to the gas phase streamtube resulting from the condensation of a single gaseous species.

Subroutine VAPOR is called at each integration step to determine location of current thermodynamic state relative to liquid-vapor or solid-vapor coexistence line on the pressure, temperature (P, T) surface.

Once condensing vapor becomes saturated, the critical droplet radius and nucleation rate are computed. The addition function components are not calculated until the nucleation rate surpasses a threshold value EJMIN (input under \$PROPEL). The addition functions are computed from the following:

$$\dot{m} = dg/dx$$

$$\dot{M} = \dot{m}V + g \frac{(1+m)}{\rho V} dp/dx$$

$$\dot{H} = (1 - 2g) \dot{m}h' - (1 + \bar{m}) \dot{g} \frac{dh'}{dT} \frac{dT}{dx}$$

$$\dot{S}_i = \dot{m} , \text{ for } i = \text{condensing species}$$

$$= 0 , \text{ for remaining species}$$

The rate of change of the condensed mass fraction is obtained from

$$\frac{dg}{dx} = \frac{4\pi\rho_L}{\rho V} \left[\frac{1}{3} r^{**}(x) J(x) \frac{A(x)}{A_o} + \frac{dr}{dx} \int_{x_o}^x r(x, \xi)^2 J(\xi) \frac{A(\xi)}{A_o} d\xi \right]$$

The liquid droplet properties are obtained from Subroutine DROPS.

(20) Subroutine VAPOR (PV, PVS, DPVSDT, TS, IP, JJ, ISAT)

This routine computes for a specified species JJ the vapor pressure (PV), saturated vapor properties, and the location of the current state with respect to both the triple point and the liquid-vapor or solid-vapor coexistence line. Vapor pressure is computed from

$$P_v = C_i \frac{R_i}{R} P$$

For pressures and temperatures above the triple point, the saturated vapor pressure (PVS) corresponding to temperature T, derivative of PVS with respect to T, and saturated vapor temperature (TS) corresponding to pressure P are obtained from expressions of the form

$$PVS = C_1 + C_2/T + C_3/T^2$$

$$TS = 1. / \left[C_4 + C_5 \ln(PV) + C_6 \ln^2(PV) \right]$$

$$DPVSDT = -PVS (C_2 - 2.0 C_3/T) / T^2$$

At or below the triple point, the following expressions are used

$$PVS = \exp(C_8 - C_7/T)$$

$$TS = C_7 / \left[C_8 - \ln(PV) \right]$$

$$DPVSDT = PVS C_7 / T^2$$

where the constants C_1 through C_8 are determined from data and are input under \$PRØPEL. Preliminary values of these constants for water vapor are stored internally and need not be entered.

The additional parameters in the calling statement are

IP = 0 Current state corresponds to triple point

= 1 Above triple point

= 2 Below triple point

ISAT = 0 Vapor is unsaturated

= 1 Vapor is saturated

(21) Subroutine DROPS

This subroutine computes liquid droplet properties and derivatives as a function of temperature. Above the triple point, latent heat and density are computed from

$$L = A_1 - A_2 T - A_3 T^2$$

$$\rho = A_4 - A_5 T_D + A_6 T_D^2$$

$$\sigma = A_{11} - A_{12} T_D$$

At or below the triple point, the following are used

$$L = A_7 - A_8 T$$

$$\rho = A_9 - A_{10} T_D$$

$$\sigma = A_{11} - A_{12} T_D$$

First and second derivatives with respect to temperature are obtained by differentiating the above expressions. The coefficients A_1 through A_{12} are input under \$PRØPEL. Preliminary values of these constants for water vapor are stored internally.

c. Plotting Subroutines Descriptions

(1) Subroutine LINK 50

This subroutine reads the quantities saved for plotting from logical unit IPTAPE into the proper buffer areas and calls subroutine DSCPLT for the actual plotting.

(2) Subroutine DSCPLT

This subroutine is a generalized plotting routine utilizing Calcomp software to produce plots. It requires subroutines SCAL and MAXMIN.

(3) Subroutine MAXMIN

This subroutine finds the maximum and minimum entries in an array.

(4) Subroutine SCAL(XMAX, XMIN, XI, DX, XO, XE)

Given the maximum and minimum of a variable and the number of units (inches, cm., etc.) available for plotting, this routine:

1. Determines the most efficient scale per plotting unit of the form $1.0 \cdot 10^a$, $2.0 \cdot 10^a$, $5.0 \cdot 10^a$ where a is an integer.
2. Adjusts the minimum scale value so that the plot begins at a multiple of the scale value.

Calling Sequence:

XMAX = the maximum value of the variable (input)

XMIN = the minimum value of the variable (input)

XI = the number of units (in., cm, etc.) available for plotting (input)

DX = the scale selected for the plot grid (output)

XO = the first plot grid value (output)

XE = the last plot grid value (output)

The algorithm used is given below:

$$W = \frac{XMAX - XMIN}{XI}$$

Then select $s = 1, 2, \text{ or } 5$ such that

$W = DX$ is a minimum

where

$$A = 1 + \log\left(\frac{W}{s}\right)$$

$B = [A]$, $[A]$ = the greatest integer strictly less than A ,
e. g. $[1.2] = 1$, $[0] = -1$

or

$$B = |A| - 1 \text{ if } A = |A| \text{ or } A < 0$$

$$C = s 10^B$$

$$D = \left\lfloor \frac{XMIN}{C} \right\rfloor C$$

or

$$D = \left(\left\lfloor \frac{XMIN}{C} \right\rfloor - 1 \right) C \text{ if } C \cdot D > XMIN$$

$$E = W/C$$

and

$$DX = C$$

$$XO = D$$

$$XE = E$$

also

$$\text{if } W=0 \text{ then } DX=XO=XE=0$$

C.6 PROGRAM USER'S MANUAL

This program was developed on the CDC 6500 computer using the FORTRAN IV language. Conversion to another computer system should be straight forward provided sufficient core storage (120,000 words) is available. Program overlay extends three levels deep including the executive level, when used as a subprogram to CONTAM.

The description of the operation mode and input to the computer program is divided into the following six Subsections:

C. 6. 1 OPERATION MODE—Automatic or manual.

C. 6. 2 \$THERMO—Namelist input which controls the thermodynamic data input.

C. 6. 3 THERMODYNAMIC DATA—Optional.

- C. 6. 4 TITLE CARD—Also serves for plot labels.
- C. 6. 5 SPECIES CARDS—Species to be considered and their initial concentrations.
- C. 6. 6 REACTION CARDS—Input of reactions and rate data.
- C. 6. 7 \$PROPEL—Namelist input for a specific case.

Card listings for the complete input for several sample cases are given in Section C. 7.

a. Operation Mode

Two modes of operation (automatic or manual) are available and specified through input variable KMØDE in the executive program, CONTAM.

(1) Manual Mode (KMØDE = 1)

In the manual mode of operation the KINCON subprogram is independent of the other subprograms. The user is free to specify, via input data (cards), the streamtube initial conditions, boundary conditions, and program options. A complete set of data (inputs described in Subsections C. 6b through C. 6g) is required for each streamtube calculation. However, if a specific nozzle/plume streamtube, generated by either the nozzle or plume portion of MULTRAN is desired; subprogram SLINES may be utilized in conjunction with MULTRAN to specify initial conditions and pressure distribution while operating in the manual mode. The variable NSL, which specifies the number of streamtubes processed by subprogram SLINES, is input through either the executive program or SLINES and is tested to determine if input data from SLINES via TAPE 8 is to be used in the manual mode of operation.

If NSL = 0, TAPE 8 will not be read and all data must be input.

If NSL \neq 0, the initial values (Z, PI, T, V, and EXIT), as well as the streamtube pressure distribution (NTB, ZTB (I), and PTB (I)) are read from TAPE 8. If successive cases are run, TAPE 8 will be read successively until either the final case is completed or the number of streamtubes on TAPE 8 is exhausted. It should be noted that any or all data read from Tape 8 may be overridden by card input.

(2) Sequential Mode (KMØDE = 0)

The automatic mode of operation is designed to calculate both chemical-kinetic and single-species condensation effects (a two-pass calculation performed in that order) for a number of streamtubes calculated by MULTRAN and SLINE subprograms. This mode requires only one set of input data and is utilized in conjunction with subprogram SLINES (or a TAPE 8 previously generated by SLINES).

In the automatic mode, KINCON will accept input data describing initial gas-phase composition, chemical reaction and rate coefficients, and pertinent integration control parameters (described in Subsections C.6.b through C.6.g). Initial streamtube conditions and pressure distribution are read from TAPE 8, and kinetics calculation is then performed along the pressure-defined streamline. During the kinetics calculation pass the vapor pressure of the condensible species is compared with the saturated vapor surface to determine the vapor state. Once the saturated vapor state is reached, the streamtube conditions at the saturation point (location, temperature, pressure, velocity, and species composition) are written onto TAPE 1. The streamtube area ratio, referenced to the saturation point, is then computed and written on TAPE 1 during the subsequent integration.

TAPE 1 thus contains, at the completion of the kinetics pass, the initial conditions and area ratio distribution for the streamtube beginning at the saturation point.

If the saturation point is countered on the kinetics pass, a second pass is made to compute condensation. This pass, utilizing TAPE 1 generated during the kinetics pass, invokes frozen-chemistry and single-species condensation options to compute condensation effects along the area defined streamtube. Following the completion of the condensation calculation, initial conditions for the next streamtube are read from TAPE 8 and the calculation procedure is repeated until all streamtubes have been completed. If the saturation point is not reached on a given kinetics pass, the condensation calculation pass is not performed and the program proceeds to the next streamtube.

Inputs in the automatic mode consist of all inputs described in Subsections C.6.b through C.6.f and a limited number of inputs in \$PROPEL. Inputs required in \$PROPEL are the following:

RSTAR	Axial distance normalizing factor (nozzle throat radius)
PRINT VARIABLES	(ND1, ND2, ND3)
INTEGRATION VARIABLES	(HI, HMIN, HMAX, DEL, JF)

Inputs that are available but not required include MISCELLANEOUS VARIABLES (except IFLAST), INTERMEDIATE OUTPUT VARIABLES, and certain CONDENSATION OPTION VARIABLES.

b. \$THERMØ

Permits the generation of a master thermodynamic file or the use of a tape file previously generated master thermodynamic file.

<u>Variable</u>		<u>Value</u>	<u>Description</u>
NUCHEM	=	1	A master thermodynamic file will be generated for this case on tape unit 4. Species and thermodynamic data will be read from unit INTAPE (nominal=5, the input file) and a new thermodynamic file will be generated on unit 4. The new thermodynamic file will be end-filed and rewound after generation.
	=	0	A previously generated master thermodynamic file will be used for this case. The master thermodynamic file must be file TAPE 4. No other input variables are required for this option.
MAXSP	=	Input	If a master thermodynamic file is to be generated this variable specifies the number of species for the master file.
LIST	=	1	A list of species named for those species master file will be output.
	=	0	This output will be deleted.
LISTX	=	1	Thermodynamic functions (CP, H, F) will be output for each species (one page per species, 52 lines per page). Species names, molecular weights, and heats of formation will also be printed.
	=	-1	Only a table of species names, molecular weights, and heats of formation will be printed.
	=	0	The above output will be deleted.
INTAPE	=	Input	Tape file from which thermodynamic data is to be read (nominal = 5).

\$END

c. Thermodynamic Data

For a NUCHEM = 1 option in \$THERMØ the program will read MAXSP Master Species cards containing: species symbolic identifier, molecular weight, and $\Delta H^\circ F_{298}$, and then read MAXSP sets of thermodynamic data (CP, H, F) checking names and card sequences. The Master Species cards must be sequenced sequentially in columns 41-50 (I10 format) and must correspond directly to the order in which the thermodynamic data is to be read. Thermodynamic functions consist of 10 cards per function, 5 values per card corresponding to temperature values of 100 → 5,000°K at 100°K

intervals. Table C-I lists the species for which thermodynamic data is currently available. For species which do not appear in Table C-I, this input may be obtained directly from the JANAF tables. Table C-II is a sample listing of the thermodynamic function input for the species N₂.

Master Species Cards

<u>Column</u>	<u>Information</u>
1 - 10	Not used.
11 - 16	Species Symbolic Identifier, 6 alphanumeric characters (left justified).
17 - 20	Not used.
21 - 30	Species molecular weight (F) format.
31 - 40	Species ΔH°_{F298} (F) format, K cal/mole.
41 - 50	Right justified sequence number used for sequence checking on input (I10 format).
51 - 80	Not used.

It should be noted that a species is identified by the name assigned by the user. In general this name is the chemical symbol, e.g., O, O₂, H, H₂. However, it may be useful to define a dummy species with all the properties of another species but which may be treated in a special manner, e.g., the percentage of the total amount of a species which is designated as an inert (possibly to simulate incomplete mixing or combustion). This may be done by defining species O and OX where OX is identical to O except in name, but does not appear in any reaction.

Master Thermodynamic Function Cards

<u>Column</u>	<u>Information</u>
1	Not used.
2 - 10	Function value at $(100 + 500(n-1))^\circ\text{K}$, $n = \text{card number}$.
11	Not used.
12 - 20	Function value at $(200 + 500(n-1))^\circ\text{K}$.
21	Not used.
22 - 30	Function value at $(300 + 500(n-1))^\circ\text{K}$.
31	Not used.
32 - 40	Function value at $(400 + 500(n-1))^\circ\text{K}$.
41	Not used.
42 - 50	Function value at $(500 + 500(n-1))^\circ\text{K}$.
51 - 60	Not used.
61 - 66	Species symbolic identifier, left justified.
67 - 68	Not used.
69 - 70	Function Definition CP, H, or F, left justified.
73 - 76	The word CARD.
77 - 78	Card number 1-10 right justified.
79 - 80	Not used.

Species symbolic identifier, function definition, and card numbers are checked for consistency on input.

Table C-L SPECIES RESIDING ON MASTER THERMODYNAMIC TAPE

1 H ₂	19 SF ₄	37 HCL ₃	55 C ₂ F ₂	73 COF ₂	90 ALF
2 H ₂	20 SF ₆	38 HF	56 O ₃	74 NO ₃	91 ALF ₂
3 O ₂	21 C	39 PF ₂	57 H ₂ O	75 NH	92 ALF ₃
4 O ₂	22 C ₂	40 PF ₃	58 NO ₂ -	76 NH ₂	93 ALGCL
5 O ₂	23 C ₂	41 H ₂ OCL	59 NA	77 NH ₃	94 ALOF
6 O ₂	24 C ₂	42 HOF	60 NA+	78 NH	95 ALCLF
7 A ₂ / O ₂	25 C ₂	43 HCLF	61 HAO	79 NH ₂	96 ALCL ₂ F
8 F ₂	26 C ₂	44 HCL ₂ F	62 CF ₂	80 NH ₃	97 ALCL ₂ F ₂
9 H ₂	27 C ₂	45 HCL ₂ F ₂	63 CF ₃	81 H ₂ NO	98 OH-
10 F ₂	28 C ₂	46 F	64 CF ₄	82 C ₂ H ₂	99 CH ₂
11 F ₂	29 C ₂ H ₂	47 CL	65 C ₂ F ₄	83 C ₂ H ₃	100 HAO ₂
12 F ₂	30 C ₂	48 CL ₂	66 NO ₂	84 AL	101 NH
13 F ₂ +	31 H ₂ O	49 F	67 N ₂ O	85 AL ₂	102 H ₂ Z
14 F ₂ -	32 H ₂ O	50 HCL	68 HCO	86 AL ₂ O	103 H ₂
15 H ₂	33 H ₂	51 CLF	69 HCO+	87 ALCL	104 OHX
16 F ₂	34 H ₂ O	52 H ₂ OCL	70 C ₂ H	88 ALCL ₂	105 PHOTON
17 F ₂	35 H ₂ CL	53 CNF	71 H ₃ O+	89 ALCL ₃	106 O ₂
18 F ₂	36 H ₂ CL ₂	54 CF	72 H ₂ O ₂		

Table C-II. SAMPLE LISTING FOR THERMODYNAMIC
FUNCTION CARDS FOR N₂

6,9560,	6,9570,	6,9610,	6,9900,	7,0690,	N2	CP	CARD 1
7,1960,	7,3500,	7,5120,	7,6700,	7,8150,	N2	CP	CARD 2
7,9450,	8,0610,	8,1620,	8,2520,	8,3300,	N2	CP	CARD 3
8,3980,	8,4580,	8,5120,	8,5590,	8,6010,	N2	CP	CARD 4
8,6380,	8,6720,	8,7030,	8,7310,	8,7560,	N2	CP	CARD 5
8,7790,	8,8000,	8,8200,	8,8380,	8,8550,	N2	CP	CARD 6
8,8710,	8,8850,	8,9000,	8,9140,	8,9270,	N2	CP	CARD 7
8,9390,	8,9500,	8,9620,	8,9720,	8,9830,	N2	CP	CARD 8
8,9930,	9,0020,	9,0120,	9,0210,	9,0300,	N2	CP	CARD 9
9,0390,	9,0480,	9,0570,	9,0660,	9,0740,	N2	CP	CARD10
-1,3790,	-.6850,	.0130,	.7100,	1,4130,	N2	H	CARD 1
2,1250,	2,8530,	3,5960,	4,3550,	5,1290,	N2	H	CARD 2
5,9170,	6,7180,	7,5290,	8,3500,	9,1790,	N2	H	CARD 3
10,0150,	10,8590,	11,7070,	12,5600,	13,4180,	N2	H	CARD 4
14,2800,	15,1460,	16,0150,	16,8860,	17,7610,	N2	H	CARD 5
18,6380,	19,5170,	20,3980,	21,2800,	22,1650,	N2	H	CARD 6
23,0510,	23,9390,	24,8290,	25,7190,	26,6110,	N2	H	CARD 7
27,5050,	28,3990,	29,2950,	30,1910,	31,0890,	N2	H	CARD 8
31,9880,	32,8880,	33,7880,	34,6900,	35,5930,	N2	H	CARD 9
36,4960,	37,4000,	38,3060,	39,2120,	40,1190,	N2	H	CARD10
41,9570,	42,8670,	43,7700,	44,6830,	45,5960,	N2	F	CARD 1
47,1430,	47,7310,	48,3030,	48,8530,	49,3780,	N2	F	CARD 2
49,8790,	50,3570,	50,8130,	51,2480,	51,6650,	N2	F	CARD 3
52,0650,	52,4480,	52,8160,	53,1710,	53,5130,	N2	F	CARD 4
53,8420,	54,1600,	54,4600,	54,7650,	55,0550,	N2	F	CARD 5
55,3350,	55,6060,	55,8700,	56,1270,	56,3760,	N2	F	CARD 6
56,6190,	56,8560,	57,0870,	57,3120,	57,5320,	N2	F	CARD 7
57,7470,	57,9570,	58,1620,	58,3620,	58,5590,	N2	F	CARD 8
58,7510,	58,9400,	59,1240,	59,3050,	59,4820,	N2	F	CARD 9
59,6570,	59,8270,	59,9950,	60,1600,	60,3220,	N2	F	CARD10

d. Title Card

The title card contains free field information which will be written as a header label for the program output. The first 40 characters will be written as a label on each plot if plotting is requested.

e. Species Cards

This input is prefixed by a single card with SPECIES in columns 1 to 7 and with the words MASS FRACTIONS or MOLE FRACTIONS in columns 9-22. If the identifier for mass or mole fractions is omitted, mass fractions are assumed. Up to 40 species cards may be input. Only those species specified by input species cards will be considered. The order of the input species cards is independent of the order in which the species appear on the master thermodynamic data file. However, the order of the input species cards does define the species order for the specific calculation, and other input referencing individual species must refer to the order of the input species cards. Species Cards are described below:

<u>Column</u>	<u>Function</u>
1 - 10	Not used.
11 - 16	Symbol (left justified).
17 - 20	Not used.
21 - 60	Value of initial species concentration (if zero must be input as 0.0) free field F or E format.
61 - 80	User identification if desired.

Symbols for Species Identification

A chemical species is identified symbolically by six alphanumeric characters as follows:

The species symbol must agree with that given on its master species card (columns 11-16) used in generating the master thermodynamic file. If the species is ionized, the degree of ionization is indicated by a + (or -) sign followed by an integer describing the degree of ionization (if no integer is given the species will be assumed singly ionized). The species symbol may not contain the characters * or =. The special species symbol PHOTON is reserved for specifying radiative reactions.

Examples:

<u>Symbol</u>	<u>Interpretation</u>
CL	Cl
NA+	NA ⁺
K+2	K ⁺⁺
CL2-2	Cl ₂ ⁻
H2O2	H ₂ O ₂

f. Reaction Cards

This input is prefixed by a single card with REACTIØNS in columns 1 to 9. Up to 15 dissociation reactions and a total 150 reactions may be input following this card. Only one card per reaction is permitted. Cards specifying dissociation-recombination reactions must precede cards specifying exchange reactions. The content and format of the reaction cards are defined as follows:

(1) Each card is divided into five fields, separated by commas. Each field contains:

Field 1	the reaction.
Field 2	A = followed by the value of A.
Field 3	N = followed by the value of N.
Field 4	B = followed by the value of B, the activation energy (Kcal/mole).
Field 5	available for comments.

Rules for specifying the reaction are given in C.6. e(2) below. The values A, N, and B define the reverse reaction rate, k, as

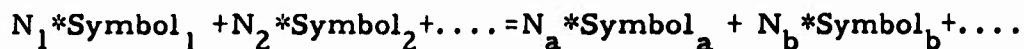
$$k = A \cdot T^{-N} \cdot e^{-(B/RT)}$$

All three reaction rate parameters must be input. The numeric value of each parameter may be specified in either I, F, or E format. If E format is used, the E must appear before the exponent.

There may be no blanks between the characters A and equal sign, the N and equal sign, and the B and equal sign.

Input rate parameters are in units of cc, °K, mole, sec.

(2) The general form of a reaction is:



where the left-hand side represents reactants and the right-hand side represents products.

Each symbol must be as defined on an input species card (see the description of SPECIES CARDS).

The multipliers, N, must be integers and represent stoichiometric coefficients. If no stoichiometric coefficient is given, the value 1 is assumed.

It is required that

$$N_1 + N_2 + \dots \leq 10$$

and

$$N_a + N_b + \dots \leq 10$$

Examples:

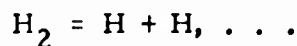
<u>Reaction</u>	<u>Interpretation</u>
NA++CL- = NACL	$Na^+ + Cl^- = NaCl$
B+2+M-2 = BM	$B^{++} + M^{--} = BM$
BE+2+2*ØH- = BEØHØH	$Be^{++} + 2ØH^- = Be (ØH)_2$

(3) The dissociation-recombination reactions specifying third-body terms must precede other types of reactions, and must be followed by the directive:

Column 1

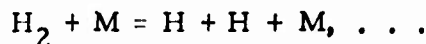
END TBR REAX

All reactions prior to the above directive will have a third-body term added to each side of the reaction. For example:



END TBR REAX

is the same as



where M is a generalized third body. Specific third-body effects may be included by inputting specific third-body reaction rate ratios XMM (J, I).

(4) Radiative reactions may be considered using the special species PHØTØN. The PHØTØN may only appear on the left-hand side of the equal sign for a reaction.

(5) The reaction set is terminated by a card containing LAST CARD in columns 1 to 9.

g. \$PRØPEL

<u>Case Variables</u>	<u>Units</u>
*Z	Initial normalized axial position
*PI	Initial pressure
*T	Initial temperature
*V	Initial velocity
RSTAR	Axial distance normalizing factor (normally throat radius for nozzle calculations)
	ft/sec
	Inches

*EXIT	Normalized axial distance for run termination	None
NØCHEM	= 1 if a frozen chemistry case is desired	None

Plot Variables (plotting not available in automatic mode of operation)

IFP	= 1	Plotting requested
ITP	= 1	Plot temperature
IRØP	= 1	Plot density
ICHEMP (1)	=	Species numbers for desired species concentration plots, up to 30 species
IXP	= 1	Plot functions vs normalized distance
MLP	= 1	Plot species MØLE fractions
MSP	= 1	Plot species MASS fractions

Print Variables

ND1	Print every ND3 rd step beginning with the ND1 st step
ND2	until the ND2 nd step. (The initial conditions and the
ND3	EXIT point are always printed.)

Integration Variables

HI	Initial normalized step size
HMIN	Minimum normalized step size
HMAX	Maximum normalized step size
DEL	Relative error criterion
JF	= 0 all variables considered for step size control
	= 1 only fluid dynamic variables considered for step size control.

The variable which controls the step size; i. e., has the maximum relative error; is printed in the normal output under Integration Parameters, labeled Governing Equation. The number: variable correspondence is as follows: 1=T; 2=RO; 3=V, 4=Species 1; 5=Species 2; . . . NSP + 3 = Species NSP.

Table Input Variables

*NTB	Number of input table entries for pressure table (101).
JPFLAG	Determines the type of differentiation used to obtain derivatives for all input tables. Reference should be made to Mass, Momentum, Energy and Species Addition Functions for other input tables controlled by JPFLAG.

*Values are read from TAPE 8 and need not be input when operated in automatic mode (KMØDE = 0) or in a manual mode (KMØDE = 1) and using streamtube data from TAPE 8 (NSL ≠ 0). If input, they will override TAPE 8 values for first streamtube only.

= 1 derivatives of input table obtained by simple difference formulae with second derivatives defined as 0. Normally used in automatic mode.

= 2 derivatives of input tables obtained by SPLINE fit ($NTB \leq 20$).

= 3 derivatives input along with tables.

= 4 derivatives of input tables obtained by parabolic differentiation ($NTB \leq 20$).

*PSCALE = Multiplicative constant for the input pressure table.

*ZTB (1) = Normalized axial positions for input tabular values for pressure table (always input).

*PTB (1) = Pressure table (PSIA) (always input).

*DPTB (1) = Pressure table derivative (for JPFLAG = 3 option).

Miscellaneous Variables

XMM (J,I) Reaction rate ratio effect on reaction J of species I.

TU (1) Temperature above which approximate extension of JANAF tables will occur for each species (nominal = 9,000°R).

IFLAST For overlay reasons must be set = 1 on the last case of a run.

TSTOP Time at which a run will arbitrarily be terminated (CP time). Ignore in automatic mode.

Intermediate Output

IDQDX = 1 Print total derivatives.

IDXJDX = 1 Print individual reaction net production rates.

IEQOUT = 1 Print equilibrium constant and its temperature dependence in internal units.

IRATE = 1 Print reaction forward and reverse rates in internal units.

*Values are read from TAPE 8 and need not be input when operated in automatic mode ($KMODE = 0$) or in a manual mode ($KMODE = 1$) and using streamtube data from TAPE 8 ($NSL \neq 0$). If input, they will override TAPE 8 values for first streamtube only.

IMASDX = 1 For an IADDF = 1 option print chemical and addition function components of total derivatives.

IØPXF = 1 Print influence coefficient vectors.

IØPVAR (1) = Set consecutive entries equal to K for variables for which influence coefficient vectors are to be output, where

<u>K</u>	<u>Variable</u>
1	V
2	RØ
3	T
4	Species number 1
.	.
.	.
.	.
NSP+3	Species number NSP

For example: IØPVAR(1) = 4, 3, will output influence coefficient vectors for species number 1 and for temperature.

Mass, Momentum, Energy, and Species Addition Functions

Variable

IADDF = 1 Addition functions will be input.

IXTB = Number of entries in addition function tables ≤ 40 .

IADDØP = 0 Addition functions input via tables.

 = 1 Addition functions defined via multiplicative factors. See EFACT (I), XMFACT (I), SPFACT (I, J) below. Note that IXTB factors must be input.

 = 2 A subroutine for addition calculation will be supplied by the user.

XADSCL = Multiplicative scale factor for all addition functions. Note that input of XADSCL as 1.0/(p. V. A) will provide automatic normalization (per unit initial streamtube mass flux) for input addition functions.

ADDX (I) = Table of normalized axial stations for all input addition functions.

ADDMAS (I)	=	Mass addition rate, per unit normalized length, per unit initial streamtube mass flux (unitless).
ADDE (I)	=	Energy addition rate, per unit normalized length, per unit initial streamtube mass flux (BTU/lb).
ADDEX (I)	=	Auxiliary energy addition rate, per unit normalized length, per unit initial streamtube mass flux (BTU/lb) which will be added to the energy addition rate ADDE (I). Note that ADDEX (I) is independent of EFACT (I) for IADDOP = 1 option and will be added to ADDE (I) before modification by XADSCL.
ADDMOM (I)	=	Momentum flux, per unit normalized length, per unit initial streamtube mass flux (ft/sec).
NPINT (I)	=	Species number (for current case) to relate species addition functions to specific species. See example under ADDSP (I, J).
NSPADD	=	Number of entries in NPINT (I) table.
ADDSP (I, J)	=	Species mass addition rate per unit normalized length, per unit initial streamtube mass flux (unitless).
		I=1, . . . IXTB corresponding to number of entries
		J=1, . . . NSPADD
		e. g. , NSPADD = 2
		NPINT = 3, 5
		ADDSP (I, 1) corresponds to Species 3
		ADDSP (I, 2) corresponds to Species 5
EFACT (I)	=	For IADDOP = 1, ADDE (I) computed as ADDMAS(O) *EFACT(I).
XMFACT (I)	=	For IADDOP = 1, ADDMOM (I) computed as ADDMAS (I) *XMFACT (I).
SPFACT (I, J)	=	For IADDOP = 1, ADDSP (I, J) computed as ADDMAS (I) *SPFACT (I, J).
IHTOTF	= 1	Restart flag indicating that a case is being restarted and directing the initial enthalpy to be HTOTX.
HTOTX	=	Initial enthalpy if a case has been restarted (ft ² /sec ²).

DMASDX (I)	=	For JPFLAG = 3 option, derivative of the mass addition rate $d(ADDMAS)/d\bar{x}$.
DEDXT (I)	=	For JPFLAG = 3 option, derivative of the total energy addition rate $d(ADDE+ADDEX)/d\bar{x}$.
DMØMDX (I)	=	For JPFLAG = 3 option, derivative of the momentum addition rate $d(ADDMØM)/d\bar{x}$.
DSPDX (I, J)	=	For JPFLAG = 3 option, derivative of the species addition rate $d(ADDSP)/d\bar{x}$.

Generalized Oblique Shock Calculation

A generalized oblique shock calculation is specified by input of a pressure table containing a pressure discontinuity, and a pointer designating the shock location.

		UNITS
NSHØCK	=	Pointer designating the last entry in the pressure table prior to the shock. For example:
		$\frac{P_2}{P_1} = \frac{PTB(NSHØCK+1)}{PTB(NSHØCK)}$ <p>Entries NSHØCK and NSHØCK+1 in the pressure table must have the same axial position.</p>
SHKBUG	=	1.0 provides intermediate output. None 0.0 provides no intermediate output.
SMAXIT	=	Maximum number of iterations during a generalized oblique shock calculation. None
SKEPS(1)	=	Relative convergence criterion for temperature iteration during a generalized oblique shock calculation. None
SKEPS(2)	=	Relative convergence criterion for overall iteration during a generalized oblique shock calculation. None

Normal Shock Stagnation Streamline Calculation

The normal shock stagnation streamline calculation option performs a normal shock calculation from specified upstream and downstream velocities and continues the calculation as a velocity defined streamtube.

			<u>UNITS</u>
NSTAGV	=	1 specifies a normal shock stagnation streamline calculation.	None
VEL1	=	Upstream velocity for the normal shock calculation.	ft/sec
VTB(1)	=	Array defining the velocity as a function of normalized axial distance. VTB(1) is defined as the downstream velocity for the normal shock calculation.	ft/sec
NVTB	=	Number of entries in the velocity profile NVTB ≤ 101 .	None

Reaction Screening Input Variables

If a reaction screening calculation is requested, the program performs a two-pass calculation. The first pass utilizes the complete reaction set and determines those reactions which must be retained to satisfy the input criteria for each species screened. The second pass redoes the first calculation with an edited reaction set and provides a summary page comparing both calculations.

			<u>UNITS</u>
ISCRF	=	1, specifies a reaction screening case for ISCSP (I) species.	None
ISCSP(1)	=	Species number for those species to be screened ≤ 40 .	None
EPSCR(1)	=	Relative retention criterion for each species to be screened. Defined as the maximum change in mass fraction relative to production or destruction of the species per unit normalized length for all reactions involving the corresponding species ≤ 40 .	None
ISCBUG	=	1, provides intermediate output during the reaction screening procedure.	None

Area Defined Option Input

Area Defined Calculation With Mass, Energy or Momentum Addition:

ITAREA	=	Input maximum number of iterations for area ratio calculation. A nonzero value for ITAREA triggers the area ratio iteration logic. After maximum iterations, the program outputs an error message, accepts the most recent values, and continues.
ABAR(1)	=	Area ratio table (A/A_0).
XARTAB(1)	=	Normalized axial coordinates for the input area ratio table.
DABARX(1)	=	Derivative with respect to normalized axial distance of the input area ratio table (if input derivative option used).
NPATAB	=	Number of entries in area ratio table ≤ 40 .
ICALDA	=	0 derivative of area ratio table controlled by JPFLAG.
	=	1, 2, 3, 4 replaces JPFLAG control for area ratio table ONLY.
AREPS	=	Relative convergence criterion for area ratio iteration.

Single Species Condensation Option

Condensation calculations require the use of both the mass, momentum, and energy addition option and the area-defined streamtube option. The pertinent parameters for these options are included below:

*IADDF	= 1	Addition function option will be utilized.
*IADDOP	= 3	Single species condensation routines will provide addition functions.
*ITAREA	=	Maximum number of iterations for area ratio calculation.
*XARTAB(1)	=	Normalized axial coordinate for input area ratio table.
*ABAR(1)	=	Area ratio table (A/A_0).

*Values for these variables are calculated internally when operated in automatic mode (KMØDE = 0) and need not be input.

*NPATAB = Number of entries in area ratio table ≤ 40 .
 *DABARX (1) = Derivative with respect to normalized axial distance of input area ratio table (if input derivative option used).
 AREPS = Relative convergence criterion for area ratio iteration.
 *NØCHEM = 1 Frozen chemistry option is utilized.
 ICØND = Number signifying the location of condensing species with respect to the species input order.

The following inputs describe the vapor/liquid properties. A preliminary set of constants for water is stored internally and will be used if the following inputs are ignored. If improved values for water are available or if a different condensing species is being considered, some or all of the following may be input:

TLIM = Limiting temperature for saturated vapor test. State of condensible vapor will not be tested above TLIM (units = °R).
 EJMIN = Threshold value for nucleation rate below which condensation effects will not be computed (units = 1/ft³-sec).
 ETA = Condensation (or sticking) coefficient for water vapor/liquid.
 PCØNST (I) = Array of constants utilized in describing vapor state (see subroutine VAPØR).
 PCØNST (1) = C₁ (atm)
 PCØNST (2) = C₂ (atm - °R)
 PCØNST (3) = C₃ (atm - (°R)²)
 PCØNST (4) = C₄ (1/°R)
 PCØNST (5) = C₅ (1/°R)
 PCØNST (6) = C₆ (1/°R)
 PCØNST (7) = C₇ (°R)
 PCØNST (8) = C₈ (-)

*Values for these variables are calculated internally when operated in automatic mode (KMØDE = 0) and need not be input.

PCØNST (9)	=	Triple point pressure (poundal/ft ²)
PCØNST (10)	=	Triple point temperature (°R)
DCØNST (I)	=	Array of constants utilized in describing liquid droplet properties (see Subroutine DRØPS)
DCØNST (1)	=	A ₁ (BTU/lb)
DCØNST (2)	=	A ₂ (BTU/lb)-°R)
DCØNST (3)	=	A ₃ (BTU/lb)-°R ²)
DCØNST (4)	=	A ₄ (lb/ft ³)
DCØNST (5)	=	A ₅ (lb/ft ³) - °R)
DCØNST (6)	=	A ₆ (lb/ft ³ - °R ²)
DCØNST (7)	=	A ₇ (BTU/lb)
DCØNST (8)	=	A ₈ (BTU/lb - °R)
DCØNST (9)	=	A ₉ (lb/ft ³)
DCØNST (10)	=	A ₁₀ (lb/ft ³ - °R)
DCØNST (11)	=	A ₁₁ (Poundal/ft)
DCØNST (12)	=	A ₁₂ (Poundal/ft - °R)
DCØNST (13)	=	Condensed phase heat capacity (BTU/lb - °R)

C. 7 SAMPLE CASES

A sample case illustrating the abilities of the KINCON program as a subprogram to CONTAM has been presented in the program description of CONTAM, Section 7.0. In this mode, the KINCON program analyzes the nonequilibrium chemical kinetics and condensation of plume species for prediction of contamination effects on bodies submerged in bipropellant plumes. Several additional KINCON program options are available when run in the manual mode as an independent program. Sample cases are included in this appendix to illustrate these options.

a. Reaction-Rate Screening Case

Computer input card listing and selected output for the rate screening of pure-air chemistry system are presented in Tables C-III through C-V.

The original system consists of a set of 14 species and 37 reactions as presented in the card-image listing in Table C-III. The complete reaction set is utilized on the first calculation pass. Those reactions which must be retained to satisfy the input criteria for each species screened are determined. A second pass recomputes the case using the edited reaction set and provides a summary page comparing both results.

Output for a rate-screening case differs from a standard kinetics run only by the addition of intermediate reaction-rate printout for each screened species at each output station and a summary page comparing the results of the original and edited reaction sets. Table C-IV contains the reaction rate output for screened species E-(electron) at axial position 20.0. A similar page is output for each remaining screened species. The summary page is included in Table C-V.

b. Oblique Shock Case

Card image listing for an oblique shock calculation in air is included in Table C-VI. A discontinuity in the input pressure table identifies the shock location as shown in pressure table output, Table C-VII. Results of the shock calculation are presented in Table C-VIII. The output for the integration to and from the shock is the same as the standard kinetics output and has been omitted.

c. Normal Shock-Stagnation Streamline Case

Card-image listing for a normal shock stagnation streamline calculation in air is included in Table C-IX. The streamline downstream of the normal shock is defined through an input velocity distribution table. Velocity table is output as shown in Table C-X. The normal shock calculation output is included in Table C-XI. The remaining output for this case is of the same format as the standard kinetics run and has been omitted.

d. Automated Kinetics and Condensation Case

The following sample case was completed to illustrate the operation of the KINCON subprogram in the automatic mode including both kinetics and water vapor condensation passes in a single case. The test case corresponds to a streamline bounding 90% of the total mass flow for a typical MMH/NTO engine. The initial streamtube temperature was purposely reduced from the original combustion chamber value to ensure condensation within the region of interest.

A card-image listing of the case is shown in Table C-XII. The streamline conditions (initial pressure, temperature, and velocity) including the pressure distribution were obtained from the output of the MULTRAN subprogram and are presented in Table C-XIII. Printout of the input data and the pressure distribution table were omitted since that information is available in Tables C-XII and C-XIII. The initial streamline conditions for the kinetics pass are presented in Table C-XIV.

Table C-III. CARD LISTING FOR RATE-SCREENING CASE

PURE AIR SCREENING		PROGRAM SCREEN	
SPECIES			
O2	1.765500E		
O2	0.227936E		
O2	4.037183E-4		
O2	1.418422E-4		
O2	1.100173E-7		
O2	3.921925E-7		
O2	2.260473E-11		
O2	1.867942E-1		
O2	7.175542E-12		
O2	1.002474E-7		
O2	7.536630E-9		
O2	1.00075E-10		
O2	4.275525E-6		
O2	9.99519E-11		
REACTIONS			
O2 = O + O	A = 1.1E+17, B = 1.2, H = 0.0		
N2 = N + N	A = 1.5E+17, B = 1.2, H = 0.0		
NO = N + O	A = 4.0E+14, B = 0.0, H = 0.0		
NO2 = NO + O	A = 1.5E+15, B = 1.0, H = -1.79		
NO = NO + O	A = 5.67E+20, B = 2.5, H = 0.0		
O3 = O + O2	A = 1.0E+19, B = 2.0, H = 0.0	I = ALL	12.49
O2 = O2 + E	A = 3.5E+10, B = 0.0, H = 0.0		14.24
O = O + E	A = 3.0E+10, B = 0.0, H = 0.0		15.23
NO2 = NO2 + E	A = 1.45E+10, B = 0.0, H = 0.0	NAME2 (NO2 REM)	16.77
NO2 = NO + O	A = 3.0E+14, B = 0.0, H = 2.0		17.151
END TBR REAA			
NO + O = O2 + E	A = 1.0E+14, B = -1.5, H = 5.94		1 4
N2 + O = NO + N	A = 1.3E+14, B = 0.0, H = 0.0		12 5
N2 + O2 = NO + NO	A = 5.0E+10, B = 0.0, H = 79.5		20 6
NO + NO = N2O + O	A = 1.2E+14, B = 0.0, H = 27.0		21 51
NO + NO = N + NO2	A = 3.0E+12, B = 0.0, H = 0.0		22 52
NO + O2 = O + NO2	A = 1.0E+10, B = 0.0, H = 1.15		23 56
O2 + O2 = O + O3	A = 2.15E+14, B = 0.0, H = 5.44		24 54
NO + O2 = N + NO2	A = 3.0E+11, B = 0.0, H = 1.0		25 55
NO2 + O2 = NO + O3	A = 4.5E+11, B = 0.0, H = 2.37		26 57
NO3 + O2 = O2 + O3	A = 4.2E+10, B = 0.0, H = 0.0		27 139
N2 + O2 = N2 + O	A = 3.0E+17, B = 0.0, H = 24.0		28 50
N2O + O = N + NO2	A = 4.0E+10, B = 0.0, H = 0.0		29 53
N2 + NO = N2O + O	A = 1.2E+0, B = 0.0, H = 0.0		30 141
O2 + E = O + O	A = 4.4E+13, B = 0.0, H = 0.0		31 70
O3 + E = O + O2	A = 4.0E+3, B = -0.53, H = 9.36		32 79
O3 + E = O2 + O	A = 1.0E+14, B = 0.0, H = 0.0		33 40
N2O + E = O + NO2	A = 6.0E+0, B = 0.0, H = 0.0		34 81
NO2 + E = O + O2	A = 1.0E+14, B = 0.0, H = 0.0		35 159
NO + E = O + O	A = 9.0E+14, B = 0.0, H = 0.0		36 160

Table C-III--Concluded

NO2 + E = O = + A1, A = 9.6E+13, B = 0.0, C = 0.0,	37	142
O2 + O = O2 = + O, A = 4.3E+13, B = 0.0, C = 0.0,	38	142
O2 + NO2 = O2 = + NO2, A = 4.5E+14, B = 0.0, C = 0.0,	39	131
NO2 = O = NO2 + O =, A = 7.2E+14, B = 0.0, C = 0.0,	40	154
N + O = NO + O =, A = 1.44E+21, B = 1.0, C = 0.0,	41	7
NO + O2 = NO + O2 =, A = 3.6E+17, B = 1.0, C = 0.0,	42	129
NO + O = NO + O =, A = 3.4E+17, B = 1.0, C = 0.0,	43	129
NO + NO2 = NO + NO2 =, A = 3.6E+17, B = 1.0, C = 0.0,	44	142
LAST CARD		
PSPROCEL		
NT=5, PTF(1)=5*1.0, ZTR(1)=0.0,10.0,20.0,30.0,1.0E4, Z=0.0, PI=1.0,		
PI = 1.0, PSWA=50.0, PDS=1, EXITS=0.45, IS47L=0.0, VS3200.0, RSTAR=12.0,		
HI=0.1, HMIN=0.1, HMAX=0.0, DEL=0.005, JF=1,		
ISCRF=1, ICSF(1)=4.0,7.6,12.17,14, EPSCP(1)=4*1.0E-2,3*1.0E-2,		
NC3=2, JF=1,		
JCGUX=1,		
SEN		

The water vapor saturation point is reached at station 24.988 as shown in the station output, Table C-XV. Conditions at the saturation point are saved as initial conditions for subsequent condensation calculation pass. An area ratio table is constructed as the integration continues downstream as can be seen by the area ratio printout. Table C-XVI shows the termination of the kinetics pass when the static temperature dropped below 180°R. The condensation calculation pass begins at the saturation point and follows the area ratio table computed during the kinetics pass. Table C-XVII presents this area ratio table plus the first derivative as output at the beginning of the condensation pass. Initial conditions for the condensation pass are included in Table C-XVIII; intermediate printout of pertinent water vapor properties and nucleation rate are also shown. Variables include

PV	=	vapor pressure (atm)
PVS	=	saturated vapor pressure (atm)
PRATIO	=	PV/PVS
RS	=	critical droplet radius (cm)
EJ	=	nucleation rate (1/cm ³ sec)
TS	=	saturated vapor temperature (°R)

As the flow continues to expand to higher degrees of supersaturation, the nucleation rate increases triggering droplet growth (condensation). Tables C-XIX and C-XX present the output at typical locations in the condensing region. These tables illustrate the additional printout in the condensing region (where nucleation rate is greater than threshold value). The

Table C-IV. SAMPLE REACTION-SCREENING OUTPUT

REACTIONS INVOLVING SPECIES E ⁻		AT AXIAL POSITION	2.00000E-61
PRODUCTION		DESTRUCTION	
D(C(I))/DX	REACTION	D(C(I))/DX	REACTION
5.69563475E-21	25	7.53288253E-20	5
5.18730759E-20	9	4.95092844E-14	34
2.19782288E-18	28	6.41667151E-14	24
1.91513964E-17	29		
5.43746279E-17	27		
1.55960595E-15	26		
1.00310791E-14	8		
2.20229032E-14	30		
2.32151000E-14	7		
NET PRODUCTION		5.69021127E-14	
NET DESTRUCTION		1.13676075E-13	

Table C-V. FINAL SUMMARY OUTPUT AFTER SCREENING - RESULTS
OF ORIGINAL AND SCREENED RUNS

VARIABLE	ORIG FINAL COND	SCREENED FINAL COND
VEL	3.80000000E+03	3.80000000E+03
DENS	1.17993504E-05	1.17993504E-05
TEMP	4.70000501E+03	4.70000501E+03
N2	7.60000253E-01	7.60000253E-01
O2	2.25934373E-01	2.25934373E-01
NO	4.04039502E-03	4.04039501E-03
N	5.62376673E-07	5.62376794E-07
U	1.00229198E-02	1.00229198E-02
NO+	3.90949443E-07	3.90950464E-07
U2-	2.80312862E-10	2.80494462E-10
O-	2.03467463E-09	2.03513961E-09
E-	7.05313769E-12	7.05313731E-12
NO2	1.08509134E-06	1.08509778E-06
N2O	1.06161532E-08	1.06141731E-08
NO2-	1.02571348E-10	1.02570492E-10
O3	5.70692828E-09	5.70186569E-09
NO3	9.98470043E-11	9.99081900E-11

THE FOLLOWING REACTIONS WERE OMITTED ON THE SCREENED CALCULATION

REACTION	5
REACTION	9
REACTION	10
REACTION	18
REACTION	19
REACTION	20
REACTION	25
REACTION	27
REACTION	28
REACTION	29
REACTION	35

Table C-VI. CARD LISTING FOR OBLIQUE SHOCK CALCULATION IN AIR

```

STERMO
NLCHENR, L151E1,
SEND
BLUNT BODY INVISCID FIELD STREAMTUBE NO. 20
SPECIES MASS FRACTIONS
  02      .781184
  02      .209476
  00      .0
  0      .0
  0      .0
  00+     .0
  F=      .0
  ANGUA   .00934

REACTIONS
N2 = 2*N;
O2 = 2*O;
NC = N + O;
END TBR REAX
NC + O = O2 + N;
N2 + O = NO + N;
N2 + O2 = 2*NO;
N + O = NO + C;
LAST CARD
$PROPEL
Z=0.0, P1=7.2004, T=431.41, V=22500., RSTAR=5, EXITE=.056928, PSCALE=.00694444,
M1=1, E=4, MINEL1, E=4, MAXE1, 0, DELT=0.1, NUS=10, JPELAG=1,
NSHCKK=3,
TCOMB(1)=4500.,
NTH=10,
ZTB(1)=.01, .015,
ZTB(3)=0.0, 0.0, 1.491951, 5.548852, 11.607338, 21.724300, 31.837449, 52.050573,
PTB(1)=9.2004, 5.2004,
PTB(3)=9.2004, 10.96, 147.18, 157.68, 100.42, 117.28, 144.11, 158.45,
EXITE 49.7663,
SEND

```

Table C-VII. PRESSURE TABLE

*****		SHOCK OCCURS AT TABLE ENTRY	3	*****
I	X	P		DP/DX
1	-1.00000000E+00	9.20040000E+00	0.	
2	-5.07000000E-01	9.20040000E+00	0.	
3	0.	9.20040000E+00	0.	
4	0.	1.80960000E+02		-2.26413425E+01
5	1.49196100E+00	1.47180000E+02		-1.11897475E+01
6	6.54885200E+00	1.07680000E+02		-4.62266508E+00
7	1.16073380E+01	1.00420000E+02		6.32600681E+01
8	2.17843020E+01	1.17280000E+02		2.16953827E+00
9	3.18374490E+01	1.44310000E+02		1.35712132E+00
10	5.20605730E+01	1.58450000E+02		6.99199590E-01

FORTTRAN symbols correspond to the symbols used in the analysis in the following manner for primary variables of interest;

RPRIME = r'

XMBAR = \bar{m}

HINT = $\int_0^x \dot{H} dx$

G = g

DHPDX = dh'/dx

DGDx = dg/dx

DRDX = dr/dx

RSTAR = r^{**}

JRATE = J

Table C-VIII. SHOCK CALCULATION

BEGIN SHOCK CALCULATION, AXIAL POSITION = 0.00000

CALCULATED SHOCK CONDITIONS

SHOCK ANGLE (DEG)	1.07112538E+01
DEFLECT ANG (DEG)	8.47695096E+00
P2/P1	1.96687101E+01

PROPERTY	UPSTREAM	DOWNSTREAM
PRESSURE (PSIA)	6.38916258E+02	1.25664586E+00
TEMPERATURE (DEG-R)	4.31411921E+02	1.75017828E+03
DENSITY (LBM/FT3)	3.98120375E+04	1.93016028E+03
MACH NUMBER	2.20478049E+01	1.10106903E+01
FROZEN GAMMA	1.40065148E+00	1.33856013E+00

HPRIME = h'

DHPDT = dh'/dT

XMDOT = \dot{m}

XMOM = \dot{M}

E = \dot{H}

All values of variables printed out under the above symbols are in the internal computing units of poundal, pound mass, BTU, foot, and second.

Table C-X. INPUT VELOCITY DISTRIBUTION TABLE

V E L O C I T Y T A B L E			
1	1,	1,70160000E+03	-3,35797665E+04
2	2,57000000E+03	1,61560000E+03	-3,35603113E+04
3	2,14000000E+03	1,52910000E+03	-3,35603113E+04
4	7,71000000E+03	1,44280000E+03	-3,35408560E+04
5	1,02000000E+02	1,35670000E+03	-3,34924903E+04
6	1,26500000E+02	1,27070000E+03	-3,34435798E+04
7	1,54200000E+02	1,18480000E+03	-3,34241245E+04
8	1,79900000E+02	1,09590000E+03	-3,34144893E+04
9	2,05600000E+02	1,01310000E+03	-3,33630335E+04
10	2,31300000E+02	9,27500000E+02	-3,33073930E+04
11	2,57000000E+02	8,41900000E+02	-3,32484925E+04
12	2,82700000E+02	7,56500000E+02	-3,31906615E+04
13	3,08400000E+02	6,71300000E+02	-3,31422947E+04
14	3,34100000E+02	5,86200000E+02	-3,30739300E+04
15	3,59800000E+02	5,01300000E+02	-3,29766537E+04
16	3,85500000E+02	4,16700000E+02	-3,29182879E+04
17	4,11200000E+02	3,32100000E+02	-3,28415564E+04
18	4,36900000E+02	2,48100000E+02	-3,26264591E+04
19	4,62600000E+02	1,64400000E+02	-3,16881323E+04
20	4,88300000E+02	8,41950000E+01	-3,19044356E+04
21	5,14000000E+02	0,	-3,27407004E+04

Table C-XI. SAMPLE OUTPUT FOR NORMAL SHOCK CALCULATION

NORMAL SHOCK CALCULATION - REFINED STEP		
CALCULATED SHOCK CONDITIONS		
PROPERTY	REFINED STEP	REFINED STEP
$M_1 = 5.000000$ (GIVEN)	$5.000000E+00$	$5.000000E+00$
$M_2 = 1.577730$ (FROM M_1)	$1.577730E+00$	$1.577730E+00$
$P_2/P_1 = 5.750000$ (FROM M_1)	$5.750000E+00$	$5.750000E+00$

Reproduced from
best available copy.

Table C-XII. KINCON SAMPLE CASE-DATA LISTING

```

STATION 8
AUTOMATED KINCON TEST CASE
SUCCESS MASS FRACTIONS
CO2 .0452
H2O .2738
O2 .2017
H2 .020
N2 .42509761
NO .002
OH .00967
O2 .000764
C 1.69E-11
H .00115
N 1.39E-6
O .000617

REACTIONS
O2 = 2*O, A=3.3E17, N=1.0, B=0.0, REACTION 1
N2 = 2*N, A=9.6E17, N=1.0, B=0.0, REACTION 2
NO = N + O, A=7.2E15, N=0.5, B=0.0, REACTION 3
H2 = 2*H, A=5.0E18, N=1.0, B=0.0, REACTION 4
H2O = H + OH, A=1.17E17, N=0.0, B=0.0, REACTION 5
OH = H + O, A=2.3E16, N=0.0, B=0.0, REACTION 6
CO2 = CO + O, A=5.1E15, N=0.0, B=3.5A, REACTION 7
CO = C + O, A=6.0E8, N=0.0, B=50., REACTION 8
END TBR REAX
NO + O = O2 + N, A=3.0E11, N=0.5, B=7.13, REACTION 9
NO + N = N2 + O, A=9.0E13, N=0.0, B=75.5, REACTION 10
N2 + O2 = 2*NO, A=1.0E13, N=0.0, B=79.48A, REACTION 11
CO + O2 = CO2 + O, A=1.9E13, N=0.0, B=54.15, REACTION 12
CC + N = C + NO, A=1.3E10, N=0.5, B=0.5, REACTION 13
CO + O = C + O2, A=2.4E13, N=0.0, B=1.99, REACTION 14
CC + H = C + OH, A=1.2E14, N=0.0, B=25.83, REACTION 15
CO2 + H = CO + OH, A=9.6E11, N=0.0, B=1.08, REACTION 16
OH + O = H + O2, A=2.24E14, N=0.0, B=16.8, REACTION 17
OH + H2 = H2O + H, A=8.41E13, N=0.0, B=20.1, REACTION 18
2*OH = H2O + O, A=9.75E13, N=0.0, B=18.7, REACTION 19
H2 + O = OH + H, A=7.33E12, N=0.0, B=0.0, REACTION 20
H2 + O2 = 2*OH, A=4.98E23, N=2.5, B=85.7, REACTION 21
NO + CO = CO2 + N, A=1.0E13, N=0.0, B=9.93, REACTION 22
NO + H = OH + N, A=3.4E13, N=0.0, B=1.38, REACTION 23
CC + CO = CO2 + C, A=1.0E13, N=0.0, B=9.93, REACTION 24

AST CARD
SPROPEL
RSTAR=0.0972, JPFLAG=1, DEL=.01, ND3=10, W1=.0001, WMIN=.0001, HMAX=1.0,
TCOND(1)=12*0., T=2500.,
AREPS=.001, ETA=0.1, TCOND(1)=12*0., IDCOND=2,
SEND

```

Table C-XIII. STREAMLINE GENERATION PROGRAM

CP TIME = 33,799

PP TIME = 192,713

~~STREAMLINE(1) = 98.00000 PERCENT OF THE TOTAL MASS FLOW~~
~~ZINIT = 0.000000 (NONDIMENSIONAL * S/RC)~~
~~PINIT = 67.524369 (PSIA)~~
~~TINIT = 5453.270529 (DEG. R)~~
~~VINIT = 2587.734814 (FT/SEC)~~
~~ZFINAL = 44.569804 (NONDIMENSIONAL * Z/RC)~~
~~NOKSK = 78 (NO. OF PRESSURE TABLE POINTS)~~

POINT NO.	AXIAL DISTANCE (Z/RC)	RADIAL DISTANCE (R/RC)	STREAMLINE DISTANCE (S/RC)	PRESSURE (PSIA)
1	6.237351E+01	1.010896E+00	0.	6.752437E+01
2	5.613616E+01	9.992094E+01	6.345886E+02	6.550104E+01
3	4.989881E+01	9.884265E+01	1.247576E+01	6.466242E+01
4	4.366146E+01	9.792893E+01	1.897968E+01	6.246165E+01
5	3.742411E+01	9.713276E+01	2.526764E+01	6.019785E+01
6	3.118675E+01	9.645190E+01	3.154204E+01	5.839127E+01
7	2.494940E+01	9.589293E+01	3.780439E+01	5.614706E+01
8	1.871205E+01	9.545219E+01	4.405729E+01	5.386846E+01
9	1.247470E+01	9.512855E+01	5.030288E+01	5.155861E+01
10	6.237351E+02	9.492547E+01	5.654367E+01	4.951774E+01
11	3.552714E+15	9.484006E+01	6.278160E+01	4.715078E+01
12	6.237351E+02	9.487171E+01	6.901903E+01	4.478359E+01
13	1.247470E+01	9.502609E+01	7.525830E+01	4.274839E+01
14	1.871205E+01	9.529274E+01	8.150134E+01	4.038052E+01
15	2.494940E+01	9.567407E+01	8.775046E+01	3.804044E+01
16	3.118675E+01	9.617624E+01	9.400784E+01	3.573715E+01
17	3.742411E+01	9.680336E+01	1.002766E+00	3.374438E+01
18	4.366146E+01	9.753766E+01	1.065571E+00	3.152130E+01
19	4.989881E+01	9.838889E+01	1.128522E+00	2.935697E+01
20	5.613616E+01	9.935746E+01	1.191643E+00	2.726202E+01
21	6.237351E+01	1.003425E+00	1.255478E+00	2.448532E+01
22	6.681853E+01	1.006635E+00	1.299366E+00	2.406621E+01
23	8.230535E+01	1.047388E+00	1.459507E+00	1.980347E+01
24	8.840405E+01	1.063762E+00	1.522653E+00	1.899437E+01
25	9.959586E+01	1.095271E+00	1.638922E+00	1.758742E+01
26	1.109730E+00	1.126632E+00	1.756937E+00	1.667694E+01
27	1.226214E+00	1.158689E+00	1.877752E+00	1.572458E+01
28	1.345742E+00	1.191324E+00	2.001655E+00	1.479170E+01
29	1.468845E+00	1.224672E+00	2.129195E+00	1.386588E+01
30	1.596016E+00	1.258866E+00	2.260882E+00	1.295506E+01
31	1.727683E+00	1.294023E+00	2.397162E+00	1.206744E+01
32	1.864462E+00	1.330303E+00	2.538672E+00	1.120840E+01
33	2.007078E+00	1.367891E+00	2.686158E+00	1.037866E+01

Table C-XIII--Concluded

34	2,156435E+00	1,407000E+00	2,840550E+00	9,581216E+00
35	2,313262E+00	1,447797E+00	3,002596E+00	8,816376E+00
36	2,478760E+00	1,490560E+00	3,173530E+00	8,084436E+00
37	2,655024E+00	1,535843E+00	3,355528E+00	7,368069E+00
38	2,845226E+00	1,584638E+00	3,551879E+00	6,652436E+00
39	3,048344E+00	1,636619E+00	3,761543E+00	5,974779E+00
40	3,269320E+00	1,693105E+00	3,989624E+00	5,314822E+00
41	3,508983E+00	1,754318E+00	4,236981E+00	4,702522E+00
42	3,773142E+00	1,821724E+00	4,509604E+00	4,121188E+00
43	4,065000E+00	1,896143E+00	4,810801E+00	3,581002E+00
44	4,392306E+00	1,979536E+00	5,148564E+00	3,075581E+00
45	4,761856E+00	2,073639E+00	5,529907E+00	2,610257E+00
46	5,185288E+00	2,181412E+00	5,966838E+00	2,183015E+00
47	5,675233E+00	2,306087E+00	6,472396E+00	1,797046E+00
48	6,251182E+00	2,452654E+00	7,066704E+00	1,451938E+00
49	6,625002E+00	2,547389E+00	7,452340E+00	1,272373E+00
50	7,074635E+00	2,660688E+00	7,916029E+00	1,086394E+00
51	7,815313E+00	2,849148E+00	8,680306E+00	8,667201E-01
52	8,571396E+00	3,041428E+00	9,460456E+00	7,013092E-01
53	9,265366E+00	3,218157E+00	1,017658E+01	5,882468E-01
54	9,975806E+00	3,399777E+00	1,090986E+01	4,941469E-01
55	1,068503E+01	3,581162E+00	1,164192E+01	4,249876E-01
56	1,067373E+01	3,574772E+00	1,165490E+01	4,264300E-01
57	1,076811E+01	3,604541E+00	1,175387E+01	5,163831E-01
58	1,113066E+01	3,702849E+00	1,212951E+01	4,638904E-01
59	1,125574E+01	3,738687E+00	1,225963E+01	4,641027E-01
60	1,142516E+01	3,787626E+00	1,243527E+01	4,589467E-01
61	1,156782E+01	3,829747E+00	1,258472E+01	4,641766E-01
62	1,180306E+01	3,899483E+00	1,283008E+01	4,481104E-01
63	1,207228E+01	3,977769E+00	1,311045E+01	4,302594E-01
64	1,242947E+01	4,074703E+00	1,348056E+01	5,042020E-01
65	1,285652E+01	4,183837E+00	1,392133E+01	4,871803E-01
66	1,314293E+01	4,257693E+00	1,421712E+01	4,860031E-01
67	1,357414E+01	4,370228E+00	1,466277E+01	4,534370E-01
68	1,411218E+01	4,512423E+00	1,521928E+01	4,268618E-01
69	1,478154E+01	4,686822E+00	1,591098E+01	3,980918E-01
70	1,663745E+01	5,120941E+00	1,781699E+01	2,243533E-01
71	1,816543E+01	5,496204E+00	1,939037E+01	1,536901E-01
72	1,906691E+01	5,647968E+00	2,030454E+01	1,482508E-01
73	2,135328E+01	6,248347E+00	2,266842E+01	1,130785E-01
74	2,379229E+01	6,939570E+00	2,520350E+01	4,096669E-02
75	2,684459E+01	8,144826E+00	2,848513E+01	1,523652E-02
76	2,942882E+01	9,186441E+00	3,127138E+01	9,973209E-03
77	3,145359E+01	9,973589E+00	3,344378E+01	7,958811E-03
78	4,158523E+01	1,454961E+01	4,456980E+01	2,352045E-03

Table C-XIV. INITIAL CONDITIONS KINETIC STREAMTUBE CALCULATION AXIAL POSITION = 0.
INPUT NORMALIZING AXIAL SCALE FACTOR (FT) 8.10000E-03

FLOW PROPERTIES				KINETIC COUPLING TERMS			
WASH NUMBER	0.00000000E+00	COUPLING TERM A	0.00000000E+00	COUPLING TERM B	-2.00000000E+00		
PRESSURE (PSIA)	0.75843600E+01						
VELOCITY (FT/SEC)	2.50773400E+00						
TEMPERATURE (K)	0.00000000E+00	INTERACTION PARAMETERS					
DENSITY (LB/FT ³)	4.95011000E-02						
ENTHALPY-H ₂ (BTU/LB)	0.10422100E+02	CURRENT STEP SIZE	1.00000000E+04				
GAS-MOLE-FRACTION	0.00000000E+00	PERCENT CHANGE	0.00000000E+00				
HEAT CAPACITY (BTU/LB-DEG)	4.98487710E-01	1.0 = SUMMATION C(1)	-1.00000000E+11				
PROGEN GAMMA	1.30000000E+00	MAXIMUM RELATIVE ERROR	0.00000000E+00				
GAS-TEMPERATURE (K)	0.00000000E+00	GOVERNING EQUATION	0.00000000E+00				
SUM C(1)*H(1) (FT ² /SEC)	-3.10439960E+07						
CHEMICAL COMPOSITION							
NO.	SPECIES	MASS FRACTION	MOLE FRACTION	MOLEC/CC	NO.	SPECIES	MASS FRACTION
							MOLE FRACTION
1	O ₂	0.000000E+00	0.000000E+00	7.07010E+17	2	H ₂ O	0.000000E+01
3	CO	0.000000E+00	0.000000E+00	3.44000E+18	4	HS	0.000000E+02
5	N ₂	0.000000E+00	0.000000E+00	7.25000E+18	6	NO	0.000000E+03
7	OH	0.000000E+00	0.000000E+00	2.71000E+17	8	O ₂	0.000000E+04
9	C	0.000000E+00	0.000000E+00	4.72300E+18	10	H	0.000000E+03
11	N	0.000000E+00	0.000000E+00	4.74100E+13	12	O	0.000000E+04

Table C-XV. KINETIC STREAMTUBE CONDITIONS AXIAL POSITION 2.41693E+01

FLOW PROPERTIES		KINETIC COUPLING TERMS							
MACH NUMBER	5.7408214E+00	COUPLING TERM A	7.660971895E+00						
PRESSURE (PSIA)	6.78062174E+02	COUPLING TERM B	-7.81593792E+06						
VELOCITY (FT/SEC)	7.44408137E+03	INTEGRATION PARAMETERS							
TEMPERATURE (DEG-R)	4.07065590E+02	CURRENT STEP SIZE							
DENSITY (LB/FT3)	2.33488281E+04	PERCENT ENTHALPY CHANGE							
ENTHALPY-H0 (BTU/LB)	-1.78964723E+01	1.0 = SUMMATION C(I)							
GAS MOLECULAR WEIGHT	1.98930856E+01	MAXIMUM RELATIVE ERROR							
HEAT CAPACITY(BTU/LB-DEGR)	3.66045862E+01	GOVERNING EQUATION							
FROZEN GAMMA	1.37535284E+00								
GAS CONDUCTIVITY(FT2/SEC-R)	2.49942170E+03								
SUM C(I)*W(I) (FT2/SEC2)	-5.47937080E+07								
CHEMICAL COMPOSITION									
NO.	SPECIES	MASS FRACTION	MOLE FRACTION	MOLEC/CC	NO.	SPECIES	MASS FRACTION	MOLE FRACTION	MOLEC/CC
1	CO2	7.116331E+02	3.216600E+02	4.0189E+15	2	H2O	2.827214E+01	3.121782E+01	3.9004E+16
3	CO	1.0779046E+01	1.408496E+01	1.7561E+16	4	H2	1.999614E+02	1.973140E+01	2.4653E+16
5	N2	4.250984E+01	3.018460E+01	3.7713E+16	6	NO	2.001244E+03	1.326677E+03	1.6576E+14
7	OH	1.748476E+06	2.045071E+06	2.5551E+11	8	C2	3.837964E+04	2.385905E+04	2.9810E+13
9	C	4.028950E+12	6.674861E+12	8.3393E+05	10	H	7.285474E+04	1.437A03E+02	1.7964E+15
11	N	1.076187E+08	2.664416E+08	3.3290E+09	12	O	7.349727E+07	9.138047E+07	1.1417E+11
SATURATION POINT H2O AT Z = 2.4988500E+01									
P = 4.9890143E+02				T = 4.5431785E+02		V = 7.4871328E+03			
Z = 2.4988500E+01				AREA RATIO =		1.000000E+00			
Z = 2.5193300E+01				AREA RATIO =		1.0577367E+00			
Z = 2.5304500E+01				AREA RATIO =		1.1238470E+00			
Z = 2.5602900E+01				AREA RATIO =		1.1971106E+00			
STEP SIZE HALVED AT Z = 2.56029000E+01									

Table C-XVI. KINETIC STREAMTUBE CONDITIONS AXIAL POSITION 3.52285E+01

FLOW PROPERTIES				KINETIC COUPLING TERMS					
HIGH NUMBER				COUPLING TERM A					
PRESSURE (PSIA)				COUPLING TERM B					
VELOCITY (FT/SEC)				INTEGRATION PARAMETERS					
TEMPERATURE (DEG-R)				CURRENT STEP SIZE					
DENSITY (LB/FT3)				PERCENT ENTHALPY CHANGE					
ENTHALPY-HO (BTU/LB)				1.0 - SUMMATION C(I)					
GAS MOLECULAR WEIGHT				MAXIMUM RELATIVE ERROR					
HEAT CAPACITY(BTU/LB-DEGR)				GOVERNING EQUATION					
PROZEN GAMMA									
GAS CONST+FT2/SEC2-DEG-R)									
SUM C(I)*H(I) (FT2/SEC2)									
CHEMICAL COMPOSITION									
NO.	SPECIES	MASS FRACTION	MOLE FRACTION	MOLEC/CC	NO.	SPECIES	MASS FRACTION	MOLE FRACTION	MOLEC/CC
1	CO2	7.116333E-02	3.216602E-02	9.13960E+14	2	H2O	2.827214E-01	3.121783E-01	9.1197E+15
3	CO	1.878046E-01	1.408486E-01	4.1036E+15	4	H2	1.999619E-02	1.973145E-01	5.7638E+15
5	N2	4.250984E-01	3.018461E-01	8.8172E+15	6	NO	2.001243E-03	1.326677E-03	3.8754E+13
7	OH	1.636699E-06	1.914335E-06	5.9920E+10	8	O2	3.837965E-04	2.385906E-04	6.9695E+12
9	C	4.828744E-12	6.624384E-12	1.9496E+05	10	H	7.285886E-04	1.4373727E-02	4.1997E+14
11	N	1.869501E-08	2.624922E-08	7.7553E+08	12	O	8.333111E-07	1.036071E-06	3.0265E+10
TEMPERATURE 176.204 IS OUTSIDE THERMAL TABLES									
Za	3.6847700E+01	AREA RATIO=	6.9523233E+00						
Za	3.6866900E+01	AREA RATIO=	7.3103800E+00						
Za	3.7486100E+01	AREA RATIO=	7.7188414E+00						
Za	3.8503300E+01	AREA RATIO=	8.1616624E+00						
Za	3.9324500E+01	AREA RATIO=	8.6731070E+00						
Za	4.0243200E+01	AREA RATIO=	9.2586885E+00						
Za	4.0962900E+01	AREA RATIO=	9.9366756E+00						
Za	4.1782100E+01	AREA RATIO=	1.0732400E+01						

Table C-XVII. AREA RATIO TABLE

1	x	1	DA/PA CALCED
1	2,49895000E+01	1,00000000E+00	0,
2	2,51933000E+01	1,05773674E+00	3,02360939E+01
3	2,53981000E+01	1,12784784E+00	3,48868291E+01
4	2,56029000E+01	1,19711063E+00	3,75357475E+01
5	2,58077000E+01	1,27759346E+00	4,12841205E+01
6	2,60125000E+01	1,36421039E+00	4,52880593E+01
7	2,62173000E+01	1,46309663E+00	4,93586234E+01
8	2,64221000E+01	1,56438331E+00	5,34413881E+01
9	2,66269000E+01	1,66199256E+00	5,74269561E+01
10	2,68317000E+01	1,80360412E+00	6,11919442E+01
11	2,70365000E+01	1,93263476E+00	6,46070464E+01
12	2,72413000E+01	2,06423459E+00	6,75455096E+01
13	2,74461000E+01	2,20930117E+00	6,98907936E+01
14	2,76509000E+01	2,35450728E+00	7,15425464E+01
15	2,78557000E+01	2,50233944E+00	7,24198945E+01
16	2,80605000E+01	2,65113916E+00	7,24603912E+01
17	2,82653000E+01	2,79913720E+00	7,16138891E+01
18	2,84701000E+01	2,94446965E+00	7,12483409E+01
19	2,87261000E+01	3,12754171E+00	7,43507550E+01
20	2,89421000E+01	3,32514552E+00	7,96910279E+01
21	2,92893000E+01	3,57434158E+00	8,32199993E+01
22	2,95965000E+01	3,83644914E+00	8,48097857E+01

Table C-XVII—Concluded

23	2,99037000E+01	4,09743291E+00	8,37479712E+01
24	3,02100000E+01	4,35099667E+00	8,80741677E+01
25	3,05181000E+01	4,58940859E+00	7,27663481E+01
26	3,09277000E+01	4,87258586E+00	6,17132385E+01
27	3,14397000E+01	5,15815788E+00	5,32842647E+01
28	3,19517000E+01	5,41739749E+00	4,85100428E+01
29	3,25661000E+01	5,70457492E+00	4,17098491E+01
30	3,33853000E+01	6,01534988E+00	3,44497609E+01
31	3,44093000E+01	6,33955291E+00	3,51928117E+01
32	3,60477000E+01	6,95232330E+00	3,95030554E+01
33	3,48649000E+01	7,31038888E+00	4,62962691E+01
34	3,76861000E+01	7,71084136E+00	5,19581533E+01
35	3,85053000E+01	8,16166239E+00	5,87320313E+01
36	3,93245000E+01	8,67318696E+00	6,69575694E+01
37	4,01437000E+01	9,25869520E+00	7,71221106E+01
38	4,09629000E+01	9,93667562E+00	8,99477990E+01
39	4,17821000E+01	1,07323999E+01	9,71343169E+01

Table C-XVIII. INITIAL CONDITIONS KINETIC STREAMTUBE CALCULATION AXIAL POSITION = 2.4985E+01 INPUT NORMALIZING AXIAL SCALE FACTOR (FT) 8.10000E-03

FLOW PROPERTIES				KINETIC COUPLING TERMS					
MACH NUMBER				COUPLING TERM 1					
PRESSURE (PSIA)				COUPLING TERM 0					
VELOCITY (FT/SEC)									
TEMPERATURE (DEG-R)				INTEGRATION PARAMETERS					
DENSITY (LB/FT3)				CURRENT STEP SIZE					
ENTHALPY (BTU/LB)				PERCENT ENTHALPY CHANGE					
GAS MOLECULAR WEIGHT				1.0 - SUMMATION C(I)					
HEAT CAPACITY (BTU/LB-DEGR)				MAXIMUM RELATIVE ERROR					
PROGEN GAMMA				CONVERGING EQUATION					
GAS COMPOSITION (FT2/SEC2)									
SUM C(I)*M(I) (FT2/SEC2)									
CHEMICAL COMPOSITION									
NO.	SPECIES	MASS FRACTION	MOLE FRACTION	MOLEC/CC	NO.	SPECIES	MASS FRACTION	MOLE FRACTION	MOLEC/CC
1	COR	7.110331E-02	3.210601E-02	3.1793E+15	2	H2O	2.027214E+01	3.121702E+01	3.0017E+10
3	CO	1.070044E-01	1.408400E-01	1.3035E+16	4	H2	1.000610E+00	1.000445E+01	1.0000E+10
5	H2	4.250904E-01	3.010461E-01	2.0797E+16	6	NO	2.001243E+03	1.326077E+03	1.3097E+10
7	OH	1.720320E-06	2.021497E-06	1.9990E+11	8	O2	3.037064E+04	2.309009E+04	2.3593E+13
9	C	4.000000E-03	6.074431E-13	4.0000E+08	10	H	3.000000E+04	1.437301E+00	1.4103E+15
11	N	1.074230E-00	2.001670E-00	2.0275E+00	12	O	7.512097E+07	9.340099E+07	9.2212E+10
MOR = 0.				AREA RATIO = 1.00000E+00					
Z = 2.498500E+01				PVS = 1.0002130E+03				PRATIO = 1.1461902E+00	
IYACT = 0				RNO = 9.9025604E-07				EJO = 0.	
Z = 2.498500E+01				PVS = 1.0002177E+03				PRATIO = 1.1461960E+00	
IYACT = 0				RNO = 9.9021973E-07				EJO = 0.	
Z = 2.498500E+01				PVS = 1.0002133E+03				PRATIO = 1.1462139E+00	
IYACT = 0				RNO = 9.9000740E-07				EJO = 0.	
Z = 2.498500E+01				PVS = 1.0002000E+03				PRATIO = 1.1462402E+00	
IYACT = 0				RNO = 9.9700000E-07				EJO = 0.	
Z = 2.498500E+01				PVS = 1.0001000E+03				PRATIO = 1.1463302E+00	
IYACT = 0				RNO = 9.9731904E-07				EJO = 0.	
Z = 2.498500E+01				PVS = 1.0001023E+03				PRATIO = 1.1464742E+00	
IYACT = 0				RNO = 9.9640001E-07				EJO = 0.	

Table G-XIX. KINETIC STREAMTUBE CONDITIONS AXIAL POSITION 2.70052E+01

FLOW PROPERTIES									
KINETIC COUPLING TERMS									
MACM NUMBER									
PRESSURE (PSIA)									
VELOCITY (FT/SEC)									
TEMPERATURE (K)									
DENSITY (LB/FT ³)									
ENTHALPY (BTU/LB)									
GAS MOLECULAR WEIGHT									
HEAT CAPACITY (BTU/LB-DEGR)									
FROZEN GAMMA									
GAS CONDUCTIVITY (BTU/FT-SEC)									
SUM C(1)M(1) (1/2/SEC ²)									
CHEMICAL COMPOSITION									
NO. SPECIES MASS FRACTION MOLE FRACTION MOLEC/CC									
1 CO2 7.110430E+02 3.210694E+02 1.3315E+15 2 H2O 2.027104E+01 3.121007E+01 1.2922E+16									
3 CO 1.070070E+01 1.405510E+01 5.0101E+15 4 H2 1.000045E+02 1.978174E+01 0.1679E+19									
5 N2 4.251040E+01 3.010511E+01 1.2495E+16 6 NO 2.001274E+03 1.326599E+03 5.4910E+13									
7 OH 1.720346E+00 2.021531E+00 8.3001E+10 8 O2 3.850022E+04 2.305945E+04 9.8765E+12									
9 C 4.020026E+12 6.474832E+12 2.7620E+05 10 H 7.200470E+04 1.437005E+02 5.9517E+14									
11 N 1.074207E+00 2.601723E+00 1.1010E+09 12 O 7.513071E+07 9.341151E+07 3.8667E+10									
MORPH = 0.152007E+05 MORPH=1 = 9.99995E+01 AREA RATIO = 1.00004E+00									
Z = 2.7007250E+01 PVS = 3.4550150E+04 PVS = 0.0252110E+07 PRATIO = 4.000044E+02 TERM1 = 9.9241550E+21									
TERM2 = 2.700520E+01 DELZ = 2.000000E+03 RPRINT = 1.460714E+12 MINI = 1.060324E+01 S = 1.520000E+05									
BB = 1.0210070E+13 DMOD = 0.000000E+00 DEBY = 0.000000E+00 DEBY = 0.000000E+00 TERM2 = 1.520000E+05									
BB = 1.7871034E+20 RSTAN = 9.8331763E+10 J RATE = 4.6754794E+22 J RATE = 4.6754794E+22 TERM3 = 1.7871034E+20									
DMODT = -1.3965942E+04 TRAC = 9.9997633E+01 E = 0.3030054E+01 TERM4 = -1.7490037E+08									
XMDO7 = -1.1004737E+04 XMOD = -0.0341514E+01 E = 0.3030054E+01									
Z = 2.7007250E+01 PVS = 3.4550150E+04 PVS = 0.0252110E+07 PRATIO = 4.000044E+02 TERM5 = 9.9241550E+21									
TERM6 = 1.0210070E+13 DELZ = 2.000000E+03 RPRINT = 1.460714E+12 MINI = 1.060324E+01 S = 1.520000E+05									
Z = 2.7007250E+01 PVS = 3.4517047E+04 PVS = 0.0252110E+07 PRATIO = 4.0010707E+02 TERM6 = 1.520000E+05									
TERM7 = 1.0210070E+13 DMOD = 0.000000E+00 DEBY = 0.000000E+00 DEBY = 0.000000E+00 TERM7 = 1.7871034E+20									
Z = 2.7011250E+01 PVS = 3.4477620E+04 PVS = 0.0252110E+07 PRATIO = 4.0704408E+02 TERM8 = 9.9241550E+21									
TERM9 = 1.0210070E+13 DELZ = 2.000000E+03 RPRINT = 1.460714E+12 MINI = 1.060324E+01 S = 1.520000E+05									
STEP SIZE VALVED AT Z = 2.7011250E+01									
Z = 2.7007250E+01 PVS = 3.4477620E+04 PVS = 0.0252110E+07 PRATIO = 4.0363704E+02 TERM8 = 9.9241550E+21									
TERM9 = 1.0210070E+13 DMOD = 0.000000E+00 DEBY = 0.000000E+00 DEBY = 0.000000E+00 TERM9 = 1.7871034E+20									
Z = 2.7010250E+01 PVS = 3.4457931E+04 PVS = 0.0252110E+07 PRATIO = 4.0540304E+02 TERM9 = 1.520000E+05									
TERM10 = 1.0210070E+13 DELZ = 2.000000E+03 RPRINT = 1.460714E+12 MINI = 1.060324E+01 S = 1.520000E+05									
Z = 2.7011250E+01 PVS = 3.4437420E+04 PVS = 0.0252110E+07 PRATIO = 4.0710037E+02 TERM10 = 9.9241550E+21									
TERM11 = 1.0210070E+13 DMOD = 0.000000E+00 DEBY = 0.000000E+00 DEBY = 0.000000E+00 TERM11 = 1.7871034E+20									
Z = 2.7011250E+01 PVS = 3.4437420E+04 PVS = 0.0252110E+07 PRATIO = 4.0710037E+02 TERM11 = 1.520000E+05									
TERM12 = 1.0210070E+13 DELZ = 2.000000E+03 RPRINT = 1.460714E+12 MINI = 1.060324E+01 S = 1.520000E+05									
Z = 2.7011250E+01 PVS = 3.4437420E+04 PVS = 0.0252110E+07 PRATIO = 4.0710037E+02 TERM12 = 9.9241550E+21									
TERM13 = 1.0210070E+13 DMOD = 0.000000E+00 DEBY = 0.000000E+00 DEBY = 0.000000E+00 TERM13 = 1.7871034E+20									
Z = 2.7011250E+01 PVS = 3.4437420E+04 PVS = 0.0252110E+07 PRATIO = 4.0710037E+02 TERM13 = 1.520000E+05									
TERM14 = 1.0210070E+13 DELZ = 2.000000E+03 RPRINT = 1.460714E+12 MINI = 1.060324E+01 S = 1.520000E+05									
Z = 2.7011250E+01 PVS = 3.4437420E+04 PVS = 0.0252110E+07 PRATIO = 4.0710037E+02 TERM14 = 9.9241550E+21									
TERM15 = 1.0210070E+13 DMOD = 0.000000E+00 DEBY = 0.000000E+00 DEBY = 0.000000E+00 TERM15 = 1.7871034E+20									
Z = 2.7011250E+01 PVS = 3.4437420E+04 PVS = 0.0252110E+07 PRATIO = 4.0710037E+02 TERM15 = 1.520000E+05									
TERM16 = 1.0210070E+13 DELZ = 2.000000E+03 RPRINT = 1.460714E+12 MINI = 1.060324E+01 S = 1.520000E+05									
Z = 2.7011250E+01 PVS = 3.4437420E+04 PVS = 0.0252110E+07 PRATIO = 4.0710037E+02 TERM16 = 9.9241550E+21									
TERM17 = 1.0210070E+13 DMOD = 0.000000E+00 DEBY = 0.000000E+00 DEBY = 0.000000E+00 TERM17 = 1.7871034E+20									
Z = 2.7011250E+01 PVS = 3.4437420E+04 PVS = 0.0252110E+07 PRATIO = 4.0710037E+02 TERM17 = 1.520000E+05									
TERM18 = 1.0210070E+13 DELZ = 2.000000E+03 RPRINT = 1.460714E+12 MINI = 1.060324E+01 S = 1.520000E+05									
Z = 2.7011250E+01 PVS = 3.4437420E+04 PVS = 0.0252110E+07 PRATIO = 4.0710037E+02 TERM18 = 9.9241550E+21									
TERM19 = 1.0210070E+13 DMOD = 0.000000E+00 DEBY = 0.000000E+00 DEBY = 0.000000E+00 TERM19 = 1.7871034E+20									
Z = 2.7011250E+01 PVS = 3.4437420E+04 PVS = 0.0252110E+07 PRATIO = 4.0710037E+02 TERM19 = 1.520000E+05									
TERM20 = 1.0210070E+13 DELZ = 2.000000E+03 RPRINT = 1.460714E+12 MINI = 1.060324E+01 S = 1.520000E+05									
Z = 2.7011250E+01 PVS = 3.4437420E+04 PVS = 0.0252110E+07 PRATIO = 4.0710037E+02 TERM20 = 9.9241550E+21									
TERM21 = 1.0210070E+13 DMOD = 0.000000E+00 DEBY = 0.000000E+00 DEBY = 0.000000E+00 TERM21 = 1.7871034E+20									
Z = 2.7011250E+01 PVS = 3.4437420E+04 PVS = 0.0252110E+07 PRATIO = 4.0710037E+02 TERM21 = 1.520000E+05									
TERM22 = 1.0210070E+13 DELZ = 2.000000E+03 RPRINT = 1.460714E+12 MINI = 1.060324E+01 S = 1.520000E+05									
Z = 2.7011250E+01 PVS = 3.4437420E+04 PVS = 0.0252110E+07 PRATIO = 4.0710037E+02 TERM22 = 9.9241550E+21									
TERM23 = 1.0210070E+13 DMOD = 0.000000E+00 DEBY = 0.000000E+00 DEBY = 0.000000E+00 TERM23 = 1.7871034E+20									
Z = 2.7011250E+01 PVS = 3.4437420E+04 PVS = 0.0252110E+07 PRATIO = 4.0710037E+02 TERM23 = 1.520000E+05									
TERM24 = 1.0210070E+13 DELZ = 2.000000E+03 RPRINT = 1.460714E+12 MINI = 1.060324E+01 S = 1.520000E+05									
Z = 2.7011250E+01 PVS = 3.4437420E+04 PVS = 0.0252110E+07 PRATIO = 4.0710037E+02 TERM24 = 9.9241550E+21									
TERM25 = 1.0210070E+13 DMOD = 0.000000E+00 DEBY = 0.000000E+00 DEBY = 0.000000E+00 TERM25 = 1.7871034E+20									
Z = 2.7011250E+01 PVS = 3.4437420E+04 PVS = 0.0252110E+07 PRATIO = 4.0710037E+02 TERM25 = 1.520000E+05									
TERM26 = 1.0210070E+13 DELZ = 2.000000E+03 RPRINT = 1.460714E+12 MINI = 1.060324E+01 S = 1.520000E+05									
Z = 2.7011250E+01 PVS = 3.4437420E+04 PVS = 0.0252110E+07 PRATIO = 4.0710037E+02 TERM26 = 9.9241550E+21									
TERM27 = 1.0210070E+13 DMOD = 0.000000E+00 DEBY = 0.000000E+00 DEBY = 0.000000E+00 TERM27 = 1.7871034E+20									
Z = 2.7011250E+01 PVS = 3.4437420E+04 PVS = 0.0252110E+07 PRATIO = 4.0710037E+02 TERM27 = 1.520000E+05									
TERM28 = 1.0210070E+13 DELZ = 2.000000E+03 RPRINT = 1.460714E+12 MINI = 1.060324E+01 S = 1.520000E+05									
Z = 2.7011250E+01 PVS = 3.4437420E+04 PVS = 0.0252110E+07 PRATIO = 4.0710037E+02 TERM28 = 9.9241550E+21									
TERM29 = 1.0210070E+13 DMOD = 0.000000E+00 DEBY = 0.000000E+00 DEBY = 0.000000E+00 TERM29 = 1.7871034E+20									
Z = 2.7011250E+01 PVS = 3.4437420E+04 PVS = 0.0252110E+07 PRATIO = 4.0710037E+02 TERM29 = 1.520000E+05									
TERM30 = 1.0210070E+13 DELZ = 2.000000E+03 RPRINT = 1.460714E+12 MINI = 1.060324E+01 S = 1.520000E+05									
Z = 2.7011250E+01 PVS = 3.4437420E+04 PVS = 0.0252110E+07 PRATIO = 4.0710037E+02 TERM30 = 9.9241550E+21									
TERM31 = 1.0210070E+13 DMOD = 0.000000E+00 DEBY = 0.000000E+00 DEBY = 0.000000E+00 TERM31 = 1.7871034E+20									
Z = 2.7011250E+01 PVS = 3.4437420E+04 PVS = 0.0252110E+07 PRATIO = 4.0710037E+02 TERM31 = 1.520000E+05									
TERM32 = 1.0210070E+13 DELZ = 2.000000E+03 RPRINT = 1.460714E+12 MINI = 1.060324E+01 S = 1.520000E+05									
Z = 2.7011250E+01 PVS = 3.4437420E+04 PVS = 0.0252110E+07 PRATIO = 4.0710037E+02 TERM32 = 9.9241550E+21									
TERM33 = 1.0210070E+13 DMOD = 0.000000E+00 DEBY = 0.000000E+00 DEBY = 0.000000E+00 TERM33 = 1.7871034E+20									
Z = 2.7011250E+01 PVS = 3.4437420E+04 PVS = 0.0252110E+07 PRATIO = 4.0710037E+02 TERM33 = 1.520000E+05									
TERM34 = 1.0210070E+13 DELZ = 2.000000E+03 RPRINT = 1.460714E+12 MINI = 1.060324E+01 S = 1.520000E+05									
Z = 2.7011250E+01 PVS = 3.4437420E+04 PVS = 0.0252110E+07 PRATIO = 4.0710037E+02 TERM34 = 9.9241550E+21									
TERM35 = 1.0210070E+13 DMOD = 0.000000E+00 DEBY = 0.000000E+00 DEBY = 0.000000E+00 TERM35 = 1.7871034E+20									
Z = 2.7011250E+01 PVS = 3.4437420E+04 PVS = 0.0252110E+07 PRATIO = 4.0710037E+02 TERM35 = 1.520000E+05									
TERM36 = 1.0210070E+13 DELZ = 2.000000E+03 RPRINT = 1.460714E+12 MINI = 1.060324E+01 S = 1.520000E+05									
Z = 2.7011250E+01 PVS = 3.4437420E+04 PVS = 0.0252110E+07 PRATIO = 4.0710037E+02 TERM36 = 9.9241550E+21									
TERM37 = 1.0210070E+13 DMOD = 0.000000E+00 DEBY = 0.000000E+00 DEBY = 0.000000E+00 TERM37 = 1.7871034E+20									
Z = 2.7011250E+01 PVS = 3.4437420E+04 PVS = 0.0252110E+07 PRATIO = 4.0710037E+02 TERM37 = 1.520000E+05									
TERM38 = 1.0210070E+13 DELZ = 2.000000E+03 RPRINT = 1.460714E+12 MINI = 1.060324E+01 S = 1.520000E+05									
Z = 2.7011250E+01 PVS = 3.4437420E+04 PVS = 0.0252110E+07 PRATIO = 4.0710037E+02 TERM38 = 9.9241550E+21									
TERM39 = 1.0210070E+13 DMOD = 0.000000E+00 DEBY = 0.000000E+00 DEBY = 0.000000E+00 TERM39 = 1.7871034E+20									
Z = 2.7011250E+01 PVS = 3.4437420E+04 PVS = 0.0252110E+07 PRATIO = 4.0710037E+02 TERM39 = 1.520000E+05									
TERM40 = 1.0210070E+13 DELZ = 2.000000E+03 RPRINT = 1.460714E+12 MINI = 1.060324E+01 S = 1.520000E+05									
Z = 2.7011250E+01 PVS = 3.4437420E+04 PVS = 0.0252110E+07 PRATIO = 4.0710037E+02 TERM40 = 9.9241550E+21									
TERM41 = 1.0210070E+13 DMOD = 0.000000E+00 DEBY = 0.000000E+00 DEBY = 0.000000E+00 TERM41 = 1.7871034E+20									
Z = 2.7011250E+01 PVS = 3.4437420E+04 PVS = 0.0252110E+07 PRATIO = 4.0710037E+02 TERM41 = 1.520000E+05									
TERM42 = 1.0210070E+13 DELZ = 2.000000E+03 RPRINT = 1.460714E+12 MINI = 1.060324E+01 S = 1.520000E+05									
Z = 2.7011250E+01 PVS = 3.4437420E+04 PVS = 0.0252110E+07 PRATIO = 4.0710037E+02 TERM42 = 9.9241550E+21									
TERM43 = 1.0210070E+13 DMOD = 0.000000E+00 DEBY = 0.000000E+00 DEBY = 0.000000E+00 TERM43 = 1.7871034E+20									
Z = 2.7011250E+01 PVS = 3.4437420E+04 PVS = 0.0252110E+07 PRATIO = 4.0710037E+02 TERM43 = 1.520000E+05									
TERM44 = 1.0210070E+13 DELZ = 2.000000E+03 RPRINT = 1.460714E+12 MINI = 1.060324E+01 S = 1.520000E+05									
Z = 2.7011250E+01 PVS = 3.4437420E+04 PVS = 0.0252110E+07 PRATIO = 4.0710037E+02 TERM44 = 9.9241550E+21									
TERM45 = 1.0210070E+13 DMOD = 0.000000E+00 DEBY = 0.000000E+00 DEBY = 0.000000E+00 TERM45 = 1.7871034E+20									
Z = 2.7011250E+01 PVS = 3.4437420E+04 PVS = 0.0252110E+07 PRATIO = 4.0710037E+02 TERM45 = 1.520000E+05									
TERM46 = 1.0210070E+13 DELZ = 2.000000E+03 RPRINT = 1.460714E+12 MINI = 1.060324E+01 S = 1.520000E+05									
Z = 2.7011250E+01 PVS = 3.4437420E+04 PVS = 0.0252110E+07 PRATIO = 4.0710037E+02 TERM46 = 9.9241550E+21									
TERM47 = 1.0210070E+13 DMOD = 0.000000E+00 DEBY = 0.000000E+00 DEBY = 0.000000E+00 TERM47 = 1.7871034E+20									
Z = 2.7011250E+01 PVS = 3.4437420E+04 PVS = 0.0252110E+07 PRATIO = 4.0710037E+02 TERM47 = 1.520000E+05									
TERM48 = 1.0210070E+13 DELZ = 2.000000E+03 RPRINT = 1.460714E+12 MINI = 1.060324E+01 S = 1.520000E+05									
Z = 2.7011250E+01 PVS = 3.4437420E+04 PVS = 0.0252110E+07 PRATIO = 4.0710037E+02 TERM48 = 9.9241550E+21									
TERM49 = 1.0210070E+13 DMOD = 0.000000E+00 DEBY = 0.000000E+00 DEBY = 0.000000E+00 TERM49 = 1.7871034E+20									
Z = 2.7011250E+01 PVS = 3.4437420E+04 PVS = 0.0252110E+07 PRATIO = 4.0710037E+02 TERM49 = 1.520000E+05									
TERM50 = 1.0210070E+13 DELZ = 2.000000E+03 RPRINT = 1.460714E+12 MINI = 1.060324E+01 S = 1.520000E+05									
Z = 2.7011250E+01 PVS = 3.4437420E+04 PVS = 0.0252110E+07 PRATIO = 4.0710037E+02 TERM50 = 9.9241550E+21									
TERM51 = 1.0210070E+13 DMOD = 0.000000E+00 DEBY = 0.000000E+00 DEBY = 0.000000E+00 TERM51 = 1.7871034E+20									
Z = 2.7011250E+01 PVS = 3.4437420E+04 PVS = 0.0252110E+07 PRATIO = 4.0710037E+02 TERM51 = 1.520000E+05									
TERM52 = 1.0210070E+13 DELZ = 2.000000E+03 RPRINT = 1.460714E+12 MINI = 1.060324E+01 S = 1.520000E+05									
Z = 2.7011250E+01 PVS = 3.4437420E+04 PVS = 0.0252110E+07 PRATIO = 4.0710037E+02 TERM52 = 9.9241550E+21									
TERM53 = 1.0210070E+13 DMOD = 0.000000E+00 DEBY = 0.000000E+00 DEBY = 0.000000E+00 TERM53 = 1.7871034E+20									
Z = 2.7011250E+01 PVS = 3.4437420E+04 PVS = 0.0252110E+07 PRATIO = 4.0710037E+02 TERM53 = 1.520000E+05									
TERM54 = 1.0210070E+13 DELZ = 2.000000E+03 RPRINT = 1.460714E+12 MINI = 1.060324E+01 S = 1.520000E+05									
Z = 2.7011250E+01 PVS = 3.4437420E+04 PVS = 0.0252110E+07 PRATIO = 4.0710037E+02 TERM54 = 9.9241550E+21									
TERM55 = 1.0210070E+13 DMOD = 0.000000E+00 DEBY = 0.000000E+00 DEBY = 0.000000E+00 TERM55 = 1.7871034E+20									
Z = 2.7011250E+01 PVS = 3.4437420E+04 PVS = 0.0252110E+07 PRATIO = 4.0710037E+02 TERM55 = 1.520000E+05									
TERM56 = 1.0210070E+13 DELZ = 2.000000E+03 RPRINT = 1.460714E+12 MINI = 1.060324E+01 S = 1.520000E+05									
Z = 2.7011250E+01 PVS = 3.4437420E+04 PVS = 0.0252110E+07 PRATIO = 4.0710037E+02 TERM56 = 9.9241550E+21									
TERM57 = 1.0210070E+13 DMOD = 0.000000E+00 DEBY = 0.000000E+00 DEBY = 0.000000E+00 TERM57 = 1.7871034E+20									
Z = 2.7011250E+01 PVS = 3.4437420E+04 PVS = 0.0252110E+07 PRATIO = 4.0710037E+02 TERM57 = 1.520000E+05									
TERM58 = 1.0210070E+13 DELZ = 2.000000E+03 RPRINT = 1.460714E+12 MINI = 1.060324E+01 S = 1.520000E+05									
Z = 2.7011250E+01 PVS = 3.4437420E+04 PVS = 0.0252110E+07 PRATIO = 4.0710037E+02 TERM58 = 9.9241550E+21									
TERM59 = 1.0210070E+13 DMOD = 0.000000E+00 DEBY = 0.000000E+00 DEBY = 0.000000E+00 TERM59 = 1.7871034E+20									
Z = 2.7011250E+01 PVS = 3.4437420E+04 PVS = 0.0252110E+07 PRATIO = 4.0710037E+02 TERM59 = 1.520000E+05									
TERM60 = 1.0210070E+13 DELZ = 2.000000E+03 RPRINT = 1.460714E+12 MINI = 1.060324E+01 S = 1.520000E+05									
Z = 2.7011250E+01 PVS = 3.4437420E+04 PVS = 0.0252110E+07 PRATIO = 4.0710037E+02 TERM60 = 9.9241550E+21									
TERM61 = 1.0210070E+13 DMOD = 0.000000E+00 DEBY = 0.000000E+00 DEBY = 0.000000E+00 TERM61 = 1.7871034E+20									
Z = 2.7011250E+01 PVS = 3.4437420E+04 PVS = 0.0252110E+07 PRATIO = 4.0710037E+02 TERM61									

Table C-XX. KINETIC STREAMTUBE CONDITIONS AXIAL POSITION 2.90277E+01

FLOW PROPERTIES										KINETIC COUPLING TERMS																													
MACH NUMBER					7.30520003E+00					COUPLING TERM A					0:																								
PRESSURE (PSIA)					6.50610240E+03					COUPLING TERM B					0:																								
VELOCITY (FT/SEC)					7.65220390E+03					INTEGRATION PARAMETERS																													
TEMPERATURE (DEGR)					3.00030010E+03																																		
DENSITY (LB/FT3)					5.91070152E+03																																		
ENTHALPY (BTU/LB)					-0.27515332E+01					CURRENT STEP SIZE					9.00000000E+04																								
GAS MOLECULAR WEIGHT					1.00025023E+01					PERCENT ENTHALPY CHANGE					-2.71502002E+00																								
HEAT CAPACITY (BTU/LB-DEGR)					3.57063000E+01					1.0 = SUMMATION C(1)					-4.23403471E+12																								
FROZEN GAMMA					1.30600720E+00					MAXIMUM RELATIVE ERROR					1.31014552E+03																								
GAS COMPOSITION (DEGR)					3.00000000E+03					GOVERNING EQUATION					3																								
SUM C(1)=C(1) (FT2/SEC2)					-5.62210244E+07																																		
CHEMICAL COMPOSITION																																							
NO. SPECIES					MASS FRACTION					MOLE FRACTION					NO. SPECIES					MASS FRACTION					MOLE FRACTION														
1 CO2					7.131691E+02					3.224260E+02					6.1000E+14					2 H2O					2.011733E+01					3.105300E+01					5.0004E+15				
3 CO					1.003310E+01					1.400046E+01					2.7041E+15					4 H2					2.003031E+02					1.077044E+01					3.7942E+15				
5 N2					4.260159E+01					3.029566E+01					5.0073E+15					6 NO					2.005563E+03					1.320039E+03					2.5525E+13				
7 OH					1.732051E+06					2.026316E+06					3.0392E+10					8 O2					3.046240E+04					2.391592E+04					4.5903E+12				
8 C					4.030003E+12					6.000331E+12					1.2041E+05					10 H					7.301000E+04					1.441200E+02					2.7442E+14				
11 N					1.070304E+00					2.60024E+00					5.1200E+00					12 O					7.520173E+07					9.363262E+07					1.7972E+10				
MBAR = 2.15560E+03					MBAR+1 = 9.97044E+01					AREA RATIO = 3.36225E+00																													
2 TERM2 = 2.0027750E+01					DELZ = 0					5.00000000E+04					RPIME = 4.1365600E+12					TERM1 = 3.4093905E+24																			
3 TERM3 = 2.0000000E+00					XMBAR = 0					-2.155605E+03					MINY = 1.501274E+01					G = 2.155605E+03																			
4 TERM4 = 2.0000000E+00					DMB1 = 0					0.0000000E+00					DOEX = 1.307300E+03					DOEX = 1.307300E+03																			
5 TERM5 = 1.3242010E+21					ASTAR = 0					7.1500377E+10					J RATE = 7.0799803E+23					MBRIME = -1.7472215E+00																			
6 TERM6 = -1.307459E+04					TFAC = 0					9.9063642E+01																													
7 TERM7 = -1.307300E+03					XMON = 0					-1.0460240E+01					E = 0					9.4144203E+00																			

C.8 REFERENCES

- C-1. J. R. Kliegel, and H. M. Frey. One-Dimensional Reacting Gas Nonequilibrium Performance Program. 02874-6003-R000, March, 1967, TRW Systems, Redondo Beach, Calif.
- C-2. J. R. Kliegel, H. M. Frey, G. R. Nickerson, and T. J. Tyson. ICRPG One-Dimensional Kinetic Nozzle Analysis Computer Program. Published by Dynamic Science, under contract NAS7-443, July 1968.
- C-3. H. M. Frey and G. R. Nickerson. SCREEN, A Computer Program for the Screening of Chemically Reacting Gas Mixtures. Published by Dynamic Science under Contract to McDonnell Douglas Astronautics Company, TR-141-1-CS, February, 1970.
- C-4. J. O. Hirschfelder, C. F. Curtiss, and R. B. Bird. Molecular Theory of Gases and Liquids. Wiley, (New York), 1954.
- C-5. S. S. Penner. Chemistry Problems in Jet Propulsion. Pergamon, (New York), 1957.
- C-6. S. W. Benson and T. Fueno. "Mechanism of Atom Recombination by Consecutive Vibrational Deactivations." Journal of Chemical Physics, Vol. 36, 1962, pp 1597-1607.
- C-7. J. Frankel. Kinetic Theory of Liquids. Oxford University Press. (London), 1946.
- C-8. H. G. Stever. Condensation in High-Speed Flows. High-Speed Aerodynamics and Jet Propulsion. Vol. III, Princeton University Press, (Princeton, N. J.), 1958.
- C-9. P. G. Hill. "Condensation of Water Vapor During Supersonic Expansion in Nozzles." Journal of Fluid Mechanics, Vol 25, 1966.
- C-10. T. J. Tyson and J. R. Kliegel. "An-Implicit Integration Procedure for Chemical Kinetics." AIAA 6th Aerospace Sciences Meeting, Paper No. 68-180, January 1968.

Appendix D

SURFACE

**DEPOSITION AND SURFACE EFFECTS
COMPUTER PROGRAM**

CONTENTS

D. 1	INTRODUCTION	533
D. 1. a	Objectives	533
D. 1. b	Data Base	533
D. 1. c	Output	533
D. 1. d	Program Outline/Summary	534
D. 1. e	Program Physical Configuration	534
D. 2	ANALYSIS	535
D. 2. a	Satellite Structure	535
D. 2. b	Projection Configuration	535
D. 2. c	Structural Materials	535
D. 2. d	Optical and Thermal Coefficients for Structural Materials	538
D. 2. e	Physicochemical Properties of Propellants and Deposits	538
D. 2. f	Optical and Thermal Coefficients for Deposits	538
D. 2. g	Other Data	538
D. 2. h	Initial Assignment of Materials	538
D. 2. i	Suppression of Listing	538
D. 2. j	Optical/Thermal Surface Parameters	539
D. 2. k	Effective Values of Heat Transfer Coefficients	539
D. 2. l	Transmission Through Transparent Segments (Windows, Optical Ports)	539
D. 2. m	Test/Precalculated Surface State	539
D. 2. n	Optical/Thermal Surface Parameters and Heat Transfer Coefficients	539
D. 2. o	Reinitialization	540
D. 2. p	Exposure Sequence	540
D. 2. q	Plume Impingement Locations	540
D. 2. r	Space Effects Locations	541
D. 2. s	Transformation of Coordinates (Plume Exposure Only)	541
D. 2. t	Surface Properties	541
D. 2. u	Surface Effects	541
D. 2. v	Abrasion	542
D. 2. w	Condensation	542
D. 2. x	Deposition	543
D. 2. y	Net Effects	543

D. 2. z	Space Exposure Effects	543
D. 2. aa	Recycling/Termination	543
D. 2. ab	Program Operations Information	543
D. 3	PROGRAM FUNCTIONS	544
D. 3. a	Outline	544
D. 3. b	First Principal Overlay (0, 0) – Program TM42	544
D. 3. c	Principal Overlay (0, 0)	546
D. 3. d	Primary Overlay (1, 0) – Program P4210	554
D. 3. e	Primary Overlay (14, 0)	555
D. 3. f	Primary Overlay (2, 0) – Program P4220	557
D. 3. g	Secondary Overlay (2, 1) – Program P4221	559
D. 3. h	Primary Overlay (3, 0) – Program P4230	561
D. 3. i	Primary Overlay (11, 0)	561
D. 3. j	Primary Overlay (4, 0) – Program P4240	567
D. 3. k	Primary Overlay (7, 0)	567
D. 3. l	Overlays (11, 0) to (11, 2)	570
D. 3. m	Secondary Overlay (10, 2) – Program P42102	570
D. 3. n	Primary Overlay (5, 0)	570
D. 3. o	Primary Overlay (12, 0) = Program P42120	577
D. 3. p	Primary Overlay (13, 0)	579
D. 3. q	Primary Overlay (15, 0) = Program P42150	584
D. 3. r	Secondary Overlay (10, 1) = Program P42101	584
D. 3. t	Primary Overlay (6, 0) = Program P4260	585
D. 3. v	Primary Overlay (16, 0) = Program P42160	586
D. 3. w	Primary Overlay (10, 0) = Program P42100	586
D. 4	PROGRAM USER'S MANUAL	586
D. 4. a	General	586
D. 5. b	Input Data Descriptions	586
D. 5. c	Data Categories	587
D. 5. e	DATA Statements	588
D. 5. f	Assignment of Constant Values to Variables	590
D. 5. g	Punched Card Input to File TAPE17 = INPUT	593

D. 5. h	DATA Files	597
D. 5. i	File ADATA = TAPE16	598
D. 5. j	File INDATA = TAPE5	624
D. 5. l	File CDATA = TAPE9	634
D. 5. m	File DDATA = TAPE10	638
D. 5. n	File EDATA = TAPE11.	642
D. 5. o	Summary of File Assignments in SURFACE	643
D. 5. p	Operation of SURFACE	646
D. 5	TEST CASE	653
D. 6	REFERENCES	696

FIGURES

D-1	Table of Contents of SURFACE Master Tape	536
D-2	Satellite Coordinate System	537
D-3	Program Card for SURFACE (P1942)	545
D-4	Part A. Program Segment Linkage Pattern	547
	Part B. Program Segment Linkage Pattern	548
	Part C. Program Segment Linkage Pattern	549
	Part D. Program Segment Linkage Pattern	550
	Part E. Program Segment Linkage Pattern	551
D-5	Typical DATA Assignments	591
D-6	Directives for Correcting File DDTA:	599
D-7	Structural and Plume/Deposit Constituents	601
D-8	File ADATA - Initial Section	602
D-9	Satellite Configuration	603
D-10	Storage Locations in SURDES for Satellite Configuration Data	605
D-11	ADATA Input of Satellite Configuration	606
D-12	ADATA Input of Satellite Projections	608
D-13	Storage Locations in MATERIAL for Mechanical Properties	609
D-14	ADATA Input of Mechanical Properties	611
D-15	ADATA Input of Phys-Chem Properties	613
D-16	Storage Locations in CHEMIC for Chemical Properties	614
D-17	ADATA Input of Chemical Properties	615
D-18	ADATA Input of Molecular Weights and of Wear Equation Constants	616

D-19	Storage Locations in SCRPT E for Wear Rate Constants	618
D-20	Storage Locations in PRØPTY for Optical/Thermal Constants	620
D-21	Part A. ADATA Input of Optical and Thermal Constants	621
	Part B. ADATA Input of Optical and Thermal Constants	622
	Part C. ADATA Input of Optical and Thermal Constants	623
D-22	Assignment of Exposure Sequences	625
D-23	ADATA Input of Program Sequencing Control Parameters	626
D-24	INPUT1 Input Card Format	628
D-25	INDATA Cards for INPUT1 Edited Input	630
D-26	Material Code Assignments	633
D-27	Operation of Flag KTEST	635
D-28	BDATA Input File	636
D-29	Locations in EFFECT for Various Surface Conditions	638
D-30	CDATA Input File	639
D-31	DDATA Input File	640
D-32	EDATA Input File	644
D-33	Control Cards to Run SURFACE From File Copy with No Modifications	647
D-34	Calls to Subroutines and Overlays Listed by Auxillary Program PX4.	648
D-35	Additional Control Cards to Initiate a Checkpoint File and Namelist Input	650
D-36	Control Cards for Modification of SURFACE	652
D-37	Structure of OLDPL of Surface (1 of 2)	654
D-38	LISTIT Output from SURFACE Master File (Page 1 of 5)	656

D-39	Control Cards for Replacement of a DATA Deck	661
D-40	Initialization Listing	663
D-41	Satellite Configuration Listing (Page 1 of 3)	665
D-42	Properties of Materials (Page 1 of 10)	668
D-43	Derived Coefficients and Properties of Deposit Constituents (Page 1 of 5)	678
D-44	Revised Data Input by NAMELIST	683
D-45	Assignment of Calculation Cycles	684
D-46	Initial Material Assignment to Spacecraft Exterior (Page 1 of 2)	686
D-47	Satellite Exterior Conditions (Page 1 of 3)	688
D-48	Summary of Initial Satellite Condition	691
D-49	Assignment of Post-Exposure Conditions	692
D-50	Comparison of Selected Segments Before and After Assignment of Post-Exposed Conditions	693
D-51	Summary of Effects Caused by Assigned Post- Exposure Conditions	694
D-52	Exposure Time and Time Increment	695
D-53	Segments Impinged for Selected Thrustors and Plume Configurations	697
D-54	Segments Impinged by Plume	698
D-55	Transformation of Coordinates, Thrustor Based to Satellite Based	699
D-56	Locations of Impinged Segments, Thrustor Based Coordinate System	700

TABLES

D-I	Surface Program Overlay Structure	546
-----	-----------------------------------	-----

Appendix D

SURFACE

DEPOSITION AND SURFACE EFFECTS COMPUTER PROGRAM

D. 1 INTRODUCTION

The computer program SURFACE described in this appendix is a subprogram to the Plume Contamination Effects Prediction Computer Program, CØNTAM. It computes the effect of direct plume impingement on sensitive satellite surfaces in terms of changes in the thermal and optical properties of the surfaces.

a. Objectives

1. Analyze and model the direct impingement interaction of the plume from a chemical thruster with typical satellite surface configurations and materials to predict changes which occur on the satellite surface by chemical deposition and mechanical abrasion.
2. Analyze and model the surface changes which occur during subsequent periods when the thruster is not operating.
3. Analyze and model the behavior of satellite optical ports and thermal control surfaces subsequent to their being affected by plume impingement and space exposure sequences to predict changes in transmissivity and thermal balance factors.

b. Data Base

Required input to the SURFACE Subprogram includes:

1. The gasdynamic, thermodynamic, and chemical constitution description of a plume as computed by the MULTRAN (Appendix B) and KINCØN (Appendix C) subprograms.
2. A configurational and material description of the external sensitive surfaces of the spacecraft.

c. Output

The SURFACE Subprogram of the CØNTAM program includes determination of plume impingement effects in two related areas:

1. Surface chemical/mechanical effects on a satellite caused by direct plume impingement or exposure to the space environment.
2. Optical/thermal effects on satellite functioning caused by the surface chemical/mechanical changes.

d. Program Outline/Summary

The program is a generalized system model consisting of:

1. A general configurational description of a satellite with multiple thrusters and functional projections such as solar cell arrays — up to 175 separate structural elements can be treated.
2. A variety of structural materials commonly used on the exteriors of satellites, such as alloys, thermal control paints, platings, viewport materials, and solar cell materials. These may be combined to model multilayer surfaces. Up to 25 different materials may be used.
3. A variety of typical plume constituents which may be gases, vapors, or condensed droplets/particles. Up to 25 different constituents may be treated.
4. The configuration of the plume and its local properties are a necessary input. This information may be obtained by examination of the KINCON and MULTRAN subprograms.
5. Program output consists of a description of the current condition at up to 175 satellite locations. The description includes, for each location, structure composition and surface state, deposit chemical composition, deposit quantity, deposit state and surface condition, surface and substrate temperatures, thermal radiation coefficients for heat balance calculations, and optical transmissivity coefficients for sensor efficiency calculations. Average values for thermal and optical coefficients are also listed.

e. Program Physical Configuration

The SURFACE program consists of about 7 boxes of punched cards. (The size of an object deck in punched form has not been estimated.) The standard data supplied with the program consists of about 1/2 box of cards. If a complete set of plume characteristics data is prepared from KINCON and MULTRAN and used as input to SURFACE in punched card form, this will add one to four more boxes.

The physical size of the program when in card form makes it preferable to store the program and data in a magnetic tape or disc file when it is in use, and just to keep a backup copy on punched cards.

The tape file of SURFACE prepared at MDAC is a multi-file master file which has the structure illustrated in Figure D-1. This figure, a Table of Contents for the tape, is the first file on the tape, and it is normal practice at MDAC to copy this contents file to output every time the tape is used.

It is advisable to keep this table up to date by correcting it whenever modifications are made to the program or data and a new file created with the modified contents. This is readily done because the second file on the master tape is the UPDATE \emptyset PL for the Table of Contents. (The Deck Name is STR.)

D.2 ANALYSIS

a. Satellite Structure

SURFACE accepts data input to describe the external surface of the satellite. The surface is divided into a preselected, arbitrary number of locations given in a cylindrical coordinate system. Additional inputs include the locations of all projections from the surface, the height of such projections, and the angle they present to the main axis of the satellite. The initial surface temperature at each location is noted. The program prints a set of tables showing all configuration data.

In the satellite-based cylindrical coordinate system, the origin is placed at the forward vertex of the satellite, with the satellite axis lying on the X-axis. The cylindrical coordinates of any point in this system are given in terms of (X, R, θ) , with θ measured in radians in the plane of the Y-Z axis from an arbitrary zero (see Figure D-2).

For purposes of defining the various conditions and effects on the surface of the satellite, the exterior is divided into segments, each with a specified area. Each segment is given an identification number, and its location is recorded in the cylindrical coordinates of its centroid. The shapes of the segments are appropriate to the surfaces on which they lie—curved squares on the cylindrical surface, annular segments and circles for the ends, etc. The assignments are completely flexible and can be changed by simply changing the data cards. In general, there is no need to describe the satellite exterior completely. If the areas which can interact with the plume are already known, then the input can be limited to these areas.

b. Projection Configuration

Data are input to describe the configuration and structure of projections above the satellite surface, including sensors, solar cells, and thrusters. These are also broken down into conveniently sized segments. Tables are printed showing the data for each projection.

c. Structural Materials

Data are input to describe the structural-mechanical properties of typical materials used for exterior structures of satellites. Materials include aluminum, gold plating, solar-cell cover glasses, infrared ports, windows, ultraviolet ports, and white and black thermal-control coatings, plastics, etc. Typical or handbook data are currently input. Definitive data for specific alloys or compositions can be added easily when information on their behavior is required. The input data are listed.

STRUCTURE	STR	2
RUMFAC	STR	3
(13/6/73)	STR	4
TAPL NO.	STR	5
FILE NO. FILE NAME CONTENTS	STR	6
(FID)	STR	7
1 STRUCT STRUCTURE OF TAPE (THIS TABLE)	STR	8
2 STRUCT CLEPL OF STRUCT FOR USE WITH UPDATE	STR	9
3 OLUP1 CLEPL OF RUN VERSION OF FORTRAN PROGRAM	STR	10
FOR USE WITH UPDATE	STR	11
(13/6/73)	STR	12
4 CMPL COMPILER FILE OF FORTRAN PROGRAM GENERATED	STR	13
BY UPDATE FOR USE WITH RUN COMPILER	STR	14
(13/6/73)	STR	15
5 ADATA COMPILE FILE FOR USE BY OVERLAYS 0/0, 1/0, 2/0	STR	16
AND 3/0 EXCEPT FOR TABLE SECTION IN 3/0	STR	17
(13/6/73)	STR	18
6 BDATA FOR USE BY OVERLAY 3/0	STR	19
(13/12/72)	STR	20
7 CDATA FOR USE BY OVERLAYS 4/0 AND 10/0	STR	21
(13/3/72)	STR	22
8 DDATA FOR USE BY OVERLAY 5/0	STR	23
(13/5/73)	STR	24
9 EDATA FOR USE BY OVERLAY 14/0	STR	25
(13/12/72)	STR	26
10 INDATA FOR USE BY INPUTS	STR	27
(13/4/72)	STR	28
11 ADDEL CLEPL OF ADATA FOR USE WITH UPDATE	STR	29
(13/5/73)	STR	30
12 BDUPL CLEPL OF BDATA	STR	31
(13/12/72)	STR	32
13 CDUPL CLEPL OF CDATA	STR	33
(13/3/72)	STR	34
14 DDUPL CLEPL OF DDATA	STR	35
(13/5/73)	STR	36
15 EBUPL CLEPL OF EDATA	STR	37
(13/12/72)	STR	38
16 INDUPL CLEPL OF INDATA	STR	39
(13/4/72)	STR	40
17 P4TEXT ONACODE FOR EXECUTION-TIME ABORT TO FIND HOW	STR	41
FAR PROGRAM RAN BEFORE THE ERROR, (COMPILE FILE)	STR	42
(13/5/73)	STR	43
18 EXT0PL CLEPL OF P4TEXT	STR	44
(13/5/73)	STR	45
19 PX4 RCP OF P4TEXT, READY TO LOAD	STR	46
(13/5/73)	STR	47
20 LGUPR RCP OF *SURFACE*, READY TO LOAD	STR	48
64 LOGICAL RECORDS LONG, INCLUDING *ZERO*	STR	49
LEASTIN OVERLAY CARDS, BUT EXCLUDING 0,0,0	STR	50
(13/6/73)	STR	51
21 N01TH RCP OF INITIAL CLOSING PROGRAM	STR	52
2 LOGICAL RECORDS LONG	STR	53
(13/5/73)	STR	54
22 TH0PL CLEPL OF N01TH	STR	55
(13/6/73)	STR	56
NOTE--DATES ARE FOR LATEST MODIFICATION TO EACH FILE.	STR	57
NOTE--IF UPDATE IS USED FOR MODIFYING DATA FILES, THE RCP PARAMETER	STR	58
MUST BE USED TO PREVENT OVERWRITING DATA RECORDED IN COLUMNS 72-80.	STR	59
----	STR	60
-----	STR	61
-----	STR	62
-----	STR	63
-----	STR	64
-----	STR	65
-----	STR	66
-----	STR	67
-----	STR	68
-----	STR	69
-----	STR	70
-----	STR	71
-----	STR	72
-----	STR	73
-----	STR	74
-----	STR	75
-----	STR	76
-----	STR	77
-----	STR	78
-----	STR	79
-----	STR	80
-----	STR	81
-----	STR	82
-----	STR	83
-----	STR	84
-----	STR	85
-----	STR	86
-----	STR	87
-----	STR	88
-----	STR	89
-----	STR	90
-----	STR	91
-----	STR	92
-----	STR	93

Figure D-1. Table of Contents of SURFACE Master Tape

C	38	1/0	
C	39	1/0	
C	40	1/0	FOR PURPOSES OF CALCULATION, CYLINDRICAL COORDINATES ARE USED, THE
C	41	1/0	CRIGIN IS PLACED AT THE VERTEX OF THE NOSE, WITH THE SATELLITE AXIS
C	42	1/0	LYING ON THE Y-AXIS, THE COORDINATES OF ANY POINT IN THIS SYSTEM
C	43	1/0	ARE GIVEN IN TERMS OF (X,R,THETA), WITH THETA MEASURED IN RADIAN
C	44	1/0	FROM THE HORIZONTAL Y-AXIS.
C	45	1/0	
C	46	1/0	
C	47	1/0	
C	48	1/0	AXIS / P(X,R,THETA) 1/0
C	49	1/0	
C	50	1/0	
C	51	1/0	
C	52	1/0	
C	53	1/0	
C	54	1/0	AX AXIS
C	55	1/0	
C	56	1/0	
C	57	1/0	
C	58	1/0	
C	59	1/0	
C	60	1/0	
C	61	1/0	
C	62	1/0	
C	63	1/0	

Figure D-2. Satellite Coordinate System

d. Optical and Thermal Coefficients for Structural Materials

Data are input to define properties such as a solar absorptivity (α_s), thermal emissivity (ϵ_{TH}), transmittivity (τ), and reflectivity (ρ) at selected wavelengths, etc., as functions of surface finish for the structural materials. Typical or handbook data are currently supplied. Specific data inputs for selected compositions of materials can be added as required. The input data are listed.

e. Physicochemical Properties of Propellants and Deposits

Data are input to define the physical and chemical properties of plume species and deposits at selected reference temperatures. Properties of propellants at other temperatures are then calculated. However, there are insufficient data for some of the condensed reaction products to allow accurate extrapolation of these properties, and data for these materials are treated as constant with temperature.

f. Optical and Thermal Coefficients for Deposits

Data are input to define thermal and optical coefficients— α_s , ϵ_{TH} , τ , and ρ —as functions of temperature. Input data are listed.

g. Other Data

When certain data normally input in c. to f. are not supplied, appropriate values are estimated from other data that are input. Thus, if the critical temperature is not supplied, it can be internally estimated from the 3/2's rule and the boiling point: $T_c = 3/2 T_B$. As another example, missing optical transmissivities at various wavelengths are estimated from the refractive index. A listing of missing property data for each material is made.

h. Initial Assignment of Materials

Data are input to assign specific structural materials to each satellite segment. As many as three layers of materials may be assigned to any segment. Usually only one or two layers of structural materials are input, leaving at least one layer for deposits formed by the plume. The data are entered into two arrays; one is the surface description array SURDES, and the other is a transfer matrix used to search for properties corresponding to the materials and their conditions.

A table is printed showing the materials assigned to each segment of the satellite and projections, and the initial surface condition (finish or roughness, and temperature).

i. Suppression of Listing

The tables listing initial input data can be suppressed by a flag set during initialization. This reduces redundant output when the same initial conditions are used in a sequence of runs. Error, warning, and timing messages are not suppressed.

j. Optical/Thermal Surface Parameters

This routine takes the transfer matrix of materials assignments to segments and searches the stored optical and thermal coefficients for the appropriate data. Interpolations/extrapolations are conducted if the specific data needed have not been entered during input. (The optical and thermal properties of structural materials are tabulated as functions of surface finish; the properties of the deposits are given as functions of surface temperature.) The data appropriate to specific segments are entered in the array SURDES.

The interpolation/extrapolation routines include the following features:

1. No extrapolation of optical/thermal properties is done below the value given for the lowest temperature or surface finish in the tables; the minimum value is used.
2. Extrapolation above the highest temperature/surface finish is a simple linear ratio from the values for the two greatest temperatures/surface finishes.
3. Interpolation is by ratio from the nearest adjacent values, using essentially the method given by Wiberg (Reference D-1).

The new description of the surface is printed out.

k. Effective Values of Heat Transfer Coefficients

This routine calculates the values for solar absorptivity and thermal emissivity and their ratio, averaged over the whole satellite exterior (excluding projections). The calculated values are printed out.

l. Transmission Through Transparent Segments (Windows, Optical Ports)

The percentage transmission of an incident normal ray through the actual thickness of transparent material is calculated at eight wavelengths (infrared to ultraviolet) and the results are listed. Averaged values are calculated for devices which extend over more than one segment.

m. Test/Precalculated Surface State

Card data are input describing the physical state of selected structural segments. Such data include presence of deposits, thickness of deposit and/or thickness of original surface, surface finish, and surface temperature. The data are listed.

A flag is set during initialization to activate or bypass this module.

n. Optical/Thermal Surface Parameters and Heat Transfer Coefficients

The program then returns to the calculation of surface parameters and coefficients above, this tests for the precalculated surface state, and lists the values obtained.

o. Reinitialization

If the precalculated results module (m and n above) is active, the results from this module may be discarded after listing, or they may be used as the basic condition prior to plume and space exposure. A flag set during initialization selects the mode to be followed.

p. Exposure Sequence

A set of input data define the exposure sequences to be undergone by the satellite. The definitions include types of exposure (plume or space), their sequence and durations. Flags and counters are set by these inputs to select the sequence of computation routines appropriate to the sequence of exposures.

q. Plume Impingement Locations

Those satellite segments upon which the plume impinges directly are identified by considering the configurations of the plume and satellite. Only these identified segments are used in calculation of plume impingement effects.

The intercept of the plume with the satellite is calculated. The variables used are satellite configuration, thruster location, and plume geometry. A paraboloid shape for the plume is assumed. The latus-rectum of the plume paraboloid, which defines the shape of the plume, is equal to four times P. P is a function of thruster size, configuration, etc., and of the time in the cycle (pulse transient).

The locations impinged by the plume are functions of the geometry of the plume and the configuration of the satellite. The border of the impinged area is founded by simultaneous solution of the equations for the plume and the surface. The array SURDES is searched to find all segments whose coordinates are on or inside the border. These segment identification numbers are put into the array called AFFSEG.

The computation is done in two separate modules. The first is the intersection of the plume with the satellite surface. Currently this module is restricted to satellites of near cylindrical cross section. The second module determines the intersection with projections. The computation assumes an approximately plane surface on the projection which can lie at any solid angle to the axis of the plume. The configuration of the system used for these calculations is the data originally entered in the program. There is no provision for recalculating the intersection of movable projections after they have changed position.

Impingement on one location by the plumes from two separate thrusters fired simultaneously is not treated; however, sequential firing of two or more thrusters is treated.

r. Space Effects Locations

The satellite segments which have a surface deposit formed by previous plume exposure cycles are identified. Only these segments are used in calculation of space exposure effects.

The identification is done simply by searching the array SURDES, which lists current surface state, for the presence of deposited materials as the topmost layer of a segment.

s. Transformation of Coordinates (Plume Exposure Only)

The MULTRAN and KINCØN subprograms treat the plume in thruster-based cylindrical coordinates. In order to identify the locations of impinged satellite surfaces in the plume, a transformation to satellite-based coordinates is performed on the plume flow field. These calculations require inclusion of a radial angle in the plume coordinates because the cylindrical symmetry of the isolated plume is lost in the presence of the satellite structure. The origin for measuring this angle is defined by the plane in which the central axis of the thruster and the central axis of the satellite both lie.

t. Surface Properties

The physical and mechanical properties of the surfaces of the affected segments are found and entered in the array SEARCH. These properties determine the type of interaction with the plume.

u. Surface Effects

KINCØN and MULTRAN outputs are used to determine data on the characteristics of the plume at the location of each impinged segment at each time slice. If complete data on the plume characteristics are not available, the program assumes that conditions prevailing at the previous time increment or at the adjacent segment (or both) apply to the segment of interest. This allows the program to be run with as few as a single set of plume characteristics—in such a case there is automatic provision for startup and trail-off transients.

As a first step, the abrasion wear is calculated for a single time increment of approximately a microsecond (the exact width is controlled by the user). The amount of abrasion in this interval is then compared with a standard wear depth value, input by the user (and defaulting to 10⁻¹⁰ inch). If wear is less than the specified amount, the program considers wear as insignificant and branches to calculation of condensation from the plume vapor. (The two processes are treated as mutually exclusive.) After completing the condensation routines, direct deposition of plume droplets is calculated.

The results of the three processes are stored temporarily. The effects are then calculated for the next time interval, using the results from the previous interval as the base.

v. Abrasion

All abrasion is assumed to be the result of impacting particles (droplets). There are no provisions for abrasive wear resulting from gas impact or for thermal ablation. If abrasion occurs, the impacting drops are assumed to depart along with the abraded surface material. The wear relation used is the fatigue wear term of Neilson and Gilchrist (Reference D-2). The rate of material removed per weight of impinging condensed phase is calculated by means of tabulated values for the fatigue wear parameter for the several materials, plus constants for the equation used to calculate the value at specific velocities.

The wear rate constant (lbm material removed per lbm material impinged) for a particular material is a function of the impingement velocity up to a lower critical velocity; it then becomes constant. The critical velocity is a property of the material undergoing abrasion. Some data available suggest that there are upper critical velocities at which the form of the wear equation changes, but the data are insufficient for definitive application, therefore the program does not model the changes.

In the calculation of abrasion effects, the droplets are grouped into two size categories: the uncombusted material (large) and the condensed combustion products (small). An average diameter is used for each size category.

Two effects are calculated—the wear depth and the resulting surface finish. If the abrasion is sufficient to completely remove the surface layer, subsequent calculations are conducted with the characteristics of the newly exposed layer.

w. Condensation

The model used for the condensation process is one which uses the analogy between heat and mass transfer, based on Trebal's model (Reference D-3). The model uses heat transfers coefficients, without requiring input data on mass transfer or deposition rates.

The determination of deposition requires the diffusivities of the condensing species in the gas stream. These are calculated from the boiling point, molecular radius, and density. The assumption is made that each condensable species diffuses independently through a medium consisting solely of nitrogen gas. Next, using the specific heat, viscosity, and molecular weight of the plume, the Prandtl number and Schmidt number are calculated.

For each condensable species, separate film heat transfer coefficients are calculated based on plume properties and on substrate properties. The one based on plume properties is used to define a mass transfer coefficient. Then using the bulk heat transfer behavior of the substrate, the heat of condensation of the species of interest, and the heat and mass transfer coefficients, the rates of deposition of both heat and mass are obtained by simultaneous solution of the equations, with vapor pressure of the condensing species used as the pivot in the calculations. The process is carried out for each species, then the results are summed. The final substrate and surface temperatures are also calculated.

Chemical reactions between respective species as they condense are also computed to define the final composition of the deposit. The calculations are repeated for each time increment in the pulse, using the appropriate plume characteristics.

x. Deposition

The direct contact of plume particulates is then treated. Droplets which are not moving fast enough to cause abrasion wear are assumed to have a probability of adhering to the surface. The probability is calculated as a function of droplet mass, droplet velocity, and impingement angle; then the total quantity of deposited material is determined from the probability and the droplet mass flux.

The calculations are repeated for each time increment.

y. Net Effects

After exposure to the plume is complete, reactions between species deposited at various times and by various processes are calculated to define the final deposit condition.

The surface finish of the deposit is calculated, based primarily on temperature and deposit thickness.

The total quantity (depth) of surface deposit at each segment is compared with a user-input standard, typically about 10^{-6} in. If the quantity deposited is smaller than the standard, then the deposit is ruled negligible and the data are deleted.

z. Space Exposure Effects

The model used for space exposure effects is primarily a calculation of evaporation rate of volatile deposits as a function of surface temperature, heat transfer from the substrate, and vapor pressure and heat of evaporation of the deposits. A zero back pressure is assumed. The method of calculation is similar to that used for evaporation of surface films in the thruster chamber (see Appendix A).

aa. Recycling/Termination

The program prints a summary of the calculations carried out for the completed exposure. It then checks for instructions about further exposure cycles, and proceeds to follow the instructions. If all cycles are complete, a closing summary is printed.

ab. Program Operations Information

A clock is kept to measure the length of time each overlay requires, and this information is listed after return from the overlay. To keep core and disc space reservations to the minimum required for program execution, internal field length redefinition (SRFL) and disc file release (DRØPIT) are used extensively. Appropriate messages are printed in the Day File when these routines are called. The field length redefinition routine SRFL, when

used to increase the field length, sets all locations in the newly acquired core region to zero. SFRL is written in COMPASS and included in SURFACE.

A counter is used to keep track of all calls to external routines which are part of the program (library and system calls are not monitored). At normal termination, this count is listed by a program subroutine. For abnormal termination, going to EXIT, a small auxiliary program prints the same information.

The standard CDC library function EXP has a serious drawback: If the value supplied for exponentiation is less than or equal to -675.82 , the result is set to zero, but no warning is given of this action. (A warning notice is printed if the value is too large.) A modified version of EXP which does give a warning message has been coded (in COMPASS) and this function is included in the SURFACE program.

Overlay calls to levels which are 8_{10} or greater are coded in octal numbers, using a terminal B (e. g., CALL OVERLAY (fid, 12B, 1)) to avoid the confusion inherent when the calls are decimal while the Overlay identification cards are octal. *

The Program Card for SURFACE includes as parameters the names of all files on which Overlays are stored, even those which are not released by DRØPIT (see Figure D-3). This listing on the Program Card was found to be necessary to prevent random losses of unlisted Overlay files when DRØPIT was used on an Overlay file that was listed.

D. 3 PROGRAM FUNCTIONS

a. Outline

This section contains descriptions of the various modules—overlays and subroutines—in SURFACE. These descriptions are given in the order of their presentation in Table D-1, which shows the Overlays which function for each major subtask.

The calling sequences for overlays and subroutines is outlined in Figure D-4.

b. First Principal Overlay (0, 0)—Program TM42

There is an additional preliminary 0, 0 level Overlay, not shown in Table D-1, which can be used to set initial timing before even starting to copy the main program 0, 0 Overlay into core. Its use is optional. If it is used, it calls the main program automatically.

This module prints the data and a summary of the CP and PP time used since the job started, prior to starting on the SURFACE program proper.

Program TM42 calls Program P1942.

*Note: In this Appendix, all overlays are referred to by their octal level numbers used in define the overlay, e. g., OVERLAY (ABC, 11, 2) is referred to as (11, 2).

PROGRAM P1942(TAPE1, TAPE2, TAPE3, TAPE4, INDATA, TAPE5=INDATA, OUTPUT,	0/0	14
STAPE6=OUTPUT, TAPE7=EDATA, TAPE8=BDATA, CDATE, TAPE9=CIATA, DDATA,	0/0	15
STAPE10=BDATA, ECATA, TAPE11=EDATA, TAPE12=COUNT, TAPE13=COUNT, ADATA,	0/0	16
STAPE16=ADATA, INPUT, TAPE17=INPUT, TAPE18=FLG, TAPE20=FLG, FLF,	0/0	17
STAPE21=FLF, FLG, TAPE22=FLG, FLE, TAPE23=FLE, CHEEP, TAPE24=CCHEEP, FLO,	0/0	18
STAPE25=FLO, PUNCH, TAPE26=PUNCH, TAPE30, TAPE31, TAPE32, FI, AT, FLB, FLZ,	0/0	19
FI)	0/0	20
	0/0	21
	0/0	22

Figure D-3. Program Card for SURFACE (P1942)

Table D-I
SURFACE PROGRAM OVERLAY STRUCTURE

Initiation and Program Executive	0, 0
Structure and Properties Input	2, 1 1, 0 14, 0 2, 0
Materials Assignment and Initial Surface Conditions	3, 0 11, 0-11, 2
Precalculated Post Exposure Data and Surface Conditions	4, 0 7, 0 11, 0-11, 2 10, 2
Plume Exposure Sequence and Surface Conditions (This sequence loops back on itself several times)	5, 0-5, 5 12, 0 15, 0 7, 0 11, 0-11, 2 10, 1
Space Exposure Sequence and Surface Conditions	6, 0 7, 0 11, 0-11, 2 10, 1
Termination	16, 0 10, 0

c. Principal Overlay (0, 0)

(1) Program P1942

This routine initializes most storage and control variables and flags. It reads in the data defining the exposure sequence to be followed and sets up the appropriate sequence of calls to primary overlays. These data are on file ADATA (TAPE16).

It is possible to turn off listing of some of the normal outputs which describe materials properties and satellite structure, and also the computations with precalculated exposure data. It is done by adding a single card to the 0, 0 Overlay. This can be useful for reducing the amount of paper generated when several computer runs are to be made with the same initial data. The card assigns the value 7 to I6F. The usual location of use it is noted in the (0, 0) listing. Reversion to normal listing at any point can be caused by inserting a card equating I6F to 6; in any case reversion occurs automatically upon entry to operating sequences which calculate plume or space exposure effects.

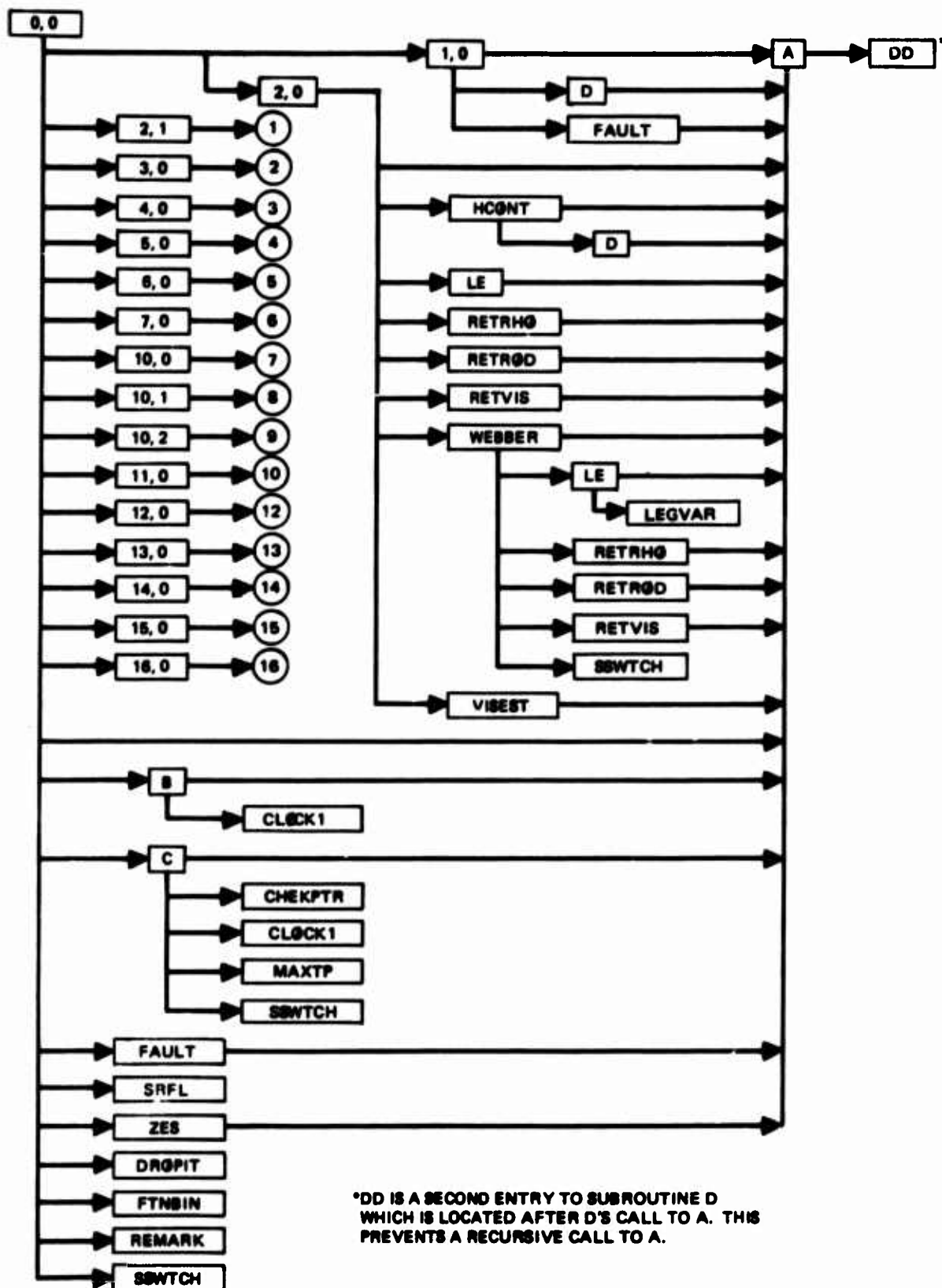


Figure D-4. Part A. Program Segment Linkage Pattern

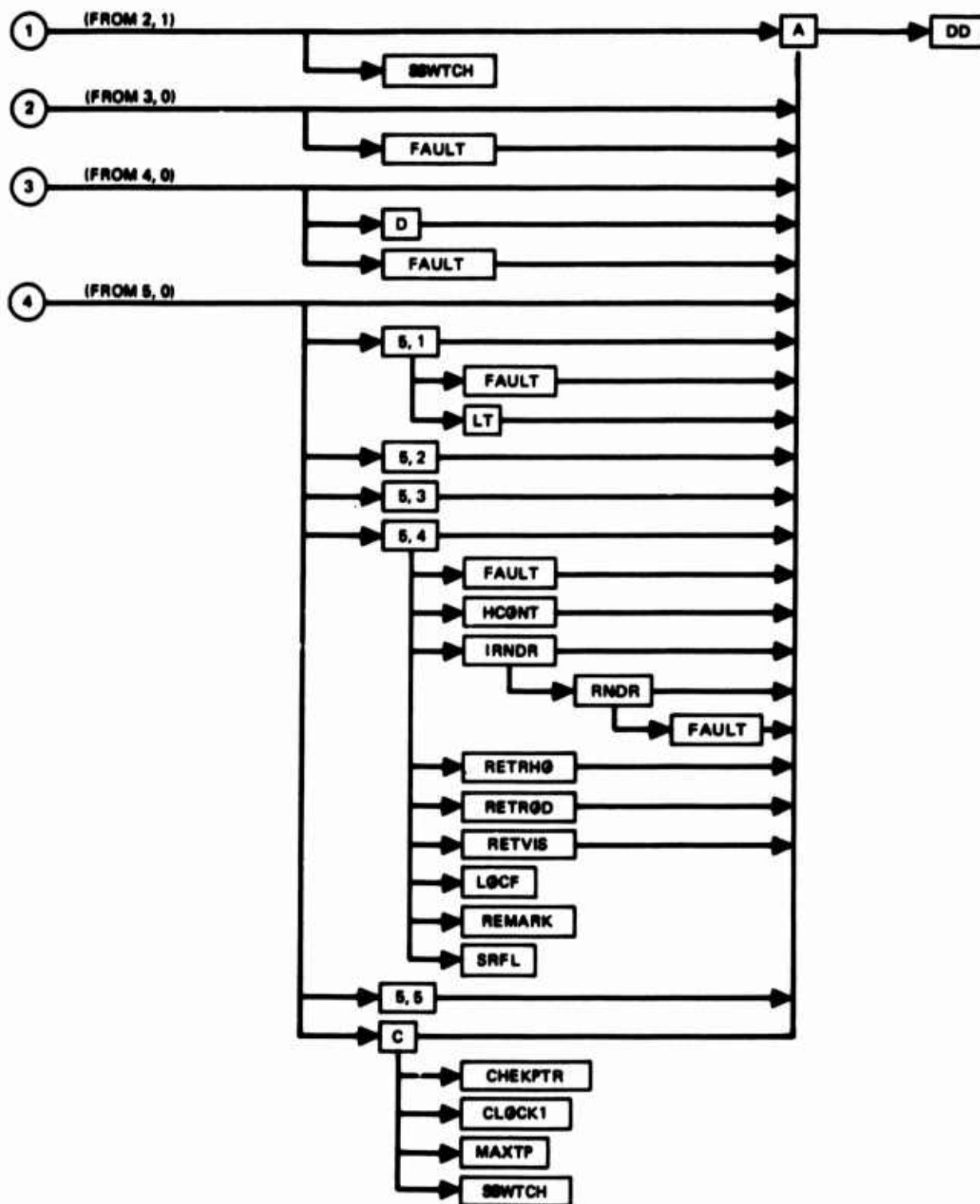


Figure D-4. Part B. Program Segment Linkage Pattern

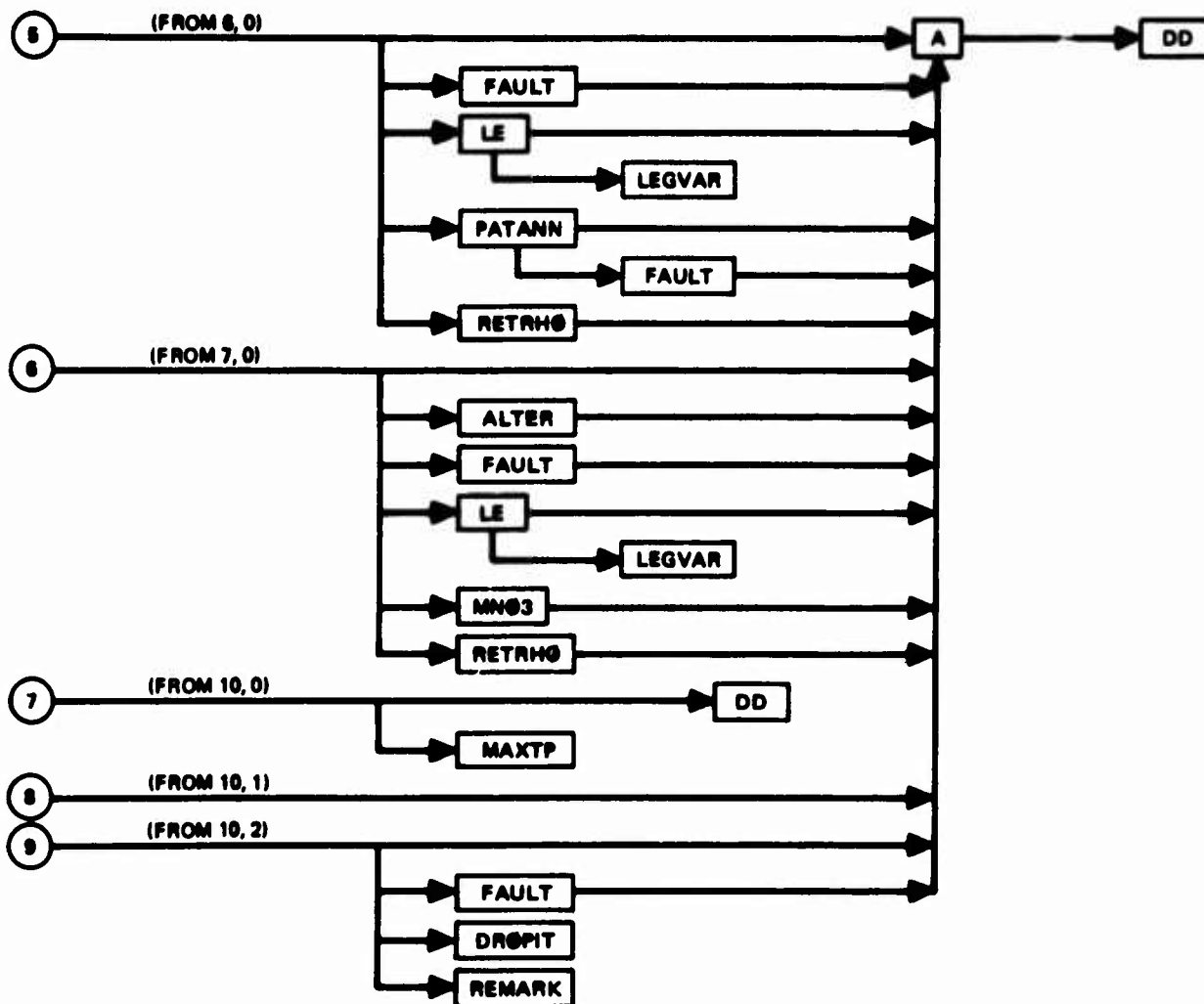


Figure D-4. Part C. Program Segment Linkage Pattern

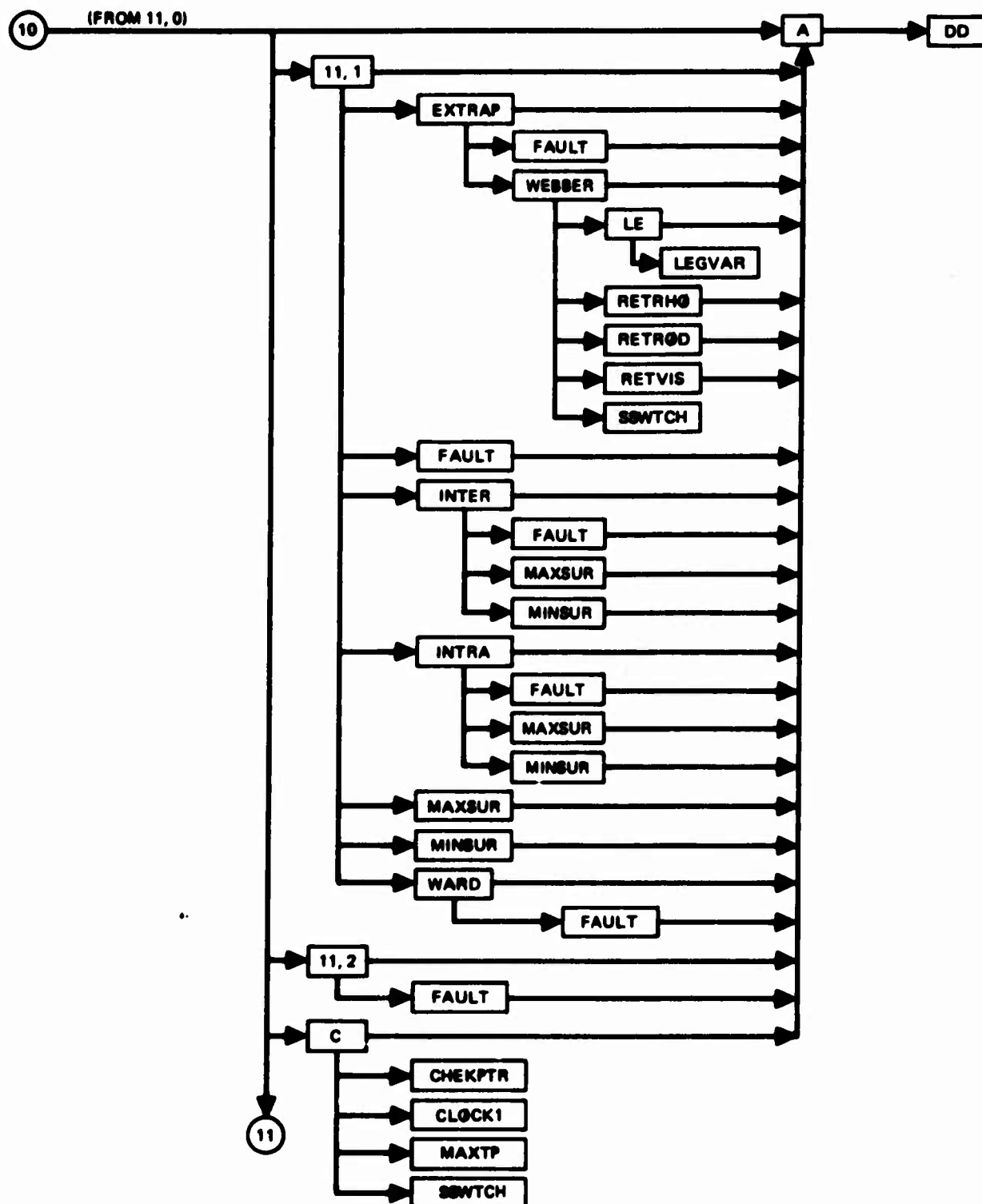


Figure D-4. Part D. Program Segment Linkage Pattern

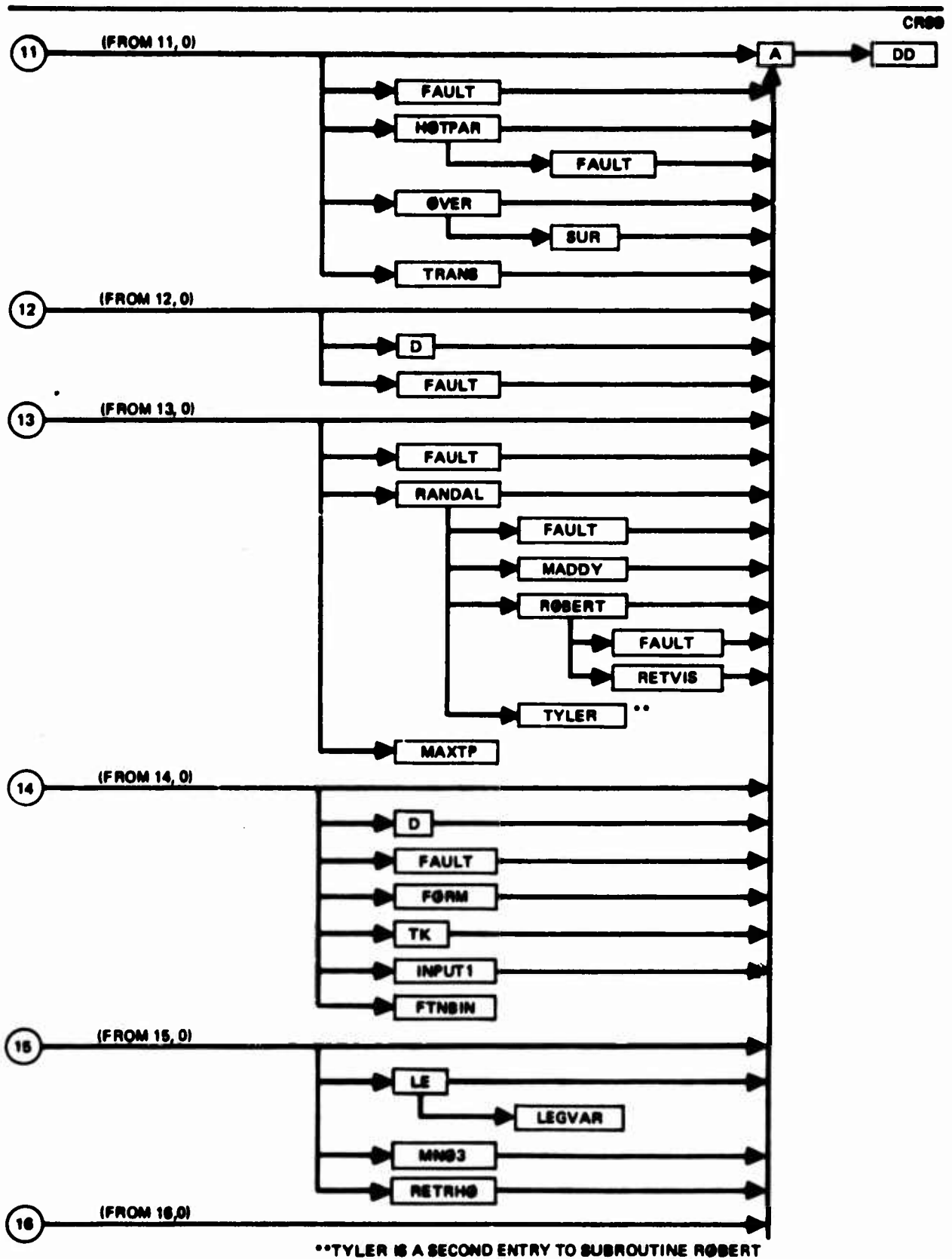


Figure D-4. Part E. Program Segment Linkage Pattern

Overlay (0,0) calls all primary overlays, the secondary overlays (2,1), (10,1), and (10,2), and the subroutines A, B, C, D, and ZES.

(2) Subroutine A

This subroutine writes the file (CØUNT = TAPE15) which records the number of calls to Overlays and Subroutines. It is called by all program units. It calls Subroutine D in case of a fatal error.

(3) Subroutine B

This subroutine initializes the clock for timing program operation. It calls Subroutine A.

(4) Subroutine C

This subroutine has two functions: (1) It keeps track of and prints the time needed to process each primary and secondary overlay and the total PP and CP time used on the job after finishing each overlay. (2) It will write a CHECKPØINT file of the SURFACE program if switched on to do so. The file is taken after return from the nth Overlay call, where n lies between 3 and 6, inclusive, and is repeated at every tenth subsequent return from an Overlay call. Each new CHECKPØINT file is written over the previous one. The CHECKPØINT file operation is enabled by turning on any Switch with a number from 3 to 6.

Subroutine C calls Subroutine A.

(5) Subroutine D

This subroutine prints a Dayfile listing of the numbered STØP's in the program and their corresponding sources. It calls Subroutine A.

(6) Subroutine ZES

This subroutine interprets the data which define the next exposure sequence and sets the flag which calls the appropriate computing sequence. It calls Subroutine A.

(7) Function HCØNT (TEMP)

This subroutine calculates the enthalpy HCØNT (= H) of the condensed phase of volatile plume constituents as a function of the temperature:

- (a) If $T (= TEMP)$ is below the melting point of the material, then $H = T * C_{psolid}$
- (b) If T is equal to or greater than the melting point, then $H = \text{Melting Point} * C_{psolid} + H_{fusion} + (T - M. P.) * C_{pliquid}$

The calculation is done using SI units.

Function HCØNT calls Subroutines A and D.

(8) Function RETRHØ (RTEMP)

This subroutine approximates the SI reduced density of a liquid as a function of reduced temperature, RTEMP, along the saturation line, based on the curve of Hougen and Watson. The calculation is identical to REDRHØ in TCC.

Function RETRHØ calls Subroutine A.

(9) Function RETRØD (RTEMP)

This subroutine calculates an approximation of the reduced density difference (liquid-vapor) as a function of reduced temperature along the saturation line. The calculation is identical to REDRØD used in TCC.

Function RETRØD calls Subroutine A.

(10) Function RETVIS (RTEMP)

This subroutine calculates the reduced viscosity (SI units) of a fluid as a function of reduced temperature. The value resulting is that for the liquid along the saturation line up to the critical temperature, and for the vapor along P_0 above the critical temperature. The computation is identical to REDVIS in TCC.

Function RETVIS calls Subroutine A.

(11) Function RNDR (X, N)

This subroutine will round off a real number, X, of any size to a real number containing N significant digits, without changing the location of the decimal point. The statement functions IRNDR, RNDI, IRNDI are used in conjunction with RNDR for input or output of integer variables.

Function RNDR calls Subroutine A.

(12) Subroutine FAULT (PØSN)

This subroutine is called when certain types of program-defined errors are detected. These errors may be fatal or nonfatal. For both types, an error message, giving the location of the error, is printed. The program is transferred to a termination step if the error is fatal. If it is nonfatal, the count of nonfatal errors is increased and the program returns to computation. However, if the error count reaches an input-data defined limit (defaulting to 10), the error is treated as fatal and computation is terminated. PØSN is the statement number (coded in Hollerith) at the location of the error. It is assigned in the calling routine immediately prior to the call to FAULT.

Subroutine FAULT calls Subroutine A.

(13) Subroutine LE (X, N)

This subroutine is used to check the validity of a real variable X (whether it is in range, indefinite, or infinite) before the variable is used in calculations, setting N to 0, -1 or +1 respectively. It calls the library routine LEGVAR for the check.

Subroutine LE calls Subroutine A.

(14) Subroutine VISEST (LOGV, N, X, Y, I)

This subroutine is used to calculate the viscosities of mixtures of liquids, given the viscosities X and Y of the component liquids. The number of concentrations calculated is given by I, which defaults to 10 if no value for I is supplied. The logical variable LOGV switches printing of the results off/on; if LOGV is .TRUE., the results are printed. When N is set to 1, a demonstration calculation using N₂O₄ and MMH is carried out.

Subroutine VISEST calls Subroutine A.

(15) Subroutine WEBBER (RTEMP, X, Y, LOGV)

This subroutine is used to calculate the reduced values of a number of physical properties of liquid or gaseous plume/deposit constituents at the reduced temperature RTEMP. Either one or two substances (X and Y) can be handled at once. All the results are stored in the array REDPRP.

The routine checks to determine whether the particular temperature/constituent pair has already been computed before proceeding.

The logical variable LOGV switches on listing of the results when it is .TRUE..

The properties for which reduced property values are calculated are vapor pressure, density, density ratio if two substances are being treated, viscosity, and surface tension.

Vapor pressures is calculated by use of the Calingaert-Davis equation:

$$\ln P = A - B/(T - 43.)$$

This is applied by evaluating A and B at the boiling point of the fluid, then the A and B are used at the temperature of interest.

Density and viscosity are obtained by calls to the functions RETRHØ and RETVIS.

Subroutine WEBBER also calls Subroutines A, LE, and RETRØD

d. Primary Overlay (1, 0) — Program P4210

This routine reads and stores input data which have the following names and functions:

FACTR - controls width of time slice on space exposure

DECPH - significant abrasion depth lower limit

DEDPTH - significant deposition depth lower limit

NAME - symbolic names of structural features, structural materials, and plume/deposit constituents

(7) The parachor, PCHØR, is calculated by means of the relation

$$\text{PCHØR} = \frac{(\text{Molecular Weight} * \text{Surface Tension})^{1/4}}{\text{Critical Density} * \text{RETRØD (Reduced Room Temperature)}}$$
$$= (\text{AMW} * \text{TENS}) ** 0.25 / (\text{RCRIT} * \text{RETRØD (TRED)})$$

(8) The liquid enthalpy, vapor pressure, specific gravity, viscosity, and surface tension are calculated at a series of temperatures for N₂O₄, MMH, and water, using the equations and subroutines described earlier, and the results are printed.

(9) The latent heat content of the vapor, DELH, at room temperature is calculated by means of the relationship.

$$\text{DELH} = \text{specific heat (vapor)} * \text{room temperature} * \text{enthalpy at absolute zero} - (\text{specific heat (solid)}) * \text{freezing point} + \text{latent heat of freezing} + \text{specific heat (liquid)} * (\text{room temperature} - \text{freezing point})$$

Subroutines are used so the equation is

$$\text{DELH} = \text{HVAP (TEMP (ATM))} - \text{HCØNT (TEM)}.$$

(10) A call to Subroutine WEBBER is made, and the density, viscosity, and surface tension are calculated at assigned temperatures, read from file ADATA (TAPE16).

(11) A call to Subroutine VISEST is used for calculating the viscosity of mixtures of liquids from the viscosities of the component liquids.

Program P4220 calls Subroutines A, HCØNT, RETRHØ, RETRØD, RETVIS, LE, WEBBER, and VISEST.

g. Secondary Overlay (2, 1) — Program P4221

This overlay is used to read in NAMELIST values of changed data from the INPUT file (TAPE17) and stores them on TAPE18 for access by user routines. It is activated by turning on SWITCH 1 by means of the SCØPE control card.

①

SWITCH, 1.

If desired, it will also list the values supplied. This is controlled by the value of the flag RDWRT—if RDWRT is greater than zero, the input is printed.

There are eight NAMELIST sets, which include the following variables.

NAST1 — Used by **OVERLAY (0, 0)** for changing exposure cycle assignments:

1. **NP1** - number of sequences to be run
2. **NPSEQ** - sequence of exposure cycles
3. **ISXTST** - number of space exposing
4. **IPXTST** - number of plume exposures
5. **IGOTST** - total number of exposure cycles

NAST2 — Used by **OVERLAY (4, 0)** for changing assigned effect inputs:

1. **IIS** - total number of segments affected
2. **EFFECT** - conditions on segments

NAST3 — Used by **OVERLAY (5, 0)** for changing values for the variables:

1. **TOTIME** - plume operating time
2. **DELTIME** - time slice width for plume exposure calculations

NAST4 — Used by **OVERLAY (5, 0)** for changes in assignments to the variables:

1. **P** - quarter latus-rectum of the plume
2. **DELP** - change of **P** from cycle to cycle
3. **NTR** - I.D. number of active thruster (source of plume)

NAST5 — Used by **OVERLAY (10, 2)** for checking whether the assigned data used in **OVERLAY (4, 0)** are to be the basis for further calculations instead of using the initial conditions:

ISTST - flag to select which data for the base

NAST6 and **NAST7** — Used by **OVERLAY (12, 0)** for input of new or additional plume characteristics data in addition to card input and data supplied by **KINCØN**:

1. **IP1S** - identifies cycle number
2. **IP2S** - identifies segment to which initially input plume characteristic data apply
3. **J1** - new cycle number
4. **K1** - new segment
5. **PLMCHR** - new plume characteristics

NAST8—Used by ØVERLAY (11, 0) to control evaluation of averaged thermal transfer coefficients.

1. PRJFLG - flag to turn on processing of averaged thermal coefficients on a projection
2. MS11 - SURDES location of segment with lowest ID number to be included
3. MS21 - SURDES location of highest segment ID to be included

Program P4221 calls Subroutines A and D.

h. Primary Overlay (3, 0)—Program P4230

This overlay reads in the assignment of structural materials and initial surface roughness and temperature for specified segments of the satellite surface and projections from file BDATA (TAPE8). The data are added to the array SURDES which already contains the coordinates of each segment. The data are also placed in the transfer array SEEK, which is used to search for the properties (optical and thermal) which the surface exhibits. SEEK is buffered out onto TAPE12.

No computations are conducted in P4230, other than to check the ID's and locations of individual segments.

Program P4230 calls Subroutines A and FAULT.

i. Primary Overlay (11, 0)

The set of overlays and subroutines based on Primary Overlay (11, 0) function to calculate the current state of each segment in terms of optical and thermal energy transmission coefficients, based on the current physical and chemical condition of the surface of the segment, resulting from initial preparation or plume or space exposure.

(1) Program P42110

The program first reads in from TAPE12 the latest values for SURDES (surface description), SEEK (the segments affected by the latest sequence of exposures), and several constants and auxiliary arrays. A check is made that the data in SURDES are consistent, and that a top layer still exists for each segment. If the top layer has been destroyed, (e. g., by abrasion), the second layer is moved into the top position, etc. The calculations of the state of each segment are made by table interpolation during multiple calls to the secondary Overlays (11, 1) and (11, 2) and associated Subroutines, and the numerical results are returned in the array VALUE. A final check is made to ensure that segment ID's match in the arrays SURDES, SEEK, and VALUE, then the data are entered into SURDES.

The temperature of the surface is checked, and the emissivity is corrected for temperature.

The data are then printed out in a large tabulation in which each segment is described completely—location, deposit thickness, materials, surface condition, optical and thermal constants. In cases of slight abrasion, where the thickness might require printing a string of 5 to 19 nine's or else rounding up to no apparent effect, a special routine prints the value in the form:

n·n9(6)9nn

where the bracketed 6 indicates 6 additional nines in between the two printed nines. Subroutines ØVER and SUR perform this task, storing the results in arrays SUR^H and SUR^I.

Subsequent to printing the data for each segment, the average values over the whole satellite for absorptivity and emissivity are calculated by summing and dividing by the number of segments, and listed. The calculation is done in subroutine HØTPAR. The results are EFALFA for the average solar absorptivity, EFEPSN for the average thermal emissivity, and EFRATØ for their ratio. The results are printed. The percent change in EFRATØ from the baseline value is calculated and printed.

The program next checks TAPE18 for the presence of NAMELIST NAST8 directives which cause a calculation of the average heat transfer coefficients for projections. If the directive is present (PRJFLG > 0) the program recalls HØTPAR and calculates EFALFA, EFEPSN, and EFRATØ for specified projection locations. This call can also be used for calculating the constants for specified limited regions of the hull of the satellite.

Next, all transparent segments are isolated, and the percent transmission for normally incident rays of light through any deposits and the transparent structure elements are calculated at seven wavelengths, from far infrared to ultraviolet. When there are several segments of one transmission type (such as a solar cell array) the average transmission for the group of segments for each wavelength is calculated and printed. These calculations are done in the Subroutine TRANS.

All subroutines local to (11,0) and its secondaries are attached to (11,0). These include EXTRAP, HØTPAR, INTER, INTRA, MAXSUR, MINSUR, ØVER, SUR, TRANS, and WARD. They are described following the sections on (11,1) and (11,2).

Overlays and Subroutines called from P42110: P42111 (ØVERLAY (11,1)), P42112 (ØVERLAY (11,2)); A, C, ØVER, FAULT, HØTPAR, and TRANS.

(2) Secondary Overlay (11,1) – Program P42111

This program initiates the search for property data which correspond to the current surface condition. The array VALUE is used to hold the results of the search. The array ALPHA is used to hold data originally read in as PRØPTY, CHEMIC or MATERIAL, now stored on files, and read in as required for current searching needs. The data contained in ALPHA become the primary source of information on the surface state.

The data in array SEEK are first checked to be sure that the layers of materials correspond to those in SURDES, except of course, for new deposits or removal by abrasion/evaporation. Subroutine WARD makes this test, and performs simple corrections.

Then, working with one segment at a time, and on each segment from the top layer down, one layer at a time, the material present is identified by its code number. If it is a deposit that is present, the substance present in highest concentration is taken to represent the deposit. Deposit temperature is obtained by octal masking of the appropriate location in the array SEEK.

A check is made to be certain that the surface condition sought is legal (not a negative number). If illegal, a warning message is printed and the segment is bypassed.

If the condition is legal, the file TAPE2 (which contains optical/thermal properties) is searched until the material corresponding to that on the segment is found. The data for this material are copied to array ALPHA. A flag called HOLD is set with the material's code number: this will be checked when the next segment is processed, and if the material and HOLD are the same, the file search will be skipped.

The surface condition of the segment is compared with the entries in ALPHA. If a match is found, the properties corresponding to the condition are copied to array VALUE. Where a specific property value is not available for the surface condition of interest, interpolation/extrapolation from values for other surface conditions must be carried out—Subroutines MINSUR, MAXSUR, INTER, INTRA, and EXTRAP are used for such calculations—the specific routines called depend on the type of calculation needed.

In similar fashion, if the surface condition does not correspond exactly to an entry in ALPHA, extrapolation/interpolation is used to identify its exact relation to the entries in ALPHA, then the surface state data are calculated. After completion of the calculations, the results are entered into the array VALUE.

The calculation recycles until data for all layers of all segments have been entered into VALUE, then a return to OVERLAY (11,0) is made.

PROGRAM P42111 calls Subroutines A, WARD, MINSUR, INTER, MAXSUR, EXTRAP, INTRA, and FAULT.

(3) Secondary Overlay (11, 2) — Program P42112

This program enters the data on surface state from VALUE into SURDES. It first checks the information currently in SURDES against the entries in VALUE, and if they are the same, no further action is taken. A check is then made of whether the sequence of materials in VALUE is possible (e. g., that no cases exist where the top layer is aluminum and the second is a deposit). Such errors will abort the program. Then the sequence of layers in VALUE is compared with the sequence in SURDES. After allowing for deposition and erosion, if the sequences do not correspond, the data in VALUE are bypassed and the next segment is taken up.

If deposits exist on the segment in both SURDES and VALUE, their identities are compared. They should be the same, both plume and space exposure routines call Overlays (15, 0) and (7, 0) to make sure of this. However, post exposure data supplied as input data in Overlay (4, 0) does not call those overlays, so in that case the concordance may not exist. If such is the case, some simplified assumptions about the chemistry of deposit interactions are made, and the final products calculated. If this process has occurred, the data on surface state in VALUE are incorrect, and the routine returns to (11, 0) with flag GETGET set to cause another call to (11, 1).

Eventually the material identity test is satisfied.

Then (11, 2) transfers the data in VALUE to the array SURDES and returns.

Program P42112 calls Subroutines A and FAULT.

(4) Subroutine EXTRAP

This subroutine, called from (11, 1), is used to interpolate/extrapolate physical/chemical properties as a function of temperature required to determine the surface state. It reads TAPE3 until it finds the material ID number, then puts the data into the array CHEM, then calls Subroutine WEBBER to do the actual computations. The results are returned in the array REDPRP.

Subroutine EXTRAP calls Subroutines A, FAULT, and WEBBER.

(5) Subroutine HØTPAR

This subroutine is called by the Overlay (11, 0). It calculates the overall effective values for α , ϵ , and the α/ϵ ratio corresponding to a particular set of surface conditions. Local values of α , ϵ , and the area of each segment are read from the file SURDES. The products of α times area and of ϵ times area for each segment are separately summed, then divided by the total area. Normally, the complete main body of the satellite is used for the calculations, and projections such as solar cell arrays are ignored. However, by using Namelist input NAST8, the routine can be commanded to calculate the coefficients for any subsection of the satellite, including and/or limited to projections.

Subroutine HØTPAR calls Subroutines A and FAULT.

(6) Subroutine INTER

This subroutine, called from Overlay (11, 1), is used to interpolate values for surface optical/thermal properties when no values corresponding to the surface finish of interest are available in the tabulation. It searches to find the closest lower and higher values, and the corresponding finishes. A factor is calculated from the finishes

$$Q = \frac{R_{\phi} - R_L}{R_U - R_L}$$

The surface property required is then calculated.

$$S_{\phi} = (S_U - S_L) * Q + S_L$$

where S indicates the surface property, R the finish, L the lower value, and U the upper value.

Subroutine INTER calls Subroutines A, FAULT, MINSUR, and MAXSUR.

(7) Subroutine INTRA

This subroutine, called from overlay (11, 1), is used to interpolate values for surface optical/thermal properties when interpolation is necessary on the surface finish entry as well as the desired property entry. The interpolation routines are the same as in INTER.

Subroutine INTRA calls Subroutines A, FAULT, MINSUR, and MAXSUR.

(8) Subroutine MAXSUR

This subroutine, called from Overlay (11, 1) or by Subroutines INTER and INTRA in turn called from (11, 1), is used when there is no value of a selected surface thermal/optical property corresponding to the surface finish of interest. It searches through the tabulation to find the property entry which corresponds to a surface finish which is less than but as close as possible to the surface finish of interest.

Subroutine MAXSUR calls Subroutine A.

(9) Subroutine MINSUR

This subroutine, called from Overlay (11, 1), INTER and INTRA, is the mirror image of MAXSUR. It is used to find the value of a surface property corresponding to the least increase in surface finish, when a value corresponding exactly to the surface finish is not available.

Subroutine MINSUR calls Subroutine A.

(10) Subroutine OVER

This subroutine, called from Overlay (11, 0), is used to display a long series of the numeral 9 in condensed form, avoiding the requirement for a printing format of 20 positions to prevent rounding up. This is used for printing the thickness of materials after exposure to the plume, where a minor amount of abrasion can give a long series of 9's. The routine encodes the number in decimal form, then decodes it as a one-dimensional array of individual numbers. It then inspects each number in turn, starting at the most significant. It counts the number of 9's in any sequence of 9's only, and if the number of 9's is greater than 5, it sets up the special format. Any number other than 9 in the sequence counted resets the counter to zero.

The special format consists of modification, suitable for computer printout, of the number structure found in some mathematics publications,

$$x \cdot x 9_n 9 x x$$

where the subscript in n is a number which indicates how many nines lie between the two nines printed on the line (that is, there are $n + 2$ nines in the sequence). The x 's indicate any other numeral. In SURFACE, the above structure is presented as

$$x \cdot x 9 (n) 9 x x$$

The procedure works only for real numbers—extension to exponential numbers (scientific notation) would not be difficult but does not seem to be needed.

Subroutine ØVER calls Subroutines A and SUR.

(11) Subroutine SUR

This subroutine, called from ØVER, stores the number describing the thickness of a layer in one of two arrays, SURH or SURI, for transmission to Overlay (11,0). The array is selected by means of a flag which is set by the use to which the number will be put.

Subroutine SUR calls Subroutine A.

(12) Subroutine TRANS

The subroutine, called from Overlay (11,0), calculates the percent transmission of light (UV, visible, and IR) through all layers of transparent locations on the satellite—sensors, solar cell arrays, and windows. The approach is based on the usual relation for intensity at any depth;

$$\frac{I}{I_0} = e^{-kt}$$

which is applied to each layer, including deposits, and on extra loss of intensity at all interfaces. The loss at each interface is calculated from the reflectivity appropriate to the wavelength—if reflectivity data are not supplied, it is taken as 4 percent for internal interfaces and 2 percent for external interfaces.

The results are returned to (11,0) for display printing, but are not stored.

Subroutine TRANS calls Subroutine A.

(13) Subroutine WARD

This subroutine, called from Overlay (11, 1), is used to transfer all lower layers upward one layer in the segment description if the data indicate a zero or negative thickness for a top layer in the array SEEK. It checks the results for consistency with the data in SURDES.

Subroutine WARD calls Subroutine A and FAULT.

j. Primary Overlay (4, 0)—Program P4240

This overlay has the function of accepting input data which define the postexposure condition of the exterior of the satellite when this data originates from sources other than program SURFACE. Such data may be input simply to test the overall program or may have been generated from other sources, such as tests, or even from previous runs of SURFACE. The data are input from file CDATE (TAPE9).

Prior to input of the data, the initial state of the satellite surface as contained in SURDES is written out and stored in TAPE4. This feature allows use of the defined postexposure state simply to test the program, and then later to calculate exposure effects on a pristine surface. If this is done, the initial state is restored downstream by a call in Overlay (10, 2).

The data read in by Overlay (4, 0) are stored directly in the array EFFECT, which is same array for storing the results from plume or space exposure. The input data are listed.

Program P4240 calls Subroutines A, D, and FAULT, and calls in TAPE12 to obtain the current values in SURDES for writing on TAPE4.

As mentioned in the description of the main Overlay (0, 0), the call to Overlay (4, 0) can be bypassed if assigned condition calculations are not wanted.

k. Primary Overlay (7, 0)

(1) Program P4270

This program calculates the final chemical composition of deposits on satellite segments after a plume or space exposure cycle, and writes the results in appropriate locations of the arrays SURDES and EFFECT. The computations include calculation of chemical reactions between pre-existing and newly deposited layers.

There are a number of steps in the calculations in this program.

(a) This array EFFECT is checked for the presence of data with which to calculate.

(b) Local, temporary arrays are copied from SURDES and EFFECT.

(c) The presence of deposits is tested.

The following steps are carried out for each affected segment before returning to the main overlay.

(d) If there are no deposits, appropriate changes in SURDES are made in response to data in EFFECT and program returns to Overlay (0,0).

(e) If there are deposits, a check is made for their presence both prior to and after the exposure.

(f) If deposits are present only prior to the exposure, the exposure has removed them. The appropriate changes in SURDES are entered and the program returns to (0,0).

(g) If deposits are present only after exposure, exposure has caused their formation. The layer structure is checked for consistency, then SURDES is modified and the program returns to (0,0).

(h) If deposits are present both before and after exposure, their constituents and percentage composition are equated to a set of local variables.

(i) The segment temperature is noted, the melting point of all deposit constituent and density-temperature coefficients are read in from TAPE3.

(j) The surface temperature is compared with the melting points of the deposit constituents. If all constituents are solids, no reactions will occur, and the following calculations are made.

1. The mass of each constituent is determined from the percent concentrations in the new and old deposits.

2. The masses of species present in both old and new layers are summed.

3. The total mass and the percent concentrations of all species are calculated.

4. The two most abundant species are identified (plus water, if present).

5. The identities and concentrations of the two most abundant species, plus the concentration of water, are stored in SURDES and EFFECT, and the program returns to (0,0).

(k) If at least one constituent is liquid, chemical reactions are possible. The species present are checked to see if there are any mutually reactive substances.

Allowed reactions are

N_2O_4 + any base \rightarrow base nitrate

HN_3 + any base \rightarrow base nitrate

$HCL/HCL \cdot aq + NH_3/NH_4OH \rightarrow$ ammonium chloride

N_2O_4 + water \rightarrow nitric acid

Displacement reactions and redox reactions are not allowed.

(l) If no reactions can occur, the calculations summarized in (j) 1 to 5 are carried out.

(m) If reactions are possible, the following calculations are made:

1. The mass of each constituent present is determined.
2. Identical species are identified and their masses are summed.
3. Using a table of allowed reactions and their priorities, the following calculations are made:

The equivalent concentrations of the reactive species are calculated.

It is assumed that the reaction goes to completion. The final concentration of the reactant in excess is calculated.

The product is identified and its concentration is calculated.

(n) The remaining reactants are checked in a return to steps (k) through (m).

(o) After all reaction calculations have been completed, the program steps to the routines described under (j).

(p) The information on deposit species and concentrations is stored in condensed fashion by octal masking to reduce array size requirements.

Program P4270 calls Subroutines A, FAULT, REPLACE, LE, RETRH0 and MN03.

(2) Subroutine MNØ3

This subroutine checks whether more than one type of base nitrate is present, and if such are detected, they are combined as the mixed fuel nitrate deposit species.

Subroutine MNØ3 calls Subroutine A.

(3) Subroutine REPLACE

This subroutine is used to move the structural and deposit layers in array SURDES upward or downward when this is required because of removal of a layer or formation of a new deposit.

Subroutine REPLACE calls Subroutine A.

l. Overlays (11,0) to (11,2)

Overlays (11,0) to 11,2) are called at this time. See their descriptions in Section D. 3. i.

m. Secondary Overlay (10,2)—Program P42102

This program checks whether the post exposure conditions input in Program P4240 are to be used as the base condition prior to further exposure calculations, or that they should be discarded and the initial conditions reinstated. The flag ISTST is used. This is read from TAPE9(=CDATA), and then NAMELIST NAST5 is checked for any changes. If ISTST is zero, the initial conditions are to be used, and they are brought back in from TAPE4, where they were stored during operation of P4240. If ISTST is greater than zero, the data on TAPE4 are ignored and the program returns to (0,0).

Program P42102 calls Subroutine A.

n. Primary Overlay (5,0)

The sequence of routines called in this region of the program calculate the effects of plume exposure on the satellite exterior. The sequence includes calls to Overlays (7,0), and (11,0) to (11,2), all previously described.

The primary and secondary level 5 overlays will be described first, then the associated subroutines. Following these will be other primary overlays which are used.

(1) Program P4250

This overlay controls the sequence of calculations for plume exposure effects and performs basic calculations related to the timing of the events. The program expects to find information about the plume, supplied by TCC or KINCØN on TAPE30. It first checks for the thruster "on" time, TØTIME, the selected time increment, DELTIME, and the ID number of the

thruster which is operating, NTR. If these values are not found on TAPE30, the data input in Overlay (0,0) supplies TØTIME, and TAPE10(=DDATA) is read for DELTME. Then, NAMELIST NAST8 is checked for updated values of TØTIME and DELTME. If no value for TØTIME is supplied, the run is terminated after printing an appropriate message. If DELTME is not supplied, a default value is used.

The number of calculation cycles, NUMCYC, is determined by the relation

$$\text{NUMCYC} = \text{TØTIME} / \text{DELTME}.$$

Preliminaries being completed, the clock is started:

$$\text{TIME} = \text{TIME} + \text{DELTME}$$

where TIME was previously equal to zero.

Data on the plume configuration is now required from KINCØN.

*The first data needed are the latus-rectum of the plume, assuming it has a paraboloid shape. A tape is made upon which is listed each time interval and a zero value of P, which is one-fourth the latus rectum at that time. This is written out on TAPE 31.

*The program later reads TAPE31, expecting to find nonzero values for P. If P is found equal to zero, and there was no previous P, the program reads DDATA for a value of P.

If a previous value for P exists which was not supplied by TAPE31, DDATA is read to find DELP, which is the change in P per time increment, unless DELP has already been input.

*A check is also made to be certain that a value for NTR was read in from TAPE30 earlier. If the value of NTR is zero, a value is read from DDATA (TAPE10).

If the calculation is in the first exposure cycle it is assumed that the available value of P corresponds to the current plume shape. When DELP has been input, implying that SURFACE must calculate the plume shape, the change in P for each subsequent cycle is calculated at the end of the calculations for the current cycle, as described later.

The thruster location is read from storage, using the thruster ID number, NTR, as the key.

The next step is to determine which segments of the satellite surface are impinged by the plume, knowing the thruster location and plume configuration. Program P4251 (Overlay (5,1)) is called in to do this calculation, and the results are stored in the Array AFFSEG (affected segments) and listed in the Output. The program will actually accept several inputs of P and NTR and calculate and list the plume-surface intercepts. If this feature is used, the program assumes that the last such input is the one to be used for calculation of plume effects.

Because KINCØN and upstream subprograms use a coordinate system based on the thruster, and do not relate to the satellite on which the thruster is mounted, routines to transform coordinates from thruster-based systems to satellite-based systems and vice versa are needed. These are available in Overlays (5,2) and (5,3). Because the transformation requirements may vary from run to run, there is a flag, ITRNCL, which selects the needed routines. If ITRNCL is negative, only satellite-based to thruster-based are computed; if ITRNCL is zero, none are computed; if ITRNCL = 1, both types will be run, and a value of 2 limits the calculations to thruster-based to satellite-based. The value of ITRNCL is tested; if zero, a new value is sought on TAPE10. Note that input of a 'new' value of zero is allowed.

For demonstration or testing purposes of thruster-to-satellite based coordinates, TAPE10 is read to provide a thruster ID number and an index equal to number of locations which will be transformed in the demonstration.

Then the thruster based coordinates are input from TAPE10, and Overlay (5,2) = Program P4252 is called to calculate the transformations. On return, the results are listed. Then a check is made for further requirements for these transformations. When completed the program moves to the inverse calculation, if it is required.

Here, the data in AFFSEG on actual plume-satellite intercepts are used for the calculation, done by calling in Overlay (5,3) = Program P4253. Again, the results are listed.

At this point, NAMELIST NAST4 is checked for changed value assignments for P, DELP and NTR.

*When the above sequences are completed, if a set of P values at different times are available from KINCØN, as discussed earlier, then TAPE31 is read at each time interval to find P, and Overlays (5,1) and (5,3) are called, and the thruster based coordinates for all affected segments are determined at each time interval, and immediately written out on TAPE32. This procedure is done until all the affected segment locations for time slices have been written to the file.

*The file Tape 32 is actually an enquiry sent to KINCØN: the program will expect to get data on the plume characteristics for each location and time interval on TAPE14 when overlay (12,0) is processed downstream.

The program then checks SURDES to determine whether the surface temperature has changed since the last time cycle, and calculates a new average temperature. Those material properties for structural and previous deposits which affect further plume-surface interactions are identified, and the current values, as determined by the surface temperature, are calculated in Overlays (5,4), (5,5), and the final steps in this primary overlay. Representative listings are made and then the program returns to the principal (0,0) Overlay.

Subprogram SURFACE, because of its core size requirements, has been modified to run independently of the remainder of CØNTAM, instead of in conjunction with the other subprograms under the control of

the CØNTAM executive. All portions of SURFACE which were designed to communicate directly with other CONTAM subprograms have been rendered inoperative. They are still present in the program, but they have been changed to CØMMENT cards. These inactive portions can be found at the following locations:

Overlay (5,0) - Program P4250

Cards 250 to 261
Card 268
Cards 302 to 326
Card 349
Cards 571 to 582

Overlay (12,0) - Program P42120

Cards 207 to 219

Overlay (13,0) - Program P42120

Cards 147 to 159

The descriptive paragraphs above which have been marked with an asterisk do not apply when this modification is in effect.

Because direct automatic communication between SURFACE and other subprograms of CØNTAM is now impossible, the execution of SURFACE has been modified to facilitate indirect, manual communication. This has been done by setting up three modes of operation, with the mode controlled by data in the physical punched card file INPUT (TAPE17) of the control flag STPFLG (an integer).

If STPFLG = 0, the program runs as a complete unit. Default data on plume characteristics for calculating impingement effects is read from input file EDATA (TAPE11). Note that if the currently deactivated interprogram communication routines are reactivated, plume characteristics data from other subprograms will be read from file TAPE14, and EDATA will be ignored.

If STPFLG = 1, the program runs only as far as calculation of the plume-satellite intercepts in Overlay (5,0). At this point, all data in Common and variable storage is copied to file TAPE30 and TAPE30 is confirmed, the coordinates of the intercept locations are calculated in terms of the thruster based coordinate system and listed. Then the program stops. Note that TAPE30 must have been established as a RESERVE physical tape or a common or permanent disc file because the data stored on it will be required in the third mode of operation.

The listed output data on the coordinates of plume-surface intercepts are used to determine the characteristics of the plume at these locations by some manual method of interrogating the other program in CØNTAM. These characteristics are then coded into punched cards in the format described for

file EDATA (see Section D. 4. n) and this punched card file is input to replace the default file which is currently supplied with the program. If all data inputs being used in the form of physical cards, the EDATA decks are exchanged. If the data input are card images on magnetic tape or disc, the file corresponding to default EDATA is not copied from the master file (SKIPF, fid, 1, 17, B. is inserted in the control card file where appropriate) and the new card deck is copied to disc by use of the control card COPYBR, INPUT, EDATA.

If STPFLG = 2, SURFACE reads the stored values of Common and variable storage from file TAPE30, then resumes execution in Overlay (5, 0) at a location immediately following the location of the STOP in the second mode. When plume characteristics information is required for calculations (Overlays (12, 0) and (13, 0)), the data will be sought on file EDATA; presumably the program will find the data prepared manually as described above.

Program P4250 calls Overlays (5, 1), (5, 2), (5, 3), (5, 4), and (5, 5) and subroutines A, FAULT, and C.

(2) Secondary Overlay (5. 1)—Program P4251

This program calculates the intercepts of the thruster plume with the surface of the satellite and with projections from the surface as a function of the plume configuration. The location of the center point of each segment is the reference point for the calculation; if the center is on or inside the plume boundary, the whole segment is assumed to be affected by the plume.

The method is based on the calculation of the intercepts of two circles, the planar cross sections of the satellite and plume. Each segment is tested to see if it is "inside" the boundaries of the plume by the following sequence of steps:

1. The segment x coordinate is checked to ascertain that it is aft of the thruster.
2. The radius of the plume is calculated at a position corresponding to the x coordinate of the segment:

$$R = \sqrt{2 p (x - a)}$$

where a is the x coordinate of the plume vertex.

$$AR = \text{SQRT} (2. * P * (SR2 - TX))$$

3. The plume radius is checked against the thruster standoff and the local satellite radius to see if the plume contacts the satellite surface.
4. The limits of plume contact with the satellite on either side of the line joining the satellite and plume central

axes are calculated as angular displacements from that line.

Plume contact limit angle = $\cos^{-1} \left(\frac{(\text{Thruster offset})^2 + (\text{Satellite Radius})^2 - (\text{plume radius})^2}{2(\text{Thruster offset})(\text{Satellite Radius})} \right)$

$$ALP = \arccos \left(\frac{TR^2 + SR^2 - AR^2}{2 \cdot TR \cdot SR} \right)$$

5. If the diameter of the plume is so large that it impinges beyond the midline of the satellite, the impingement is limited to the midline.
6. The θ coordinate of the segment is tested to see if it lies in the range defined by the θ coordinate of the thruster plus/minus the plume contact limit angle.
7. If the segment meets the above tests, its ID is entered into the array AFFSEG (affected segment).

An analogous computation is used to find projection segments impinged by the plume; the intercept calculated is that of a paraboloid with a plane at a known angle to the axis of the paraboloid.

Program P4251 calls Subroutines A, FAULT, and LT.

(3) Secondary Overlay (5,2) - Program P4252

This routine, called from Overlay (5,0), transforms the coordinates of any point reported in cylindrical coordinates based on a specified thruster to a cylindrical coordinate system based on the satellite.

If X_S , R_S , and θ_S are the required satellite-based coordinates of the point, and Z_T , R_T , and θ_T are the known thruster-based coordinates of the point, with the thruster coordinate Z parallel in 3-space to the satellite X , and if the satellite-based coordinates of the origin of the thruster-based system are X_O , R_O , and θ_O , then the transformation equations are:

$$X_S = X_O + Z_T$$

$$R_S = \sqrt{2 \left(R_O^2 + R_T^2 + 2 R_O R_T \cos(\theta_O - \theta_T) \right)}$$

$$\theta_S = \tan^{-1} \frac{R_O \sin \theta_O + R_T \sin \theta_T}{R_O \cos \theta_O + R_T \cos \theta_T}$$

Program P4252 calls Subroutine A.

(4) Secondary Overlay (5, 3) = Program P4253

This routine is the converse of P4252, and calculates thruster-based coordinates of a point from the satellite-based coordinates.

If X_S , R_S and θ_S apply to the satellite system

X_O , R_O and θ_O are the origin of the thruster in the satellite system

Z_T , R_T and θ_T are the required thruster-based coordinates

$$Z_T = X_S - X_O$$

$$R_T = (R_S^2 + R_O^2 - 2 R_S R_O \cos(\theta_S - \theta_O))$$

$$\theta_T = \tan^{-1} \frac{R_S \sin \theta_S - R_O \sin \theta_O}{R_S \cos \theta_S - R_O \cos \theta_O}$$

The program uses data in AFFSEG for impinged segments as the source of X_S , R_S , and θ_S .

Program P4253 calls Subroutine A.

(5) Secondary Overlay (5, 4) = Program P4254

This program supplies physical and mechanical properties of structural and deposited materials which are needed to calculate the effects of impingement by the plume. The properties are corrected to the current surface temperature if the temperature factors have been input.

The methods for calculation deposit properties are those discussed earlier in Overlay (2, 0). The properties of interest for deposits are the enthalpy of the deposit and of the vapor, the enthalpy of deposition, the specific gravity, the viscosity, and the surface tension.

The materials properties at the specific temperature are evaluated by using the temperature coefficients for the equation:

$$\text{Property Value}_{(T)} = A + BT + CT^2 + \frac{D}{T} + \frac{E}{T^2}$$

The coefficients have been entered in the input array MATERIAL and stored on TAPE1. The properties of interest are the melting point, Vickers hardness, bulk modulus, surface energy, heat capacity, and thermal conductivity.

If temperature coefficients are not available, room-temperature data are used.

The properties data are stored in the array SEARCHD and buffered out on TAPE19.

Program P4254 calls Subroutines A, FAULT, IRNDR, RETRØD, RETVIS, RETRHØ, and HCØNT.

(6) Secondary Overlay (5, 5) = Program P4255

This program changes the values of the constants in the abrasion rate in response to temperature changes on the surface.

A temperature factor is calculated by the equation

$$\text{Factor} = 1 - 0.25 (\text{Surface Temperature} - 520) / 520$$

This factor is also applied as follows:

$$\text{Upper Velocity Limit}_T = \text{Lower velocity limit}_0 \times (\text{Factor})^{1.2}$$

$$\text{Hyper Velocity Limit}_T = \text{Upper velocity limit}_0 \times (\text{Factor})^{1.25}$$

$$\text{Lower Velocity Limit}_T = \text{Lower velocity limit}_0 \times (\text{Factor})^{0.8}$$

These formulas were devised for this program from available data; no such formulas were found in the literature. The lower velocity limit figure is related closely to the effect of temperature on hardness and surface energy.

The modified values for the upper and hypervelocity limits are stored in VUP1A and VUP2A. The lower limit is placed in SKRPTE (I, 3), other SKRPTE constants are passed to SKRPTE unchanged.

Program P4255 calls Subroutine A.

(7) Subroutine LT

This subroutine tests the total number of segments impinged by the plume against the maximum the program can handle, which is 50.

If more than 50 have been identified in Program (5, 1), this subroutine truncates the number to 50 and stops the calculation of affected segments. A message is printed warning of the truncation.

Subroutine LT calls Subroutine A.

o. Primary Overlay (12, 0) = Program P42120

This program is designed to acquire data about characteristics of the plume at the locations on the satellite where Program P4250 calculated that impingement occurs. The primary data input occurs on TAPE14, which

is supposed to have been written by KINCØN in response to TAPE32. If data are not available on TAPE14, there is a default to reading data from cards (file EDATA = TAPE11). These default data are then stored on TAPE14.

The data required consist of the following:

Diameter of Small Droplets (from condensate)	=	PLMCHR(1)	=	SPRPDM
Diameter of Large Droplets (from incomplete combustion, etc.)	=	PLMCHR(2)	=	LDRPDM
Velocity of SD	=	PLMCHR(3)	=	SDVEL
Velocity of LD	=	PLMCHR(4)	=	LDVEL
Angle of Impingement, SD	=	PLMCHR(5)	=	SDAIMP
Angle of Impingement, LD	=	PLMCHR(6)	=	LDAIMP
Flow Velocity, SD	=	PLMCHR(7)	=	SDMAPS
Flow Velocity, LD	=	PLMCHR(8)	=	LDMAPS
Plume Concentration for 25 mass fraction species of plume constituents	=	PLMCHR(9)	to	(33)
	=	PMCMP (1)	to	(25)
Chemical Composition of Small Drops, Species	=	PLMCHR(34)	to	(52)
		by 2's	=	SDCMP
		(1, 1) to (10, 1)		
Concentration	=	PLMCHR(35)	to	(53)
		by 2's	=	SDCMP
		(1, 2) to (10, 2)		
Chemical Composition, LD, Species	=	PLMCHR(54)	to	(72)
		by 2's	=	LDCMP
		(1, 1) to (10, 1)		
Concentration	=	PLMCHR(55)	to	(73)
		by 2's	=	LDCMP
		(1, 2) to (10, 2)		
Plume Temperature		PLMCHR(84)	=	PMTMP
Plume Pressure		PLMCHR(85)	=	PMPRS
Plume Density		PLMCHR(86)	=	PMRHØ
Plume Viscosity		PLMCHR(87)	=	PMVIS

(Unused at present, PLMCHR(74) to (83) and (88) to (90).)

These data are required for each impinged segment and each time slice. If data are not input for certain time intervals or segment locations, the program will use data for an earlier time segment or a lower segment number of both.

Program P42120 prints a listing of representative plume characteristics.

Program P42120 calls Subroutines A, FAULT, and D.

P. Primary Overlay (13,0)

(1) Program P42130

This program and its subroutines calculate the results of the plume-surface interaction in terms of surface abrasion, condensation on the surface from plume vapors and deposition on the surface of plume-carried droplets.

A simplifying assumption is made--if the conditions of the plume as it impinges a satellite segment lead to abrasion, neither deposition nor condensation can occur during the same time element on the same segment.

The primary overlay buffers in the data required for calculations and storage then it calls subroutine RANDAL to perform the surface effect calculations. RANDAL in turn calls MADDY and ROBERT.

If deposition or condensation occur, it is necessary to calculate the results of chemical interactions between depositing species, and between new and previous deposits. When this is done, data are stored, a flag called MCFLG is set and a return is made to the principle overlay for calls to Overlays (15, 0) and (7, 0) which perform the chemical calculations. When these two routines are finished, the flags cause (13, 0) to be recalled and the computation reenters at the location from which the return to (0, 0) was made. This sequence is necessary due to the core size requirements of (13, 0), (7, 0) and (15, 0). The latter two cannot fit in as secondary overlays to (13, 0).

Calculations are performed for all segments during a single plume operating time element. Then the total time (sum of all time elements computed) is compared to the thruster duration. If they are equal, the exposure is complete and the programs prints a note of this and returns to (0, 0) for calculation of the surface state. If the exposure has not reached completion, the program checks to see if the plume characteristics input was from cards or from KINCØN. A check is also made as to whether there will be a change in the plume configuration in the next cycle. Depending on the source of the data and the shape of the plume, the flags JMP2 or JMP3 are set and a return is made to (0, 0) to get the data needed for the next time element.

The main overlay calls in Overlay (5, 0 et seq) for input from KINCØN or if there is no change in plume geometry for card data input, the calculations go to (5, 4) and (5, 5) and the last part of (5, 0) to set up the current surface mechanical conditions before redoing the plume effects. If

the plume configuration changes (for card input), Overlays (5, 1) and (5, 3) are called to calculate the new set of affected segments, then the surface mechanical conditions are determined. The program then returns to (0, 0). If there are new segments affected, the calculation calls in P42120 to check for new card data on plume characteristics, then returns to (0, 0). In either case, P42130 is then recalled to calculate the plume effects during the next time element.

Program P42130 calls (in effect) Programs P4250, P4270, and P42150, and Subroutines A, FAULT and RANDAL.

(2) Subroutine RANDAL

This routine calls in information from TAPE12, TAPE14, and TAPE19 on the properties of the plume, the surface, and the current state of the surface. The plume characteristics are loaded to the variables described under Overlay (12, 0).

The calculations of the effects of the plume on the segment surface are then initiated.

The first step is calculations of the abrasion wear, using the fatigue wear term from the Nielson-Gilchrist equation (Reference D-2).

$$\text{Wear} = (\text{Time slice})^2 * \text{Particle flow concentration (lb/sec)} \\ \times (\text{Particle velocity (impingement angle} \\ - \text{correction factor)})^2 / (\text{Wear constant (1/lb)} \\ \times (\text{Velocity/Velocity constant}) \text{Wear exponent})$$

The wear for the two particle sizes is summed, and the abrasion depth is calculated by dividing by the area.

The abrasion depth is then compared with a standard value, which was either input to the program, or the default value of 10⁻¹⁰ inches. If the depth worn away is less than this value, it is taken as negligible, and the program turns to calculating deposition and condensation by means of a call to Subroutine ROBERT.

If abrasion is sufficient, the surface finish resulting from the abrasion is calculated, based on the assumptions:

(a) The surface roughening due to contact by a drop is proportional to the drop radius and a stepped function of the drop velocity.

(b) Once a local region has been roughened by an impact of certain size and velocity, additional impacts of similar size and velocity do not cause additional roughening.

(c) The probability of impact by a droplet is independent of the previous history of the surface location.

From these assumptions and the data on the plume characteristics, the final finish is calculated as follows

SURFIN = Roughening factor = drop diameter
 If velocity is greater than upper velocity limit,
 roughening factor = $2.5 * \text{diam}$
 If velocity is greater than hypervelocity limit,
 roughening factor = $5 * \text{diam}$

The total mass of droplets per second per unit plume area (perpendicular to the plume):

(PIMP) = Mass/second-ft² * time slice.

The area of the segment impacted:

(AIMP) = PIMP * π * drop diam. * Cos (impingement angle)

The fraction of the segment area impacted:

(FAMP) = AIMP/Segment area

The final finish is then:

Area * Old Finish * (1 - FAMP (small) - FAMP (large)
 + FAMP (small) * SURFIN (small)
 + FAMP (large) * SURFIN (large)

After determining the surface resulting from abrasion, a call is made to a special entry in Subroutine RANDAL (CALL TYLER) to set up the cycle through Overlays 15, 0 and 7, 0 which determine the chemical effects of the abrasion.

As mentioned earlier in this section, if abrasion is not significant, condensation from plume vapors is calculated in Subroutine ROBERT. After the return from ROBERT, the present subroutine, RANDAL calculates the extent of deposition of material from droplets in the plume.

The weight deposited is proportional to the ratio of the difference between the droplet velocity and the lower limit divided by the velocity lower limit. This velocity ratio, multiplied by the droplet concentration, the time, and the sine of the impingement angle, provides the mass depositing. Separate calculations are made for the large and small drop distributions. After each a call is made to subroutine MADDY, where the composition of the deposit is determined from the plume characteristics data, followed by the CALL TYLER route to (7, 0) and (15, 0) to calculate the chemical composition of the deposited layer.

The routine sets some counters for use by overlay (13, 0) and returns to (13, 0).

Subroutine RANDAL calls subroutines A, FAULT, RØBERT, and MADDY and the special entry TYLER to RØBERT.

(3) Subroutine MADDY

The subroutine looks up the data on droplet composition and calculates the mass of each species deposited, then selects the 4 (or 5, if water is one of the deposits) most abundant species and enters their ID numbers and masses into CØMMØN/10/for use by Overlays (7, 0) and (15, 0) in calculating the final composition of the deposits.

Subroutine MADDY calls Subroutine A.

(4) Subroutine RØBERT

This routine calculates the condensation of plume constituents from the plume vapor onto the satellite surface. The relations used assume an identity of heat transfer and mass transfer processes. Because of this, mass transfer coefficients are not required; heat transfer coefficients are sufficient.

The discussion by Trebal upon which this algorithm is based assumes only one species condenses (or evaporates) although the equations are generalized for an indefinite number of species. However, the degrees of freedom are too great for the number of data for the plume, so the simplifying assumption has been made that each condensable species acts independently of all others during all steps of the process. Only at the end, when the temperature of the condensed film of each substance is calculated, are mutual effects considered. After a film temperature for each species is obtained, the various temperatures are averaged, and this average is used for the final cycle of deposit quantity calculations. For certain species, not all of the data needed for calculation of deposition is available. Certain factors, such as liquid viscosity, are hard to obtain for species such as carbon. The program maintains running averages of certain variables, and these are available as approximations when specific data are not supplied or calculable.

In the first step, the molecular diffusivity of each species at the plume temperature is calculated from the boiling point, molecular radius, molecular weight, plume temperature and pressure, and a collision function. The calculation assumes that the species being treated exists in an environment of nitrogen gas--none of the other condensable species are part of the calculation.

The mean specific heat and the mean molecular weight of the plume are calculated from those properties of the plume constituents and their concentrations. The plume viscosity is also calculated if not supplied by KINCØN, by calculating the viscosity of each species at the plume temperature and correcting the nitrogen viscosity for the species at their concentrations.

The plume Reynolds number is then derived

$$REN\phi = \frac{\text{Plume velocity} * \text{Plume density} * 3600}{\text{Mean molecular weight} * \text{Plume viscosity}}$$

in which a characteristic length of 1 foot is assumed, as appropriate for typical satellite dimensions.

The coefficient of mass factor $C\phi FMT$ is calculated from the Reynolds number, using the vertical plate correlation, with corrections for the angle of impingement. The data used to derive the equations are found in the ASHRAE guide and Data Book and the ASHRAE Handbook of Fundamentals.

The Prandtl number of the plume is calculated as

$$PRNDT = \frac{\text{Plume specific heat} * \text{Plume Viscosity} * 3600}{17593}$$

The Schmidt number for each species is calculated from the formula

$$SCHMDT = \frac{\text{Viscosity of } N_2}{\text{Plume density} * \text{Species diffusivity}}$$

and then used to determine the formal mass transfer coefficient, ZLS , for each species

$$ZLS = \frac{3600. * C\phi FMT * \text{Plume Velocity} * \text{Plume density}}{\text{Mean Molecular Weight}} * \left(\frac{1}{SCHMDT} \right)^{2/3}$$

where $C\phi FMT$ is a mass transfer factor calculated from the Reynolds number and the angle of impingement,

$$C\phi FMT = \frac{(1 + 0.07 \sin(\text{impingement angle}) * 0.664}{REN\phi}$$

The heat transfer coefficient of each plume species is calculated and the values are summed. The relation used is

$$\frac{\text{Plume Velocity} * \text{Plane Density} * \text{Specific Heat} * \text{Mole Fraction} * \text{Mass transfer coefficient}}{\text{Schmidt}^{2/3} * \text{Prandtl} * \text{Mass flow rate}}$$

The rate of heat transfer into the satellite structure is then calculated. A thermal conductance is calculated on the assumption that existent deposits and coatings conduct toward the interior of the satellite, using input data thermal conductivities and known thicknesses. The bottom layer, usually aluminum, is assumed to conduct "radially" along the satellite surface, through one half of its area in contact with other segments, and the contacting segments are assumed to be at the prevailing satellite structure temperature.

It is then assumed that the species depositing from the plume will be at a temperature intermediate between the plume temperature and the satellite wall temperature. The temperature will be such that at the rate of condensation of condensing species, which is controlled by the vapor pressure of the condensing species at the film temperature, the heat input from cooling the species and releasing the heat of condensation must balance the heat flow into the satellite structure from the film temperature to the main satellite temperature.

To calculate this, a film temperature is assumed, and the deposition rate and hence the heat flux rates are calculated. If the heat flows do not balance, the temperature is corrected in the direction which will bring them closer to balance, and the process repeated until a balance is struck. This film temperature is stored, and the process repeated for all condensing species.

When all species have been calculated, the various film temperatures are averaged, and this mean value is taken as the most probable temperature. New deposition rates are calculated for each species at the mean temperature, and then the mass of each material and total quantity of heat deposited is calculated.

The data are stored for use by Overlays (7,0), (15,0) and (13,0).

Then flags are set, and the previously described return to (0,0) and calling of the chemical reaction overlays occurs. After (7,0) and (15,0) have been completed, the calculation returns to Subroutine RØBERT for wrap up and return to RANDAL.

q. Primary Overlay (15,0) = Program P42150

This program determines whether there are any chemical reactions which can occur between species currently depositing, and if such reactions are possible, calculates the products and their concentrations. It is a simplified version of Overlay (7,0); the latter also considers the reactions between new and previous deposits. The logic followed and the chemical reactions calculated are the same as in (7,0), but fewer checks, comparisons and calculations need to be made; see (7,0) for a description of the calculations and logic.

Overlay (15,0) calls Subroutines A, LE, FAULT, and MNØ3, and Function RETRHØ.

r. Secondary Overlay (10,1) = Program P42101

This routine calculates accumulated exposure time for the whole program after completion of each exposure cycle. It is for checking purposes after the calculations are all completed. It also sets the loop counter back to zero.

Overlay (10, 1) calls subroutine A.

s. This completes the sequence of calculation routines for plume exposure, which started with the initial call to (5,0), and the program returns to (0,0).

The next sequence is the calculation of space exposure effects. This is a simpler set of routines, because of the initial assumption that conditions external to the spacecraft remain constant at a pressure and temperature originally input in Overlay (14,0). It is important to note that although α and ϵ are known for the satellite, no accounting is made of radiant heat transfer to or from the satellite or of heat input to the satellite shell from internal processes. All temperature changes in the shell are assumed due to mass transfer processes on the satellite exterior. It is beyond the scope of SURFACE to include radiant and convective heat transfer, although the importance of such processes are acknowledged. There are a number of effective computer programs to calculate radiant heat transfer to and from satellites and the plume, space, the sun, and the earth, and it would be an important step to integrate CONTAM with such a program.

t. Primary Overlay (6, 0) = Program P4260

This program and its subroutine PATANN have the function of determining the effects of exposure to a space environment on deposits originating from plume exposure. The program does not consider the effect of space conditions on structural materials, even when it is known that such materials can change. The steps used are the following:

1. The array SURDES is screened for segments with deposits and all calculations are limited to such segments.
2. Chemical and physical chemical properties related to volatility are called in from TAPE3.
3. Surface heat loss by evaporation of volatile species must balance heat inflow from the satellite structure, resulting in an equilibrium surface temperature. These heat fluences are calculated in, the same fashion as is done for the evaporation of intra-thruster deposits in program TCC.
4. With the surface temperature established the rate of evaporation becomes constant.
5. The amount of material lost of each volatile species is calculated for each time slice.
6. The equations used are described fully in TCC. (See Appendix A.)

The assumption is made that drastic chemical changes are not likely to be caused by evaporation of volatiles, so it is unnecessary to calculate whether or not new chemical reactions can occur after each time slice. Instead, the complete space exposure is calculated in (6,0).

At the end of the exposure time, Subroutine PATANN is called to store the exposure results, then (6, 0) returns to (0, 0).

Overlay (6, 0) calls Subroutines A, FAULT, LE and PATANN, and function RETRHØ.

u. Following completion of the space exposure calculations, the main overlay calls in Overlays (7, 0) to check for chemical changes, then (11, 0 et. seq) use called to determine the current surface state, and finally (10, 1) is called to accumulate the total exposure time.

The main Overlay (0, 0) then sequences plume and space exposures until all instructions have been fulfilled. It then calls the termination routine.

v. Primary Overlay (16, 0) = Program P42160

This Overlay copies appropriate data from array SURDES to array EFFECT so that EFFECT contains the latest data for all segments. EFFECT is then copied to the PUNCH file in the same format as the input from CDATE in Overlay (4, 0). This allows the results from one set of calculations to be used as the initial conditions for a subsequent set.

w. Primary Overlay (10, 0) = Program P42100

This routine wraps up the program by printing a listing of the number of calls to all overlays and subroutines, the total exposure times accumulated, and a closing logo.

D.4 PROGRAM USER'S MANUAL

a. General

The SURFACE program is the fourth link of the CØNTAM computer program. It may be run as a subprogram to CØNTAM under control of subroutine EXEC, or as an independent program. It was developed on a CDC 6500 computer using FØRTRAN IV language. The SURFACE program requires 275,000 words of core storage. Conversion to another computer system should be straightforward, providing that sufficient core is available. Two subroutines written in the CDC assembly language CØMPASS are not essential to the program and can be eliminated readily.

b. Input Data Descriptions

Six named files plus the standard INPUT card file are used for basic formatted data input to SURFACE. Use of several files is necessary to allow a variety of sequences of exposure calculations, all of which require data inputs, without simultaneously requiring major reshuffling of the data input file whenever a different sequence of calculations is to be carried out.

The input files are identified as follows:

<u>External fid</u>	<u>Program (Internal) fid</u>
INPUT	17
ADATA	16
INDATA	5
BDATA	8
CDATA	9
DDATA	10
EDATA	11

In addition, when SURFACE is run under CØNTAM EXEC in conjunction with the other subprograms, unformatted data supplied from these programs are read from two files

<u>External fid</u>	<u>Internal fid</u>
TAPE31	31
TAPE14	14

If TAPE14 is not supplied, or if the data on it are incomplete, SURFACE generates a complete set of data and stores it on TAPE14 for later use. The input file DDATA is used instead of TAPE31 when SURFACE is run without the other CØNTAM subprograms.

Data statements are used for some values, but they are primarily initializations to zero or else default values.

c. Data Categories

The following inputs are the major categories required for SURFACE:

Propellant Properties and Thrustor Characteristics

External Materials

Satellite Configuration

Projection(s) Configuration(s)

Structural Materials

Propellant Temperature (Test Case)

Optical/Thermal Properties

Segment Structure

Program Option Selection

Modified Surface Conditions (Test Case)

Program Option Selections

Pulse Characteristics
 Program Option Selection
 Coordinate Transformation
 Thruster to Satellite
 Satellite to Thruster
 Molecular Weight
 Wear Constants
 Plume Characteristics
 Velocity Limits
 Heat Transfer Coefficients
 Plume Physical Properties
 Plume Configuration Change

d. In the following sections, the inputs and their functions are described, the input format is given where required, and typical inputs are illustrated. The order of presentation in this manual is DATA statements, program ASSIGNMENT statements, and then the input files in the order in which they are listed in the two tables in (b). Note that this order for the files is not necessarily in the same order in which the program will access the files, because the latter is determined by the data themselves.

e. DATA Statements

Only data which are used in computation are presented. Data used for variable FORMAT statements, Hollerith data, control of files and buffers, and program sequencing etc., are omitted here.

<u>Variable</u>	<u>Use</u>	<u>Initial Value</u>
LINK 0, 0		
ACP(I), I = 1, 25	Constant in denominator of Calingaert-David equation	43.
PI	Trigonometric calculations	3.141592
R	Universal Gas Constant	8.31436×10^7
CMETL	Convert inches to centimeters	2.540005
CMETA	Convert square inches to square centimeters	6.4516258
CMETV	Convert in ³ to cm ³	16.387162

<u>Variable</u>	<u>Use</u>	<u>Initial Value</u>
CMETM	Convert pounds mass to grams	453.5924
CMETF	Convert pounds force to dynes	444822.
CENTCG	Convert cal/gm to Btu/lb	1.8
CMETP	Convert psia to millibars	6.8947×10^4
CRAD	Convert degrees of arc to radians	0.0174532925
CKTR	Convert Kelvin to Rankine	1.8
CSGTED	Convert specific gravity or g/cc to lb/ft ³	62.427961
CVPTE	Convert poise to lb(m)/ft-sec	6.72×10^{-2}
CSTTE	Convert dyne/cm to lb(m)/in	5.71015×10^{-6}
TØTIME	Duration of plume or space exposure cycle (sec)	0
L		0
DELTMA	Duration of pulse slice used in computation	0
EXTYPE	Type of exposure	0
	<u>Values</u>	<u>Meaning</u>
	-1	End of program
	0	Initial conditions
	1	Assigned conditions
	2	Plume exposure
	3	Space exposure
IPXCT	Number of plume exposure cycles completed	0
ISXCT	Number of space exposure cycles completed	0
P	Quarter latus rectum of plume	0
DELP	Change in P for next time slice	0
ITRNCL	Flag to control type of coordinate transformations to be computed	0

<u>Variable</u>	<u>Use</u>	<u>Initial Value</u>
IF6	Flag to control listing of initial conditions data	6

IF6 = 6 lists all data
IF6 = 7 stops listing of initial conditions

SUBROUTINE WEBBER

REDPRP(I), I = 1, 2500	Initialize <u>REDUCED</u> <u>PROPERTIES</u> array	-1.
------------------------	--	-----

LINK 2, 0

A	{ Variables used as parameters for identification of materials in call to VISEST }	0
B		0

LINK 6, 0

SURH(I), SURI(I), I = 1, 20	Initial zero values for variables used to carry coded thickness of deposits for listing	20*6
-----------------------------	---	------

Typical DATA assignments are shown in Figure D-5.

f. Assignment of Constant Values to Variables

<u>Variable</u>	<u>Use</u>	<u>Assigned Value</u>	<u>At Card</u>
LINK 0, 0			
STPFLG	Controls mode of execution of SURFACE	0	0/0.770
	<u>Value</u> <u>Effect</u>		
	0 Run complete program.		
	1 Stop after calculating plume intercepts.		
	2 Start at location immediately after above stop.		
NTR	ID number of thruster currently operating	0	0/0.842
IGOTST, IPXTST, ISXTST	Total number of all cycles, plume exposure cycles and space exposure cycles, respectively.	0	0/0.845, 847

DATA PI/3,141592/,R/8.31436E7/,CMETL/2,540005/,CMETA/6.4516258/ 0/0 641
DATA CPETV/16,387162/,CMETH/453,5924/,CMETF/444822./,CENTCG/1,8/ 0/0 642
DATA CMETR/6,8947E4/,CRAD/,0174532925/,CKTR/1,8/,CSGTED/62,427961/0/0 643
DATA CVPTE/6,72E-2/,CSTTE/5,71015E-6/ 0/0 644

Figure D5. Typical DATA Assignments

<u>Variable</u>	<u>Use</u>	<u>Assigned Value</u>	<u>At Card</u>						
RDWRT	Flag to allow/stop listing of NAMELIST correction inputs	1	0/0.941						
	<table><tr><th><u>Value</u></th><th><u>Effect</u></th></tr><tr><td>0</td><td>No listing</td></tr><tr><td>1</td><td>Listing produced</td></tr></table>	<u>Value</u>	<u>Effect</u>	0	No listing	1	Listing produced		
<u>Value</u>	<u>Effect</u>								
0	No listing								
1	Listing produced								
NPIS	Total cycles to be calculated; reset to maximum value of 10 if data input would result in a greater value.	(10)	0/0.969						
TIME	Time since start of latest exposure cycle calculation. Set to zero prior starting the cycle	0.0	0/0.1028						
I6F	Resume listing of results from calculations if currently turned off. I6F is the "unit number" for certain write statements. If set to 7, listing is turned off.	6	0/0.1125						
NØJ	Used in GØ TØ NØJ statement in certain sub-routines and overlays to cause jump back to statement 231 in Link 0,0	ASSIGN 231	0/0.1218						
	LINK 1,0								
DEDPH	Default value for lower limit for effective deposit depth	(1 x 10 ⁻⁹ in)	1/0.306						
SURDES(I, 7)	Default value for surface temperature	529.2K	1/0.668						
	LINK 14,0								
DATA(119)	Default value for thermal conductivity of liquid N ₂ Ø ₄	6 x 10 ⁻⁴	14/0.627						
DATA(139)	Default thermal conductivity of MMH	0.279 x 10 ⁻⁴	14/0.657						
DATA(140)	Default accommodation coefficient for boiling deposit	0.1	14/0.659						

SCRPTE(I, 3), I ≤ 25	Default value for velocity lower limit for structural materials	400	14/0.1160
SCRPTE(I, 3), I > 25	Default value for velocity lower limit for deposits	650	14/0.1163
SCRPTE(I, 4)	Default value for wear rate exponent	-3.19	14/0.1164

LINK 7,0

Starting at Statement Numbers 1460 (Card 7/0.789) arbitrary factors for calculation of final surface finish are assigned on the basis of surface temperature, deposit thickness, and deposit melting point. No good general method to calculate these factors is available.

Starting at Statement Numbers 1670, (Card 7/0.941) and at 1720 (Card 7/0.969) the variables ACIDR and BASER are assigned constants which depend on the specific acid and base for which calculations are being made. The values assigned to ACIDR and BASER are the equivalent weights of the acid and base.

Starting at Statement Number 1910, (Card 7/0.1078) the molecular weights of the products are assigned to the variable PRØD.

LINK 15,0

Identical equivalent weight and molecular weight assignments to those in Link 7.0 are made starting at Statement Numbers 600, 625, and 710. (Cards 15/0.501, .529, and .638, respectively)

Subroutine TRANS

At several locations, the amount of energy transmitted through transparent interfaces is assigned for cases where measured values are not available. Transmittance values of 0.96 are assigned for all cases except for infrared and visible light from vacuum to condensed phase, which is assigned a value 0.98.

g. Punched Card Input to File TAPE17 = INPUT

This data input is primarily a set of NAMELIST inputs for supplying a few changes to the standard data inputs. The latter are normally resident as card images on a set of files, and if only a few changes are required it is often easier to use this NAMELIST capability rather than change the basic data files. See Section D-3.g for a description of the eight NAMELIST's used. When NAMELIST input is to be used, the card SWITCH,1. should be included in the control deck.

The card file is also used input the Mode Control flag, STPFLG, which is described in Section D.3.n.(1).

The card file deck should be arranged with the STPFLG card first, followed by the NAMELIST cards in any order. STPFLG must be present for the program to run.

Note that Link (2, 1) of SURFACE actually reads in the NAMELIST portion of the INPUT file as a unit, and then stores it unchanged on TAPE18. The links which use NAMELIST read from TAPE18.

<u>Variable</u>	<u>Read Format</u>	<u>Notes</u>
STPFLG	10X, I5	Values of 0, 1, 2 are accepted (Negative values are treated as 0)
	NAMELISTS	Standard CDC NAMELIST formats with \$ in column 2 at start, etc., are used.
NPIS1	NAST1 (Called in 0, 0)	Corresponds to NPIS, the total number of exposure cycles to be calculated. Maximum value is 10.
NPSEQ1(I, J)	NAST1	Corresponds to NPSEQ and details the exposure details. Maximum value of I is 10, of J is 3. NPSEQ1(I, 1) is cycle number (I, 2) is type of exposure (I, 3) is exposure duration
ISXTS1	NAST1	Corresponds to ISXTST, the total number of space exposure cycles
IPXTS1	NAST1	Corresponds to IPXTST, the total number of plume exposure cycles
IGØTS1	NAST1	Corresponds to IGØTST, the total number of cycles, including initial set up and assigned exposure conditions
IIS1	NAST2 (Called in 4, 0)	Corresponds to IIS, the number of affected segments on the satellite. The maximum value is 175.
EFFEC1(I, J)	NAST2	Corresponds to EFFECT(I, J) I is IIS J corresponds to the particular condition to be entered, its maximum value is 11. It is used as follows: J = 1 is Segment X Coordinate 2 is R coordinate 3 is Ø coordinate 4 is segment ID 5 is temperature 6 is top layer material 7 is top layer thickness 8 is top layer surface finish

<u>Variable</u>	<u>Read Format</u>	<u>Notes</u>
		9 is 2nd layer material 10 is 2nd layer thickness 11 is 2nd layer surface finish
TØTIM1	NAST3 (Called in 5, 0)	Corresponds to TØTIME, the total duration of the current motor pulse. It is the same as NPSEQ(I, 3) discussed above, but if only the duration of exposure is to be changed, this is a more convenient input.
DELTM1	NAST3	Corresponds to DELTIME, the "time slice" used for calculations of exposure effects. Reset to 1/2 of TØTIME if greater than TØTIME.
P1	NAST4 (Called in 5, 0)	Corresponds to P, the 1/4 latus rectum of the thruster plume
DELP1	NAST4	Corresponds to DELP, the amount that P <u>decreases</u> for each time slice during start-up transients
NTR1	NAST4	Corresponds to NTR, the ID number of the active thruster during the current plume exposure. Program will stop if the value is greater than the total number entered during input of the satellite description.
ISTS1	NAST5 (Called in 10, 2)	Corresponds to ISTST, the flag which controls whether assigned conditions data are to be discarded or used as the basic conditions for further exposures. ISTST = 0 - discard > 0 - use as base
IP11	NAST6 (Called in 12, 0)	Corresponds to IP1 and identifies the calculation cycle for which the data to be input will apply
IP21	NAST6	Corresponds to IP2, the ID of the affected segment
IP31	NAST6	Corresponds to IP3, the specific plume property of interest.

Input of IP11 or IP21 is used to change the time slice and segment ID assignment of plume characteristics data which is already input in the regular data file, TAPE11(=EDATA.) If the characteristics are to be changed, or new ones entered, NAST7 must be used.

<u>Variable</u>	<u>Read Format</u>	<u>Notes</u>
J1J	NAST7 (Called in by 12, 0)	Corresponds to IP1, the time slice or cycle number. Used as J1 in the pro- gram to avoid resetting IP1
K1K	NAST7	Corresponds to IP2, the segment ID. Used as K1
PLMCH1(IP3)	NAST7	Corresponds to PLMCHR(IP3), the plume characteristics. These are assigned as follows:

PLMCHR

- (1) -- small drop diameter (in)
- (2) -- large drop diameter (in)
- (3) -- small drop velocity and gas
velocity (ft/sec)
- (4) -- large drop velocity (ft/sec)
- (5) -- angle of tangent of path of
small drop measured rela-
tive to plume axis. Also for
gas (radians)
- (6) -- tangent angle for large drop
(radians)
- (7) -- mass flow rate for small
drops (lbs/sq ft-sec)
- (8) -- mass flow, large drops
(lbs/ft-sec)
- (9) -- N_2O_4 concentration in plume
gas (mass fraction)
- (10) -- HN_3
- (11) -- MMH (items 10-31 in units
of mass fraction)
- (12) -- MMH. H_2O
- (13) -- MMH Nitrate
- (14) -- MMH Nitrate, hydrated
- (15) -- Water
- (16) -- Ammonia
- (17) -- Ammonia hydroxide
- (18) -- NH_4NO_3
- (19) -- NH_4NO_3 , hydrated
- (20) -- Mixed fuel nitrates, hydrated
- (21) -- AL_2O_3
- (22) -- HCL
- (23) -- Hydrochloric acid azeotrope
- (24) -- Iron oxide
- (25) -- Carbon
- (26) -- NH_4CL
- (27) -- NH_4CL , hydrated
- (28) -- N_2H_4
- (29) -- $N_2H_4. H_2O$

Note: Items 10-31 have the units of mass fraction

<u>Variable</u>	<u>Read Format</u>	<u>Notes</u>
		30 -- $N_2H_4.HN\emptyset_3$
		31 -- $N_2H_4.HN\emptyset_3$ hydrated
		32 -- Unassigned
		33 -- Unassigned
		34 to 53 are the composition of the small drops; up to 10 components can be handled. The ID of each component is entered into the even numbered locations (34, 36 --- 52) and the corresponding weight fraction concentration is entered in the next, odd, location (35, 37, --- 53).
		54 to 73 are the composition of the large drops, entered in the same way as the small ones.
Note: Odd numbered items from 35 to 73 have the units mass percentage.		
		74 to 83 are unassigned
		84 -- plume temperature ($^{\circ}R$)
		85 -- plume pressure (PSIA)
		86 -- plume density (lb/ft ³)
		87 -- plume viscosity (lb/ft-sec)
		88 to 90 Unassigned
NPRFL	NAST8 (Called in by 11, 0)	Corresponds to NPRFLG, the flag which indicates that absorptivity and transmissivity ratios are to be calculated for projections and/or limited region of the satellite body. Integer
		NPRFLG = 0 -- Do not determine for other regions
		≥ 1 -- Calculate for special regions
MS11	NAST8	Corresponds to MSS1, the lower segment ID for special regions. Integer
MS21	NAST8	Corresponds to MSS2, the upper segment ID. Integer
PRJNM	NAST8	Corresponds to PRNAME, the title for the listing of the special region. Maximum of 8 Hollerith characters.

h. DATA Files

These files are typically used in the form of disc files, copied from the multiframe magnetic tape of the program SURFACE and all its auxiliaries. There also are UPDATE \emptyset PL's of the DATA files on the tape. These \emptyset PL's can be used to make corrections to the DATA files -- the output COMPILE file is

then named, for example, ADATA by means of the UPDATE parameter C = ADATA. When UPDATE is used to change the DATA files, it is essential to use the D parameter to ensure that data in columns 73-80 is not destroyed. A typical control card sequence for updating one of the DATA files is illustrated in Figure D-6.

The listing given in the figure shows only directives for updating the specific data file, and does not include other processes which would usually be done at the same time, such as executing the program with the new data, and generating a new magnetic tape on which the new DDATA replaces the old, and DDNPL replaces DDØPL.

The UPDATE deck names for the various data files are

<u>File Name</u>	<u>Deck Name</u>
ADATA	AD
BDATA	BD
CDATA	CRCD1
DDATA	DD
EDATA	ED
INDATA	IND

i. File ADATA = TAPE16

This formatted file contains a description of the satellite configuration and the physical, chemical, and mechanical properties of the materials of construction and of plume/deposit constituents.

A maximum of 175 separate locations on the satellite can be identified; 25 each structural materials and plume/deposit constituents can be handled.

ADATA also contains the instructions for the computing sequence, and several program control flags.

In the description which follows, the discussion is separated into sections which correspond to the various divisions of the data on the file

(1) Initialization

<u>Variable</u>	<u>Format Structure</u>	<u>Comments</u>
None (in 0,0)	(////)	Skip file title cards
IERTST (in 0,0)	(5X, 15)	Maximum number of minor errors before program self-aborts. Defaults to 10.
IT1; FACTR(K), K = 1, IT1	5X, 15, 5X, 9F7.0	FACTR controls the duration of the time slices during space exposure in (6,0) as a function of temperature

```

JOB CARD:(PARAMETERS:JFL=10000,MAXFL=40000, )
ID CARD:(FACILITY OPTIONS)
REQUEST:A,M,I. (REEL NO, )
RETURN:A
RETURN:A
COPIES COMPLETE MULTIFILE FROM TAPE TO DISC1
FREES THE TAPE DRIVE.
RETURN:A
COPIES OF B, OUTPUT. LIST THE FIRST FILE, WHICH IS A TABLE OF CONTENTS.
SKIPF: B, 0, 17, B. SKIP TO OLD VERSION OF DDATA.
COPIES OF B, OUTPUT. LIST OLD DDATA TO USE AS COMPARISON.
SKIPF: B, 0, 17, B. SKIP TO OLDPL OF DDATA.
COPIES OF B, DDOPL. MAKE OLDPL AN INDEPENDENT FILE.
RETURN:A. FREE THE DISC SPACE.
RFL: 40000. FIELD LENGTH FOR UPDATE.
UPDATE(D,E,F,U,P=DDOPL,N=DDNPL,C=DDATA,L=A123)
RFL: 10000.
COPIES OF DDATA. OUTPUT. LIST NEW DDATA FOR CHECKING.
7/8/9 END OF RECORD
OLD DDCR1
// CORRECTION DIRECTIVES
//
// SEQUENCE DD
7/8/9 END OF RECORD
6/7/8/9 END OF JOB/FILE

```

M 12-1123

Figure D-6. Directives for Correcting File DDTA:

<u>Variable</u>	<u>Format Structure</u>	<u>Comments</u>
DECPATH, DEDPTH (in 1, 0)	7X, F9.0, 7X F9.0	DECPATH is used in (13, 0) to test whether abrasion is signif- icant or whether deposition is the primary effect DEDPTH is used in (13, 0) to test whether deposition is significant
NAME (in 1, 0) Four calls: NAME (I, 1), I = 1, 13 NAME (I, 1), I = 14, 15, NAME (I, 3), I = 1, 3; NAME (I, 2), I = 1, 7 NAME (I, 2), I = 8, 19 NAME (I, 2), I = 20, 23	13A6	NAME carries the titles used for materials, constituents, and projections from the satellite NAME (I, 1) is materials NAME (I, 2) is projections NAME (I, 3) is constituents Unused locations are set to UNASND. The 2-D array NAME (25, 3) is equivalenced to the linear array ALNAME(75) for computations in which the single dimension will save time.

In addition the linear array NAAM(5) is equivalenced to negative locations of ALNAME by (NAAM(5), ALNAME(1)) and the values

```

NAAM(1) = 6HERØDED
(2) = 6H HØLE
(3) = 6H NØNE
(4) = 6HUNASND
(5) = 6H (blank)

```

set by a DATA statement in Link (0, 0). These latter names are used to print the effects of abrasion.

The materials and constituents currently used in SURFACE and stored in array NAME are shown in Figure D-7. A copy of a listing of the first section of ADATA is presented in Figure D-8 to show the appearance of the file. (The names are abbreviated in the program.)

(2) Model Satellite Configuration

The structure used in the standard data is a model satellite. The features of its structure are shown in Figure D-9.

The description of the basic satellite is read from ADATA and is entered into the array SURDES (SURface DEScription), but it only partially

C	1/0	313
C	1/0	314
C	1/0	315
C	1/0	316
C	1/0	317
C	1/0	318
C	1/0	319
C	1/0	320
C	1/0	321
C	NAMES CORRESPONDING TO THE VARIOUS STRUCTURAL MATERIALS	1/0	322
C	PLUME DEPOSITS, AND SURFACE-ATTACHED COMPONENTS ARE	1/0	323
C	READ IN AND ASSIGNED TO THE VARIABLE ARRAY "NAME"	1/0	324
C	NAME(1,1) STRUCTURAL MATERIALS; NAME(1,2) DEPOSITS	1/0	325
C	NAME(1,3) PROJECTION/COMPONENT TYPES	1/0	326
C	1/0	327
C	NAME(1,1) IS ALUMINUM	1/0	328
C	NAME(2,1) IS WINDOW	1/0	329
C	NAME(3,1) IS SOLAR CELL	1/0	330
C	NAME(4,1) IS INFRA RED PORT	1/0	331
C	NAME(5,1) IS ULTRA-VIOLET PORT	1/0	332
C	NAME(6,1) IS TEFLON	1/0	333
C	NAME(7,1) IS GOLD PLATE	1/0	334
C	NAME(8,1) IS BLACK COATING	1/0	335
C	NAME(9,1) IS WHITE COATING	1/0	336
C	NAME (10,1) IS KAPTAN	1/0	337
C	NAMES(11,1)-(29,1) ARE UNASSIGNED	1/0	338
C	NAME (1,2) IS N2O4	1/0	339
C	NAME (2,2) IS NITRIC ACID (HYDRATED N2O4)	1/0	340
C	NAME (3,2) IS MMH	1/0	341
C	NAME (4,2) IS HYDRATED MMH	1/0	342
C	NAME (5,2) IS MMH2,NITRATE	1/0	343
C	NAME (6,2) IS HYDRATED MMH2,NITRATE	1/0	344
C	NAME (7,2) IS WATER	1/0	345
C	NAME (8,2) IS AMMONIA	1/0	346
C	NAME (9,2) IS AMMONIUM HYDROXIDE	1/0	347
C	NAME (10,2) IS AMMONIUM NITRATE	1/0	348
C	NAME (11,2) IS HYDRATED NH4NO3	1/0	349
C	NAME (12,2) IS MIXED FUEL NITRATES (HYDRATED)	1/0	350
C	NAME (13,2) IS ALUMINA	1/0	351
C	NAME (14,2) IS HYDROGEN CHLORIDE	1/0	352
C	NAME (15,2) IS HYDROCHLORIC ACID AZEOTROPE	1/0	353
C	NAME (16,2) IS IRON OXIDE	1/0	354
C	NAME (17,2) IS CARBON	1/0	355
C	NAME (18,2) IS AMMONIUM CHLORIDE	1/0	356
C	NAME (19,2) IS HYDRATED AMMONIUM CHLORIDE	1/0	357
C	NAME (20,2) IS HYDRAZINE	1/0	358
C	NAME (21,2) IS HYDRAZINE HYDRATE	1/0	359
C	NAME (22,2) IS HYDRAZINE NITRATE	1/0	360
C	NAME (23,2) IS HYDRATED HYDRAZINE NITRATE	1/0	361
C	NAMES (24,2) AND (25,2) ARE UNASSIGNED	1/0	362
C	NAME(1,3) IS THRUSTOR	1/0	363
C	NAME(2,3) IS RADIO ANTENNA	1/0	364
C	NAME(3,3) IS SOLAR CELL ARRAY	1/0	365
C	NAME(4,3)-(29,3) ARE UNASSIGNED	1/0	366
C	1/0	367

Figure D-7. Structural and Plume/Deposit Constituents

AB-7A

IERTST= 12
 ITLO= 7FACTR 6.E5 3.E5 1.E5 1.E4 1.E3 10. 11
 DECPHM= 1.E9LECPH42 3.E11
 ALUMINWINDCWSULCELIRPORTLVPORTTEFLONGOLD BLACK WHITE KAPTANUNASNDUNASNDUNASND
 UNASNDUNASNDTHESSTRAN4AESOLARY N204 HN03 H44 MH4420MH443MH44 AQWATER
 AMONIANNH4OH NH4NC3AMN.AQXFLUCAL203 HCL HCL,ACFE203 CARBONNH4CL AQAMCL
 N2H4 N2H4C3N3H5C3AQH4NT

9330AD
9332AD
9334AD

ND

AC AD AB AC AD AB AD AD

SECRET

Figure D-8. File ADAData – Initial Section

C	1/0	377
C	1/0	378
C	1/0	379
C	1/0	380
C	1/0	381
C	1/0	382
C	1/0	383
C	1/0	384
C	1/0	385
C	1/0	386
C	1/0	387
C	1/0	388
C	1/0	389
C	1/0	390
C	1/0	391
C	1/0	392
C	1/0	393
C	1/0	394
C	1/0	395
C	1/0	396
C	1/0	397
C	1/0	398
C	1/0	399
C	1/0	400
C	1/0	401
C	1/0	402
C	1/0	403
C	1/0	404
C	1/0	405
C	1/0	406
C	1/0	407

CONFIGURATION AND
SURFACE DESCRIPTION

.....

BASIC
SATELLITE CONFIGURATION

.....

FOR PURPOSES OF LOCATING THE VARIOUS CONDITIONS AND EFFECTS ON THE
SURFACE OF THE SATELLITE, THE EXTERIOR IS DIVIDED INTO SEGMENTS, EACH
WITH AN AREA OF 1 SQ FT. EACH SEGMENT IS GIVEN AN ID AND ITS LOCATION
RECORDED IN THE CYLINDRICAL COORDINATES OF ITS MID-POINT. THE SHAPES
THE SEGMENTS ARE APPROPRIATE TO THE SURFACES THEY LIE ON--SQUARES ON
CYLINDRICAL SURFACE, ANNULAR SEGMENTS AND CIRCLES FOR THE ENDS. THE
SATELLITE IS A CYLINDER WITH A CONICAL NOSE AND FLAT DISC AFT

RADIUS	=	1.6 FT
CYLINDER LENGTH	=	10 FT
NOSE LENGTH	=	0.825 FT
TOTAL LENGTH	=	10.825 FT
AREA OF NOSE	=	9 SQ FT
AREA OF CYLINDER	=	100 SQ FT
AREA OF AFT DISC	=	8 SQ FT
CONE ANGLE	=	2.162 RAD

Figure D-9. Satellite Configuration

fills the array. The materials present on the exterior and their current condition will be entered later. In addition, data on projection from the basic surface are read in separately.

<u>Variable</u>	<u>Format</u>	<u>Comments</u>
M1S, M2S (in 1, 0)	5X, 15, 5X, 15	M1S is the number of segments to be input = 116. M2S is the number of data points in each line of the array. M2S = 11
TØTAR (in 1, 0)	10X, F10.0	Total area of basic satellite.
SURDES (M1, M2), M2 = 1, M2S (read in M1S times) (in 1, 0)	10F8.0/F8.0	Satellite configuration data.

Figure D-10 explains the assignment of various data values to locations in the array SURDES.

A part of the current input for the above variables is illustrated in Figure D-11. Note particularly the presence of values other than -1. in columns 8-11 for segment with ID numbers (column 1) of 5 and 116. These values indicate the presence of projections from these particular segments of the satellite. Subsequent inputs will supply further data about these projections. In this and subsequent inputs, and in program execution, values of -1. for data usually indicate that data are lacking.

(3) Projections from Satellite Surface

In the next set of reads, data about projections from the satellite surface are input. At present, the projections can consist of thrusters, antennas, and solar cell arrays.

The current satellite model has eight ACS thrusters, four aimed aft and four forward, located 90 degrees apart around the girth of the satellite 3.6 feet from the apex, and a ninth thruster for translation centered on the tail of the satellite. There is also one antenna and one solar cell array.

The information about the projections is input in the following fashion:

The eighth column of the array SURDES is read for each segment, starting at the one with the lowest ID number. When a value different from -1. is found in column 8, a READ of TAPE16 is made to input data about the projection located on that segment.

<u>Variable</u>	<u>Format</u>	<u>Comment</u>
PRJN, TRX, TRR, TRTHET (Read in 1, 0)	10X, A6, 5X, F10.0, 2 (5X, F5.0)	

C	M2S # 1 IS SEGMENT ID	1/0	444
C		1/0	445
C	M2S #2 IS THE X COORDINATE OF THE CENTER OF THE SEGMENT	1/0	446
C	M2S #3 IS THE R COORDINATE OF THE CENTER OF THE SEGMENT	1/0	447
C	M2S #4 IS THE ANGLE (THETA) COORDINATE OF THE SEGMENT CENTER	1/0	448
C	M2S #5 IS THE SEGMENT AREA (MINIMUM = 1 SQ FT)	1/0	449
C	M2S #6 IS THE DISTANCE TO THE VERTEX OF THE NEAREST PLUME, PROJ	1/0	450
C	JECTED ON THE X AXIS (A NEGATIVE VALUE MEANS THAT THE SEGMENT	1/0	451
C	UPSTREAM OF THE FLOW FIELD)	1/0	452
C	M2S #7 IS THE SURFACE TEMPERATURE OF THE SEGMENT	1/0	453
C	M2S #8 IS THE HEIGHT OF ANY PROJECTION ON THE SEGMENT	1/0	454
C	M2S #9-11 ARE THE DIRECTION COSINES OF THE NORMAL TO THE PLAN	1/0	455
C	WHICH IS TANGENT TO THE PROJECTION	1/0	456
C	9 = LAMBDA	1/0	457
C	10 = MU	1/0	458
C	11 = NU	1/0	459

Figure D-10. Storage Locations in SURDES for Satellite Configuration Data

[illegible]

Figure D-11. ADATA Input of Satellite Configuration

The word read in as PRJN is compared with the word 6HTHRSTR. If the words match, the information read in is stored in the form input, where TRX, TRR and TRTHET are the thruster X-, R- and θ - coordinates. One set is indexed and stored for each input of this type. The implicit assumption is made that the plume direction is aft. If the R coordinate for the thruster location is larger than the satellite radius, a second thruster firing forward, with the same configurational constants, is assumed and entered in the file.

If the word read in by PRJN is not 6HTHRSTR, the other data read in are transformed as indicated

AREA = TRX
M11S = TRR
M22S = TRTHET

Then another set of variables is read in; there are M11S separate reads for these new data, which consist of configurational information similar to that read in for the original segments on the satellite body.

<u>Variable</u>	<u>Format</u>	<u>Comment</u>
SURDES(MM1, MM2), MM2 = 1, MM22S	F7.0, F9.0, F8.0, F9.0, F6.0, F9.0, F8.0	

If the seventh column (temperature) is null, a default value of 529.2°R is assigned. No data for columns 8 to 11 are expected or accepted; that is, there are no projections on top of projections.

The process of reading in data on projections is continued until all of the original segments in SURDES have been checked for the presence of projections. Current inputs are shown in the excerpt from ADATA in Figure D-12.

(4) Material Properties

The next set of inputs consists of information about the properties of structural materials. The data are read into the array MATERIAL (26, 20, 7). After input is complete, the data are stored on the unformatted file TAPE1 to save storage space in core. (Other data are read into an equivalenced array later.) The structure of the properties input is explained in the program segment shown in Figure D-13.

The level MT3 = 7 is not currently assigned.

<u>Variable</u>	<u>Format</u>	<u>Comment</u>
MT1S, MT2S (in 14, 0)	10X, I5, 10X, I5	MT1S = 10, MT2S = 9
MATERIAL (I, J, K), J=1, MT2S read in K=6 times, read in I=MT1S times (in 14, 0)	F3.0, F7.0, 2E10.7, F6.0 2F8.3, E10.7, F5.2	

C	THE DATA CURRENTLY ENTERED IN THE PROGRAM FOR PROPERTIES ARE	14/0 369
C	NOMINAL OR HANDBOOK VALUES FOR REPRESENTATIVES OF CLASSES OF	14/0 370
C	MATERIALS OF INTEREST. PROPERTIES OF SPECIFIC MATERIALS	14/0 371
C	(ALLOYS, COATINGS, CERAMICS, ETC.) SHOULD BE ENTERED IF SPE-	14/0 372
C	CIFIC PLUME EFFECTS ON SUCH MATERIALS ARE TO BE CALCULATED.	14/0 373
C		14/0 374
C		14/0 375
C	*****	14/0 376
C		14/0 377
C	MECHANICAL STRUCTURE MATERIALS	14/0 378
C		14/0 379
C	*****	14/0 380
C		14/0 381
C	MATERIAL IS THE ARRAY OF PROPERTIES OF STRUCTURAL MATERIALS	14/0 382
C	IT IS STORED ON TAPE 1	14/0 383
C	MT18 CORRESPONDS TO THE NUMBER OF MATERIALS IN THE TABLE	14/0 384
C	MT2 IS THE SPECIFIC PROPERTY	14/0 385
C	MT2 = 1 IS THE CODE NUMBER (CORRESPONDS TO NAME(1,1))	14/0 386
C	MT2 = 2 IS THE MELTING POINT	14/0 387
C	MT2 = 3 IS THE VICKERS HARDNESS	14/0 388
C	MT2 = 4 IS THE BULK MODULUS	14/0 389
C	MT2 = 5 IS THE SURFACE ENERGY & SURFACE TENSION	14/0 390
C	MT2 = 6 IS THE HEAT CAPACITY	14/0 391
C	MT2 = 7 IS THE THERMAL CONDUCTIVITY	14/0 392
C	MT2 = 8 IS THE YIELD STRENGTH	14/0 393
C	MT2 = 9 IS THE DENSITY	14/0 394
C	MT3 CONTAINS THE CONSTANTS FOR THE PARAMETRIC EQUATION RELATING	14/0 395
C	CHANGE OF MATERIAL PROPERTIES WITH TEMPERATURE	14/0 396
C		14/0 397
C	$PROP(F(T)) = A + B \cdot T + C \cdot T^2 + D/T + E/(T^2)$	14/0 398
C		14/0 399
C	MT3 = 1 IS THE VALUE FOR THE PROPERTY AT ROOM TEMPERATURE (290 R, 80 F)	14/0 400
C		14/0 401
C	MT3 = 2 IS A	14/0 402
C	MT3 = 3 IS B	14/0 403
C	MT3 = 4 IS C	14/0 404
C	MT3 = 5 IS D	14/0 405
C	MT3 = 6 IS E	14/0 406

Figure D-13. Storage Locations in MATERIAL for Mechanical Properties

The data used were obtained from a variety of standard handbooks, including the Handbook of Chemistry, Handbook of Chemistry and Physics, Handbook of Applied Engineering Science, Chemical Engineers Handbook, Plastics Encyclopedia, Space Materials Handbook, ASHRAE Guide and Data Book, Military Handbook 5, Materials Selector issue of Materials Engineering, Mechanical Engineers Handbook, etc.

A single equation for thermal effects was selected to avoid carrying separate equations for each property, or even for each material and property combination. The constants were calculated from data reported at several temperatures, and least-squares fitted the equation by a small interactive computer program.

As shown by the copy of this part of the ADATA input (Figure D-14) for some materials insufficient data were found to calculate the correlations coefficients. In these cases, the room temperature constants are stored in MT3 = 2, and zeroes are left for MT3 = 3 to 6.

(5) Chemical Properties of Propellant/Plume Constituents

The next data input in sequence is from the file INDATA, read in by the INPUT1 input editor. This input will be described in detail later, after completing the description of the ADATA file. It basically consists of certain physical chemical properties of N_2O_4 and MMH.

Following the above input and subsequent to the assignment of the input values to specific variables, formatted input of similar data from ADATA for other plume/deposit constituents takes place. The inputs alternate between reading how many items will be read in on the next line, and the actual values read in. The input of number of items is shown only once in the following table.

<u>Variable</u>	<u>Format</u>	<u>Comments</u>
NUDA (Read in 14/0)	5X, I5	Number of NU Data in next line; maximum value is 5
I, CP(I) J=1, NUDA (two lines)	5(I5, F10.0)	I corresponds to the code for the constituents in NAME(I, 2). CP = vapor specific heat
In subsequent lines, the following variables are input:		
EPCRT (1 line)	same	Critical pressure, psia
FREZT (1 line)		Freezing point, °K
FRZEN (1 line)		Latent Heat of Melting, cal/g
RHØL (3 lines)		Specific gravity, liquid
TENS (2 lines)		Surface tension, dynes/cm
SHS (1 line)		Specific heat, solid, cal/g-°K
TBØIL (1 line)		Boiling point, °K
VAPEN (1 line)		Heat of evaporation, cal/g
VISL (2 lines)		Viscosity, poise

This portion of the ADATA input file is shown in Figure D-15.

Note that if two successive lines of data have the same number of items, it is not necessary to read in a new value of NUDA (cards 349 and 350), but that no harm is done if a duplicate value of NUDA is read (cards 344 and 346).

The next input consists of a number of additional physical-chemical properties of plume/deposit constituents, read in as the array CHEMIC (26, 20, 7), equivalenced to MATERIAL, and then stored, unformatted, on TAPE3. Figure D-16 illustrates the assignment of types of data to specified locations in CHEMIC.

The method to input the CHEMIC data is basically similar to that used for MATERIAL.

<u>Variable</u>	<u>Format</u>	<u>Comments</u>
JC1S, JC2S (Read in 14, 0)	10X, 15, 10X, 15	JC1S = 23 (number of constituents) JC2S = 13 (number of properties) Note JC3S = 6; the seventh layer is not used at present
CHEMIC(I, J, K), J = 1, JC2S (Do K = 6 times) (Do I = 23 times)	10F8.4/4F8.4	Note 2 cards for each read

The data were obtained from a variety of standard sources; Gmelin, Beilstein, Chemical Abstracts, Batelle; Propellant Handbook, CPIA: Propellant Manual, Handbook of Chemistry, Handbook of Chemical Engineering, Handbook of Chemistry and Physics, Manufacturers' literature, Kirk-Othmer, JANNAF Tables, etc. The constants for the variation of solid properties with temperature were calculated in the same fashion as described above for structural materials.

A few portions of the ADATA input to CHEMIC are illustrated in Figure D-17.

(6) Molecular Weight

The next input is that of vapor state molecular weights (MØLWT) of the plume/deposit constituents (see Figure D-18).

<u>Variable</u>	<u>Format</u>	<u>Comments</u>
MØLWT(I), I = 1, 7 (Read in 14.0) 8, 12 13, 19 20, 23	7(5X, F5.0)	4 cards

MØLWT is equivalenced to AMW because parts of the program were written with one name for these data, and parts with the other.

NUDAS	7	1.4836	8	.5232	14	.2939	20	.472	2	.412	AD	338
NUDAS	3										AD	339
NUDAS	9	-.161	10	.1113	13	.229					AD	340
NUDAS	5										AD	341
NUDAS	7	.223.	6	1635.7	14	1193.7	18	537.	20	2135.	AD	342
NUDAS	1										AD	343
NUDAS	22	70.7									AD	344
NUDAS	1										AD	345
NUDAS	16	44.6									AD	346
NUDAS	3										AD	347
NUDAS	2	1.451	4	1.140	7	.9887	3	.6814	9	.889	AD	348
NUDAS	11	1.336	14	1.439	15	1.213	19	1.067	20	1.0045	AD	349
NUDAS	21	1.647	10	1.41							AD	350
NUDAS	5										AD	351
NUDAS	2	69.	7	72.	8	14.1	11	57.	15	65.5	AD	352
NUDAS	5	65.	1	56.4	19	50.76	20	66.67	21	74.2	AD	353
NUDAS	1										AD	354
NUDAS	16	.155									AD	355
NUDAS	3										AD	356
NUDAS	16	4069.	21	114.4	22	147.					AD	357
NUDAS	2										AD	358
NUDAS	15	56.7	18	71.9							AD	359
NUDAS	5										AD	360
NUDAS	2	.177	7	.01062	8	.020	11	.00972	15	.01067	AD	361
NUDAS	3										AD	362
NUDAS	19	.00664	19	.0023	20	.20					AD	363
NUDAS	1										AD	364
NUDAS	1										AD	365

Figure D-15. ADATA Input of Phys-Chem Properties

C	14/0	719
C	.	14/0	720
C	.	14/0	721
C	PHYS=CHEM	14/0	722
C	PROPERTIES OF	14/0	723
C	SPECIFIC DEPOSITS	14/0	724
C	.	14/0	725
C	.	14/0	726
C	14/0	727
C		14/0	728
C	CHEMIC IS THE ARRAY OF PHYS=CHEM PROPERTIES OF DEPOSIT	14/0	729
C	IT IS STORED ON TARE 3	14/0	730
C	JC18 CORRESPONDS TO THE NUMBER OF MATERIALS IN THE TABLE	14/0	731
C	JC2 CONTAINS THE SPECIFIC PROPERTIES	14/0	732
C	JC2# 1 IS THE MATERIAL CODE NUMBER(SAME AS NAME(1,2))	14/0	733
C	JC2# 2 IS THE FREEZING POINT	14/0	734
C	JC2# 3 IS THE SOLID DENSITY	14/0	735
C	JC2# 4 IS THE CRITICAL TEMPERATURE	14/0	736
C	JC2# 5 IS THE NORMAL BOILING POINT	14/0	737
C	JC2# 6 IS THE HEAT OF FUSION	14/0	738
C	JC2# 7 IS THE HEAT OF VAPORIZATION	14/0	739
C	JC2# 8 IS THE THERMAL CONDUCTIVITY OF THE SOLID PHASE	14/0	740
C	JC2# 9 IS THE THERMAL CONDUCTIVITY OF THE LIQUID PHASE	14/0	741
C	JC2# 10 IS THE HEAT CAPACITY OF THE SOLID PHASE	14/0	742
C	JC2# 11 IS THE HEAT CAPACITY OF THE LIQUID PHASE	14/0	743
C	JC2# 12 IS THE REFRACTIVE INDEX	14/0	744
C	JC2# 13 IS THE MOLECULAR RADIUS	14/0	745
C	JC2# 14 IS THE LIQUID DENSITY	14/0	746
C	JC3 CONTAINS THE CONSTANTS FOR THE PARAMETRIC EQUATION	14/0	747
C	RELATING SOLID DEPOSIT PROPERTIES TO TEMPERATURE	14/0	748
C		14/0	749
C	$PROP(F(T)) = A + B \cdot T + C \cdot T^2 + D/T + E/(T^2)$	14/0	750
C		14/0	751
C	JC3 # 1 IS THE VALUE AT 340 R(80 F)	14/0	752
C	JC3 # 2 IS A	14/0	753
C	JC3 # 3 IS B	14/0	754
C	JC3 # 4 IS C	14/0	755
C	JC3 # 5 IS D	14/0	756
C	JC3 # 6 IS E	14/0	757
C		14/0	758
C	PROPERTIES OF LIQUID DEPOSITS AS FUNCTIONS OF TEMPERATURE	14/0	759
C	ARE CALCULATED FROM REDUCED(CRITICAL) PROPERTIES	14/0	760

Figure D-16. Storage Locations in CHEMIC for Chemical Properties

JC1S=	23	JC2S=	13								AD	366
1,	471.37	116.6	776.4	529.2	63.51	178.2	.000252	.002509	0.295		AD	367
0.79	1.425	3.710									AD	368
1,							11317E=8		.407426		AD	369
1,							1364.5=V		8.093E=4		AD	370
1,							-209E=11		-7.00E=7		AD	371
1,							.100453		-206.806		AD	372
1,							-51.126V		24459.5		AD	373
2,	416.2	116.6	-1.	569.	32.9	236.2	-1.	.00336	0.658		AD	374
0.42	1.402	4.785									AD	375
2,											AD	376
2,											AD	377
2,											AD	378
2,											AD	379
2,											AD	380
2,											AD	381
2,											AD	382
2,											AD	383
2,											AD	384
2,											AD	385
2,											AD	386
2,											AD	387
2,											AD	388
2,											AD	389
2,											AD	390
↑ 60 CARDS OMITTED												
6,	351.6	-1.	730.0	431.5	194.6	589.3	.00193	.00097	.688		AD	451
1.064	1.325	2.075									AD	452
8,	-1.	-1.	-1.	-1.	-1.	849.38	-1.	27875E=7	-1.		AD	453
7.4877	-1.	-1.									AD	454
8,								-3004E=9	-1.		AD	455
-1.02E=2											AD	456
8,								2551E=13	-1.		AD	457
1.543E=5											AD	458
6,								-1.218468	-1.		AD	459
-248.17											AD	460
8,								31.6037	-1.		AD	461
-156523.											AD	462
↑ 168 CARDS OMITTED												
23,	563.										AD	631
.56	-1.	4.0011									AD	632
23,											AD	633
23,											AD	634
23,											AD	635
23,											AD	636
23,											AD	637
23,											AD	638
23,											AD	639
23,											AD	640
23,											AD	641
23,											AD	642

Figure D-17. ADATA Input of Chemical Properties

Reproduced from
best available copy.

N02= 49, HMO3= 63, PHM=	46, MHM20	64, HMA3	109, PAM0154, M20= 10,	AD	643
NH2= 17, HMA0= 35, HMA02	60, HMA03	98, HMA08	252,	AD	644
A1203101,9 HCL	36,5HCLAC	21,7FE203		AD	645
NH2= 32, AGHYE	50, PYA03	95, AGHYN	113,	AD	646
1= 0,0 CSTSCAPTE		3,50VMIN		AD	647
1= 2,0 CSTSCAPTE		5,54VMIN	SLOPE -3,3125	AD	648
1= 3,0 CSTSCAPTE		5,54VMIN	SLOPE -3,5625	AD	649
1= 4,0 CSTSCAPTE		5,54VMIN	SLOPE -3,5625	AD	650
1= 5,0 CSTSCAPTE		5,54VMIN	SLOPE -3,5625	AD	651
1= 6,0 CSTSCAPTE		1,5E5VMIN	1,E3SLOPE -2,5	AD	652
1= 7,0 CSTSCAPTE		3,50VMIN	SLOPE -3,3125	AD	653
1= 8,0 CSTSCAPTE		1,2E4VMIN	2,E2SLOPE -2,5	AD	654
1= 9,0 CSTSCAPTE		1,2E4VMIN	2,E2SLOPE -2,5	AD	655
1= 10, CSTSCAPTE		1,50E5VMIN	SLOPE -2,51	AD	656
1= 1,0CSTSCAPTE		1,54VMIN	SLOPE -1,	AD	657
1= 2,0CSTSCAPTE		1,54VMIN	SLOPE -3,	AD	658
1= 3,0CSTSCAPTE		1,54VMIN	SLOPE -3,	AD	659
1= 4,0CSTSCAPTE		1,54VMIN	SLOPE -3,	AD	660
1= 5,0CSTSCAPTE		1,54VMIN	SLOPE -3,	AD	661
1= 6,0CSTSCAPTE		1,54VMIN	SLOPE -3,	AD	662
1= 7,0CSTSCAPTE		1,54VMIN	SLOPE -3,	AD	663
1= 8, CSTSCAPTE	-1,	VMIN	SLOPE -1,	AD	664
1= 9, CSTSCAPTE	-1,	VMIN	SLOPE -1,	AD	665
1= 10, CSTSCAPTE	-1,	VMIN	SLOPE -1,	AD	666
1= 11, CSTSCAPTE	-1,	VMIN	SLOPE -1,	AD	667
1= 12, CSTSCAPTE	-1,	VMIN	SLOPE -1,	AD	668
1= 13, CSTSCAPTE	-1,	VMIN	SLOPE -1,	AD	669
1= 14, CSTSCAPTE	-1,	VMIN	SLOPE -1,	AD	670
1= 15, CSTSCAPTE	-1,	VMIN	SLOPE -1,	AD	671
1= 16, CSTSCAPTE	-1,	VMIN	SLOPE -1,	AD	672
1= 17, CSTSCAPTE	-1,	VMIN	SLOPE -1,	AD	673
1= 18, CSTSCAPTE	-1,	VMIN	SLOPE -1,	AD	674
1= 19, CSTSCAPTE	-1,	VMIN	SLOPE -1,	AD	675
1= 20, CSTSCAPTE	-1,	VMIN	SLOPE -1,	AD	676
1= 21, CSTSCAPTE	-1,	VMIN	SLOPE -1,	AD	677
1= 22, CSTSCAPTE	-1,	VMIN	SLOPE -1,	AD	678
1= 23, CSTSCAPTE	-1,	VMIN	SLOPE -1,	AD	679
1= 0,				AD	680

Figure D-18. ADATA Input of Molecular Weights and of Wear Equation Constants

(7) Wear Rate Equation Constants

Following the molecular weights, constants for the Nielson-Gilchrist wear rate equation are supplied from ADATA for both structural materials and solid deposits. However, there are few data for the latter substances, and approximations are supplied in the program. The constants were obtained by plotting the observed wear rates from published rain drop and dust erosion tests and observations as functions of input velocity (log-log scale) and then reading off or hand calculating appropriate constants.

The data (see Figure D-18) are read into the array SCRPTTE.

SCRPTTE's dimensions are 50 x 5. The material code column in card images for SCRPTTE corresponds to the value of J in array NAME(J, 1) for structural materials and (J, 2) for deposits; thus there can be two cards with the same values in the first column. The earliest such card in the input file contains data on structural materials, the second card contains data on deposit materials. Figure D-19 illustrates the locations in SCRPTTE for specific constants

<u>Variable</u>	<u>Format</u>	<u>Comment</u>
SCRPTTE(I, J), J = 1, 4 Repeat I = 1, 50 times	5X, F5.0, 10X, G10.0, 5X, G10.0, 5X, F10.0	If the value for SCRPTTE(1, 1) is zero, input ceases even though 50 cards have not been read.

When the example of the inputs from ADATA in Figure D-18 are examined, it may be seen that no data have been entered for a number of the deposit constituents. Values internally calculated by the program from the hardness are entered, if hardness is available. If not assignment of default values is done.

If 50 cards are read for SCRPTTE, there is a skip read to bypass the "end of SCRPTTE" card with zero in the first location.

The two velocities at which a change in form of the Nielson-Gilchrist equation occurs are next read. These are used for all substrates.

<u>Variable</u>	<u>Format</u>	<u>Comment</u>
VUP1, VUP2	5X, F10.0, 5X, F10.0	VUP1 is less than VUP2. The values were obtained by inspection of data on high velocity micrometeoroid impact effects. When more data available, different values for different substrate materials will probably be found.

```

C
C THE ARRAY SCRPT E (SCRIPT E) STORES THE DATA USED TO DETERMINE
C CONSTANTS FOR THE WEAR EQUATION.
C 1A SCRPT E CORRESPONDS TO 1 IN THE MATERIAL NAME CODE,
C
C SCRPT E INDICES FOR THE EQUATION
C  $B = \frac{VEL}{VEL - LOWER LIMIT} \cdot EXP$ 
C WHICH APPLIES IF THE VELOCITY RATIO IS LESS THAN CNE, (IF
C RATIO IS ONE OR GREATER, E IS CONSTANT)
C M = 1 IS MATERIAL CODE
C M = 2 IS WEAR RATE TERM E
C M = 3 IS VELOCITY LOWER LIMIT (FT/SEC)
C M = 4 IS WEAR RATE EXPONENT
C
14/011111
14/011112
14/011113
14/011114
14/011115
14/011116
14/011117
14/011118
14/011119
14/011120
14/011121
14/011122
14/011123
14/011124

```

Figure D-19. Storage Locations in SCRPT E for Wear Rate Constants

(8) Optical/Thermal Properties

The next batch of cards images in ADATA contain optical and thermal properties for the structural materials and deposit constituents. The data are read into the array PRØPTY(51, 20, 2) which is also equivalenced to MATERIAL. After approximation of missing data by means of several routines, the data are stored in unformatted fashion on TAPE2. Figure D-20 describes the assignment of particular properties in array PRØPTY.

In this portion of the ADATA file, the materials to which the properties apply are not identified in the input. (For the benefit of the user, the name is given on a portion of the card which is not read.) The data are presented in the order of the materials in the array NAME, and if NAME contains the word UNASND, input is bypassed. The program supplies the material ID numbers as it proceeds, and puts them in the array.

There are two read statements associated with each material. The first read reports to the program on how many data cards and how many columns of data on each will be found by the second read. The first read can report that no data cards exist; in such cases the second read is skipped. The lack of data is not surprising in some instances; few people have considered that hydrochloric acid is a likely coating for a satellite, and studied its absorptivity and emissivity, etc. The ADATA file is illustrated in Figure D-21.

<u>Variable</u>	<u>Format</u>	<u>Comments</u>
N1S, N2S (Read in 14, 0)	5X, I5, 5X, I5	N1S = number of data cards, max = 5 . If zero, the read of PRØPTY is skipped. N2S = number of columns of data, max = 20.
PRØPTY(N1, N2, N3), N2 = 2, N2S + 1 read N1 times (N3 is either 1 or 2, corresponding to structural or deposit materials, respectively: it is set in the program)		if N2S. LE. 8 Format = 8F10.4 if N2S. GT. 8 Format = 8F10.4/ 8F10.4

(9) Temperature Effects

For a demonstration of the capability of calculation of properties of plume/deposit constituents at various temperatures by Subroutine WEBBER, (called by Link 2, 0), two temperatures are read in from ADATA and then used in the calculation.

<u>Variable</u>	<u>Format</u>	<u>Comments</u>
TTANK(1), TTANK(2) (Read in 2, 0)	10X, F10.0, 10X, F10.0	These inputs are in °K

C	PROPTY IS THE ARRAY OF OPTICAL/THERMAL CONSTANTS	14/01268
C	IT IS STORED ON TARE 2	14/01269
C		14/01270
C		14/01271
C	N19 IS THE NUMBER OF ENTERIES IN THE TABLE	14/01272
C	N2 = 1 IS THE CODE NUMBER OF THE MATERIAL. IT IS	14/01273
C	CONSTANT THROUGHOUT EACH TABLE AND CORRESPONDS TO	14/01274
C	THE ENTRY WITH THE SAME NUMBER IN NAME.	14/01275
C	N2 = 2 IS EITHER THE SURFACE FINISH (FOR STRUCTURAL	14/01276
C	MATERIALS AND COATINGS), OR THE SURFACE TEMPERATURE	14/01277
C	(FOR DEPOSITS)	14/01278
C	N2 = 3 IS ALPHA(S), THE SOLAR ABSORPTIVITY	14/01279
C	N2 = 4 IS EPSILON(TN), THE THERMAL EMISSIVITY	14/01280
C	N2 = 5 IS DIFFUSE REFLECTIVITY	14/01281
C	N2 = 6 IS THE SOLAR REFLECTIVITY	14/01282
C	N2 = 7 IS THE THERMAL REFLECTIVITY	14/01283
C	N2 = 8 IS THE THERMAL CONDUCTIVITY	14/01284
C	N2 = 9 IS REFRACTIVE INDEX (VISIBLE)	14/01285
C	N2 = 10-17 ARE TRANSMITTANCES (PER INCH OF THICKNESS	14/01286
C	N2 = 10 AT 15 MICRON (IR)	14/01287
C	N2 = 11 AT 5 MICRON (IR)	14/01288
C	N2 = 12 AT 2 MICRON (IR)	14/01289
C	N2 = 13 AT 1 MICRON (IR)	14/01290
C	N2 = 14 AT 0.5 MICRON (VISIBLE)	14/01291
C	N2 = 15 AT 0.1 MICRON (UV)	14/01292
C	N2 = 16 AT 0.05 MICRON (UV)	14/01293
C	N2 = 17 AT 0.01 MICRON (UV)	14/01294
C		14/01295

Figure D-20. Storage Locations in PROPTY for Optical/Thermal Constants

VPU1=	3.63VPU2=	9.E09							AD	
N15=	29 N28= 16								ALUMINUMAC	
0.	0.	0.	0.	-1.0	-1.0	-1.0	0.407	0.	AD	681
-1.0	0.1	0.011	0.05	0.93	-1.0	0.98	-1.0	-1.0	AD	682
-1.0	1.0	0.015	0.05	-1.0	0.92	-1.0	-1.0	-1.0	AD	683
-1.0	2.0	0.020	-1.0	0.85	-1.0	0.96	-1.0	-1.0	AD	684
-1.0	3.0	0.030	-1.0	-1.0	-1.0	-1.0	-1.0	-1.0	AD	685
-1.0	4.0	0.050	-1.0	0.73	0.83	0.95	-1.0	-1.0	AD	686
-1.0	5.0	0.070	-1.0	-1.0	-1.0	-1.0	-1.0	-1.0	AD	687
-1.0	6.0	0.100	-1.0	-1.0	-1.0	-1.0	-1.0	-1.0	AD	688
-1.0	7.0	0.120	0.05	0.53	-1.0	0.98	-1.0	-1.0	AD	689
-1.0	8.0	0.140	0.05	-1.0	-1.0	-1.0	-1.0	-1.0	AD	690
-1.0	9.0	0.160	0.06	-1.0	-1.0	-1.0	-1.0	-1.0	AD	691
-1.0	10.0	0.170	-1.0	-1.0	-1.0	-1.0	-1.0	-1.0	AD	692
-1.0	11.0	0.180	-1.0	-1.0	-1.0	-1.0	-1.0	-1.0	AD	693
-1.0	12.0	0.190	0.08	-1.0	-1.0	-1.0	-1.0	-1.0	AD	694
-1.0	13.0	0.200	-1.0	-1.0	-1.0	-1.0	-1.0	-1.0	AD	695
-1.0	14.0	0.210	-1.0	-1.0	-1.0	-1.0	-1.0	-1.0	AD	696
-1.0	15.0	0.220	-1.0	-1.0	0.76	-1.0	-1.0	-1.0	AD	697
-1.0	20.0	0.260	0.10	-1.0	-1.0	-1.0	-1.0	-1.0	AD	698
-1.0	25.0	0.290	-1.0	-1.0	-1.0	-1.0	-1.0	-1.0	AD	699
-1.0	30.0	0.330	-1.0	0.50	-1.0	0.20	-1.0	-1.0	AD	700
-1.0	35.0	0.360	-1.0	-1.0	-1.0	-1.0	-1.0	-1.0	AD	701
-1.0	40.0	0.380	-1.0	-1.0	-1.0	-1.0	-1.0	-1.0	AD	702
-1.0	50.0	0.420	0.21	-1.0	-1.0	-1.0	-1.0	-1.0	AD	703
-1.0	60.0	0.450	-1.0	-1.0	0.50	-1.0	-1.0	-1.0	AD	704

Figure D-21. Part A. ADATA Input of Optical and Thermal Constants

-1.0	-1.0								AD	730
-1.0	-1.0	-0.500	-1.0	-1.0	-1.0	-1.0	-1.0	-1.0	AD	731
-1.0	-1.0	0.560	-1.0	-1.0	-1.0	-1.0	-1.0	-1.0	AD	732
100.0	-1.0		-1.0	-1.0	-1.0	-1.0	-1.0	-1.0	AD	733
-1.0	-1.0	0.670	0.54	-1.0	-1.0	-1.0	-1.0	-1.0	AD	734
-1.0	-1.0	0.750	-1.0	-1.0	-1.0	-1.0	-1.0	-1.0	AD	735
-1.0	-1.0		-1.0	-1.0	-1.0	-1.0	-1.0	-1.0	AD	736
-1.0	-1.0	0.800	-1.0	-1.0	-1.0	-1.0	-1.0	-1.0	AD	737
-1.0	-1.0		-1.0	-1.0	-1.0	-1.0	-1.0	-1.0	AD	738
-1.0	-1.0		-1.0	-1.0	-1.0	-1.0	-1.0	-1.0	AD	739
N15=	2 125=	16							AD	740
0.1	0.02		0.69	0.08	0.0018	0.0	0.00102	1.547	AD	741
0.0	0.0		0.07	.53	.96	0.0	0.0	0.0	AD	742
10.0	0.09		1.85	0.10	0.0010	0.0	-1.0	-1.0	AD	743
0.0	0.0		0.06	.44	0.0	0.0	0.0	0.0	AD	744
N15=	1 125=	16							AD	745
10.0	0.1		1.95	-1.0	-1.0	-1.0	0.0242	2.45	AD	746
0.0	0.0		0.25	.64	.45	0.0	0.0	0.0	AD	747
N15=	1 125=	16							AD	748
2.5	0.05		0.5	-1.0	-1.0	-1.0	0.98	2.72	AD	749
0.005	0.005		0.75	0.75	0.25	0.00	0.0	0.0	AD	750
N15=	1 125=	16							AD	751
1.0	0.005		0.51	-1.0	-1.0	-1.0	0.026	1.4585	AD	752
0.0	0.0		0.0	.05	.9	.85	.25	.005	AD	753
N15=	1 125=	16							AD	754
50.0	.28		.07	-1.0	-1.0	-1.0	0.0192	-1.0	AD	755
0.0	0.0		0.0	0.0	0.0	0.0	0.0	0.0	AD	756
N15=	2 125=	16							AD	757
0.1	0.1		0.02	0.90	0.607	-1.0	0.606	-1.0	AD	758
0.0	0.0		0.0	0.0	0.0	0.0	0.0	0.0	AD	759
1.0	0.26		0.04	0.85	0.607	-1.0	-1.0	0.00	AD	760
0.0	0.0		0.0	0.0	0.0	0.0	0.0	0.0	AD	761
N15=	2 125=	16							AD	762
10.0	0.64		0.65	0.05	-1.0	-1.0	0.0233	0.00	AD	763
0.0	0.0		0.0	0.0	0.0	0.0	0.0	0.0	AD	764
0.000	0.80		0.77	0.02	-1.0	-1.0	-1.0	0.00	AD	765
0.0	0.0		0.0	0.0	0.0	0.0	0.0	0.0	AD	766
N15=	2 125=	16							AD	767
10.0	0.12		0.93	0.05	-1.0	-1.0	0.0067	0.00	AD	768
0.0	0.0		0.0	0.0	0.0	0.0	0.0	0.0	AD	769
0.000	0.21		0.45	0.02	-1.0	-1.0	-1.0	0.00	AD	770
0.0	0.0		0.0	0.0	0.0	0.0	0.0	0.0	AD	771
N15=	1 125=	16							AD	772
10.0	-1.0		.7	-1.0	-1.0	-1.0	0.00299967	1.78	AD	773
0.0	0.000		0.0	0.0009	0.0006	0.0	0.0	0.0	AD	774
N15=	1 125=	7							AD	775
960.0	-1.0		-1.0	-1.0	0.0795	-1.0	0.00239		AD	776
									AD	777

Figure D-21. Part B

[illegible]

22 CARDS OMITTED

Figure D-21. Part C

(10) Exposure Sequencing

The next data on ADATA are the controls for the exposure sequences to be computed. There are two reads; the first, NP1S, is the total number of cycles to be run, where this number includes initial conditions, assigned conditions, and both space and plume exposures. Subsequently, the details of the exposure sequences are read in.

<u>Variable</u>	<u>Format</u>	<u>Comment</u>
NP1S (Read in 0, 0)	5X, 15	Maximum value allowed is 10
NPSEQ(I, J), J = 1, 3 (read NP1S times in 0, 0)	3(10X, F5.0)	J = 1 is ID number of cycle J = 2 is type of exposure, EXTYPE J = 3 is exposure duration for plume on space exposure cycles = TØTIME

Figure D-22 shows the values associated with EXTYPE.

The final data controls preparation of a punched deck which contains the latest version of the array EFFECT. This array contains the information calculated in the program describing the state of the satellite surface after the last exposure cycle. This deck of punched cards can be used as the file CDATA (TAPE9) and when input in this fashion, the information can be used as the assigned initial condition prior to additional exposures.

Preparation of the punched deck is controlled by the flag NEFPN.

<u>Variable</u>	<u>Format</u>	<u>Comments</u>
NEFPN	10X, 15	Zero inhibits punching . 1 or greater causes punching. Normal setting is 1.

The data currently used for the control input reads, described above, are illustrated in Figure D-23.

Following this last data input from file ADATA = TAPE16, the routine DRØPIT is called to return the file and release the disc space it occupied. Note that this action does not release the core space assigned to the FET (File Environment Table) or to the buffer for the file, thus the core requirements for the program are unchanged.

j. File INDATA = TAPE5

This file is used to supply properties of N₂O₄ and MMH. The INPUT1 editor is used, which requires special formatting of the data cards. The following information explains the requirements for using INPUT1.

(1) Description of INPUT 1

INPUT1 clears a specified area of core and reads REAL or INTEGER numbers from INPUT1 cards into this storage area.

C	ASSIGNMENT OF EXPOSURE SEQUENCES	0/0 1006
C	0/0 1007
C	0/0 1008
C	EXTYPE DECLARES TYPE OF EXPOSURE	0/0 1009
C	EXTYPE = *1 INDICATES END OF COMPUTATION	0/0 1010
C	EXTYPE = 0 INDICATES INITIAL CONDITIONS	0/0 1011
C	EXTYPE = 1 INDICATES ASSIGNED CONDITIONS	0/0 1012
C	EXTYPE = *2 INDICATES PLUME EXPOSURE	0/0 1013
C	EXTYPE = *3 INDICATES SPACE EXPOSURE	0/0 1014
C	0/0 1015

Figure D-22. Assignment of Exposure Sequences

TANKER	860.0	TANKS	273.2	
AP18	0			AD 031
IGOR	1	EXTYPE	0; TOTIME	AD 038
IGOR	2	EXTYPE	1; TOTIME	AD 033
IGOR	3	EXTYPE	2; TOTIME	AD 034
IGOR	4	EXTYPE	3; TOTIME	AD 038
IGOR	5	EXTYPE	4; TOTIME	AD 030
SNFPN	1	8		AD 032
				AD 039

Figure D-23. ADATA Input of Program Sequencing Control Parameters

(2) Use

CALL INPUT1 (X, Y, Z) where:

- X is the first element of an array where the input data is to be placed; DATA(1) in SURFACE.
- Y is the last element of the above-mentioned array; DATA(202) in SURFACE.
- Z is the array dimensioned large enough to hold any data which goes into X through Y. This Z array will hold the reference run data. This is DATBAG in SURFACE.

The arrays X and Z must be dimensioned at the start of the program. The dimensions of Z are not mentioned in the call to INPUT1.

(3) Restrictions

1. Within each reference run (including the zero reference run), the case numbers must be in increasing order.
2. After a program calls INPUT1, no data may be input from the TAPE5 except by INPUT1.

(4) Error Indications

All INPUT1 data cards will be examined. If an error is found which is clearly in a certain case, that case will be not executed; if that case number = 0, that is, it defines a reference run, then no case in that reference run will be executed. If the reference run or case number changes illegally, no case will be executed after the illegal change. This subprogram may not find more than one error per card.

The following error messages are possible:

MINUS PUNCH IN SECOND COLUMN OF FRACTION
BAD PUNCH IN EXPONENT
REF RUN NUMBER HAS CHANGED INCORRECTLY
REF RUN AND CASE NUMBERS ARE BOTH ZERO
NO REF RUN STORAGE HAS BEEN PROVIDED
CASES NOT IN INCREASING ORDER
BAD PUNCH IN FIRST COLUMN OF FRACTION
LOCATION IS IN ERROR
ILLEGAL CHAR IN DATA BELOW

(5) Method

Data numbers to be read by INPUT1 must be on cards punched as shown in Figure D-24.

Each card must have a one punched in column 1, and the reference run and case numbers punched in columns 69-73. Punches in columns 66-68 and 74-80 are not examined. Each card has four fields, and data numbers

[illegible]

Figure D-24. INPUT1 Input Card Format

may be entered one per field. A completely blank field is ignored, while a field used to enter a data number must contain no blanks. Each field consists of three subfields:

1. LQC,
2. NUMBER
3. E

For purposes of explanation assume i is punched in the LQC subfield, n is punched in the NUMBER subfield, and e is punched in the E subfield. The number i denotes which element of the x array is to be set equal to the data number in this field. (This is X , the first INPUT1 argument.) Thus i is a subscript of X , so i must be greater than zero and equal to or less than the subscript associated with the INPUT1 argument Y . The only acceptable value of e is XX or a number in the range $-38 \leq e \leq 38$. If e is XX, the data number in this field is interpreted as an INTEGER whose value is n . If $-38 \leq e \leq 38$, the data number in this field is interpreted as a REAL whose value is n times 10^e . (Here n is interpreted as though a decimal point preceded the first digit.) All other values of e are unacceptable and will result in error printouts. Either e or n , or both may be negative numbers. The minus sign is indicated by punching both a minus punch and a number punch in the first column of the subfield.

The data supplied to the INPUT1 editor were first prepared for an early version of the TCC subprogram, and contained a number of entries pertaining to thruster design and operation that are not required by SURFACE. The unneeded entries have been removed from the INDATA deck, but some of the spaces for these entries are still reserved in the array DATA.

The card images in INDATA are shown in Figure D-25.

The data supplied by the INDATA file are the following:

<u>Item Number</u>	<u>Description</u>	<u>Units</u>
9	External Pressure	psia
10	Surface Temperature	$^{\circ}\text{K}$
<u>MMH Properties</u>		
109	Boiling Point	$^{\circ}\text{K}$
110	Freezing Point	$^{\circ}\text{K}$
111	Critical Temperature	$^{\circ}\text{K}$
112	Critical Pressure	psia
113	Vapor Cp	$\text{cal/g} \cdot ^{\circ}\text{K} = \text{Btu/lb} \cdot ^{\circ}\text{R}$

Figure D-25. INDATA Cards for INPUT1 Edited Input

<u>Item Number</u>	<u>Description</u>	<u>Units</u>
114	Liquid Specific Heat	cal/g-°K = Btu/lb - °R
115	Not used	
116	Molecular Weight Vapor	g/g-mole = lb/lb mole
117	Latent Heat of Evaporation at Boiling Point	cal/g
118	Latent Heat of Fusion at Freezing Point	cal/g
119	Liquid Thermal Conductivity	cal/sec-g-°K
120	Vaporization Accommodation Coefficient	none
121	Reference Temperature for Physical Properties	°K
122	Density, liquid	g/cc
123	Viscosity, liquid	poise
124	Surface Tension, liquid-air	dyne/cm
	<u>N₂O₄ Properties</u>	
129	Boiling Point	°K
130	Freezing Point	°K
131	Critical Temperature	°K
132	Critical Pressure	psia
133	Vapor Cp	cal/g-°K = Btu/lb-°R
134	Liquid Specific Heat	cal/g-°K = Btu/lb-°R
135	Not used	
136	Molecular Weight, Vapor	g/g mole = lb/lb-mole
137	Latent Heat of Evaporation at Boiling Point	cal/g
138	Latent Heat of Fusion at Freezing Point	cal/g
139	Liquid Thermal Conductivity	cal/sec-g-°K

<u>Item Number</u>	<u>Description</u>	<u>Units</u>
140	Vaporization Accommodation Coefficient	none
141	Reference Temperature for Physical Properties	$^{\circ}\text{K}$
142	Density, liquid	g/cc
143	Viscosity, liquid	poise
144	Surface Tension, liquid-air	dyne/cm
	<u>MMH·N₂O₄·H₂O Deposit</u>	
185	Density	g/cc
186	Specific heat of gas evolved when deposit is pyrolyzed	cal/g- $^{\circ}\text{K}$ = Btu/lb $^{\circ}\text{R}$
187	Latent heat of pyrolysis	cal/g
	<u>Operations</u>	
201	Default pulse duration	sec
202	Default time slice width	sec

k. File BDATA = TAPE8

This file contains the assignment of structural materials to specified satellite segments, and their initial surface condition. The data are assigned to the array SURDES (175, 66) corresponding to the segment ID numbers. (See Section D. 4. i for initial input to SURDES.) The new data are located in SURDES in the following locations

SURDES (M1, 12) = Code number of material into player

13 = Thickness of top layer

14 = Surface finish of top layer

30 = Code number of material in second layer

31 = Thickness of second layer

32 = Surface finish of second layer

Positions 48, 49, and 50 are corresponding locations for third layer data, but none are currently input. Later in the computation, condensate or deposits form the top layer and the structural materials are pushed down one layer. The material ID numbers correspond to those given in Figure D-26 and in array ALNAME.

C	MATERIAL	CODE	PLUME CONST, CODE	3/0	127
C	ALUMINUM	1	3/0	128
C	WINDOWS	2	N2O4	3/0	129
C	SOLAR CELL	3	N2O4, AQ	3/0	130
C	IR PORT	4	MMH	3/0	131
C	UV PORT	5	MMH HYDRATE	3/0	132
C	TEFLON	6	MMH NITRATE	3/0	133
C	GOLD PLATE	7	MMH NIT, AQ	3/0	134
C	BLACK COAT	8	WATER	3/0	135
C	WHITE COAT	9	AMMONIA	3/0	136
C	KAPTAN	10	NH4OH	3/0	137
C	UNASSIGNED	11=25	NH4NO3	3/0	138
C			NH4NO3, AQ	3/0	139
C			MIXED AQNO3	3/0	140
C			AL2O3	3/0	141
C			HCL	3/0	142
C			HCL, AQ(AZI)	3/0	143
C			FE2O3	3/0	144
C			CARBON	3/0	145
C			NH4CL	3/0	146
C			NH4CL, 2H2O	3/0	147
C			N2H4	3/0	148
C			N2H4, H2O	3/0	149
C			N2H5NO3	3/0	150
C			N2H5NO3, AQ	3/0	151
C			UNASSIGNED	3/0	152
C			UNASSIGNED	3/0	153

Figure D-26. Material Code Assignments

<u>Variable</u>	<u>Format</u>	<u>Comments</u>
None (Read in 3, 0)	(//)	Skips the file leader cards
SURDES (M1, 12), M1 = 1, M1S	20F4.0	Material code input. A value of -99, will terminate the input.
Unnamed	(%)	Skip the -99, if M1S values found, Repeated after every SURDES read.
SURDES (M1, 13), M1 = 1, M1S	8E10.7	Thickness
SURDES (M1, 14), M1 = 1, M1S	16F5.0	Finish
SURDES (M1, 30), M1 = 1, 9	20F4.0	Second layer material. To save file space, M1 values are limited to those segments which have second layers.
SURDES (M1, 30), M1 = 41, M3S	20F4.0	
SURDES (M1, 31), M1 = 1, 9	8E10.7	Second layer thickness
SURDES (M1, 31), M1 = 41, M3S		
SURDES (M1, 32), M1 = 1, 9	16F5.0	Second layer finish
SURDES (M1, 32), M1 = 41, M3S		
KTEST	5X, 15	Flag to control further input of segment materials KTEST = 0: no further data KTEST 1: more data, number of inputs = KTEST
MZ3, MZ2, MZ1, (SSR(MZ), MZ = 1, MZ2) (Read in 3, 0)	3(5X, 15) 5G10.0	--

The function of KTEST and the variables MZ1, MZ2 and MZ3 are summarized in Figure D-27.

After appropriate tests and modifications of indices, SURDES (MZ3, n), where n is a function of MZ1 and MZ2, is set equal to SSR (MZ).

The current input supplied by BDATA is shown in Figure D-28.

1. File CDATA = TAPE9

This file is used to supply descriptions of the surface state corresponding to exposure to plume or space. It inputs such information as deposits, thickness, surface finish, temperature, etc., which are usually calculated by the program. These special inputs are then used as the basis for calculating the final surface condition--optical and thermal coefficients, etc. The input can be derived from previous SURFACE runs, from test data, or from other sources. This input can be used for a demonstration calculation or can be used as the basic state prior to further exposures. This selection is controlled by the flag ISTST, input either on NAMELIST NAST5 or later in file CDATA.

C	IF KTEST IS GREATER THAN ZERO, ADDITIONAL DATA ABOUT	3/0	236
C	SEGMENT MATERIALS WILL BE HEAD IN. THIS STEP MAY BE	3/0	237
C	USED TO CHANGE EARLIER INPUTS OR TO ADD INFORMATION	3/0	238
C	ABOUT NEW SEGMENTS. KTEST IS SET EQUAL TO THE NUMBER	3/0	239
C	OF SEGMENTS FOR WHICH NEW DATA IS TO BE INPUT.	3/0	240
C		3/0	241
C	MZ1 IS THE LOCATION IN SURDES OF THE FIRST DATA POINT	3/0	242
C	MZ2 IS THE NUMBER OF CONTIGUOUS DATA POINTS	3/0	243
C	MZ3 IS THE SEGMENT ID	3/0	244
C	NOTE THAT NON-CONTIGUOUS DATA REQUIRE SEPARATE INPUTS	3/0	245
C		3/0	246

Figure D-27. Operation of Flag KTEST

The data on CDATE is read into the array EFFECT (175, 15). The assignment of specific variables to locations in EFFECT is detailed in Figure D-29.

<u>Variable</u>	<u>Format</u>	<u>Comments</u>
None (Read in 4, 0)	(//)	Skips the file header cards
IIS, I2S	5X, I5, 5X, I5	IIS is the number of affected segments I2S is the number of data points for each segment.
EFFECT (I1, I2) I2 = 1, I2S Do IIS times (Read in at 4, 0)	5G10.6/3G10.6	If I2S is less than 9 file will not read properly
ISTST (Read in 10, 2)	10X, I5	Flat to select whether surface condition calculated from assigned input is used as basis for further calculations, or whether original pristine input is used. ISTST = 0; use original conditions ISTST 1; use conditions resulting from assigned state input.

The complete CDATE file is shown in Figure D-30.

m. File DDATA = TAPE10

This input shown in Figure D-31, contains the primary data defining the operating conditions for plume exposure and also some data used to demonstrate the capabilities of the coordinate transformation routines.

<u>Variable</u>	<u>Format</u>	<u>Comments</u>
None (Read in 5, 0)	(//)	Skips file header cards.
DELTIME	10X, F10.0	Time increment for thruster calculations
DELP or DUM	5X, F10.0	DELP = Change in latus rectum, between time increments during startup and tailoff. If DELP already input, this read is to a dummy variable.
NTR, P	10X, I5, 10X, F10.0	NTR is thruster ID number P2 is 1/4 latus rectum

C	IN ARRAY EFFECT	4/0	38
C	12 = 1 IS X COORDINATE	4/0	39
C	12 = 2 IS Y COORDINATE	4/0	40
C	12 = 3 IS ZETA COORDINATE	4/0	41
C	12 = 4 IS SEGMENT ID	4/0	42
C	12 = 5 IS TEMPERATURE OF TOP STRUCTURAL LAYER	4/0	43
C	12 = 6-8 ARE FIRST LAYER	4/0	44
C	12 = 9-11 ARE SECOND LAYER	4/0	45
C	12 = 6-9 ARE MATERIAL CODE NUMBER	4/0	46
C	12 = 7-10 ARE THICKNESS	4/0	47
C	12 = 8-11 ARE TEMPERATURE OR SURFACE FINISH	4/0	48
C		4/0	49
C		4/0	50

Figure D-29. Locations in EFFECT for Various Surface Conditions



CR00

C DATA									
1.57	1.00	1.57000	42.	600.	1.1	0.095	100.	CR001	1
4.329	1.00	1.57000	42.	600.	1.1	0.095	100.	CR001	2
1.57	1.00	1.57000	42.	600.	1.1	0.095	100.	CR001	3
1.57	1.00	1.57000	42.	600.	1.1	0.095	100.	CR001	4
1.57	1.00	1.57000	42.	600.	1.1	0.095	100.	CR001	5
1.57	1.00	1.57000	42.	600.	1.1	0.095	100.	CR001	6
1.57	1.00	1.57000	42.	600.	1.1	0.095	100.	CR001	7
1.57	1.00	1.57000	42.	600.	1.1	0.095	100.	CR001	8
1.57	1.00	1.57000	42.	600.	1.1	0.095	100.	CR001	9
1.57	1.00	1.57000	42.	600.	1.1	0.095	100.	CR001	10
1.57	1.00	1.57000	42.	600.	1.1	0.095	100.	CR001	11
1.57	1.00	1.57000	42.	600.	1.1	0.095	100.	CR001	12
1.57	1.00	1.57000	42.	600.	1.1	0.095	100.	CR001	13
1.57	1.00	1.57000	42.	600.	1.1	0.095	100.	CR001	14
1.57	1.00	1.57000	42.	600.	1.1	0.095	100.	CR001	15
1.57	1.00	1.57000	42.	600.	1.1	0.095	100.	CR001	16
1.57	1.00	1.57000	42.	600.	1.1	0.095	100.	CR001	17
1.57	1.00	1.57000	42.	600.	1.1	0.095	100.	CR001	18
1.57	1.00	1.57000	42.	600.	1.1	0.095	100.	CR001	19
1.57	1.00	1.57000	42.	600.	1.1	0.095	100.	CR001	20
1.57	1.00	1.57000	42.	600.	1.1	0.095	100.	CR001	21
1.57	1.00	1.57000	42.	600.	1.1	0.095	100.	CR001	22
1.57	1.00	1.57000	42.	600.	1.1	0.095	100.	CR001	23
1.57	1.00	1.57000	42.	600.	1.1	0.095	100.	CR001	24
1.57	1.00	1.57000	42.	600.	1.1	0.095	100.	CR001	25

Figure D-30. C DATA Input File

[illegible]

Figure D-31. DDATA Input File

<u>Variable</u>	<u>Format</u>	<u>Comments</u>
		These data are used to calculate plume-satellite intercepts. Several sets can be calculated, because the program returns and reads new NTR and P until a value of 999 is found in NTR.
ITRNCL	10X, I5	<p>ITRNCL is a flag which selects which coordinate transformation routines will be computed.</p> <p>ITRNCL = -1: Satellite to thruster</p> <p>= 0: None</p> <p>= 1: Thruster to satellite and satellite to thruster</p> <p>= 2: Thruster-to-satellite only</p> <p>If <u>SURFACE</u> is computing the effects of a second plume exposure, ITRNCL is automatically set to -1. and the read is skipped.</p>
N, NR	3(10X, I5)	This input supplies the thruster number (NR) and the number of data sets to follow (N) for the calculation of thruster coordinate system based coordinates
ZZ, RR, THE (read in 5,0)	4(10X, F10.0)	This input supplies demonstration data consisting of coordinates of locations in the thruster-based coordinate system. The values are used to calculate the coordinates of the same locations in the satellite-based coordinate system. The read is only made if ITRNCL is positive, and it is made N times.

After the data set for ZZ, etc., is exhausted, the program returns and reads N, NR again. This sequence continues until a value of -1 is read for N. No further data are read from DDATA on the plume exposure currently being computed.

For each additional plume exposure cycle, four more cards will be read; the inputs required are DELTME (one card), DELP (one card), NTR and P (one card), and a NTR = 999 card to end the input for the cycle.

The copy of file DDATA in Figure D-31 has input for two cycles; the second cycle input starts at card DD. 16.

n. File EDATA = TAPE11.

File EDATA is used to supply information about the characteristics of the thruster plume at the locations where it impinges satellite surfaces. The data in the file were selected from typical output of subprograms KINCØN and MULTRAN as recorded in the 1972 final report on CØNTAM.

The SURFACE program needs one set of plume descriptive data for each impinged segment for each time interval, and will accept any number of inputs up to that quantity. If fewer are input the program will use the inputs actually available for locations/time intervals which were not supplied.

<u>Variable</u>	<u>Format</u>	<u>Comments</u>
blank (Read in 12,0)	(//)	Skip past file heading
NPMCR (Read in 12,0)	10X, 15	Total number of sets of plume characteristics to be read in at this time.
IP1S, IP2S, IP3S (Read in 12, 0)	3(10X, 15)	IP1S = Time slice number IP2S = Affected segment number in array EFFECT (not segment ID) IP3S = Number of individual data points. (This variable is not operative.)
PLMCHR (IP3), IP3 = 1, 90 (Read in 12, 0)	10F8.0 (9 cards)	Specific plume characteristics

A single set of 9 cards is first read in. Then the program checks to see if more data are to be available (is NPMCR greater than 1?). If not, the values of IP1S and IP2S are ignored and the array PLMCHR is filled for the

range IP1 = 1, N1; IP2 = 1, N2; where N1 = number of cycles and N2 = number of affect segments, generated from the values of PLMCHR and written on TAPE14. If more than one set are to be input, the program writes PLMCHR to the tape up to the input values of IP1S and IP2S. Then the program reads EDATA for new values of IP1, IP2, and PLMCHR. This cycle is repeated until a value of -1 for IP1 is found, which indicates that no more PLMCHR values are available. The current value is written out to fill the file.

The copy of file EDATA shown in Figure D-32 has two sets of input for the first plume exposure cycle, and a single set for the second cycle.

The variables that are assigned to specific locations in PLMCHR are given in detail in Section D. 4. g.

o. Summary of File Assignments in SURFACE

Functions of all the files assigned to SURFACE are summarized below.

<u>Number (Internal)</u>	<u>Name (External)</u>	<u>Function</u>
1	-	Storage for array MATERIAL
2	-	Storage for array PROPTY
3	-	Storage for array CHEMIC
4	-	Storage for array SURDES
5	INDATA	INPUT1 data input
6	OUTPUT (Line printer)	Listing results
7	-	Dummy file when listing not desired
8	BDATA	Standard data input (Formatted)
9	CDATA	Standard data input (Formatted)
10	DDATA	Standard data input (Formatted)
11	EDATA	Standard data input (Formatted)
12	-	Buffered storage for common blocks OED and OEF
13	-	Buffered storage for common block R6
14	-	Storage for array PLMCHR. Generated in <u>SURFACE</u> or other <u>CONTAM</u> subprograms.
15	COUNT	Buffered storage of count of calls to overlays and subroutines.

[illegible]

Figure D-32. EDATA Input File

<u>Number (Internal)</u>	<u>Name (External)</u>	<u>Function</u>
16	ADATA	Standard data input (Formatted)
17	INPUT (Card reader)	NAMELIST card input of changes
18	-	NAMELIST inputs from 17 are stored on 18 and read from 18
19	-	Buffered storage of array SEARCHD
20	FLG	Overlay (2, 1) (Object module)
21	FLG	Overlays (4, 0), (10, 2) (Object modules)
22	FLC	Overlays (5, 0), (5, 1), (5, 2), (5, 3), (5, 4), (5, 5), (12, 0), (13, 0) (Object modules)
23	FLE	Overlay (6, 0) (Object module)
24	CHEEP	CHECKPOINT save of program
25	FLØ	Overlays (0, 0), (1, 0), (2, 0), (3, 0), (14, 0) (Object modules)
26	PUNCH (Card punch)	Card deck of array EFFECT (Formatted)
30		Buffered storage of variables when program is to be stopped after calculating intercepts and input of same variables when restarted
31*	-	Communication with other subprograms in CØNTAM about thruster operation
32*	-	Inquiry to other CØNTAM subprograms about plume characteristics
-	FLA	Overlays (11, 0), (11, 1), (11, 2) (Object modules)
-	FLB	Overlay (7, 0) (Object module)
-	FLD	Overlay (10, 0), (10, 1), (16, 0) (Object modules)
-	FLZ	Overlay (15, 0) (Object module)
-	DAYFILE (Not named on Program Card)	Listing of file releases, RFL's and termination causes.

*These two files are referenced in sections of the program which are currently not operational.

Figure D-3 is a copy of the Program Card showing the assignments by parameters. Three files are not mentioned on the Program Card. These are TAPE13, TAPE14 and TAPE 19. These three files are equivalenced by EQUBUFF to other files which have finished their functions at the times EQUBUFF is called.

p. Operation of SURFACE

In the following sections, it is assumed that SURFACE and its auxiliaries are stored in a master file on magnetic tape or in disc Permanent Files.

(1) No Modifications/Corrections

This is the most straightforward method, with defaults in their standard conditions, and all that is required is to copy the needed individual program and data files from the Master File. The program will most likely be executed in this fashion for test or demonstration runs. Of course, the punched data card input for STPFLG must be supplied. The deck to operate in this manner is shown in Figure D-33. The example is based on the assumption that SURFACE is stored on a magnetic tape file. If, instead, it is stored on a disc Permanent File, the REQUEST card shown should be replaced with an appropriate ATTACH card.

The cards marked with circled numbers are included for certain special reasons:

Number ①, CØPYSBF the first file to listing output, is included so the user will obtain the Table of Contents to the multi-file master file for more complex operations in the future. If this listing is not wanted, the CØPYSBF card can be replaced with a SKIPF, A, 1, 17, B card.

Number ②. The file named PX4 consists of a small program to print a count of the calls made to each of the overlays and subroutines during execution, and a statement of what routine was being processed when execution stopped. It uses the information stored on File CØUNT by Subroutine A of SURFACE. PX4 is designed to be used after an EXIT card so that it is only called if the run is aborted for some reason. A similar routine included in SURFACE is called when normal termination occurs.

The advantage of the count of calls to subroutines and overlays is that it is easier to determine what part of the execution had been reached. The normal error statements on the CDC computers will tell at what address an error occurred, but if the address is in a routine called 100 times, it is often difficult to track the cause of the problem when it is not known at what stage in the execution that the call occurred. If use of PX4 is not desired, the CØPYBF can be replaced by SKIPF, A, 1, 17, B. and the short deck after the EXIT(S) card can be omitted. Figure D. 34 is a typical output from PX4.

Number ③. The file RØMTM contains a small program which prints the total CP and PP times used prior to initiating the execution of the main program. It then calls in the main program for execution. The first action in the main program is to set internal clocks and again give the totals for CP and PP time. It is sometimes found that there is an appreciable time interval between the two sets of CP and PP times. If use of RØMTM is not desired, the CØPYBF should be replaced by a SKIPF card, the LØAD of

```

JOB CARD,      IFL = 10000, MAXFL = 275000,
ID CARD,
(7A) REQUEST, SUR, HY,      (NUMBER)
REWIND, SUR,
COPY, SUR, A,
RETURN, SUR,
REWIND, A,
(1) COPYSRF, A, OUTPUT,      TABLE OF CONTENTS
SKIPF, A, 3, 17, B,
COPYBF, A, ADATA,
COPYBF, A, BDATA,
COPYBF, A, CDATA,
(11) COPYBF, A, DDATA,
COPYBF, A, EDATA,
COPYBF, A, INDATA,
SKIPF, A, 3, 17, B,
(2) COPYBF, A, PX4,          LOAD MODULE(ROM)
COPYBF, A, LGOPR,          LOAD MODULE(ROM)
(3) COPYBF, A, RCHTM,        LOAD MODULE(ROM)
RETURN, A,
REWIND, ADATA, BDATA, CDATA, DDATA, EDATA, INDATA, COUNT,
RFL, 275000,
SETCORE,
LOAD, LGOPR,
NOGO,
(4) SETCORE,
LOAD, RCHTM,
NOGO,
(6) RETURN, LGOPR, RCHTM,
REDUCE,
(5) TP1,
EXIT(S)
RFL, 60000,
(2) REWIND, COUNT,
MAP, OFF,
SETCORE,
REDUCE,
(2) PX4,
(11A) 7/8/9                END OF RECORD
                                EXECUTION JOB DECK
(8A) STPFLG= 0
7/8/9                END OF RECORD
6/7/8/9            END OF JOB/FILE

```

Figure D-33. Control Cards to Run SURFACE From File Copy with No Modifications

OVERLAY(1,0)	ENTERED	1	TIMES.
OVERLAY(2,0)	ENTERED	1	TIMES.
OVERLAY(3,0)	ENTERED	1	TIMES.
OVERLAY(4,0)	ENTERED	1	TIMES.
OVERLAY 5,0	ENTERED	1	TIMES.
OVERLAY 7,0	ENTERED	1	TIMES.
OVERLAY 11,0	ENTERED	2	TIMES.
OVERLAY 10,2	ENTERED	1	TIMES.
OVERLAY 2,1	ENTERED	2	TIMES.
OVERLAY 14,0	ENTERED	1	TIMES.
VISCEST	ENTERED	2	TIMES.
WEBBER	ENTERED	2	TIMES.
ZES	ENTERED	3	TIMES.
HCONT	ENTERED	65	TIMES.
REIRHO	ENTERED	57	TIMES.
RETROD	ENTERED	46	TIMES.
RETVIS	ENTERED	44	TIMES.
OVERLAY 11,2	ENTERED	148	TIMES.
OVERLAY 11,1	ENTERED	2	TIMES.
HOTPAR	ENTERED	2	TIMES.
INTER	ENTERED	80	TIMES.
INTRA	ENTERED	291	TIMES.
MAXSUR	ENTERED	331	TIMES.
MINSUR	ENTERED	319	TIMES.
OVERLAY(5,1)	ENTERED	3	TIMES.
OVERLAY(5,3)	ENTERED	1	TIMES.
OVERLAY(5,2)	ENTERED	3	TIMES.
WARD	ENTERED	2	TIMES.
OVER	ENTERED	551	TIMES.
SUB A	ENTERED	6960	TIMES.
SUB B	ENTERED	1	TIMES.
SUB C	ENTERED	21	TIMES.
SUB LY	ENTERED	59	TIMES.
SUB TRANS	ENTERED	44	TIMES.
SUB TK	ENTERED	311	TIMES.
SUR	ENTERED	551	TIMES.
SUB LE	ENTERED	168	TIMES.
ALTER	ENTERED	25	TIMES.
FORM	ENTERED	644	TIMES.
INPUT1	ENTERED	1	TIMES.

(RETURN AFTER A CALL TO ANOTHER ROUTINE IS
NOT INCLUDED IN THE COUNT OF ENTRIES)

LAST ROUTINE ENTERED WAS OVERLAY 5,0
PENULTIMATE ROUTINE WAS SUB C

Figure D.34. Calls to Subroutines and Overlays Listed by Auxillary Program PX4.

RØMTM at Number ④ should be omitted, and the card TP1 at Number ⑤, which initiates execution, must be replaced by a card reading "FLØ." The execution initiation cards mentioned (TP1 and FLØ) are the file names on which the principal Overlays reside. They are defined on the cards ØVERLAY (file name, 0,0).

Number ⑥. After loading the programs, it is advisable to RETURN the program RØM's because they are no longer needed and they are simply using up disc storage space.

(2) SCØPE Card Changes to Default Operations

There are two changes in operation which are controlled by the addition of SWITCH cards in the SCØPE control card deck. If the card SWITCH,1 is inserted, NAMELIST input will be expected from the Input card deck. If SWITCH,n., with "n" having any value from 3 to 6 is inserted, a Checkpoint-Restart tape file will be made at periodic intervals. It is necessary to supply a magnetic tape named CHEEP for the checkpoint file. Both SWITCH cards can be included, but be certain that two SWITCH cards with values greater than 1 are not present.

The cards illustrated in Figure D-35 are typical examples. The three cards indicated by Number ⑦ will turn on both the checkpoint option and a read of NAMELIST input. They should be placed in the control deck (Figure D-33) at the location marked with a Number ⑦A in that figure. Typical NAMELIST cards are shown at Number ⑧ of Figure D-35, these should be inserted at location Number ⑧A in Figure D-33.

The particular Checkpoint SWITCH, 5. card will cause the Checkpoint file to be written after completing five ØVERLAY calls, and then after every subsequent six ØVERLAY calls. The NAMELIST cards illustrated will prevent calculation of space exposure effects by overriding standard input, and cause evaluation of average solar absorptivity and thermal emissivity on the solar cell array, a location which is normally bypassed in the evaluation.

(3) Modification of the Program

When modifications to the program are required, such as turning off portions of the Output listing by assigning IF6 = 7, the UPDATE processor should be used, with the ØLDPL drawn from the third file in the program master file. Unless the modification are very extensive and involve a large fraction of the 62 decks which make up the ØI DPL, the "Selective" ("Normal") or the "Quick" mode should be used. The decision between "Selective" or "Quick" modes should be made on the basis of whether or not the NEWPL generated during UPDATE processing is to be saved. If it is to be saved, the "Selective" mode should be used. In either mode, only those decks actually modified will be written to the CØMPILE file by UPDATE. The CØMPILE file should then be compiled by the RUN compiler, and the resulting RØM of the changed routines merged into the current RØM by the CØPYL processor.

If the changes include introduction of a new program unit (external function, subroutine, or overlay), CØPYL will not function successfully, and CØPYN must be used.

⑦ REQUEST, CHEEP, HY, CK, (RESERVE)
~~SWITCH, 5,~~
~~SWITCH, 1.~~

⑧ INAST1 IPXYS1 = 03
~~I NAST0 NPAFL = 1, NS11 = 117, NS21 = 125, PRJNM = 6MSOLARY 5~~

Figure D.35. Additional Control Cards to Initiate a Checkpoint File and Namelist Input

The control card listing in Figure D-36 will modify a few cards in two routines, prepare a new program library and a new ROM, and then generate a new master tape. The LISTIT routine is used to check the contents of the new tape.

In the series of operations controlled by the deck shown in Figure D-36, the following points may be noted. Number ① The new tape file is called using the RESERVE parameter with the \$ for S, and it is not made permanent by CONFIRM until after the LISTIT is performed successfully at Number ② .

Number ③ The file Table of Contents is updated to reflect the dates at which the new versions of the program were prepared.

Number ④ The new Master File is first generated as a multifile disc file named STRCP and later copied to the tape. This reduces the number of times that the magnetic tape unit is accessed. At facilities which do not restrict loading of magnetic tapes to the first steps of the job, the request for the new tape can be delayed until Number ⑤ , thus leaving a drive unit available for other users.

Number ⑥ . SURFACE should be compiled with minimum length buffers. The ROM supplied by MDAC was compiled with all tape buffers set at 1001g words. If larger buffers are desired, the whole program must be recompiled, and the load and execution field lengths must be increased by 30000g for each 1000g increase in buffer size.

Number ⑦ . The load module or ROM generated at this operation has the same field name (fid) as the one described in Section D. 4. b. (1) above (see Figure D-33), and can be called into load and execution in the fashion illustrated. However, both PX4 and ROMTM would have to be copied from Master File A by the additional control cards Number ⑧ and ⑨ in Figure D-36, which should be inserted at locations Number ⑧A and ⑨A . The job deck which includes the STPFLG card will then follow the last UPDATE job deck.

Figure D-37 is the data on the structure of the OLDPL of SURFACE when the latest version was generated. Figure D-38 is the output from a LISTIT of the master file for SURFACE.

(4) Modifications to DATA Files

This was discussed in Section D. 4.

(5) Temporary Replacement of DATA Files

If a completely new deck of data cards equivalent to one of the DATA files is to be used, but if the use is for only a few runs and the original file is not to be replaced, the DATA file from the master is not copied, and the COPYBF card is replaced by a SKIPF and a COPYBR, INPUT card which causes a deck to be read in from the input stack. Warning, do not use COPYBF on the input stack unless all cards up to the end-of-job 6/7/8/9 are to be copied to a single file. For example, if a replacement file for DDATA has been punched by a previous run of the program, then Number ⑪ in Figure D-33 would be replaced by

```

JOB CARD, IFL=10000, MAXFL=70000,
ID CARD, (FACILITY OPTIONS)
REQUEST, SUR, MY, (NUMBER)
① REQUEST, NEWSUR, MY, (RESERVE)
REWIND, SUR, NEWSUR,
COPY, SUR, A,
RETURN, SUR, FREE THE TAPE DRIVE
REWIND, A,
COPYSF, A, OUTPLT, TABLE OF CONTENTS
COPYSF, A, STRCT1, OLDPL FOR T=0=C
③ RPL, 40000,
UPDATE(D, E, F, U, P, STRCT1, N, STRCT2, C, STRCP)
RPL, 10000,
COPYSF, STRCP, OUTPUT, TABLE OF CONTENTS FOR NEW TAPE
④ COPYSF, STRCT2, STRCP,
RETURN, STRCT1, STRCT2,
COPYSF, A, OLDPL, OLDPL FOR SURFACE
RPL, 40000,
UPDATE(D, E, F, U, P, OLDPL, N, NEWSUR, C, CHPN)
RPL, 10000,
COPYSF, NEWSUR, STRCP, NEWPL FOR SURFACE
COPYSF, CHPN, STRCP,
RETURN, OLDPL, NEWSUR,
REWIND, CHPN,
SKIP, A, 3, 17, 0, SKIP OLD COMPILE FILES
⑧ COPYSF, A, STRCP, 19, DATA FILES AND PX4 (OLDPLS AND COMPILES)
RPL, 70000,
⑥ RUN(1, 1001, CHPN, LOOP, 1) LOOP HAS ONLY THE CHANGED ROUTINES
RPL, 10000,
⑨ COPYSF, A, L00A,
REWIND, L00A, L00A,
⑦ COPYL, L00A, L00A, L00PR, MERGE TO CREATE COMPLETE, MODIFIED ROM
REWIND, L00PR,
COPYSF, L00PR, STRCP,
COPYSF, A, STRCP, 2,
RETURN, A, CHPN, L00A, L00B,
⑤ REWIND, STRCP,
COPY, STRCP, NEWSUR,
REWIND, NEWSUR,
LISTIT, NEWSUR, OUTPUT, 88,
② CONFIRM, NEWSUR,
7/8/9
// CORRECTION SET FOR TABLE OF CONTENTS -- UPDATE JOB DECK
// IDENT STRCP
// DELETE STR, 7
// (NEWDATE)
// 20 (NEWDATE)
// 34 (NEWDATE)
// 70 (NEWDATE)
// SEQUENCE STR
7/8/9
// CORRECTION SET FOR SURFACE -- UPDATE JOB DECK
// IDENT COR1
// 0/0, 027
// 10F = 7
// 1/0, 005
// IF (TRR(NTR).LE.0) TRR(NTR) = SURDES(M1,3) * 0.75
7/8/9
0/7/8/9
⑧ SKIP, A, 3, 17, 0,
COPYSF, A, PX4,
⑨ COPYSF, A, ROMTH,
SKIP, A, 3, 17, 0,

```

Figure D-36. Control Cards for Modification of SURFACE

①
COPYBR, INPUT, DDATA.
SKIPF, A, 1, 17, B.

and the new deck including a 7/8/9 card, would be placed at Number ①1A .

If the new deck is to replace the previous deck of the same name in the master file, UPDATE must be used to generate the program libraries (NEWPL and OLDPL) and the sequenced COMPILE file. For this case, the file named in the COPYBR should not be DDATA. Figure D-39 shows the appropriate set of cards for this operation. These also would replace Number ①1 in Figure D-33. The UPDATE job deck directives in Figure D-39 must then be placed immediately following the new DDATA deck in the job stream, which is located at Number ①1A (Figure D-33).

D. 5 TEST CASE

Subprogram SURFACE was executed independently of the CONTAM executive. Hence, the data for running the sample case were modified from that used for other subprograms. First: certain parameters were arbitrarily assigned. This was done for either of one of two reasons:

a. The parameter is not meaningful for other subprograms, and so was not used earlier.

Parameter	Program Variable	Assigned Value	Input Method
Active Thrustor Identification	NTR	2	NAMelist/NASt4 Input of NTR1
Plume Exposure Duration	TØTIME	2×10^{-3} sec	NAMelist/NASt3 Input of TØTIM1
Plume Exposure Time Increment	DELTIME	2×10^{-4} sec	NAMelist/NASt3
Space Exposure Duration	TØTIME	6×10^5 sec	ADATA Input
Space Ambient Pressure	PE	1×10^{-6} psia	INDATA Input

b. The parameter is not specifically defined in other subprograms, so an estimated value was developed by inspection of the related output from the other subprograms.

CORRECTION IDENTS ARE LISTED IN CHRONOLOGICAL ORDER OF INSERTION

YAIRSS	C/D	SA	SE	SC	SD	MCN	RHO
WCF	WIS	END	EFF	LE	VI	WBR	ZS
WAF	WFL	1/0	14/0	FRM	TK	2/0	2/1
W/C	4/0	5/0	5/1	LT	5/2	5/3	5/4
W/B	6/0	EAT	7/0	MLO	6PL	10/0	10/1
12/2	11/0	EXT	HCT	IER	IRA	MAX	MIN
W/P	WVR	WNS	WARD	11/1	11/2	12/0	13/0
WAT	WADY	WCA	15/0	WAI	WU	18/0	16/0

1 FUGED IDENTS WERE FOUND

BECKS ARE LISTED IN THE ORDER OF THEIR OCCURRENCE ON A NEW PROGRAM LIBRARY IF CNE IS CREATED BY THIS UPDATE

YAIRSS	C/D	SA	SB	SC	SD	MCN	RHO
WCF	WIS	END	ERR	LE	VI	WBR	ZS
WAF	WFL	1/0	14/0	IF1	FRP	TK	2/0
W/C	4/0	4/0	5/0	5/1	LT	5/2	5/3
W/B	6/0	EAT	7/0	6/0	WAO	RPL	10/0
12/2	11/0	EXT	EXT	ACT	IER	IRA	MAX
W/P	WVR	WNS	TRANS	WARD	11/1	11/2	12/0
WAT	WADY	WCA	15/0	WAI	WU	18/0	16/0

BECKS WRITTEN TO COMPILE FILE

YAIRSS	C/D	SA	SB	SC	SD	MCN	RHO
WCF	WIS	END	ERR	LE	VI	WBR	ZS
WAF	WFL	1/0	14/0	IF1	FRP	TK	2/0
W/C	4/0	4/0	5/0	5/1	LT	5/2	5/3
W/B	6/0	EAT	7/0	6/0	WAO	RPL	10/0
12/2	11/0	EXT	EXT	ACT	IER	IRA	MAX
W/P	WVR	WNS	TRANS	WARD	11/1	11/2	12/0
WAT	WADY	WCA	15/0	WAI	WU	18/0	16/0

THIS UPDATE REQUIRED 3410CE NCRS OF CORE.
Figure D-37. Structure of OLDPL of Surface (1 of 2)

UNLABELED OLDPL

MASTER AUDIT, IDENT CARD TOTAL

UPDATE V1.2

06/07/73 13.55.50

PAGE 3

SUMMARY OF UPDATE IDENTIFIERS WITHIN DECK - TOTALS

IDENTIFIER	TOTAL	ACTIVE
WALKER	0	0
C/C	1342	1342
SA	19	18
SM	14	14
SC	119	118
SD	29	29
ECN	33	33
MND	17	17
MOD	14	14
VIS	14	14
MAD	40	39
BMP	29	28
LE	0	0
VI	137	135
MBP	249	241
LS	19	18
BXP	113	113
MFL	44	44
1/0	484	478
14/0	1555	1534
FMI	15	15
TA	12	11
2/0	308	495
2/1	169	165
2/2	420	413
4/C	200	193
5/0	675	654
5/1	199	192
LT	19	18
5/2	59	59
5/3	52	51
5/4	363	350
5/5	51	49
6/0	346	320
PAT	150	148
7/0	1391	1369
MND	18	17
MPL	18	18
10/0	109	100
10/1	84	84
10/2	96	92
11/0	470	448
BAT	89	88
POY	93	91
IEP	60	58
INA	76	74
PAX	20	19
PID	22	21
CMV	89	88
SLT	21	21
THUS	91	90
NAED	44	43
11/1	343	313
11/2	196	188
12/0	468	458
14/0	200	193
NAT	498	482
PADY	67	66
POI	497	488
15/0	886	886
PAI	18	18
VW	288	288
IP1	166	166
16/0	46	46
	14116	13755

Figure D-37. Structure of OLDPL of Surface (2 of 2)

06/12/73 LISTIT OF FILE SCL PAGE NO, 1

RECORD NO.	LEVEL NO.	LENGTH	PACKAGE	CHNSUP	CREATION DATE
1	0	900 1684	000000	0616	
2	17	0		0	
LEVEL 17CHNSUP LENGTH IS 900 1684					
***** END FILE *****					

06/12/73 LISTIT OF FILE SCL PAGE NO, 2

RECORD NO.	LEVEL NO.	LENGTH	PACKAGE	CHNSUP	CREATION DATE
1	0	347 933	000000	1414	
2	17	0		0	
LEVEL 17CHNSUP LENGTH IS 347 933					
***** END FILE *****					

06/12/73 LISTIT OF FILE SCL PAGE NO, 3

RECORD NO.	LEVEL NO.	LENGTH	PACKAGE	CHNSUP	CREATION DATE
1	0	00044 280774	000000	1207	
2	17	0		0	
LEVEL 17CHNSUP LENGTH IS 00044 280774					
***** END FILE *****					

06/12/73 LISTIT OF FILE SCL PAGE NO, 4

RECORD NO.	LEVEL NO.	LENGTH	PACKAGE	CHNSUP	CREATION DATE
1	0	00044 280774	000000	1207	
2	17	0		0	
LEVEL 17CHNSUP LENGTH IS 00044 280774					
***** END FILE *****					

06/12/73 LISTIT OF FILE SCL PAGE NO, 5

RECORD NO.	LEVEL NO.	LENGTH	PACKAGE	CHNSUP	CREATION DATE
1	0	0378 20202	000000	310	
2	17	0		0	
LEVEL 17CHNSUP LENGTH IS 0378 20202					
***** END FILE *****					

06/12/73 LISTIT OF FILE SCL PAGE NO, 6

RECORD NO.	LEVEL NO.	LENGTH	PACKAGE	CHNSUP	CREATION DATE
1	0	090 1202	000000	377	
2	17	0		0	
LEVEL 17CHNSUP LENGTH IS 090 1202					
***** END FILE *****					

06/12/73 LISTIT OF FILE SCL PAGE NO, 7

RECORD NO.	LEVEL NO.	LENGTH	PACKAGE	CHNSUP	CREATION DATE
1	0	250 372	000000	1124	
2	17	0		0	
LEVEL 17CHNSUP LENGTH IS 250 372					
***** END FILE *****					

Figure D-38. LISTIT Output from SURFACE Master File (Page 1 of 5)

04/12/73

LISTIT OF FILE SCL

PAGE NO, 8

RECORD NO.	LEVEL NO.	LENGTH	PACKAGE	CHRGUP	CREATION DATE
1	0	100 244	000000	1739	
2	17	0		0	
LEVEL 17CHRGUP LENGTH IS					
000000 END FILE 0000					

04/12/73

LISTIT OF FILE SCL

PAGE NO, 9

RECORD NO.	LEVEL NO.	LENGTH	PACKAGE	CHRGUP	CREATION DATE
1	0	370 962	000000	3736	
2	17	0		0	
LEVEL 17CHRGUP LENGTH IS					
000000 END FILE 0000					

04/12/73

LISTIT OF FILE SCL

PAGE NO, 10

RECORD NO.	LEVEL NO.	LENGTH	PACKAGE	CHRGUP	CREATION DATE
1	0	110 196	0100000	6944	02940000
2	17	0		0	
LEVEL 17CHRGUP LENGTH IS					
000000 END FILE 0000					

04/12/73

LISTIT OF FILE SCL

PAGE NO, 11

RECORD NO.	LEVEL NO.	LENGTH	PACKAGE	CHRGUP	CREATION DATE
1	0	3920 6711	000000	1726	
2	17	0		0	
LEVEL 17CHRGUP LENGTH IS					
000000 END FILE 0000					

04/12/73

LISTIT OF FILE SCL

PAGE NO, 12

RECORD NO.	LEVEL NO.	LENGTH	PACKAGE	CHRGUP	CREATION DATE
1	0	499 763	000000	7989	
2	17	0		0	
LEVEL 17CHRGUP LENGTH IS					
000000 END FILE 0000					

04/12/73

LISTIT OF FILE SCL

PAGE NO, 13

RECORD NO.	LEVEL NO.	LENGTH	PACKAGE	CHRGUP	CREATION DATE
1	0	119 167	000000	9811	
2	17	0		0	
LEVEL 17CHRGUP LENGTH IS					
000000 END FILE 0000					

04/12/73

LISTIT OF FILE SCL

PAGE NO, 14

RECORD NO.	LEVEL NO.	LENGTH	PACKAGE	CHRGUP	CREATION DATE
1	0	71 187	000000	9374	
2	17	0		0	
LEVEL 17CHRGUP LENGTH IS					
000000 END FILE 0000					

Figure D-38. LISTIT Output from SURFACE Master File (Page 2 of 5)

04/12/73 LISTIT OF FILE SCL PAGE NO, 15

RECORD NO.	LEVEL NO.	LENGTH	PACKAGE	GROUP	ORIGIN
	OCTAL	DECIMAL OCTAL(16)			DATE
1	0	209 319	*****	8147	
2	17	0		0	
	LEVEL	17HNCUP LENGTH IS	209 319		
	*****	END FILE *****			

04/12/73 LISTIT OF FILE SCL PAGE NO, 16

RECORD NO.	LEVEL NO.	LENGTH	PACKAGE	GROUP	ORIGIN
	OCTAL	DECIMAL OCTAL(16)			DATE
1	0	102 146	*****	1936	
2	17	0		0	
	LEVEL	17HNCUP LENGTH IS	102 146		
	*****	END FILE *****			

04/12/73 LISTIT OF FILE SCL PAGE NO, 17

RECORD NO.	LEVEL NO.	LENGTH	PACKAGE	GROUP	ORIGIN
	OCTAL	DECIMAL OCTAL(16)			DATE
1	0	790 1426	*****	5936	
2	17	0		0	
	LEVEL	17HNCUP LENGTH IS	790 1426		
	*****	END FILE *****			

04/12/73 LISTIT OF FILE SCL PAGE NO, 18

RECORD NO.	LEVEL NO.	LENGTH	PACKAGE	GROUP	ORIGIN
	OCTAL	DECIMAL OCTAL(16)			DATE
1	0	420 694	*****	6232	
2	17	0		0	
	LEVEL	17HNCUP LENGTH IS	420 694		
	*****	END FILE *****			

04/12/73 LISTIT OF FILE SCL PAGE NO, 19

RECORD NO.	LEVEL NO.	LENGTH	PACKAGE	GROUP	ORIGIN
	OCTAL	DECIMAL OCTAL(16)			DATE
1	0	772 1484	P47EXT	9923	
2	17	0		0	
	LEVEL	17HNCUP LENGTH IS	772 1484		
	*****	END FILE *****			

Figure D-38. LISTIT Output from SURFACE Master File (Page 3 of 5)

06/12/73

LISTIT OF FILE SCL

PAGE NO, 20

RECORD NO.	LEVEL NO.	LENGTH	PAGE	CHNSUP	CREATION DATE
	CCTAL	DECIMAL CCTAL (H)			
13	0	02	122	A	4432
14	0	01	122	F	7834
15	0	01	122	C	4087
16	0	01	122	C	8432
17	0	01	122	C	3340
18	0	01	122	REVMHC	4112
19	0	01	122	REVMHC	4481
20	0	01	122	REVMHC	4875
21	0	01	122	REVMHC	9446
22	0	01	122	REVMHC	4372
23	0	01	122	REVMHC	7732
24	0	01	122	REVMHC	1432
25	0	01	122	REVMHC	7945
26	0	01	122	REVMHC	252
27	0	01	122	REVMHC	8885
28	0	01	122	REVMHC	2376
29	0	01	122	REVMHC	
30	0	01	122	REVMHC	1380
31	0	01	122	REVMHC	
32	0	01	122	REVMHC	335
33	0	01	122	REVMHC	9787
34	0	01	122	REVMHC	6275
35	0	01	122	REVMHC	6840
36	0	01	122	REVMHC	
37	0	01	122	REVMHC	5316
38	0	01	122	REVMHC	
39	0	01	122	REVMHC	1895
40	0	01	122	REVMHC	
41	0	01	122	REVMHC	2141
42	0	01	122	REVMHC	
43	0	01	122	REVMHC	5324
44	0	01	122	REVMHC	
45	0	01	122	REVMHC	8841
46	0	01	122	REVMHC	
47	0	01	122	REVMHC	2067
48	0	01	122	REVMHC	5063
49	0	01	122	REVMHC	
50	0	01	122	REVMHC	2066
51	0	01	122	REVMHC	
52	0	01	122	REVMHC	7735
53	0	01	122	REVMHC	
54	0	01	122	REVMHC	8490
55	0	01	122	REVMHC	
56	0	01	122	REVMHC	3625
57	0	01	122	REVMHC	
58	0	01	122	REVMHC	5366
59	0	01	122	REVMHC	5261
60	0	01	122	REVMHC	
61	0	01	122	REVMHC	7213
62	0	01	122	REVMHC	1122

06/12/73
06/12/73

06/12/73

LISTIT OF FILE SCL

PAGE NO, 21

RECORD NO.	LEVEL NO.	LENGTH	PAGE	CHNSUP	CREATION DATE
	CCTAL	DECIMAL CCTAL (H)			
63	0	01	122	ALTER	2465
64	0	01	122	ALTER	
65	0	01	122	ALTER	4313
66	0	01	122	ALTER	
67	0	01	122	ALTER	1107
68	0	01	122	ALTER	
69	0	01	122	ALTER	5012
70	0	01	122	ALTER	
71	0	01	122	ALTER	1227
72	0	01	122	ALTER	7602
73	0	01	122	ALTER	7013
74	0	01	122	ALTER	4433
75	0	01	122	ALTER	4772
76	0	01	122	ALTER	5776
77	0	01	122	ALTER	3101
78	0	01	122	ALTER	6603
79	0	01	122	ALTER	6017
80	0	01	122	ALTER	7607
81	0	01	122	ALTER	4736
82	0	01	122	ALTER	
83	0	01	122	ALTER	5903
84	0	01	122	ALTER	
85	0	01	122	ALTER	1079
86	0	01	122	ALTER	
87	0	01	122	ALTER	6703
88	0	01	122	ALTER	
89	0	01	122	ALTER	22
90	0	01	122	ALTER	142
91	0	01	122	ALTER	1013
92	0	01	122	ALTER	3643
93	0	01	122	ALTER	
94	0	01	122	ALTER	3120
95	0	01	122	ALTER	1223
96	0	01	122	ALTER	
97	0	01	122	ALTER	6677
98	0	01	122	ALTER	

LEVEL 174400 LENGTH 15 51455 142743
***** END FILE *****

Figure D-38. LISTIT Output from SURFACE Master File (Page 4 of 5)

01/12/73

LISTIT OF FILE SCL

PAGE NO. 22

RECORD NO.	LEVEL NO.	LENGTH	PACKAGE	CHRSUM	CREATION DATE
1>	0	113	143	000000	0244
2	0	113	143	000000	0244
3	17	0	0	0	0
LEVEL 17 CHRSUM LENGTH IS 113 143					
***** END FILE *****					

01/12/73

LISTIT OF FILE SCL

PAGE NO. 23

RECORD NO.	LEVEL NO.	LENGTH	PACKAGE	CHRSUM	CREATION DATE
1	0	113	143	000000	0244
2	17	0	0	0	0
LEVEL 17 CHRSUM LENGTH IS 113 143					
***** END FILE *****					

Figure D-38. LISTIT Output from SURFACE Master File (Page 5 of 5)


```
SKIPF,A,1,17,B.  
COPYBR,INPUT,INDD.  
REWIND INDD.  
RFL,40000.  
UPDATE(D,E,F,U,N=DDOPL,C=DDATA,L=A12)  
RFL,10000.
```

```
*/          UPDATE JOB DECK FOR INSERTION OF NEW DDATA  
*DECK DD  
*READ INDD  
7/8/9
```

Figure D-39. Control Cards for Replacement of a DATA Deck

<u>Parameter</u>	<u>Program Variable</u>	<u>Assigned Value</u>	<u>Input Method</u>
Plume Shape Specification 1/4 Latus Rectum	P	1.0	NAMELIST/NAST4 Input of P1
Plume Shape Change During Startup and Tailoff; Change in Latus Rectum	DELP	0.001	NAMELIST/NAST4 Input of DELP1

Second: Using the input data files described earlier with the above specific values, SURFACE was executed with STPFLG = 1. This resulted in execution proceeding only as far as calculation of the satellite surface segments which are impinged by the thruster plume, and their coordinates in the thruster-based coordinate system. These data were listed, current values of all variables were stored on a magnetic tape, and then the program stopped automatically.

The list of locations of impinged segments was then used as the basis of a manual search of KINCON and MULTRAN output listings to find the plume characteristics at the locations and times corresponding to plume time slices. The method of determining these data is described in the main section of the description of the test case.

The plume characteristics data were then punched on cards in the correct format for file EDATA.

A second run of SURFACE was then made with STPFLG = 2, with the new EDATA file replacing the default data supplied with the program, and using the magnetic tape to supply values of variables which had been stored earlier.

In this run, computations started immediately after the location at which the previous run was halted.

The listings from the two runs are discussed separately below:

RUN WITH STPFLG = 1 FOR CALCULATION OF PLUME-SURFACE INTERCEPTS

The option to list all normally-generated output was left turned on (16F = 6); hence the listing is complete. In the illustrations given in this report, some redundant portions are truncated to save space.

Initialization and Timing (Figure D-40)

The first three statements (date, time prior to entry, and rollout warning) are generated in the auxiliary (0,0) overlay, Program TM42. The note about long operating times and rollouts is borne out almost at once; the excessive time for running (2,1) is due to a rollout, see the section of the dayfile indicating a 14 minute rollout inserted to the left of the listing of the time needed for (2,1). The remainder of the timing messages are generated in the main program. Overlay (2,1) is used to input all the NAMELIST modifications to the data.

IF ANY OPERATING TIMES SEEM UNREASONABLY LONG
CHECK THE DAYFILE FOR ROLLOUTS IN THE SAME CLOCK
TIME PERIOD

CP TIME USED = 37.91 SECONDS
PP TIME USED = 275.03 SECONDS
SINCE JOB STARTED

CP TIME USED = 30.95 SECONDS
PP TIME USED = 270.90 SECONDS
SINCE JOB STARTED

SSSSSSSS	PPPPPPPP	AAAA	CCCCCCC	EEEEEEEE	SSSSSSSS	MM	MM	0000000	00000000
SSSSSSSS	PPPPPPPP	AAAAA	CCCCCCCC	EEEEEEEE	SSSSSSSS	MMM	MMM	00000000	00000000
SS	PP	AA	CC	EE	SS	MM	MM	00	00
SS	PP	AA	CC	EE	SS	MM	MM	00	00
SSSSSSSS	PPPPPPPP	AAAAA	CCCC	EEEE	SSSSSSSS	MM	MM	00	00
SSSSSSSS	PPPPPPPP	AAAAA	CCCC	EEEE	SSSSSSSS	MM	MM	00	00
SS	PP	AA	CC	EE	SS	MM	MM	00	00
SS	PP	AA	CC	EE	SS	MM	MM	00	00
SSSSSSSS	PP	AA	CC	CCCCC	EEEEEEEE	SSSSSSSS	MM	MM	00000000
SSSSSSSS	PP	AA	CC	CCCCC	EEEEEEEE	SSSSSSSS	MM	MM	00000000

663

Satellite Configuration Description

The next operation is reading in the configuration of the satellite used in the calculations. The data are read from file ADATA. Figure D-41 presents the input data as tabulations which consist of a description of the satellite exterior.

Note that the presence of 'projections' from the satellite surface is signalled by numbers other than -1. appearing in the column headed "Height of Projection" in the main table "Satellite Configuration." Following the main table, details are given about the projections; the details include the ID number of the segment to which they are attached (compare column 1 of the main table).

Properties of Structural Materials and Plume/Deposit Constituents

The properties of materials and constituents which will form the basis for calculation of exposure effects are next listed. The data were read from ADATA and INDATA. Approximations for data not supplied are performed after the inputs are completed, and the information given in Figure D-42 includes both input and approximated data. The listing is in the order physical properties of structural materials, phys-chem properties of plume/deposit constituents, wear rate properties of all substance, and optical and thermal constants for all materials. The last section of this part lists significant data which were not input and which could not be approximated.

Coefficients and Physical-Chemical Properties of Deposit Materials

The values for representative constants which are internally generated from the input data are listed. The listing is presented as Figure D-43. The listed values can be compared with available literature values for a check of the accuracy of the program computations. Flagrant variation can indicate errors in either the input data or in a computation module.

Data Revisions

The revised data supplied by means of NAMELIST input are listed, because the flag RDWRT is greater than zero. These revisions alter the values input from the data files or the defaults assigned in the program. Figure D-44 shows the revision inputs. Remember that these revisions do not affect data storage or execution paths until the point at which execution tests for their existence and then replaces the old values. Hence the other data file input listings still show the original values as supplied.

Assignment of Calculation Cycles

The basic set of calculation cycles, read from file ADATA, is next interpreted and listed. These data can be superseded by NAMELIST inputs, and in this particular case, they are (see section above on Data Revisions). The listing of calculation cycles is illustrated in Figure D-45.

SATELLITE CONFIGURATION

S E G M E N T					X DIST SEGMENT TO PLUME VERTEX (FT)	SURFACE TEMPER ATURE (DEG R)	HEIGHT OF PROJECTION (FT)	DIRECTION COSINES OF NORMAL TO PROJECTION TANGENT PLANE		
ID NO.	X COORD. (FT)	Y COORD. (FT)	THETA (RAD)	AREA (SQ FT)				LAMBDA	MU	MU
1	0.000	0.000	0.00000	1	-3.000	520.0	-1.0	-1.0	-1.0	-1.0
2	.305	.590	1.04720	1	-3.295	520.0	-1.0	-1.0	-1.0	-1.0
3	.305	.590	3.14159	1	-3.295	520.0	-1.0	-1.0	-1.0	-1.0
4	.305	.590	5.23600	1	-3.295	520.0	-1.0	-1.0	-1.0	-1.0
5	.620	1.200	.62830	1	-2.900	520.0	9.4	1.0000	0.0000	0.0000
6	.620	1.200	1.00490	1	-2.900	520.0	-1.0	-1.0	-1.0	-1.0
7	.620	1.200	3.14159	1	-2.900	520.0	-1.0	-1.0	-1.0	-1.0
8	.620	1.200	4.39810	1	-2.900	520.0	-1.0	-1.0	-1.0	-1.0
9	.620	1.200	5.65460	1	-2.900	520.0	-1.0	-1.0	-1.0	-1.0
10	1.325	1.600	.31416	1	-2.275	520.0	-1.0	-1.0	-1.0	-1.0
11	1.325	1.600	.94248	1	-2.275	520.0	-1.0	-1.0	-1.0	-1.0
12	1.325	1.600	1.57080	1	-2.275	520.0	-1.0	-1.0	-1.0	-1.0
13	1.325	1.600	2.19911	1	-2.275	520.0	-1.0	-1.0	-1.0	-1.0
14	1.325	1.600	2.82743	1	-2.275	520.0	-1.0	-1.0	-1.0	-1.0
15	1.325	1.600	3.45575	1	-2.275	520.0	-1.0	-1.0	-1.0	-1.0
16	1.325	1.600	4.08407	1	-2.275	520.0	-1.0	-1.0	-1.0	-1.0
17	1.325	1.600	4.71240	1	-2.275	520.0	-1.0	-1.0	-1.0	-1.0
18	1.325	1.600	5.34070	1	-2.275	520.0	-1.0	-1.0	-1.0	-1.0
19	1.325	1.600	5.96902	1	-2.275	520.0	-1.0	-1.0	-1.0	-1.0
20	2.325	1.600	.31416	1	-1.275	520.0	-1.0	-1.0	-1.0	-1.0
21	2.325	1.600	.94248	1	-1.275	520.0	-1.0	-1.0	-1.0	-1.0
22	2.325	1.600	1.57080	1	-1.275	520.0	-1.0	-1.0	-1.0	-1.0
23	2.325	1.600	2.19911	1	-1.275	520.0	-1.0	-1.0	-1.0	-1.0
24	2.325	1.600	2.82743	1	-1.275	520.0	-1.0	-1.0	-1.0	-1.0
25	2.325	1.600	3.45575	1	-1.275	520.0	-1.0	-1.0	-1.0	-1.0
26	2.325	1.600	4.08407	1	-1.275	520.0	-1.0	-1.0	-1.0	-1.0
27	2.325	1.600	4.71240	1	-1.275	520.0	-1.0	-1.0	-1.0	-1.0
28	2.325	1.600	5.34070	1	-1.275	520.0	-1.0	-1.0	-1.0	-1.0
29	2.325	1.600	5.96902	1	-1.275	520.0	-1.0	-1.0	-1.0	-1.0
30	3.325	1.600	.31416	3	-.275	520.0	1.5	NOT	APPLICABLE	
31	3.325	1.600	.94248	1	-.275	520.0	-1.0	-1.0	-1.0	-1.0
32	3.325	1.600	1.57080	3	-.275	520.0	1.5	NOT	APPLICABLE	
33	3.325	1.600	2.19911	1	-.275	520.0	-1.0	-1.0	-1.0	-1.0
34	3.325	1.600	2.82743	1	-.275	520.0	-1.0	-1.0	-1.0	-1.0
35	3.325	1.600	3.45575	3	-.275	520.0	1.5	NOT	APPLICABLE	
36	3.325	1.600	4.08407	1	-.275	520.0	-1.0	-1.0	-1.0	-1.0
37	3.325	1.600	4.71240	3	-.275	520.0	1.5	NOT	APPLICABLE	
38	3.325	1.600	5.34070	1	-.275	520.0	-1.0	-1.0	-1.0	-1.0
39	3.325	1.600	5.96902	1	-.275	520.0	-1.0	-1.0	-1.0	-1.0
40	4.325	1.600	.31416	1	.725	520.0	-1.0	-1.0	-1.0	-1.0
41	4.325	1.600	.94248	1	.725	520.0	-1.0	-1.0	-1.0	-1.0
42	4.325	1.600	1.57080	1	.725	520.0	-1.0	-1.0	-1.0	-1.0
43	4.325	1.600	2.19911	1	.725	520.0	-1.0	-1.0	-1.0	-1.0
44	4.325	1.600	2.82743	1	.725	520.0	-1.0	-1.0	-1.0	-1.0
45	4.325	1.600	3.45575	1	.725	520.0	-1.0	-1.0	-1.0	-1.0
46	4.325	1.600	4.08407	1	.725	520.0	-1.0	-1.0	-1.0	-1.0
47	4.325	1.600	4.71240	1	.725	520.0	-1.0	-1.0	-1.0	-1.0
48	4.325	1.600	5.34070	1	.725	520.0	-1.0	-1.0	-1.0	-1.0
49	4.325	1.600	5.96902	1	.725	520.0	-1.0	-1.0	-1.0	-1.0
50	5.325	1.600	.31416	1	1.725	520.0	-1.0	-1.0	-1.0	-1.0
51	5.325	1.600	.94248	1	1.725	520.0	-1.0	-1.0	-1.0	-1.0
52	5.325	1.600	1.57080	1	1.725	520.0	-1.0	-1.0	-1.0	-1.0
53	5.325	1.600	2.19911	1	1.725	520.0	-1.0	-1.0	-1.0	-1.0
54	5.325	1.600	2.82743	1	1.725	520.0	-1.0	-1.0	-1.0	-1.0
55	5.325	1.600	3.45575	1	1.725	520.0	-1.0	-1.0	-1.0	-1.0
56	5.325	1.600	4.08407	1	1.725	520.0	-1.0	-1.0	-1.0	-1.0
57	5.325	1.600	4.71240	1	1.725	520.0	-1.0	-1.0	-1.0	-1.0
58	5.325	1.600	5.34070	1	1.725	520.0	-1.0	-1.0	-1.0	-1.0
59	5.325	1.600	5.96902	1	1.725	520.0	-1.0	-1.0	-1.0	-1.0
60	6.325	1.600	.31416	1	2.725	520.0	-1.0	-1.0	-1.0	-1.0
61	6.325	1.600	.94248	1	2.725	520.0	-1.0	-1.0	-1.0	-1.0
62	6.325	1.600	1.57080	1	2.725	520.0	-1.0	-1.0	-1.0	-1.0
63	6.325	1.600	2.19911	1	2.725	520.0	-1.0	-1.0	-1.0	-1.0
64	6.325	1.600	2.82743	1	2.725	520.0	-1.0	-1.0	-1.0	-1.0
65	6.325	1.600	3.45575	1	2.725	520.0	-1.0	-1.0	-1.0	-1.0
66	6.325	1.600	4.08407	1	2.725	520.0	-1.0	-1.0	-1.0	-1.0
67	6.325	1.600	4.71240	1	2.725	520.0	-1.0	-1.0	-1.0	-1.0
68	6.325	1.600	5.34070	1	2.725	520.0	-1.0	-1.0	-1.0	-1.0
69	6.325	1.600	5.96902	1	2.725	520.0	-1.0	-1.0	-1.0	-1.0
70	7.325	1.600	.31416	1	3.725	520.0	-1.0	-1.0	-1.0	-1.0
71	7.325	1.600	.94248	1	3.725	520.0	-1.0	-1.0	-1.0	-1.0
72	7.325	1.600	1.57080	1	3.725	520.0	-1.0	-1.0	-1.0	-1.0
73	7.325	1.600	2.19911	1	3.725	520.0	4.0	.9820	.1000	.0500
74	7.325	1.600	2.82743	1	3.725	520.0	-1.0	-1.0	-1.0	-1.0
75	7.325	1.600	3.45575	1	3.725	520.0	-1.0	-1.0	-1.0	-1.0
76	7.325	1.600	4.08407	1	3.725	520.0	-1.0	-1.0	-1.0	-1.0
77	7.325	1.600	4.71240	1	3.725	520.0	-1.0	-1.0	-1.0	-1.0
78	7.325	1.600	5.34070	1	3.725	520.0	-1.0	-1.0	-1.0	-1.0
79	7.325	1.600	5.96902	1	3.725	520.0	-1.0	-1.0	-1.0	-1.0
80	8.325	1.600	.31416	1	4.725	520.0	-1.0	-1.0	-1.0	-1.0
81	8.325	1.600	.94248	1	4.725	520.0	-1.0	-1.0	-1.0	-1.0
82	8.325	1.600	1.57080	1	4.725	520.0	-1.0	-1.0	-1.0	-1.0
83	8.325	1.600	2.19911	1	4.725	520.0	-1.0	-1.0	-1.0	-1.0

Figure D-41. Satellite Configuration Listing (Page 1 of 3)

84	8.325	1.000	2.02743	1	4.725	520.0	-1.0	-1.0	-1.0	-1.0
85	8.325	1.000	3.45575	1	4.725	520.0	-1.0	-1.0	-1.0	-1.0
86	8.325	1.000	4.08407	1	4.725	520.0	-1.0	-1.0	-1.0	-1.0
87	8.325	1.000	4.71240	1	4.725	520.0	-1.0	-1.0	-1.0	-1.0
88	8.325	1.000	5.34070	1	4.725	520.0	-1.0	-1.0	-1.0	-1.0
89	8.325	1.000	5.96902	1	4.725	520.0	-1.0	-1.0	-1.0	-1.0
90	9.325	1.000	.31416	1	5.725	520.0	-1.0	-1.0	-1.0	-1.0
91	9.325	1.000	.94240	1	5.725	520.0	-1.0	-1.0	-1.0	-1.0
92	9.325	1.000	1.57000	1	5.725	520.0	-1.0	-1.0	-1.0	-1.0
93	9.325	1.000	2.19911	1	5.725	520.0	-1.0	-1.0	-1.0	-1.0
94	9.325	1.000	2.82743	1	5.725	520.0	-1.0	-1.0	-1.0	-1.0
95	9.325	1.000	3.45575	1	5.725	520.0	-1.0	-1.0	-1.0	-1.0
96	9.325	1.000	4.08407	1	5.725	520.0	-1.0	-1.0	-1.0	-1.0
97	9.325	1.000	4.71240	1	5.725	520.0	-1.0	-1.0	-1.0	-1.0
98	9.325	1.000	5.34070	1	5.725	520.0	-1.0	-1.0	-1.0	-1.0
99	9.325	1.000	5.96902	1	5.725	520.0	-1.0	-1.0	-1.0	-1.0
100	10.325	1.000	.31416	1	6.725	520.0	-1.0	-1.0	-1.0	-1.0
101	10.325	1.000	.94240	1	6.725	520.0	-1.0	-1.0	-1.0	-1.0
102	10.325	1.000	1.57000	1	6.725	520.0	-1.0	-1.0	-1.0	-1.0
103	10.325	1.000	2.19911	1	6.725	520.0	-1.0	-1.0	-1.0	-1.0
104	10.325	1.000	2.82743	1	6.725	520.0	-1.0	-1.0	-1.0	-1.0
105	10.325	1.000	3.45575	1	6.725	520.0	-1.0	-1.0	-1.0	-1.0
106	10.325	1.000	4.08407	1	6.725	520.0	-1.0	-1.0	-1.0	-1.0
107	10.325	1.000	4.71240	1	6.725	520.0	-1.0	-1.0	-1.0	-1.0
108	10.325	1.000	5.34070	1	6.725	520.0	-1.0	-1.0	-1.0	-1.0
109	10.325	1.000	5.96902	1	6.725	520.0	-1.0	-1.0	-1.0	-1.0
110	10.825	1.195	.52300	1	6.725	520.0	-1.0	-1.0	-1.0	-1.0
111	10.825	1.195	1.57000	1	6.725	520.0	-1.0	-1.0	-1.0	-1.0
112	10.825	1.195	2.61000	1	6.725	520.0	-1.0	-1.0	-1.0	-1.0
113	10.825	1.195	3.65200	1	6.725	520.0	-1.0	-1.0	-1.0	-1.0
114	10.825	1.195	4.71240	1	6.725	520.0	-1.0	-1.0	-1.0	-1.0
115	10.825	1.195	5.75900	1	6.725	520.0	-1.0	-1.0	-1.0	-1.0
116	10.825	0.000	0.00000	2	6.725	520.0	2.5	NOT APPLICABLE		

NOTE VALUES OF -1.0 INDICATE NO DATA ENTERED.

EXTERNAL TOTAL AREA = 125.00 SQUARE FEET

PROJECTIONS

AERIAL AT SEGMENT NO. 5

S E G M E N T					X DIST SEGMENT TO PLUME VERTEX (FT)	SURFACE TEMPER- ATURE (DEG R)
ID NO.	X COORD. (FT)	R COORD. (FT)	THETA (RAD)*	AREA (SQFT)		
501	.599	5.300	-6.28300	1	-2.959	529.2
502	.641	5.300	6.28300	1	-3.001	529.2

* NEGATIVE VALUE FOR ANGLE SIGNALS THAT SEGMENT IS ON
SIDE OF PROJECTION FACING AWAY FROM THE PLUME.

AREA OF AERIAL IS 2.0 SQUARE FEET.

THRUSTER NO.	SEGMENT NO.	X (FT)	R (FT)	THETA (RAD)

PLUME AFT

1	30	3.600	2.100	.314160
2	32	3.600	2.100	1.571000
3	35	3.600	2.100	3.142000
4	37	3.600	2.100	4.712000

Figure D-41. Satellite Configuration Listing (Page 2 of 3)

SOLCEL AT SEGMENT NO. 73

S E G M E N T					X DIST	SURFACE
ID	X	R	THETA	AREA	SEGMENT	TEMPER-
NO.	COORD.	COORD.	(RAD)*	(SQFT)	TO PLUME	ATURE
	(FT)	(FT)			VERTEX	(DEG R)
					(FT)	
7301	6.886	2.502	2.19911	1	3.286	550.0
7302	6.608	4.161	1.49900	1	3.000	560.0
7303	6.603	4.056	2.19911	1	3.003	560.0
7304	6.598	3.951	2.89900	1	2.998	560.0
7305	6.420	5.122	1.50100	1	2.020	560.0
7306	6.415	5.038	2.19911	1	2.015	560.0
7307	6.410	4.954	2.89700	1	2.010	560.0
7308	6.232	6.100	1.50300	1	2.032	560.0
7309	6.227	6.020	2.19911	1	2.027	560.0
7310	6.222	5.940	2.89500	1	2.022	560.0
7311	6.723	6.200	-2.89500	1	3.123	510.0
7312	6.718	6.119	-2.19911	1	3.118	510.0
7313	6.713	6.038	-1.50300	1	3.113	510.0
7314	6.911	5.235	-2.89700	1	3.311	510.0
7315	6.906	5.137	-2.19911	1	3.306	510.0
7316	6.901	5.039	-1.50100	1	3.301	510.0
7317	7.099	4.275	-2.89900	1	3.499	510.0
7318	7.094	4.155	-2.19911	1	3.494	510.0
7319	7.089	4.035	-1.49900	1	3.489	510.0
7320	7.372	2.681	-2.19911	1	3.772	520.0

* NEGATIVE VALUE FOR ANGLE SIGNALS THAT SEGMENT IS ON
SIDE OF PROJECTION FACING AWAY FROM THE PLUME.

AREA OF SOLCEL IS 20.0 SQUARE FEET.

THRUSTER	SEGMENT	X	R	THETA
NO.	NO.	(FT)	(FT)	(RAD)

PLUME AFT

5	116	11.050	1.0000E-05	0.000000
---	-----	--------	------------	----------

PLUME FORWARD

6	30	3.600	2.100	.314160
7	32	3.600	2.100	1.571000
8	35	3.600	2.100	3.142000
9	37	3.600	2.100	4.712000

TOTAL SATELLITE AREA, INCLUDING PROJECTIONS, IS 147.00 SQUARE FEET.

STRUCTURE ELEMENTS CURRENTLY USED

MAIN STRUCTURE	PROJECTIONS
BASIC SEGMENTS	THRUSTORS
WINDOWS	RADIO ANTENNAE
INFRA RED PORTS	SOLAR CELL ARRAYS
ULTRA VIOLET PORTS	SUPPORTS

HICKORY-DICKORY SAYS 7.20 SECONDS
FOR RUNNING OVERLAY(1.0)
FINISHED AT CLOCK TIME 11-24-48.0

CP TIME USED = 124.18 SECONDS
PP TIME USED = 41.35 SECONDS
SINCE JOB STARTED

Figure D-41. Satellite Configuration Listing (Page 3 of 3)

MATERIALS AND DEPOSITS USED IN PROGRAM

MATERIALS	DEPOSITS
ALUMIN	N204
WINDOW	MN03
SOLCEL	MMH
IMPORT	MMH20
UVPORT	MMH03
TEFLON	MMH,40
GOLD	WATER
BLACK	AMONIA
WHITE	NH00H
NAPTAN	NH003
UNASND	MMH,40

PROPERTIES OF STRUCTURAL MATERIALS

MATERIAL	CODE NO.	MELTING POINT (DEG R)	VICKERS HARDNESS (KG/50MM)	BULK MODULUS (PSI)	SURFACE TENSION (DYNE/CM)	HEAT CAPACITY (BTU/LB-DEG)	THERMAL CONDUCTIVITY (BTU-IN/80FT-DEG-SEC)	YIELD STRENGTH (PSI)	DENSITY (LB/CUFT)
ALUMIN	1	1270.00	27.000E+01	98.000E+05	900.000	.215	.457	47.000E+03	169.00
WINDOW	2	1700.00	55.000E+01	99.000E+05	200.000	.170	.002	50.000E+03	162.00
SOLCEL	3	1520.00	49.000E+01	23.000E+05	200.000	.180	.002	80.000E+02	139.00
IMPORT	4	425.00	45.000E+01	64.000E+04	200.000	.200	.008	80.000E+02	390.00
UVPORT	5	1350.00	40.000E+01	99.000E+05	200.000	.180	.003	80.000E+02	135.00
TEFLON	6	970.00	40.000E+01	65.000E+04	15.000	.250	.001	20.000E+02	143.00
GOLD	7	2440.00	50.000E+00	11.000E+06	1120.000	.031	.006	30.000E+02	1230.00
BLACK	8	6700.00	20.000E+01	10.000E+05	190.000	.360	.023	12.000E+03	110.00
WHITE	9	5270.00	20.000E+01	10.000E+05	190.000	.250	.007	12.000E+03	356.00
NAPTAN	10	1140.00	10.000E+00	51.000E+03	80.000	.310	.002	75.000E+02	88.70

NOTE VALUES OF -1.0 INDICATE NO DATA ENTERED,
OR INTERNALLY GENERATED.

REFERENCE RUN NO. 1 CASE NO. 1

OPERATING CONDITIONS

EXTERNAL PRESSURE WALL TEMPERATURE
(PSIA) (DEG R)
1.000000E-06 520.200000

DEFAULT INSTRUCTIONS

STOP TIME TIME INTERVAL
(SEC) (SEC)
.020000 .004000

MMH PROPERTIES

BOILING POINT (DEG R)	FREEZING POINT (DEG R)	CRITICAL TEMP. (DEG R)	CRITICAL PRESS. (PSIA)
640.000000	397.000000	1052.000000	1195.000000
VAPOR CP. (BTU/LB-DEG)	LIQUID CP. (BTU/LB-DEG)	SOLID CP. (BTU/LB-DEG)	MOL. WEIGHT (LB/LB-MOLE)
.905000	.600000	.522292	46.074000
LATENT HEAT VAP. (BTU/LB)	LATENT HEAT FUS. (BTU/LB)	LIG. THERM. COND. ACCON. COEFF. (BTU-IN/80FT-DEG-SEC)	
370.000000	97.300000	.000404	.100000
REFERENCE TEMP. (DEG R)	SPECIFIC GRAVITY	VISCOSITY (LBM/FT-SEC)	SURFACE TENSION (LB(N)/IN)
540.000000	.870000	.000600	.000190

N204 PROPERTIES

BOILING POINT (DEG R)	FREEZING POINT (DEG R)	CRITICAL TEMP. (DEG R)	CRITICAL PRESS. (PSIA)
529.200000	471.370000	776.000000	1441.300000

Figure D-42. Properties of Materials (Page 1 of 10)

VAPOR CP. (BTU/LB-DEG) .295000	LIQUID CP. (BTU/LB-DEG) .378300	SOLID CP. (BTU/LB-DEG) .295000	VAP. MOL. WEIGHT (LB/LB-MOLE) 46.005000
LATENT HEAT VAP. (BTU/LB) 178.200000	LATENT HEAT FUS. (BTU/LB) 68.510000	LIG. THERM. COND. ACCOM. COEFF. (BTU-IN/SGFT-DEG-SEC) .002509	.100000
REFERENCE TEMP. (DEG R) 540.000000	SPECIFIC GRAVITY 1.434000	VISCOSITY (LBH/FT-SEC) .000265	SURFACE TENSION (LBH/IN) .000100

PHYSICO-CHEMICAL PROPERTIES OF PLUME DEPOSITS

NAME	CODE	FREEZING POINT (DEG R)	SOLID DENSITY (LB/CUFT)	CRITICAL TEMP. (DEG R)	BOILING POINT (DEG R)	FUSION HEAT (BTU/LB)	VAPORIZN HEAT (BTU-IN/SGFT-SEC-DEG)	CONDUCTIVITY SOL. LIQ. (BTU-IN/SGFT-SEC-DEG)	HEAT CAPACITY SOL. LIQ. (BTU/LB-DEG)	REFRACTIVE INDEX LIQ.	MOLECULAR RADIUS (ANGSTR.)	LIQUID DENSITY (LB/CUFT)
N2O4	1	471.4	118.6	776.4	529.2	68.5	178.2	2.52E-04 2.51E-03	.295 .750	1.420	3.710	49.522
HN03	2	418.2	118.3	851.5	549.0	92.9	296.2	1.17E-02 3.36E-03	.650 .420	1.402	4.085	41.207
MMH	3	397.0	75.3	1052.0	648.0	97.3	378.0	1.49E-03 4.04E-04	.350 .700	1.430	4.607	54.312
MMHM20	4	382.0	62.4	1108.0	900.0	-1.0	180.0	2.38E-03 6.66E-04	.395 .704	1.403	5.150	64.925
MMHM03	5	597.0	62.4	1350.0	900.0	82.5	180.0	-1.0 1.60E-04	.967 .732	-1.0	5.298	-1.0
MMH, A0	6	-1.0	62.4	1350.0	900.0	-1.0	180.0	-1.0 1.13E-04	.809 .821	-1.0	5.644	-1.0
WATER	7	491.0	57.2	1165.0	671.0	143.2	971.3	4.16E-03 1.13E-03	.490 1.000	1.333	1.140	62.347
AMONIA	8	351.9	51.0	730.0	431.5	194.6	589.3	1.93E-03 9.70E-04	.600 1.044	1.325	2.074	42.563
MMHOM	9	349.5	63.2	989.7	475.0	104.0	640.0	2.45E-03 7.00E-04	1.341 1.015	1.357	1.190	54.937
MMHM03	10	797.0	107.8	1080.0	720.0	32.8	180.0	4.84E-03 1.38E-03	.415 .641	1.414	4.100	88.023
MMH, A0	11	598.0	62.4	1029.1	686.1	-1.0	180.0	4.71E-03 1.34E-03	.420 .707	1.177	4.340	81.551
MMFU00	12	-1.0	62.4	1350.0	900.0	-1.0	180.0	1.49E-04 4.20E-05	.793 .600	-1.0	5.298	62.420
AL2O3	13	4150.0	247.5	664E+1	4430.0	461.0	180.0	1.30E-03 3.72E-04	.190 .333	1.700	6.300	-1.0
MCL	14	291.6	62.4	584.3	330.4	23.4	190.7	4.31E-04 1.23E-04	.191 .192	1.411	1.350	102.319
MCL, A0	15	450.0	62.4	875.0	699.4	120.0	177.7	3.24E-03 7.28E-04	.753 .570	1.365	1.600	75.725
FE2O3	16	3260.0	327.0	12960.0	8440.0	1500.0	180.0	9.01E-03 2.58E-03	.155 .117	3.010	6.500	-1.0
CARBON	17	1000.0	140.6	12075.0	8050.0	-1.0	180.0	1.20E-02 3.43E-03	.170 .129	-1.0	3.000	-1.0
MMHCL	18	1050.0	95.3	1633.0	1100.0	-1.0	142.0	4.69E-03 1.34E-03	.307 .530	1.371	3.240	-1.0
ABACCL	19	803.0	62.4	1035.3	690.2	135.0	180.0	4.60E-03 1.26E-03	.434 .724	1.370	3.495	66.611
MMH0	20	494.3	71.5	1117.0	696.0	170.0	550.0	1.91E-03 5.47E-04	.470 .730	1.404	3.996	62.709
MMH, A0	21	395.1	62.4	1057.5	705.0	-1.0	180.0	2.50E-03 7.32E-04	1.030 .700	1.424	3.234	102.010
MMH03	22	618.0	62.4	1115.0	743.0	-1.0	180.0	-1.0 -1.0	-1.0 -1.0	-1.0	3.763	-1.0
MMHNT	23	563.0	62.4	1350.0	900.0	-1.0	180.0	-1.0 1.20E-04	.766 .580	-1.0	4.001	-1.0

NOTE: VALUES OF -1.0 INDICATE NO DATA ENTERED.
OR INTERNALLY GENERATED.
(A), DECOMPOSITION TEMPERATURE.
(B), HEAT OF ABLATION OR DECOMPOSITION.
(C), SUBLIMATION.

HEAR CONSTANTS OF MATERIALS ON SURFACE

NAME	ID	HEAR CONSTANT (FT-LB/LB)	VELOCITY LIMIT (FT/SEC)	EXPONENT (BLOPF)	MOLECULAR WEIGHT (VAPOR)
ALUMIN	1	3.000E+06	400	-3.3125	---
MMHND	2	5.000E+04	170	-3.5625	---
BOLCEL	3	5.000E+04	170	-3.5625	---
MMHPORT	4	4.000E+04	170	-3.5625	---
MMHPORT	5	5.000E+04	170	-3.5625	---
TEFLON	6	1.500E+05	1000	-2.5000	---
BOLD	7	3.000E+06	400	-3.3125	---
PLATING					
BLACK	8	1.200E+04	200	-2.5000	---
COATING					
WHITE	9	1.200E+04	200	-2.5000	---
COATING					
KAPTON	10	1.500E+05	900	-2.5100	---

DEPOSITS

N2O4	1	1.000E+04	220	-3.0000	46.0
HN03	2	1.000E+04	220	-3.0000	63.0
MMH	3	1.000E+04	220	-3.0000	46.0
MMHM20	4	1.000E+04	220	-3.0000	64.0
MMHM03	5	1.000E+04	220	-3.0000	109.0
MMH, A0	6	1.000E+04	220	-3.0000	154.0
WATER	7	1.000E+04	220	-3.0000	18.0
AMONIA	8	1.500E+05	170	-3.1900	17.0
MMHOM	9	1.500E+05	160	-3.1900	35.0
MMHM03	10	1.500E+05	123	-3.1900	80.0
MMH, A0	11	1.500E+05	161	-3.1900	90.0
MMFU00	12	1.500E+05	161	-3.1900	252.0
AL2O3	13	1.500E+05	81	-3.1900	101.9
MCL	14	1.500E+05	161	-3.1900	36.5
MCL, A0	15	1.500E+05	161	-3.1900	21.7
FE2O3	16	1.500E+05	70	-3.1900	160.0

Figure D-42. Properties of Materials (Page 2 of 10)

CARBON	17	1.500E+05	107	-3.1900	88.0
NHACL	18	1.500E+05	130	-3.1900	53.5
AGACL	19	1.500E+05	101	-3.1900	89.5
NZMR	20	1.500E+05	150	-3.1900	32.0
NZMRAD	21	1.500E+05	101	-3.1900	50.0
NHSHO3	22	1.500E+05	101	-3.1900	95.0
ADHMYT	23	1.500E+05	101	-3.1900	113.0

NOTE VALUES OF -1.0 INDICATE NO DATA ENTERED,
OR INTERNALLY GENERATED.

HIGH VELOCITY LOWER LIMITS FOR ALL MATERIALS

HIGH VELOCITY (FT/SEC)	HYPER VELOCITY (FT/SEC)
3000	900000

SURFACE PROPERTIES INPUT

ALUMIN

FINISH (MU-IN)	SURFACE ABSORB- TIVITY (SOLAR)	EMISS- IVITY (THERM)	REFLECTIVITY		THERMAL COND. BTU-IN/ SQFT-DEG-SEC	REFRACT. INDEX	TRANSMISSIVITY AT MICRON WAVELENGTHS OF PER INCH OF THICKNESS								
			DIFFUSE	SPECULAR			15 (IR)	5 (IR)	2 (IR)	1 (IR)	0.5 (VIS)	0.2 (UV)	0.05 (UV)	0.01 (UV)	
0.0	.0100	.0400	-1.0	.0900	.0400	.4570	0.0	0.0	0.0	0.0	0.0	0.0	0.0	0.0	0.0
.50	.0110	.0350	.9300	.0600	.0650	-1.0	-1.0	-1.0	-1.0	0.0	0.0	0.0	0.0	0.0	0.0
1.00	.0475	.0500	-1.0	.0525	.0500	-1.0	-1.0	-1.0	-1.0	0.0	0.0	0.0	0.0	0.0	0.0
2.00	.0200	.0400	.4500	.0800	.0400	-1.0	-1.0	-1.0	-1.0	0.0	0.0	0.0	0.0	0.0	0.0
3.00	.0300	-1.0	-1.0	.0700	-1.0	-1.0	-1.0	-1.0	-1.0	0.0	0.0	0.0	0.0	0.0	0.0
4.00	.1100	.0500	.7300	.0400	.0500	-1.0	-1.0	-1.0	-1.0	0.0	0.0	0.0	0.0	0.0	0.0
5.00	.0700	-1.0	-1.0	.0300	-1.0	-1.0	-1.0	-1.0	-1.0	0.0	0.0	0.0	0.0	0.0	0.0
6.00	.1000	-1.0	-1.0	.0000	-1.0	-1.0	-1.0	-1.0	-1.0	0.0	0.0	0.0	0.0	0.0	0.0
7.00	.1200	.0850	.5000	.0800	.0150	.9500	-1.0	-1.0	-1.0	0.0	0.0	0.0	0.0	0.0	0.0
8.00	.1400	.0500	-1.0	.0400	.0500	-1.0	-1.0	-1.0	-1.0	0.0	0.0	0.0	0.0	0.0	0.0
9.00	.1600	.0600	-1.0	.0400	.0400	-1.0	-1.0	-1.0	-1.0	0.0	0.0	0.0	0.0	0.0	0.0
10.00	.1700	-1.0	-1.0	.0300	-1.0	-1.0	-1.0	-1.0	-1.0	0.0	0.0	0.0	0.0	0.0	0.0
11.00	.1800	-1.0	-1.0	.0200	-1.0	-1.0	-1.0	-1.0	-1.0	0.0	0.0	0.0	0.0	0.0	0.0
12.00	.1900	.0800	-1.0	.0100	.0200	-1.0	-1.0	-1.0	-1.0	0.0	0.0	0.0	0.0	0.0	0.0
13.00	.2000	-1.0	-1.0	.0000	-1.0	-1.0	-1.0	-1.0	-1.0	0.0	0.0	0.0	0.0	0.0	0.0
14.00	.2100	-1.0	-1.0	.0700	-1.0	-1.0	-1.0	-1.0	-1.0	0.0	0.0	0.0	0.0	0.0	0.0
15.10	.2300	-1.0	-1.0	.0700	-1.0	-1.0	-1.0	-1.0	-1.0	0.0	0.0	0.0	0.0	0.0	0.0
20.10	.2600	-1.0	-1.0	.0400	-1.0	-1.0	-1.0	-1.0	-1.0	0.0	0.0	0.0	0.0	0.0	0.0
25.00	.2900	-1.0	-1.0	.0020	-1.0	-1.0	-1.0	-1.0	-1.0	0.0	0.0	0.0	0.0	0.0	0.0
30.00	.3300	.2000	.5000	.0700	.0000	-1.0	-1.0	-1.0	-1.0	0.0	0.0	0.0	0.0	0.0	0.0
35.00	.3600	-1.0	-1.0	.0400	-1.0	-1.0	-1.0	-1.0	-1.0	0.0	0.0	0.0	0.0	0.0	0.0
40.00	.3800	-1.0	-1.0	.0200	-1.0	-1.0	-1.0	-1.0	-1.0	0.0	0.0	0.0	0.0	0.0	0.0
50.00	.4200	.2100	-1.0	.0000	.0700	-1.0	-1.0	-1.0	-1.0	0.0	0.0	0.0	0.0	0.0	0.0
60.00	.4750	-1.0	-1.0	.0250	-1.0	-1.0	-1.0	-1.0	-1.0	0.0	0.0	0.0	0.0	0.0	0.0
80.00	.5000	-1.0	.5000	-1.0	-1.0	-1.0	-1.0	-1.0	-1.0	0.0	0.0	0.0	0.0	0.0	0.0
100.00	.5000	-1.0	.0400	-1.0	-1.0	-1.0	-1.0	-1.0	-1.0	0.0	0.0	0.0	0.0	0.0	0.0
130.00	.6700	.3400	.3300	-1.0	.0400	-1.0	-1.0	-1.0	-1.0	0.0	0.0	0.0	0.0	0.0	0.0
150.00	.7500	-1.0	.2500	-1.0	-1.0	-1.0	-1.0	-1.0	-1.0	0.0	0.0	0.0	0.0	0.0	0.0
100.00	.0000	-1.0	.2000	-1.0	-1.0	-1.0	-1.0	-1.0	-1.0	0.0	0.0	0.0	0.0	0.0	0.0

NOTE VALUES OF -1.0 INDICATE NO DATA ENTERED,
OR INTERNALLY GENERATED.

WINDOW

FINISH (MU-IN)	SURFACE ABSORB- TIVITY (SOLAR)	EMISS- IVITY (THERM)	REFLECTIVITY		THERMAL COND. BTU-IN/ SQFT-DEG-SEC	REFRACT. INDEX	TRANSMISSIVITY AT MICRON WAVELENGTHS OF PER INCH OF THICKNESS								
			DIFFUSE	SPECULAR			15 (IR)	5 (IR)	2 (IR)	1 (IR)	0.5 (VIS)	0.2 (UV)	0.05 (UV)	0.01 (UV)	
.10	.5091	.0400	.0800	.4900	.1100	.8010	1.5470	0.0	0.0	.0700	.5300	.9600	0.0	0.0	0.0
10.00	.5441	.0400	.1000	.4550	.1100	-1.0	1.5470	0.0	0.0	.0600	.4400	.6000	0.0	0.0	0.0

NOTE VALUES OF -1.0 INDICATE NO DATA ENTERED,
OR INTERNALLY GENERATED.

Figure D-42. Properties of Materials (Page 3 of 10)

SOLCEL

SURFACE (MU-IN)	ABSORB- (SOLAR)	EMISS- (THERM)	REFLECTIVITY (DIFFUSE SPECULAR)	THERMAL COND. BTU-IN/	REFRACT. INDEX	TRANSMITTANCE							
						PER INCH OF THICKNESS AT MICRON WAVELENGTHS OF							
						15	5	2	1	0.5	0.2	0.05	0.01
						(IR)	(IR)	(IR)	(IR)	(VIS)	(UV)	(UV)	(UV)

NOTE VALUES OF -1.0 INDICATE NO DATA ENTERED,
OR INTERNALLY GENERATED.

IRPORT

SURFACE (MU-IN)	ABSORB- (SOLAR)	EMISS- (THERM)	REFLECTIVITY (DIFFUSE SPECULAR)	THERMAL COND. BTU-IN/	REFRACT. INDEX	TRANSMITTANCE							
						PER INCH OF THICKNESS AT MICRON WAVELENGTHS OF							
						15	5	2	1	0.5	0.2	0.05	0.01
						(IR)	(IR)	(IR)	(IR)	(VIS)	(UV)	(UV)	(UV)

NOTE VALUES OF -1.0 INDICATE NO DATA ENTERED,
OR INTERNALLY GENERATED.

UVPORT

SURFACE (MU-IN)	ABSORB- (SOLAR)	EMISS- (THERM)	REFLECTIVITY (DIFFUSE SPECULAR)	THERMAL COND. BTU-IN/	REFRACT. INDEX	TRANSMITTANCE							
						PER INCH OF THICKNESS AT MICRON WAVELENGTHS OF							
						15	5	2	1	0.5	0.2	0.05	0.01
						(IR)	(IR)	(IR)	(IR)	(VIS)	(UV)	(UV)	(UV)

NOTE VALUES OF -1.0 INDICATE NO DATA ENTERED,
OR INTERNALLY GENERATED.

TEFLON

SURFACE (MU-IN)	ABSORB- (SOLAR)	EMISS- (THERM)	REFLECTIVITY (DIFFUSE SPECULAR)	THERMAL COND. BTU-IN/	REFRACT. INDEX	TRANSMITTANCE							
						PER INCH OF THICKNESS AT MICRON WAVELENGTHS OF							
						15	5	2	1	0.5	0.2	0.05	0.01
						(IR)	(IR)	(IR)	(IR)	(VIS)	(UV)	(UV)	(UV)

NOTE VALUES OF -1.0 INDICATE NO DATA ENTERED,
OR INTERNALLY GENERATED.

GOLD PLATING

SURFACE (MU-IN)	ABSORB- (SOLAR)	EMISS- (THERM)	REFLECTIVITY (DIFFUSE SPECULAR)	THERMAL COND. BTU-IN/	REFRACT. INDEX	TRANSMITTANCE							
						PER INCH OF THICKNESS AT MICRON WAVELENGTHS OF							
						15	5	2	1	0.5	0.2	0.05	0.01
						(IR)	(IR)	(IR)	(IR)	(VIS)	(UV)	(UV)	(UV)

NOTE VALUES OF -1.0 INDICATE NO DATA ENTERED,
OR INTERNALLY GENERATED.

Figure D-42. Properties of Materials (Page 4 of 10)

BLACK COATING

SURFACE FINISH (MU-IN)	ABSORB- TIVITY (SOLAR)	EMISS- TIVITY (THERM)	R E F L E C T I V I T Y		THERMAL COND. BTU-IN/ SQFT-DEG-SEC	REFRACT. INDEX	T R A N S M I T T A N C E							
			SOLAR	DIFFUSE SPECULAR			PER INCH OF THICKNESS AT MICRON WAVELENGTHS OF							
							15	5	2	1	0.5	0.2	0.05	0.01
							(IR)	(IR)	(IR)	(IR)	(VIS)	(UV)	(UV)	(UV)

NOTE VALUES OF -1.0 INDICATE NO DATA ENTERED,
OR INTERNALLY GENERATED.

WHITE COATING

SURFACE FINISH (MU-IN)	ABSORB- TIVITY (SOLAR)	EMISS- TIVITY (THERM)	R E F L E C T I V I T Y		THERMAL COND. BTU-IN/ SQFT-DEG-SEC	REFRACT. INDEX	T R A N S M I T T A N C E							
			SOLAR	DIFFUSE SPECULAR			PER INCH OF THICKNESS AT MICRON WAVELENGTHS OF							
							15	5	2	1	0.5	0.2	0.05	0.01
							(IR)	(IR)	(IR)	(IR)	(VIS)	(UV)	(UV)	(UV)

NOTE VALUES OF -1.0 INDICATE NO DATA ENTERED,
OR INTERNALLY GENERATED.

KAPTON

SURFACE FINISH (MU-IN)	ABSORB- TIVITY (SOLAR)	EMISS- TIVITY (THERM)	R E F L E C T I V I T Y		THERMAL COND. BTU-IN/ SQFT-DEG-SEC	REFRACT. INDEX	T R A N S M I T T A N C E							
			SOLAR	DIFFUSE SPECULAR			PER INCH OF THICKNESS AT MICRON WAVELENGTHS OF							
							15	5	2	1	0.5	0.2	0.05	0.01
							(IR)	(IR)	(IR)	(IR)	(VIS)	(UV)	(UV)	(UV)

NOTE VALUES OF -1.0 INDICATE NO DATA ENTERED,
OR INTERNALLY GENERATED.

N804 DEPOSIT

TEMPERATURE (DEG R)	ABSORB- TIVITY (SOLAR)	EMISS- TIVITY (THERM)	R E F L E C T I V I T Y		THERMAL COND. BTU-IN/ SQFT-DEG-SEC	REFRACT. INDEX	T R A N S M I T T A N C E							
			SOLAR	DIFFUSE SPECULAR			PER INCH OF THICKNESS AT MICRON WAVELENGTHS OF							
							15	5	2	1	0.5	0.2	0.05	0.01
							(IR)	(IR)	(IR)	(IR)	(VIS)	(UV)	(UV)	(UV)

NOTE VALUES OF -1.0 INDICATE NO DATA ENTERED,
OR INTERNALLY GENERATED.

N803 DEPOSIT

TEMPERATURE (DEG R)	ABSORB- TIVITY (SOLAR)	EMISS- TIVITY (THERM)	R E F L E C T I V I T Y		THERMAL COND. BTU-IN/ SQFT-DEG-SEC	REFRACT. INDEX	T R A N S M I T T A N C E							
			SOLAR	DIFFUSE SPECULAR			PER INCH OF THICKNESS AT MICRON WAVELENGTHS OF							
							15	5	2	1	0.5	0.2	0.05	0.01
							(IR)	(IR)	(IR)	(IR)	(VIS)	(UV)	(UV)	(UV)

NOTE VALUES OF -1.0 INDICATE NO DATA ENTERED,
OR INTERNALLY GENERATED.

Figure D-42. Properties of Materials (Page 5 of 10)

MMH DEPOSIT

TEMPERATURE	ABSORBANCE	EMISSIVITY	REFLECTIVITY	DIFFUSE	SPECULAR	THERMAL COND.	REFRACT. INDEX	PER INCH OF THICKNESS	AT MICRON WAVELENGTHS OF	0.5	0.2	0.05	0.01
(DEG R)	(SOLAR)	(THERM)	(SOLAR)	(DIFFUSE)	(SPECULAR)	(BTU-IN/	(INDEX)	(IR)	(IR)	(IR)	(IR)	(UV)	(UV)
						SOFT-DEG-SEC		15	5	2	1	0.5	0.2
500.00	.7751	.9600	50.1185	.2249	.0311	.0017	1.4300	.0289	.0291	.0291	.0294	.0294	.0275
800.00	.7709	.9711	50.1115	.2231	.0289	-1.0	1.4100	.0290	.0292	.0292	.0294	.0294	.0275

NOTE VALUES OF -1.0 INDICATE NO DATA ENTERED,
OR INTERNALLY GENERATED.

MMH20 DEPOSIT

TEMPERATURE	ABSORBANCE	EMISSIVITY	REFLECTIVITY	DIFFUSE	SPECULAR	THERMAL COND.	REFRACT. INDEX	PER INCH OF THICKNESS	AT MICRON WAVELENGTHS OF	0.5	0.2	0.05	0.01
(DEG R)	(SOLAR)	(THERM)	(SOLAR)	(DIFFUSE)	(SPECULAR)	(BTU-IN/	(INDEX)	(IR)	(IR)	(IR)	(IR)	(UV)	(UV)
						SOFT-DEG-SEC		15	5	2	1	0.5	0.2
500.00	-1.0	-1.0	-1.0	-1.0	-1.0	.0028	-1.0	-1.0	-1.0	-1.0	-1.0	-1.0	-1.0
800.00	-1.0	-1.0	-1.0	-1.0	-1.0	-1.0	-1.0	-1.0	-1.0	-1.0	-1.0	-1.0	-1.0

NOTE VALUES OF -1.0 INDICATE NO DATA ENTERED,
OR INTERNALLY GENERATED.

MMH203 DEPOSIT

TEMPERATURE	ABSORBANCE	EMISSIVITY	REFLECTIVITY	DIFFUSE	SPECULAR	THERMAL COND.	REFRACT. INDEX	PER INCH OF THICKNESS	AT MICRON WAVELENGTHS OF	0.5	0.2	0.05	0.01
(DEG R)	(SOLAR)	(THERM)	(SOLAR)	(DIFFUSE)	(SPECULAR)	(BTU-IN/	(INDEX)	(IR)	(IR)	(IR)	(IR)	(UV)	(UV)
						SOFT-DEG-SEC		15	5	2	1	0.5	0.2
500.00	-1.0	-1.0	-1.0	-1.0	-1.0	-1.0	-1.0	-1.0	-1.0	-1.0	-1.0	-1.0	-1.0
800.00	-1.0	-1.0	-1.0	-1.0	-1.0	-1.0	-1.0	-1.0	-1.0	-1.0	-1.0	-1.0	-1.0

NOTE VALUES OF -1.0 INDICATE NO DATA ENTERED,
OR INTERNALLY GENERATED.

MMH40 DEPOSIT

TEMPERATURE	ABSORBANCE	EMISSIVITY	REFLECTIVITY	DIFFUSE	SPECULAR	THERMAL COND.	REFRACT. INDEX	PER INCH OF THICKNESS	AT MICRON WAVELENGTHS OF	0.5	0.2	0.05	0.01
(DEG R)	(SOLAR)	(THERM)	(SOLAR)	(DIFFUSE)	(SPECULAR)	(BTU-IN/	(INDEX)	(IR)	(IR)	(IR)	(IR)	(UV)	(UV)
						SOFT-DEG-SEC		15	5	2	1	0.5	0.2
500.00	.4500	.7500	50.2750	.5500	.2500	-1.0	3.0030	.0500	.0500	.0000	0.0	.0227	.0195
800.00	.6014	.7524	50.1990	.5981	.2476	-1.0	2.9830	.0219	.0222	.0223	.0220	.0220	.0196

NOTE VALUES OF -1.0 INDICATE NO DATA ENTERED,
OR INTERNALLY GENERATED.

WATER DEPOSIT

TEMPERATURE	ABSORBANCE	EMISSIVITY	REFLECTIVITY	DIFFUSE	SPECULAR	THERMAL COND.	REFRACT. INDEX	PER INCH OF THICKNESS	AT MICRON WAVELENGTHS OF	0.5	0.2	0.05	0.01
(DEG R)	(SOLAR)	(THERM)	(SOLAR)	(DIFFUSE)	(SPECULAR)	(BTU-IN/	(INDEX)	(IR)	(IR)	(IR)	(IR)	(UV)	(UV)
						SOFT-DEG-SEC		15	5	2	1	0.5	0.2
492.00	.7400	.9500	50.1200	.2400	.0500	.0042	1.3330	.0293	.0295	.0295	.0297	.0297	.0280
500.00	.7434	.9502	50.1103	.2366	.0450	.0011	1.3276	.0293	.0295	.0295	.0297	.0297	.0280
672.00	.7704	.9630	50.1148	.2296	.0370	0.0	1.3106	.0294	.0295	.0296	.0297	.0297	.0281

NOTE VALUES OF -1.0 INDICATE NO DATA ENTERED,
OR INTERNALLY GENERATED.

Figure D-42. Properties of Materials (Page 6 of 10)

AMONIA DEPOSIT

TEMPERATURE (DEG R)	ABSORB- TIVITY (SOLAR)	EMISS- IVITY (THERM)	REFLECTIVITY SOLAR DIFFUSE SPECULAR	THERMAL COND. BTU-IN/ SQFT-DEG-SEC	REFRACT. INDEX	PER INCH OF THICKNESS AT MICRON WAVELENGTHS OF	15 (IR)	5 (IR)	2 (IR)	1 (IR)	0.5 (VIS)	0.2 (UV)	0.05 (UV)	0.01 (UV)
540.00	.7845	.9816	50.1078	.2155	.0194	1.3250	.0293	.0295	.0295	.0297	.0297	.0280	.0279	.0278
800.00	.7862	.9827	50.1069	.2138	.0173	1.3042	.0294	.0296	.0296	.0298	.0298	.0280	.0280	.0279

NOTE VALUES OF -1.0 INDICATE NO DATA ENTERED,
OR INTERNALLY GENERATED.

NH4OH DEPOSIT

TEMPERATURE (DEG R)	ABSORB- TIVITY (SOLAR)	EMISS- IVITY (THERM)	REFLECTIVITY SOLAR DIFFUSE SPECULAR	THERMAL COND. BTU-IN/ SQFT-DEG-SEC	REFRACT. INDEX	PER INCH OF THICKNESS AT MICRON WAVELENGTHS OF	15 (IR)	5 (IR)	2 (IR)	1 (IR)	0.5 (VIS)	0.2 (UV)	0.05 (UV)	0.01 (UV)
540.00	.7810	.9772	50.1091	.2182	.0228	1.3570	.0292	.0294	.0294	.0296	.0296	.0279	.0277	.0276
800.00	.7835	.9794	50.1082	.2165	.0206	1.3362	.0293	.0294	.0295	.0297	.0297	.0280	.0278	.0277

NOTE VALUES OF -1.0 INDICATE NO DATA ENTERED,
OR INTERNALLY GENERATED.

NH4NO3 DEPOSIT

TEMPERATURE (DEG R)	ABSORB- TIVITY (SOLAR)	EMISS- IVITY (THERM)	REFLECTIVITY SOLAR DIFFUSE SPECULAR	THERMAL COND. BTU-IN/ SQFT-DEG-SEC	REFRACT. INDEX	PER INCH OF THICKNESS AT MICRON WAVELENGTHS OF	15 (IR)	5 (IR)	2 (IR)	1 (IR)	0.5 (VIS)	0.2 (UV)	0.05 (UV)	0.01 (UV)
540.00	.7966	.9957	50.1017	.2034	.0043	1.1413	.0300	.0301	.0301	.0302	.0302	.0291	.0290	.0288
800.00	.7975	.9968	50.1013	.2025	.0032	1.1205	.0300	.0301	.0301	.0302	.0302	.0292	.0291	.0290

NOTE VALUES OF -1.0 INDICATE NO DATA ENTERED,
OR INTERNALLY GENERATED.

AMN,AG DEPOSIT

TEMPERATURE (DEG R)	ABSORB- TIVITY (SOLAR)	EMISS- IVITY (THERM)	REFLECTIVITY SOLAR DIFFUSE SPECULAR	THERMAL COND. BTU-IN/ SQFT-DEG-SEC	REFRACT. INDEX	PER INCH OF THICKNESS AT MICRON WAVELENGTHS OF	15 (IR)	5 (IR)	2 (IR)	1 (IR)	0.5 (VIS)	0.2 (UV)	0.05 (UV)	0.01 (UV)
540.00	-1.0	-1.0	-1.0	-1.0	-1.0	.0047	-1.0	-1.0	-1.0	-1.0	-1.0	-1.0	-1.0	-1.0
800.00	-1.0	-1.0	-1.0	-1.0	-1.0	-1.0	-1.0	-1.0	-1.0	-1.0	-1.0	-1.0	-1.0	-1.0

NOTE VALUES OF -1.0 INDICATE NO DATA ENTERED,
OR INTERNALLY GENERATED.

MKFUAQ DEPOSIT

TEMPERATURE (DEG R)	ABSORB- TIVITY (SOLAR)	EMISS- IVITY (THERM)	REFLECTIVITY SOLAR DIFFUSE SPECULAR	THERMAL COND. BTU-IN/ SQFT-DEG-SEC	REFRACT. INDEX	PER INCH OF THICKNESS AT MICRON WAVELENGTHS OF	15 (IR)	5 (IR)	2 (IR)	1 (IR)	0.5 (VIS)	0.2 (UV)	0.05 (UV)	0.01 (UV)
540.00	-1.0	-1.0	-1.0	-1.0	-1.0	.0001	-1.0	-1.0	-1.0	-1.0	-1.0	-1.0	-1.0	-1.0
800.00	-1.0	-1.0	-1.0	-1.0	-1.0	-1.0	-1.0	-1.0	-1.0	-1.0	-1.0	-1.0	-1.0	-1.0

Figure D-42. Properties of Materials (Page 7 of 10)

NOTE VALUES OF -1.0 INDICATE NO DATA ENTERED,
OR INTERNALLY GENERATED.

AL2O3 DEPOSIT

TEMPERATURE (DEG R)	ABSORB- TIVITY (SOLAR)	EMISS- IVITY (THERM)	REFLECTIVITY SOLAR DIFFUSE SPECULAR	THERMAL COND. BTU-IN/ SQFT-DEG-SEC	REFRACT. INDEX	PER INCH OF THICKNESS AT MICRON WAVELENGTHS OF	15 (IR)	5 (IR)	2 (IR)	1 (IR)	0.5 (VIS)	0.2 (UV)	0.05 (UV)	0.01 (UV)
540.00	.9000	.0000	50.0100	.0200	.0000	1.7000	0.0	0.0	0.0	0.0	0.0	0.0	0.0	0.0
850.00	.0000	.1100	50.4500	.0120	.0900	0.0	1.6752	0.0	0.0	0.0	0.0	0.0	0.0	0.0
1370.00	.0000	.1900	50.0100	.0200	.0100	0.0	1.6176	0.0	0.0	0.0	0.0	0.0	0.0	0.0
3600.00	.5000	.2000	50.2500	.5000	.7200	0.0	1.4552	0.0	0.0	0.0	0.0	0.0	0.0	0.0

NOTE VALUES OF -1.0 INDICATE NO DATA ENTERED,
OR INTERNALLY GENERATED.

MCL DEPOSIT

TEMPERATURE (DEG R)	ABSORB- TIVITY (SOLAR)	EMISS- IVITY (THERM)	REFLECTIVITY SOLAR DIFFUSE SPECULAR	THERMAL COND. BTU-IN/ SQFT-DEG-SEC	REFRACT. INDEX	PER INCH OF THICKNESS AT MICRON WAVELENGTHS OF	15 (IR)	5 (IR)	2 (IR)	1 (IR)	0.5 (VIS)	0.2 (UV)	0.05 (UV)	0.01 (UV)
540.00	.7769	.0711	50.1114	.2231	.0209	1.4110	.0290	.0292	.0292	.0294	.0294	.0275	.0274	.0272
800.00	.7700	.0735	50.1106	.2212	.0205	-1.0	1.3902	.0291	.0292	.0293	.0295	.0299	.0277	.0274

NOTE VALUES OF -1.0 INDICATE NO DATA ENTERED,
OR INTERNALLY GENERATED.

MCL40 DEPOSIT

TEMPERATURE (DEG R)	ABSORB- TIVITY (SOLAR)	EMISS- IVITY (THERM)	REFLECTIVITY SOLAR DIFFUSE SPECULAR	THERMAL COND. BTU-IN/ SQFT-DEG-SEC	REFRACT. INDEX	PER INCH OF THICKNESS AT MICRON WAVELENGTHS OF	15 (IR)	5 (IR)	2 (IR)	1 (IR)	0.5 (VIS)	0.2 (UV)	0.05 (UV)	0.01 (UV)
540.00	.7811	.0763	50.1095	.2109	.0237	1.3650	.0292	.0293	.0294	.0296	.0296	.0278	.0277	.0275
800.00	.7829	.0786	50.1086	.2171	.0214	-1.0	1.3442	.0293	.0294	.0295	.0296	.0296	.0279	.0276

NOTE VALUES OF -1.0 INDICATE NO DATA ENTERED,
OR INTERNALLY GENERATED.

PE203 DEPOSIT

TEMPERATURE (DEG R)	ABSORB- TIVITY (SOLAR)	EMISS- IVITY (THERM)	REFLECTIVITY SOLAR DIFFUSE SPECULAR	THERMAL COND. BTU-IN/ SQFT-DEG-SEC	REFRACT. INDEX	PER INCH OF THICKNESS AT MICRON WAVELENGTHS OF	15 (IR)	5 (IR)	2 (IR)	1 (IR)	0.5 (VIS)	0.2 (UV)	0.05 (UV)	0.01 (UV)
500.00	.5040	.0300	50.2400	.4900	.3700	0.0990	3.0100	0.0	0.0	0.0	0.0	0.0	0.0	0.0
1390.00	.6000	.0500	50.1000	.3200	.1500	0.0	2.9430	0.0	0.0	0.0	0.0	0.0	0.0	0.0
2650.00	.7120	.0900	50.1040	.2800	.1100	0.0	2.8420	0.0	0.0	0.0	0.0	0.0	0.0	0.0

NOTE VALUES OF -1.0 INDICATE NO DATA ENTERED,
OR INTERNALLY GENERATED.

CARBON DEPOSIT

Figure D-42. Properties of Materials (Page 8 of 10)

TEMPERATURE (DEG R)	ABSORB- TIVITY (SOLAR)	EMISS- IVITY (THERM)	REFLECTIVITY SOLAR DIFFUSE SPECULAR	THERMAL COND. BTU-IN/ SOFT-DEG-SEC	REFRACT. INDEX	PER INCH OF THICKNESS AT	TRANSMITTANCE MICRON WAVELENGTHS OF	PER INCH OF THICKNESS AT	TRANSMITTANCE MICRON WAVELENGTHS OF	PER INCH OF THICKNESS AT	TRANSMITTANCE MICRON WAVELENGTHS OF	PER INCH OF THICKNESS AT	TRANSMITTANCE MICRON WAVELENGTHS OF	PER INCH OF THICKNESS AT	TRANSMITTANCE MICRON WAVELENGTHS OF
						15 (IR)	5 (IR)	2 (IR)	1 (IR)	0.5 (VIS)	0.2 (UV)	0.05 (UV)	0.01 (UV)		
500.00	.9700	0.0	.8100	.0300	0.0	.0120	-1.0	0.0	0.0	0.0	0.0	0.0	0.0	0.0	0.0
720.00	.6480	.8100	50.1700	.3520	.1900	0.0	0.0	0.0	0.0	0.0	0.0	0.0	0.0	0.0	0.0
1170.00	.6400	.8000	50.1800	.3610	.2000	0.0	0.0	0.0	0.0	0.0	0.0	0.0	0.0	0.0	0.0
1620.00	.6320	.7900	50.1840	.3680	.2100	0.0	0.0	0.0	0.0	0.0	0.0	0.0	0.0	0.0	0.0

NOTE VALUES OF -1.0 INDICATE NO DATA ENTERED,
OR INTERNALLY GENERATED.

NHACL DEPOSIT

TEMPERATURE (DEG R)	ABSORB- TIVITY (SOLAR)	EMISS- IVITY (THERM)	REFLECTIVITY SOLAR DIFFUSE SPECULAR	THERMAL COND. BTU-IN/ SOFT-DEG-SEC	REFRACT. INDEX	PER INCH OF THICKNESS AT	TRANSMITTANCE MICRON WAVELENGTHS OF	PER INCH OF THICKNESS AT	TRANSMITTANCE MICRON WAVELENGTHS OF	PER INCH OF THICKNESS AT	TRANSMITTANCE MICRON WAVELENGTHS OF	PER INCH OF THICKNESS AT	TRANSMITTANCE MICRON WAVELENGTHS OF	PER INCH OF THICKNESS AT	TRANSMITTANCE MICRON WAVELENGTHS OF
						15 (IR)	5 (IR)	2 (IR)	1 (IR)	0.5 (VIS)	0.2 (UV)	0.05 (UV)	0.01 (UV)		
500.00	.7805	.9757	50.1097	.2195	.0243	.0047	1.3710	.0292	.0293	.0294	.0296	.0296	.0278	.0276	.0275
800.00	.7824	.9779	50.1088	.2176	.0221	-1.0	1.3502	.0292	.0294	.0294	.0296	.0296	.0279	.0276	.0276

NOTE VALUES OF -1.0 INDICATE NO DATA ENTERED,
OR INTERNALLY GENERATED.

AGANCL DEPOSIT

TEMPERATURE (DEG R)	ABSORB- TIVITY (SOLAR)	EMISS- IVITY (THERM)	REFLECTIVITY SOLAR DIFFUSE SPECULAR	THERMAL COND. BTU-IN/ SOFT-DEG-SEC	REFRACT. INDEX	PER INCH OF THICKNESS AT	TRANSMITTANCE MICRON WAVELENGTHS OF	PER INCH OF THICKNESS AT	TRANSMITTANCE MICRON WAVELENGTHS OF	PER INCH OF THICKNESS AT	TRANSMITTANCE MICRON WAVELENGTHS OF	PER INCH OF THICKNESS AT	TRANSMITTANCE MICRON WAVELENGTHS OF	PER INCH OF THICKNESS AT	TRANSMITTANCE MICRON WAVELENGTHS OF
						15 (IR)	5 (IR)	2 (IR)	1 (IR)	0.5 (VIS)	0.2 (UV)	0.05 (UV)	0.01 (UV)		
500.00	.7799	.9749	50.1100	.2201	.0251	.0045	1.3700	.0291	.0293	.0293	.0295	.0295	.0277	.0276	.0274
800.00	.7817	.9772	50.1091	.2183	.0228	-1.0	1.3572	.0292	.0294	.0294	.0296	.0296	.0279	.0277	.0276

NOTE VALUES OF -1.0 INDICATE NO DATA ENTERED,
OR INTERNALLY GENERATED.

N2M4 DEPOSIT

TEMPERATURE (DEG R)	ABSORB- TIVITY (SOLAR)	EMISS- IVITY (THERM)	REFLECTIVITY SOLAR DIFFUSE SPECULAR	THERMAL COND. BTU-IN/ SOFT-DEG-SEC	REFRACT. INDEX	PER INCH OF THICKNESS AT	TRANSMITTANCE MICRON WAVELENGTHS OF	PER INCH OF THICKNESS AT	TRANSMITTANCE MICRON WAVELENGTHS OF	PER INCH OF THICKNESS AT	TRANSMITTANCE MICRON WAVELENGTHS OF	PER INCH OF THICKNESS AT	TRANSMITTANCE MICRON WAVELENGTHS OF	PER INCH OF THICKNESS AT	TRANSMITTANCE MICRON WAVELENGTHS OF
						15 (IR)	5 (IR)	2 (IR)	1 (IR)	0.5 (VIS)	0.2 (UV)	0.05 (UV)	0.01 (UV)		
500.00	.7717	.9667	50.1141	.2283	.0353	.0019	1.4644	.0286	.0289	.0290	.0292	.0292	.0272	.0271	.0269
800.00	.7738	.9672	50.1131	.2262	.0328	-1.0	1.4436	.0286	.0290	.0291	.0293	.0293	.0273	.0272	.0270

NOTE VALUES OF -1.0 INDICATE NO DATA ENTERED,
OR INTERNALLY GENERATED.

N2M4A0 DEPOSIT

TEMPERATURE (DEG R)	ABSORB- TIVITY (SOLAR)	EMISS- IVITY (THERM)	REFLECTIVITY SOLAR DIFFUSE SPECULAR	THERMAL COND. BTU-IN/ SOFT-DEG-SEC	REFRACT. INDEX	PER INCH OF THICKNESS AT	TRANSMITTANCE MICRON WAVELENGTHS OF	PER INCH OF THICKNESS AT	TRANSMITTANCE MICRON WAVELENGTHS OF	PER INCH OF THICKNESS AT	TRANSMITTANCE MICRON WAVELENGTHS OF	PER INCH OF THICKNESS AT	TRANSMITTANCE MICRON WAVELENGTHS OF	PER INCH OF THICKNESS AT	TRANSMITTANCE MICRON WAVELENGTHS OF
						15 (IR)	5 (IR)	2 (IR)	1 (IR)	0.5 (VIS)	0.2 (UV)	0.05 (UV)	0.01 (UV)		
500.00	.7757	.9696	50.1122	.2243	.0304	.0026	1.4200	.0289	.0291	.0292	.0294	.0294	.0275	.0273	.0272
800.00	.7776	.9720	50.1112	.2224	.0280	-1.0	1.4032	.0290	.0292	.0292	.0295	.0295	.0276	.0274	.0273

NOTE VALUES OF -1.0 INDICATE NO DATA ENTERED,
OR INTERNALLY GENERATED.

Figure D-42. Properties of Materials (Page 9 of 10)

N3M503 DEPOSIT

TEMPERATURE (DEG R)	ABSORPTIVITY (SOLAR)	EMISSIVITY (THERM)	REFLECTIVITY DIFFUSE	REFLECTIVITY SPECULAR	THERMAL COND. BTU-IN/	REFRACTIVE INDEX SOFT-DEG-BEC	PER INCH OF THICKNESS AT MICRON WAVELENGTHS OF	PER INCH OF THICKNESS AT MICRON WAVELENGTHS OF	PER INCH OF THICKNESS AT MICRON WAVELENGTHS OF	PER INCH OF THICKNESS AT MICRON WAVELENGTHS OF	PER INCH OF THICKNESS AT MICRON WAVELENGTHS OF	PER INCH OF THICKNESS AT MICRON WAVELENGTHS OF	PER INCH OF THICKNESS AT MICRON WAVELENGTHS OF	PER INCH OF THICKNESS AT MICRON WAVELENGTHS OF	PER INCH OF THICKNESS AT MICRON WAVELENGTHS OF
							15 (IR)	5 (IR)	2 (IR)	1 (IR)	0.5 (VIS)	0.2 (UV)	0.05 (UV)	0.01 (UV)	
540.00	-1.0	-1.0	-1.0	-1.0	-1.0	-1.0	-1.0	-1.0	-1.0	-1.0	-1.0	-1.0	-1.0	-1.0	-1.0
800.00	-1.0	-1.0	-1.0	-1.0	-1.0	-1.0	-1.0	-1.0	-1.0	-1.0	-1.0	-1.0	-1.0	-1.0	-1.0

NOTE VALUES OF -1.0 INDICATE NO DATA ENTERED,
OR INTERNALLY GENERATED.

ASHMT DEPOSIT

TEMPERATURE (DEG R)	ABSORPTIVITY (SOLAR)	EMISSIVITY (THERM)	REFLECTIVITY DIFFUSE	REFLECTIVITY SPECULAR	THERMAL COND. BTU-IN/	REFRACTIVE INDEX SOFT-DEG-BEC	PER INCH OF THICKNESS AT MICRON WAVELENGTHS OF	PER INCH OF THICKNESS AT MICRON WAVELENGTHS OF	PER INCH OF THICKNESS AT MICRON WAVELENGTHS OF	PER INCH OF THICKNESS AT MICRON WAVELENGTHS OF	PER INCH OF THICKNESS AT MICRON WAVELENGTHS OF	PER INCH OF THICKNESS AT MICRON WAVELENGTHS OF	PER INCH OF THICKNESS AT MICRON WAVELENGTHS OF	PER INCH OF THICKNESS AT MICRON WAVELENGTHS OF	PER INCH OF THICKNESS AT MICRON WAVELENGTHS OF
							15 (IR)	5 (IR)	2 (IR)	1 (IR)	0.5 (VIS)	0.2 (UV)	0.05 (UV)	0.01 (UV)	
540.00	-1.0	-1.0	-1.0	-1.0	-1.0	-1.0	-1.0	-1.0	-1.0	-1.0	-1.0	-1.0	-1.0	-1.0	-1.0
800.00	-1.0	-1.0	-1.0	-1.0	-1.0	-1.0	-1.0	-1.0	-1.0	-1.0	-1.0	-1.0	-1.0	-1.0	-1.0

NOTE VALUES OF -1.0 INDICATE NO DATA ENTERED,
OR INTERNALLY GENERATED.

UNAVAILABLE SIGNIFICANT DATA NEITHER INPUT NOR INTERNALLY APPROXIMATED

HYDRATED MONOMETHYL HYDRAZINE -- HEAT OF FUSION.

MONOMETHYLHYDRAZINE NITRATE -- THERMAL CONDUCTIVITY (SOL); REFRACTIVE INDEX (D LINE); BOILING POINT; CRITICAL PRESSURE;
VISCOSITY (LIQUID); SURFACE TENSION (LIQUID).

HYDRATED MONOMETHYLHYDRAZINE NITRATE--MELTING POINT; THERMAL CONDUCTIVITY (SOL); REFRACTIVE INDEX (D LINE);
BOILING POINT; CRITICAL PRESSURE; VISCOSITY (LIQUID); SURFACE TENSION (LIQUID);
HEAT OF FUSION.

AMMONIUM NITRATE --VISCOSITY (LIQUID).

HYDRATED AMMONIUM NITRATE - HEAT OF FUSION.

HYDRATED MIXED NITRATES -- MELTING POINT; REFRACTIVE INDEX (D LINE); VISCOSITY (LIQUID); SURFACE TENSION (LIQUID);
HEAT OF FUSION.

ALUMINUM OXIDE -- BOILING POINT; VISCOSITY (LIQUID); SURFACE TENSION (LIQUID).

HYDROGEN CHLORIDE -- VISCOSITY (LIQUID); SURFACE TENSION (LIQUID).

IRON OXIDE -- BOILING POINT; VISCOSITY (LIQUID); SURFACE TENSION (LIQUID).

CARBON -- REFRACTIVE INDEX (D LINE); BOILING POINT; VISCOSITY (LIQUID); SURFACE TENSION (LIQUID);
HEAT OF FUSION.

AMMONIUM CHLORIDE -- BOILING POINT; VISCOSITY (LIQUID); SURFACE TENSION (LIQUID); HEAT OF FUSION;

HYDRAZINE HYDRATE -- VISCOSITY (LIQUID); HEAT OF FUSION.

HYDRAZINE NITRATE -- SPECIFIC HEAT (SOLID); THERMAL CONDUCTIVITY (SOL); REFRACTIVE INDEX (D LINE); BOILING POINT;
LIQUID HEAT CAPACITY; THERMAL CONDUCTIVITY (LIG); VISCOSITY (LIQUID); SURFACE TENSION (LIQUID); HEAT OF FUSION;

HYDRATED HYDRAZINE NITRATE -- THERMAL CONDUCTIVITY (SOL); REFRACTIVE INDEX (D LINE); BOILING POINT; VISCOSITY (LIQUID);
SURFACE TENSION (LIQUID); HEAT OF FUSION.

MICKORY-DICKORY SAYS 483.60 SECONDS
FOR RUNNING OVERLAY 14.0
FINISHED AT CLOCK TIME 11-32-51.6

CP TIME USED = 150.96 SECONDS
PP TIME USED = 83.94 SECONDS
SINCE JOB STARTED

KNUDSEN-LANGMUIR COEFFICIENTS

FLUID	CN6TV	CN6TM
N2O4	2.9673899015E-05	3.1429169E-05
NNO3	3.4726896547E-06	3.6373957E-05
NNH	2.9673899015E-05	2.8571429E-06
NNHH2O	1.5001421788E-06	8.2537901E-06
NNHHO3	4.5678196402E-06	1.9784219E-06
NNH,40	5.4294527618E-06	1.3994642E-06
WATER	1.8562306998E-06	2.5969584E-06
AMONIA	1.8639319864E-06	3.6741052E-06
NN4OH	2.5883900442E-06	2.4415072E-06
NN4NO3	3.9132779160E-06	1.7149235E-05
NNH,40	4.3312049401E-06	1.6573279E-05
NNFUA0	6.9453791094E-06	5.1061763E-07
AL2O3	4.4165463296E-06	4.6132859E-06
NCL	2.6432736752E-06	1.4441706E-06
NCL,40	2.0381003569E-06	1.1659992E-05
FE2O3	5.5342107022E-06	3.1949308E-05
CARBON	3.0312120396E-06	4.2518764E-05
NN4CL	3.2001666100E-06	2.1075260E-05
AGAMCL	4.1391123630E-06	1.5576575E-05
N2H4	2.4749742664E-06	2.2200593E-06
N2H440	3.0937178330E-06	9.0753651E-06
N3H5O3	4.2643957435E-06	-1.0
AGMYNT	4.6508777094E-06	1.4980728E-06

NOTE--VALUES OF -1.0 INDICATE THAT THE TERM
COULD NOT BE CALCULATED BECAUSE ESSENTIAL
DATA WERE NOT SUPPLIED

CALINGEART-DAVIS COEFFICIENTS

$$LN(P) = A + (B/(T-43.0)) \text{ FOR } P \text{ IN MM; } T \text{ IN DEG K}$$

NAME	A	B
N2O4	26.795586	-3254.696353
NNO3	25.070959	-3070.394268
NNH	24.439086	-3363.502319
NNHH2O	37.557346	-10844.005645
NNHHO3	-1.0	-1.0
NNH,40	-1.0	-1.0
WATER	25.698530	-3914.416532
AMONIA	24.130496	-2026.677054
NN4OH	21.901157	-1783.122984
NN4NO3	25.910388	-4313.145316
NNH,40	26.682285	-4346.666454
NNFUA0	26.704724	-5084.357388
AL2O3	31.976900	-43884.439245
NCL	22.901782	-1315.601431
NCL,40	32.504642	-6453.586427
FE2O3	34.863481	-96257.003310
CARBON	33.844486	-88656.500510
NN4CL	24.163152	-5871.134691
AGAMCL	25.757619	-4061.174983
N2H4	26.112422	-4221.482134
N2H440	25.854350	-4105.980660
N3H5O3	26.027094	-4515.857023
AGMYNT	26.764724	-5084.357388

NOTE--VALUES OF -1.0 INDICATE THAT THE TERM
COULD NOT BE CALCULATED BECAUSE ESSENTIAL
DATA WERE NOT SUPPLIED

CRITICAL TEMP.
DEG RCRITICAL PRESS
PSIA

	CRITICAL TEMP. DEG R	CRITICAL PRESS PSIA
N2O4	776.400000	1441.300000
NNO3	853.500000	905.723700
NNH	1052.000000	1195.000000
NNHH2O	1108.000000	1128.642240
NNHHO3	1350.000000	-1.000000
NNH,40	1350.000000	-1.000000
WATER	1165.000000	3226.000000
AMONIA	730.000000	1635.700000
NN4OH	989.700000	1394.744316
NN4NO3	1080.000000	1125.166714
NNH,40	1029.150000	1074.362773
NNFUA0	1350.000000	1394.980911
AL2O3	6645.000000	6689.195434
NCL	584.300000	1198.700000

Figure D-43. Derived Coefficients and Properties of Deposit Constituents (Page 1 of 5)

MCL, A0	875.000000	897.207071
FE2O3	12960.000000	13004.123489
CARBON	12075.000000	12119.328958
NH4CL	1033.000000	507.000000
AOAMCL	1035.000000	1080.506959
N2H4	1117.000000	2135.000000
N2H4A0	1057.500000	1102.686580
N3H5O3	1115.000000	1100.776967
AOHMYT	1350.000000	1394.980911

NOTE--VALUES OF-1.0 INDICATE THAT THE TERM
COULD NOT BE CALCULATED BECAUSE ESSENTIAL
DATA WERE NOT SUPPLIED

VAPOR ENTHALPY AT ABSOLUTE ZERO
(BTU/LB)

N2O4	273.023
MN03	403.184
MMH	140.366
MMH2O	-1.0
MMHNO3	161.622
MMH, A0	121.337
WATER	1210.59
AMONIA	884.941
NH4OH	1263.56
NH4NO3	390.376
AMN, A0	-1.0
MXFUAR	-1.0
AL2O3	541.470
MCL	213.145
MCL, A0	79.2801
FE2O3	-1.0
CARBON	-1.0
NH4CL	-1.0
AOAMCL	-1.0
N2H4	776.821
N2H4A0	122.056
N3H5O3	-1.0
AOHMYT	-1.0

NOTE--VALUES OF-1.0 INDICATE THAT THE TERM
COULD NOT BE CALCULATED BECAUSE ESSENTIAL
DATA WERE NOT SUPPLIED

VAPOR PRESSURE AT THE FREEZING POINT
(PSIA)

N2O4	2.19063
MN03	.101570
MMH	3.53371E-03
MMH2O	4.38744E-17
MMHNO3	-1.0
MMH, A0	-1.0
WATER	8.38919E-02
AMONIA	.740905
NH4OH	.354986
NH4NO3	53.5362
AMN, A0	1.06927
MXFUAR	-1.0
MCL	2.02428
MCL, A0	5.47244E-05
FE2O3	2.05031E-14
NH4CL	214.302
AOAMCL	1.30221E-02
N2H4	3.85329E-02
N2H4A0	1.205017E-04
N3H5O3	.860579
AOHMYT	1.93380E-03

NOTE--VALUES OF-1.0 INDICATE THAT THE TERM
COULD NOT BE CALCULATED BECAUSE ESSENTIAL
DATA WERE NOT SUPPLIED

PARACHOR

N2O4	73.790115	MN03	124.280390
MMH	127.675718	MMH2O	159.108415
MMHNO3		MMH, A0	

Figure D-43. Derived Coefficients and Properties of Deposit Constituents (Page 2 of 5)

-1.000000	-1.000000
WATER	AMONIA
52.501363	51.829613
NH4OH	NH4NO3
112.931140	178.697982
AMN.AO	MXFUAO
206.182410	-1.000000
AL2O3	MCL
-1.000000	-1.000000
MCL.AO	FE2O3
50.893141	-1.000000
CARBON	NH4CL
-1.000000	-1.000000
AGAMCL	N2H4
250.906647	91.829603
N2H4AO	N3H5O3
89.899936	-1.000000
AGHMYT	
-1.000000	

NOTE--VALUES OF -1.0 INDICATE THAT THE TERM
COULD NOT BE CALCULATED BECAUSE ESSENTIAL
DATA WERE NOT SUPPLIED

DERIVED MMH PROPERTIES

REDUCED TEMP.	TEMPERATURE (DEG R)	LIO. ENTHALPY (BTU/LB)	VAP. ENTHALPY (BTU/LB)	VAPOR PRESSURE (PSIA)	SPECIFIC GRAVITY	VISCOSITY (LBM/FT-SEC)	SURFACE TENSION (LBM/IN)
.300000	315.000	112.085	462.388	5.455410E-06	.988563	1.09998	3.236435E-04
.400000	420.000	256.086	567.062	1.313494E-02	.932980	2.881702E-03	2.567667E-04
.500000	526.000	329.724	671.736	.820367	.877397	8.113349E-04	2.088325E-04
.600000	631.200	403.366	776.410	10.6515	.821814	2.888386E-04	1.545765E-04
.700000	736.400	477.006	881.084	61.0007	.766231	1.769939E-04	1.168122E-04
.800000	841.600	550.646	985.758	216.066	.710648	1.162207E-04	8.643056E-05
.900000	946.800	624.286	1090.43	563.530	.329241	8.019608E-05	4.223650E-05
.999999	1052.00	697.925	1195.10	1194.99	1.138293E-03	5.754644E-05	9.092751E-15
1.000000	1052.00 (CRITICAL TEMP.)	944.514	946.516	1195.00 (CRITICAL PRESS.)	2.910106E-07	1.294791E-05	1.256507E-31
1.010000	1062.52	-----	1205.57	-----	0.	1.307739E-05	-----

DERIVED N2O4 PROPERTIES

REDUCED TEMP.	TEMPERATURE (DEG R)	LIO. ENTHALPY (BTU/LB)	VAP. ENTHALPY (BTU/LB)	VAPOR PRESSURE (PSIA)	SPECIFIC GRAVITY	VISCOSITY (LBM/FT-SEC)	SURFACE TENSION (LBM/IN)
.300000	232.920	68.7114	341.734	2.746280E-10	1.84410	1.09998	4.372654E-04
.400000	310.560	91.6152	366.638	7.699040E-05	1.74061	1.09998	3.469182E-04
.500000	398.200	114.519	387.542	4.096244E-02	1.63673	1.09998	2.713390E-04
.600000	485.840	137.423	410.445	1.77267	1.53304	1.09998	2.088439E-04
.700000	573.480	261.647	433.349	21.8645	1.42935	2.594643E-04	1.578216E-04
.800000	621.120	319.877	456.253	131.595	1.32567	1.703739E-04	1.167738E-04
.900000	698.760	374.107	479.157	585.757	.614177	1.175635E-04	5.706452E-05
.999999	776.399	436.336	502.060	1841.29	2.123410E-03	8.436824E-05	1.228495E-14
1.000000	776.400 (CRITICAL TEMP.)	469.199	469.199	1841.30 (CRITICAL PRESS.)	5.428688E-07	1.898899E-05	1.697631E-31
1.010000	784.164	-----	504.351	-----	0.	1.917888E-05	-----

Figure D-43. Derived Coefficients and Properties of Deposit Constituents (Page 3 of 5)

DERIVED WATER PROPERTIES

REDUCED TEMP.	TEMPERATURE (DEG R)	LIQ. ENTHALPY (BTU/LB)	VAP. ENTHALPY (BTU/LB)	VAPOR PRESSURE (PSIA)	SPECIFIC GRAVITY	VISCOSITY (LBH/FT-SEC)	SURFACE TENSION (LBH/IN)
.300000	309.500	171.255	1379.61	1.192027E-05	1.09902	109990	6.046761E-04
.400000	406.000	228.340	1635.95	2.80316E-02	1.03790	109990	4.797276E-04
.500000	502.500	475.240	1492.29	1.03663	.976141	4.378775E-04	3.752234E-04
.600000	699.000	991.790	1548.63	25.0046	.91392	1.554545E-04	2.800015E-04
.700000	815.500	708.290	1604.97	150.111	.852466	9.552362E-05	2.182489E-04
.800000	932.000	224.790	1661.31	951.536	.790626	6.272835E-05	1.616817E-04
.900000	1048.50	961.290	1717.65	1482.97	.566294	4.328186E-05	7.891214E-05
.999999	1165.00	1057.79	1773.99	3225.99	1.266399E-03	3.105782E-05	1.698035E-14
1.000000	1165.00 (CRITICAL TEMP.)	1415.89	1415.89	3226.00 (CRITICAL PRESS.)	3.237915E-07	6.987987E-06	2.347593E-31
1.010000	1176.65	-----	1779.62	-----	0.	7.057867E-04	-----

FUEL VAPOR HEAT CONTENT (BTU/LB)	OXIDIZER VAPOR HEAT CONTENT (BTU/LB)	WATER VAPOR HEAT CONTENT (AT 540 DEG R)
453.00000	170.10000	1102.30000

CALCULATED VALUES AT TEMPERATURES OF MMH = 1000.000 DEG M. N2O4 = 491.768 DEG R.				
MMH PRESS (PSIA)	N2O4 PRESS (PSIA)	MMH DENSITY (LB/CUFT)	N2O4 DENSITY (LB/CUFT)	MMH / N2O4 DENSITY RATIO
1195.00000	1441.30000	14.02751	93.54352	6.66858
MMH VISC. (LBM/FT-SFG)	N2O4 VISC. (LBM/FT-SFG)	MMH SURF TENS. (LBM/IN)	N2O4 SURF TENS. (LBM/IN)	
.0000058	.0003555	.0029053	.0034253	

TEMPERATURE INPUT OF 500,000 DEG R TO SUBROUTINE -DBRNEN- CALLED FROM -DBENLAY(2,0)- FOR CALCULATION OF REDUCED PROPERTIES IS NOT SIGNIFICANTLY DIFFERENT FROM A PREVIOUS INPUT FOR THE SAME SUBSTANCES. THE NEW VALUE HAS BEEN RESET TO THE PREVIOUS ENTRY OF 500,000 DEG R.

MMH + N2O4
CONTAMINANT PROPERTIES
(ESTIMATED)

DENSITY (LBM/CUFT)	VAPOR CP. (HTH/LM=DFG)	LATENT HEAT OF VAPORIZATION	DECOMP. TEMP. (NEG R)
02.827961	1.000300	180.000000	900.000000
VISCOSITY 1 0 PCT MMH .000205	VISCOSITY 2 9 PCT MMH .000304	VISCOSITY 3 18 PCT MMH .000344	VISCOSITY 4 27 PCT MMH .000383
VISCOSITY 5 36 PCT MMH .000423	VISCOSITY 6 45 PCT MMH .000462	VISCOSITY 7 55 PCT MMH .000502	VISCOSITY 8 64 PCT MMH .000541
VISCOSITY 9 73 PCT MMH .000580	VISCOSITY 10 82 PCT MMH .000620	VISCOSITY 11 91 PCT MMH .000659	VISCOSITY 12 100 PCT MMH .000699

VISCOSITIES ARE GIVEN LB(MASS)/FT-SEC

MIXTURE OF AA = AMONIA AND BB = 42H4

Figure D-43. Derived Coefficients and Properties of Deposit Constituents (Page 4 of 5)

ESTIMATED MIXTURE VISCOSITIES

0 PCT 9AA0 17 PCT 9AA0 33 PCT 9AA0 50 PCT 9AA0
 .000400 .050024 .040760 .030912

67 PCT 9AA0 83 PCT 9AA0 100 PCT 9AA0
 .021056 .011200 .001344

VISCOSITIES ARE GIVEN LN(MASS)/FT-SEC

HICKORY-DICKORY SAYS 401.40 SECONDS
FOR RUNNING OVERLAY(2.0)
FINISHED AT CLOCK TIME 11-39-33.0

CP TIME USED = 156.35 SECONDS
PP TIME USED = 100.96 SECONDS
SINCE JOB STARTED

REVISED DATA INPUT WITH NAMELIST

```
SNAST3
TOTIM1 = 0.2E-02.
DELTIM1 = 0.2E-03.
SEND
```

```
SNAST4
P1      = 0.142E+00.
DELP1   = 0.1E-02.
NTR1    = 2.
SEND
```

```
HICKORY-DICKORY SAYS      6.00 SECONDS
FOR RUNNING OVERLAY 2.1
FINISHED AT CLOCK TIME 11-39-39.0
```

```
CP TIME USED = 156.64 SECONDS
PP TIME USED = 107.95 SECONDS
SINCE JOB STARTED
```

Figure D-44. Revised Data Input by NAMELIST

CALCULATION CYCLE	EXPOSURE /OPERATION	DURATION (SEC.)
1	INITIAL	-1.0000
2	ASSIGNED	-1.0000
3	PLUME	70.000
4	SPACE	6.000000E+05
5	WRAP-UP	-1.0000

Figure D-45. Assignment of Calculation Cycles

Spacecraft Exterior Materials and Conditions, Initial State

The assignment of materials and their thickness, surface temperature, and surface finish at specified segments of the satellite is performed in Link 3, 0 with data input from file BDATA. This input is listed for inspection in Figure D-46.

Initial Condition of Satellite Exterior

The data on the assignment of structural materials to the satellite and the properties of the materials are used by Link 11, 0 and its subsidiary programs to calculate the condition of each segment of the surface. The results of the calculations include the solar absorptivity, thermal emissivity, diffuse and specular solar reflectivity, thermal reflectivity, thermal conductivity and transmissivity at several wavelengths. This information is listed for each segment (see Figure D-47 for a portion of this listing).

The condition is then summarized in a listing of the average solar absorptivity, thermal emissivity, and their ratio for the whole satellite. Then the percent transmission for a set of 8 different wavelengths of light through all transparent segments is listed. These outputs are presented in Figure D-48.

Assigned Satellite Conditions

The assigned post-exposure conditions for specific satellite locations, input from file TAPE9 (CDATA) by execution of Link (4, 0), and used to test the functioning of the subsequent calculation routines in Links (7, 0) and (11, 0) are listed next. This input can be the satellite condition data generated in a previous run of the program, but that feature is not used in the Test Case run. The input is listed, as shown in Figure D-49. These data are then used to calculate the condition of the exterior, and then a segment-by-segment printout of the condition is again made. Figure D-50 shows the results of the assigned post-exposure condition at three of the segments, numbers 51, 52, and 53, identified in Figure D-49. The data in Figure D-50 consists first of the condition for the three segments in the pristine or original condition, then the condition for the same segments after the assigned exposure. The changes are those caused by the alteration of the surface condition.

The summary of current conditions, Figure D-51, includes not only the average α and ϵ values, and their ratio, but also the percent change in the ratio compared to the initial or baseline condition.

The execution then enters Link (10, 2) and checks to see whether the assigned conditions should be used as the base for further calculations or whether the initial conditions should be reestablished. The flag ISTST, read from file TAPE9, is zero, so the initial conditions are reestablished.

Plume Exposure Sequences

The total exposure duration and the calculation time increment are listed, see Figure D-52. Note that these are the true values to be used; in this case they are the specific corrected values supplied by NAMELIST/NAST3, not those input from ADATA.

Figure D-48. Initial Material Assignment to Spacecraft Exterior (Page 1 of 2)

89	520.00	BLACK	.0070	40.00	ALUMIN	.1000	16.00	NONE	-1.0	-1.0
90	520.00	BLACK	.0070	40.00	ALUMIN	.1000	16.00	NONE	-1.0	-1.0
91	520.00	BLACK	.0070	40.00	ALUMIN	.1000	16.00	NONE	-1.0	-1.0
92	520.00	BLACK	.0070	40.00	ALUMIN	.1000	16.00	NONE	-1.0	-1.0
93	520.00	BLACK	.0070	40.00	ALUMIN	.1000	16.00	NONE	-1.0	-1.0
94	520.00	BLACK	.0070	40.00	ALUMIN	.1000	16.00	NONE	-1.0	-1.0
95	520.00	BLACK	.0070	40.00	ALUMIN	.1000	16.00	NONE	-1.0	-1.0
96	520.00	BLACK	.0070	40.00	ALUMIN	.1000	16.00	NONE	-1.0	-1.0
97	520.00	BLACK	.0070	40.00	GOLD	.0075	10.00	NONE	-1.0	-1.0
98	520.00	BLACK	.0070	40.00	GOLD	.0075	10.00	NONE	-1.0	-1.0
99	520.00	BLACK	.0070	40.00	ALUMIN	.1000	16.00	NONE	-1.0	-1.0
100	520.00	WHITE	.0050	32.00	ALUMIN	.1000	16.00	NONE	-1.0	-1.0
101	520.00	WHITE	.0050	32.00	ALUMIN	.1000	16.00	NONE	-1.0	-1.0
102	520.00	WHITE	.0050	32.00	ALUMIN	.1000	16.00	NONE	-1.0	-1.0
103	520.00	WHITE	.0050	32.00	ALUMIN	.1000	16.00	NONE	-1.0	-1.0
104	520.00	WHITE	.0050	32.00	ALUMIN	.1000	16.00	NONE	-1.0	-1.0
105	520.00	WHITE	.0050	32.00	ALUMIN	.1000	16.00	NONE	-1.0	-1.0
106	520.00	WHITE	.0050	32.00	ALUMIN	.1000	16.00	NONE	-1.0	-1.0
107	520.00	WHITE	.0050	32.00	ALUMIN	.1000	16.00	NONE	-1.0	-1.0
108	520.00	WHITE	.0050	32.00	ALUMIN	.1000	16.00	NONE	-1.0	-1.0
109	520.00	WHITE	.0050	32.00	ALUMIN	.1000	16.00	NONE	-1.0	-1.0
110	520.00	GOLD	.0003	1.00	ALUMIN	.1000	16.00	NONE	-1.0	-1.0
111	520.00	GOLD	.0003	1.00	ALUMIN	.1000	16.00	NONE	-1.0	-1.0
112	520.00	GOLD	.0003	1.00	ALUMIN	.1000	2.00	NONE	-1.0	-1.0
113	520.00	GOLD	.0003	1.00	ALUMIN	.1000	2.00	NONE	-1.0	-1.0
114	520.00	GOLD	.0003	1.00	ALUMIN	.1000	2.00	NONE	-1.0	-1.0
115	520.00	GOLD	.0003	1.00	ALUMIN	.1000	2.00	NONE	-1.0	-1.0
116	520.00	GOLD	.0003	1.00	ALUMIN	.1000	2.00	NONE	-1.0	-1.0
501	520.20	BLACK	.0060	20.00	ALUMIN	.0210	32.00	NONE	-1.0	-1.0
502	520.20	BLACK	.0060	20.00	ALUMIN	.0205	32.20	NONE	-1.0	-1.0
7301	550.00	TEFLON	.0400	10.00	ALUMIN	.0700	120.00	NONE	-1.0	-1.0
7302	560.00	SOLCEL	.0500	10.00	UNASND	-1.0	-1.0	UNASND	-1.0	-1.0
7303	560.00	SOLCEL	.0500	10.00	UNASND	-1.0	-1.0	UNASND	-1.0	-1.0
7304	560.00	SOLCEL	.0500	10.00	UNASND	-1.0	-1.0	UNASND	-1.0	-1.0
7305	560.00	SOLCEL	.0500	10.00	UNASND	-1.0	-1.0	UNASND	-1.0	-1.0
7306	560.00	SOLCEL	.0500	10.00	UNASND	-1.0	-1.0	UNASND	-1.0	-1.0
7307	560.00	SOLCEL	.0500	10.00	UNASND	-1.0	-1.0	UNASND	-1.0	-1.0
7308	560.00	SOLCEL	.0500	10.00	UNASND	-1.0	-1.0	UNASND	-1.0	-1.0
7309	560.00	SOLCEL	.0500	10.00	UNASND	-1.0	-1.0	UNASND	-1.0	-1.0
7310	560.00	SOLCEL	.0500	10.00	UNASND	-1.0	-1.0	UNASND	-1.0	-1.0
7311	510.00	SOLCEL	.0500	10.00	UNASND	-1.0	-1.0	UNASND	-1.0	-1.0
7312	510.00	SOLCEL	.0500	10.00	UNASND	-1.0	-1.0	UNASND	-1.0	-1.0
7313	510.00	SOLCEL	.0500	10.00	UNASND	-1.0	-1.0	UNASND	-1.0	-1.0
7314	510.00	SOLCEL	.0500	10.00	UNASND	-1.0	-1.0	UNASND	-1.0	-1.0
7315	510.00	SOLCEL	.0500	10.00	UNASND	-1.0	-1.0	UNASND	-1.0	-1.0
7316	510.00	SOLCEL	.0500	10.00	UNASND	-1.0	-1.0	UNASND	-1.0	-1.0
7317	510.00	SOLCEL	.0500	10.00	UNASND	-1.0	-1.0	UNASND	-1.0	-1.0
7318	510.00	SOLCEL	.0500	10.00	UNASND	-1.0	-1.0	UNASND	-1.0	-1.0
7319	510.00	SOLCEL	.0500	10.00	UNASND	-1.0	-1.0	UNASND	-1.0	-1.0
7320	520.00	TEFLON	.0400	10.00	ALUMIN	.0700	120.00	NONE	-1.0	-1.0

NOTE VALUES OF -1.0 INDICATE NO DATA ENTERED.

HICKORY-DICKORY SAYS 4.00 SECONDS
FOR RUNNING OVERLAY(3.0)
FINISHED AT CLOCK TIME 11-39-43.0

CP TIME USED = 150.10 SECONDS
PP TIME USED = 100.90 SECONDS
SINCE JOB STARTED
MAXIMUM EXECUTION FIELD LENGTH REQUIRED = 202406

HICKORY-DICKORY SAYS 1020.00 SECONDS
FOR RUNNING OVERLAY 11.0
FINISHED AT CLOCK TIME 12-10-12.0

CP TIME USED = 171.99 SECONDS
PP TIME USED = 157.44 SECONDS
SINCE JOB STARTED

HICKORY-DICKORY SAYS 592.20 SECONDS
FOR RUNNING OVERLAY 11.2
FINISHED AT CLOCK TIME 12-20- 4.0

CP TIME USED = 174.05 SECONDS
PP TIME USED = 166.46 SECONDS
SINCE JOB STARTED

Figure D-46. Initial Material Assignment to Spacecraft Exterior (Page 2 of 2)

CURRENT CONDITION OF SATELLITE EXTERIOR

INITIAL CONDITIONS

ID	X	R	THETA	AREA	PLUME X	TEMP	PRJN HGT	LAMBDA	MU	NU
1	0.000	0.000	0.00000	1	-3.000	520.0	-1.0	-1.0	-1.0	-1.0

MATL NAME	DEPTH	FINISH	ABRY	EMISY	DIFRF	SPECRF	TRMRF	TRMCD	RFIND	IS	S	Z	1	.5	.2	.05	.01	TEMP
7 GOLD	.000300000	1.00	.336	.040	.050	.663	.960	.006	0.0	0.0	0.0	0.0	0.0	0.0	0.0	0.0	0.0	520
1 ALUMIN	.100000000	2.00	.020	.040	.050	.980	.960	.598	0.0	0.0	0.0	0.0	0.0	0.0	0.0	0.0	0.0	520
NO THIRD LAYER																		

ID	X	R	THETA	AREA	PLUME X	TEMP	PRJN HGT	LAMBDA	MU	NU
2	.305	.590	1.04720	1	-3.295	520.0	-1.0	-1.0	-1.0	-1.0

MATL NAME	DEPTH	FINISH	ABRY	EMISY	DIFRF	SPECRF	TRMRF	TRMCD	RFIND	IS	S	Z	1	.5	.2	.05	.01	TEMP
7 GOLD	.000300000	1.00	.336	.040	.050	.663	.960	.006	0.0	0.0	0.0	0.0	0.0	0.0	0.0	0.0	0.0	520
1 ALUMIN	.100000000	2.00	.020	.040	.050	.980	.960	.598	0.0	0.0	0.0	0.0	0.0	0.0	0.0	0.0	0.0	520
NO THIRD LAYER																		

ID	X	R	THETA	AREA	PLUME X	TEMP	PRJN HGT	LAMBDA	MU	NU
3	.305	.590	3.14159	1	-3.295	520.0	-1.0	-1.0	-1.0	-1.0

MATL NAME	DEPTH	FINISH	ABRY	EMISY	DIFRF	SPECRF	TRMRF	TRMCD	RFIND	IS	S	Z	1	.5	.2	.05	.01	TEMP
7 GOLD	.000300000	1.00	.336	.040	.050	.663	.960	.006	0.0	0.0	0.0	0.0	0.0	0.0	0.0	0.0	0.0	520
1 ALUMIN	.100000000	2.00	.020	.040	.050	.980	.960	.598	0.0	0.0	0.0	0.0	0.0	0.0	0.0	0.0	0.0	520
NO THIRD LAYER																		

↑
 PORT 12: OMITTED

ID	X	R	THETA	AREA	PLUME X	TEMP	PRJN HGT	LAMBDA	MU	NU
8	.620	1.200	4.39816	1	-2.980	520.0	-1.0	-1.0	-1.0	-1.0

MATL NAME	DEPTH	FINISH	ABRY	EMISY	DIFRF	SPECRF	TRMRF	TRMCD	RFIND	IS	S	Z	1	.5	.2	.05	.01	TEMP
2 WINDOW	.150000000	5.00	.526	.090	.120	.474	.110	.002	1.547	0.0	0.0	.005	.005	.001	0.0	0.0	0.0	520
NO SECOND LAYER																		
NO THIRD LAYER																		

ID	X	R	THETA	AREA	PLUME X	TEMP	PRJN HGT	LAMBDA	MU	NU
9	.620	1.200	5.69440	1	-2.980	520.0	-1.0	-1.0	-1.0	-1.0

MATL NAME	DEPTH	FINISH	ABRY	EMISY	DIFRF	SPECRF	TRMRF	TRMCD	RFIND	IS	S	Z	1	.5	.2	.05	.01	TEMP
7 GOLD	.000300000	1.00	.336	.040	.050	.663	.960	.006	0.0	0.0	0.0	0.0	0.0	0.0	0.0	0.0	0.0	520
1 ALUMIN	.100000000	2.00	.020	.040	.050	.980	.960	.598	0.0	0.0	0.0	0.0	0.0	0.0	0.0	0.0	0.0	520
NO THIRD LAYER																		

ID	X	R	THETA	AREA	PLUME X	TEMP	PRJN HGT	LAMBDA	MU	NU
10	1.325	1.600	3.1416	1	-2.275	520.0	-1.0	-1.0	-1.0	-1.0

MATL NAME	DEPTH	FINISH	ABRY	EMISY	DIFRF	SPECRF	TRMRF	TRMCD	RFIND	IS	S	Z	1	.5	.2	.05	.01	TEMP
1 ALUMIN	.100000000	10.00	.236	.090	.549	.764	.910	.950	0.0	0.0	0.0	0.0	0.0	0.0	0.0	0.0	0.0	520
NO SECOND LAYER																		
NO THIRD LAYER																		

Figure D-47. Satellite Exterior Conditions (Page 1 of 3)

ID	X	R	THETA	AREA	PLUME X	TEMP	PRJN HGT	LAMBDA	MU	NU										
11	6.325	1.000	0.04248	1	2.275	520.0	-1.0	-1.0	-1.0	-1.0										
MATERIAL NAME DEPTH FINISH ABBRY EMISY DIFRF SPECRF TMRPF TMCND RFIND 15 5 2 1 .5 .2 .05 .01 TEMP																				
1 ALUMIN	.100000000	10.00	.236	.090	.549	.764	.910	.950	0.0	0.0	0.0	0.0	0.0	0.0	0.0	0.0	0.0	0.0	0.0	520
NO SECOND LAYER																				
NO THIRD LAYER																				
.....																				
↑ PORTION OMITTED																				
67	6.325	1.000	4.71840	1	2.725	520.0	-1.0	-1.0	-1.0	-1.0										
MATERIAL NAME DEPTH FINISH ABBRY EMISY DIFRF SPECRF TMRPF TMCND RFIND 15 5 2 1 .5 .2 .05 .01 TEMP																				
1 ALUMIN	.100000000	10.00	.236	.090	.549	.764	.910	.950	0.0	0.0	0.0	0.0	0.0	0.0	0.0	0.0	0.0	0.0	0.0	520
NO SECOND LAYER																				
NO THIRD LAYER																				
.....																				
68	6.325	1.000	5.34070	1	2.725	520.0	-1.0	-1.0	-1.0	-1.0										
MATERIAL NAME DEPTH FINISH ABBRY EMISY DIFRF SPECRF TMRPF TMCND RFIND 15 5 2 1 .5 .2 .05 .01 TEMP																				
5 UVPORY	.500000000	.50	.055	.910	-1.0	.945	.090	.003	1.459	0.0	0.0	0.0	.050	.990	.050	.250	.005			520
NO SECOND LAYER																				
NO THIRD LAYER																				
.....																				
69	6.325	1.000	5.46902	1	2.725	520.0	-1.0	-1.0	-1.0	-1.0										
MATERIAL NAME DEPTH FINISH ABBRY EMISY DIFRF SPECRF TMRPF TMCND RFIND 15 5 2 1 .5 .2 .05 .01 TEMP																				
1 ALUMIN	.100000000	10.00	.236	.090	.549	.764	.910	.950	0.0	0.0	0.0	0.0	0.0	0.0	0.0	0.0	0.0	0.0	0.0	520
NO SECOND LAYER																				
NO THIRD LAYER																				
.....																				
70	7.325	1.000	3.31416	1	3.725	520.0	-1.0	-1.0	-1.0	-1.0										
MATERIAL NAME DEPTH FINISH ABBRY EMISY DIFRF SPECRF TMRPF TMCND RFIND 15 5 2 1 .5 .2 .05 .01 TEMP																				
0 BLACK	.007000000	40.00	.907	.789	.027	.093	.211	.023	0.0	0.0	0.0	0.0	0.0	0.0	0.0	0.0	0.0	0.0	0.0	520
1 ALUMIN	.100000000	10.00	.236	.090	.549	.764	.910	.950	0.0	0.0	0.0	0.0	0.0	0.0	0.0	0.0	0.0	0.0	0.0	520
NO THIRD LAYER																				
.....																				
71	7.325	1.000	0.04248	1	3.725	520.0	-1.0	-1.0	-1.0	-1.0										
MATERIAL NAME DEPTH FINISH ABBRY EMISY DIFRF SPECRF TMRPF TMCND RFIND 15 5 2 1 .5 .2 .05 .01 TEMP																				
0 WHITE	.100000000	32.00	.100	.939	.037	.040	.041	.007	0.0	0.0	0.0	0.0	0.0	0.0	0.0	0.0	0.0	0.0	0.0	520
1 ALUMIN	.100000000	10.00	.236	.090	.549	.764	.910	.950	0.0	0.0	0.0	0.0	0.0	0.0	0.0	0.0	0.0	0.0	0.0	520
NO THIRD LAYER																				
.....																				
72	7.325	1.000	1.57600	1	3.725	520.0	-1.0	-1.0	-1.0	-1.0										
MATERIAL NAME DEPTH FINISH ABBRY EMISY DIFRF SPECRF TMRPF TMCND RFIND 15 5 2 1 .5 .2 .05 .01 TEMP																				
0 BLACK	.007000000	40.00	.907	.789	.027	.093	.211	.023	0.0	0.0	0.0	0.0	0.0	0.0	0.0	0.0	0.0	0.0	0.0	520
1 ALUMIN	.100000000	10.00	.236	.090	.549	.764	.910	.950	0.0	0.0	0.0	0.0	0.0	0.0	0.0	0.0	0.0	0.0	0.0	520
NO THIRD LAYER																				
.....																				

Figure D-47. Satellite Exterior Conditions (Page 2 of 3)

↑
PORTION OMITTED

ID	X	R	THETA	AREA	PLUME X	TEMP	PRJN HGT	LAMBDA	NU	NU
7302	6.641	5.300	6.20300	1	3.001	929.2	-1.0	-1.0	-1.0	-1.0

MATL NAME	DEPTH	FINISH	ABRY	EMISY	DIFRF	SPECRF	TMRP	TMCND	RFIND	IS	S	Z	1	.5	.2	.05	.01	TEMP
0 BLACK	.000000000	20.00	.946	.034	.044	.054	.166	.023	0.0	0.0	0.0	0.0	0.0	0.0	0.0	0.0	0.0	529
1 ALUMIN	.020500000	32.20	.343	.201	.500	.657	.799	.950	0.0	0.0	0.0	0.0	0.0	0.0	0.0	0.0	0.0	
NO THIRD LAYER																		

ID	X	R	THETA	AREA	PLUME X	TEMP	PRJN HGT	LAMBDA	NU	NU
7301	6.606	2.502	2.19911	1	3.206	950.0	-1.0	-1.0	-1.0	-1.0

MATL NAME	DEPTH	FINISH	ABRY	EMISY	DIFRF	SPECRF	TMRP	TMCND	RFIND	IS	S	Z	1	.5	.2	.05	.01	TEMP
0 TEFLON	.040000000	10.00	.280	.070	-1.0	.720	.130	.002	-1.0	0.0	0.0	0.0	0.0	0.0	0.0	0.0	0.0	550
1 ALUMIN	.060711100	120.00	.633	.324	.367	.525	.676	.950	0.0	0.0	0.0	0.0	0.0	0.0	0.0	0.0	0.0	
NO THIRD LAYER																		

ID	X	R	THETA	AREA	PLUME X	TEMP	PRJN HGT	LAMBDA	NU	NU
7302	6.608	4.161	1.89900	1	3.000	900.0	-1.0	-1.0	-1.0	-1.0

MATL NAME	DEPTH	FINISH	ABRY	EMISY	DIFRF	SPECRF	TMRP	TMCND	RFIND	IS	S	Z	1	.5	.2	.05	.01	TEMP
0 SOLCEL	.050000000	10.00	.100	.050	-1.0	.900	.150	.002	2.450	0.0	0.0	.250	.650	.650	0.0	0.0	0.0	500
NO SECOND LAYER																		
NO THIRD LAYER																		

ID	X	R	THETA	AREA	PLUME X	TEMP	PRJN HGT	LAMBDA	NU	NU
7303	6.603	4.056	2.19911	1	3.003	900.0	-1.0	-1.0	-1.0	-1.0

MATL NAME	DEPTH	FINISH	ABRY	EMISY	DIFRF	SPECRF	TMRP	TMCND	RFIND	IS	S	Z	1	.5	.2	.05	.01	TEMP
0 SOLCEL	.050000000	10.00	.100	.050	-1.0	.900	.150	.002	2.450	0.0	0.0	.250	.650	.650	0.0	0.0	0.0	500
NO SECOND LAYER																		
NO THIRD LAYER																		

↑
PORTION OMITTED

NOTE VALUES OF -1.0...0 INDICATE NO DATA ENTERED

.....

Figure D-47. Satellite Exterior Conditions (Page 3 of 3)

EFFECTIVE HEAT TRANSFER CONSTANTS

SUM OF SEGMENT AREAS = 125.00

EFFECTIVE SOLAR ABSORPTIVITY = .348
 EFFECTIVE THERMAL EMISSIVITY = .423

AVERAGE VALUE ALPHA/EPSILON RATIO FOR WHOLE SPACECRAFT = .0232

PERCENT TRANSMISSION THROUGH TRANSPARENT SEGMENTS

SEGMENT	MATERIAL	1SMU	3MU	2MU	1MU	.5MU	.2MU	.05MU	.01MU
0	WINDOW	.	.	1.418	28.98	69.87	.	.	.
23	IMPORT	22.98	54.21	88.48	88.48	98.55	.	.	.
68	UVPORT	.	.	.	19.53	89.25	86.74	47.04	6.652
7302	SOLCEL	.	.	76.14	79.86	92.00	.	.	.
7303	SOLCEL	.	.	76.14	79.86	92.00	.	.	.
7304	SOLCEL	.	.	76.14	79.86	92.00	.	.	.
7305	SOLCEL	.	.	76.14	79.86	92.00	.	.	.
7306	SOLCEL	.	.	76.14	79.86	92.00	.	.	.
7307	SOLCEL	.	.	76.14	79.86	92.00	.	.	.
7308	SOLCEL	.	.	76.14	79.86	92.00	.	.	.
7309	SOLCEL	.	.	76.14	79.86	92.00	.	.	.
7310	SOLCEL	.	.	76.14	79.86	92.00	.	.	.
7311	SOLCEL	.	.	76.14	79.86	92.00	.	.	.
7312	SOLCEL	.	.	76.14	79.86	92.00	.	.	.
7313	SOLCEL	.	.	76.14	79.86	92.00	.	.	.
7314	SOLCEL	.	.	76.14	79.86	92.00	.	.	.
7315	SOLCEL	.	.	76.14	79.86	92.00	.	.	.
7316	SOLCEL	.	.	76.14	79.86	92.00	.	.	.
7317	SOLCEL	.	.	76.14	79.86	92.00	.	.	.
7318	SOLCEL	.	.	76.14	79.86	92.00	.	.	.
7319	SOLCEL	.	.	76.14	79.86	92.00	.	.	.
MEAN	SOLCEL	.	.	76.14	79.86	92.00	.	.	.

HICKORY-DICKORY SAYS 320.00 SECONDS
 FOR RUNNING OVERLAY 11.0
 (PRIMARY OVERLAY ONLY)

HICKORY-DICKORY SAYS 2749.00 SECONDS
 FOR RUNNING OVERLAY 11.0
 INCLUDING ALL SECONDARY OVERLAYS
 FINISHED AT CLOCK TIME 12-25-33.6

CP TIME USED = 193.14 SECONDS
 PP TIME USED = 198.85 SECONDS
 SINCE JOB STARTED

Figure D-48. Summary of Initial Satellite Condition

SPACECRAFT EXTERIOR MATERIALS

ASSIGNED CONDITIONS

SEGMENT NO.	TEMPERATURE (DEG R)	T O P L A Y E R		2 - N D L A Y E R		
		MATERIAL	DEPTH (IN)	FINISH (MU-IN)	MATERIAL DEPTH (IN)	FINISH (MU-IN)
42	600.0	ALUMIN	9.500E-02	100.00	NONE	-1.0
51	610.0	WHITE	2.000E-03	80.00	ALUMIN	.100
52	650.0	ALUMIN	9.500E-02	250.00	NONE	-1.0
53	610.0	ERODED	0.	-1.00	ALUMIN	.100
61	700.0	ALUMIN	9.000E-02	50.00	NONE	-1.0
62	900.0	ALUMIN	7.900E-02	190.00	NONE	-1.0
63	700.0	ALUMIN	9.000E-02	50.00	NONE	-1.0
72	650.0	HOLE	-5.000E-02	-1.00	NONE	-1.0
82	610.0	ALUMIN	.100	90.00	NONE	-1.0
92	500.0	BLACK	5.700E-03	32.00	ALUMIN	.100

NOTE VALUES OF -1.0 INDICATE NO DATA ENTERED.

HICKORY-DICKORY SAYS 7.00 SECONDS
FOR RUNNING OVERLAY 7.0
FINISHED AT CLOCK TIME 12-25-48.6

CP TIME USED = 195.07 SECONDS
PP TIME USED = 204.19 SECONDS
SINCE JOB STARTED

HICKORY-DICKORY SAYS 47.40 SECONDS
FOR RUNNING OVERLAY 11.1
FINISHED AT CLOCK TIME 12-26-36.0

CP TIME USED = 202.08 SECONDS
PP TIME USED = 222.96 SECONDS
SINCE JOB STARTED

HICKORY-DICKORY SAYS 3.00 SECONDS
FOR RUNNING OVERLAY 11.2
FINISHED AT CLOCK TIME 12-26-39.0

CP TIME USED = 202.06 SECONDS
PP TIME USED = 223.71 SECONDS
SINCE JOB STARTED

Figure D-49. Assignment of Post-Exposure Conditions

PRISTINE CONDITION

ID	X	R	THETA	AREA	PLUME X	TEMP	PRJN HGT	LAMBDA	MU	NU
51	5.325	1.000	.74240	1	1.725	520.0	-1.0	-1.0	-1.0	-1.0

MATL NAME	DEPTH	FINISH	ABSRY	EMISY	DIFRF	SPECRF	TMRHF	TMRCHD	RFIND	15	5	2	1	.5	.2	.05	.01	TEMP
0 WHITE	.005000000	32.00	.100	.930	.037	.040	.001	.007	0.0	0.0	0.0	0.0	0.0	0.0	0.0	0.0	0.0	520
1 ALUMIN	.100000000	10.00	.230	.090	.549	.764	.910	.950	0.0	0.0	0.0	0.0	0.0	0.0	0.0	0.0	0.0	520
NO SECOND LAYER																		
NO THIRD LAYER																		

ID	X	R	THETA	AREA	PLUME X	TEMP	PRJN HGT	LAMBDA	MU	NU
52	5.325	1.000	1.57080	1	1.725	520.0	-1.0	-1.0	-1.0	-1.0

MATL NAME	DEPTH	FINISH	ABSRY	EMISY	DIFRF	SPECRF	TMRHF	TMRCHD	RFIND	15	5	2	1	.5	.2	.05	.01	TEMP
1 ALUMIN	.100000000	10.00	.230	.090	.549	.764	.910	.950	0.0	0.0	0.0	0.0	0.0	0.0	0.0	0.0	0.0	520
NO SECOND LAYER																		
NO THIRD LAYER																		

ID	X	R	THETA	AREA	PLUME X	TEMP	PRJN HGT	LAMBDA	MU	NU
53	5.325	1.000	2.19911	1	1.725	520.0	-1.0	-1.0	-1.0	-1.0

MATL NAME	DEPTH	FINISH	ABSRY	EMISY	DIFRF	SPECRF	TMRHF	TMRCHD	RFIND	15	5	2	1	.5	.2	.05	.01	TEMP
0 WHITE	.005000000	32.00	.100	.930	.037	.040	.001	.007	0.0	0.0	0.0	0.0	0.0	0.0	0.0	0.0	0.0	520
1 ALUMIN	.100000000	10.00	.230	.090	.549	.764	.910	.950	0.0	0.0	0.0	0.0	0.0	0.0	0.0	0.0	0.0	520
NO SECOND LAYER																		
NO THIRD LAYER																		

RESULT OF ASSIGNED POST EXPOSURE CONDITION

ID	X	R	THETA	AREA	PLUME X	TEMP	PRJN HGT	LAMBDA	MU	NU
51	5.325	1.000	.74240	1	1.725	610.0	-1.0	-1.0	-1.0	-1.0

MATL NAME	DEPTH	FINISH	ABSRY	EMISY	DIFRF	SPECRF	TMRHF	TMRCHD	RFIND	15	5	2	1	.5	.2	.05	.01	TEMP
0 WHITE	.005000000	32.00	.210	.950	.020	.790	.050	.007	0.0	0.0	0.0	0.0	0.0	0.0	0.0	0.0	0.0	610
1 ALUMIN	.100000000	10.00	.370	.204	.500	.624	.795	.950	0.0	0.0	0.0	0.0	0.0	0.0	0.0	0.0	0.0	610
NO SECOND LAYER																		
NO THIRD LAYER																		

ID	X	R	THETA	AREA	PLUME X	TEMP	PRJN HGT	LAMBDA	MU	NU
52	5.325	1.000	1.57080	1	1.725	650.0	-1.0	-1.0	-1.0	-1.0

MATL NAME	DEPTH	FINISH	ABSRY	EMISY	DIFRF	SPECRF	TMRHF	TMRCHD	RFIND	15	5	2	1	.5	.2	.05	.01	TEMP
1 ALUMIN	.100000000	250.00	.000	.340	.200	.525	.600	.950	0.0	0.0	0.0	0.0	0.0	0.0	0.0	0.0	0.0	650
NO SECOND LAYER																		
NO THIRD LAYER																		

ID	X	R	THETA	AREA	PLUME X	TEMP	PRJN HGT	LAMBDA	MU	NU
53	5.325	1.000	2.19911	1	1.725	610.0	-1.0	-1.0	-1.0	-1.0

MATL NAME	DEPTH	FINISH	ABSRY	EMISY	DIFRF	SPECRF	TMRHF	TMRCHD	RFIND	15	5	2	1	.5	.2	.05	.01	TEMP
1 ALUMIN	.100000000	30.00	.370	.204	.500	.624	.795	.950	0.0	0.0	0.0	0.0	0.0	0.0	0.0	0.0	0.0	610
NO SECOND LAYER																		
NO THIRD LAYER																		

Figure D-50. Comparison of Selected Segments Before and After Assignment of Post-Exposed Conditions

EFFECTIVE HEAT TRANSFER CONSTANTS

SUM OF SEGMENT AREAS = 125.00

EFFECTIVE SOLAR ABSORPTIVITY = .357
 EFFECTIVE THERMAL EMISSIVITY = .801

AVERAGE VALUE ALPHA/EPSILON RATIO FOR WHOLE SPACECRAFT = .0000

PERCENT CHANGE IN ALPHA/EPSILON RATIO FROM BASELINE VALUE = 7.970

PERCENT TRANSMISSION THROUGH TRANSPARENT SEGMENTS

SEGMENT	MATERIAL	1SMU	5MU	2MU	1MU	.5MU	.2MU	.05MU	.01MU
0	WINDOW	.	.	1.410	20.00	60.07	.	.	.
23	INPORT	22.90	54.21	80.40	80.40	50.55	.	.	.
60	UVPORT	.	.	.	19.53	89.25	86.70	87.00	6.052
7302	SOLCEL	.	.	70.10	79.00	92.00	.	.	.
7303	SOLCEL	.	.	70.10	79.00	92.00	.	.	.
7304	SOLCEL	.	.	70.10	79.00	92.00	.	.	.
7305	SOLCEL	.	.	70.10	79.00	92.00	.	.	.
7306	SOLCEL	.	.	70.10	79.00	92.00	.	.	.
7307	SOLCEL	.	.	70.10	79.00	92.00	.	.	.
7308	SOLCEL	.	.	70.10	79.00	92.00	.	.	.
7309	SOLCEL	.	.	70.10	79.00	92.00	.	.	.
7310	SOLCEL	.	.	70.10	79.00	92.00	.	.	.
7311	SOLCEL	.	.	70.10	79.00	92.00	.	.	.
7312	SOLCEL	.	.	70.10	79.00	92.00	.	.	.
7313	SOLCEL	.	.	70.10	79.00	92.00	.	.	.
7314	SOLCEL	.	.	70.10	79.00	92.00	.	.	.
7315	SOLCEL	.	.	70.10	79.00	92.00	.	.	.
7316	SOLCEL	.	.	70.10	79.00	92.00	.	.	.
7317	SOLCEL	.	.	70.10	79.00	92.00	.	.	.
7318	SOLCEL	.	.	70.10	79.00	92.00	.	.	.
7319	SOLCEL	.	.	70.10	79.00	92.00	.	.	.
	MEAN SOLCEL	.	.	70.10	79.00	92.00	.	.	.

NICKORY-DICKORY SAYS 99.00 SECONDS
 FOR RUNNING OVERLAY 11.0
 (PRIMARY OVERLAY ONLY)

NICKORY-DICKORY SAYS 150.00 SECONDS
 FOR RUNNING OVERLAY 11.0
 INCLUDING ALL SECONDARY OVERLAYS
 FINISHED AT CLOCK TIME 12-20-10.6

CP TIME USED = 221.69 SECONDS
 PP TIME USED = 256.01 SECONDS
 SINCE JOB STARTED

NICKORY-DICKORY SAYS 5.40 SECONDS
 FOR RUNNING OVERLAY 10.2
 FINISHED AT CLOCK TIME 12-20-24.0

CP TIME USED = 222.40 SECONDS
 PP TIME USED = 257.27 SECONDS
 SINCE JOB STARTED

Figure D-51. Summary of Effects Caused by Assigned Post-Exposure Conditions

The satellite segments impinged by the plume for various combinations of thruster operation and plume geometry input from file DDATA are then calculated and printed. This facility can be used to identify the segments of the satellite most frequently exposed to plume impingement. The test case has two such demonstrations, and the results are shown in Figure D-53.

The specified test case thruster i. d. and plume configuration, input by NAMELIST/NAST4, are then used for calculation the i. d. 's of the segments impinged by the plume, to be used for calculating the plume exposure effects. These data are printed and identified as the base for further calculations, see Figure D-54.

The capability of coordinate transformation from thruster based coordinates is next demonstrated in the output, based on data input by file DDATA. This is an ancillary routine which requires specific inputs of the thruster coordinates; it does not form part of the calculation of plume impingement effects. The listing from this routine is shown in Figure D-55.

The next listing (Figure D-56) is that of the coordinates of the satellite segments which were identified as being impinged by the plume (Figure D-54). The coordinates are given in the thruster based coordinate system for use in selecting appropriate plume characteristics from KINCON AND MULTRAN.

This output terminates the run for the case where STPFLG = 1. The program is then rerun with STPFLG = 2 and with the plume characteristics supplied as a new version of file EDATA

RUN WITH STPF6G = 2 FOR CALCULATION OF EXPOSURE EFFECTS

The plume characteristics data used as EDATA input for this run are shown in Figure D-57.

D.6 REFERENCES

- D-1. K. B. Wiberg, "Subroutine LOCATN," Computer Programming for Chemists, W. A. Benjamin, Inc., New York (1965).
- D-2. J. H. Neilson and A. Gilchrist, Wear, Vol. 11, pp. 111-122 (1968).
- D-3. R. E. Trebal, Illustration 3.6 Mass Transfer Operations, McGraw Hill, 2nd Edition (1968).

SATELLITE SEGMENTS AFFECTED BY THE PLUME FROM THRUSTER NO. 2 WHEN P = 1.25 IC ACS,			
69	61	62	43
71	72	73	44
81	82	88	44
90	91	92	93
94	100	101	102
103	104		
PROJECTION SEGMENTS IMPINGED BY THRUSTER NO. 2 WHEN P = 1.250			
7301	7302	7303	7305
7306	7308		
A 01 INDICATES NO SEGMENTS ARE IMPINGED			
DEMONSTRATION CALCULATION			
SATELLITE SEGMENTS AFFECTED BY THE PLUME FROM THRUSTER NO. 1 WHEN P = .25 IC ACS,			
=1			
PROJECTION SEGMENTS IMPINGED BY THRUSTER NO. 1 WHEN P = .200			
=1			
A 01 INDICATES NO SEGMENTS ARE IMPINGED			
HICKORY=CICKORY SAYS 40.20 SECONDS FOR RUNNING OVERLAY(2,1) FINISHED AT CLOCK TIME 0-36-50.8			
CP TIME USED = 177.38 SECONDS PP TIME USED = 249.14 SECONDS SINCE JOB STARTED			
HICKORY=CICKORY SAYS 0.00 SECONDS FOR RUNNING OVERLAY(2,1) FINISHED AT CLOCK TIME 0-36-50.8			
CP TIME USED = 177.48 SECONDS PP TIME USED = 249.29 SECONDS SINCE JOB STARTED			

Figure D-53. Segments Impinged for Selected Thrusters and Plume Configurations

SATELLITE SEGMENTS AFFECTED BY THE PLUME
 FROM THRUSTER NO. 2 WHEN P = .14
 IC ACB,

PROJECTION SEGMENTS IMPINGED BY THRUSTER NO. 2 WHEN P = .142
 7302

* 02 INDICATES NO SEGMENTS ARE IMPINGED

WICKORY-DICKORY SAYS 1.20 SECONDS
 FOR RUNNING OVERLAYS
 FINISHED AT CLOCK TIME 0-37-0.0

CP TIME USED = 177.60 SECONDS
 PP TIME USED = 249.44 SECONDS
 SINCE JOB STARTED

OPERATING THRUSTER FOR SUBSEQUENT CALCULATION OF EFFECTS

Figure D-54. Segments Impinged by Plume

COORDINATE TRANSFORMATION

THRUSTOR SYSTEM TO SATELLITE SYSTEM

THRUSTOR NUMBER 3

AXIAL COORDINATE		RADIAL COORDINATE		ANGULAR COORDINATE	
ZZ (FT)	Y (FT)	RR (FT)	R (FT)	TME (RAD)	TMETA (RAD)
4.0700	7.6700	1.5000	3.3095	2.9870	-.1225
5.1000	8.7000	1.0000	1.1023	.0500	-.0240
1.7300	5.3300	1.0000	3.1000	3.1416	.0000

DEMONSTRATION CALCULATION

HICKORY-DICKORY SAYS 1.20 SECONDS
 FOR RUNNING OVERLAY(S.2)
 FINISHED AT CLOCK TIME 12-28-40.0

CP TIME USED = 220.49 SECONDS
 PP TIME USED = 263.65 SECONDS
 SINCE JOB STARTED

HICKORY-DICKORY SAYS 0.00 SECONDS
 FOR RUNNING OVERLAY(S.3)
 FINISHED AT CLOCK TIME 12-28-40.0

CP TIME USED = 224.53 SECONDS
 PP TIME USED = 264.17 SECONDS
 SINCE JOB STARTED

Figure D-55. Transformation of Coordinates, Thrustor Based to Satellite Based

THRUSTER-BASED COORDINATES
OF PLUME-IMPINGED SEGMENTS

FROM THRUSTER NO. 2 WHEN P# 114

SEG ID	AXIAL DIST Z (FT)	RADIAL DIST R (FT)	ANGULAR COCRD THE(RAD)
7302	3.00820	.71581	1.13957

* ANGLE FROM LINE JOINING
AXES OF SATELLITE AND THRUSTER

USE COORDINATES Z AND R IN DETERMINATION OF PLUME CHARACTERISTICS
FOR INPLT TO REPLACE DEFAULT VALUES C# EDATA = IAP#11

Figure D-56. Locations of Impinged Segments, Thruster Based Coordinate System

EDATA FROM KINCON/MULTRA

	1	2	31	32	33
1.0E-04	1.0E-04	1.0E-04	1.0E-04	1.0E-04	1.0E-04
0.0					
0.0					
0.0					
1.0E-04	1.0E-04	1.0E-04	1.0E-04	1.0E-04	1.0E-04
0.0					
0.0					
0.0					

Appendix E

**HYDRAZINE MONOPROPELLANT
ENGINE ANALYSIS**

N₂H₄

**A VAPORIZED MONOPROPELLANT AND INITIAL PULSE
MODEL COMPUTER PROGRAM**

CONTENTS

E. 1	INTRODUCTION	709
	E. 1. a Estimating Cold Start Transients	710
	E. 1. b Hot Starts	710
E. 2	ANALYSIS	710
	E. 2. a Scope	710
	E. 2. b Feed System	713
	E. 2. c Physical Properties	714
	E. 2. d Propellant Stream Distribution and Breakup	714
	E. 2. e Monopropellant Decomposition	715
	E. 2. f Testing for Cold Start Spikes	715
	E. 2. g Simulating Cold Start Transients and the Associated Contamination	716
	E. 2. h Chamber Calculations	717
E. 3	CATALYST BED BREAKUP LITERATURE SEARCH	717
	E. 3. a Types of Catalyst Losses	718
E. 4	MODEL DEVELOPMENT	718
E. 5	CELL LOADER STRUCTURE	718
E. 6	PROGRAM SUBROUTINES	720
	E. 6. a N2H4	720
	E. 6. b INLETM	720
	E. 6. c GCALC	720
	E. 6. d DERIVM	720
	E. 6. e PDERIV	720
	E. 6. f DERIVO	720
	E. 6. g OSTEP	720
	E. 6. h SPIKE	720
	E. 6. i TRAP	720
	E. 6. j RDPNCH	721
	E. 6. k OTPUT	721
	E. 6. l UNBAR	721
	E. 6. m Block Data	721

E. 7	PROGRAM USER'S MANUAL	721
	E. 7. a Inputs	721
	E. 7. b Steady-State Data	723
E. 8	CONTAM INTERFACING	724
E. 9	SAMPLE CASES	724
	E. 9. a Steady State Program	724
	E. 9. b Monopropellant Engine, Hot Catalyst Bed	724
	E. 9. c Monopropellant Engine, Cold Catalyst Bed	725
E. 10	REFERENCES	725

FIGURES

E-1a	Final Verification Test	711
E-1b	Variation of Chamber Pressure With Time	712

TABLES

E-1	Processes Needed for a Transient Monopropellant Contamination Model	719
------------	--	------------

Appendix E

HYDRAZINE MONOPROPELLANT ENGINE ANALYSIS

A Vaporized Monopropellant and Initial Pulse Model Computer Program

E. 1 INTRODUCTION

The current program N2H4 is used to model the contaminant production, i. e., the hydrazine droplets, hydrazine vapor, and ammonia from an N_2H_4 catalytic reactor.

The program N2H4 is a modification of the code written by Kesten, Smith, and Smith (Reference E-1) at the United Aircraft Research Laboratories (UARL). The UARL program was based on a model of the vapor phase region only. The modeling of a monopropellant engine considering only the vapor phase places its utility in the same state as models of a bipropellant system starting with premixed gases. That is, a very substantial amount of the phenomena critical to the process are excluded from the model.

MDAC has modified the UARL program with the addition of the following elements.

- a. Time-dependent inertial-resistive feed line modeling
- b. Time-dependent injection stream velocities
- c. The estimation of cold start spikes - from empirical UARL data
 1. Time to pressure rise
 2. Peak Pressure
 3. Propellant accumulation
 4. Contaminant discharge (associated with initial cold start transient)

The program with the current additions can be utilized for either cold or hot starts. The initial conditions which are given as input permits the program to determine whether the start will be smooth (hot) or rough (cold). If a smooth start is indicated, the program calculates the start and steady state operation in the manner programmed by Kesten. If a rough start is indicated, the program provides working information about the initial pressure surge, but it is incapable of following this with the subsequent

steady operation; it shuts down and prints out the characteristics of the rough start.

a. Estimating cold start transients

The following parameters are estimated by correlations of UARL data.

1. Time to pressure rise
2. Peak pressure
3. Contaminant discharges associated with cold start transient.

b. Hot starts

Hot starts and the subsequent steady operation may be simulated with the modified program to the same level of accuracy as in the original Kesten program. The program still contains the UARL assumption of "instantaneous evaporation" and hence overestimates the speed of hydrazine decomposition. The program cannot handle system instabilities.

The difficulty of application of the UARL model to real transient situations is illustrated in Figures E-1a and E-1b taken from References E-2 and E-3, respectively. In Figure E-1a attention is directed to the experimental curve of chamber pressure. Note (1) the time delay from opening of the propellant valve to the rise in pressure and (2) the shape of the pressure pulse. Compare this curve to the theoretical pressure pulse calculated via the UARL code as shown in Figure E-1b. The program does not properly simulate the experimental data for this case.

E. 2 ANALYSIS

a. Scope

The monopropellant subprogram at its current state must be considered quasi-steady-state. It is necessary to include a substantial subprogram to compute steady state conditions as inputs to the time dependent "main" program. This program uses numerical integration techniques centered around the catalyst bed reaction kinetics and associated mass and heat fluxes.

The initial flow of propellant is calculated beginning with the valve opening. The propellant is assumed to accelerate through inertial, resistive feed lines. The monopropellant is fed into the chamber through orifices which are direct extensions of the feed tubes. In the absence of experimental data, the injected streams are assumed to impact into the catalyst bed, with stream breakup parameters falling between a splash plate and a shower head model.

The injection velocity is such that in an unpacked chamber a droplet of liquid propellant would traverse a 2-inch-long chamber in the order of 1 millisecond.

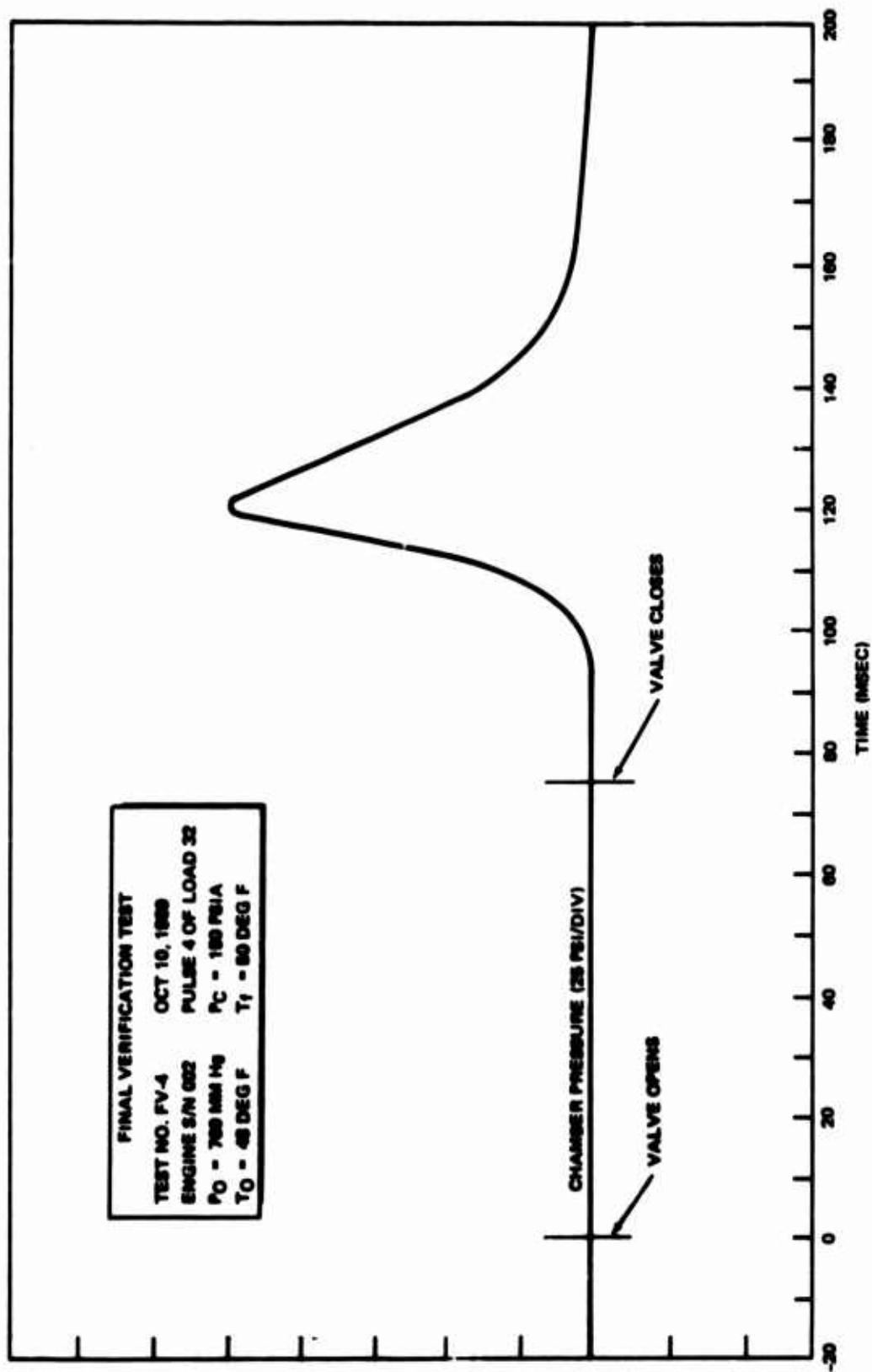


Figure E-1a. Final Verification Test

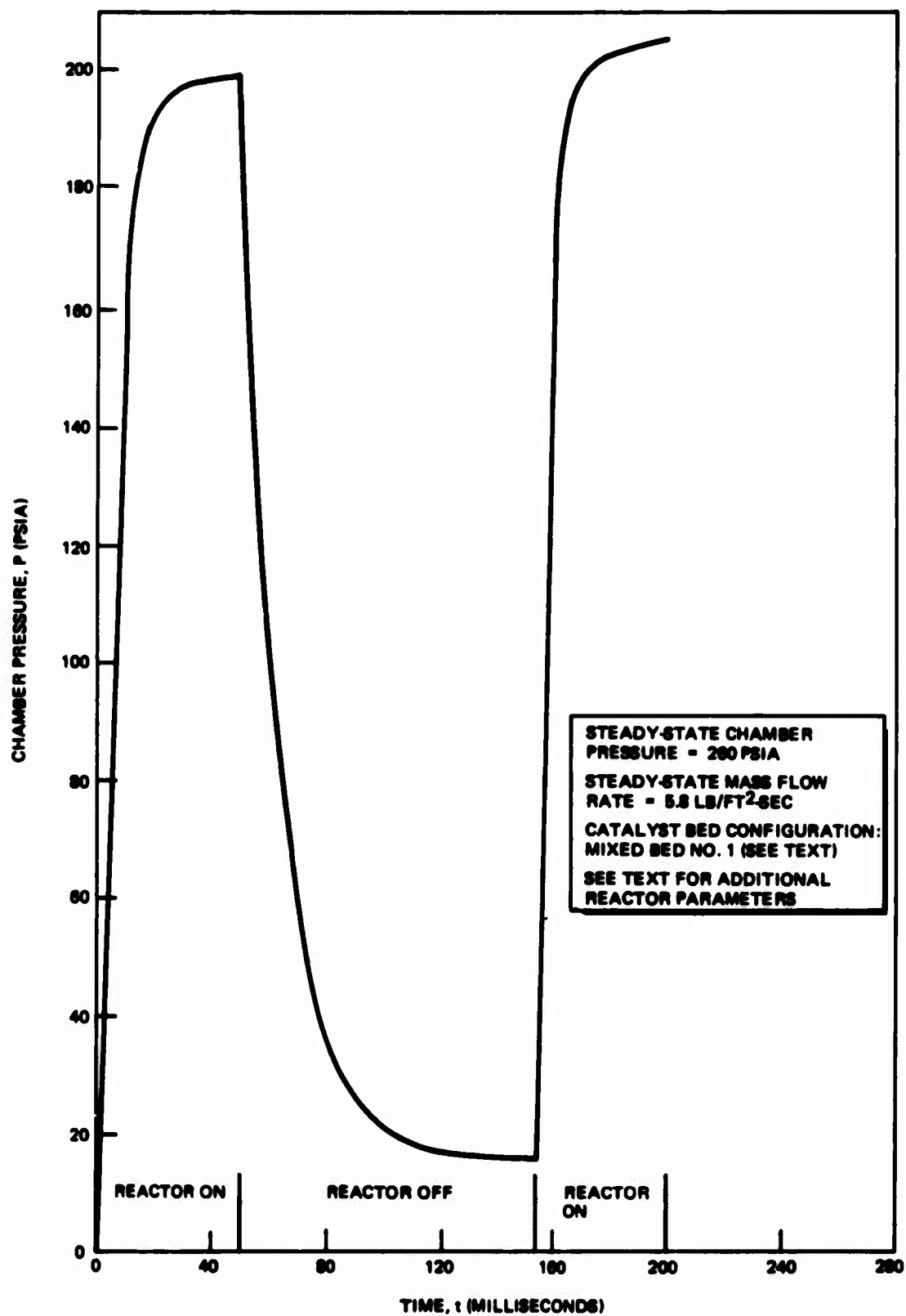


Figure E-1b. Variation of Chamber Pressure With Time

In the estimation of startups constrained by evaporation, assumptions most favorable to rapid evaporation were used, and evaporation limitations were used as the test for cold starts. The processes of distribution and evaporation of liquid hydrazine are considered crucial to a model capable of accurately predicting dynamic behavior in the cold start of a catalyst-pack hydrazine motor.

The hot vapor catalyst bed reactions used included both heterogenous and homogenous decomposition of hydrazine. Consideration was also given to the decomposition of ammonia and the heat transfer between catalyst particles and the surrounding gases.

The heat flux to the wall and atmosphere was treated in a lumped manner, with the chamber wall being considered an isothermal heat sink.

The mass flow of gas was calculated as a function of time and axial distance with the changes in composition and temperature based upon the catalyst bed processes controlling rates. There is no gas acceleration treatment in either the chamber or the throat, nor calculation of the pressure drop across the catalyst bed.

Gas composition profiles are calculated for each interval of model time. The gas composition at the throat section gives values for undecomposed hydrazine and ammonia expelled as contaminant. An infinite evaporation rate of hydrazine was assumed and this produced a tendency to underestimate the residual hydrazine and ammonia. In the case of cold starts, the MDAC modifications yield estimates of the liquid contamination attributable to the initial pressure spike.

The crucial limitations in the model are (1) lack of liquid phase dispersion and breakup, (2) lack of competition between wetted catalyst reactions and vapor-catalyst reactions, (3) lack of detailed evaporation processes, and (4) the chamber gas dynamics are treated as slug-flow i. e., gas velocity and composition differences only in the radial dimension. These deficiencies grossly limit the ability of this program to model start transients (particularly cold starts), pulse transients, or low frequency instabilities.

There is no capability in this program to treat situations in which the initial ambient pressure is less than the propellant vapor pressure. Low-temperature stops have been added by MDAC to avoid meaningless computer output in these regimes.

Performance estimation requires that the downstream end thermochemical data be manually combined with assumed motor parameters

b. Modeling the System Processes

1. Feed System

The feed systems are approximated with single lumped parameters representing the inertial and resistive aspects of the feed system, i. e.,

$$\frac{dq}{dt} = \frac{P_t - P_c - 1/2 \rho R q |q|}{\rho \Sigma L/A} \quad (E-1)$$

where

q = volumetric flow rate through line

P_t = tank pressure

P_c = chamber pressure

R = a coefficient representing steady flow pressure drop in the line

$\Sigma L/A$ = the summation of the segment length divided by cross-sectional area for the series of segments which make up the feed system.

A common design style of monopropellant feed system consists of a cluster of long small bore tubes which directly feed the injector orifices. The feed valves are treated as simple "off-on" devices, and at the present level of sophistication of the program it is felt that no further accuracy would be gained by use of a valve ramp function. The resistive aspects of the feed system was determined from experimental flow rates versus pressure drops for test engines. The current feed system will compute the line fill time for any degree of line void which is input to the program. The feed will follow the time history of the chamber and compute the flow rate as a function of time and chamber pressure, i.e.,

$$q = \phi(t, P_c). \quad (E-2)$$

This inertial/resistive feed system is the basis for computing inputs in the INLETM subroutine. It provides means of estimating the accumulation of propellants in the chamber in a cold start situation.

c. Physical Properties

In those segments of the program developed by UARL, physical properties of propellants and products were introduced in tabular form. The sections added at MDAC have approximated the physical properties of hydrazine and the associated chemical products as algebraic functions of temperature, using the relations developed by Priem (Reference E-4).

d. Propellant Stream Distribution and Breakup

The injection velocity of the hydrazine feed is computed. At present, there is no propellant spray distribution system in this model. However, propellant evaporation rates are used for testing the accumulation of propellants on cold start. The assumption that droplet sizes lie between shower head and splash ring values leads to the approximation:

$$D = 0.25 D_o, \quad (E-3)$$

where

D = median droplet diameter, and

D_o = orifice diameter of the injector

e. Monopropellant Decomposition

The monopropellant decomposition packed bed model was developed by Kesten (Reference E-1). The calculation is time and distance dependent but as stated earlier is based solely on the vapor phase condition and the mass, enthalpy, and species balances are treated in slug flow. The rates of mass and heat flux between the interstitial gases and the particle surfaces are treated as transport-process-controlled for the hydrazine catalysis. The much slower catalytic decomposition of ammonia is treated as controlled by chemical kinetics.

The UARL model assumes that the hydrazine vaporizes so rapidly that this process can be assumed to occur in zero axial distance. Subsequently, hydrazine decomposes exothermically either heterogeneously at the catalyst surface or homogeneously in the gas phase. The ammonia breaks up endothermically on the catalyst surfaces.

f. Testing for Cold Start Spikes

In the MDAC extension of the program, start spikes are assumed to be due to the accumulation of liquid hydrazine in the chamber, and are estimated by calculating the amount of evaporation of liquid hydrazine occurring in the time needed for it to pass through the fine particle stage of the catalyst bed. Arbitrarily it has been assumed that sufficient hydrazine must evaporate to yield the heat required to vaporize 50 percent of the propellant fed to the chamber in order to avoid a hard start. In practice, about 1/6 of the propellant must evaporate in the transit time through the catalyst fine zone to avoid triggering the cold start test calculation. The drop velocity is assumed to be equal to injection velocity.

The "flight" distance or "effective" bed path length is assumed to be twice the physical thickness of the fine particle zone, due to the tortuous path.

The evaporation of drops with forced convective heating has been investigated by Cramer (Reference E-5) and Webber (Reference E-6), and the mass rate of change is given by

$$\dot{M} = \left(\frac{\pi K}{c_p} \right) D \left[2.0 + 0.5 N_{R_e}^{0.5} \right] \ln \left[1 + \left(\frac{c_p}{\Delta H} \right) \Delta T \right] \quad (E-4)$$

where

\dot{M} = mass rate of change with time,

k = thermal conductivity of the boundary layer about the drop,

- c_p = specific heat at constant pressure,
 D = drop diameter,
 N_{R_e} = Reynolds number,
 ΔH = heat of vaporization,
 ΔT = difference between medium and droplet surface temperature.

The evaporation rates existing in a hydrazine catalyst bed at or near steady-state conditions will be slow compared to bipropellant engines. Under cold start conditions, evaporation rates are orders of magnitude slower. In the test for cold start flooding, the thermal conductivity, K , of the boundary layer around the hydrazine drop is taken to be that of air. This assumption is justified because normally cold starts occur when the temperature is less than 560°R , and in this case the hydrazine vapor never exceeds 5 percent of the mole fraction of the hydrazine-air mixture.

At the present time the program is limited to (1) a single hard-start transient with a cold catalyst bed or (2) hot start calculations assuming instantaneous vaporization of hydrazine. The temperature value of 560°R is an experimentally determined figure below which the engine will normally experience a hard start. Should the model later be expanded to cover multiple pulses or transient calculations leading to the equilibrium state, the following information should be noted:

When the temperature of the hydrazine is of the order of the boiling point, the correct value of K would be that given by Priem (Reference E-1) derived from the properties of hydrazine vapor. As the engine continues to heat, i. e., when the catalyst temperature reaches 1,700 to 1,900 $^\circ\text{R}$, this value will be too low, and the effect of decomposition products must be considered. The thermal decomposition products NH_3 , N_2 , and H_2 have a substantially higher value of K than N_2H_4 alone.

g. Simulating Cold Start Transients and the Associated Contamination

When the cold start test routine senses a condition indicating the accumulation of liquid hydrazine in the catalyst bed i. e., the hydrazine temperature is less than 560°R , the program computes the accumulation of liquid hydrazine by integrating the propellant feed rate from propellant entrance time to pulse cut off or pulse spike time, whichever comes first. Referring above to the feed system model, the volumetric feed rate, q , at time, t , is given by integrating Equation (E-1).

The accumulation of propellants in the cold chamber in preparation for a chug and spike is obtained by the summation

$$M_{\text{puddle}} = \rho \int_{t_1}^{t_2} q dt \quad (\text{E-5})$$

where:

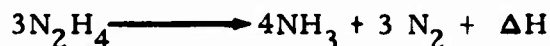
M_{puddle} = accumulating mass of liquid N_2H_4 ,

t_1 = time of first arrival of propellant to chamber after filling feed lines,

t_2 = time to propellant flow cutoff (either due to pulse cutoff or chamber pressure spike whichever is first).

The times to spiking and the peak pressure were fitted to empirical data gathered on a 5-lb and a 100-lb engine reported by UARL (Reference E-3). These data were collected over a temperature range from 495° to 560°R. The time to pressure rise was curve fitted as a function of temperature, and the peak pressure was fitted as a function of time to pressure rise.

The contaminants discharged from the chamber from a cold start surge are estimated by calculating the fraction of the puddle mass (M_{puddle}) which must react to generate enough gas and temperature to produce the pressure spike, assuming the reaction,



Gaseous ammonia will be blown out at the cold start spike. It is assumed that the upstream catalyst particles will have had the longest time to heat up. Much of the pressure surge will, therefore, be upstream of the bulk of the accumulating puddle mass, and consequently, an estimated one half of the residual unreacted puddle mass will be blown out as liquid N_2H_4 . That portion of the residual puddle mass which is not blown out of the chamber with the initial chug is assumed to evaporate and react (on a longer time scale) to produce a slower discharge of gaseous NH_3 and N_2 . Experimental monitoring of liquid hydrazine spray under these conditions has been reported at a recent Plume Interference Conference (Reference E-7).

If the chamber or propellants are warm enough to pass the cold start test routine, the calculation will proceed immediately to the UARL time-dependent hydrazine reactor program. This program has now been coupled with inertial/resistive feed system so that it more realistically reflects feed fluid dynamics. The program is, however, still without an integrated liquid-phase distribution and evaporation scheme.

h. Chamber Calculations

The UARL time-dependent program generates a time-axial distance calculating matrix for particle temperature, interstitial gas temperature, interstitial composition, and mass flow rates. An average chamber pressure is calculated for each time point. Gas velocity effects in the chamber are not estimated and the contraction region or throat are not treated.

E.3 CATALYST BED BREAKUP LITERATURE SEARCH

The effective-use life of the catalyst bed is the most frequent limiting factor for service life of a hydrazine monopropellant reactor. The bulk of

the literature on catalyst bed breakup does not mention or consider catalyst breakup debris in the rocket exhaust or as a plume effect. The recent conference on plume effects (Reference E-7) contains the only specific mention of catalyst particles in the rocket exhaust. The rest of the literature in this area deals only with loss of effectiveness of the catalyst bed.

a. Types of Catalyst Losses

A survey of the current literature indicates that catalyst loss is due to mechanical abrasion, systems vibration, and spalling due to thermal cycling. References E-8, E-9, E-10, and E-11 suggest a source of these phenomena are low-frequency instabilities; Reference E-15 quotes system support vibration; and references E-13 and E-15 also trace sources of the loss phenomena to high-velocity stream erosion and thermal shock.

The losses are correlated with the particular system design and mode of operation. References E-9 through E-12 and E-16 through E-18 cite various losses of the catalyst particle masses ranging from a low of 0.1 percent mass loss/min to values as high as 50 percent of the total mass during unstable runs.

References E-13 and E-19 indicate that there can be substantial function loss or drop in performance for monopropellant engines. The figures are put in the range of 50 to 67 percent over several minutes of run time.

The accumulation of damage from mechanical and thermal sources associated with transient phenomena appears far more important than the total run time. There is insufficient information presently available to weight particular conditions on an a priori basis.

The current state of the literature on catalyst breakup is relatively sparse in detailed information on catalyst particle breakup mechanics and loss exhaust rates. Consequently, the best approach at this time would be to develop a system by system statistical model built upon the available empirical data.

E.4 MODEL DEVELOPMENT

Table E-1 illustrates the various phenomena that were modeled in the original UARL program; those which have been added by MDAC; and those which are recommended for future inclusion.

E.5 CELL LOADER STRUCTURE

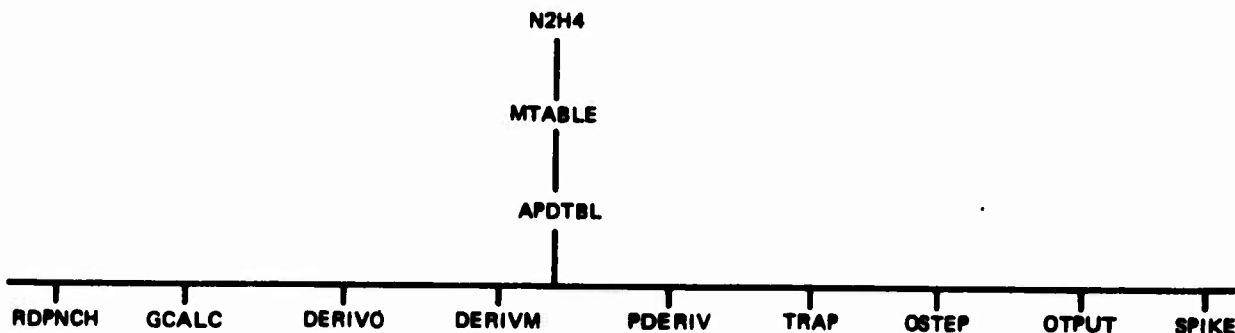


Table E-1
PROCESSES NEEDED FOR A TRANSIENT
MONOPROPELLANT CONTAMINATION MODEL

Process	U A R L	Added Current	Recommended Addition
Feed System			
Inertial/Resistive Flow	No	Yes	Yes
Dribble Start	No		Yes
Dribble Cutoff	No		Yes
Injection			
Stream Breakup Atomization	No	Yes	Yes
Low-Pressure Flashing	No		Yes
Chamber Gas Dynamics	No	No	Yes
Drop Mechanics			
Breakup	No		Yes
Acceleration	No		Yes
Evaporation	No	Yes	
Drop Size Distribution	No		Yes
Vacuum Start	No		Yes
Wall Effects			
Heat Transfer	Yes (isothermal)		Real Transients
Wetting			
Liquid Drag Breakoff	No		Yes
Evaporation	No		Yes
Decomposition of N_2H_4			
Liquid N_2H_4	Yes		
Vapor Heterogenous	Yes		
Homogeneous	Yes		
Decomposition of NH_3			
Vapor Heterogenous	Yes		
Homogenous	Yes		
Heat Exchange - Gas/Catalysts	Yes		
Calculation of Cold Start			
Conditions	No	Yes	
Contaminant	No	Yes	
Run Contaminants	No		Yes
Transient Operations	No ¹		Yes
Performance Calculations	No		Yes
Affects of Chamber			
Dynamics on Catalyst Bed	No	Yes ²	Yes
Dimensional Effects	No		Yes

¹ The program is based on steady state inputs and will not calculate a "true" transient operation.

² Only most primitive calculations have currently been made.

E.6 PROGRAM SUBROUTINES

a. N2H4

This is the main routine and contains all MDAC modifications. It controls program decision making for both continuous and pulse operation cases; it also calculates all times, temperatures, concentrations, pressures, etc., using values generated in the various subroutines. Input/output is controlled by this routine.

b. INLETM

This routine calculates the inlet conditions of the bed at the start of each time increment.

c. GCALC

This routine calculates the mass flow rate used in particle and interstitial equations.

d. DERIVM

This routine calculates certain functions used in the particle temperature and concentration equations.

e. PDERIV

This routine calculates partial derivatives of interstitial temperature and concentration with respect to axial position.

f. DERIVO

This routine is not used in the present version of N2H4, but is retained for possible future use with multiple pulse applications.

g. OSTEP

This routine interpolates to obtain temperatures, concentrations, etc., when the accumulated time has "overstepped" the duty cycle interrupt time. The routine is used only for pulse operation.

h. SPIKE

This routine is not used in the present version of N2H4, but is retained for possible future use with multiple-pulse applications.

i. TRAP

This routine is used to integrate certain functions using the trapezoidal rule.

j. RDPNCH

This routine is not used in the present version of N2H4, but is retained for possible future use with multiple-pulse applications.

k. OUTPUT

This routine retrieves and prints information stored on drum during the course of program calculations.

l. UNBAR

This is an interpolation routine used to obtain values from a table.

m. Block Data

Many of the arrays and parameters contained in the labeled common's are input via block data. In particular these data cover tables of:

1. Temperature vs Viscosity
2. Utilization Factor (log)
3. Temperature vs N₂H₄ Heat of Reaction
4. Temperature vs NH₃ Heat of Reaction
5. Temperature vs N₂H₄ Specific Heat
6. Temperature vs NH₃ Specific Heat
7. Temperature vs N₂ Specific Heat
8. Temperature vs H₂ Specific Heat
9. Vapor Pressure vs Temperature

E.7 PROGRAM USER'S MANUAL

a. Inputs

Input to N2H4 is carried out via the NAMELIST mode. However, it should be mentioned that certain of the original control parameters of the UARL code have been arbitrarily set within the MDAC program. This was done to make the former compatible with the modifications made in the latter. Certain of the parameter values are obtained from the steady state program, STDST, explained further on. The NAMELIST's and their corresponding parameter lists are as follows:

1. NAMELIST/ENGINE

Parameter	Identity
ZO	Axial distance to injector end (ft)
GOSS	Mass flow rate, obtained from STDST (lb/ft ²)
MBSS	Steady state average molecular weight obtained from STDST
PSS	Pressure chamber, steady state obtained from STDST (Psia)
TSS	Steady state downstream temperature obtained from STDST (°R)
TVAP	Vaporization temperature obtained from STDST (°R)

HIV	Enthalpy at liquid-vapor/vapor interface (Btu/lbm)
F	Distributed feed rate (lbm/ft ³ -sec)
HF	Enthalpy of the feed (Btu/lbm)
TF	not used in present calculation
ENMX1,	
ENMX2,	
ENMX3	not used in current calculation
PF	pressure of propellant feed (psia)
ZEND	not used in present calculation
VC	volume of chamber (free volume)
AC	Cross-sectional area, of reactor (ft ²)
MW	chamber wall thermal mass (lbm)
CW	Chamber wall specific heat (Btu/lbm-°R)
AW	Chamber wall total surface area (ft ²)
TA	Ambient temperature in chamber (°R)
HA	Forced convection heat transfer coefficient (Btu/ft ² -sec-°R)
HA1	Natural convection heat transfer coefficient (Btu/ft ² -sec-°R 1.25)
HA2	Radiative heat transfer coefficient (Btu/ft ² -sec-°R ⁴)
TPI	Initial catalyst temperature (°R)
PCI	Initial chamber pressure (psia)
CPHYI	Initial hydrazine concentration in the catalyst (lbm/ft ³)
CPAMI	Initial ammonia concentration in catalyst (lbm/ft ³)
CIAMI	Initial interstitial ammonia concentration (lbm/ft ³)
CPN2I	Initial nitrogen concentration in the catalyst (lbm/ft ³)
CIN2I	Initial interstitial nitrogen concentration (lbm/ft ³)
CPH2I	Initial hydrogen concentration in catalyst (lbm/ft ³)
CIH2I	Initial interstitial hydrogen concentration (lbm/ft ³)
AG	Acceleration due to gravity (ft/sec ²)
DORIF	Diameter of orifice (ft)
ORINO	Number of orifices (No. /ft ²)
FDLINL	Feedline length (ft)
FULFR	Fraction of feed line full at start
TLIQ	Temperature of liquid hdyrazine (°R)
TPULS	Time of pulse signal (sec)
FINZON	Thickness of fine particle bed (ft)
CIHYI	Initial Interstitial hydrazine concentration (lbm/ft ³)

2. NAMELIST/CATALYST

Parameter	Identity
M	Time mesh dimension
N	Axial distance mesh dimension
NOFZ	Number of axial stations used in input tables
Z(75)	Axial stations in total solution mesh
Z1(37)	Axial stations used in table inputs
RADT(37)	Catalyst particle radii (ft)
SURFT(37)	Total external catalyst particle surface areas/unit Volume of catalyst bed (ft ² /ft ³)
VOIDT(37)	Interparticle void fractions

3. NAMELIST/CONTROL

Parameter	Identity
DRUM	Fortran logical unit designator (default value = 11)
MPRNT	Print indicator (default value = 0 gives summary printout, MPRNT = 1 gives much more detailed printout)
NPASS	total number of passes through mesh defined by M and N
DELT(20)	Time increments between each NPAS integration (sec)

b. Steady-State Data

The program STDST supplies the needed steady state input values required by the Monopropellant Engine program N2H4. STDST has not been incorporated into CONTAM (i.e., driven by the EXEC program) because there is only one set of equilibrium conditions for a given engine design, and once these values are determined, any transient problem may be solved using these steady state conditions.

STDST, except for the conversion to NAMELIST input, is the UARL Steady State one-dimensional program (Reference E-20), and the reader is directed to the reference for the details of the program.

It should be noted that this program does not lend itself to overlaying in that many subroutines continually call upon other subroutines during a run. Consequently, STDST has been supplied in a stand-alone non-cell loader program, and requires a memory capacity of 150,000 words on a CDC 6500 computer.

The input to the program is given via the NAMELIST/STEADY/. The variables in this list are as follows:

NCASE	Number of data cases with each run, use NCASE = 1
NOFZ	Number of axial stations used in the table inputs
ZO	Axial distance to the end of buried injector (ft)
GO	Inlet mass flow rate (lbm/ft ² -sec)
FC	Rate of feed of hydrazine from buried injectors (lbm/ft ³ -sec)
HF	Enthalpy of liquid hydrazine entering catalyst bed (btu/lbm) set to zero for cold flow
TF	Temperature of liquid hydrazine entering bed (°R)
ENMX1	Constant used to determine the size of axial station increments in the liquid region. It equals 200. Increasing this number would result in a decrease in size of axial station increments (and an increase in computer run time).
ENMX2	Constant used to determine the size of axial station increments in the liquid-vapor region. It equals 40. Increasing this number would result in a decrease in size of axial station increments (and an increase in computer run time).
ENMX3	Constant used to determine the size of axial station increments in the vapor region. It equals 80. Increasing this number would result in a decrease in size of axial station increments (and an increase in computer run time).

PRES	Inlet chamber pressure (psia)
ZEND	Catalytic bed length (ft)
ZPOS	Number of independent variables in tables
RADII	Catalyst particle radius (ft)
SURFAR	Catalyst particle surface area per unit of volume of bed (ft ² /ft ³)
VOIDFR	Interparticle void fraction

E.8 CONTAM INTERFACING

The monopropellant engine model is not nearly to the same level of development as that of the bipropellant. Consequently, in determining the inputs for the MULTRAN portion of CONTAM certain assumptions and approximations must be made. The following list is a suggested NAMELIST input for the MULTRAN portion of CONTAM when the MDAC modifications are put to use in the program N2H4.

```
$DATA CAPN= 0.6 , CPG=18, 150 , CPL=S. A. B.* , CPS=S. A. B. , GAMMA=
1.206, GMGO=4.24E-5 , HPL=S. A. B. , HPS= S. A. B. , PR=0.7 , RCAP=
3102
```

*Same as bipropellant

E.9 SAMPLE CASES

The sample cases shown are those used by Kesten, et al (References E-1 and E-20). The steady state program, STDST, is illustrated first, and then the program N2H4. Two examples of N2H4 are shown; a "hot" catalyst bed run, the original Kesten program; and the "cold" bed or the program with the MDAC modifications.

a. Steady State Program

The following list identifies the required STDST outputs and their corresponding name for the N2H4 program input.

N2H4 Input	STDST Output
GOSS	GO in the INPUT CONSTANTS
MBSS	MBAR printed out at end of output
PSS	last PRES printed out
TSS	last TEMP printed out.

b. Monopropellant Engine, Hot catalyst Bed

The term "hot catalyst bed" refers to the cases when the parameters TF (feed temperature), TA (ambient temperature), TPI (bed particle temperature), and TLIQ (liquid fuel temperature) are all greater than 561°R.

The output has been edited and during a run considerably more printout will be obtained. With the hot bed there are no droplets produced. If the user wishes to make a contamination run for the hydrazine, ammonia,

nitrogen, and hydrogen vapors, the last value on each of the interstitial lists should be used. In the case shown these values appear just before the "completion of pass 1" message.

The figures given are in units of lbm/ft³. The droplet sizes should be set to vanishingly small, and the rest of CONTAM will calculate for the vapor phase only.

c. Monopropellant Engine, Cold Catalyst Bed

When temperature parameters listed above fall below 560°R, the Monopropellant Engine program will use the MDAC modifications. In this case the output is much simplified. The time required to reach the pressure peak of the start transient is shown, the pressure obtained, the amounts of liquid hydrazine and ammonia produced, and the amount of ammonia vapor produced.

At the present time there is some evidence (Reference E-7) to suggest that very small droplets are formed during a cold start transient. Since the Monopropellant program has no capability to calculate droplet sizes, it is recommended that the diameter of 20 microns be assumed for the droplets.

E.10 REFERENCES

- E-1 D. B. Smith, E. J. Smith, and A. J. Kesten. Analytic Study of Catalytic Reactors for Hydrazine Decomposition, Computer Program Manual, Transient Model. United Aircraft Research Laboratories Report H910481-37, May 1969
- E-2 A. V. Kesten. Analytic Study of Catalytic Reactors for Hydrazine Decomposition Third Annual Progress Report. United Aircraft Research Laboratories Report N910461-38, May 1969
- E-3 J. J. Sangiovanni and A. J. Kesten. Study of Hydrazine Reactor Vacuum Start Characteristics First Annual Progress Report. United Aircraft Research Laboratories Report H910758
- E-4 R. J. Priem. Propellant Vaporization as a Criterion for Rocket Engine Design; Calculations of Chamber Length to Vaporize Various Propellants. NACA TN 3883, September 1958
- E-5 F. B. Cramer and P. Baker. Combustion Processes in a Bipropellant Liquid Rocket Engine, Multi-Tech, Inc. JPL Report No. 900, January 1967
- E-6 R. J. Hoffman, W. D. English, R. G. Oeding, and W. T. Webber. Plume Contamination Effects Prediction (McDonnell Douglas Astronautics Company). AF RPL TR 71-109, December 1971
- E-7 Plume Interference Assessment and Mitigation Conference. Calspan Corporation, March 6, 1973
- E-8 Catalyst Durability Test Report. Rocket Research Corporation Report 66-R-61, June 1966

- E-9 Development of Design and Scaling Criteria for Monopropellant Hydrazine Reactors Employing Shell 405 Spontaneous. Rocket Research Corporation. RRC 66-R-76
- E-10 H. Greer. The Aerospace Corporation Shell 405 Catalyst Evaluation Program. Report No. TOR 0066(5305)-2, January 1970 AD 865376
- E-11 W. L. Owens. "A Combustion Stability Analysis for Catalytic Monopropellant Thrustors." AIAA Paper 71-701 AIAA 7th Propulsion Joint Specialist Conference. June 1971
- E-12 H. Greer. An Investigation of the First Pulse Characteristics of Monopropellant Hydrazine Reactors. Aerospace Corporation Report No. TR-0066(5305)-1, July 1969, AD 859-733.
- E-13 H. Greer. Performance Drop off in a Monopropellant Hydrazine Reactor. Aerospace Corporation Report No. TOR-0066(5305), May 1970 AD 869-982
- E-14 B. W. Schmitz and W. W. Wilson. Long Life Monopropellant Hydrazine Engine Development. Rocket Reserve Report RRC-71-R-257, September 1971, AD 731-287
- E-15 D. C. Morrissey, et al. "Development of the Titan III Transtage ALS Hydrazine Monopropellant Rocket Engine Modules." AIAA paper 69-422, AIAA 5th Propulsion Joint Specialist Conference, June 1969
- E-16 L. B. Katter and D. A. Williams. Development of Long Life Catalyst Beds for Monopropellant Hydrazine Reactors. Rocket Research Corporation Report 69-R 178, January 1969
- E-17 S. M. King, P. C. Max, and D. Taylor. The Aerospace Corporation Shell 405 Catalyst Evaluation Program Vol. 1 Physical Properties. Aerospace Corporation Report No. TR 0066(5210-10)-4-Vol, August 1969, AD 858913
- E-18 L. Kusak, R. A. Dickerson, and R. N. Gurnitz. "Long Life Firings of a Catalytic Reactor for Monopropellant Hydrazine." AIAA Paper 72-1045, AIAA/SAE 8th Joint Propulsion Specialist Conference, November 1972
- E-19 R. A. Carlson and W. Baker. Space Environment Operation of Experimental Hydrazine Reactors. Final Report April 1967, TRW Systems Group Report 4712, 4-67-28
- E-20. E. J. Smith, D. B. Smith, and A. S. Kesten. Analytical Study of Catalytic Reactors for Hydrazine Decomposition; one and two-Dimensional Steady-State Programs. United Aircraft Research Laboratories Report G 910461-30, August 1968

TEST RUN OF STEADY STATE PROGRAM BY KRYVEN, APRIL 1973

MP	ML	MV	TF	TVAP	CPL	PRESSURE	MP	PC	GO
0.	2.12020E-02	7.12970E-02	9.30000E-02	8.20000E-02	7.32000E-01	1.00000E-02	1.00000E-01	1.	3.00000E-00
R	ALPHA3	CEM	DIF3	DIF4	WM4	MP3	WM2	MP1	ZMP
1.07300E-01	2.14000E-10	3.30000E-04	1.70000E-04	9.50000E-05	3.20400E-01	1.70320E-01	2.00100E-01	2.01000E-00	2.90000E-01
ASH	BOM	ALPHA1	ALPHA2	M1	M2	K3	EPHX1	EPHX2	GMX3
2.90000E-03	5.00000E-01	1.00000E-10	1.00000E-11	1.00000E-00	1.00000E-00	-1.00000E-00	2.00000E-02	4.00000E-01	0.00000E-01

0.
20

2 VS A TABLE

0.	5.30000E-03	1.13000E-02	0.	1.00000E-00	2.00000E-01	0.	0.	0.	0.
1.11900E-01	1.25000E-01	1.30100E-01	1.92700E-01	1.00000E-02	4.39000E-02	5.75000E-02	7.11000E-02	0.47000E-02	9.03000E-02
1.00000E-03	1.00000E-03	1.00000E-03	1.00000E-03	1.00000E-03	1.00000E-03	1.00000E-03	1.00000E-03	1.00000E-03	1.00000E-03
0.40000E-03	0.40000E-03	0.40000E-03	0.40000E-03	0.40000E-03	0.40000E-03	0.40000E-03	0.40000E-03	0.40000E-03	0.40000E-03

2 VS AP TABLE

0.	5.30000E-03	1.13000E-02	0.	1.00000E-00	2.00000E-01	0.	0.	0.	0.
1.11900E-01	1.25000E-01	1.30100E-01	1.92700E-01	1.00000E-02	4.39000E-02	5.75000E-02	7.11000E-02	0.47000E-02	9.03000E-02
2.10000E-03	2.10000E-03	2.10000E-03	2.10000E-03	2.10000E-03	2.10000E-03	2.10000E-03	2.10000E-03	2.10000E-03	2.10000E-03
0.40000E-03	0.40000E-03	0.40000E-03	0.40000E-03	0.40000E-03	0.40000E-03	0.40000E-03	0.40000E-03	0.40000E-03	0.40000E-03

2 VS DELTA TABLE

0.	5.30000E-03	1.13000E-02	0.	1.00000E-00	2.00000E-01	0.	0.	0.	0.
1.11900E-01	1.25000E-01	1.30100E-01	1.92700E-01	1.00000E-02	4.39000E-02	5.75000E-02	7.11000E-02	0.47000E-02	9.03000E-02
3.40000E-01	3.40000E-01	3.40000E-01	3.40000E-01	3.40000E-01	3.40000E-01	3.40000E-01	3.40000E-01	3.40000E-01	3.40000E-01
0.40000E-03	0.40000E-03	0.40000E-03	0.40000E-03	0.40000E-03	0.40000E-03	0.40000E-03	0.40000E-03	0.40000E-03	0.40000E-03

[illegible]

STATEADY

```

NCASE = 1.
NPFZ = 20.
Z0 = 0.0.
00 = 0.3E+01.
PC = 0.0.
HP = 0.0.
TF = 0.53E+03.
ENHX1 = 0.2E+03.
ENHX2 = 0.0E+02.
ENHX3 = 0.0E+02.
PRES = 0.1E+03.
ZEND = 0.25E+00.
ZPOB = 0.0. 0.55E-02. 0.11E-01. 0.107E-01. 0.108E-01. 0.439E-01.
0.575E-01. 0.711E-01. 0.07E-01. 0.903E-01. 0.1119E+00.
0.1255E+00. 0.1391E+00. 0.1527E+00. 0.1663E+00. 0.1799E+00.
0.1935E+00. 0.2207E+00. 0.2343E+00. 0.25E+00. 0.0. 0.0.
RADI = 0.1E-02. 0.1E-02. 0.1E-02. 0.1E-02. 0.64E-02. 0.64E-02.
0.64E-02. 0.64E-02. 0.64E-02. 0.64E-02. 0.64E-02. 0.64E-02.
0.64E-02. 0.64E-02. 0.64E-02. 0.64E-02. 0.64E-02. 0.64E-02.
0.64E-02. 0.64E-02. 0.0. 0.0. 0.0.
SURFAR = 0.21E+04. 0.21E+04. 0.21E+04. 0.21E+04. 0.33E+03. 0.33E+03.
0.33E+03. 0.33E+03. 0.33E+03. 0.33E+03. 0.33E+03. 0.33E+03.
0.33E+03. 0.33E+03. 0.33E+03. 0.33E+03. 0.33E+03. 0.33E+03.
0.33E+03. 0.33E+03. 0.0. 0.0. 0.0.
VOIDPR = 0.34E+00. 0.34E+00. 0.34E+00. 0.34E+00. 0.34E+00. 0.34E+00.
0.34E+00. 0.34E+00. 0.34E+00. 0.34E+00. 0.34E+00. 0.34E+00.
0.34E+00. 0.34E+00. 0.34E+00. 0.34E+00. 0.34E+00. 0.34E+00.
0.34E+00. 0.34E+00. 0.0. 0.0. 0.0.

```

SEND

ENTERING LIQUID REGION							
Z	TEMP	M	DMDZ	Z	TEMP	M	DMDZ
0.	5.30000E+02	0.	3.77509E+04				
	TEMP	M	DMDZ				
2.512030E+04	5.420397E+02	9.40405E+00	5.30919E+04				
	TEMP	M	DMDZ				
4.270030E+04	5.59010E+02	1.09010E+01	9.43200E+04				
	TEMP	M	DMDZ				
5.272010E+04	5.607015E+02	2.04349E+01	1.437071E+05				
	TEMP	M	DMDZ				
5.931290E+04	5.816947E+02	3.79029E+01	2.211349E+05				
	TEMP	M	DMDZ				
6.359235E+04	5.940015E+02	4.730905E+01	3.225400E+05				
	TEMP	M	DMDZ				
6.692677E+04	6.075019E+02	5.682440E+01	4.077077E+05				
	TEMP	M	DMDZ				
6.884974E+04	6.203999E+02	6.627024E+01	6.753092E+05				
	TEMP	M	DMDZ				
6.994075E+04	6.332034E+02	7.572730E+01	9.621124E+05				
	TEMP	M	DMDZ				
7.092661E+04	6.461049E+02	8.517100E+01	1.315590E+06				
	TEMP	M	DMDZ				
7.164413E+04	6.590392E+02	9.441152E+01	1.824710E+06				
	TEMP	M	DMDZ				
7.216112E+04	6.719074E+02	1.040465E+02	2.424999E+06				
	TEMP	M	DMDZ				
7.255000E+04	6.847091E+02	1.134769E+02	3.160479E+06				
	TEMP	M	DMDZ				
7.284779E+04	6.976240E+02	1.239629E+02	4.130432E+06				
	TEMP	M	DMDZ				
7.307904E+04	7.104790E+02	1.323234E+02	5.779910E+06				
	TEMP	M	DMDZ				

7.323070E+04	7.233105E+02	1.417390E+02	7.914132E+06
Z	TEMP	M	ENDZ
7.330402E+04	7.301530E+02	1.911520E+02	9.332052E+06
Z	TEMP	M	ENDZ
7.300400E+04	7.400000E+02	1.005627E+02	1.176000E+07
Z	TEMP	M	ENDZ
7.354402E+04	7.610220E+02	1.009710E+02	1.910097E+07
Z	TEMP	M	ENDZ
7.360070E+04	7.740229E+02	1.793795E+02	1.077941E+07
Z	TEMP	M	ENDZ
7.360005E+04	7.074010E+02	1.007895E+02	2.293013E+07
Z	TEMP	M	ENDZ
7.360059E+04	0.003002E+02	1.001900E+02	2.099047E+07
Z	TEMP	M	ENDZ
7.373343E+04	0.131327E+02	2.079920E+02	3.420109E+07
Z	TEMP	M	ENDZ
7.374011E+04	0.200000E+02	2.120000E+02	3.034039E+07

ENTERTAIN LIQUID-VAPOR REGION

Z	TEMP	H	MPV
7.13772E-04	0.20000E+02	2.59630E+02	9.34717E+02
7.30992E-04	0.20000E+02	3.06632E+02	1.06043E+01
7.48170E-04	0.20000E+02	3.53635E+02	2.00415E+01
7.65348E-04	0.20000E+02	4.00637E+02	3.73667E+01
7.82526E-04	0.20000E+02	4.47639E+02	4.67358E+01
7.99704E-04	0.20000E+02	4.94641E+02	5.60305E+01
8.16882E-04	0.20000E+02	5.41643E+02	6.54322E+01
8.34060E-04	0.20000E+02	5.88645E+02	7.47773E+01
8.51238E-04	0.20000E+02	6.35647E+02	8.41245E+01
8.68416E-04	0.20000E+02	6.82649E+02	9.34717E+01
8.85594E-04	0.20000E+02	7.29651E+02	1.00000E+00

ENTERING VAPOR REGION

2
7.90041742E+04 0.20000000E+02 1.00000000E+02 7.15470000E+02 3.13799194E+03 C1 C2 C3 C4
TEMP PRES M 4.30000000E+02 9.33000000E+02 1.03433000E+01

MFRAC1 MFRAC2 MFRAC3 MFRAC4 FRAC3D
1.37026024E-01 1.37026024E-01 2.75623040E-01 4.40023095E-01 -3.95271300E-15

2
9.07424074E+04 0.00450000E+02 0.00000000E+02 7.38979111E+02 3.29001030E+03 C1 C2 C3 C4
TEMP PRES M 4.33340000E+02 9.00400000E+02 1.47394200E+01

MFRAC1 MFRAC2 MFRAC3 MFRAC4 FRAC3D
1.50410040E-01 1.44297200E-01 2.76321000E-01 4.20932100E-01 2.10705390E-02

2
1.00000000E+04 0.13507000E+02 0.00000000E+02 7.02400000E+02 3.33700100E+03 C1 C2 C3 C4
TEMP PRES M 4.27007010E+02 9.00000000E+02 1.33001070E+01

MFRAC1 MFRAC2 MFRAC3 MFRAC4 FRAC3D
1.01979000E-01 1.50340700E-01 2.77437115E-01 4.10230090E-01 4.02330100E-02

2
1.22700240E+04 0.00000000E+02 0.00000000E+02 7.09043000E+02 3.30030170E+03 C1 C2 C3 C4
TEMP PRES M 4.22002400E+02 9.00000000E+02 1.23022270E+01

MFRAC1 MFRAC2 MFRAC3 MFRAC4 FRAC3D
1.78480190E-01 1.59062770E-01 2.70000015E-01 3.92000700E-01 5.97497000E-02

2
1.30212000E+04 0.00000000E+02 0.00000000E+02 8.00420100E+02 3.30700100E+03 C1 C2 C3 C4
TEMP PRES M 4.13027000E+02 9.13027000E+02 1.11100000E+01

MFRAC1 MFRAC2 MFRAC3 MFRAC4 FRAC3D
1.02102100E-01 1.61000410E-01 2.00020010E-01 3.70000000E-01 0.91027000E-02

2 1.00000787E-03 1.04100799E+03 PRES 0.00077100E-01 0.32010012E+02 3.40801374E+03 C1 C2 C3 C4
4.29000000E+02 4.11000000E+02 4.29000000E+02 4.29000000E+02

MFRAC1 MFRAC2 MFRAC3 MFRAC4 FRAC3D
1.91093703E-01 1.64864405E-01 2.02070215E-01 3.99771076E-01 0.06033201E-02

2 1.73010137E-03 1.00266790E+03 PRES 0.00000041E-01 0.54400470E+02 3.40001499E+03 C1 C2 C3 C4
4.00000000E+02 4.11000000E+02 4.11000000E+02 4.11000000E+02

MFRAC1 MFRAC2 MFRAC3 MFRAC4 FRAC3D
1.99317693E-01 1.70065190E-01 2.05225212E-01 3.44491049E-01 9.04103099E-02

2 1.90000000E-03 1.12000000E+03 PRES 0.00000000E-01 0.70000000E+02 3.40000000E+03 C1 C2 C3 C4
3.99000000E+02 3.99000000E+02 3.99000000E+02 3.99000000E+02

MFRAC1 MFRAC2 MFRAC3 MFRAC4 FRAC3D
2.07202500E-01 1.79951000E-01 2.0730304E-01 3.39664198E-01 9.94109537E-02

2 1.00000000E-03 1.10000000E+03 PRES 0.00000000E-01 0.80000000E+02 3.40000000E+03 C1 C2 C3 C4
3.99000000E+02 3.99000000E+02 3.99000000E+02 3.99000000E+02

MFRAC1 MFRAC2 MFRAC3 MFRAC4 FRAC3D
2.14000000E-01 1.79041040E-01 2.90000000E-01 3.13430700E-01 1.07130057E-01

2 1.20000000E-03 1.20000000E+03 PRES 0.00000000E-01 0.80000000E+02 3.40000000E+03 C1 C2 C3 C4
3.99000000E+02 3.99000000E+02 3.99000000E+02 3.99000000E+02

MFRAC1 MFRAC2 MFRAC3 MFRAC4 FRAC3D
2.21739405E-01 1.00010037E-01 2.9299337E-01 3.0166722E-01 1.14104230E-01

2 1.00000000E-03 1.24000000E+03 PRES 0.00000000E-01 0.90000000E+02 3.40000000E+03 C1 C2 C3 C4
3.99000000E+02 3.99000000E+02 3.99000000E+02 3.99000000E+02

MFRAC1 MFRAC2 MFRAC3 MFRAC4 MFRAC5D
2.20906707E-01 1.00090000E-01 2.95132375E-01 2.00204399E-01 1.20042329E-01

Z
TEMP PRES C1 C2 C3 C4
1.2023090E+03 9.99740300E+01 9.74010070E+02 3.36007907E+03 3.0109210E+02 3.00010010E+02 0.20047399E+02

MFRAC1 MFRAC2 MFRAC3 MFRAC4 MFRAC5D
2.35194800E-01 1.91004323E-01 2.97027927E-01 2.79233200E-01 1.26674000E-01

Z
TEMP PRES C1 C2 C3 C4
1.32090070E+03 9.90279000E+01 9.9700090E+02 3.3930710E+03 3.7700002E+02 3.9104970E+02 9.70234400E+02

MFRAC1 MFRAC2 MFRAC3 MFRAC4 MFRAC5D
2.4100040E-01 1.99017001E-01 3.00034215E-01 2.02010401E-01 1.30402300E-01

Z
TEMP PRES C1 C2 C3 C4
1.3902001E+03 9.99700000E+01 1.0211700E+03 3.34000000E+03 3.7900000E+02 3.4100000E+02 9.3900000E+02

MFRAC1 MFRAC2 MFRAC3 MFRAC4 MFRAC5D
2.4703010E-01 1.9907272E-01 3.0203070E-01 2.9000000E-01 1.39000010E-01

Z
TEMP PRES C1 C2 C3 C4
1.00710700E+03 9.99210000E+01 1.00470000E+03 3.30000000E+03 3.0000000E+02 3.3077000E+02 4.9000000E+02

MFRAC1 MFRAC2 MFRAC3 MFRAC4 MFRAC5D
2.5422101E-01 2.0200000E-01 3.0407227E-01 2.9700000E-01 1.4330000E-01

Z
TEMP PRES C1 C2 C3 C4
1.0000000E+03 9.99000000E+01 1.00000000E+03 3.31000000E+03 3.0000000E+02 3.3077000E+02 4.9000000E+02

MFRAC1 MFRAC2 MFRAC3 MFRAC4 MFRAC5D
2.6043007E-01 2.0000000E-01 3.0047010E-01 2.9000000E-01 1.4000000E-01

Z
TEMP
PRES
M
C1
C2
C3
C4
8.7958488E-03 1.4721027E-03 9.0000000E-01 1.0020722E+03 3.3020720E+03 3.0220720E+02 3.220041070E+02 4.2192297E+02

MFRAC1 MFRAC2 MFRAC3 MFRAC4 FRAC3D
2.0664919E-01 8.1047400E-01 3.00001207E-01 2.1427407E-01 1.5399070E-01

Z
TEMP
PRES
M
C1
C2
C3
C4
4.00500477E-03 1.5002910E+03 9.0022900E-01 1.1337400E+03 3.0024337E+03 3.50000317E+02 3.1034200E+02 3.00003100E+02

MFRAC1 MFRAC2 MFRAC3 MFRAC4 FRAC3D
2.72001047E-01 8.14020010E-01 3.1034110E-01 2.0275100E-01 1.5041424E-01

Z
TEMP
PRES
M
C1
C2
C3
C4
4.80005002E-03 1.54015410E+03 9.0024000E-01 1.1304400E+03 3.00330010E+03 3.50000317E+02 3.0000730E+02 3.3700000E+02

MFRAC1 MFRAC2 MFRAC3 MFRAC4 FRAC3D
2.79170210E-01 2.17003300E-01 3.1102375E-01 1.9140247E-01 1.0497923E-01

Z
TEMP
PRES
M
C1
C2
C3
C4
4.8479147E-03 1.0007000E+03 9.01500110E-01 1.1031741E+03 3.07500200E+03 3.50000317E+02 3.0000000E+02 3.0000000E+02

MFRAC1 MFRAC2 MFRAC3 MFRAC4 FRAC3D
2.05540004E-01 2.21007507E-01 3.13170621E-01 1.0020000E-01 1.70735543E-01

Z
TEMP
PRES
M
C1
C2
C3
C4
4.04300732E-03 1.01020011E+03 9.0000000E-01 1.1000200E+03 3.0700410E+03 3.4000047E+02 2.07040030E+02 3.0100000E+02

MFRAC1 MFRAC2 MFRAC3 MFRAC4 FRAC3D
2.0200370E-01 2.30070007E-01 3.1422440E-01 1.0015373E-01 1.70735543E-01

Z
TEMP
PRES
M
C1
C2
C3
C4
5.19740041E-03 1.0004170E+03 9.00041110E-01 1.2300070E+03 3.0000000E+03 3.4000047E+02 2.0000000E+02 3.7000000E+02

MFRAC1 MFRAC2 MFRAC3 MFRAC4 FRAC3D
2.980705E-01 2.280953E-01 3.149841E-01 1.302100E-01 1.030900E-01

TEMP PRES M C1 C2 C3 C4
3.493994E-03 1.091492E-03 9.003500E-01 1.234407E-03 3.204400E-03 3.430300E-02 2.040977E-02 2.350302E-02

MFRAC1 MFRAC2 MFRAC3 MFRAC4 FRAC3D
3.090027E-01 2.310304E-01 3.154222E-01 1.470000E-01 1.000671E-01

TEMP PRES M C1 C2 C3 C4
9.090407E-03 1.727319E-03 9.070201E-01 1.290227E-03 3.200210E-03 3.418304E-02 2.708304E-02 2.207937E-02

MFRAC1 MFRAC2 MFRAC3 MFRAC4 FRAC3D
3.120001E-01 2.392123E-01 3.154009E-01 1.304109E-01 1.071400E-01

TEMP PRES M C1 C2 C3 C4
6.240201E-03 1.703025E-03 9.090304E-01 1.202103E-03 3.200001E-03 3.309102E-02 2.710971E-02 2.043709E-02

MFRAC1 MFRAC2 MFRAC3 MFRAC4 FRAC3D
3.201103E-01 2.300403E-01 3.151741E-01 1.290103E-01 2.090100E-01

TEMP PRES M C1 C2 C3 C4
6.670071E-03 1.790700E-03 9.000200E-01 1.300009E-03 3.274913E-03 3.300207E-02 2.002207E-02 1.000000E-02

MFRAC1 MFRAC2 MFRAC3 MFRAC4 FRAC3D
3.270020E-01 2.400307E-01 3.153001E-01 1.190300E-01 2.190007E-01

TEMP PRES M C1 C2 C3 C4
7.150201E-03 1.000700E-03 9.010000E-01 1.200000E-03 3.200000E-03 3.300000E-02 2.000000E-02 1.000000E-02

MFRAC1 MFRAC2 MFRAC3 MFRAC4 FRAC3D
3.301302E-01 2.401302E-01 3.120303E-01 1.000100E-01 2.200303E-01

MFRAC1 MFRAC2 MFRAC3 MFRAC4 FRAC3D
4,0019497E-01 2,74490351E-01 2,01372259E-01 3,37420103E-02 3,21944340E-01

TEMP PRES M C1 C2 C3 C4
1,40560907E-02 2,07009049E-03 9,43490002E-01 1,49010790E-03 3,80024375E-03 3,24700900E-02 1,03450020E-02 2,50042040E-03

MFRAC1 MFRAC2 MFRAC3 MFRAC4 FRAC3D
4,34226339E-01 2,02014410E-01 2,03204095E-01 1,90542470E-02 3,65031956E-01

TEMP PRES M C1 C2 C3 C4
1,4763701E-02 2,07002408E-03 9,42090000E-01 1,49020397E-03 3,59127000E-03 3,24706332E-02 1,02939022E-02 2,52099010E-03

MFRAC1 MFRAC2 MFRAC3 MFRAC4 FRAC3D
4,35162900E-01 2,03177170E-01 2,0232079E-01 1,9277392E-02 3,66700716E-01

TEMP PRES M C1 C2 C3 C4
1,40912119E-02 2,0700551E-03 9,42201002E-01 1,49033790E-03 3,59020490E-03 3,24022738E-02 1,02234703E-02 2,4700921E-03

MFRAC1 MFRAC2 MFRAC3 MFRAC4 FRAC3D
4,30090139E-01 2,03430900E-01 2,01599701E-01 1,80070494E-02 3,60533362E-01

TEMP PRES M C1 C2 C3 C4
1,49900099E-02 2,07001017E-03 9,41591159E-01 1,49039490E-03 3,60120004E-03 3,24970092E-02 1,01830222E-02 2,42009900E-03

MFRAC1 MFRAC2 MFRAC3 MFRAC4 FRAC3D
4,37000200E-01 2,03092405E-01 2,00734000E-01 1,00490700E-02 3,7023970E-01

TEMP PRES M C1 C2 C3 C4
1,50917410E-02 2,07010002E-03 9,39999007E-01 1,49091300E-03 3,61007040E-03 3,20044370E-02 1,70009111E-02 2,80010071E-03

MFRAC1 MFRAC2 MFRAC3 MFRAC4 FRAC3D
4,30730025E-01 2,04451325E-01 2,00300095E-01 1,70013000E-02 3,75439213E-01

TEMP 2 2.070400E+02 1.37020400E+01 1.400400E+03 3.20202000E+02 1.77030000E+02 2.19000000E+03

MFRAC1 MFRAC2 MFRAC3 MFRAC4 FRAC3D
4.42300214E-01 2.05101314E-01 2.95040027E-01 1.04020400E-02 3.00500119E-01

TEMP 2 2.070400E+02 1.37020400E+01 1.400400E+03 3.20202000E+02 1.77030000E+02 2.19000000E+03

MFRAC1 MFRAC2 MFRAC3 MFRAC4 FRAC3D
4.50100397E-01 2.07200100E-01 2.40091030E-01 1.30090047E-02 3.95402032E-01

TEMP 2 2.070400E+02 1.37020400E+01 1.400400E+03 3.20202000E+02 1.77030000E+02 2.19000000E+03

MFRAC1 MFRAC2 MFRAC3 MFRAC4 FRAC3D
4.57003095E-01 2.00147022E-01 2.42400052E-01 1.13043000E-02 4.00275107E-01

TEMP 2 2.070400E+02 1.37020400E+01 1.400400E+03 3.20202000E+02 1.77030000E+02 2.19000000E+03

MFRAC1 MFRAC2 MFRAC3 MFRAC4 FRAC3D
4.50403171E-01 2.00000570E-01 2.40350005E-01 1.00002020E-02 4.13600314E-01

TEMP 2 2.070400E+02 1.37020400E+01 1.400400E+03 3.20202000E+02 1.77030000E+02 2.19000000E+03

MFRAC1 MFRAC2 MFRAC3 MFRAC4 FRAC3D
4.61090000E-01 2.90420000E-01 2.30370222E-01 9.52000200E-03 4.10009520E-01

TEMP 2 2.070400E+02 1.37020400E+01 1.400400E+03 3.20202000E+02 1.77030000E+02 2.19000000E+03

MFRAC1 MFRAC2 MFRAC3 MFRAC4 MFRAC3D
4.6824150E-01 2.9222582E-01 2.3237493E-01 7.1304304E-03 4.3182329E-01

Z
TEMP PRES M C1 C2 C3 C4
4.8893211E-02 2.0744132E-03 9.8822763E-01 1.4937939E-03 2.7746880E-03 3.2487874E-02 1.9228827E-02 8.8897661E-04

MFRAC1 MFRAC2 MFRAC3 MFRAC4 MFRAC3D
4.7439356E-01 2.0388260E-01 2.2642302E-01 9.3892242E-03 4.4369880E-01

Z
TEMP PRES M C1 C2 C3 C4
6.6994749E-02 2.0952242E-03 9.8977491E-01 1.4818239E-03 2.8473147E-03 3.2411259E-02 1.3888781E-02 1.8813399E-04

MFRAC1 MFRAC2 MFRAC3 MFRAC4 MFRAC3D
4.9162423E-01 2.0882710E-01 2.8889261E-01 1.4883234E-03 4.8183748E-01

Z
TEMP PRES M C1 C2 C3 C4
9.3180680E-02 2.0276688E-03 9.8871172E-01 1.4626589E-03 3.0881889E-03 3.2291398E-02 1.2832138E-02 8.8892941E-05

MFRAC1 MFRAC2 MFRAC3 MFRAC4 MFRAC3D
9.8580376E-01 3.8889479E-01 1.9397165E-01 9.2979128E-04 9.1324846E-01

Z
TEMP PRES M C1 C2 C3 C4
1.7189883E-01 1.9872515E-03 7.8889577E-01 1.4828789E-03 3.8661182E-03 3.1922581E-02 9.8894998E-03 8.

MFRAC1 MFRAC2 MFRAC3 MFRAC4 MFRAC3D
9.3774934E-01 3.8794988E-01 1.9478991E-01 8. 9.8884842E-01

Z
TEMP PRES M C1 C2 C3 C4
2.5888888E-01 1.9888888E-03 7.8888888E-01 1.3788888E-03 1.8888888E-03 8.8873318E-02 7.7733888E-03 8.

MFRAC1 MFRAC2 MFRAC3 MFRAC4 MFRAC3D
8.8498917E-01 3.1888888E-01 1.3488888E-01 8. 8.4341342E-01

229 FROM VAPOR REGION

2.8904174E-049, 0742408E-041, 0665908E-031, 2270025E-031, 3921393E-031, 5506973E-031, 7301614E-031, 9055045E-032, 0040202E-032, 2092112E-03
2.4506077E-032, 0502231E-032, 0502231E-032, 0600077E-033, 2000020E-033, 0104017E-033, 7593432E-034, 0050040E-034, 2600100E-034, 5272175E-03
0.6400070E-033, 1974024E-033, 1720000E-033, 0000000E-033, 0000000E-033, 0000000E-033, 0000000E-033, 0000000E-033, 0000000E-033, 0000000E-033
9.7930131E-031, 0030245E-031, 0284073E-031, 4086000E-031, 4707000E-031, 0671380E-031, 4970930E-031, 5301761E-031, 5620302E-031, 0000000E-03
1.7501570E-032, 1407009E-032, 3372540E-032, 2000000E-032, 0000000E-032, 0000000E-032, 0000000E-032, 0000000E-032, 0000000E-032, 0000000E-032
1.7500000E-031, 0110402E-032, 1077000E-032, 0000000E-031, 0000000E-031, 0000000E-031, 0000000E-031, 0000000E-031, 0000000E-031, 0000000E-031

STEADY STATE VALUES FOR PEAR AND S AT END OF BED
MEAN = 3.21145E+01 S = 3.00900E+00

***** OPERATIONS COMPLETE *****

```

IDENT M012CL
* CELL LOADER DIRECTIVES FOR 150K CONTAM, I.E. FULL N2M4
* BC1 BLK RELMAX,
*   SAVEIT,CONSAT,CTPVIN,VTABLE,VTABLE,PTABLE,PTABLE,CTSTOP,CPRMT,
*   COMY,COMEC,CONCAS,MINFO,RXIND,SPINRX,RCOEFF,RATES,CPASS,
*   CAREPS,CARIT,XMBAR,PCOND,VSTAG,CSMOCK,CSCR,COPYX,TOKIN,
*   TLIMIT,TBR,TAPES,HEIGHT,SNAMES,MEMBER,PFAC,CHAXSP,LINFO,
*   CPMF,COMF,CINFO,CEND,CDELM,AAB,2DEB,DOLOOP,TOPLY,CLCMP,
*   PLSCAL,CHEMF,ADMTOT,ADFACT,ADXTAB,ADDRV,ADDTAB,ADDFLG,
*   BLOCK0
* BC2 BLK
* BC3 BLK BLANK,NAME4,NAME3,NAME2,NAME1,NAME0,NAMEA,NAMEP,ERR,
* BC4 BLK CONCE,STFOUT,STFOUT,BLKTHM,CDATEP,CXMBAR,
* BC7 BLK THMSP,TABLES,
* BC8 BLK THMS,
* BC9 BLK CNE,
* BC10 BLK DROP,MHAXXZ,EFOUT,MUST,XEND,SPEED,FNALBT,COMPLU,CHO,CINT,
* BC12 BLK BLOCK1,BLOCK2,BLOCK3
* BC13 BLK MTABLE,APDTBL,BLOCK1,BLOCK2,BLOCK3,BLOCK4,BLOCK5
* L61 SEG TTAPES-BC7,
* L63 SEG STFSET-BC8,
* L13 SEG GRAPHS
* L641 SEG PACKIP-010,
* L642 SEG MAIN-011,
* L31 SEG TD2-(PARTIL,M2MAIN)
* L3 SEG TDMIN-BC3-(L31,TD2P)
* L4 SEG N2M4-BC13-(RDPNCH,SCALC,DERIVD,DERIVM,PDERTV,TRAP,OSTEP,OTPUT,
*   SPIKE)
* L6 SEG SCREEN-BC1-(L61,INPUT,L63,L645,LINKS0)
* L7 SEG BILINK,
* L8 SEG MNLINK,
* L645 SEG AF073C-BC4-(L641,L642)
* L12 SEG MASTER-BC12-(START,WRITER,INJECT,DROPLT,METNAL,CHAMBR)
* L1 SEG FCC-BC2-(HEADER,L12,L13)
* SEG M012-(L1,L3,L4,L7,L8,XMKS,L6,SURF)
* ENDCELL

```

ENGINE

Z0	= 0.0.
QJ8	= 0.509E+01,
W03	= 0.1239E+02,
P38	= 0.24E+01,
T08	= 0.193E+04,
TVAP	= 0.80E+03,
W14	= 0.3304E+03,
F	= 0.0,
W7	= 0.0,
Z7	= 0.33E+03,
BMX1	= 0.2E+03,
BMX2	= 0.4E+02,
BMX3	= 0.0E+02,
PP	= 0.209E+03,
Z8D	= 0.22E+00,
Y0	= 0.49E+02,
AC	= 0.32E+01,
W4	= 0.4E+00,
Q4	= 0.33E+00,
AV	= 0.3E+00,
TA	= 0.53E+03,
MA	= 0.0.
MA1	= 0.11E+03,
MA2	= 0.0,
Z01	= 0.33E+03,
PG1	= 0.147E+02,
QPHY1	= 0.0,
QPHY1	= 0.0.
QPHY1	= 0.0,
QPHY1	= 0.97E+01,
QPHY1	= 0.0E+01.

CPH2I = 0.0.
CIN2I = 0.0.
AG = 0.3217E+02,
DOMIP = 0.15E+02,
ORINO = 0.12E+04,
FDLIML = 0.1667E+00,
FULFR = 0.0,
YLIQ = 0.57E+03,
TPULS = 0.1E+00,
PINZON = 0.2003E-01,
CINVI = 0.0.
SEND

NOFZ 21.

[illegible]

5040

SCONTRL

DRUM = 11.

MPRNT = 1.

MPASS = 0.

DELT = 0.1E-03, 0.5E-03, 0.1E-02, 0.2E-02, 0.5E-02, 0.1E-01, 0.1E-01,
0.2E-01, 0.0, 0.0, 0.0, 0.0, 0.0, 0.0, 0.0, 0.0, 0.0,
0.0, 0.0.

SEND

G VALUES FOR TIME INCREMENT 7

4.57101E+00	4.56984E+00	4.56818F+00	4.56745E+00	4.56616E+00	4.56494E+00	4.56398E+00	4.56225E+00	4.56001E+00	4.55988E+00
4.56004E+00	4.55835E+00	4.55645E+00	4.55435E+00	4.55215E+00	4.54985E+00	4.54745E+00	4.54495E+00	4.54235E+00	4.53975E+00
4.53413E+00	4.53066E+00	4.52635E+00	4.52135E+00	4.51575E+00	4.50955E+00	4.50285E+00	4.49565E+00	4.48795E+00	4.47975E+00
4.47005E+00	4.46095E+00	4.45075E+00	4.43955E+00	4.42735E+00	4.41415E+00	4.40005E+00	4.38505E+00	4.36925E+00	4.35265E+00
3.34231E+00	3.25211E+00	3.06192E+00	2.87172E+00	2.78152E+00					

WALL TEMPERATURE = 5.70002E+02

G VALUES FOR TIME INCREMENT 8

4.56984E+00	4.56818E+00	4.56645E+00	4.56475E+00	4.56305E+00	4.56135E+00	4.55965E+00	4.55795E+00	4.55625E+00	4.55455E+00
4.55285E+00	4.55115E+00	4.54945E+00	4.54775E+00	4.54605E+00	4.54435E+00	4.54265E+00	4.54095E+00	4.53925E+00	4.53755E+00
4.53585E+00	4.53415E+00	4.53245E+00	4.53075E+00	4.52905E+00	4.52735E+00	4.52565E+00	4.52395E+00	4.52225E+00	4.52055E+00
4.51855E+00	4.51685E+00	4.51515E+00	4.51345E+00	4.51175E+00	4.51005E+00	4.50835E+00	4.50665E+00	4.50495E+00	4.50325E+00
4.50155E+00	4.49985E+00	4.49815E+00	4.49645E+00	4.49475E+00	4.49305E+00	4.49135E+00	4.48965E+00	4.48795E+00	4.48625E+00
3.34231E+00	3.25211E+00	3.06192E+00	2.87172E+00	2.78152E+00					

WALL TEMPERATURE = 5.70002E+02

G VALUES FOR TIME INCREMENT 9

4.56818E+00	4.56645E+00	4.56475E+00	4.56305E+00	4.56135E+00	4.55965E+00	4.55795E+00	4.55625E+00	4.55455E+00	4.55285E+00
4.55185E+00	4.55015E+00	4.54845E+00	4.54675E+00	4.54505E+00	4.54335E+00	4.54165E+00	4.53995E+00	4.53825E+00	4.53655E+00
4.53055E+00	4.52885E+00	4.52715E+00	4.52545E+00	4.52375E+00	4.52205E+00	4.52035E+00	4.51865E+00	4.51695E+00	4.51525E+00
4.51355E+00	4.51185E+00	4.51015E+00	4.50845E+00	4.50675E+00	4.50505E+00	4.50335E+00	4.50165E+00	4.49995E+00	4.49825E+00
4.49655E+00	4.49485E+00	4.49315E+00	4.49145E+00	4.48975E+00	4.48805E+00	4.48635E+00	4.48465E+00	4.48295E+00	4.48125E+00
3.34231E+00	3.25211E+00	3.06192E+00	2.87172E+00	2.78152E+00					

WALL TEMPERATURE = 5.70002E+02

G VALUES FOR TIME INCREMENT 10

4.56645E+00	4.56475E+00	4.56305E+00	4.56135E+00	4.55965E+00	4.55795E+00	4.55625E+00	4.55455E+00	4.55285E+00	4.55115E+00
4.54505E+00	4.54335E+00	4.54165E+00	4.53995E+00	4.53825E+00	4.53655E+00	4.53485E+00	4.53315E+00	4.53145E+00	4.52975E+00
4.52715E+00	4.52545E+00	4.52375E+00	4.52205E+00	4.52035E+00	4.51865E+00	4.51695E+00	4.51525E+00	4.51355E+00	4.51185E+00
4.50985E+00	4.50815E+00	4.50645E+00	4.50475E+00	4.50305E+00	4.50135E+00	4.49965E+00	4.49795E+00	4.49625E+00	4.49455E+00
4.49255E+00	4.49085E+00	4.48915E+00	4.48745E+00	4.48575E+00	4.48405E+00	4.48235E+00	4.48065E+00	4.47895E+00	4.47725E+00
3.34231E+00	3.25211E+00	3.06192E+00	2.87172E+00	2.78152E+00					

WALL TEMPERATURE = 5.70002E+02

G VALUES FOR TIME INCREMENT 11

4.56475E+00	4.56305E+00	4.56135E+00	4.55965E+00	4.55795E+00	4.55625E+00	4.55455E+00	4.55285E+00	4.55115E+00	4.54945E+00
4.53315E+00	4.53145E+00	4.52975E+00	4.52805E+00	4.52635E+00	4.52465E+00	4.52295E+00	4.52125E+00	4.51955E+00	4.51785E+00
4.51615E+00	4.51445E+00	4.51275E+00	4.51105E+00	4.50935E+00	4.50765E+00	4.50595E+00	4.50425E+00	4.50255E+00	4.50085E+00
4.49885E+00	4.49715E+00	4.49545E+00	4.49375E+00	4.49205E+00	4.49035E+00	4.48865E+00	4.48695E+00	4.48525E+00	4.48355E+00
4.48125E+00	4.47955E+00	4.47785E+00	4.47615E+00	4.47445E+00	4.47275E+00	4.47105E+00	4.46935E+00	4.46765E+00	4.46595E+00
3.34231E+00	3.25211E+00	3.06192E+00	2.87172E+00	2.78152E+00					

WALL TEMPERATURE = 5.70002E+02

G VALUES FOR TIME INCREMENT 12

4.56305E+00	4.56135E+00	4.55965E+00	4.55795E+00	4.55625E+00	4.55455E+00	4.55285E+00	4.55115E+00	4.54945E+00	4.54775E+00
4.52125E+00	4.51955E+00	4.51785E+00	4.51615E+00	4.51445E+00	4.51275E+00	4.51105E+00	4.50935E+00	4.50765E+00	4.50595E+00
4.50425E+00	4.50255E+00	4.50085E+00	4.49915E+00	4.49745E+00	4.49575E+00	4.49405E+00	4.49235E+00	4.49065E+00	4.48895E+00
4.48725E+00	4.48555E+00	4.48385E+00	4.48215E+00	4.48045E+00	4.47875E+00	4.47705E+00	4.47535E+00	4.47365E+00	4.47195E+00
4.46995E+00	4.46825E+00	4.46655E+00	4.46485E+00	4.46315E+00	4.46145E+00	4.45975E+00	4.45805E+00	4.45635E+00	4.45465E+00
3.34231E+00	3.25211E+00	3.06192E+00	2.87172E+00	2.78152E+00					

WALL TEMPERATURE = 5.70002E+02

G VALUES FOR TIME INCREMENT 13

4.56135E+00	4.55965E+00	4.55795E+00	4.55625E+00	4.55455E+00	4.55285E+00	4.55115E+00	4.54945E+00	4.54775E+00	4.54605E+00
4.50765E+00	4.50595E+00	4.50425E+00	4.50255E+00	4.50085E+00	4.49915E+00	4.49745E+00	4.49575E+00	4.49405E+00	4.49235E+00
4.49065E+00	4.48895E+00	4.48725E+00	4.48555E+00	4.48385E+00	4.48215E+00	4.48045E+00	4.47875E+00	4.47705E+00	4.47535E+00
4.46315E+00	4.46145E+00	4.45975E+00	4.45805E+00	4.45635E+00	4.45465E+00	4.45295E+00	4.45125E+00	4.44955E+00	4.44785E+00
4.44615E+00	4.44445E+00	4.44275E+00	4.44105E+00	4.43935E+00	4.43765E+00	4.43595E+00	4.43425E+00	4.43255E+00	4.43085E+00
3.34231E+00	3.25211E+00	3.06192E+00	2.87172E+00	2.78152E+00					

[illegible]

~~WALT TERPENTINE CO. 5, 7003 E 072~~

VALUES FOR TIME INCREMENT Δt

[illegible]

AVAILABLE TEMPERATURE 05.70004E+02

ALL MO-597VA IN VALUES LOW THE INCREASE 15

4.54577E+00	4.54544E+00	4.5428E+00	4.5399E+00	4.53871E+00	4.53743E+00	4.53615E+00	4.53402E+00
4.53345E+00	4.53040E+00	4.5282E+00	4.5253E+00	4.5231E+00	4.52196E+00	4.51907E+00	4.5172E+00
4.5120E+00	4.5075E+00	4.5052E+00	4.5021E+00	4.5004E+00	4.49940E+00	4.49808E+00	4.49637E+00
4.47808E+00	4.4761E+00	4.4721E+00	4.4704E+00	4.4680E+00	4.4660E+00	4.4640E+00	4.46237E+00
4.42272E+00	4.4203E+00	4.4224E+00	4.4200E+00	3.9103E+00	3.7767E+00	3.4335E+00	3.5093E+00

ALL INFORMATION CONTAINED HEREIN IS UNCLASSIFIED

THE UNIVERSITY OF CHICAGO

G VALUES FOR TIME INCREMENT 16	
4.5470E+00	4.5393E+00
4.5423E+00	4.5379E+00
4.5380E+00	4.5362E+00
4.5340E+00	4.5345E+00
4.5300E+00	4.5328E+00
4.5260E+00	4.5310E+00
4.5227E+00	4.5294E+00
4.5195E+00	4.5278E+00
4.5165E+00	4.5261E+00
4.5135E+00	4.5245E+00
4.5105E+00	4.5228E+00
4.5075E+00	4.5210E+00
4.5045E+00	4.5194E+00
4.5015E+00	4.5178E+00
4.4985E+00	4.5161E+00
4.4955E+00	4.5145E+00
4.4925E+00	4.5128E+00
4.4895E+00	4.5110E+00
4.4865E+00	4.5094E+00
4.4835E+00	4.5078E+00
4.4805E+00	4.5061E+00
4.4775E+00	4.5045E+00
4.4745E+00	4.5028E+00
4.4715E+00	4.5010E+00
4.4685E+00	4.4994E+00
4.4655E+00	4.4978E+00
4.4625E+00	4.4961E+00
4.4595E+00	4.4945E+00
4.4565E+00	4.4928E+00
4.4535E+00	4.4910E+00
4.4505E+00	4.4894E+00
4.4475E+00	4.4878E+00
4.4445E+00	4.4861E+00
4.4415E+00	4.4845E+00
4.4385E+00	4.4828E+00
4.4355E+00	4.4810E+00
4.4325E+00	4.4794E+00
4.4295E+00	4.4778E+00
4.4265E+00	4.4761E+00
4.4235E+00	4.4745E+00
4.4205E+00	4.4728E+00
4.4175E+00	4.4710E+00
4.4145E+00	4.4694E+00
4.4115E+00	4.4678E+00
4.4085E+00	4.4661E+00
4.4055E+00	4.4645E+00
4.4025E+00	4.4628E+00
4.3995E+00	4.4610E+00
4.3965E+00	4.4594E+00
4.3935E+00	4.4578E+00
4.3905E+00	4.4561E+00
4.3875E+00	4.4545E+00
4.3845E+00	4.4528E+00
4.3815E+00	4.4510E+00
4.3785E+00	4.4494E+00
4.3755E+00	4.4478E+00
4.3725E+00	4.4461E+00
4.3695E+00	4.4445E+00
4.3665E+00	4.4428E+00
4.3635E+00	4.4410E+00
4.3605E+00	4.4394E+00
4.3575E+00	4.4378E+00
4.3545E+00	4.4361E+00
4.3515E+00	4.4345E+00
4.3485E+00	4.4328E+00
4.3455E+00	4.4310E+00
4.3425E+00	4.4294E+00
4.3395E+00	4.4278E+00
4.3365E+00	4.4261E+00
4.3335E+00	4.4245E+00
4.3305E+00	4.4228E+00
4.3275E+00	4.4210E+00
4.3245E+00	4.4194E+00
4.3215E+00	4.4178E+00
4.3185E+00	4.4161E+00
4.3155E+00	4.4145E+00
4.3125E+00	4.4128E+00
4.3095E+00	4.4110E+00
4.3065E+00	4.4094E+00
4.3035E+00	4.4078E+00
4.3005E+00	4.4061E+00
4.2975E+00	4.4045E+00
4.2945E+00	4.4028E+00
4.2915E+00	4.4010E+00
4.2885E+00	4.3994E+00
4.2855E+00	4.3978E+00
4.2825E+00	4.3961E+00
4.2795E+00	4.3945E+00
4.2765E+00	4.3928E+00
4.2735E+00	4.3910E+00
4.2705E+00	4.3894E+00
4.2675E+00	4.3878E+00
4.2645E+00	4.3861E+00
4.2615E+00	4.3845E+00
4.2585E+00	4.3828E+00
4.2555E+00	4.3810E+00
4.2525E+00	4.3794E+00
4.2495E+00	4.3778E+00
4.2465E+00	4.3761E+00
4.2435E+00	4.3745E+00
4.2405E+00	4.3728E+00
4.2375E+00	4.3710E+00
4.2345E+00	4.3694E+00
4.2315E+00	4.3678E+00
4.2285E+00	4.3661E+00
4.2255E+00	4.3645E+00
4.2225E+00	4.3628E+00
4.2195E+00	4.3610E+00
4.2165E+00	4.3594E+00
4.2135E+00	4.3578E+00
4.2105E+00	4.3561E+00
4.2075E+00	4.3545E+00
4.2045E+00	4.3528E+00
4.2015E+00	4.3510E+00
4.1985E+00	4.3494E+00
4.1955E+00	4.3478E+00</

00-170668-3 - 20160820092

100

[illegible]

10-3000-12 9-10-66 021000Z 00Z

[illegible]

004326017

ALL INFORMATION CONTAINED

C VALUES FOR TIME INCREMENT 19				
4.5328E+00	4.5317E+00	4.5299E+00	4.5293E+00	4.5291E+00
4.5308E+00	4.5298E+00	4.5280E+00	4.5274E+00	4.5272E+00
4.5288E+00	4.5277E+00	4.5259E+00	4.5253E+00	4.5251E+00
4.5033E+00	4.4997E+00	4.4957E+00	4.4902E+00	4.4844E+00
4.4674E+00	4.4601E+00	4.4525E+00	4.4434E+00	4.4338E+00
4.4044E+00	4.4033E+00	4.4025E+00	4.4022E+00	4.4020E+00
4.4015E+00	4.4013E+00	4.4012E+00	4.4011E+00	4.4010E+00
4.4009E+00	4.4008E+00	4.4007E+00	4.4006E+00	4.4005E+00
4.4004E+00	4.4003E+00	4.4002E+00	4.4001E+00	4.4000E+00
4.3999E+00	4.3998E+00	4.3997E+00	4.3996E+00	4.3995E+00
4.3994E+00	4.3993E+00	4.3992E+00	4.3991E+00	4.3990E+00
4.3989E+00	4.3988E+00	4.3987E+00	4.3986E+00	4.3985E+00
4.3984E+00	4.3983E+00	4.3982E+00	4.3981E+00	4.3980E+00
4.3979E+00	4.3978E+00	4.3977E+00	4.3976E+00	4.3975E+00
4.3974E+00	4.3973E+00	4.3972E+00	4.3971E+00	4.3970E+00
4.3969E+00	4.3968E+00	4.3967E+00	4.3966E+00	4.3965E+00
4.3964E+00	4.3963E+00	4.3962E+00	4.3961E+00	4.3960E+00
4.3959E+00	4.3958E+00	4.3957E+00	4.3956E+00	4.3955E+00
4.3954E+00	4.3953E+00	4.3952E+00	4.3951E+00	4.3950E+00
4.3949E+00	4.3948E+00	4.3947E+00	4.3946E+00	4.3945E+00
4.3944E+00	4.3943E+00	4.3942E+00	4.3941E+00	4.3940E+00
4.3939E+00	4.3938E+00	4.3937E+00	4.3936E+00	4.3935E+00
4.3934E+00	4.3933E+00	4.3932E+00	4.3931E+00	4.3930E+00
4.3929E+00	4.3928E+00	4.3927E+00	4.3926E+00	4.3925E+00
4.3924E+00	4.3923E+00	4.3922E+00	4.3921E+00	4.3920E+00
4.3919E+00	4.3918E+00	4.3917E+00	4.3916E+00	4.3915E+00
4.3914E+00	4.3913E+00	4.3912E+00		

0 2.8970E+90

MESH CALCULATIONS

10-3-10

STATION 1 7MPH 55

[illegible]

PARTICLE PYRAZINE CONCENTRATIONS --- STATIONS 1 THRU 55

[illegible]

PARTICLE ANIONA CONCENTRATIONS --- STATIONS 1 THRU 55

STATION	DATE	TIME	TYPE	REMARKS
1	10/10/50	10:00	1	1000
2	10/10/50	10:00	1	1000
3	10/10/50	10:00	1	1000
4	10/10/50	10:00	1	1000
5	10/10/50	10:00	1	1000
6	10/10/50	10:00	1	1000
7	10/10/50	10:00	1	1000
8	10/10/50	10:00	1	1000
9	10/10/50	10:00	1	1000
10	10/10/50	10:00	1	1000
11	10/10/50	10:00	1	1000
12	10/10/50	10:00	1	1000
13	10/10/50	10:00	1	1000
14	10/10/50	10:00	1	1000
15	10/10/50	10:00	1	1000
16	10/10/50	10:00	1	1000
17	10/10/50	10:00	1	1000
18	10/10/50	10:00	1	1000
19	10/10/50	10:00	1	1000
20	10/10/50	10:00	1	1000
21	10/10/50	10:00	1	1000
22	10/10/50	10:00	1	1000
23	10/10/50	10:00	1	1000
24	10/10/50	10:00	1	1000
25	10/10/50	10:00	1	1000
26	10/10/50	10:00	1	1000
27	10/10/50	10:00	1	1000
28	10/10/50	10:00	1	1000
29	10/10/50	10:00	1	1000
30	10/10/50	10:00	1	1000
31	10/10/50	10:00	1	1000
32	10/10/50	10:00	1	1000
33	10/10/50	10:00	1	1000
34	10/10/50	10:00	1	1000
35	10/10/50	10:00	1	1000
36	10/10/50	10:00	1	1000
37	10/10/50	10:00	1	1000
38	10/10/50	10:00	1	1000
39	10/10/50	10:00	1	1000
40	10/10/50	10:00	1	1000
41	10/10/50	10:00	1	1000
42	10/10/50	10:00	1	1000
43	10/10/50	10:00	1	1000
44	10/10/50	10:00	1	1000
45	10/10/50	10:00	1	1000
46	10/10/50	10:00	1	1000
47	10/10/50	10:00	1	1000
48	10/10/50	10:00	1	1000
49	10/10/50	10:00	1	1000
50	10/10/50	10:00	1	1000
51	10/10/50	10:00	1	1000
52	10/10/50	10:00	1	1000
53	10/10/50	10:00	1	1000
54	10/10/50	10:00	1	1000
55	10/10/50	10:00	1	1000
56	10/10/50	10:00	1	1000
57	10/10/50	10:00	1	1000
58	10/10/50	10:00	1	1000
59	10/10/50	10:00	1	1000
60	10/10/50	10:00	1	1000
61	10/10/50	10:00	1	1000
62	10/10/50	10:00	1	1000
63	10/10/50	10:00	1	1000
64	10/10/50	10:00	1	1000
65	10/10/50	10:00	1	1000
66	10/10/50	10:00	1	1000
67	10/10/50	10:00	1	1000
68	10/10/50	10:00	1	1000
69	10/10/50	10:00	1	1000
70	10/10/50	10:00	1	1000
71	10/10/50	10:00	1	1000

PARTICLE NITROGEN CONCENTRATIONS --- STATIONS 1 THRU 55

[illegible]

PARTICLE HYDROLYZATION CONCENTRATIONS -- STATIONS 1 THRU 55

[illegible]

INITIAL TEMPERATURES AT AXIAL STATIONS 1 THRU 55

[illegible]

INVESTIGATIONAL HYPERAZINE CONCEPTATIONS --- STATISTICS 1 TMU 9 59

[illegible]

[illegible][illegible][illegible]

CHANGES PRESSURE AT TIME T = 0. IS 14,700 PSIA

[illegible]

INTERSTITIAL AMMONIA CONCENTRATIONS --- STATIONS 1 THRU 55

0.42533E-03 0.92047E-03 0.17387E-03 7.09741E-03 7.53760E-03 7.44319E-03 0.93267E-03 0.63460E-03 0.39903E-03 0.03224E-03
 5.77603E-03 5.49687E-03 5.21441E-03 4.94963E-03 4.67601E-03 4.40524E-03 4.12390E-03 3.86779E-03 3.62870E-03 3.38690E-03
 3.13216E-03 2.89139E-03 2.65451E-03 2.42451E-03 2.18946E-03 1.96438E-03 1.73543E-03 1.52338E-03 1.31339E-03 1.12483E-03
 0.92876E-03 7.19203E-04 5.07632E-04 4.07673E-04 3.07673E-04 2.07673E-04 1.07673E-04 0.07673E-04 0.00000E+00 0.00000E+00
 1.05582E-04 7.35283E-05 4.89717E-05 2.05695E-05 7.55310E-06 3.84609E-07 1.73196E-08 1.42351E-09 1.04362E-10 6.78462E-12

INTERSTITIAL NITROGEN CONCENTRATIONS --- STATIONS 1 THRU 55

7.79139E-03 8.09041E-03 2.07904E-02 3.02621E-02 3.18713E-02 3.33902E-02 3.49023E-02 3.65244E-02 3.82299E-02 3.93690E-02
 4.10622E-02 4.25937E-02 4.42435E-02 4.59059E-02 4.71979E-02 4.87179E-02 5.02578E-02 5.17469E-02 5.32980E-02 5.48993E-02
 5.63424E-02 5.78671E-02 5.93871E-02 6.09024E-02 6.24104E-02 6.39195E-02 6.54285E-02 6.69375E-02 6.84465E-02 7.02000E-02
 7.20941E-02 7.39141E-02 7.57341E-02 7.75541E-02 7.93741E-02 8.11941E-02 8.30141E-02 8.48341E-02 8.66541E-02 8.84741E-02
 0.02421E-02 0.03567E-02 0.04713E-02 0.05859E-02 0.06995E-02 0.08131E-02 0.09267E-02 0.10403E-02 0.11539E-02 0.12675E-02
 0.24089E-02 0.25273E-02 0.26457E-02 0.27641E-02 0.28825E-02 0.29999E-02 0.31173E-02 0.32347E-02 0.33521E-02 0.34695E-02

INTERSTITIAL HYDROGEN CONCENTRATIONS --- STATIONS 1 THRU 55

0.00000E+00 0.00000E+00 0.00000E+00 0.00000E+00 0.00000E+00 0.00000E+00 0.00000E+00 0.00000E+00 0.00000E+00 0.00000E+00
 0.00000E+00 0.00000E+00 0.00000E+00 0.00000E+00 0.00000E+00 0.00000E+00 0.00000E+00 0.00000E+00 0.00000E+00 0.00000E+00
 0.00000E+00 0.00000E+00 0.00000E+00 0.00000E+00 0.00000E+00 0.00000E+00 0.00000E+00 0.00000E+00 0.00000E+00 0.00000E+00
 0.00000E+00 0.00000E+00 0.00000E+00 0.00000E+00 0.00000E+00 0.00000E+00 0.00000E+00 0.00000E+00 0.00000E+00 0.00000E+00
 0.00000E+00 0.00000E+00 0.00000E+00 0.00000E+00 0.00000E+00 0.00000E+00 0.00000E+00 0.00000E+00 0.00000E+00 0.00000E+00

CHARGE PRESENT AT TIME T = 5.00000E+04 IS 14.804 PSI

VALUES OF MEAN AT AXIAL STATIONS 1 THRU 54

2.30191E-01 2.69504E-01 2.74291E-01 2.70719E-01 2.71040E-01 2.72241E-01 2.72578E-01 2.73434E-01 2.73973E-01 2.74888E-01
 2.75803E-01 2.76718E-01 2.77633E-01 2.78548E-01 2.79463E-01 2.80378E-01 2.81293E-01 2.82208E-01 2.83123E-01 2.84038E-01
 2.79024E-01 2.76317E-01 2.73610E-01 2.70903E-01 2.68196E-01 2.65489E-01 2.62782E-01 2.60075E-01 2.57368E-01 2.54661E-01
 2.61034E-01 2.61032E-01 2.61030E-01 2.61028E-01 2.61026E-01 2.61024E-01 2.61022E-01 2.61020E-01 2.61018E-01 2.61016E-01
 2.60160E-01 2.60160E-01 2.60160E-01 2.60160E-01 2.60160E-01 2.60160E-01 2.60160E-01 2.60160E-01 2.60160E-01 2.60160E-01

[illegible][illegible][illegible][illegible][illegible][illegible][illegible]

**TYPE & SICCODE--LT SECS
OFFICE TEMPERATURES AT AXIAL STATIONS 1 THRU 95**

SPACE TEMPERATURES AT AXIAL STATIONS 1 THRU 55

[illegible][illegible][illegible][illegible]

PARTICLE NUMBER CONCENTRATIONS		STATIONS 1 THRU 55	
4.02225E-04	2.72704E-04	2.47993E-04	2.33729E-04
4.02225E-04	1.60951E-04	1.50903E-04	1.053174E-04
1.00593E-04	0.99913E-04	1.30609E-04	1.12728E-05
9.09933E-05	0.99431E-05	8.06223E-05	4.40799E-05
9.09933E-05	2.72661E-05	5.74748E-04	5.51295E-06
4.07437E-05	5.00414E-06	4.49938E-07	3.83007E-10
4.07437E-05	1.06337E-06	3.59314E-08	2.77535E-09
3.30429E-05	1.74120E-15	2.25795E-16	
3.30429E-05	4.79326E-04	1.74120E-15	2.25795E-16
4.02225E-04	2.72704E-04	2.47993E-04	2.33729E-04
4.02225E-04	1.60951E-04	1.50903E-04	1.053174E-04
1.00593E-04	0.99913E-04	1.30609E-04	1.12728E-05
9.09933E-05	0.99431E-05	8.06223E-05	4.40799E-05
9.09933E-05	2.72661E-05	5.74748E-04	5.51295E-06
4.07437E-05	5.00414E-06	4.49938E-07	3.83007E-10
4.07437E-05	1.06337E-06	3.59314E-08	2.77535E-09
3.30429E-05	1.74120E-15	2.25795E-16	
3.30429E-05	4.79326E-04	1.74120E-15	2.25795E-16

[illegible][illegible]

INTERSTITIAL AMMONIA CONCENTRATIONS --- STATIONS 1 THRU 55

0.703433E-03	0.703433E-03	1.006042E-02	1.032305E-02	1.054659E-02	1.082289E-02	1.103942E-02	1.123744E-02	1.142402E-02
1.159950E-02	1.176161E-02	1.190018E-02	1.203475E-02	1.214449E-02	1.230804E-02	1.235766E-02	1.237073E-02	1.239020E-02
1.23083E-02	1.230866E-02	1.209012E-02	1.191747E-02	1.172337E-02	1.145529E-02	1.113345E-02	1.071527E-02	1.022750E-02
0.703433E-03	0.703433E-03	1.006042E-02	1.032305E-02	1.054659E-02	1.082289E-02	1.103942E-02	1.123744E-02	1.142402E-02
2.054925E-03	2.320400E-03	1.006042E-02	1.032305E-02	1.054659E-02	1.082289E-02	1.103942E-02	1.123744E-02	1.142402E-02
0.703433E-03	0.703433E-03	1.006042E-02	1.032305E-02	1.054659E-02	1.082289E-02	1.103942E-02	1.123744E-02	1.142402E-02

INTERSTITIAL NITROGEN CONCENTRATIONS --- STATIONS 1 THRU 55

0.093404E-03	0.104040E-03	0.116040E-03	0.130400E-03	0.146040E-03	0.163040E-03	0.181040E-03	0.200040E-03	0.220040E-03
1.273195E-02	1.323471E-02	1.375040E-02	1.43702E-02	1.499040E-02	1.561040E-02	1.623040E-02	1.685040E-02	1.747040E-02
1.92020E-02	2.01019E-02	2.10018E-02	2.19017E-02	2.28016E-02	2.37015E-02	2.46014E-02	2.55013E-02	2.64012E-02
3.334040E-02	3.404040E-02	3.474040E-02	3.544040E-02	3.614040E-02	3.684040E-02	3.754040E-02	3.824040E-02	3.894040E-02
4.051640E-02	4.104040E-02	4.154040E-02	4.204040E-02	4.254040E-02	4.304040E-02	4.354040E-02	4.404040E-02	4.454040E-02
5.574276E-02	5.574015E-02	5.574015E-02	5.574015E-02	5.574015E-02	5.574015E-02	5.574015E-02	5.574015E-02	5.574015E-02

INTERSTITIAL HYDROGEN CONCENTRATIONS --- STATIONS 1 THRU 55

5.023903E-04	5.445503E-04	5.870003E-04	0.	0.	0.	0.	0.	0.
0.	0.	0.	0.	0.	0.	0.	0.	0.
0.	0.	0.	0.	0.	0.	0.	0.	0.
0.	0.	0.	0.	0.	0.	0.	0.	0.
0.	0.	0.	0.	0.	0.	0.	0.	0.

CHAMBER PRESSURE AT TIME T = 3.00000E+04 TS 15.797 PSIA

VALUES OF MBAR AT AXIAL STATIONS 1 THRU 54

2.301875E+01	2.301875E+01	2.301875E+01	2.301875E+01	2.301875E+01	2.301875E+01	2.301875E+01	2.301875E+01	2.301875E+01
2.301875E+01	2.301875E+01	2.301875E+01	2.301875E+01	2.301875E+01	2.301875E+01	2.301875E+01	2.301875E+01	2.301875E+01
2.453871E+01	2.453871E+01	2.453871E+01	2.453871E+01	2.453871E+01	2.453871E+01	2.453871E+01	2.453871E+01	2.453871E+01
2.537392E+01	2.537392E+01	2.537392E+01	2.537392E+01	2.537392E+01	2.537392E+01	2.537392E+01	2.537392E+01	2.537392E+01
2.730914E+01	2.730914E+01	2.730914E+01	2.730914E+01	2.730914E+01	2.730914E+01	2.730914E+01	2.730914E+01	2.730914E+01
2.801603E+01	2.801603E+01	2.801603E+01	2.801603E+01	2.801603E+01	2.801603E+01	2.801603E+01	2.801603E+01	2.801603E+01

[illegible]

3.406240E-07	2.404064E-06	3.433041E-06	5.357071E-06	2.155075E-06	2.971210E-06	2.009297E-06	2.702111E-06	3.073195E-06
2.575208E-06	2.730341E-06	2.735124E-06	2.815126E-06	2.170033E-06	1.905942E-06	1.832302E-06	1.790004E-06	1.708775E-06
1.616594E-06	1.326134E-06	1.735035E-06	1.732547E-06	1.452333E-06	1.159913E-06	9.742922E-07	8.76143E-07	7.80333E-07
7.702000E-07	5.707200E-07	5.026422E-07	4.000102E-07	3.17276E-07	2.807775E-07	2.572350E-07	2.374500E-07	2.173770E-07
1.379878E-08	1.137566E-08	9.256422E-08	5.802704E-08	2.759000E-08	1.047400E-08	1.030235E-08	1.030235E-08	1.030235E-08
7.741332E-04	1.133545E-04	1.077070E-05	1.080663E-06	4.500411E-10	0.612074E-11	1.300100E-11	2.673170E-12	4.703711E-13

[illegible][illegible][illegible]

INTERSTITIAL TEMPERATURES AT AXIAL STATICS 1 THRU 55	
2.00133E+02	7.00794E+02
2.00133E+02	7.03204E+02
2.00133E+02	7.05900E+02
2.00133E+02	7.08499E+02
2.00133E+02	7.10995E+02
2.00133E+02	7.13491E+02
2.00133E+02	7.15987E+02
2.00133E+02	7.18483E+02
2.00133E+02	7.20979E+02
2.00133E+02	7.23475E+02
2.00133E+02	7.25971E+02
2.00133E+02	7.28467E+02
2.00133E+02	7.30963E+02
2.00133E+02	7.33459E+02
2.00133E+02	7.35955E+02
2.00133E+02	7.38451E+02
2.00133E+02	7.40947E+02
2.00133E+02	7.43443E+02
2.00133E+02	7.45939E+02
2.00133E+02	7.48435E+02
2.00133E+02	7.50931E+02
2.00133E+02	7.53427E+02
2.00133E+02	7.55923E+02
2.00133E+02	7.58419E+02
2.00133E+02	7.60915E+02
2.00133E+02	7.63411E+02
2.00133E+02	7.65907E+02
2.00133E+02	7.68403E+02
2.00133E+02	7.70899E+02
2.00133E+02	7.73395E+02
2.00133E+02	7.75891E+02
2.00133E+02	7.78387E+02
2.00133E+02	7.80883E+02
2.00133E+02	7.83379E+02
2.00133E+02	7.85875E+02
2.00133E+02	7.88371E+02
2.00133E+02	7.90867E+02
2.00133E+02	7.93363E+02
2.00133E+02	7.95859E+02
2.00133E+02	7.98355E+02
2.00133E+02	8.00851E+02
2.00133E+02	8.03347E+02
2.00133E+02	8.05843E+02
2.00133E+02	8.08339E+02
2.00133E+02	8.10835E+02
2.00133E+02	8.13331E+02
2.00133E+02	8.15827E+02
2.00133E+02	8.18323E+02
2.00133E+02	8.20819E+02
2.00133E+02	8.23315E+02
2.00133E+02	8.25811E+02
2.00133E+02	8.28307E+02
2.00133E+02	8.30803E+02
2.00133E+02	8.33299E+02
2.00133E+02	8.35795E+02
2.00133E+02	8.38291E+02
2.00133E+02	8.40787E+02
2.00133E+02	8.43283E+02
2.00133E+02	8.45779E+02
2.00133E+02	8.48275E+02
2.00133E+02	8.50771E+02
2.00133E+02	8.53267E+02
2.00133E+02	8.55763E+02
2.00133E+02	8.58259E+02
2.00133E+02	8.60755E+02
2.00133E+02	8.63251E+02
2.00133E+02	8.65747E+02
2.00133E+02	8.68243E+02
2.00133E+02	8.70739E+02
2.00133E+02	8.73235E+02
2.00133E+02	8.75731E+02
2.00133E+02	8.78227E+02
2.00133E+02	8.80723E+02
2.00133E+02	8.83219E+02
2.00133E+02	8.85715E+02
2.00133E+02	8.88211E+02
2.00133E+02	8.90707E+02
2.00133E+02	8.93203E+02
2.00133E+02	8.95699E+02
2.00133E+02	8.98195E+02
2.00133E+02	9.00691E+02
2.00133E+02	9.03187E+02
2.00133E+02	9.05683E+02
2.00133E+02	9.08179E+02
2.00133E+02	9.10675E+02
2.00133E+02	9.13171E+02
2.00133E+02	9.15667E+02
2.00133E+02	9.18163E+02
2.00133E+02	9.20659E+02
2.00133E+02	9.23155E+02
2.00133E+02	9.25651E+02
2.00133E+02	9.28147E+02
2.00133E+02	9.30643E+02
2.00133E+02	9.33139E+02
2.00133E+02	9.35635E+02
2.00133E+02	9.38131E+02
2.00133E+02	9.40627E+02
2.00133E+02	9.43123E+02
2.00133E+02	9.4561

[illegible]

INTERSTITIAL NITROGEN CONCENTRATIONS --- STATIONS 1 THRU 55

1.00900E-02	1.01504E-02	1.02221E-02	1.04147E-02	1.08492E-02	1.11340E-02	1.14356E-02	1.17210E-02	1.19929E-02	1.22000E-02
1.25237E-02	1.27811E-02	1.30311E-02	1.32726E-02	1.35034E-02	1.37320E-02	1.39460E-02	1.41448E-02	1.43373E-02	1.45095E-02
1.46572E-02	1.47747E-02	1.48691E-02	1.49510E-02	1.49747E-02	1.49797E-02	1.49809E-02	1.47800E-02	1.45094E-02	1.42574E-02
1.37616E-02	1.34164E-02	1.30502E-02	1.26802E-02	1.23122E-02	1.19374E-02	1.15512E-02	1.11574E-02	1.07544E-02	1.03424E-02
6.44488E-02	5.56613E-02	4.83306E-02	3.12937E-02	1.98251E-02	5.07082E-02	1.16450E-04	3.48991E-05	9.82148E-06	2.60438E-06
6.48480E-07	1.51098E-07	3.27342E-08	6.55263E-09	1.20237E-09					

INTERSTITIAL NITROGEN CONCENTRATIONS --- STATIONS 1 THRU 55

0.00000E+00	0.00000E+00	0.00000E+00	0.00000E+00	0.00000E+00	0.00000E+00	0.00000E+00	0.00000E+00	0.00000E+00	0.00000E+00
1.16433E-02	1.15012E-02	1.12817E-02	1.10817E-02	1.08135E-02	1.04815E-02	1.00944E-02	9.6577E-03	9.16547E-03	8.62977E-03
1.49971E-02	1.55276E-02	1.61034E-02	1.66256E-02	1.70825E-02	1.74554E-02	1.77421E-02	1.79221E-02	1.80076E-02	1.80076E-02
4.14517E-02	4.31629E-02	4.47553E-02	4.62922E-02	4.77323E-02	4.90130E-02	5.01300E-02	5.10169E-02	5.17323E-02	5.2309E-02
5.56119E-02	5.56432E-02	5.56530E-02	5.56604E-02	5.56694E-02	5.56744E-02	5.56774E-02	5.56794E-02	5.56804E-02	5.56814E-02

INTERSTITIAL HYDROGEN CONCENTRATIONS --- STATIONS 1 THRU 55

0.00000E+00	0.00000E+00	0.00000E+00	0.00000E+00	0.00000E+00	0.00000E+00	0.00000E+00	0.00000E+00	0.00000E+00	0.00000E+00
0.00000E+00	0.00000E+00	0.00000E+00	0.00000E+00	0.00000E+00	0.00000E+00	0.00000E+00	0.00000E+00	0.00000E+00	0.00000E+00
0.00000E+00	0.00000E+00	0.00000E+00	0.00000E+00	0.00000E+00	0.00000E+00	0.00000E+00	0.00000E+00	0.00000E+00	0.00000E+00
0.00000E+00	0.00000E+00	0.00000E+00	0.00000E+00	0.00000E+00	0.00000E+00	0.00000E+00	0.00000E+00	0.00000E+00	0.00000E+00

CHARGE PRESSURE AT TIME T = 4.00000E+04 IS 16.182 PSIA

VALUES OF HBAR AT AXIAL STATIONS 1 THRU 54

2.30185E+01	2.29842E+01	2.28452E+01	2.27266E+01	2.26325E+01	2.25803E+01	2.25228E+01	2.24723E+01	2.24291E+01	2.23888E+01
2.23512E+01	2.23122E+01	2.22712E+01	2.22282E+01	2.21832E+01	2.21362E+01	2.20872E+01	2.20362E+01	2.19832E+01	2.19282E+01
2.18712E+01	2.18122E+01	2.17512E+01	2.16882E+01	2.16232E+01	2.15562E+01	2.14872E+01	2.14162E+01	2.13432E+01	2.12682E+01
2.11922E+01	2.11172E+01	2.10402E+01	2.09612E+01	2.08802E+01	2.07972E+01	2.07122E+01	2.06252E+01	2.05362E+01	2.04452E+01
2.03522E+01	2.02592E+01	2.01642E+01	2.00672E+01	1.99682E+01	1.98672E+01	1.97642E+01	1.96582E+01	1.95502E+01	1.94402E+01
1.93282E+01	1.92122E+01	1.90942E+01	1.89742E+01	1.88522E+01	1.87282E+01	1.86022E+01	1.84742E+01	1.83442E+01	1.82122E+01
1.80782E+01	1.79442E+01	1.78082E+01	1.76702E+01	1.75302E+01	1.73882E+01	1.72442E+01	1.70982E+01	1.69502E+01	1.68002E+01
1.66482E+01	1.64962E+01	1.63422E+01	1.61862E+01	1.60282E+01	1.58682E+01	1.57062E+01	1.55422E+01	1.53762E+01	1.52082E+01
1.50382E+01	1.48692E+01	1.47002E+01	1.45292E+01	1.43562E+01	1.41822E+01	1.40072E+01	1.38302E+01	1.36512E+01	1.34702E+01
1.32882E+01	1.31062E+01	1.29232E+01	1.27382E+01	1.25512E+01	1.23622E+01	1.21722E+01	1.19802E+01	1.17862E+01	1.15902E+01
1.13922E+01	1.11942E+01	1.09942E+01	1.07922E+01	1.05882E+01	1.03822E+01	1.01742E+01	9.9642E+00	9.7492E+00	9.5322E+00
9.3142E+00	9.0962E+00	8.8762E+00	8.6542E+00	8.4302E+00	8.2042E+00	7.9762E+00	7.7462E+00	7.5142E+00	7.2802E+00
7.0442E+00	6.8082E+00	6.5702E+00	6.3302E+00	6.0882E+00	5.8442E+00	5.5982E+00	5.3502E+00	5.1002E+00	4.8482E+00
4.5942E+00	4.3402E+00	4.0842E+00	3.8262E+00	3.5662E+00	3.3042E+00	3.0402E+00	2.7742E+00	2.5062E+00	2.2362E+00
1.9642E+00	1.6922E+00	1.4182E+00	1.1422E+00	8.642E+00	5.822E+00	2.982E+00	1.142E+00	0.0000E+00	0.0000E+00

[illegible][illegible][illegible]

POLYCYCLIC AROMATIC CONCENTRATIONS --- STATIONS 1 THRU 5*	
1,2,3,4,6,7,8,9,10,11,12,13,14,15,16,17,18,19,20,21,22,23,24,25,26,27,28,29,30,31,32,33,34,35,36,37,38,39,40,41,42,43,44,45,46,47,48,49,50,51,52,53,54,55,56,57,58,59,60,61,62,63,64,65,66,67,68,69,70,71,72,73,74,75,76,77,78,79,80,81,82,83,84,85,86,87,88,89,90,91,92,93,94,95,96,97,98,99,100,101,102,103,104,105,106,107,108,109,110,111,112,113,114,115,116,117,118,119,120,121,122,123,124,125,126,127,128,129,130,131,132,133,134,135,136,137,138,139,140,141,142,143,144,145,146,147,148,149,150,151,152,153,154,155,156,157,158,159,160,161,162,163,164,165,166,167,168,169,170,171,172,173,174,175,176,177,178,179,180,181,182,183,184,185,186,187,188,189,190,191,192,193,194,195,196,197,198,199,200,201,202,203,204,205,206,207,208,209,210,211,212,213,214,215,216,217,218,219,220,221,222,223,224,225,226,227,228,229,230,231,232,233,234,235,236,237,238,239,240,241,242,243,244,245,246,247,248,249,250,251,252,253,254,255,256,257,258,259,260,261,262,263,264,265,266,267,268,269,270,271,272,273,274,275,276,277,278,279,280,281,282,283,284,285,286,287,288,289,290,291,292,293,294,295,296,297,298,299,300,301,302,303,304,305,306,307,308,309,310,311,312,313,314,315,316,317,318,319,320,321,322,323,324,325,326,327,328,329,330,331,332,333,334,335,336,337,338,339,340,341,342,343,344,345,346,347,348,349,350,351,352,353,354,355,356,357,358,359,360,361,362,363,364,365,366,367,368,369,370,371,372,373,374,375,376,377,378,379,380,381,382,383,384,385,386,387,388,389,390,391,392,393,394,395,396,397,398,399,400,401,402,403,404,405,406,407,408,409,410,411,412,413,414,415,416,417,418,419,420,421,422,423,424,425,426,427,428,429,430,431,432,433,434,435,436,437,438,439,440,441,442,443,444,445,446,447,448,449,450,451,452,453,454,455,456,457,458,459,460,461,462,463,464,465,466,467,468,469,470,471,472,473,474,475,476,477,478,479,480,481,482,483,484,485,486,487,488,489,490,491,492,493,494,495,496,497,498,499,500,501,502,503,504,505,506,507,508,509,510,511,512,513,514,515,516,517,518,519,520,521,522,523,524,525,526,527,528,529,530,531,532,533,534,535,536,537,538,539,540,541,542,543,544,545,546,547,548,549,550,551,552,553,554,555,556,557,558,559,560,561,562,563,564,565,566,567,568,569,570,571,572,573,574,575,576,577,578,579,580,581,582,583,584,585,586,587,588,589,590,591,592,593,594,595,596,597,598,599,600,601,602,603,604,605,606,607,608,609,610,611,612,613,614,615,616,617,618,619,620,621,622,623,624,625,626,627,628,629,630,631,632,633,634,635,636,637,638,639,640,641,642,643,644,645,646,647,648,649,650,651,652,653,654,655,656,657,658,659,660,661,662,663,664,665,666,667,668,669,670,671,672,673,674,675,676,677,678,679,680,681,682,683,684,685,686,687,688,689,690,691,692,693,694,695,696,697,698,699,700,701,702,703,704,705,706,707,708,709,710,711,712,713,714,715,716,717,718,719,720,721,722,723,724,725,726,727,728,729,730,731,732,733,734,735,736,737,738,739,740,741,742,743,744,745,746,747,748,749,750,751,752,753,754,755,756,757,758,759,760,761,762,763,764,765,766,767,768,769,770,771,772,773,774,775,776,777,778,779,780,781,782,783,784,785,786,787,788,789,790,791,792,793,794,795,796,797,798,799,800,801,802,803,804,805,806,807,808,809,810,811,812,813,814,815,816,817,818,819,820,821,822,823,824,825,826,827,828,829,830,831,832,833,834,835,836,837,838,839,840,841,842,843,844,845,846,847,848,849,850,851,852,853,854,855,856,857,858,859,860,861,862,863,864,865,866,867,868,869,870,871,872,873,874,875,876,877,878,879,880,881,882,883,884,885,886,887,888,889,890,891,892,893,894,895,896,897,898,899,900,901,902,903,904,905,906,907,908,909,910,911,912,913,914,915,916,917,918,919,920,921,922,923,924,925,926,927,928,929,930,931,932,933,934,935,936,937,938,939,940,941,942,943,944,945,946,947,948,949,950,951,952,953,954,955,956,957,958,959,960,961,962,963,964,965,966,967,968,969,970,971,972,973,974,975,976,977,978,979,980,981,982,983,984,985,986,987,988,989,990,991,992,993,994,995,996,997,998,999,1000,1001,1002,1003,1004,1005,1006,1007,1008,1009,1010,1011,1012,1013,1014,1015,1016,1017,1018,1019,1020,1021,1022,1023,1024,1025,1026,1027,1028,1029,10	

[illegible][illegible][illegible]


```

04/21/73 SCOPE 3.3R1=HCAUT06500= VER. E 12/10/72
19.24.07.A00/17J
19.24.07.000049-0AR00-REAS
19.24.07.SER.A07671
19.24.07.MONO.5.100.500.700.60000.150000,
19.24.07.19A0012 HATYHQA 051037500007104 -GM007A 943200001
19.24.07.RESUES,MON421,M1. (05000)
19.24.07.129 ASSIGNED, MEEL 05000 )
19.24.07.A00005, HATYHQA OFF
19.24.08.REJIND(MON421)
19.24.08.COPYMF(MON421,OPR)
19.24.17.RETURN(MON421)
19.24.17.REFL.150000.
19.24.17.DEGIMAC= 000 SEC.,PP= 000 SEC.,OCTAL-FL=000M.
19.24.17.000049-0AR00-REAS
19.24.19.CELL DONE .C20 CP SEC
19.24.19.LOADER(CELOADR)
19.24.19.000049-0AR00-REAS
19.24.31.0UNRFD BLOWN ASSIGNED TO MAIN LEV 0 OVL-
19.24.31.0 BLKDATA
19.24.39.0 DANGER-NO REFERENCE TO ENTRY POINT-
19.24.40. LOAD TIME 4.611 CP SEC
19.24.40.000049-0AR00-REAS
19.24.50.00 4460 OUTPUT. 2 FRAMES GENERATED **
19.24.50.CURRENT PRU COUNT = 021
19.24.50.000049-0AR00-REAS
19.24.54.CATALOG(FILMPL,PLOT2PF,CY02,PH000000,1D=
19.24.54.SYSTEMCHK,MN1)
19.24.54.000049-0AR00-REAS
19.24.54.P4 FOUND IN SD 001
19.24.54.FILE CALLOUED AS
19.24.54.000049-0AR00-REAS
19.24.54.IN SD 001
19.24.54.R0 COUNT 0001
19.24.54.000049-0AR00-REAS
19.24.55.CP 000049.500,
19.24.55.PP 055.148 SEC.
19.24.55.MU 000.004
19.24.55.000049-0AR00-REAS
19.24.55.000049-0AR00-REAS

```

ENGINE

Z0	=	0.0.
G000	=	0.5005E+01.
M001	=	0.12235E+02.
P00	=	0.20E+02.
T00	=	0.1953E+04.
TVAP	=	0.00E+03.
MIV	=	0.73904E+03.
P	=	0.0.
HF	=	0.0.
TP	=	0.57E+03.
ENMX1	=	0.2E+03.
ENMX2	=	0.4E+02.
ENMX3	=	0.0E+02.
PP	=	0.205E+03.
ZEND	=	0.29E+00.
VC	=	0.49E-02.
AC	=	0.32E-01.
MM	=	0.4E+00.
CM	=	0.12E+00.
AW	=	0.3E+00.
TA	=	0.57E+03.
MA	=	0.0.
MA1	=	0.11E-03.
MA2	=	0.0.
TP1	=	0.57E+03.
PCI	=	0.147E+02.
CPHY3	=	0.0.
CPAM1	=	0.0.
CIARI	=	0.0.
CPM21	=	0.57E-01.
CIN21	=	0.57E-01.

WIND - 0.000000

OPH2I = 0.0,

GIN2I = 0.0,

AS = 0.3203E+03,

BORIF = 0.15E+02,

GRING = 0.12E+04,

PAJIL = 0.1663E+00,

FULPR = 0.0,

TLIO = 0.53E+03,

TRULS = 0.1E+00,

FINZON = 0.2003E+01,

GINVI = 0.0,

SENO

SCONTAL

BRUM = 65,

MPRNT = 1,

MPASS = 0,

DEL7 = 0.15-03, 0.35-03, 0.15-03, 0.35-03, 0.35-03, 0.35-03, 0.15-01,
0.25-01, 0.9575263031000-203, 1, 0.34692074062203-203,
-0.0127204774059-217, 0.9612601960836-251, -0.1014213522770E+49,
0.13252728000824-259, 1, -0.1394309991394E+50,
0.4179344790225-116, 0.1261030100640-255, 1,

END

SAMPLE CASE OF MONOPROPELLANT ENGINE PROGRAM, N2H4

PRODUCT INPUT

~~66-48-03-61-3716-462+~~

PROGRAM PARAMETERS FOR THIS RUN
CFF SURFLY MCPZ DRUK UNIT

NAME	AGE	DOB	SSN	POB	POC	POA	POB	POC	POA
ALFRED	35	1950-01-01	123456789	1950-01-01	1950-01-01	1950-01-01	1950-01-01	1950-01-01	1950-01-01
BETTY	35	1950-01-01	123456789	1950-01-01	1950-01-01	1950-01-01	1950-01-01	1950-01-01	1950-01-01
CHARLES	35	1950-01-01	123456789	1950-01-01	1950-01-01	1950-01-01	1950-01-01	1950-01-01	1950-01-01
DORIS	35	1950-01-01	123456789	1950-01-01	1950-01-01	1950-01-01	1950-01-01	1950-01-01	1950-01-01
EDWARD	35	1950-01-01	123456789	1950-01-01	1950-01-01	1950-01-01	1950-01-01	1950-01-01	1950-01-01
FLORENCE	35	1950-01-01	123456789	1950-01-01	1950-01-01	1950-01-01	1950-01-01	1950-01-01	1950-01-01
GEORGE	35	1950-01-01	123456789	1950-01-01	1950-01-01	1950-01-01	1950-01-01	1950-01-01	1950-01-01
HAROLD	35	1950-01-01	123456789	1950-01-01	1950-01-01	1950-01-01	1950-01-01	1950-01-01	1950-01-01
IRVING	35	1950-01-01	123456789	1950-01-01	1950-01-01	1950-01-01	1950-01-01	1950-01-01	1950-01-01
JANE	35	1950-01-01	123456789	1950-01-01	1950-01-01	1950-01-01	1950-01-01	1950-01-01	1950-01-01
JOHN	35	1950-01-01	123456789	1950-01-01	1950-01-01	1950-01-01	1950-01-01	1950-01-01	1950-01-01
KATHLEEN	35	1950-01-01	123456789	1950-01-01	1950-01-01	1950-01-01	1950-01-01	1950-01-01	1950-01-01
LARRY	35	1950-01-01	123456789	1950-01-01	1950-01-01	1950-01-01	1950-01-01	1950-01-01	1950-01-01
MARY	35	1950-01-01	123456789	1950-01-01	1950-01-01	1950-01-01	1950-01-01	1950-01-01	1950-01-01
NANCY	35	1950-01-01	123456789	1950-01-01	1950-01-01	1950-01-01	1950-01-01	1950-01-01	1950-01-01
OLIVER	35	1950-01-01	123456789	1950-01-01	1950-01-01	1950-01-01	1950-01-01	1950-01-01	1950-01-01
PATRICIA	35	1950-01-01	123456789	1950-01-01	1950-01-01	1950-01-01	1950-01-01	1950-01-01	1950-01-01
ROBERT	35	1950-01-01	123456789	1950-01-01	1950-01-01	1950-01-01	1950-01-01	1950-01-01	1950-01-01
SARAH	35	1950-01-01	123456789	1950-01-01	1950-01-01	1950-01-01	1950-01-01	1950-01-01	1950-01-01
THOMAS	35	1950-01-01	123456789	1950-01-01	1950-01-01	1950-01-01	1950-01-01	1950-01-01	1950-01-01
WILLIAM	35	1950-01-01	123456789	1950-01-01	1950-01-01	1950-01-01	1950-01-01	1950-01-01	1950-01-01

THE INSTRUCTIONS FOR EACH OF THE PASSES

THE PASSIS IN SUMMARIZE ON APP SECTICE NUMBERS-1-2-3-4-5-6-7-8

INITIAL CONDITIONS

IPJ	PCI	CPIVI	CINVI	CINZI	CINZI
5.700C3E+02	1.476CCCE-01	0.	0.	5.70000F+01	5.70000E+02
					0.

DATA FOR LINE HOMBATUM, DEEP EVAPORATION AND PULSE TIME

AG	SCRF	ORIG	ACCLW	FCLNL	FULFR	YLIC	YPULS	FINZON
3.21700E+01	1.50700E+03	1.20600E+03	6.34000E+31	1.69233E-01	0.	3.70000E+02	1.00000E-01	2.00300E-02

VAPOR REGION AXIAL STATIONS

[illegible]

378045 2-94-4

[illegible]

AP VS Z TABLE

[illegible]

DELTA VS Z TABLE

[illegible]

3.40000E-04
 3.40000E-01 3.40000E-01 3.40000E-01 3.40000E-01 3.40000E-01 3.40000E-01 3.40000E-01 3.40000E-01 3.40000E-01
 3.40000E-01 3.40000E-01 3.40000E-01 3.40000E-01 3.40000E-01 3.40000E-01 3.40000E-01 3.40000E-01 3.40000E-01
 3.40000E-05

TIME TO FILL FEED LINES TFL = 3.9300E-03 SECONDS

THE PROGRAM STOPPED BECAUSE EVAPORATION RATE LIMITATIONS CAUSED FLOODING OF COLD ENGINE WITH CHUGGING

TIME TO PRESSURE RISE 2.1577E-02 SECONDS

PEAK PRESSURE OF CHUG 1.5735E+02 POUNDS PER SQUARE INCH

LIQUID N2H4 SPRAY 1.1621E+03 POUNDS

HOT NH3 DRIVING SPRAY 2.1299E+04 POUNDS

SLOW NH3 AFTER VENT 7.8898E+04 POUNDS

*** OPERATIONS COMPLETE ***